RPP-RPT-59197, Rev. 1

Analysis of Past Tank Waste Leaks and Losses in the Vicinity of Waste Management Area C at the Hanford Site, Southeast Washington

Author Name:
M. M. Kozak, S. Mehta, A. Ali, A. Mayenna, M. Weber – INTERA, Inc.
W. J. McMahon – CH2M HILL Plateau Remediation Company
M. P. Bergeron, J. G. Field – Washington River Protection Solutions, LLC
M. P. Connelly – TEC-GEO, Inc.
Richland, WA 99352
U.S. Department of Energy Contract DE-AC27-08RV14800

EDT/ECN:	DRCF	UC:	
Cost Center:		Charge Code:	
B&R Code:		Total Pages:	332

Key Words: Performance Assessment, Waste Management Area C, PA, WMA C, single-shell tank, STOMP, past waste releases, past leaks, unplanned releases, process-level model, modeling codes, vadose zone, groundwater, unsaturated flow, vadose zone flow, groundwater flow, contaminant transport, scoping analysis, future prediction of impacts

Abstract: This report provides an analysis of past leaks at Waste Management Area C using the models developed for the Waste Management Area C residual waste performance assessment (RPP-ENV-58782, "Performance Assessment of Waste Management Area C, Hanford Site, Washington") and Resource Conservation and Recovery Act of 1976 (RCRA) Closure Analysis (RPP-ENV-58806, "RCRA Closure Analysis of Tank Waste Residuals Impacts at Waste Management Area C, Hanford Site, Washington").

TRADEMARK DISCLAIMER. Reference herein to any specific commercial product, process, or service by trade name, trademark, manufacturer, or otherwise, does not necessarily constitute or imply its endorsement, recommendation, or favoring by the United States Government or any agency thereof or its contractors or subcontractors.

DATE:
Oct 31, 2016
HANFORD RELEASE

APPROVED
By Janis Aardal at 2:08 pm, Oct 31, 2016

Release Approval Date Release Stamp

Approved For Public Release

RPP-RPT-59197
Revision 1

Analysis of Past Tank Waste Leaks and Losses in the Vicinity of Waste Management Area C at the Hanford Site, Southeast Washington

M. M. Kozak
S. Mehta
A. Ali
A. Mayenna
M. Weber
INTERA, Inc.

W. J. McMahon
CH2M HILL Plateau Remediation Company

M. P. Bergeron
J. G. Field
Washington River Protection Solutions, LLC

M. P. Connelly
TecGeo, Inc.

Date Published
October 2016

Prepared for the U.S. Department of Energy
Office of River Protection
Contract No. DE-AC27-08RV14800

Approved for public release; distribution unlimited

This page intentionally left blank.

EXECUTIVE SUMMARY

The U.S. Department of Energy (DOE), Office of River Protection is pursuing closure on the Single-Shell Tank (SST) Waste Management Area (WMA) C under Federal requirements and forthcoming State-approved closure plans and permits in accordance with the Hanford Federal Facility Agreement and Consent Order (HFFACO) (Ecology et al. 1989), Action Plan, Appendix I.

The Performance Assessment (PA) requirements for the closure process are outlined in Appendix I of the HFFACO. Appendix I of the HFFACO Action Plan contains language that broadens the scope of a "performance assessment" compared to its usual usage in the literature and in DOE Order 435.1, Radioactive Waste Management.

To distinguish between the two terms and avoid confusion, the term "performance assessment" will be used in this document in the following manner:

- The broadened scope of the HFFACO Action Plan Appendix I analysis will be referred to as the "Appendix I Performance Assessment" (IPA)

- The simpler "performance assessment" (PA) will refer solely to the DOE O 435.1 definition of performance assessment.

Appendix I of the HFFACO Action Plan describes the waste retrieval and closure process that is to be implemented for the Hanford Site SST system. The four components of the IPA are illustrated in Figure ES-1. The current report represents the right-most component in the figure, and is an analysis of past leaks that occurred at WMA C, intended for use in supporting Resource Conservation and Recovery Act of 1976 (RCRA) regulatory documents.

This report provides an analysis of past leaks at WMA C using the models developed for the WMA C residual waste PA (RPP-ENV-58782, "Performance Assessment of Waste Management Area C, Hanford Site, Washington") and RCRA Closure Analysis (RCA) (RPP-ENV-58806, "RCRA Closure Analysis of Tank Waste Residuals Impacts at Waste Management Area C, Hanford Site, Washington"). The report has several purposes.

First, the conceptual model developed for the PA of residual contamination has been implemented to evaluate how well it explains observed field data for the time of arrival of contaminants to groundwater, concentrations of contaminants in groundwater, and the distribution of contaminants in the vadose zone. Second, the combination of the field data and model have been used to determine bounds on input assumptions that are consistent with groundwater and soil monitoring data from past leaks. In particular, a range of models has been used to evaluate the uncertainties in the inventory and volumes of past leaks, to better constrain estimates of the existing contamination. Third, the constrained model has been used to project future impacts from the past leaks. This part of the analysis will represent an input to additional analyses for the Appendix I PA.

Figure ES-1. The Components of the Appendix I Performance Assessment.

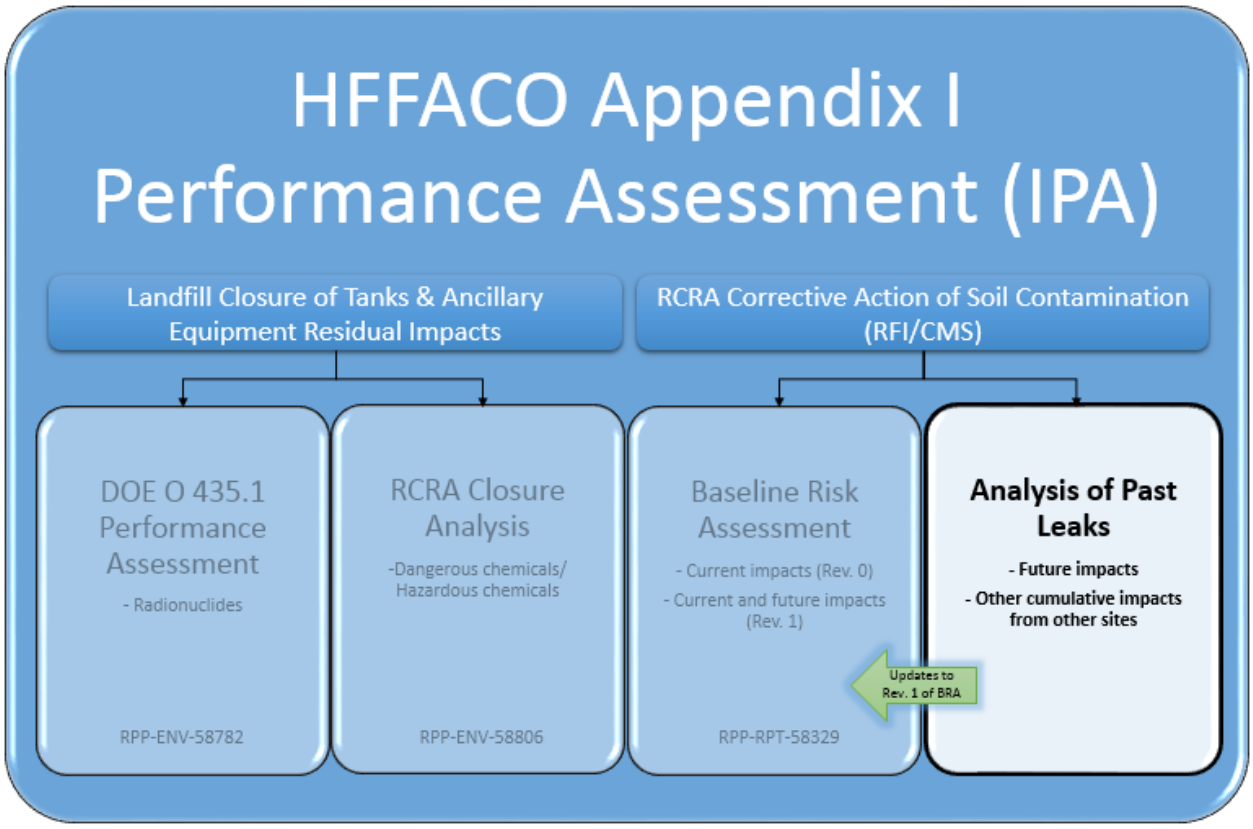

BRA = Baseline Risk Assessment
HFFACO = Hanford Federal Facility Agreement and Consent Order
RCRA = Resource Conservation and Recovery Act of 1976
RFI/CMS = RCRA Facility Investigation/Corrective Measures Study

References:
DOE O 435.1, Radioactive Waste Management.
RPP-ENV-58806, "RCRA Closure Analysis of Waste Management Area C, Hanford Site, Washington."
RPP-RPT-58329, "Baseline Risk Assessment for Waste Management Area C."

The scope of this report is limited to an assessment of past leaks at WMA C, and is intended as a companion report to the radiological PA of residual contamination (RPP-ENV-58782) and the RCA for WMA C (RPP-ENV-58806).

The analysis of past leaks has been structured to meet several goals. First, the analysis is intended to be responsive to ideas and concerns expressed in the 2009 – 2011 PA scoping sessions (see Section 1.1.1), in which specific features of WMA C were identified as requiring particular attention because of their potential to influence the migration of contaminants from WMA C. Second, the analysis is intended to be consistent, to the extent possible, with the PA (RPP-ENV-58782) and RCA (RPP-ENV-58806) for disposal of residual wastes in WMA C. Third, the goal is to provide an understanding of the key features and processes discussed in Sections 1 and 2 that influence the migration of contaminants. Fourth, the goal is to use the understanding gained by the analysis to provide a projection of the future evolution of the contamination beneath WMA C.

The strategy for this analysis of leaks at WMA C is to define and analyze a suite of-scoping cases to evaluate the uncertainties associated with past leaks. These uncertainties can be broadly considered to originate from one of the following sources.

- Uncertainties exist in the timing, inventory, and volumes of leaks. These uncertainties have been discussed at length in Revision 4 of RPP-ENV-33418.

- Uncertainties exist in past actions taken to mitigate the surface manifestations of past leaks. In particular, for several UPRs, water was added via firehose to surface contamination to wash it down into the soil column.

- Uncertainties exist in interpretations of the groundwater monitoring and vadose zone characterization data used to estimate current contamination levels resulting from the past leaks. The data represent specific locations and instances in time while the contamination continues to move.

- Uncertainties exist in the hydrogeological representation of the stratigraphy below WMA C. These uncertainties have been addressed in RPP-ENV-58782 and RPP-ENV-58806 by evaluating the consequences of alternative interpretations of the hydrogeology. This approach has continued to be used in the current report.

- Uncertainties exist in the effective values of parameters used in modeling groundwater flow and contaminant transport. These uncertainties are discussed in detail in RPP-ENV-58782 and RPP-ENV-58806.

- Uncertainties exist regarding the evolution of the groundwater system at WMA C over the past several decades, as discussed in Section 2. Anthropogenic water introduced south of WMA C created a gradient generally to the north, which has transitioned over recent decades to a gradient generally southward. The transition between these two states occurred approximately coincident with the arrival of the first contaminants at the water table. The feature of the groundwater system evolution introduces additional uncertainties about the trajectory of plumes moving in the aquifer.

The analyses of potential releases of contaminants in residual wastes presented in RPP-ENV-58782 and RPP-ENV-58806 were focused on future site conditions, and as a result did not directly address several of these sources of uncertainty; specifically, those associated with the leaks and that associated with the past evolution of the water table. However, in RPP-ENV-58782 and RPP-ENV-58806, a number of approaches to developing confidence in the data, assumptions, and methods were used, as follows.

- Many data were based on WMA C-specific site characterization, sampling, measurements and interpretations, including those for contaminant inventory, geology, hydrology and geochemistry. When data specific to WMA C were not available, data from nearby sites or comparable conditions, as well as data reported in the literature, were used.

- Data were upscaled to represent field-scale processes using scientifically-accepted approaches that have been published in peer-reviewed journals. Upscaling techniques use information from small, core-scale measurements to develop parameters that are applicable to large, field-scale models.

- The process-based modeling software, Subsurface Transport Over Multiple Phases (STOMP)©[1] code (PNNL-12030, "STOMP Subsurface Transport Over Multiple Phases Version 2.0 Theory Guide"; Pacific Northwest National Laboratory, Queried 12/18/2015, [STOMP User Guide], http://stomp.pnnl.gov/user_guide/STOMP_guide.stm; PNNL-11216, "STOMP Subsurface Transport Over Multiple Phases Application Guide"), has been benchmarked and deemed suitable for use in this PA. The STOMP© code is the pre-authorized modeling software at the Hanford Site for vadose zone and near-field groundwater modeling (Internal memorandum 1301789, "Modeling to Support Regulatory Decisionmaking at Hanford"). The STOMP© code has previously been qualified for simulation use at Hanford by CH2M HILL Plateau Remediation Company (CHPRC) (CHPRC-00269, "STOMP Requirements Traceability Matrix CHPRC Build 4").

- Sensitivity and uncertainty analyses were conducted to evaluate the effect of parameter uncertainties and alternative conceptual models on the overall performance of the system.

These approaches specifically address uncertainties in model conceptualizations and input parameters for groundwater flow and transport, but do not address uncertainties in past leaks and in past evolution of the groundwater table.

Consequently, the model used in RPP-ENV-58782 and RPP-ENV-58806 was adapted so that the water table was reflective of conditions at WMA C when first arrival of contaminants at the water table was observed. Two approaches were used. In the first approach, the water table was assumed to be fixed, and directed in the same way as the prospective water table used for future analyses, but at a higher level, which allows the analysis to represent the shorter travel time in the vadose zone that would have existed when the plumes initially arrived. This approach is intended to represent the time of first arrival and the peak of the groundwater plume, but is not necessarily to represent the spatial distribution of contamination in the groundwater. The second approach was to introduce a time-varying water table to represent the likely evolution of the aquifer gradient over the simulation period. Both of these approaches are described in more detail in Section 4.

Model results have been compared to ^{99}Tc concentrations observed in groundwater monitoring wells around WMA C because ^{99}Tc is a key risk driver, and the contamination levels observed there are considered to be the result of WMA C past leaks. The ^{99}Tc concentration data collected from groundwater monitoring wells have been used to evaluate and constrain the model inputs and assumptions that produce results that are consistent with the arrival times and concentration levels of ^{99}Tc observed historically in the vicinity of WMA C.

[1] Subsurface Transport Over Multiple Phases (STOMP)© is copyrighted by Battelle Memorial Institute, 1996.

The results of the constrained model are then also compared with other contaminant data as appropriate. The model is also used to project the consequences of past leaks to evaluate the future consequences of the past waste leaks and releases and to evaluate how the groundwater concentrations may change in the future.

The set of scoping analysis cases evaluated in the leak analysis are presented in Table ES-1. The table includes a brief explanation of each scoping analysis to provide insight into the alternative assumptions it is intended to evaluate.

Table ES-2. Description of Past Tank Waste Release Scoping Cases. (2 sheets)

Scoping Case (Abbreviation)	Scoping Case Description and Purpose
Case 1a (BaseCase_hi_inv)	Assumes general boundary conditions, hydrogeologic framework, vadose zone and groundwater flow and transport parameters used in the base case of the DOE 435.1 PA and RCRA Closure Analysis with a modification to account for the increased water table elevation in the WMA C area under current conditions. The water table has been set to approximate current conditions of ~122.5 m (401.9 ft). This case also assumes current estimates of leak inventories and volumes that includes the upper bound inventory (9.8 Ci) and volume 77,600 L (20,500 gals) developed for tank 241-C-105 (C-105).
Case 1b (BaseCase_lo_inv)	This case is similar to Case 1a but assumes current estimates of leak inventories and volumes that includes the lower bound inventory (1 Ci) and volume 7,570 L (2,000 gals) developed for tank C-105.
Cases Related to Changes in Groundwater Flux Rates	
Case 2a (GWflux_10%)	Assumes same parameterization and past leak volumes and inventories as Case 1a but with the aquifer flux set at 10th percentile values used in the uncertainty analysis developed for the DOE 435.1 PA. This case corresponds to altered aquifer flow producing minimal aquifer dilution compared to the base case.
Case 2b (GWflux_90%)	Assumes same parameterization and past leak volumes and inventories as Case 1a but with the aquifer flux set at 90th percentile values used in the uncertainty analysis developed the DOE 435.1 PA. This case corresponds to altered aquifer flow producing a higher level of aquifer dilution compared to the base case.
Cases Related to Changes in Recharge Rates	
Case 3a (EnhanceRech_150)	Assumes same parameterization and past leak volumes and inventories as Case 1a but with a recharge rate of 150 mm/yr for the tank farm area within the WMA C model domain to evaluate effect of increased anthropogenic recharge inside of the tank farm area on past releases.
Case 3b (EnhanceRech_100)	Assumes same parameterization and past leak volumes and inventories as Case 1a but with a recharge rate of 100 mm/yr applied for all areas within the WMA C model domain to evaluate effect of increased recharge outside of the tank farm area on past releases.
Case 3c (Gunite_Cap)	Assumes same parameterization and past leak volumes and inventories as Case 1a but some local changes at UPRs-E-81, -82, and -86. These changes include an additional 1,135 Lpm (300 gpm) of wash water for 4 hours at the time of release (a one-time addition of 272,550 L [72,000 gal]). Twenty years after UPRs-E-82, and -86, Gunite applied to those two surfaces is assumed to change the infiltration at those UPRs to 1 mm/y (UPR-E-81 includes no Gunite). The case investigates the effects of potential localized water use and caps at selected UPRs on those past releases.

Table ES-2. Description of Past Tank Waste Release Scoping Cases. (2 sheets)

Scoping Case (Abbreviation)	Scoping Case Description and Purpose
Cases Related to Changes in Vadose Zone Parameters/Conceptualizations	
Case 4a (ACM_II)	Assumes the same parameterization and past leak volumes and inventories as Case 1a but with the geologic interpretation developed by Nez Perce staff for Alternative Geologic Model II. This case examines the effect of a finer alternative treatment of major hydrogeologic units in the vadose zone on past releases.
Case 4b (ACM_hetero)	Assumes vadose zone parameterization in the heterogeneous hydrogeologic model interpretation developed for use in DOE 435.1 PA and RCRA Closure Analysis with Case 1a leak volumes and inventories. This case examines the effect of heterogeneous treatment of sediments in the vadose zone on past releases.
Case 4c (vzprop_50%)	Assumes same parameterization and past leak volumes and inventories as Case 1a but with vadose zone hydraulic properties at the 50th percentile values as set in the uncertainty analysis developed for the DOE 435.1 PA. This case evaluates the effect on past releases of higher vadose zone hydraulic properties than used in the base case.
Case 4d (vzprop_95%)	Assumes same parameterization and past leak volumes and inventories as Case 1 but with vadose zone hydraulic properties at the 95th percentile values as set in the uncertainty analysis developed for the DOE 435.1 PA. This case evaluates the effect on past releases of lower vadose zone hydraulic properties than used in the base case.
Case 4e (ACM_dike)	Assumes same parameterization and past leak volumes and inventories as Case 1 but with a hypothetical clastic dike placed below tank C-105. This case evaluates the effect on past releases of a possible preferential pathway for contaminants in the vicinity of tank C-105.
Case 4f (ACM_borehole)	Assumes same parameterization and past leak volumes and inventories as Case 1 but with the additional assumption of an inadequately sealed borehole at well 299-E27-70 (drywell 30-05-02), located near the past tank leak near C-105. This case evaluates the effect on past releases for another possible type of preferential pathway for contaminants in the vicinity of tank C-105.

PA = performance assessment
RCRA = Resource Conservation and Recovery Act of 1976
UPR = unplanned release
WMA = Waste Management Area

Reference: DOE 435.1, Radioactive Waste Management.

Scoping analysis Cases 1a and 1b represents a minimal change from the PA/RCA model for residual wastes presented in RPP-ENV-58782 and RPP-ENV-58806, with the level of the water table elevated to represent an appropriate travel distance to the water table for the leaks. Case 1a uses upper bound leak inventories and volumes based on an assumed upper bound ^{99}Tc inventory for the tank C-105 waste loss of 9.8 Ci and an upper bound leak volume of 77,600 L (20,500 gal). Case 1b uses the lower bound leak inventories and volumes based on an assumed lower bound ^{99}Tc inventory for the tank C-105 waste loss of 1.0 Ci and a lower bound leak volume of 7,570 L (2,000 gal).

Scoping analysis Case 1b produced concentrations substantially below observed concentrations for ^{99}Tc in observation wells. It was concluded that the lower bound estimate is inconsistent

with data, and the upper bound estimate of 10 Ci ^{99}Tc in the tank C-105 leak waste was used for all other analyses.

Cases 2a and 2b investigated the effect of changing groundwater fluxes on the model results. It was found that the higher flux rates led to a greater dilution of plume concentrations at the water table, and it is concluded that the lower groundwater flux rate provides concentration levels of ^{99}Tc that are more consistent with monitoring data observed in key monitoring well locations.

Cases 3a through 3b investigated the general effect of a higher recharge rate than used in the other scoping analysis cases. Generally it was found that the higher recharge rates led to early arrival of the plume at the water table. At a rate of 100 mm/y the difference is negligible, but at 150 mm/y the higher recharge rate generated earlier arrival times that are not consistent with monitoring data observed in key monitoring well locations.

Case 3c investigated the effect of a localized addition of water using a firehose to mitigate the operational hazard of leaks at UPRs -82 and -86, followed by the addition of Gunite caps on the UPRs. The results of the analysis case are very similar to Case 1, indicating that this past practice has had little effect on the downward migration of waste releases from the three UPRs to groundwater at WMA C.

Cases 4a through 4f investigated a number of vadose zone parameters and conceptual models of potential interest, to evaluate the potential for heterogeneities in the vadose zone to affect the plume development migration.

The results of these analysis cases compared to available monitoring data indicate the following.

- The evaluation of ACM-II in Case 4a showed that adding refinement in the Hanford H2 Sand unit does not strongly affect the results of the analysis. Neither alternative model represented in Case 4a or Case 1a was found to be clearly superior to the other in terms of explaining the monitoring well data.

- The evaluation in Case 4b of ACM using a heterogeneous representation of the vadose zone showed that adding heterogeneity resulted in an earlier arrival time than has been observed in monitoring wells and concentrations levels that were lower than those shown for Case 1a. This alternative model appears to be inconsistent with data and is not preferred for further analyses.

- The evaluation of median values of vadose zone hydraulic properties in Case 4c showed arrival time and concentration results that were not significantly different than those for Case 1a. However, the evaluation of 95th percentile values of vadose zone hydraulic properties in Case 4d showed arrival time results that were significantly different than those for Case 1a and the arrival times and concentration levels of ^{99}Tc concentrations from key monitoring wells. Therefore, the use of 95th percentile properties is not preferred for use in further analyses

The evaluation of a hypothetical clastic dike and a poorly sealed borehole located near the assumed waste release near tank C-105 in Cases 4e and 4f showed a slightly earlier arrival time at the water table and only a small effect of estimated peak concentrations. Since these scoping analysis cases produce results that are similar to cases in which these features are absent, they are not preferred to use in further analyses.

Three scoping analysis cases produced results in which the arrival time of the calculated plume appears to be substantially earlier than the observations in the wells. These scoping analysis cases are:

- Case 3a, in which the recharge was increased to 150 mm/y,
- Case 4b, in which the spatial variability of the vadose zone properties was represented by an alternative heterogeneous representation, and
- Case 4d, in which the flow properties of the vadose zone soil were set to their 95th percentile values.

The remaining scoping analysis cases evaluated in Section 4 produced comparable results to each other, and none were obviously superior to others in terms of explaining the observation well data. When uncertainties in groundwater fluxes were taken into account, these scoping analyses were capable of producing both arrival times and concentrations consistent with observed monitoring well data for ^{99}Tc.

The transient water table analysis presented in Section 5 provides the best representation of the observation well data. However, it was necessary to make assumptions that approximate the magnitude and direction of groundwater flow in order to achieve the good agreement with data. These approximations are speculative but serve to provide insight into the evolution of the monitoring well data. Key factors that most strongly influenced the comparison with downgradient wells 299-E27-23 and 299-E27-21 were:

- The local direction of flow and hydraulic gradient at WMA C at the time the releases reach the water table
- The northwesterly direction of flow inferred in other areas to the northwest of WMA C in the early 2000 time frame when releases from WMA C sources reached groundwater may not have been representative of local conditions at WMA C
- Observations of ^{99}Tc concentrations seen historically in wells on the north, south, and southeast sides of the tank suggests that the primary directions of flow in the farm may have been variable ranging from southwest to southeast at the time when past releases started to impacts groundwater
- The time varying responses and concentration levels at individual monitoring wells is directly related to the timing of dynamic changes in the flow direction and hydraulic gradients as the water continues its return to more natural conditions.

The model analysis of transient flow conditions provided in Section 5 showed that the conceptual model involving the counterclockwise rotation of the hydraulic gradient from northwest to southeast provided the best representation of observed conditions in monitoring wells near WMA C. The associated numerical model results appear capable of approximating observed field data for the time of arrival of ^{99}Tc to groundwater and concentration levels of ^{99}Tc in groundwater. The model results include several assumptions regarding the timing and inventory of the past releases, and direction and magnitude of the hydraulic gradient during the time it could not be measured. Because of these assumptions, it is unknown how accurately the model calculations represent the actual release of ^{99}Tc and its transport in the vadose zone and groundwater. The results do, however, provide some insight into the concentration levels observed in monitoring wells, and the changes in concentration that have occurred in those wells since 2000.

The concentration of ^{99}Tc observed in most of the monitoring wells appears to change too abruptly to represent the one-dimensional passing of a contaminant front. The modeling results indicate that the concentration in the wells changes so abruptly because of the direction and the magnitude of the groundwater hydraulic gradient changes. The rotation of the gradient continually changes the orientation of the groundwater plumes relative to the wells. The high concentrations measured in wells 299-E27-23 and 299-E27-13 between 2010 and 2012 likely correspond to the time when those wells were located downgradient of the sources. By 2014, the concentration in those two wells dropped markedly, while the concentration in well 299-E27-21 began increasing quickly around that same time. According to the modeling results, this pattern in the data can be explained by, and corresponds to, the further rotation of gradient from the south to the southeast.

The release from tank C-105 appears to be the dominant source of ^{99}Tc observed in groundwater in the monitoring wells. According to the inventory estimates in RPP-RPT-42294, it is the only release large enough and that occurred early enough to bring about the concentration levels observed in the monitoring wells. Whether or not the release from tank C-105 is truly the dominant source of ^{99}Tc observed at the monitoring wells is unknown. However, the modeling results do indicate that most of the ^{99}Tc observed in the monitoring wells located southwest of the farm originated from the sources inside the farm, and not from the UPRs that occurred away from the tanks. These three UPRs occurred later than the release from tank C-105, and the modeling results exhibit the implications of this. The concentration of ^{99}Tc in the wells located nearest the UPRs is dominated by the ^{99}Tc contained in the release from tank C-105. The concentration of ^{99}Tc attributed to the ^{99}Tc contained in the three UPRs peaks a few years after the concentration of ^{99}Tc peaks because of the tank C-105 release. This is later than the data indicate that the peaks occurred in the wells.

The modeling results indicate that as the water table returns to more natural conditions, the rotation of the gradient will continue to alter the primary movement of the plumes from primarily a southerly direction to a more southeasterly direction in the near future. The very high concentration levels of ^{99}Tc observed in wells 299-E27-23 and 299-E27-21, southwest and south of WMA C, respectively, are likely to be observed in wells 299-E27-24 and 299-E27-14, which are located to the southeast of WMA C.

In the assessment of impacts of past waste releases into the future, sorbing and nonsorbing contaminants were treated differently, because of the anticipated difference in the height of the water table now and in the future. As a result of this difference, the forward modeling of leaks has been undertaken using models with different water table heights for the sorbing and nonsorbing contaminants. For sorbing contaminants the PA/RCA model was used, while for nonsorbing contaminants, Scoping Case 1a was used.

The forward projection results lead to several observations, as follows.

- Model results indicate that current high concentrations of ^{99}Tc below WMA C are expected to decline over the next several decades as the contamination plume disperses in the aquifer.

- Contaminated groundwater, which is now impacted by releases from past waste leaks and losses at WMA C and in the future by upgradient sources in the B Complex area, will continue to migrate downgradient and will impact groundwater in local areas contained within the 200-PO-1 groundwater operable unit such as the A Complex area.

- There are not significant overlaps between releases from residual wastes in a closed WMA C and the releases from leaks.

- Compared to the releases from WMA C past leaks or residual wastes, the releases from upgradient sources produce more significant concentrations of all contaminants other than ^{99}Tc than the release from WMA C past leaks or residual wastes. For ^{99}Tc, the groundwater concentrations associated with past leaks are the most significant.

TABLE OF CONTENTS

PREFACE 1-1

1.0 INTRODUCTION 1-1

1.1 BACKGROUND 1-1

1.1.1 Waste Management Area C Performance Assessment Scoping Process 1-5

1.2 PURPOSE AND SCOPE OF THE REPORT 1-7

1.2.1 Purpose 1-7

1.2.2 Scope 1-7

1.3 GENERAL FACILITY DESCRIPTION 1-8

1.4 PREVIOUS ASSESSMENTS 1-12

1.4.1 Single-Shell Tank Performance Assessment 1-13

1.4.2 Tank Closure and Waste Management Environmental Impact Statement Analysis of Waste Management Area C 1-13

2.0 BACKGROUND 2-1

2.1 INVENTORY ESTIMATES FOR PAST WASTE RELEASES TO THE VADOSE ZONE 2-1

2.1.1 Tank 241-C-101 2-3

2.1.2 Tank 241-C-104 2-6

2.1.3 Tank 241-C-105 2-8

2.1.4 Tank 241-C-108 2-8

2.1.5 Tank 241-C-110 2-9

2.1.6 Tank 241-C-111 2-9

2.1.7 Tank 241-C-112 2-10

2.1.8 UPR-200-E-81 2-10

2.1.9 UPR-200-E-82 2-10

2.1.10 UPR-200-E-86 2-11

2.1.11 216-C-8 French Drain 2-11

2.1.12 Surface Level Releases 2-11

2.2 HYDROGEOLOGIC SETTING OF HANFORD'S CENTRAL PLATEAU... 2-13

2.2.1 Geologic Setting and Stratigraphic Units 2-13

2.2.2 Unconfined Aquifer System 2-14

2.3 WASTE MANAGEMENT AREA C SITE CHARACTERIZATION 2-29

2.3.1 Geology of Waste Management Area C 2-30

2.3.2 Vadose Zone Characterization at Waste Management Area C..... 2-33

2.3.3 Unconfined Aquifer at Waste Management Area C 2-49

2.3.4 Recent Interpretations of Waste Management Area C Groundwater Chemistry 2-55

3.0 FEATURES FOR ANALYSIS..... 3-1

3.1 OVERVIEW OF ANALYSIS 3-1

3.2 ADAPTATION OF THE PERFORMANCE ASSESSMENT CONCEPTUAL AND NUMERICAL MODELS USED IN THE EVALUATION OF WASTE RESIDUAL IMPACTS..... 3-3

3.3 CONCEPTUAL MODEL OF SOURCE TERM RELEASES 3-9

3.4 VADOSE ZONE CONSIDERATIONS 3-9

3.5 AQUIFER CONSIDERATIONS..... 3-10

3.5.1 Flow Considerations 3-10

3.5.2 Transport Considerations 3-10

3.6 MATHEMATICAL MODELS..... 3-12

3.6.1 Source Term..... 3-12

3.6.2 Groundwater Flow and Contaminant Transport Equations 3-13

3.6.3 Implementation of the Groundwater Pathway in STOMP© 3-15

3.7 SUMMARY OF FEATURES AND DEFINITION OF SCOPING ANALYSIS CASES 3-30

4.0 SCOPING ANALYSES OF PAST WASTE RELEASES 4-1

4.1 CASE 1: EFFECT OF LEAK INVENTORIES AND VOLUMES 4-5

4.1.1 Case Description 4-5

4.1.2 Case Results 4-7

4.2 CASE 2: EFFECT OF CHANGES IN GROUNDWATER FLUX RATES 4-8

4.2.1 Case Descriptions 4-8

4.2.2 Case Results 4-10

4.3 CASE 3: EFFECT OF CHANGES IN RECHARGE CONDITIONS 4-15

4.3.1 Case Descriptions 4-15

4.3.2 Case Results 4-16

4.4 CASE 4: EFFECT OF CHANGING VADOZE ZONE PARAMETERS AND CONCEPTUALIZATION 4-21

4.4.1 Case Description and Model Implementation 4-21

4.4.2 Case Results 4-26

4.5 SUMMARY OF ANALYSIS CASES AND ASSOCIATED OBSERVATIONS 4-39

5.0 EVALUATION OF THE EFFECTS OF TRANSIENT WATER TABLE 5-1

5.1 TRANSIENT MODEL DESCRIPTION AND IMPLEMENTATION 5-1

5.1.1 Central Plateau Groundwater Model 5-2

5.1.2 Application of the Central Plateau Groundwater Model to Waste Management Area C 5-2

5.2 EVALUATION OF THE TRANSIENT WATER TABLE HYDRAULIC GRADIENT 5-5

5.3 RESULTS OF SELECTED TRANSIENT WATER TABLE MODELS 5-11

5.3.1 Results of the Assumed Clockwise Rotation of the Transient Hydraulic Gradient Model 5-11

5.3.2 Results of the Assumed Counter-Clockwise Rotation of the Transient Hydraulic Gradient Model 5-14

5.3.3 Summary 5-23

5.3.4 Conclusion 5-23

6.0 FUTURE IMPACTS OF PAST WASTE LEAKS AND RELEASES 6-1

6.1 APPROACH TO THE FORWARD PROJECTION 6-1

6.2 IDENTIFICATION OF CONTAMINANTS OF POTENTIAL CONCERN 6-2

6.3 FUTURE PROJECTIONS OF PAST WASTE LEAKS AND RELEASES 6-4

6.3.1 Results of Groundwater Pathway Evaluation: Time before Assumed Closure of Waste Management Area C in 2020 6-5

6.3.2 Results of Groundwater Pathway Evaluation: Time after Assumed Closure of Waste Management Area C in 2020 6-11

6.3.3 Results of Groundwater Pathway Evaluation: Contaminant Flux to Groundwater 6-30

6.4 DISCUSSION OF MONITORING RESULTS WITH PROJECT MODELING RESULTS FOR NITRATE, SULFATE, AND CHROMIUM ... 6-41

7.0 OTHER SOURCES OF CONTAMINATION AT WASTE MANAGEMENT AREA C 7-1

7.1 CONTRIBUTION OF CONTAMINATION ASSOCIATED WITH UPGRADIENT SOURCES 7-1

7.1.1 Technetium-99 7-2

7.1.2 Nitrate 7-2

7.1.3 Cyanide 7-15

7.1.4 Iodine-129 7-15

7.1.5 Uranium 7-15

7.2 CONTRIBUTION OF RESIDUAL WASTES 7-30

7.2.1 Technetium-99 7-30

7.2.2 Nitrate 7-30

7.2.3 Iodine-129 7-30

7.2.4 Uranium-238/Total Uranium 7-37

7.3 COMPARISON OF UPGRADIENT SOURCES, RESIDUAL WASTES, AND PAST LEAKS 7-37

7.3.1 Technetium-99 7-37

7.3.2 Nitrate 7-41

7.3.3 Iodine-129 7-41

7.3.4 Total Uranium 7-41

7.4 SUMMARY OF PEAK CONCENTRATIONS OF CONTAMINANTS OF POTENTIAL CONCERN 7-41

8.0 SUMMARY AND OBSERVATIONS 8-1

9.0 REFERENCES 9-1

LIST OF FIGURES

Figure 1-1. Hanford Site Tank Farms. 1-3

Figure 1-2. The Components of the Appendix I Performance Assessment. 1-4

Figure 1-3. Hanford Site and its Location in Washington State. 1-9

Figure 1-4. Location Map of Waste Management Area C and Surrounding Area. 1-11

Figure 1-5. Location Map of Unplanned Release Sites of Waste Management Area C. 1-12

Figure 2-1. Schematic of Process Used to Determine Vadose Zone Inventory. 2-2

Figure 2-2. Near Surface Spectral Gamma Activity in 241-C Tank Farm. 2-12

Figure 2-3. Surface Topography and Boundaries of the 200-BP-5 Groundwater Operable Unit. 2-15

Figure 2-4. Comparison of 200-BP-5 Operable Unit Hydrostratigraphy to Hanford Site Stratigraphy. 2-17

Figure 2-5. Representative Photos of the Hanford Formation, Cold Creek Unit, Ringold Unit E, Ringold Lower Mud Unit, and Basalt. 2-18

Figure 2-6. 200-BP-5 Operable Unit Near-Field Area Hydrogeology Depicting Truncation of Ringold Units on Uplifted Basalt. 2-19

Figure 2-7. Distribution of Hydrogeologic Units at the Water Table, 2009. 2-20

Figure 2-8. Discharge History for the 216-B Pond System and Gable Mountain Pond. 2-21

Figure 2-9. Discharge History for the 216-T Pond and 216-U Pond. 2-22

Figure 2-10a. Hind Cast Water Table Map of the Hanford Site, January 1944. 2-23

Figure 2-10b. Water Table Elevations for June 1987. 2-23

Figure 2-10c. Water Table Elevations for 2013. 2-23

Figure 2-11. Water Table Elevations at Groundwater Monitoring Wells Close to U-Pond (200 West Area) and B-Pond (200 East Area). 2-25

Figure 2-12. 200-BP-5 Operable Unit Pleistocene Paleo-Erosional Surface Topography. 2-27

Figure 2-13. Groundwater Contamination for 2013 which Originated within the Central Plateau along with Central Plateau Groundwater Interest Areas. 2-28

Figure 2-14. Waste Management Area C Tanks, Infrastructure, and Associated Unplanned Releases. 2-30

Figure 2-15. Fence Diagram Showing Cross-Sections through Waste Management Areas A-AX and C. 2-31

Figure 2-16. Fence Diagram of Alternative Geologic Models for Waste Management Area C. 2-34

Figure 2-17. Vadose Zone and Groundwater Monitoring Network for Waste Management Area C. 2-35

Figure 2-18. Three-Dimensional Perspective of Waste Management Area C Tanks and Drywells Showing Occurrence of Significant (>10 pCi/g) Cesium-137 Contamination in the Vadose Zone along with Technetium-99 at Borehole C4297. 2-38

Figure 2-19. Completed Phase 2 RCRA Facility Investigation Characterization Locations.... 2-39

Figure 2-20. Completed Transitional (Phase 1.5) Characterization Locations..... 2-40

Figure 2-21. Moisture Content (% Vol) Measurements in Vadose Zone at Waste Management Area C. 2-51

Figure 2-22. Technetium-99 Concentrations above the Drinking Water Standard at Waste Management Area C Wells from January 2006 through December 2015. 2-61

Figure 2-23. Nitrate Concentrations above the Maximum Contaminant Level at Waste Management Area C Wells from January 2006 through December 2015. 2-62

Figure 2-24. Sulfate Concentrations above the Secondary Maximum Contaminant Level at Waste Management Area C Wells from January 2006 through December 2015. 2-63

Figure 2-25. Cyanide Concentrations in Waste Management Area C Wells from January 2006 through December 2015. 2-64

Figure 2-26. Technetium-99 Activity in Wells 299-E27-7, 299-E27-14, and 299-E27-24 on East and Southeast Side of Waste Management Area C. 2-65

Figure 2-27. Technetium-99 Activity in Wells 299-E27-4, 299-E24-13, and 299-E27-23 on West Side of Waste Management Area C. 2-66

Figure 2-28. Technetium-99-to-Nitrate Ratio Comparisons for Wells on West Side (299-E27-21 and 299-E27-23) and Southeast Side (299 E27-14 and 299-E27-23) of Waste Management Area C. 2-67

Figure 2-29. Cyanide-to-Nitrate Ratio Comparisons for Well 299-E27-14. 2-68

Figure 2-30. Bivariate Plots of Technetium-99/Nitrate Ratio Versus Nitrate by Year. 2-69

Figure 2-31. Bivariate Plots of Technetium-99/Sulfate Ratio Versus Sulfate by Year. 2-70

Figure 2-32. Bivariate Plots of Technetium-99/Chloride Ratio Versus Chloride by Year.....2-71

Figure 2-33. Conceptual Model for the Vadose Zone Flux Calculation.....2-73

Figure 2-34. Estimates of the Activity of Technetium-99 by Two Alternative Methods.....2-74

Figure 3-1. Schematic Conceptual Representation of Waste Management Area C and Contaminant Migration into the Environment along the Various Pathways Evaluated in the Performance Assessment.....3-5

Figure 3-2. Conceptual Model of the Waste Management Area C Site Showing Stratigraphy. 3-6

Figure 3-3. Evolution of the Groundwater Gradient In the Low-Level Waste Management Area-1 Monitoring Network.....3-7

Figure 3-4. Surface Conditions In and Around Waste Management Area C during the Construction and Operations Period. 3-8

Figure 3-5. Interpolated Numerical Three-Dimensional Post-Closure Alternative I Hydrogeologic Model. 3-17

Figure 3-6. Plan View of Waste Management Area C Performance Assessment Model Domain Showing the Horizontal Distribution and Surface Type of the Irregularly-Spaced Calculation Nodes. 3-19

Figure 3-7. Fence Diagram of Interpolated Numerical Three-Dimensional Post-Closure Alternative I Hydrogeologic Model. 3-21

Figure 3-8. Interpolated Numerical Three-Dimensional Post-Closure Alternative II Hydrogeologic Model. 3-22

Figure 3-9. Fence Diagram of Interpolated Numerical Three-Dimensional Post-Closure Alternative II Hydrogeologic Model.....3-23

Figure 3-10. Hindcast Water Table Map of the Hanford Site, January 1944. 3-31

Figure 3-11. Central Plateau Groundwater Model Calibration Results in the Vicinity of Waste Management Area C. 3-32

Figure 4-1. Decreases in Water Table Level with Time at Waste Management Area C, with a Projection to Future Conditions. 4-6

Figure 4-2. Points of Calculation for the Scoping Analyses.....4-7

Figure 4-3. Development of Technetium-99 Plumes over Selected Time Periods for Case 1a (Upper Bound Inventory for the Tank 241-C-105 Leak). 4-9

Figure 4-4. Concentrations at the Selected Points of Calculation for Case 1a (Upper Bound Inventory for the Tank 241-C-105 Leak).....4-10

Figure 4-5. Development of the Technetium-99 Plumes over Selected Time Periods for Case 1b (Lower Bound Inventory for the Tank 241-C-105 Leak). 4-12

Figure 4-6. Concentrations at the Selected Points of Calculation for Case 1b (Lower Bound Inventory for the Tank 241-C-105 Leak). 4-13

Figure 4-7. Development of the Technetium-99 Plumes at Selected Time Periods for Case 2a (10th Percentile Groundwater Flux). 4-14

Figure 4-8. Concentrations at the Selected Points of Calculation for Case 2a (10th Percentile Groundwater Flux). 4-15

Figure 4-9. Development of the Technetium-99 Plumes for Selected Time Periods for Case 2b (90th Percentile Groundwater Flux). 4-18

Figure 4-10. Concentrations at the Selected Points of Calculation for Case 2b (90th Percentile Groundwater Flux). 4-19

Figure 4-11. Surface Conditions In and Around Waste Management Area C during the Construction and Operations Period. 4-20

Figure 4-12. Development of the Technetium-99 Plumes for Selected Time Periods for Case 3a (150 mm/y Recharge). 4-22

Figure 4-13. Concentrations at Selected Points of Calculation for Case 3a (150 mm/y Recharge). 4-23

Figure 4-14. Development of the Technetium-99 Plumes for Selected Time Periods for Case 3b (100 mm/y Recharge). 4-25

Figure 4-15. Concentrations at Selected Points of Calculation for Case 3b (100 mm/y Recharge). 4-26

Figure 4-16. Development of Technetium-99 Plumes for Selected Time Periods for Case 3c (Firehose Water Addition Followed by Gunite Cover). 4-28

Figure 4-17. Concentrations at Selected Points of Calculation for Case 3c (Firehose Water Addition followed by Gunite Cover). 4-29

Figure 4-18. Depiction of Interpolated Numerical Three-Dimensional Model of Alternative Conceptual Model II for Scoping Case 4a. 4-30

Figure 4-19. Depiction of Interpolated Numerical Three-Dimensional Model of Heterogeneous Alternative Conceptual Model for Scoping Case 4b. 4-31

Figure 4-20. Depiction of Hypothetical Clastic Dike near Tank 241-C-105 Conceptualized for Scoping Case 4e. 4-33

Figure 4-21. Depiction of Hypothetical Unsealed Borehole Near Tank 241-C-105 Conceptualized for Scoping Case 4f. 4-34

Figure 4-22. Development of Technetium-99 Plumes for Selected Time Periods for Case 4a (Alternative Geologic Model II). 4-35

Figure 4-23. Concentrations at Selected Points of Calculation for Case 4a (Alternative Geologic Model II). 4-36

Figure 4-24. Development of Technetium-99 Plumes for Selected Time Periods for Case 4b (Alternative Heterogeneous Model). 4-38

Figure 4-25. Concentrations at Selected Points of Calculation for Case 4b (Alternative Heterogeneous Model). 4-39

Figure 4-26. Development of Technetium-99 Plumes for Selected Time Periods for Case 4c (Median Hydraulic Properties). 4-40

Figure 4-27. Concentrations at Selected Points of Calculation for Case 4c (Median Hydraulic Properties). 4-41

Figure 4-28. Development of Technetium-99 Plumes for Selected Time Periods for Case 4d (95th Percentile Hydraulic Properties). 4-42

Figure 4-29. Concentrations at Selected Points of Calculation for Case 4d (95th Percentile Hydraulic Properties). 4-43

Figure 4-30. Development of Technetium-99 Plumes for Selected Time Periods for Case 4e (Clastic Dike). 4-45

Figure 4-31. Concentrations at Selected Points of Calculation for Case 4e (Clastic Dike). 4-46

Figure 4-32. Development of Technetium-99 Plumes for Selected Time Periods for Case 4f (Borehole Preferential Pathway). 4-48

Figure 4-33. Concentrations at Selected Points of Calculation for Case 4f (Borehole Preferential Pathway). 4-49

Figure 4-34. Comparison of All Scoping Analysis Cases at 60 Meters Downgradient for the Tank 241-C-105 Past Release Location. 4-50

Figure 4-35. Comparison of All Scoping Analysis Cases at 120 Meters Downgradient for the Tank 241-C-105 Past Release Location. 4-51

Figure 5-1. Central Plateau Groundwater Model Calibration Results in the Vicinity of Waste Management Area C. 5-4

Figure 5-2. Alignment of the Central Plateau Groundwater Model and Waste Management Area C Unplanned Release Model Grids and Central Plateau Groundwater Model Hydraulic Head Interpolation Values Representing Calendar Year 2000 on a Triangular Mesh. 5-5

Figure 5-3. Waste Management Area C Unplanned Release Model Grid Hydraulic Head Boundary Averaging Values Representing Calendar Year 2000. 5-6

Figure 5-4. Inferred Direction of Flow During the Operations Period When the High Volume Discharge Facilities Operated. 5-10

Figure 5-5. Simulated Technetium-99 Plume in Groundwater Calendar Years 1998, 2000, 2002, 2005, 2010 and 2016 and Resulting from Waste Management Area C Unplanned Releases (Clockwise Rotation of the Hydraulic Gradient Based on Central Plateau Groundwater Model Boundary Conditions). 5-15

Figure 5-6. Comparison of Simulated Technetium-99 Concentrations in Groundwater to Measured Concentrations around the Northeast, Northwest, and Southwest of Waste Management Area C. Using Initial Conceptual Model with Clockwise Rotation of the Hydraulic Gradient. 5-17

Figure 5-7. Comparison of Simulated Technetium-99 Concentrations in Groundwater to Measured Concentrations around the Southwest and Southeast of Waste Management Area C. Using Initial Conceptual Model with Clockwise Rotation of the Hydraulic Gradient. 5-18

Figure 5-8. Simulated Technetium-99 Plume in Groundwater Calendar Years 1998, 2002, 2004, 2008, 2012 and 2016 and Resulting from Waste Management Area C Unplanned Releases (Counterclockwise Rotation of the Hydraulic Gradient). 5-19

Figure 5-9. Comparison of Simulated Technetium-99 Concentrations in Groundwater to Measured Concentrations around the Northeast, Northwest, and Southwest of Waste Management Area C. Conceptual Model with Counterclockwise Rotation of the Hydraulic Gradient. 5-21

Figure 5-10. Comparison of Simulated Technetium-99 Concentrations in Groundwater to Measured Concentrations around the Southwest and Southeast of Waste Management Area C. Conceptual Model with Counterclockwise Rotation of the Hydraulic Gradient. 5-22

Figure 6-1. Case 1a Past Leak Model Used for Nonsorbing Contaminants for the Forward Projection Compared to the Performance Assessment/RCRA Closure Analysis Model Used for the Sorbing Contaminants. 6-3

Figure 6-2. First-Arrival Time (in Calendar Year) of Radionuclides for Various K_d Values Based on Screening Analysis Using Subsurface Transport Over Multiple Phases. 6-9

Figure 6-3. Points of Calculation 100 Meters Downgradient of Waste Management Area C. 6-10

Figure 6-4. Concentration of Technetium-99 in Groundwater in the Points of Calculation at the Fenceline. 6-15

Figure 6-5. Concentration of Technetium-99 in Groundwater in the Points of Calculation 100 Meters Downgradient of the Fenceline. 6-16

Figure 6-6. Concentration of Tritium in Groundwater in the Points of Calculation at the Fenceline. 6-17

Figure 6-7. Concentration of Tritium in Groundwater in the Points of Calculation 100 Meters Downgradient of the Fenceline. 6-18

Figure 6-8. Concentration of Cobalt-60 in Groundwater in the Points of Calculation 100 Meters Downgradient of the Fenceline. 6-19

Figure 6-9. Concentration of Selenium-79 in Groundwater in the Points of Calculation 100 Meters Downgradient of the Fenceline. 6-20

Figure 6-10. Concentration of Nitrate in Groundwater in the Points of Calculation 100 Meters Downgradient of the Fenceline. 6-21

Figure 6-11. Concentration of Sulfate in Groundwater in the Points of Calculation 100 Meters Downgradient of the Fenceline. 6-22

Figure 6-12. Concentration of Chromium (as Cr^{+6}) in Groundwater in the Points of Calculation 100 Meters Downgradient of the Fenceline. 6-23

Figure 6-13. Concentration Contours of Technetium-99 along Cross-Section Planes through Unplanned Releases 200-E-81 and 200-E-82 and Tank Row 241-C-110, 241-C-107, 241-C-104 and 241-C-101 Corresponding to Year 2000. 6-24

Figure 6-14. Concentration Contours of Technetium-99 along Cross-Section Planes through Unplanned Releases 200-E-81 and 200-E-82 and Tank Row 241-C-110, 241-C-107, 241-C-104 and 241-C-101 Corresponding to Year 2016. 6-25

Figure 6-15. Concentration Contours of Nitrate along Cross-Section Planes through Unplanned Releases 200-E-81 and 200-E-82 and Tank Row 241-C-110, 241-C-107, 241-C-104 and 241-C-101 Corresponding to Year 2000. 6-26

Figure 6-16. Concentration Contours of Nitrate along Cross-Section Planes through Unplanned Releases 200-E-81 and 200-E-82 and Tank Row 241-C-110, 241-C-107, 241-C-104 and 241-C-101 Corresponding to Year 2016. 6-27

Figure 6-17. Concentration of Iodine-129 in Groundwater in the Points of Calculation at the Fenceline. 6-28

Figure 6-18. Concentration of Iodine-129 in Groundwater in the Points of Calculation 100 Meters Downgradient of the Fenceline. 6-29

Figure 6-19. Concentration of Tin-126 in Groundwater in the Points of Calculation 100 Meters Downgradient of the Fenceline. 6-31

Figure 6-20. Concentration of Uranium-238 in Groundwater in the Points of Calculation 100 Meters Downgradient of the Fenceline. 6-32

Figure 6-21. Concentration of Total Uranium in Groundwater in the Points of Calculation 100 Meters Downgradient of the Fenceline. 6-33

Figure 6-22. Concentration of Uranium-238 in Groundwater in the Points of Calculation at the Fenceline. 6-34

Figure 6-23. Concentration of Total Uranium in Groundwater in the Points of Calculation at the Fenceline. 6-35

Figure 6-24. Flux of Technetium-99 from the Vadose Zone that Enters Groundwater. 6-37

Figure 6-25. Flux of Nitrate from the Vadose Zone that Enters Groundwater. 6-38

Figure 6-26. Flux of Selenium-79 from the Vadose Zone that Enters Groundwater. 6-39

Figure 6-27. Flux of Uranium-238 from the Vadose Zone that Enters Groundwater. 6-40

Figure 7-1. 2013 200-BP-5 Operable Unit Consolidated Plume Map. 7-3

Figure 7-2. The Technetium-99 Plume at Year 2015 (Year 0 of the Simulation) for the Remedial Evaluation Case of 200-BP-5 7-4

Figure 7-3. The Technetium-99 Plume at Year 2020 (Year 5 of the Simulation) for the Remedial Evaluation Case of 200-BP-5 7-5

Figure 7-4. The Technetium-99 Plume at Year 2025 (Year 10 of the Simulation) for the Remedial Evaluation Case of 200-BP-5 7-6

Figure 7-5. The Technetium-99 Plume at Year 2035 (Year 20 of the Simulation) for the Remedial Evaluation Case of 200-BP-5 7-7

Figure 7-6. Remedial Evaluation Case Technetium-99 Concentrations at Waste Management Area C as a Function of Time. 7-8

Figure 7-7. The Nitrate Plume at Year 2015 (Year 0 of the Simulation) for the Remedial Evaluation Case of 200-BP-5. 7-9

Figure 7-8. The Nitrate Plume at Year 2025 (Year 10 of the Simulation) for the Remedial Evaluation Case of 200-BP-5. 7-10

Figure 7-9. The Nitrate Plume at Year 2030 (Year 15 of the Simulation) for the Remedial Evaluation Case of 200-BP-5. 7-11

Figure 7-10. The Nitrate Plume at Year 2035 (Year 20 of the Simulation) for the Remedial Evaluation Case of 200-BP-5. 7-12

Figure 7-11. Remedial Evaluation Case Nitrate Concentrations at Waste Management Area C as a Function of Time. 7-13

Figure 7-12. The Cyanide Plume at Year 2015 (Year 0 of the Simulation) for the Remedial Evaluation Case of 200-BP-5. 7-14

Figure 7-13. The Cyanide Plume at Year 2020 (Year 5 of the Simulation) for the Remedial Evaluation Case of 200-BP-5. 7-16

Figure 7-14. The Cyanide Plume at Year 2025 (Year 10 of the Simulation) for the Remedial Evaluation Case of 200-BP-5. 7-17

Figure 7-15. The Cyanide Plume at Year 2025 (Year 10 of the Simulation) for the Remedial Evaluation Case of 200-BP-5. 7-18

Figure 7-16. Remedial Evaluation Case Cyanide Concentrations at Waste Management Area C as a Function of Time. 7-19

Figure 7-17. The Iodine-129 Plume at Year 2015 (Year 0 of the Simulation) for the Remedial Evaluation Case of 200-BP-5. 7-20

Figure 7-18. The Iodine-129 Plume at Year 2025 (Year 10 of the Simulation) for the Remedial Evaluation Case of 200-BP-5. 7-21

Figure 7-19. The Iodine-129 Plume at Year 2035 (Year 20 of the Simulation) for the Remedial Evaluation Case of 200-BP-5. 7-22

Figure 7-20. The Iodine-129 Plume at Year 2045 (Year 30 of the Simulation) for the Remedial Evaluation Case of 200-BP-5. 7-23

Figure 7-21. Remedial Evaluation Case Iodine-129 Concentrations at Waste Management Area C as a Function of Time. 7-24

Figure 7-22. The Uranium Plume at Year 2015 (Year 0 of the Simulation) for the Remedial Evaluation Case of 200-BP-5. 7-25

Figure 7-23. The Uranium Plume at Year 2035 (Year 20 of the Simulation) for the Remedial Evaluation Case of 200-BP-5. 7-26

Figure 7-24. The Uranium Plume at Year 2045 (Year 30 of the Simulation) for the Remedial Evaluation Case of 200-BP-5. 7-27

Figure 7-25. The Uranium Plume at Year 2065 (Year 50 of the Simulation) for the Remedial Evaluation Case of 200-BP-5. 7-28

Figure 7-26. The Uranium Plume at Year 2150 (Year 135 of the Simulation) for the Remedial Evaluation Case of 200-BP-5. 7-29

Figure 7-27. Remedial Evaluation Case Total Uranium Concentrations at Waste Management Area C as a Function of Time. 7-31

Figure 7-28. Groundwater Concentration of Technetium-99 at the Highest Point of Calculation 100 Meters Downgradient from Waste Management Area C. 7-32

Figure 7-29. Extent of Technetium-99 Plume in Groundwater 1,570 Years after Closure at the Time of the Maximum Concentration at the Point of Compliance. 7-33

Figure 7-30. Maximum Predicted Groundwater Concentration of Nitrate (K_d = 0 mL/g) at All Points of Calculation 100 Meters Downgradient from Waste Management Area C from Residual Wastes. 7-34

Figure 7-31. Extent of Nitrate Plume in Groundwater 1,375 Years after Closure at the Time of the Maximum Concentration at the 100-meter Point of Calculation. 7-35

Figure 7-32. Groundwater Concentration of Iodine-129 at All Points of Calculation 100 Meters Downgradient from Waste Management Area C from Residual Wastes. 7-36

Figure 7-33a. Predicted Groundwater Concentration of Uranium-238 at the Highest Point of Calculation 100 Meters Downgradient from Waste Management Area C. ... 7-38

Figure 7-33b. Predicted Groundwater Concentration of Total Uranium at the Highest Point of Calculation 100 Meters Downgradient from Waste Management Area C. ... 7-39

Figure 7-34. Results of the Past Leak Analysis for Technetium-99 at Points of Calculation 100 Meters Downgradient, Compared to Results from the Residual Waste Analysis and Upgradient Sources. 7-40

Figure 7-35. Results of the Past Leak Analysis for Nitrate at Points of Calculation 100 Meters Downgradient, Compared to Results from the Residual Waste Analysis and Upgradient Sources. 7-42

Figure 7-36. Results of the Past Leak Analysis for Iodine-129 at Points of Calculation 100 Meters Downgradient, Compared to Results from the Residual Waste Analysis and Upgradient Sources. 7-43

Figure 7-37. Results of the Past Leak Analysis for Total Uranium at Points of Calculation 100 Meters Downgradient, Compared to Results from the Residual Waste Analysis and Upgradient Sources. 7-44

LIST OF TABLES

Table 1-1. Data Packages Produced as a Part of the Waste Management Area C Performance Assessment Scoping Process. 1-6

Table 1-2. Reference Case Inventory of Past Leaks Assumed in the Single-Shell Tank Performance Assessment. 1-13

Table 1-3. Volumes of Past Leaks Assumed in the Single-Shell Tank Performance Assessment. 1-14

Table 1-4. Inventory of Past Tank Leaks and Unplanned Releases Assumed in the Tank Closure and Waste Management Environmental Impact Statement. 1-15

Table 1-5. Volumes of Past Leaks Assumed in the Tank Closure and Waste Management Environmental Impact Statement. 1-16

Table 2-1. Constituents Evaluated in the Hanford Defined Waste Model. 2-3

Table 2-2. Average Composition of Hanford Defined Model Chemical and Radiological Constituents for Selected Waste Types. 2-4

Table 2-3. Inventory Estimates for Releases at Waste Management Area C. 2-7

Table 2-4. Summary of Field Efforts Related to Areas Investigated in Waste Management Area C RCRA Facility Investigation. 2-41

Table 2-5. Hanford Environmental Information System Laboratory Qualifier Table. 2-44

Table 2-6. Summary Statistics for Volumetric Moisture Content in the Lithologic Units Underlying Waste Management Area C. 2-50

Table 2-7. Summary Statistics from January 1, 2006 to January 1, 2016 for Constituents Discussed in SGW-59669. 2-59

Table 3-1. Abstracted Inventory of Technetium-99 Used for the Initial Analysis Cases. 3-10

Table 3-2. Distribution Coefficients (K_d) Values Used to Approximate the Transport of the Radionuclides in the Base Case. 3-11

Table 3-3. Base Case Recharge Rate (Net Infiltration) Estimates for Surface Conditions during the Pre-Construction, Operational, and Post-Closure Periods. 3-25

Table 3-4. Composite van Genuchten-Mualem Parameters for Various Strata at the Waste Management Area C Site Used in the Base Case Evaluations of Alternative Geologic Models I and II. 3-26

Table 3-5. Effective Bulk Density (E[ρb], g/cm^3) Estimates for Various Strata at Waste Management Area C Used in the Base Case Evaluations of Alternative Geologic Models I and II. 3-28

Table 3-6. Macrodispersity Estimates for Various Strata at Waste Management Area C Used in the Base Case Evaluations of Alternative Geologic Models I and II. 3-28

Table 3-7. Base Case Soil Hydraulic Properties for Aquifer Soil Type Used for Base Case at Waste Management Area C. 3-33

Table 4-1. Description of Past Tank Waste Release Scoping Cases. 4-3

Table 4-2. Comparison of the Technetium-99 Concentration Results at Selected Points of Calculation for Scoping Cases 1a and 1b. 4-11

Table 4-3. Comparison of the Technetium-99 Concentration Results at Selected Points of Calculation for Scoping Cases 2a and 2b. 4-17

Table 4-4. Assumed Recharge Rates (Net Infiltration) for Surface Conditions during the Pre-Construction, Operational Periods Used in Cases 1a, 1b, 3a, and 3b. 4-21

Table 4-5. Comparison of the Technetium-99 Concentration Results at Selected Points of Calculation for Scoping Cases 3a through 3d. 4-27

Table 4-6. van Genuchten-Mualem Parameters Corresponding to the Percentiles Selected for Cases 1a, 1b, 4c, and 4d from the Vertical Pore Water Velocity Cumulative Distribution Functions. 4-32

Table 4-7. Comparison of the Simulated Technetium-99 Concentration Results at Selected Points of Calculation for Scoping Cases 4a through 4f. 4-37

Table 4-8. Comparison of the Technetium-99 Concentration Results at Selected Points of Calculation for All Scoping Analysis Cases. 4-52

Table 5-1. Central Plateau Groundwater Model Hydraulic Head Interpolation Values and Waste Management Area C Unplanned Release Model Grid Boundary Rankings. 5-7

Table 5-2. Comparison of Central Plateau Groundwater Model Hydraulic Gradient Results (Magnitude and Direction) and Central Plateau Groundwater Model Results Modified to Rotate the Hydraulic Gradient Counterclockwise at Waste Management Area C. 5-12

Table 5-3. Central Plateau Groundwater Model Hydraulic Head Interpolation Values Modified to Rotate the Hydraulic Gradient Counterclockwise at Waste Management Area C, and Revised Model Grid Boundary Rankings. 5-13

Table 6-1. Leak Inventories of Contaminants of Concern Used in the Forward Projection Analyses. 6-7

Table 6-2. First-Arrival Time (in Calendar Year) of Radionuclides for Various K_d Values Based on Screening Analysis Using Subsurface Transport Over Multiple Phases. 6-9

Table 6-3. Width of the Nine Points of Calculation at the Waste Management Area C Fenceline. 6-11

Table 6-4. Summary Results of Radionuclides and Non-Radiological Contaminants that Arrive in Groundwater at the Waste Management Area C Fenceline before Closure. 6-12

Table 6-5. Summary Results of Radionuclides and Non-Radiological Contaminants that Arrive in Groundwater at the Waste Management Area C Fenceline after Closure. 6-36

Table 7-1. Peak Concentrations and Time of Peak of Arrival at Waste Management Area C from the Calculated Remedial Evaluation Case for Upgradient Sources. 7-15

Table 7-2. Comparison of Peak Concentrations and Approximate Calendar Year of the Occurrence of the Peak. 7-45

LIST OF TERMS

Abbreviations and Acronyms

3-D	three-dimensional
AMSL	above mean sea level
bgs	below ground surface
BRA	Baseline Risk Assessment
CCu	Cold Creek unit
CFR	Code of Federal Regulations
CHPRC	CH2M HILL Plateau Remediation Company
CMS	corrective measures study
COPC	constituent of potential concern
CPGWM	Central Plateau Groundwater Model
CRQL	contract required quantitation limit
DOE	U.S. Department of Energy
DOE-ORP	U.S. Department of Energy, Office of River Protection
DWS	drinking water standard
Ecology	State of Washington Department of Ecology
EDTA	ethylenediaminetetraacetic acid
EHM	equivalent homogeneous medium
EPA	U.S. Environmental Protection Agency
GFAA	graphite furnace atomic absorption
$H_3/CC_u/RF$	undifferentiated Hanford formation (H3), Cold Creek unit and Ringold Formation
HDW	Hanford Defined Waste
HFFACO	Hanford Federal Facility Agreement and Consent Order

HRR	High Resolution Resistivity
HSU	hydrostratigraphic unit
IDF	Integrated Disposal Facility
IDL	instrument detection limit
IPA	Appendix I Performance Assessment
K-U-T	potassium, uranium, thorium
LLWMA	Low-Level Waste Management Area
MCL	maximum contaminant level
MDA	minimum detectable activity
MDL	minimum detection limit
NAVD88	North American Vertical Datum of 1988
NRC	U.S. Nuclear Regulatory Commission
OU	operable unit
PA	performance assessment
PoCal	point of calculation
PQL	practical quantitation limit
PUREX	Plutonium Uranium Extraction (facility)
RCA	RCRA Closure Analysis
RCRA	Resource Conservation and Recovery Act of 1976
RETC	RETention Curve (code)
RFI	RCRA facility investigation
RI	Remedial Investigation
RLM	Ringold Lower Mud Unit
Rtf	upper Ringold unit

Rwia	fluvial gravel unit A
Rwie	fluvial gravel unit E
SESP	Surface Environmental Surveillance Project
SGE	Surface Geophysical Exploration
SST	single-shell tank
SST PA	Single-Shell Tank Performance Assessment
STOMP	Subsurface Transport Over Multiple Phases (code)
TC&WM EIS	DOE/EIS-0391, "Final Tank Closure and Waste Management Environmental Impact Statement for the Hanford Site, Richland, Washington"
TEDF	Treated Effluent Disposal Facility
TIC	tentatively identified compound
UPR	unplanned release
WMA	Waste Management Area
WRPS	Washington River Protection Solutions, LLC

Waste Types

IX	ion exchange waste from the cesium recovery process at B Plant
P1	PUREX high-level waste (1956-1962)
P2	PUREX high-level waste (1963-1967)
CWP1	PUREX aluminum cladding waste (1956-1960)
CWP2	PUREX aluminum cladding waste (1961-1972)
CSR	waste from B Plant ion exchange cesium recovery
PSN	P2 supernate
PSS	PUREX sludge supernate derived from washing PUREX HLW sludges in 244-AR Vault or 241-A and 241-AX tanks

PREFACE

This document is volume one of four volumes being written to support the performance assessment (PA) required under Section 2.5 of the Hanford Federal Facility Agreement and Consent Order (Ecology et al. 1989, hereinafter referred to as HFFACO) Appendix I for closure of Hanford Tank Farms. The first single-shell tank (SST) farm being closed is Waste Management Area (WMA) C. This particular volume contains an evaluation of future impacts from hazardous chemicals and dangerous waste residual contaminants in past leaks and losses at WMA C, which is needed by the State of Washington Department of Ecology (Ecology) for closure of WMA C SSTs per Washington Administrative Code (WAC) 173-303-610, "Closure and Post-Closure." The other three volumes are: 1) **DOE O 435.1 Performance Assessment** (RPP-ENV-58782, "Performance Assessment of Waste Management Area C, Hanford Site, Washington") – An evaluation of impacts from radioactive residual waste contaminants in tanks and ancillary equipment at a closed WMA C, which is needed by the U.S. Department of Energy (DOE) for closure of WMA C SSTs per DOE O 435.1, Radioactive Waste Management; 2) **RCRA Closure Analysis (RCA)** (RPP-ENV-58806, "RCRA Closure of Tank Waste Residuals Impacts at Waste Management Area C, Hanford Site Washington"), and 3) a **Baseline Risk Assessment** (RPP-RPT-58329, "Baseline Risk Assessment for Waste Management Area C"), which is an evaluation of impacts to human and ecological receptors from both non-radiological and radiological contaminants in soils at WMA C under current condition, in the absence of actions to control or mitigate releases. A more complete description of each of these documents is given in Section 1.1 of both RPP-ENV-58782 and RPP-ENV-58806.

1.0 INTRODUCTION

1.1 BACKGROUND

The U.S. Department of Energy, Office of River Protection (DOE-ORP) is pursuing closure on the SST WMA C under Federal requirements and forthcoming State-approved closure plans and permits in accordance with the HFFACO (Ecology et al. 1989), Action Plan, Appendix I. Waste Management Area C is located in the 200 East Area of the Central Plateau at Hanford and is one of 12 tank farms within 7 WMAs (A-AX, B-BX-BY, C, S-SX, T, TX-TY, and U) containing 149 SSTs and ancillary equipment built from 1943 to 1964 (see Figure 1-1).

The PA requirements for the closure process are outlined in Appendix I of the HFFACO. Appendix I of the HFFACO Action Plan contains language that broadened the scope of a "performance assessment." Section 2.5 of HFFACO Action Plan Appendix I states:

> "Ecology, as the lead agency for SST system closure, EPA, and DOE have elected to develop and maintain as part of the SST system closure plan <u>one performance assessment</u> for the purposes of evaluating whether SST system closure conditions

> are protective of human health and the environment for all contaminants of concern, both radiological and nonradiological. DOE intends that this performance assessment (PA) will document by reference relevant performance requirements defined by RCRA, HWMA, Clean Water Act, Safe Drinking Water Act, and the Atomic Energy Act of 1954 (AEA) and any other performance requirements that might be ARARs under CERCLA. The PA is of larger scope than a risk assessment required solely for nonradiological contaminants. The PA is expected to provide a single source of information that DOE can use to satisfy potentially duplicative functional and/or documentation requirements. A PA will be developed for each WMA and will incorporate the latest information available. These PAs will be approved by Ecology and DOE pursuant to their respective authorities. For Ecology approval means incorporation by reference, into the Site-Wide Permit through the closure plans.
>
> As individual components are retrieved or characterized, or other component closure activities are completed, the resulting component characterization information will be incorporated into the WMA PA to determine its relative risk compared to the entire WMA performance. In doing this, the Parties will be able to make interim closure decisions for individual components. Initially, the WMA PA will be based on assumptions and available data describing component characterization information. As each WMA proceeds toward closure, its respective PA will be updated to address all pertinent new results and findings – and will, as a minimum, incorporate the following results as they become available: actual volumes of tank waste residuals left after retrieval, results of leak investigations, new geologic and ancillary equipment waste characterization information, and the results of new barrier and tank residual stabilization and fill performance studies and tests. Final WMA closure decisions will be made after all components are retrieved and/or characterized, and all other component closure activities have been completed and a final WMA PA is completed."

Note: Underlining is added to emphasize key points in the scope of the HFFACO Action Plan Appendix I "performance assessment."

To distinguish between the two terms and avoid confusion, the term "performance assessment" will be used in this document in the following manner:

- The broadened scope of the HFFACO Action Plan Appendix I analysis will be referred to as the "Appendix I Performance Assessment" (IPA).

- The simpler "performance assessment" (PA) will refer solely to the DOE O 435.1 definition of performance assessment.

Appendix I of the HFFACO Action Plan describes the waste retrieval and closure process that is to be implemented for the Hanford Site SST system. The four components of the IPA are illustrated in Figure 1-2.

Figure 1-1. Hanford Site Tank Farms.

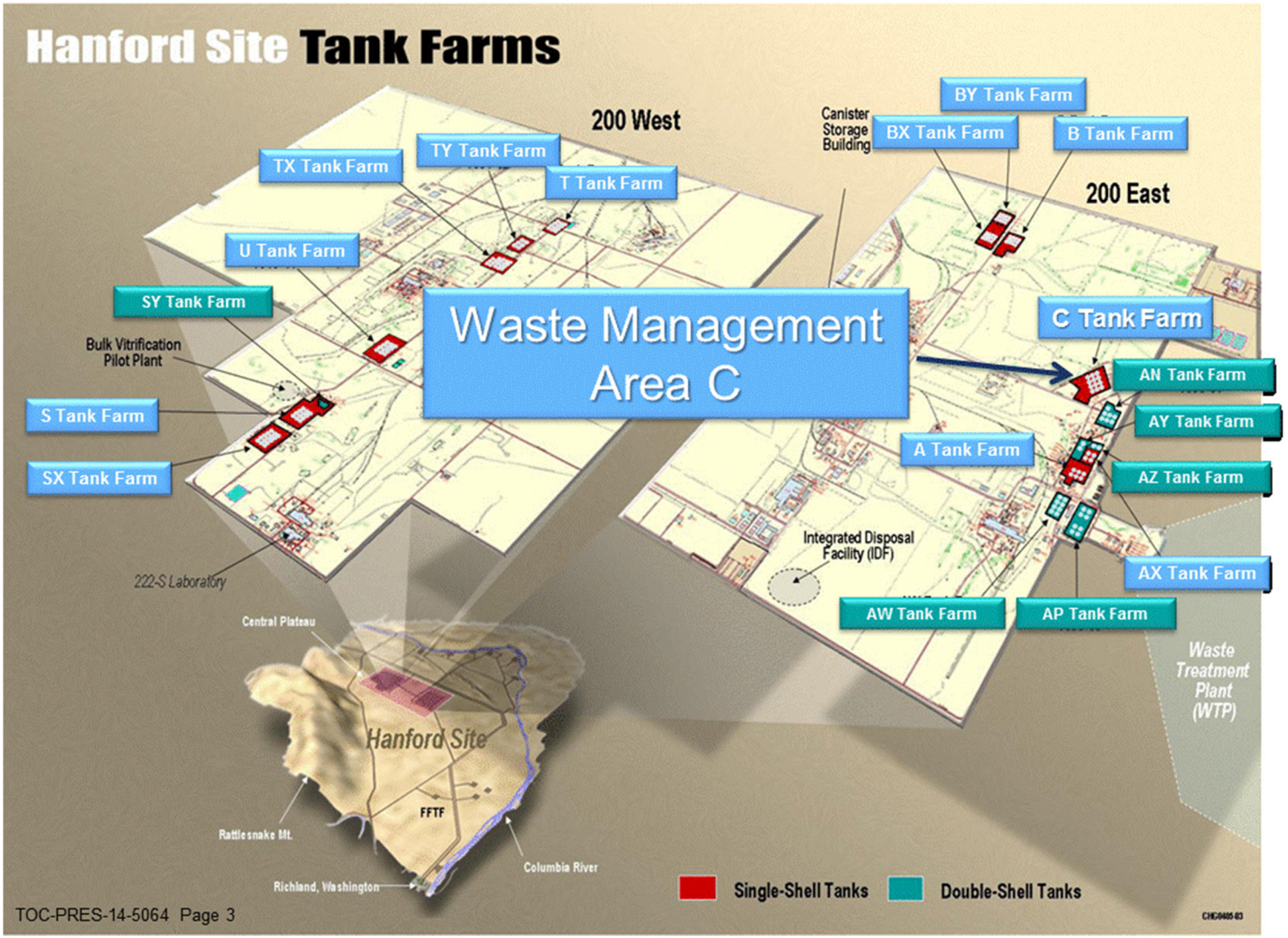

FFTF = Fast Flux Test Facility

Reference: TOC-PRES-14-5064-VA, "Waste Management Area C Performance Assessment (PA) Current Status."

Figure 1-2. The Components of the Appendix I Performance Assessment.

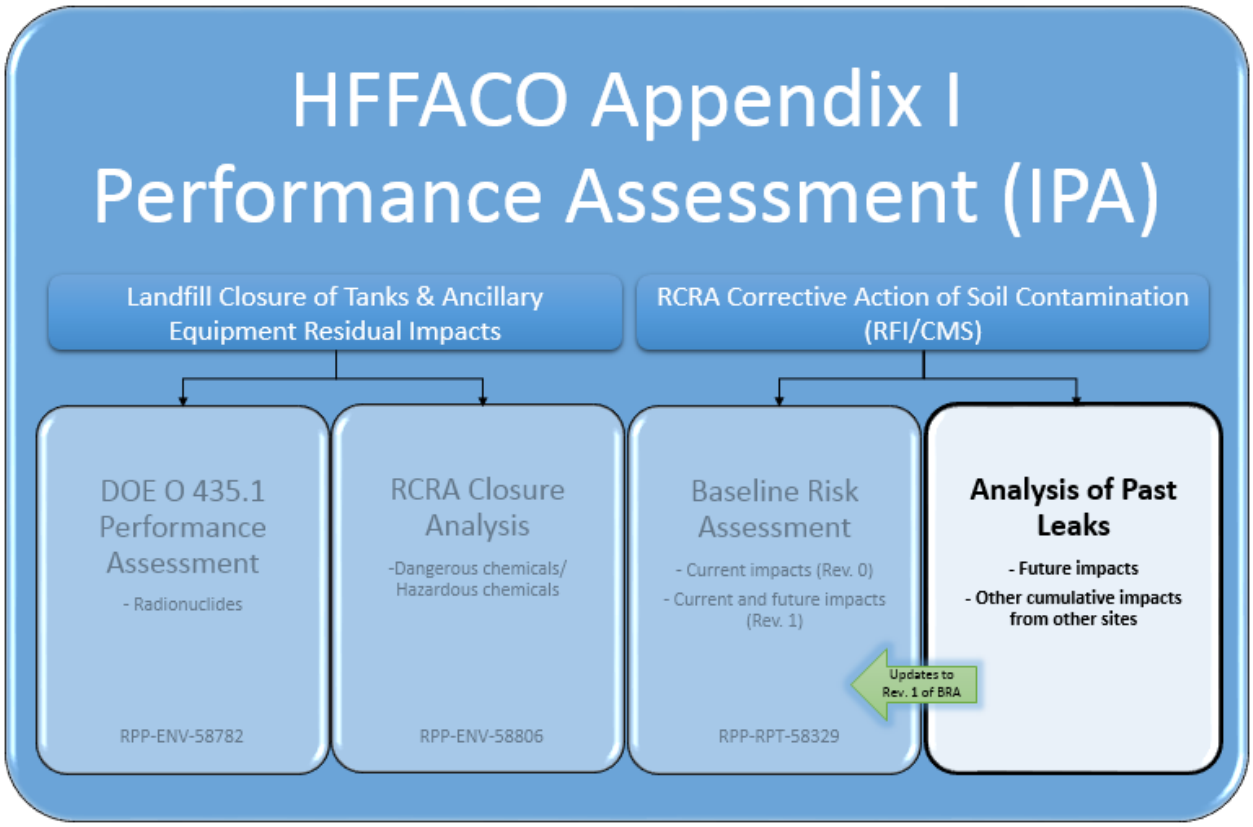

BRA = Baseline Risk Assessment
HFFACO = Hanford Federal Facility Agreement and Consent Order
RCRA = Resource Conservation and Recovery Act of 1976
RFI/CMS = RCRA Facility Investigation/Corrective Measures Study

References:
DOE O 435.1, Radioactive Waste Management.
RPP-ENV-58806, "RCRA Closure Analysis of Waste Management Area C, Hanford Site, Washington."
RPP-RPT-58329, "Baseline Risk Assessment for Waste Management Area C."

Closure decisions for the Hanford Site SST system soils will be made through the Resource Conservation and Recovery Act of 1976 (RCRA) corrective action process. The RCRA corrective action component of the IPA is documented in RPP-RPT-58339, "Phase 2 RCRA Facility Investigation Report for Waste Management Area C," Draft A and will contain 1) a baseline risk assessment and 2) an analysis of past leaks.

- **Baseline Risk Assessment** – An evaluation of impacts to human and ecological receptors from both non-radiological and radiological contaminants in soils at WMA C under current condition, in the absence of actions to control or mitigate releases. Under the U.S. Environmental Protection Agency (EPA), this is completed at contaminated waste sites prior to remediation activities to establish a need for action. An initial version of the baseline risk assessment has been prepared (RPP-RPT-58329). Revision 1 of this document will address both current and future impacts to human health and the environment.

- **Analysis of Past Leaks** – An evaluation of future impacts to human receptors from both non-radiological and radiological contaminants in soils at the closed WMA C. This evaluation of future impacts will support updates to the anticipated Revision 1 of the baseline risk assessment (RPP-RPT-58329).

1.1.1 Waste Management Area C Performance Assessment Scoping Process

The foundation of the WMA C IPA was established in a scoping process that was conducted with regulatory agencies and stakeholders between 2009 and 2011. As a part of the scoping process, a series of working sessions were conducted that addressed the following technical topic areas:

- Residual Inventory (Detailed conceptual models and data related to residual waste inventories left in WMA C tanks and ancillary equipment at closure) (May 5-7, 2009)

- Assessment Context/General Conceptual Models (September 1-3, 2009)

- Soil Inventory (Detailed conceptual models and data on waste inventories released to the environment from historical releases during operations) (October 27-29, 2009)

- Engineered System #1 (Detailed conceptual models and data on natural recharge and waste release) (January 26-28, 2010)

- Natural System (Detailed conceptual models and data on vadose zone and groundwater flow and transport) (May 25-27, 2010)

- Engineered System #2 (Continuation discussion of detailed conceptual models, data, and characteristics of the engineered systems) (July 27-29, 2010)

- Exposure Scenarios (Detailed conceptual models and data on human health exposure scenarios) (September 28-30, 2010)

- Vadose Zone and Groundwater Flow and Transport Modeling (Use of numerical and system-level codes and models to support the PA) (January 25-27, 2011)

- Ecological Risk Assessment (Detailed conceptual models and data related to ecosystem risk assessments) (May 17-19, 2011).

Regulatory agency members who participated in the scoping process included representatives from DOE, EPA, the U.S. Nuclear Regulatory Commission (NRC), and Ecology as well as their contractors. Other participants in the working sessions included representatives of the tribal nations, other stakeholders groups, and members of the interested public.

The results of the WMA C IPA scoping process have been documented in a series of data package reports that were produced in the 2009 to 2011 scoping time frame. These data packages document the outcomes of working sessions held with relevant regulatory agencies and

stakeholders. These working sessions were used to solicit input from the working session participants, and to obtain a common understanding concerning the scope, methods, and data to be used in the HFFACO Appendix I PA for WMA C. The listing of the current versions of each data package produced in each of the working sessions is summarized in Table 1-1.

Table 1-1. Data Packages Produced as a Part of the Waste Management Area C Performance Assessment Scoping Process.

Working Session Topical Area	Report Number (Year Published)	Current Revision No.	Title
Residual Inventory	RPP-RPT-42323 (2015)	3	Hanford C-Farm Tank and Ancillary Equipment Residual Waste Inventory Estimates
Assessment Context	RPP-RPT-41918 (2010)	0	Assessment Context for Performance Assessment for Waste in C Tank Farm Facilities after Closure
Soil Inventory	RPP-RPT-42294 (2016)	2	Hanford Waste Management Area C Soil Contamination Inventory Estimates
Engineered System #1	RPP-RPT-44042 (2010)	0	Recharge and Waste Release within Engineered System in Waste Management Area C
Engineered System #2	RPP-RPT-46879 (2011)	2	Corrosion and Structural Degradation within Engineered System in Waste Management Area C
Natural System	RPP-RPT-46088 (2010)	1	Flow and Transport in the Natural System at Waste Management Area C
Exposure Scenarios	RPP-RPT-47479 (2011)	1	Exposure Scenarios for the Waste Management Area C Performance Assessment
Numerical Codes	RPP-RPT-48490 (2011)	1	Technical Approach and Scope for Flow and Contaminant Transport Analysis in the Initial Performance Assessment of Waste Management Area C
Ecosystem Risk	RPP-RPT-49425 (2011)	1	Ecological Risk Assessment Approach for Hanford Waste Management Area C

Between the development of these data packages and today, updated information has become available for some of the inputs, and new conceptualizations and interpretations of data have been developed. In addition, stakeholders have expressed ideas and concerns to the project team that have led to the development of additional conceptual models and sensitivity analysis cases.

Specific areas associated with past leaks in which deviations or updates from the prior data packages occurred include the following:

- Estimates of leak inventories and volumes (RPP-ENV-33418, “Hanford C-Farm Leak Inventory Assessments Report,” Revision 4), soil inventories (RPP-RPT-42294, “Hanford Waste Management Area C Soil Contamination Inventory Estimates,” Revision 3), and groundwater plume extents and concentrations (DOE/RL-2015-07, Hanford Site Groundwater Monitoring Report for 2014; DOE/RL-2009-127, Remedial

Investigation Report for the 200-BP-5 Groundwater Operable Unit; RPP-RPT-58297, "Screening-Level Evaluation of Groundwater Monitoring Data Collected in Vicinity of WMA C") have been updated.

- Alternative models of the site stratigraphy have been implemented in collaboration with stakeholders.
- Vadose zone flow properties have been updated to better represent site-specific data.
- Aquifer flow properties have been updated to reflect new data and interpretations.

This updated information has been included in a performance assessment of tank residuals in RPP-ENV-58782.

1.2 PURPOSE AND SCOPE OF THE REPORT

1.2.1 Purpose

This document provides an analysis of past leaks at WMA C using the model developed for the WMA C residual waste PA (RPP-ENV-58782) and RCA (RPP-ENV-58806). The report has several purposes.

First, the conceptual model developed for the performance assessment of residual contamination has been implemented to evaluate how well it explains observed field data for the time of arrival of contaminants to groundwater, concentrations of contaminants in groundwater, and the distribution of contaminants in the vadose zone. Second, the combination of the field data and model have been used to determine bounds on input assumptions that are consistent with groundwater and soil monitoring data from past leaks. In particular, the model has been used to evaluate the uncertainties in the inventory and volumes of past leaks, to better constrain estimates of the existing contamination. Third, the constrained model has been used to project future impacts from the past leaks. This part of the analysis will represent an input to additional analyses for the Appendix I PA.

1.2.2 Scope

The scope of this report is limited to an assessment of past leaks at WMA C, and is intended as a companion report to the radiological PA of residual contamination (RPP-ENV-58782) and the RCA for WMA C (RPP-ENV-58806).

In the remainder of Section 1, a general description is provided of WMA C, specifically focused on information germane to the past leaks. In addition, a description is provided of previous modeling efforts on past leaks.

In Section 2, a summary is provided of the general groundwater situation associated with the past leaks analysis, a summary of current estimates of the leaks themselves, and a summary of soil and groundwater data that are used for interpreting the groundwater model.

In Section 3, a description is provided of the model implemented for the past leaks analysis. The foundation of this model is the facility-specific groundwater model developed for the analysis of residual wastes at WMA C (RPP-ENV-58782 and RPP-ENV-58806). Chapter 3 therefore represents an interpretation of the site-specific data presented in Chapter 2, along with the general understanding of groundwater behavior presented in Chapter 2.

In Section 4, a series of scoping analysis cases are presented. These scoping analysis cases apply the site-specific WMA C groundwater model to the past leaks, and compare calculations of arrival time of contamination and groundwater concentrations to evaluate which model inputs are consistent with groundwater data. These comparisons are necessarily somewhat qualitative owing to the limitations of the data, but the comparisons are intended to be as quantitative as possible.

In Section 5, a set of transient model cases of past leak behavior are presented. The transient model analysis cases attempt to approximate the flow conditions that have existed at WMA C from its construction in 1944 to present day. During this time, referred to as the operations period, the hydraulic gradient, both in direction and magnitude, appears to have been highly variable, and flow appears to have occurred in several directions.

In Section 6, a set of forward calculations to evaluate the future consequences of the leaks are presented, to evaluate how the groundwater concentrations may change in the future based on the constraints on the scoping modeling analysis cases established in Section 4.

In Section 7, results of the future impacts described in Section 6 are compared against future impacts from waste residuals anticipated to be left in tanks and ancillary equipment at closure and the potential impacts at WMA C from sources upgradient of WMA C.

Conclusions and recommendations are presented in Section 8.

1.3 GENERAL FACILITY DESCRIPTION

The Hanford Site, a facility in the DOE nuclear waste complex, encompasses ~1,500 km^2 (~586 mi^2) northwest of the city of Richland along the Columbia River in southeastern Washington State, as shown in Figure 1-3. The Federal government acquired the Site in 1943 for the production of plutonium. Production of special nuclear materials continued until the 1980s. Since the 1990s, DOE has focused on environmental remediation of the Hanford Site.

Waste Management Area C (WMA C or the 241-C Tank Farm [C Farm]), part of the SST system, is located in the Central Plateau (see Figure 1-3), near the eastern edge of the 200 East Area. One of the first tank farms built, it was constructed in 1944 and 1945.

Figure 1-3. Hanford Site and its Location in Washington State.

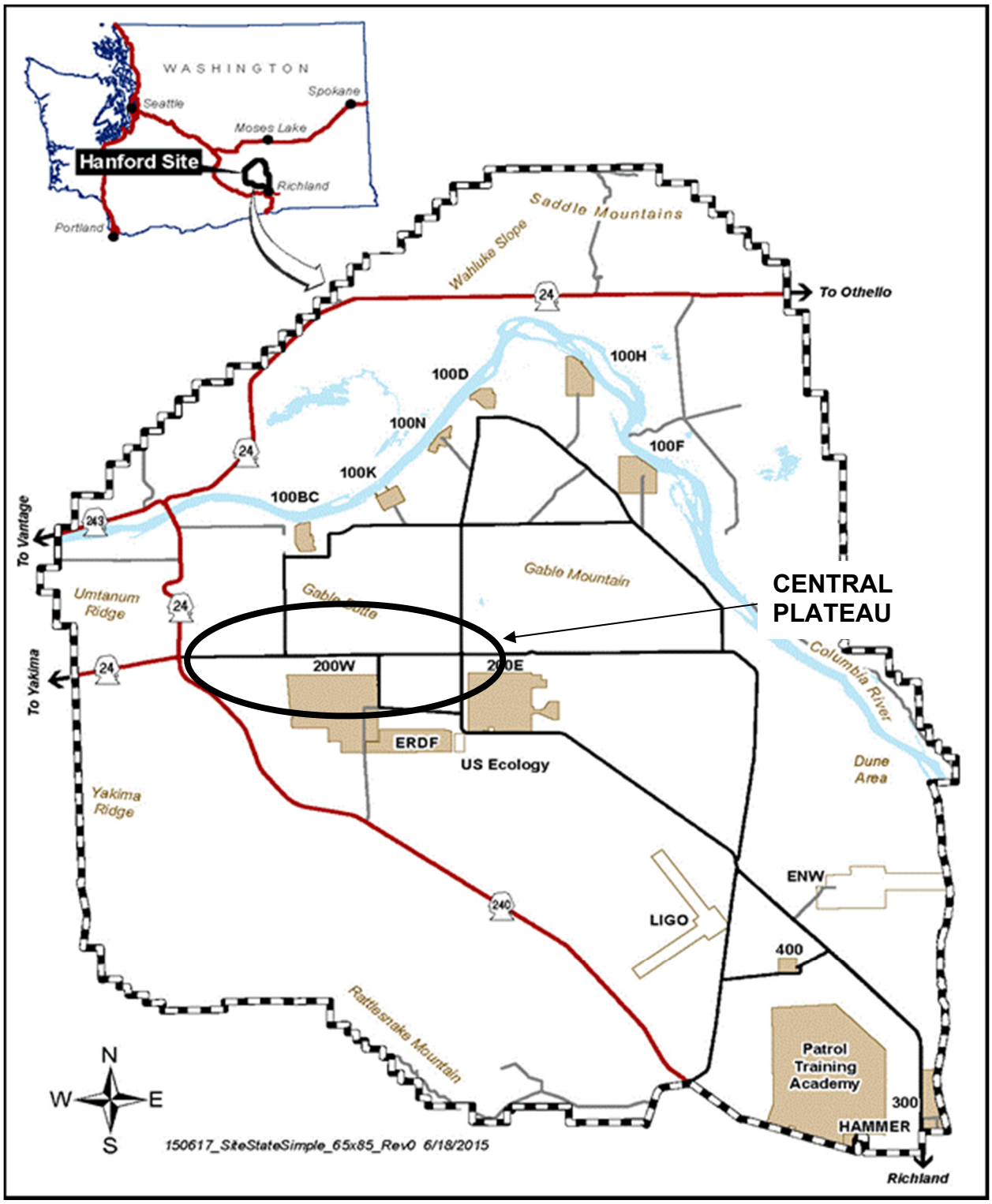

ENW = Energy Northwest Columbia Generating Station LIGO = Laser Interferometer Gravitational Wave Observatory
ERDF = Environmental Restoration Disposal Facility

The WMA C facility contains twelve 100-series tanks and four 200-series tanks (see Figure 1-4). The 100-series tanks are 23 m (75 ft) in diameter, with a maximum 5-m (16-ft) depth and 2,006,000-L (530,000-gal) design capacity. The 200-series tanks are 6 m (20 ft) in diameter with a maximum 7-m (24-ft) depth and 208,000-L (55,000-gal) design capacity. Only tanks 241-C-101 (C-101) through 241-C-106 (C-106) have concrete pits. The other 100-series tanks are equipped with centrally located salt well pump pits. The tanks sit below grade with at least 2 m (7 ft) of soil cover to provide shielding from radiation exposure to operating personnel. Tank pits are located on top of the tanks and provide access to the tanks, pumps, and associated monitoring equipment.

The SSTs were constructed in place with 0.95-cm (0.375-in.)-thick carbon steel (ASTM A283 Grade C) lining the bottom and 0.64-cm (0.25-in.)-thick carbon steel lining the sides of a reinforced-concrete shell. The tanks have concave bottoms (center of tanks lower than the perimeter) and a curving intersection of the sides and bottom, where the carbon steel plate is 0.8 cm (0.3125 in.) thick. The inlet and outlet lines are located near the top of the liners. There are four inlet lines on each tank, which are also known as nozzles. Pipelines from the diversion boxes to tanks C-101, 241-C-104 (C-104), 241-C-107 (C-107), 241-C-108 (C-108), 241-C-110 (C-110), and 241-C-111 (C-111) are supported by concrete viaducts. At ~3 m (9 ft 10 in.) from the tank wall, the viaduct surface steps down and the void space between the pipes and the viaduct surface is grouted. At this point, the viaduct begins fanning out from 0.8 m (2 ft 8 in.) wide to 2.2 m (7 ft 4 in.) wide to support the spread placement of the fill lines through the tank wall. Tanks C-101, C-104, C-107, and C-110 each have one outlet line to the next tank in series. Tanks 241-C-102 (C-102), 241-C-105 (C-105), C-108, and C-111 each have one additional inlet line and one outlet line. Tanks 241-C-103 (C-103), C-106, 241-C-109 (C-109), and 241-C-112 (C-112) each have one additional inlet line from the previous tank in the series. The lines connecting each tank are also referred to as “cascade” lines since they allowed transfer of fluids between tanks using gravity flow.

To support the transfer and storage of waste within WMA C SSTs, there is a complex waste transfer system of pipelines (transfer lines), diversion boxes, vaults, valve pits, and other miscellaneous structures. These miscellaneous features of the tank farm are referred to in this document by the general term “ancillary equipment and components.”

The 244-CR Process Tank Vault (244-CR vault) is located south of the tanks. The vault is a two-level, multi-cell, reinforced-concrete structure constructed below grade, which contains four underground tanks along with overhead piping and equipment. Two tanks (TK-CR-001 and TK-CR-011) have a capacity of 170,343 L (45,000 gal) each. The other two tanks (TK-CR-002 and TK-CR-003) have capacities of 55,494 L (14,700 gal) each. This reference estimated a capacity of 170,343 L (45,000 gal) each for two tanks (TK-CR-001 and TK-CR-011) and a capacity of 55,494 L (14,700 gal) each for the other two tanks (TK-CR-002 and TK-CR-003). HNF-EP-0182 currently lists the capacities of TK-CR-001 and TK-CR-011 as 151,400 L (40,000 gal) each and the capacities of TK-CR-002 and TK-CR-003 as 56,775 L (15,000 gal) each.

Figure 1-4. Location Map of Waste Management Area C and Surrounding Area.

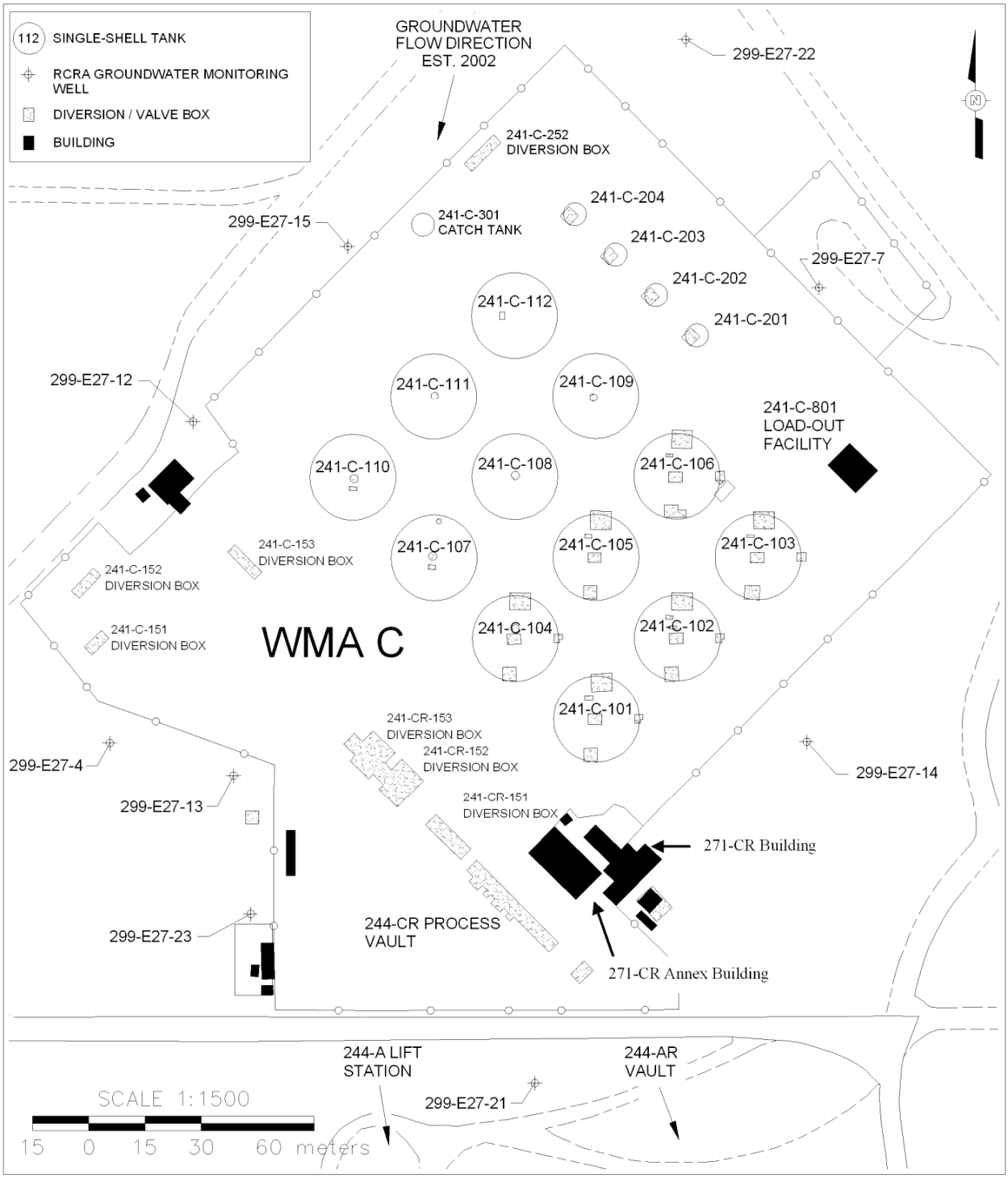

RCRA = Resource Conservation and Recovery Act of 1976 WMA = Waste Management Area

Fourteen unplanned releases (UPRs) have occurred within or near to WMA C (Figure 1-5). The largest ones are associated with leaks in pipelines or diversion boxes, with releases from

inlet/outlet ports of the SSTs, or with leaks from the SSTs. Revision 4 of RPP-ENV-33418 provides the most recent estimates of the volumes and contaminant content of these releases. A summary of Revision 4 of RPP-ENV-33418 is provided in Chapter 2.

Figure 1-5. Location Map of Unplanned Release Sites of Waste Management Area C.

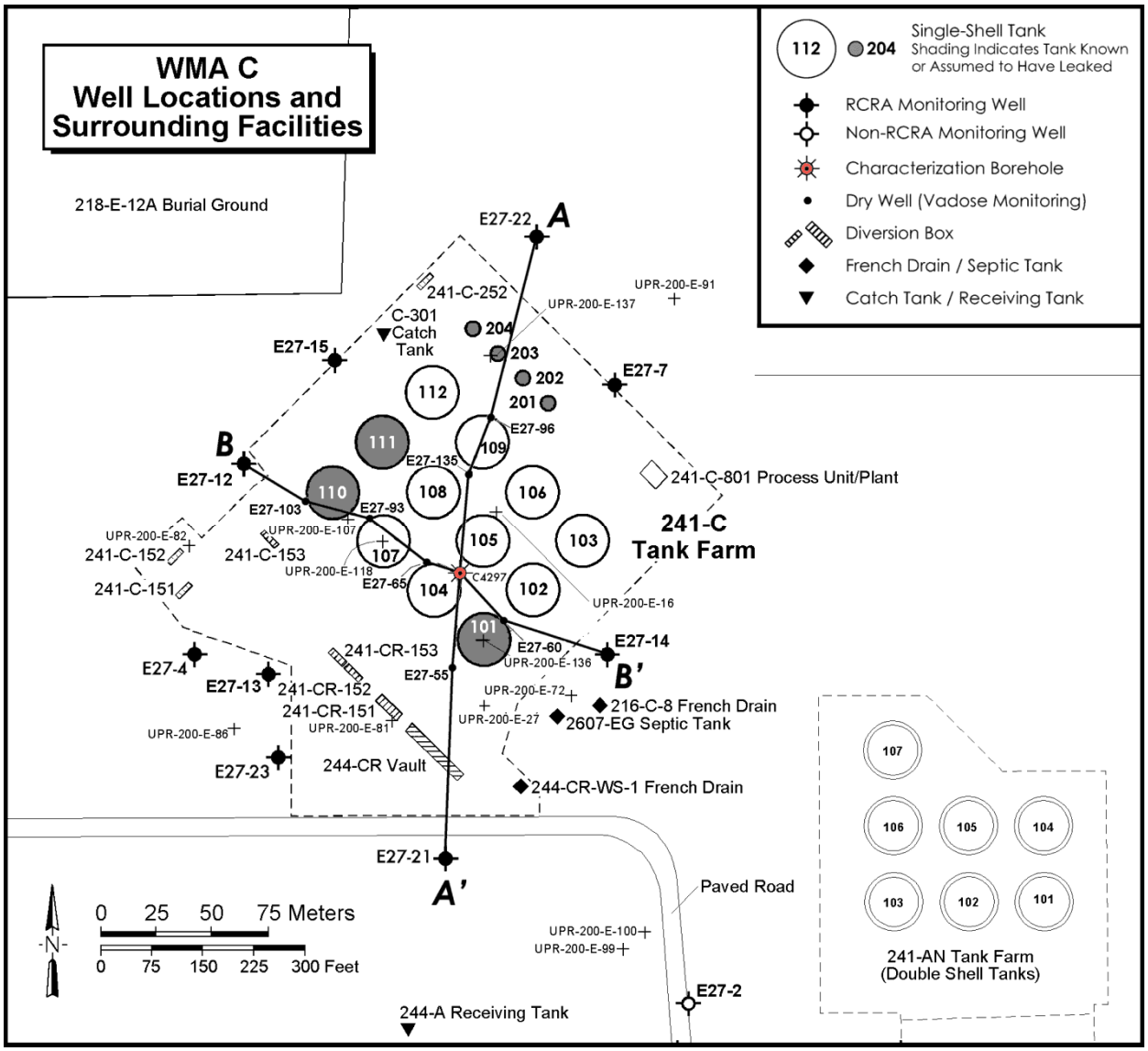

RCRA = Resource Conservation and Recovery Act of 1976 WMA = Waste Management Area

1.4 PREVIOUS ASSESSMENTS

Two principle assessments have been conducted that included consideration of past leaks at WMA C:

- DOE/ORP-2005-01, Initial Single-Shell Tank System Performance Assessment for the Hanford Site

- DOE/EIS-0391, "Final Tank Closure and Waste Management Environmental Impact Statement for the Hanford Site, Richland, Washington" (TC&WM EIS).

1.4.1 Single-Shell Tank Performance Assessment

The Single-Shell Tank Performance Assessment (SST PA) (DOE/ORP-2005-01) presented an analysis of the long-term impacts of residual wastes assumed to remain after retrieval of tank wastes and closure of the SST farms. The SST PA was intended to be a comprehensive evaluation of closure of all SST WMAs at Hanford, and included WMA C in its scope, but was not exclusively focused on it. The SST PA included four post-closure contamination sources consisting of tank residuals, ancillary equipment residuals, past UPRs, and hypothetical retrieval leaks. The SST PA assumed the presence of eight past tank leaks and four UPRs. The reference case inventories for past leaks assumed in the SST PA are presented in Table 1-2, and the assumed volumes are presented in Table 1-3. These values of the leak inventories were introduced as a source in the model at 40 m (130 ft) below surface at the start of the model (year 2000).

Table 1-2. Reference Case Inventory of Past Leaks Assumed in the Single-Shell Tank Performance Assessment.

Contaminant	Inventory	Contaminant	Inventory
Radionuclides (Ci)		Chemicals (kg)	
C-14	3.46E-1	Cr	1.11E2
Tc-99	6.93	NO_2	4.35E3
I-129	3.02E-2	NO_3	1.07E4
		U	7.88

Excerpted from DOE/ORP-2005-01, Initial Single-Shell Tank System Performance Assessment for the Hanford Site, Table 2-24.

This modeling approach was intended solely as a prospective, forward-looking analysis, and was not intended to mimic existing measured concentration data and arrival times of the plume at groundwater, and it did not match observed arrival times of ^{99}Tc at the water table.

1.4.2 Tank Closure and Waste Management Environmental Impact Statement Analysis of Waste Management Area C

The TC&WM EIS (DOE/EIS-0391) included in its scope an evaluation of all waste sources in the tank farm, including past tank leaks, retrieval leaks from the tanks, residual wastes, and UPRs associated with WMA. The inventory of the past tank leaks and UPRs used in the TC&WM EIS (see Section D.1.4 of Appendix D of DOE/EIS-0391) is presented in Table 1-4. It was assumed that all of the past leaks at WMA C occurred in 1946, and were associated with the volumes shown in Table 1-5.

Table 1-3. Volumes of Past Leaks Assumed in the Single-Shell Tank Performance Assessment.

Source	Volume (gal)*
241-C-101	1,000
241-C-105	1,000
241-C-110	2,000
241-C-111	5,500
241-C-201	550
241-C-202	450
241-C-203	400
241-C-204	350
UPR 200-E-81	36,000
UPR 200-E-82	2,600
UPR 200-E-86	18,500
UPR 200-E-107	5

Excerpted from DOE/ORP-2005-01, Initial Single-Shell Tank System Performance Assessment for the Hanford Site, Table 2-23.

* Conversion 1 gallon = 3.78541 liters

Table 1-4. Inventory of Past Tank Leaks and Unplanned Releases Assumed in the Tank Closure and Waste Management Environmental Impact Statement.

Contaminant	Inventory	Contaminant	Inventory
Past Tank Leaks			
Radionuclides (Ci)		Chemicals (kg)	
H-3	2.68E1	1-butanol	1.89E1
C-14	1.48E-1	Cr	4.15E1
Tc-99	6.61	Hg	2.12E-2
I-129	2.59E-3	NO_3	4.82E3
Np-237	2.30E-2	Pb	6.87
U-238	5.41E-3	U-total	2.88
Unplanned Releases			
Radionuclides (Ci)		Chemicals (kg)	
H-3	1.39E2	1-butanol	6.47E-1
C-14	1.90E-1	Cr	3.94E1
Tc-99	1.67	Hg	3.92E-3
I-129	2.48E-2	NO_3	9.68E3
Np-237	5.58E-3	Pb	2.16E1
U-238	1.49E-2	U-total	3.47E1

Excerpted from DOE/EIS-0391, "Final Tank Closure and Waste Management Environmental Impact Statement for the Hanford Site, Richland, Washington," Tables M-18 and M-25.

Table 1-5. Volumes of Past Tank Leaks Assumed in the Tank Closure and Waste Management Environmental Impact Statement.

All tank leaks were assumed to occur in 1946.

Source	Volume (gal)*
241-C-101	20,000
241-C-110	2,000
241-C-111	5,500
241-C-201	550
241-C-202	450
241-C-203	400
241-C-204	350

Excerpted from DOE/EIS-0391, "Final Tank Closure and Waste Management Environmental Impact Statement for the Hanford Site, Richland, Washington," Table M-4.

* Conversion 1 gallon = 3.78541 liters

2.0 BACKGROUND

This section of the report provides background information relevant to this past leak analysis including the following:

- Inventory estimates for past waste releases to the vadose zone
- A summary of the hydrologic setting for the Central Plateau
- A summary of vadose zone contamination
- A summary of aquifer conditions and contamination
- A synopsis of recent interpretations of groundwater chemistry.

2.1 INVENTORY ESTIMATES FOR PAST WASTE RELEASES TO THE VADOSE ZONE

This section summarizes inventory estimates for past leaks and releases to the soil in WMA C. The technical basis for the inventory estimates is presented in RPP-ENV-33418 and inventories for the WMA C PA are presented in RPP-RPT-44294.

Inventory estimates from past releases were determined for those facilities or areas where there was an indication that a release occurred and for which a technical basis for a soil inventory estimate could be determined. The process to estimate tank leak inventories is shown in Figure 2-1 and is described in RPP-32681, "Process to Assess Tank Farm Leaks in Support of Retrieval and Closure Planning." Information for WMA C SSTs, catch tanks, pits and diversion boxes and pipelines were reviewed to assess evidence of waste releases to the vadose zone.

The key parameters needed to estimate the inventory or mass of constituents released are: 1) the volume of a release, 2) the time a release occurred, and 3) the waste type and composition of waste released. For some tank leaks and UPRs, historical records confirm the waste loss event and data provide a strong technical basis for time of leak event, leak volume, and composition of the waste estimates. However, for many tank leaks and UPRs little data is available. Not only is there little data on many releases, but existing data is often ambiguous and incomplete.

The inventory estimates in this report are based on information available as of September 1, 2014, and were calculated for chemical and radionuclide constituents included in RPP-19822, "Hanford Defined Waste Model – Revision 5.0" (HDW) model (Table 2-1). The HDW constituents account for over 99% of the chemical and radionuclide inventory (WHC-SD-WM-TI-731, "Predominant Radionuclides in Hanford Site Waste Tanks").

The HDW Model is a spreadsheet-based engineering estimate of the chemical and radionuclide contents of the Hanford single-shell and double-shell tanks based on process reactor fuel irradiation records, separation plant dissolver charging records, separation plant and tank farm process flowsheets, and tank farm waste receipt and transfer records. The HDW includes waste type composition estimates for solids and supernate for different process waste streams in the tank farms. The predominant supernatant waste types assumed to have been released from tanks and ancillary equipment in C Farm are from the Plutonium Uranium Extraction Plant

(high-activity waste [P1 (1956-1962) and P2 (1963-1967)] and aluminum cladding waste [CWP1 (1956-1960) and CWP2 (1961-1972)]), B Plant (ion exchange cesium recovery waste [CSR]) and Stack condensate. The HDW estimates for these waste types, which are summarized in Table 2-2, provide the primary basis for the waste type composition estimates for waste released.

Figure 2-1. Schematic of Process Used to Determine Vadose Zone Inventory.

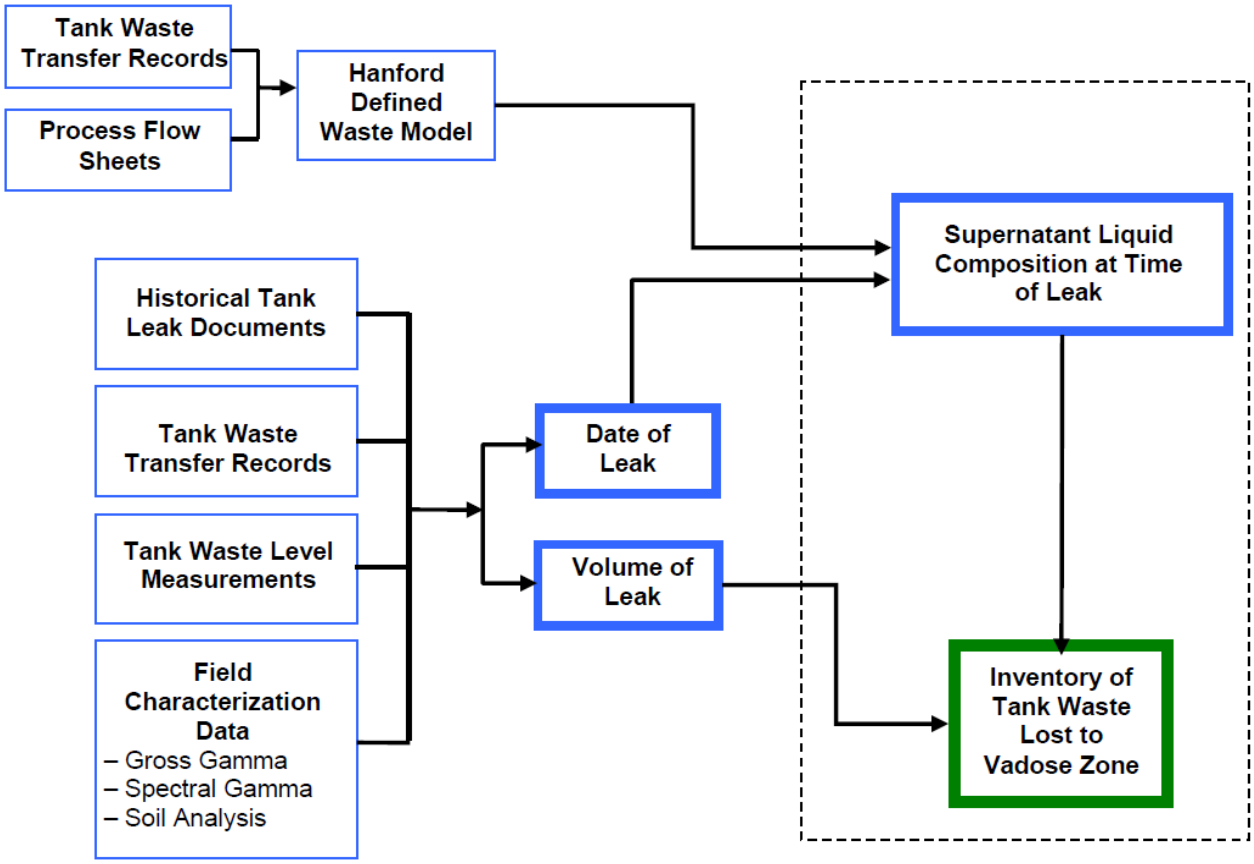

Note: Uncertainty exists in all these sources.

When sample data was identified that was considered representative of a waste release, the HDW values were adjusted based on the ratio of the analytical concentration for a constituent to the HDW concentration for that constituent. Typically, analytical data was only provided for a few constituents, but the values for all constituents were adjusted based on the ratio of ^{137}Cs concentrations or other selected analytes. This ratio is a multiplier or dilution factor comparing the HDW waste type to measured results.

The following sections and Table 2-3 summarize the basis for inventory estimates for contaminant soil releases in WMA C. Additional information for each of the releases is provided in RPP-ENV-33418. These and other releases, not included in Table 2-3, were identified in RPP-ENV-33418, Tables 6-2 and 6-3; however, volumes and inventories could only be estimated for releases shown in Table 2-3. Releases documented but not quantified include condensate discharges to the 244-CR-WS-1 drain, possible P1 and P2 waste discharges to the 241-C-801 drywell, and UPRs from air emissions, pipelines, catch tanks and diversion boxes.

Table 2-1. Constituents Evaluated in the Hanford Defined Waste Model.

Chemicals			Radionuclides			
Na	Ag	Si	H-3	Cd-113m	Ra-228	Np-237
Al	Mn	F	C-14	Sb-125	Ac-227	Pu-238
Fe	Ca	Cl	Ni-59	Sn-126	Pa-231	Pu-239
Cr	K	CCl_4	Ni-63	I-129	Th-229	Pu-240
Bi	U-Total	Butanol	Co-60	Cs-134	Th-232	Pu-241
La	NO_3	Tributyl Phosphate	Se-79	Cs-137	U-232	Pu-242
Hg	NO_2	NPH	Sr-90	Ba-137m	U-233	Am-241
Zr	CO_3	NH_3	Y-90	Sm-151	U-234	Am-243
Pb	PO_4	$Fe(CN)_6$	Zr-93	Eu-152	U-235	Cm-242
Ni	SO_4		Nb-93m	Eu-154	U-236	Cm-243
			Tc-99	Eu-155	U-238	Cm-244
			Ru-106	Ra-226		

Reference: RPP-26744, "Hanford Soil Inventory Model, Rev. 1."

2.1.1 Tank 241-C-101

Tank C-101 was classified as a confirmed leaking tank in 1968 with a leak volume of ~75,600 L (20,500 gal). The leak volume estimate appears to be based on a 34.3-cm (13.5-in.) liquid level decrease between January 1965 and September 1969 and a subsequent radioactivity increase in drywells (30-01-02, 30-01-06 and 30-01-09) around this tank. It appears that a portion of the liquid level decrease was attributed to evaporation. Tank C-101 is fitted with a condensation unit to recycle condensate back into the tank. A 34.3-cm (13.5-in.) decrease in surface level corresponds to ~140,100 L (~37,000 gal). Further evaluations and field investigations indicate that some or all of the liquid level decrease may be attributed to a spare inlet release, cascade line release, or tank leak above 137.2 cm (54 in.) from the tank bottom.

The estimated waste release volume of ~140,100 L (37,000 gal) is based on the liquid level decrease. Based on drywell readings and waste process history, the assumed waste types are 99% CWP1 and 1% P1 waste released from the spare inlet or near the inlet.

An informal integrity assessment for tank C-101 concluded, based on liquid level measurements, evaporation calculations, and low gamma activity in drywells, that the tank probably did not leak, and if it did leak the release point would have been high on the tank wall. Based on the integrity assessment, tank C-101 was retrieved using modified sluicing. Retrieval commenced on December 10, 2012 and ended on September 1, 2013. Although large volumes of water and supernate were added to the tank during sluicing operations, there was no indication of a leak during retrieval from the High Resolution Resistivity (HRR) leak detection monitoring system or other monitoring systems used.

Table 2-2. Average Composition of Hanford Defined Model Chemical and Radiological Constituents for Selected Waste Types. (3 sheets)

Constituent	Units	P1*	P2*	CWP1*	CWP2*	CSR*	Sr-Cs Rec (P2) Stack Drain**
Al(OH)4 -	g/L	0.00E+00	0.00E+00	8.10E+01	5.97E+01	3.66E+01	0.00E+00
Bi	g/L	0.00E+00	0.00E+00	0.00E+00	0.00E+00	1.06E-03	0.00E+00
butanol	g/L	0.00E+00	0.00E+00	0.00E+00	0.00E+00	1.09E+00	0.00E+00
Ca	g/L	1.50E-01	1.50E-01	1.50E-01	1.50E-01	1.50E-01	6.32E-03
Cl-	g/L	5.15E-01	9.36E-01	2.47E-01	4.10E-01	2.49E+00	0.00E+00
CO3--	g/L	2.25E-01	2.25E-01	2.25E-01	2.25E-01	1.11E+01	0.00E+00
Cr	g/L	4.18E-01	4.23E-01	1.60E-01	1.59E-01	1.65E+00	0.00E+00
DBP	g/L	0.00E+00	0.00E+00	0.00E+00	0.00E+00	3.10E+00	0.00E+00
F-	g/L	0.00E+00	0.00E+00	0.00E+00	0.00E+00	3.11E-02	0.00E+00
Fe	g/L	1.05E-01	1.05E-01	1.05E-01	1.05E-01	1.05E-01	4.80E-05
Hg	g/L	3.24E-04	3.24E-04	0.00E+00	0.00E+00	3.24E-04	8.48E-06
K	g/L	1.23E-01	2.24E-01	5.92E-02	9.82E-02	8.15E-01	9.65E-05
La	g/L	0.00E+00	0.00E+00	0.00E+00	0.00E+00	0.00E+00	0.00E+00
Mn	g/L	0.00E+00	0.00E+00	0.00E+00	0.00E+00	1.78E-02	7.07E-06
Na	g/L	1.66E+01	2.70E+01	5.47E+01	3.73E+01	9.55E+01	4.09E-04
NH3	g/L	1.43E-01	5.23E-01	1.55E-03	3.15E-04	4.19E-01	0.00E+00
Ni	g/L	1.07E-01	1.07E-01	9.05E-02	8.99E-02	1.07E-01	0.00E+00
NO2-	g/L	1.27E+01	2.83E+01	3.66E+01	1.31E+01	3.96E+01	0.00E+00
NO3-	g/L	1.09E+01	7.44E+00	4.28E+01	4.26E+01	7.77E+01	9.08E-04
OH-	g/L	3.12E+00	3.14E+00	3.19E-01	3.19E-01	1.69E+01	
Pb	g/L	2.32E-02	1.49E-01	1.49E-01	1.49E-01	1.02E-01	1.46E-05
PO4---	g/L	0.00E+00	0.00E+00	0.00E+00	0.00E+00	6.14E-01	0.00E+00
SiO3--	g/L	8.02E-01	8.02E-01	8.02E-01	0.00E+00	8.02E-01	0.00E+00
SO4--	g/L	4.22E+00	1.19E+01	8.52E-01	6.47E-01	9.04E+00	8.51E-04
Sr	g/L	4.55E-05	4.55E-05	1.17E-05	9.88E-06	4.62E-05	0.00E+00
TOC	wt%C	0.00E+00	0.00E+00	0.00E+00	0.00E+00	4.66E-01	
U total	g/L	3.10E-02	3.10E-02	3.10E-02	3.10E-02	3.10E-02	3.72E-07
Zr	g/L	0.00E+00	0.00E+00	0.00E+00	0.00E+00	1.46E-04	0.00E+00
density							
Constituent		Decayed to Year 2020					

Table 2-2. Average Composition of Hanford Defined Model Chemical and Radiological Constituents for Selected Waste Types. (3 sheets)

Constituent	Units	P1*	P2*	CWP1*	CWP2*	CSR*	Sr-Cs Rec (P2) Stack Drain**
H-3	Ci/L	1.33E-06	4.06E-06	5.73E-05	5.77E-05	6.76E-06	0.00E+00
C-14	Ci/L	2.44E-06	2.97E-06	1.57E-06	1.07E-06	3.77E-06	0.00E+00
Ni-59	Ci/L	6.12E-07	1.34E-06	6.19E-06	7.85E-06	7.02E-07	0.00E+00
Co-60	Ci/L	1.01E-06	1.97E-06	1.01E-06	1.70E-06	1.97E-06	0.00E+00
Ni-63	Ci/L	5.00E-05	1.13E-04	5.09E-04	6.64E-04	5.86E-05	0.00E+00
Se-79	Ci/L	2.39E-07	5.43E-07	6.52E-10	4.84E-10	4.50E-07	0.00E+00
Sr-90	Ci/L	1.57E-03	1.57E-03	4.03E-04	3.41E-04	1.57E-03	1.60E-05
Y-90	Ci/L	1.57E-03	1.57E-03	4.03E-04	3.41E-04	1.57E-03	1.60E-05
Zr-93	Ci/L	1.43E-05	3.23E-05	3.89E-08	2.79E-08	2.68E-05	0.00E+00
Nb-93m	Ci/L	5.23E-06	1.12E-05	1.44E-08	9.66E-09	9.56E-06	0.00E+00
Tc-99	Ci/L	7.50E-05	1.70E-04	2.84E-07	2.01E-07	1.44E-04	0.00E+00
Ru-106	Ci/L	9.29E-18	1.26E-16	9.55E-21	1.75E-18	1.00E-16	0.00E+00
Cd-113m	Ci/L	4.95E-06	1.47E-05	8.24E-07	7.94E-07	1.10E-05	0.00E+00
Sb-125	Ci/L	1.57E-08	7.38E-08	3.85E-11	1.78E-10	5.60E-08	0.00E+00
Sn-126	Ci/L	9.89E-07	2.26E-06	2.68E-09	2.00E-09	1.87E-06	0.00E+00
I-129	Ci/L	4.47E-09	1.02E-08	2.80E-07	1.75E-07	8.48E-08	0.00E+00
Cs-134	Ci/L	1.20E-10	1.71E-09	2.09E-13	2.31E-12	2.07E-11	0.00E+00
Cs-137	Ci/L	1.83E-01	4.69E-01	4.87E-04	4.08E-04	9.68E-03	1.93E-06
Ba-137m	Ci/L	1.63E-01	4.18E-01	4.35E-04	3.63E-04	8.63E-03	1.72E-06
Sm-151	Ci/L	6.35E-03	3.82E-03	2.38E-05	1.72E-05	5.10E-03	0.00E+00
Eu-152	Ci/L	4.15E-07	3.85E-07	1.42E-09	1.95E-09	4.15E-07	0.00E+00
Eu-154	Ci/L	1.76E-05	1.76E-05	5.90E-08	8.52E-08	1.76E-05	0.00E+00
Eu-155	Ci/L	2.33E-06	2.82E-06	7.44E-09	1.36E-08	2.36E-06	0.00E+00
Ra-226	Ci/L	9.35E-12	2.38E-11	8.51E-13	2.29E-12	2.08E-11	6.01E-15
Ac-227	Ci/L	2.29E-11	6.05E-11	2.28E-12	1.97E-10	6.79E-11	1.53E-14
Ra-228	Ci/L	5.90E-18	1.99E-17	9.33E-19	1.81E-09	9.93E-11	5.04E-21
Th-229	Ci/L	1.57E-13	1.45E-13	1.44E-15	4.88E-11	5.41E-12	3.66E-17
Pa-231	Ci/L	5.98E-11	1.69E-10	9.19E-12	1.81E-09	3.36E-10	4.28E-14
Th-232	Ci/L	5.98E-17	2.04E-16	1.14E-17	2.23E-10	1.51E-11	5.15E-20
U-232	Ci/L	5.72E-13	6.84E-13	3.92E-13	1.15E-09	2.16E-10	8.23E-15

Table 2-2. Average Composition of Hanford Defined Model Chemical and Radiological Constituents for Selected Waste Types. (3 sheets)

Constituent	Units	P1*	P2*	CWP1*	CWP2*	CSR*	Sr-Cs Rec (P2) Stack Drain**
U-233	Ci/L	4.86E-12	1.50E-12	2.24E-14	8.30E-08	1.61E-08	1.80E-14
U-234	Ci/L	1.01E-08	1.06E-08	1.01E-08	1.15E-08	1.10E-08	1.27E-10
U-235	Ci/L	4.32E-10	4.42E-10	4.30E-10	4.48E-10	4.61E-10	5.33E-12
U-236	Ci/L	2.23E-10	2.72E-10	2.30E-10	2.83E-10	2.99E-10	3.27E-12
Np-237	Ci/L	4.10E-07	4.57E-07	1.91E-09	1.34E-09	4.69E-07	2.38E-10
Pu-238	Ci/L	1.08E-07	2.08E-07	7.72E-08	1.05E-07	1.86E-07	1.92E-09
U-238	Ci/L	1.03E-08	1.03E-08	1.03E-08	1.03E-08	1.03E-08	1.24E-10
Pu-239	Ci/L	5.09E-06	5.03E-06	5.08E-06	5.05E-06	5.05E-06	4.63E-08
Pu-240	Ci/L	1.02E-06	1.23E-06	1.06E-06	1.19E-06	1.17E-06	1.13E-08
Am-241	Ci/L	6.53E-06	6.53E-06	6.38E-06	5.40E-06	6.53E-06	0.00E+00
Pu-241	Ci/L	1.80E-06	4.40E-06	1.84E-06	3.45E-06	3.91E-06	4.05E-08
Cm-242	Ci/L	3.37E-08	1.24E-08	1.13E-10	2.11E-10	2.30E-08	0.00E+00
Pu-242	Ci/L	3.20E-11	8.93E-11	3.30E-11	6.05E-11	8.02E-11	8.26E-13
Am-243	Ci/L	3.09E-09	3.58E-09	7.31E-11	1.48E-10	3.79E-09	0.00E+00
Cm-243	Ci/L	4.61E-10	5.21E-10	1.48E-12	7.70E-12	4.90E-10	0.00E+00
Cm-244	Ci/L	9.27E-09	9.28E-09	2.93E-11	1.81E-10	9.28E-09	0.00E+00

* Average estimates for these waste types from RPP-19822, "Hanford Defined Waste Model – Rev. 5."
** Average estimate for this waste type taken from RPP-26744, "Hanford Soil Inventory Model, Rev. 1."

P1 = Plutonium Uranium Extraction (PUREX) high-level waste (1956-1962)
P2 = PUREX high-level waste (1963-1967)
CWP1 = PUREX aluminum cladding waste (1956-1960)
CWP2 = PUREX aluminum cladding waste (1961-1972)

Source: Appendix A of RPP-RPT-42294, "Hanford Waste Management Area C Soil Contamination Inventory Estimates," Rev. 2.

2.1.2 Tank 241-C-104

Tank C-104 appears to be "sound" as previously classified. However, drywells show ^{137}Cs near the tank and ^{60}Co plumes that appear to extend from the tank cascade line and migrate outward and downward. The observed gamma activity in drywells is attributed primarily to cascade line releases from tank C-104 and may also be attributed to spare inlet overflows from tanks C-104 and C-105 and V103 pipeline leaks.

Table 2-3. Inventory Estimates for Releases at Waste Management Area C.

Waste Release	Waste Volume (gal)*	^{60}Co (Ci)	^{99}Tc (Ci)	^{129}I (Ci)	^{137}Cs (Ci)	$Fe(CN)_6$ (kg)	NO_3 (kg)	SO_4 (kg)	Total U (kg)
241-C-101	37,000	0.14	0.25	0.04	580	0	5,900	1.3	4.3
241-C-104	28,000	0.11	0.03	0.03	52	0	4,500	90	3.3
241-C-105	2,000 to 20,500	0.01 to 0.1	1 to 9.8	5.9E-4	2,700 to 27,000	0	3 to 430	690	0.18 to 1.8
241-C-108	18,000	0.07	0.02	0.02	33	0	2,900	58	2.1
241-C-110	2,000	0.05	3.4	0.003	230	0	1,800	210	0.73
241-C-112	7,000	0.03	0.0075	0.007	13	0	1,100	23	0.82
UPR-81	36,000	0.9	0.11	0.1	220	0	23,000	350	17
UPR-82	2,600	0.01	1.3	7.5E-5	3,500	0	55	88	0.2
UPR-86	17,000	0.03	2.7	1.6E-4	7,400	0	120	190	0.5
216-C-8 French Drain	>32,000	0.0	0.0	0.0	0.3	0	0.15	0.14	6.0E-05
Surface Releases	1,000	0.004	0.001	0.001	1.9	0	160	3.2	0.12
Total	201,000	1.5	18	0.2	39,000	0	40,000	1,800	31

Note: Values are rounded to two significant digits.
Radionuclide values are decayed to January 1, 2020.
No $Fe(CN)_6$ was identified in the supernate for Hanford Defined Waste waste types.

References:
RPP-ENV-33418, "Hanford C-Farm Leak Inventory Assessments Report."
RPP-19822, "Hanford Defined Waste Model – Revision 5.0."

* Conversion 1 gallon = 3.78541 liters

Tank C-104 was filled to ~2,120,000 L (560,000 gal) of CWP1 waste in 1965. No transfer was identified; however, the surface level decreased to the spare inlet elevation of ~2,014,000 L (~532,000 gal) resulting in a possible ~106,000-L (28,000-gal) release of CWP1 waste.

Waste retrieval operations for tank C-104 using a modified sluicing and chemical dissolution process began in January 2010 and were completed on August 17, 2012. Although large volumes of water and supernate were used for retrieval operations, there was no indication of a tank leak during retrieval from any of the monitoring systems used.

2.1.3 Tank 241-C-105

Tank C-105 was classified as a "sound" tank for many years. However, a high-activity ^{137}Cs plume (greater than ~10^7 pCi/g) was observed in drywell 30-05-07 near the base of the tank when it was drilled in 1974. The drywell activity was previously attributed to a cascade line release. After further field investigations and review in 2010 it was concluded that the activity around SST C-105 is from several different sources. Probable sources of waste releases to the soil include: releases from the cascade line between tanks C-104 and C-105, a leak near the base of tank C-105, releases from spare inlet nozzles, condenser leaks and leaks from Pipeline V103 (RPP-ASMT-46452, "Tank 241-C-105 Leak Assessment Completion Report"). Based on direct push logging results obtained for the assessment, the integrity assessment panel concluded that the inlet cascade line to tank C-105 leaked and tank C-105 may have leaked, and the panel recommended that the tank classification be changed to "assumed leaker."

Waste retrieval operations using a mobile arm retrieval vacuum extraction system began in June 2014 and are ongoing. To date there has been no indication of a tank leak during retrieval.

The estimated tank leak/release volume ranged from ~7,570 to 77,600 L (2,000 to 20,500 gal) of P2 supernate (PSN) based on the estimated size of the ^{137}Cs plume and a 1969 ^{137}Cs sample concentration of 4.3 Ci/gal. The upper volume estimate, provided by the Nez Perce, assumes more extensive ^{137}Cs migration under the tank. The leak volumes would be proportionally lower if the waste concentration was higher, as measured in 1963 (RPP-ENV-33418, Appendix B2.0).

2.1.4 Tank 241-C-108

Tank C-108 has previously been designated as "sound." However, drywells show ^{137}Cs near the tank at 6.7 m (22 ft) below ground surface (bgs) and ^{60}Co plumes that appear to extend from the tank bottom and migrate out and downward. Because some cascade lines are known to have released waste during times when the tanks were overfilled, and because gamma activity was observed starting just at the depth of the cascade line and adjacent to it, it was assumed that the cascade line may be the source of the observed activity at ~6.7 (~22 ft). However, drywell logging indicates continued migration of ^{60}Co in the soil over the past 40 years which appears to be from another source.

Based on geophysical logging measurements, an estimated ~68,140 L (18,000 gal) of waste may have been released. Assuming the waste was Plutonium Uranium Extraction facility (PUREX) cladding, aluminum clad fuel (1956-1960) (CWP1) waste (the type of supernate in the tank in 1965), this equates to an estimated 50 Ci of ^{137}Cs and ~0.9 Ci of ^{60}Co that may have been

released. Continued movement of the contaminant plume beneath the tank indicates that there may have been other waste releases and additional solutions (water) released.

In March 2012, tank C-108 waste retrieval was completed. During retrieval, drywell moisture monitoring and HRR monitoring are performed for leak detection. Although large volumes of supernate and other liquids were introduced to the tank during retrieval operations and liquid was recirculated in the tank to remove the remaining hard heel, no evidence of a leak during retrieval was detected by the drywell monitoring or the HRR leak detection systems; this supports the previous evaluations that the tank appears to be sound.

2.1.5 Tank 241-C-110

Tank C-110 was declared as "questionable integrity" in 1977 following the discovery of unexplained gamma activity in drywell 30-10-09. In 1984 it was declared an "assumed leaker" with an estimated leak volume of ~7,570 L (2,000 gal).

In 2008 an integrity assessment was conducted for tank C-110 (RPP-ASMT-38219, "Tank 241-C-110 Leak Assessment Report"). The assessment concluded that tank C-110 spare inlets were the apparent source for the waste release based on the tank's stable liquid level surface bracketing the period when the drywell gross gamma peak was discovered, the natural decay of the drywell gross gamma peak following discovery, and an interior tank photo showing evidence of waste in and above the tank inlet line penetrations.

There was no liquid level decrease observed and less than 1,000 pCi/g ^{137}Cs activity in drywell 30-10-09 when it was first logged in 1975. The estimated ^{137}Cs inventory is based on 1975 sample results (0.32 Ci/gal). Because a liquid level decrease was not observed, a maximum spare spare inlet release of ~7,570 L (2,000 gal) was assumed. The waste type released is assumed to be CSR supernate, the waste type in the tank in 1975.

Tank C-110 was retrieved using modified sluicing and an in-tank vehicle for mechanical and high-pressure water cleaning. Although large volumes of water and supernate were added to the tank during retrieval operations, there was no indication of a leak during retrieval from the HRR leak detection monitoring system or other monitoring systems used.

2.1.6 Tank 241-C-111

Tank 241-C-111 was designated as an "assumed leaker" in 1968, with a leak volume estimate of ~20,820 L (5,500 gal) based on a liquid level decrease. A tank integrity assessment conducted in 2008 concluded that tank C-111 likely did not leak and recommended that the tank C-111 leak integrity status be revised from "Assumed Leaker" to "Sound" (RPP-ASMT-39155, "Tank 241-C-111 Leak Assessment Report"). The report concluded that the most probable explanation for the 1965 to 1969 surface level decrease in tank C-111 was evaporation of the thermally hot waste.

Tank C-111 was sluiced in 2010 using modified sluicing. Although large volumes of water and supernate were added to the tank during sluicing operations, there was no indication of a leak

during retrieval from the HRR leak detection monitoring system or other monitoring systems used. Consequently, no soil inventory was developed for tank C-111.

2.1.7 Tank 241-C-112

Tank C-112 started receiving waste in November 1946. Tank C-112 was suspected of leaking and liquid was pumped to tank C-103 in 1975 and 1976. Later surveillance could not confirm the suspected leak, and the tank is currently considered "sound." A ^{60}Co peak was detected near tank C-112 in drywells 30-12-01 and 30-12-13. The drywells are near a known release from the tank C-112 saltwell pump pit and a transfer line leak from 252-C Diversion Box to tank C-112. Based on drywell data, an estimated ~26,500 L (7,000 gal) of CWP1-B Plant ion exchange (IX) waste was released.

Waste retrieval operations for tank C-112 using modified sluicing began December 28, 2011 and were completed on January 31, 2014. Although large volumes of water and supernate were used for retrieval operations, there was no indication of a tank leak during retrieval from any of the monitoring systems used.

2.1.8 UPR-200-E-81

RHO-CD-673, "Handbook 200 Areas Waste Sites" identifies UPR 200-E-81 (UN-216-E-9) as a ~136,275-L (36,000-gal) line leak from the PUREX Plant to tank C-102 near the 241-CR-151 diversion box (see Figure 1-6). The source was determined to be a leak in an underground transfer line from the 202-A Building to the C-102 waste storage tank via the 151-CR box. The PUREX Plant merged low-level waste flows into the remaining line available which carried organic wash and special run coating waste.

Based on RHO-CD-673, an estimated ~136,275 L (36,000 gal) and 720 Ci of ^{137}Cs was released in 1969 (220 Ci decayed to 2020). Direct push holes were drilled, logged and sampled in the vicinity of the UPR in 2008 and 2009. The direct push results appear to be consistent with the estimated ~136,275-L (36,000-gal) line leak and a CWP2 release.

2.1.9 UPR-200-E-82

A leak in cesium line V122 from tank C-105 to B Plant was discovered in December 1969, 10.7 m (~35 ft) south of the 152-C diversion box (see Figure 1-6). The pipeline leak was characterized shortly after the leak event in which waste from the pipe migrated to the surface and the site was covered with 0.6 m (2 ft) of back fill (ARH-1945, "B Plant Ion Exchange Feed Line Leak"). A Gunite cap was installed over the release site, but not for 20 years after the leak.

Based on the ARH-1945 volume estimate of ~9,840 L (2,600 gal) and a 1969 sample concentration of 4.3 Ci/gal of ^{137}Cs, an estimated 11,000 Ci of ^{137}Cs was released in 1969 (3,500 Ci decayed to 2020). Vertical direct push holes were drilled, logged and sampled in the vicinity of the UPR in 2008 and 2009. Three slant holes were also drilled under the site of the pipeline leak. The direct push results appear to be consistent with a~9,840-L (2,600-gal) PSN line leak. Higher gamma activity was expected, but the high activity may be directly under the Gunite cap and direct push holes may have been too deep to detect it.

2.1.10 UPR-200-E-86

UPR-200-E-86 (also UN-216-E-14) is identified as leakage from the 244-AR vault to the 151-C diversion box portion of the PUREX sludge supernate (PSS) line to tank C-106 (pipeline V108/812), discovered on February 25, 1971 (RHO-CD-673). The line is a 5.1 cm (2-in.) direct buried line, 2.4 m (~8 ft) below grade. The leak appeared to have occurred at a carbon steel-stainless steel weld and was estimated to have a line loss of ~65,810 L (17,385 gal) of PSS waste containing 1.35 Ci/gal of ^{137}Cs (decay date of February 1971) (RHO-CD-673).

Based on a volume estimate of 64,350 L (17,000 gal) of PSN and a 1971 sample concentration of 1.35 Ci/gal of ^{137}Cs, an estimated 23,000 Ci of ^{137}Cs may have been released (7,400 Ci decayed to 2020).

A number of vertical direct push holes were drilled, logged and sampled in the vicinity of the UPR in 2008 and 2009. Logging and sampling of the holes showed low levels of activity around the area of the suspected release, inconsistent with a release volume of ~64,350 L (17,000 gal) of PSN waste. Although there was no evidence of a large PSN leak based on the direct push data, the volume and inventory of ~64,350 L (17,000 gal) of PSN and 7,400 Ci of ^{137}Cs was determined to provide a bounding estimate for the line leak.

2.1.11 216-C-8 French Drain

The 216-C-8 French Drain is located ~22.9 m (~75 ft) southeast of the C Farm southeast perimeter fence and 250 ft east-northeast of the 244-CR vault (see Figure 1-6). The site is composed of a 1.8-m (6-ft)-diameter by 2.4-m (8-ft) -long concrete culvert, placed vertically 1.2 m (4 ft) below grade. The culvert is filled with gravel. It was placed into an 2.4-m (8-ft)-diameter by 4.8-m (16-ft)-deep excavation. A 5.1-cm (2-in.)-diameter steel vent pipe was placed vertically through the center of the culvert and extended 0.9 (3 ft) above the surface. The above-grade portion of the pipe has been removed.

Although process records are incomplete, a minimum of ~121,135 L (~32,000 gal) of treated 241-A Tank Farm Process Condensate ion exchange waste was discharged to the 216-C-8 French Drain from January 1960 through March 1965 (Interoffice memo 7G420-MEJ-06-007, "Waste Discharged to the 216-C-8 Crib" [Appendix C]). Waste sample analyses in 1961 showed a ^{137}Cs concentration of 2.57 µCi/L. The assumed waste type was Strontium - Cesium Recovery Stack drain waste from the B-Plant Process, designated in RPP-26744, "Hanford Soil Inventory Model, Rev. 1" as Sr-Cs Rec (P2) Stack Drain waste.

2.1.12 Surface Level Releases

Cross-section visualizations of near-surface gamma activity in C Farm from spectral gamma logging system drywell logging data show < 10 pCi/g of ^{137}Cs activity at 0.6 m (2 ft) bgs across the farm (Figure 2-2). In general the highest gamma activity levels were observed near tanks or where an inventory has been determined. This suggests that other, undocumented surface releases may have been smaller; contaminants have been flushed; or the waste lost contained lower levels of non-mobile gamma activity (i.e., ^{137}Cs).

Figure 2-2. Near Surface Spectral Gamma Activity in 241-C Tank Farm.

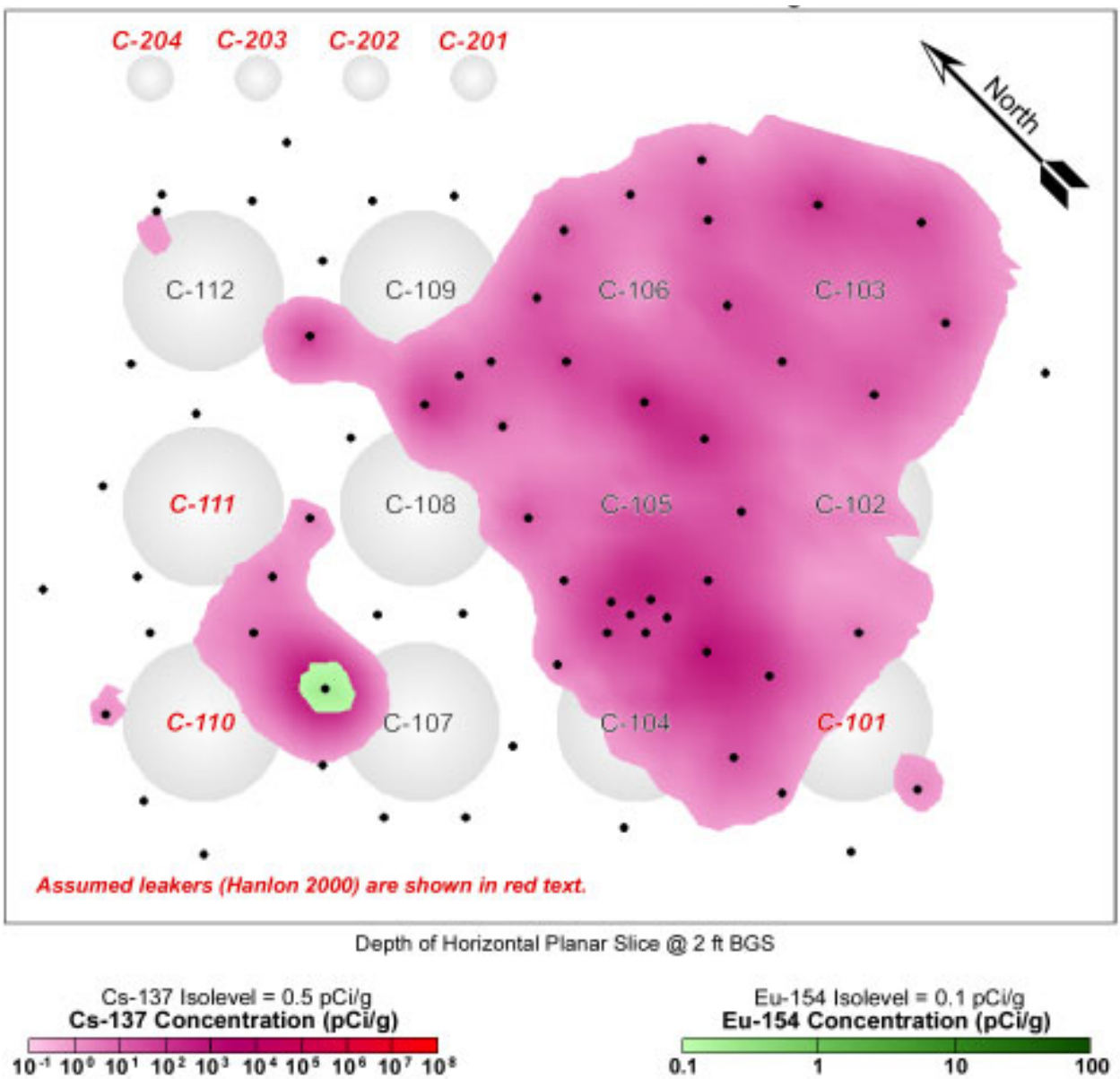

Reference: GJO-98-39-TARA/GJO-HAN-18, "Vadose Zone Characterization Project at the Hanford Tank Farms, Addendum to the C Tank Farm Report."

A ^{137}Cs activity level of 10 pCi/g in the top 3.0 m (10 ft) of soil within the perimeter of the C Farm fence (an area of ~55,740 m^2 (~600,000 ft^2)) would result in a ^{137}Cs inventory of ~2 Ci (decayed to 2020). The associated volume of waste released based on this inventory and HDW, Rev. 5 waste type composition estimates ranges from ~38 L (~10 gal) for P1 waste to ~3,785 L (~1,000 gal) for CWP1 waste. For purposes of inventory estimates it is assumed that the waste released was predominantly CWP1.

2.2 HYDROLOGIC SETTING OF HANFORD'S CENTRAL PLATEAU

This section provides a brief description of the vadose zone and unconfined aquifer in the Hanford's Central Plateau (Figure 1-3). WMA C is located within the 200-BP-Groundwater Operable Unit (OU) inside the eastern boundary of the 200 East Area (Figure 2-3). For a more complete description of the site characteristics of the Central Plateau, see Section 3.0 of RPP-ENV-58782, or RPP-ENV-58806, or DOE/RL-2009-127 Draft A.

2.2.1 Geologic Setting and Stratigraphic Units

The vadose zone and unconfined aquifer in the vicinity of WMA C are contained within the suprabasalt sediments (Figure 2-4 and 2-5). The Ringold Formation comprises the oldest suprabasalt sediments, composed of fluvially-deposited, gravel-dominated sediments designated as units A, B/D, C, and E. These high-energy deposits may be intercalated with fine-grained lake-bed (lacustrine) or overbank deposits designated as the Ringold lower mud (RLM) unit and the upper Ringold unit (Rtf). Within the WMA C near-field area, four sedimentary units are present (from oldest to youngest): fluvial gravel unit A (Rwia), RLM, fluvial gravel unit E (Rwie), and Rtf. These geologic units are designated as hydrostratigraphic units (HSUs) 9, 8, 5, and 4, respectively. Detailed lithologic descriptions of these units are provided in PNNL-12261, "Revised Hydrogeology for the Suprabasalt Aquifer System, 200-East Area and Vicinity, Hanford Site, Washington" and PNNL-19702, "Hydrogeologic Model for the Gable Gap Area, Hanford Site."

Rwia (HSU 9) is the oldest Ringold Formation unit and directly overlies the Elephant Mountain Basalt. The Rwia displays a relatively flat surface that dips toward the axis of the Cold Creek syncline (southerly). The Rwia is not present in the northern portion of the near-field area where the basalt surface has been structurally uplifted. This uplift created depositional thinning or exposed the older sediment to paleoflood removal (erosion) across this area (Figure 2-6). The Rwia ranges in thickness from over 30 m (100 ft) of the structure east and south of the 200 East Area to zero where it truncates within the near-field area. The position of the truncation boundary is approximate and is identified as the erosional limit of the post-Ringold fluvial incision from Pleistocene-age cataclysmic flooding that traversed the uplifted area. For the near-field area, Figure 2-6 depicts the stratigraphy and general structural and erosional relationships of the Ringold Formation and overlying Hanford formation sediment.

The Hanford formation (HSU 1) is the youngest geologic sequence within the 200-BP-5 OU. This unit consists of glaciofluvial sediment deposited during cataclysmic Ice Age flooding. HSU 1 is subdivided into three main facies (silt-, sand-, and gravel-dominated) that vary vertically and laterally across the region and are difficult to correlate from area to area. In the southern portion of the near-field area (southern 200 East Area), the Hanford formation sediments unconformably overly the older Ringold Formation units (Rwie, RLM, and Rwia) and may only comprise the very uppermost portion of the unconfined aquifer. In the other portions of the 200-BP-5 OU near-field area, the Hanford formation sediments were mainly deposited unconformably on top of basalt and form part or all of the sediment in the unconfined suprabasalt aquifer. The vadose zone in the 200-BP-5 OU near-field area is primarily composed of the Hanford formation. The thickness of the Hanford formation ranges from 0 m to more than 109 m (0 to 357 ft).

Clastic dikes are not known to exist in great numbers within the Hanford formation sediments of the 200-BP-5 OU but have been mapped extensively at the Hanford Site south of the 200-BP-5 OU (PNNL-14224, "Influence of Clastic Dikes on Vertical Migration of Contaminants in the Vadose Zone at Hanford"). Clastic dikes normally occur as cross-cutting, vertically oriented cracks or fissures in the formation that are typically filled with sand, silt, clay, and minor coarser debris. Their origin is not well understood but is likely associated with hydraulic ejection during or immediately following Pleistocene cataclysmic flooding, mass wasting, earthquakes, and other geologic processes. Clastic dikes occurring in vadose zone sediments have the potential to influence the movement of soil moisture and contaminants (BHI-01103, "Clastic Injection Dikes of the Pasco Basin and Vicinity – Geologic Atlas Series"), but no data exist about the potential influence of clastic dikes within the aquifer.

Holocene surficial deposits in the 200 East Area are dominated by very fine-grained to medium-grained, and occasionally silty, eolian sheet sands. These deposits have been removed or reworked over much of the area by past construction activities.

2.2.2 Unconfined Aquifer System

The base of the uppermost aquifer system is defined as the top of the uppermost basalt flow, with the top of the system being the water table. This aquifer system is bounded laterally by anticlinal basalt ridges and is ~152 m (500 ft) thick near the center of the Pasco Basin. Within the Hanford Site, this uppermost aquifer system lies at depths ranging from less than 0.3 m (1 ft) below the ground surface near West Lake and the Columbia and Yakima Rivers (Figure 2-7), to more than 107 m (350 ft) in the central portion of the Cold Creek syncline. Groundwater in the unconfined aquifer at the Hanford Site generally flows from recharge areas in the elevated region near the western boundary of the Hanford Site toward the Columbia River on the eastern and northern boundaries. The Columbia River is the primary discharge area for the unconfined aquifer. The Yakima River borders the Hanford Site on the southwest and is generally regarded as a source of recharge.

The unconfined aquifer system underlying the Hanford Site exists within sediments deposited on top of the Columbia River Basalts. It is composed primarily of the Ringold Formation and overlying Hanford formation. Figure 2-7 is a hydrogeologic map of the units present at the water table surface in 2009. In the 200 West Area, the water table occurs almost entirely in the Ringold Unit E gravels (Rwie, which corresponds to HSU 5), while in the 200 East Area, it occurs primarily in the Hanford formation and in the Ringold Unit A gravels (Rwia, which corresponds to HSU 9). Along the southern edge of the 200 East Area, the water table is in the Ringold Unit E gravels. The upper Ringold facies were eroded in most of the 200 East Area by the ancestral Columbia River and, in some places, by the Missoula floods that subsequently deposited Hanford gravels and sands on what was left of the Ringold Formation (DOE/RL-2002-39, Standardized Stratigraphic Nomenclature for Post-Ringold-Formation Sediments Within the Central Pasco Basin). Because the Hanford formation and possibly the Cold Creek unit (CCu) sand and gravel deposits are much more permeable than the Ringold gravels, the water table is relatively flat in the 200 East Area, but groundwater flow velocities are higher. Directly underneath WMA C, the unconfined aquifer occurs in the undifferentiated Hanford Gravels, CCu, and Ringold Formation (Figure 2-6).

Figure 2-3. Surface Topography and Boundaries of the 200-BP-5 Groundwater Operable Unit.

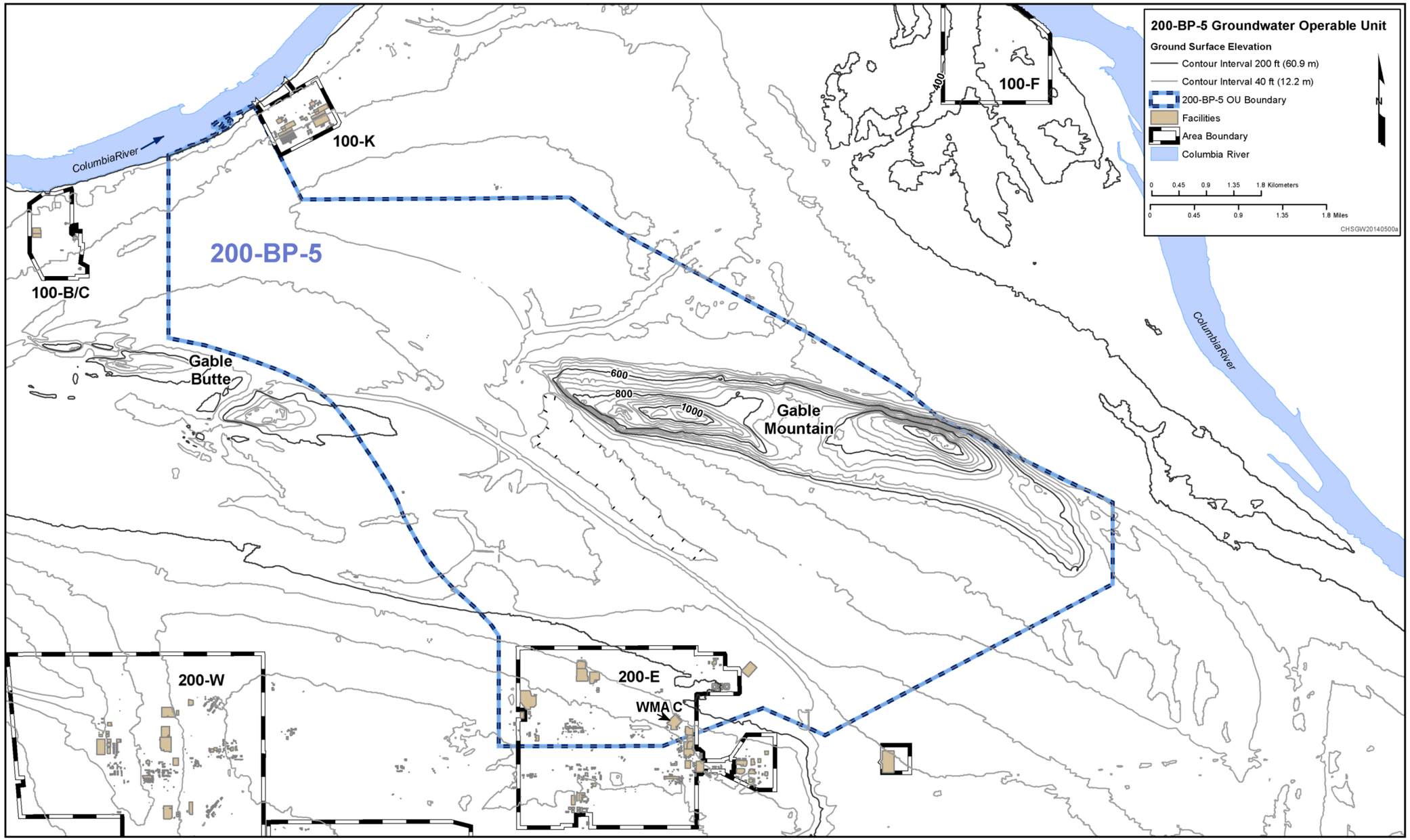

WMA = Waste Management Area

Figure 2-4. Comparison of 200-BP-5 Operable Unit Hydrostratigraphy to Hanford Site Stratigraphy.

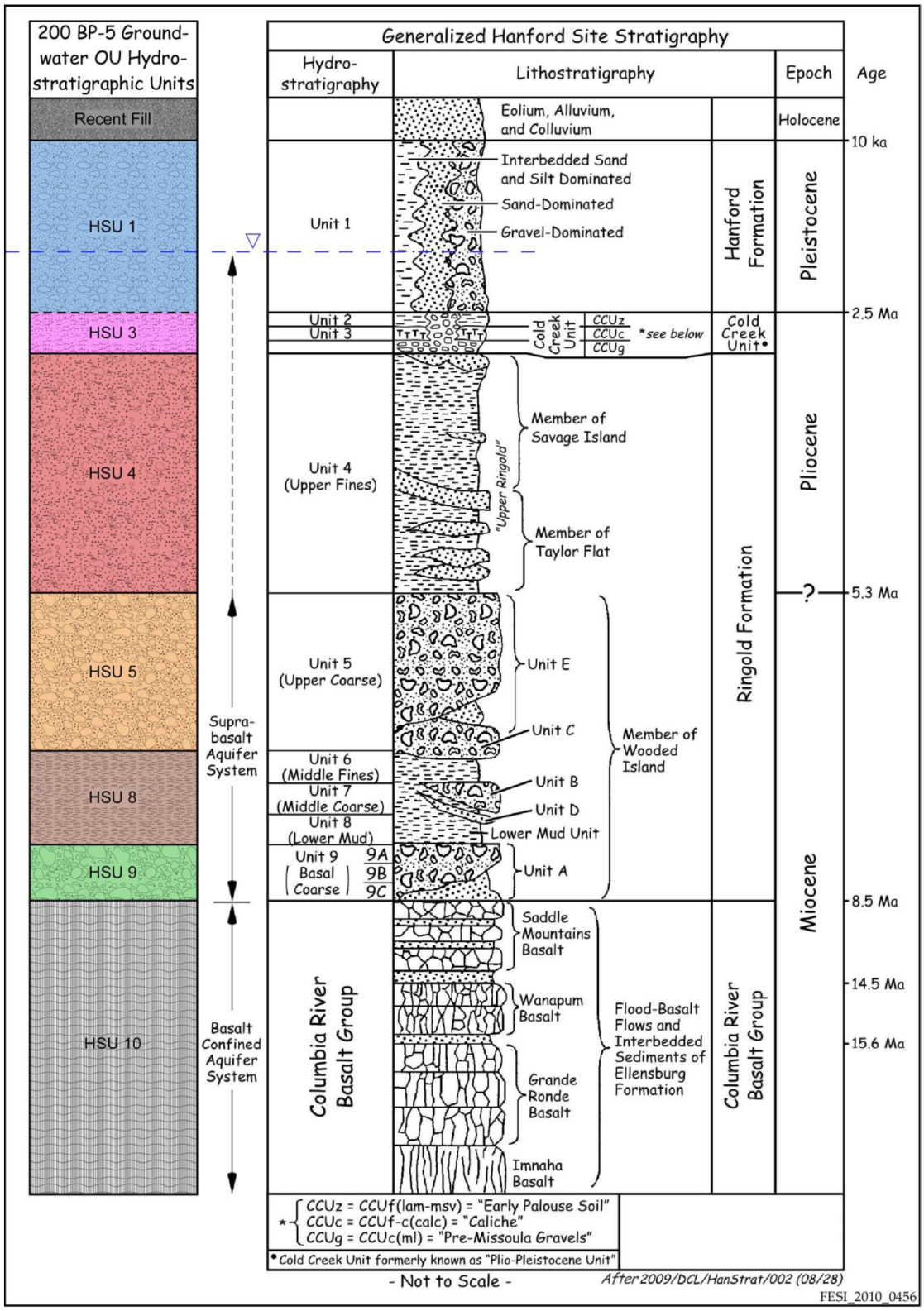

HSU = hydrostratigraphic unit OU = operable unit

Figure 2-5. Representative Photos of the Hanford Formation, Cold Creek Unit, Ringold Unit E, Ringold Lower Mud Unit, and Basalt.

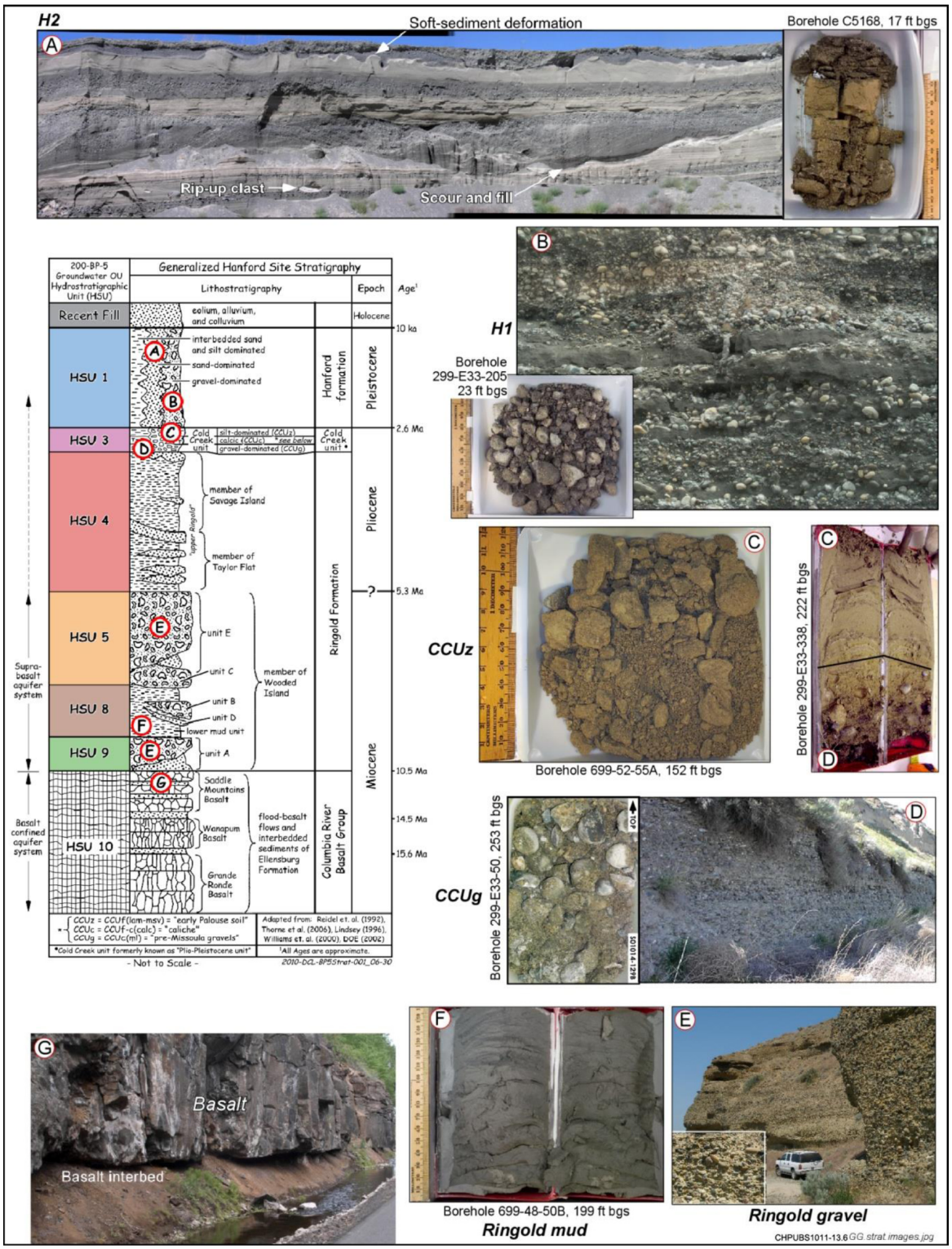

HSU = hydrostratigraphic unit OU = operable unit

Reference: PNNL-19702, "Hydrogeologic Model for the Gable Gap Area, Hanford Site."

Figure 2-6. 200-BP-5 Operable Unit Near-Field Area Hydrogeology Depicting Truncation of Ringold Units on Uplifted Basalt.

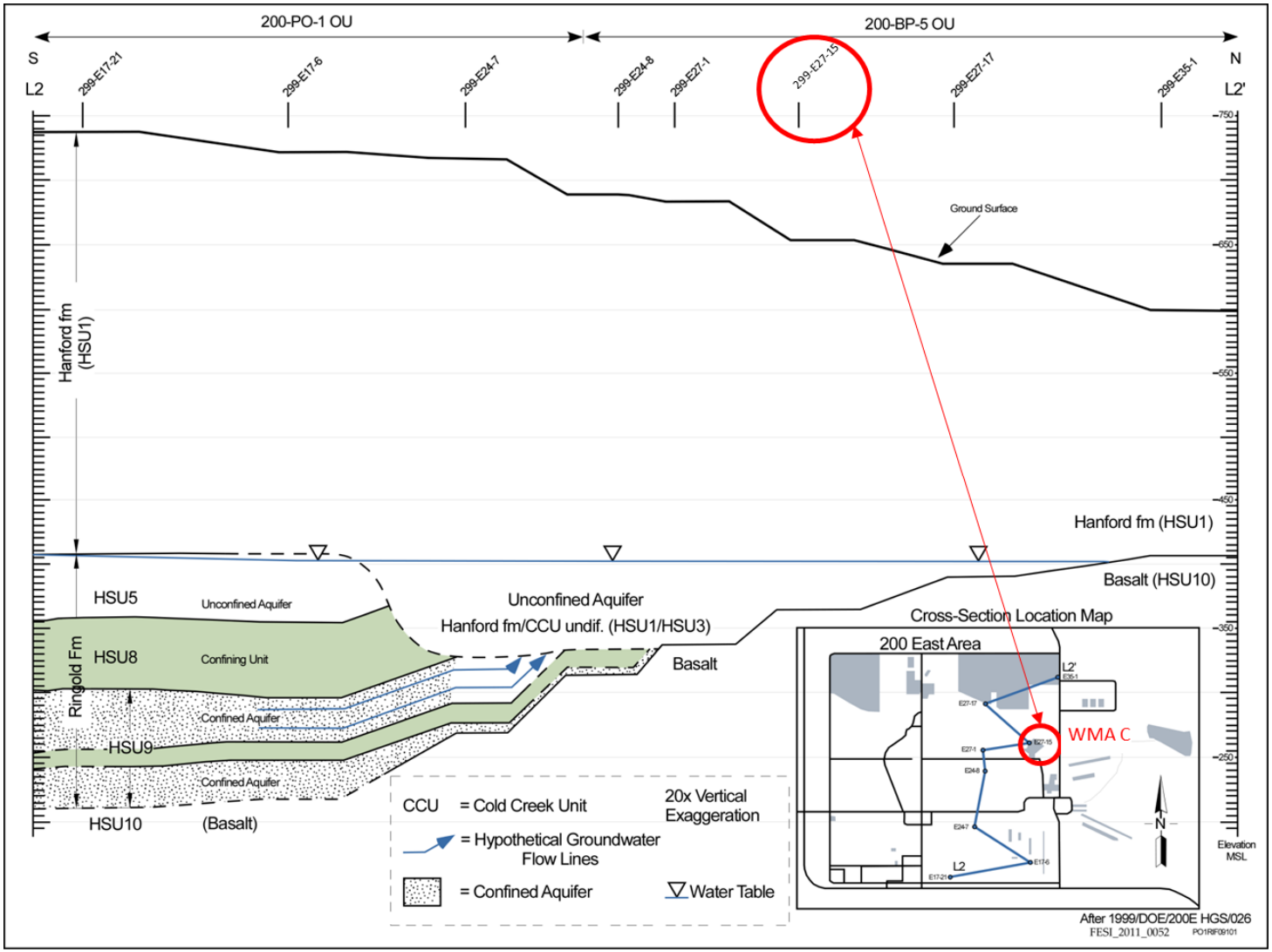

HSU = hydrostratigraphic unit OU = operable unit

Reference: PNNL-12261, "Revised Hydrogeology for the Suprabasalt Aquifer System, 200-East Area and Vicinity, Hanford Site, Washington."

Figure 2-7. Distribution of Hydrogeologic Units at the Water Table, 2009.

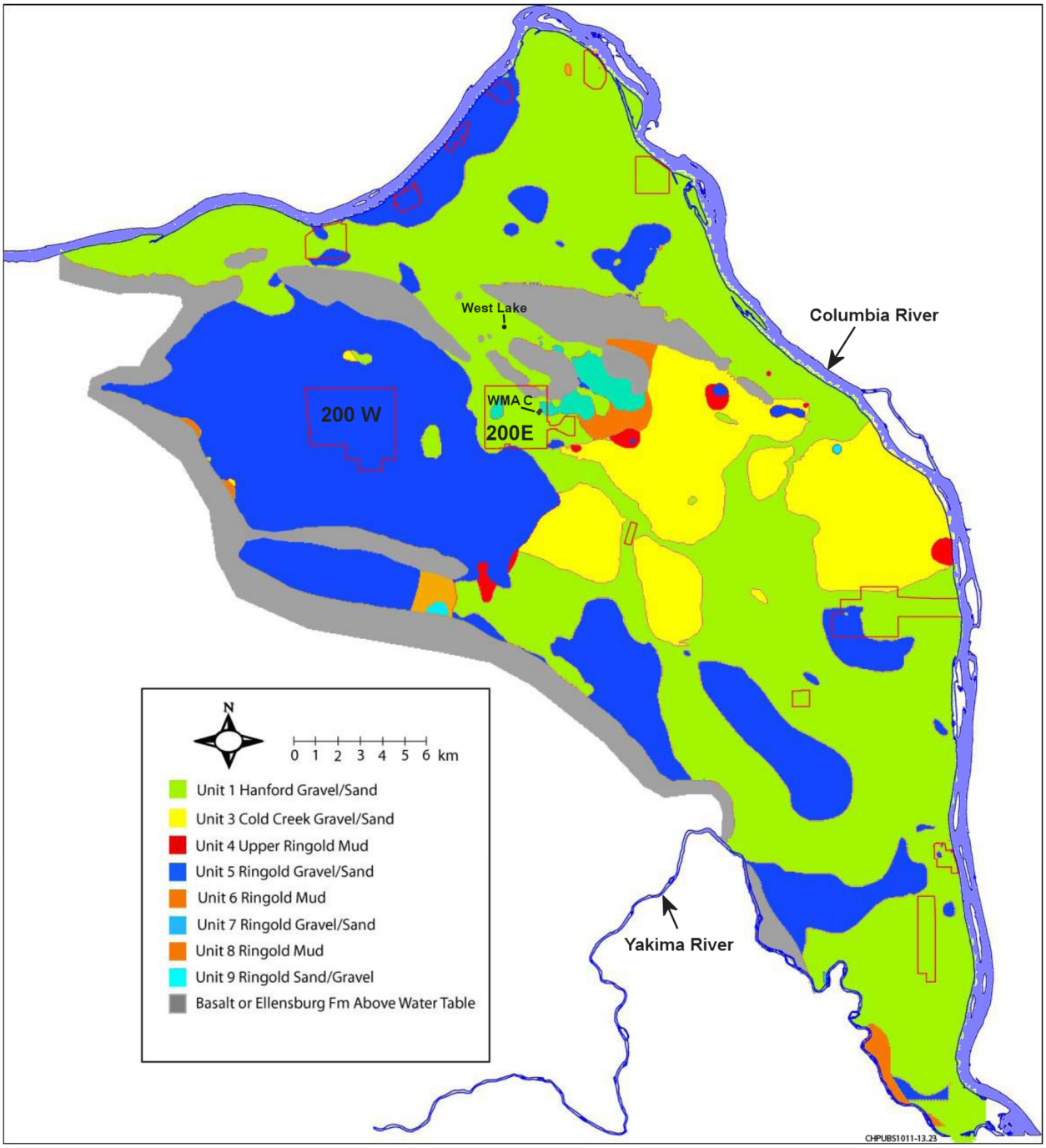

WMA = Waste Management Area

The hydrology of the 200 Areas has been strongly influenced by the discharge of large quantities of wastewater to the ground. Between 1944 and the mid-1990s, an estimated 1.68×10^{12} L (4.44×10^{11} gal) of liquid was discharged to disposal ponds, trenches, and cribs. Wastewater discharge has decreased since 1984 and currently only contributes a volume of recharge in the same range as the estimated natural recharge from precipitation. The largest volumes of discharge around the 200 East Area were to the 216-B Pond system, the 216-A-25 (Gable

Mountain) pond system, and several of the PUREX cribs in the southeast corner of 200 East Area. Figure 2-8 shows the liquid discharge history for the two ponds. The Gable Mountain Pond is estimated to have received ~293 billion L of effluent, while the 216-B Pond to have received ~256 billion L of effluent. In the 200 West Area, the largest volumes of discharge were to the 216-T Pond system and the 216-U-10 Pond (Figure 2-9). The 216-T Pond system is estimated to have received ~424 billion L of effluent (WHC-EP-0815, "Groundwater Impact Assessment Report for the 216-T-4-2 Ditch"), while the 216-U Pond to have received ~158 billion L of effluent (WHC-EP-0707, "216-U-10 Pond and 216-Z-19 Ditch Characterization Studies").

Figure 2-8. Discharge History for the 216-B Pond System and Gable Mountain Pond.

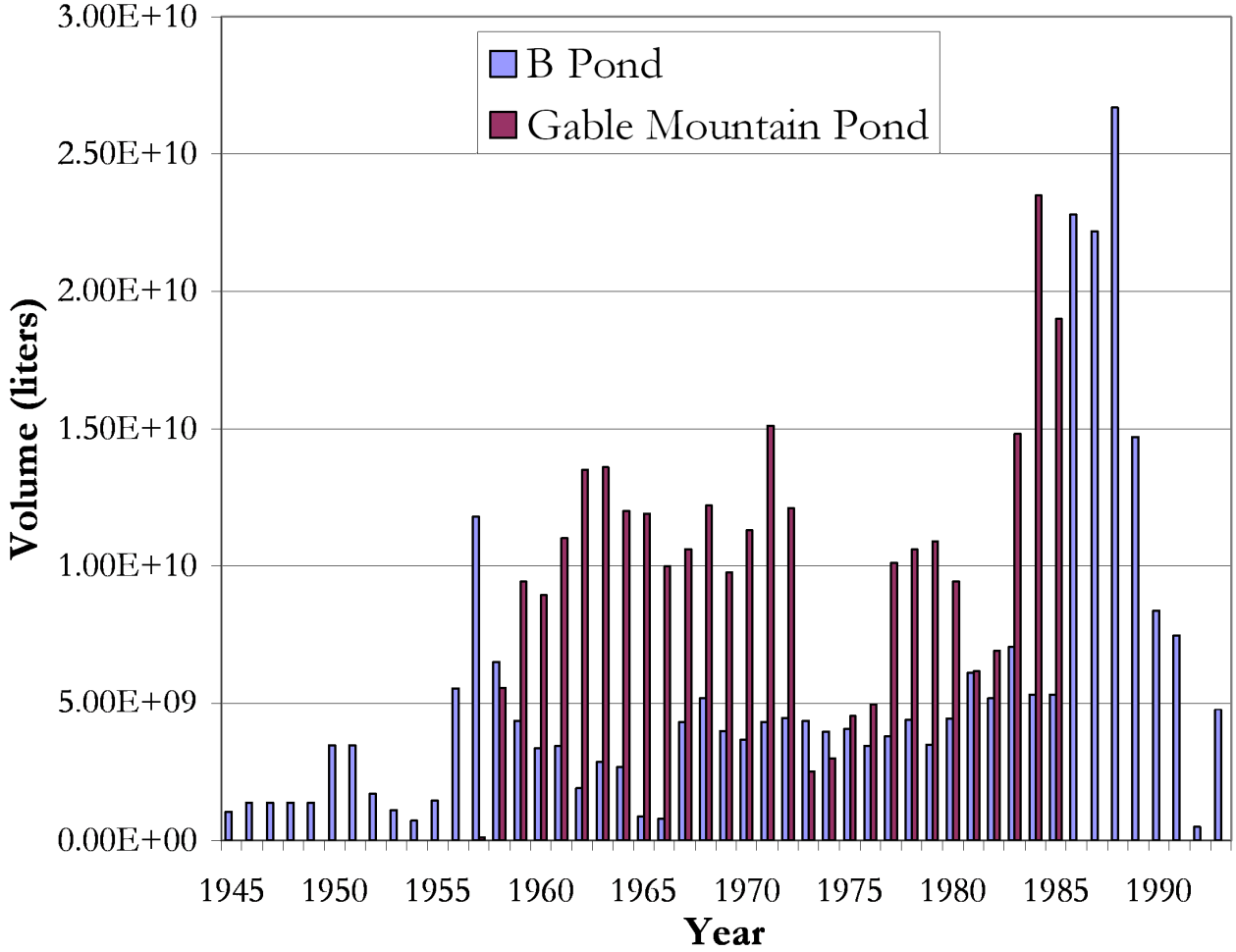

Figure 2-10 shows a series of water table elevation maps for the time periods representing pre-operational conditions, operational conditions, and present day conditions for the Hanford Site. The first water table map (Figure 2-10a) is a hind cast map of water table elevations (ERDA-1538, "Final Environmental Impact Statement, Waste Management Operations, Hanford Reservation, Richland, Washington") prior to the start of significant Hanford Site wastewater discharges. This water map includes the effects of limited irrigation near the former towns of White Bluff and Hanford, but not the effects of extensive irrigation now common in Cold and Dry Creeks. The 1944 water table contours indicate that groundwater flow is easterly toward the

Columbia River with a relatively uniform hydraulic gradient (~1.5 m/km [5 ft/mi]). Regional groundwater flow was generally toward the east-northeast, while flow north of Gable Mountain was more to the north.

Figure 2-9. Discharge History for the 216-T Pond and 216-U Pond.

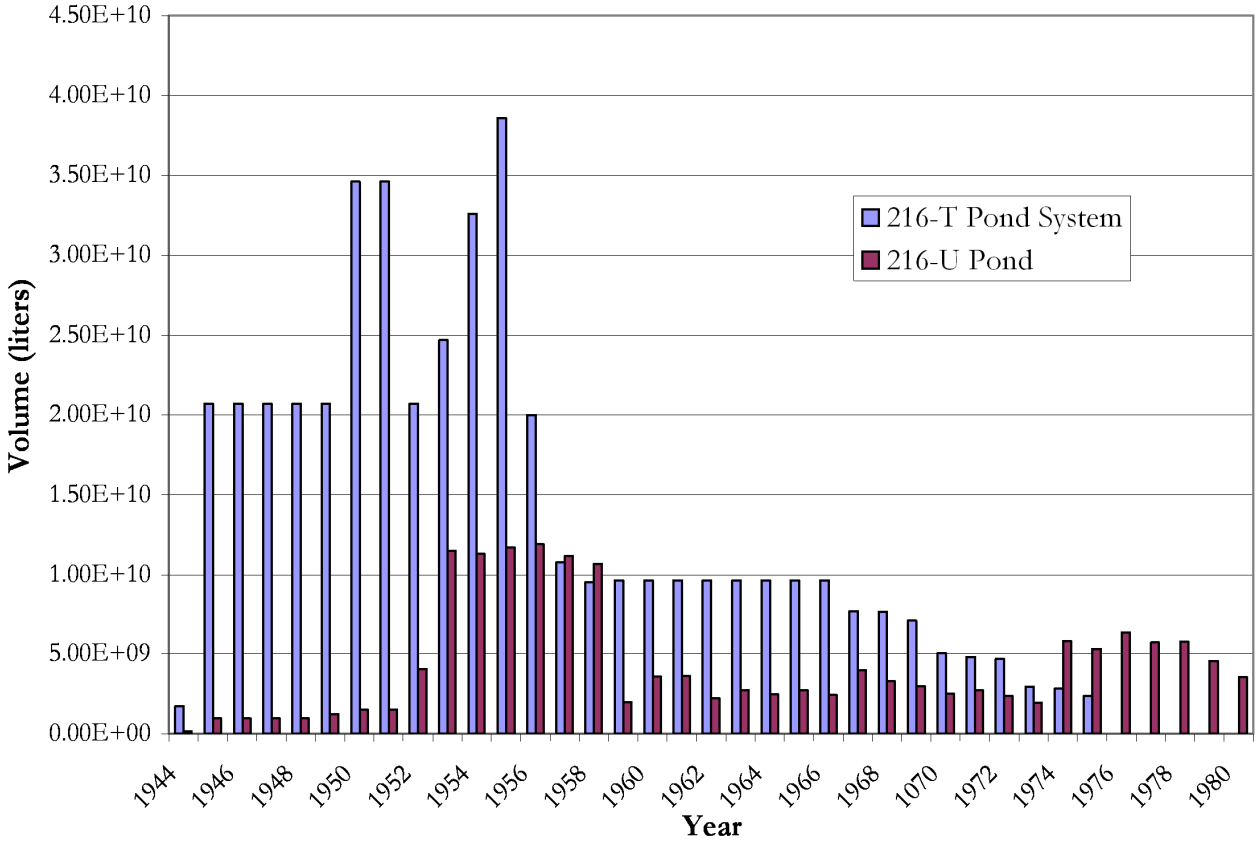

The pre-Manhattan Project water table in the 200 West Area and 200 East Area was ~123 m and 120 m above sea level, respectively (BNWL-B-360, "Selected Water Table Contour Maps and Well Hydrographs for the Hanford Reservation, 1944-1973"). In the 200 West Area, the water-table elevation increased rapidly from 1949 to 1956, but appeared to stabilize between the late 1960s and the late 1980s. Water levels began to decline in the late 1980s when wastewater discharges in the 200 West Area were reduced. In the 200 East Area, the water-table elevation increased rapidly from 1954 to 1963. The water table declined somewhat in the late 1960s and early 1970s, but then increased again in the early 1980s before beginning a final decline throughout the 1990s when wastewater discharges in the 200 East Area were reduced.

During operations, water levels in the uppermost and unconfined aquifer rose as much as 26 m and 9 m beneath the 200 West Area and 200 East Area, respectively, because of artificial recharge caused by liquid waste disposed from the mid-1940s to 1995. Figure 2-10b shows water table mounding present in the 200 Areas for June 1987. The volume of water that was discharged to the ground at the 200 West Area was actually less than that discharged at the 200 East Area. However, the lower hydraulic conductivity of the aquifer near the 200 West Area inhibited groundwater movement in this area, resulting in a higher groundwater mound.

Figure 2-10a. Hind Cast Water Table Map of the Hanford Site, January 1944.

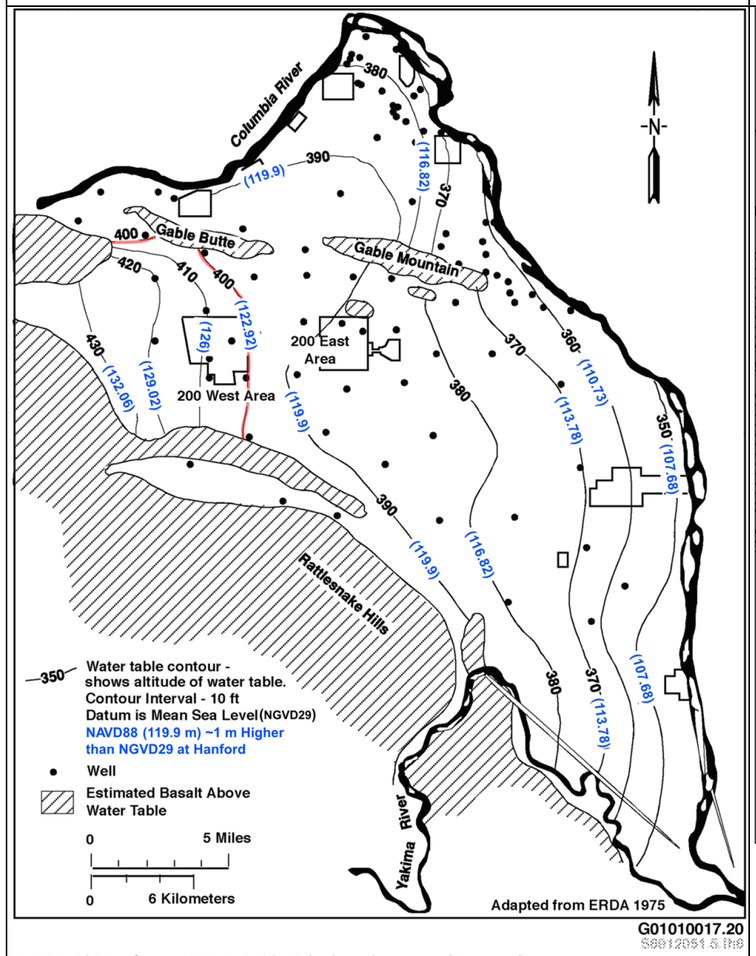

ERDA 1975 refers to ERDA-1538, "Final Environmental Impact Statement, Waste Management Operations, Hanford Reservation, Richland, Washington."

Note red contour line is to allow reader to follow changes for that contour interval through all three water table maps.

Figure 2-10b. Water Table Elevations for June 1987.

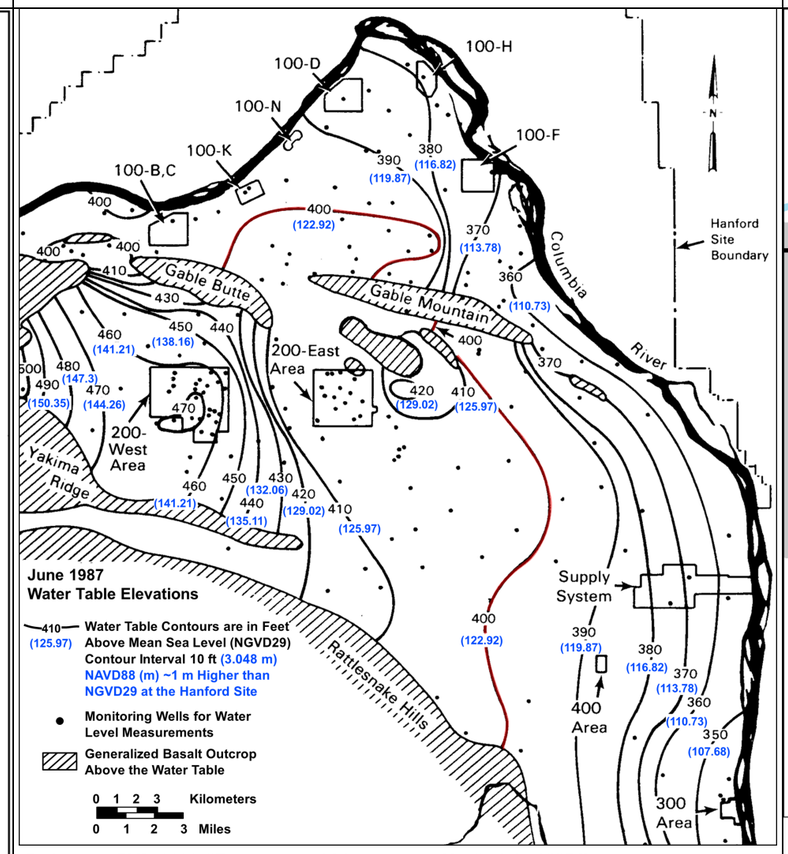

Reference: PNL-6464, "Environmental Monitoring at Hanford for 1987."

Figure 2-10c. Water Table Elevations for 2013.

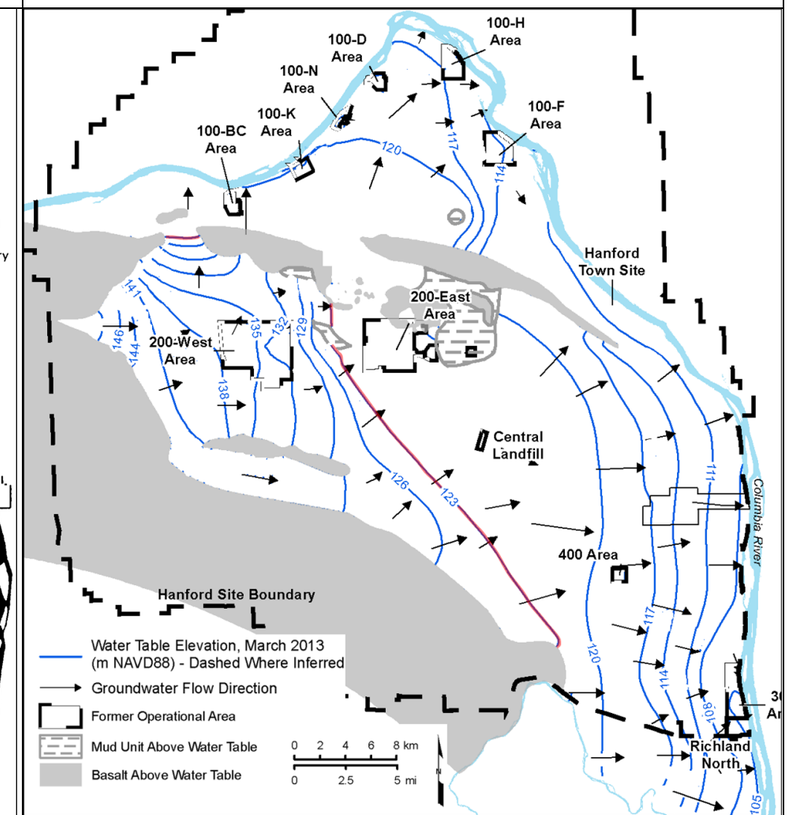

Source: DOE/RL-2014-32, Hanford Site Groundwater Monitoring Report for 2013.

Presently, groundwater in the unconfined aquifer generally flows from upland areas in the west toward the regional discharge area north and east along the Columbia River (Figure 2-10c). Steep hydraulic gradients occur in the western, eastern, and northern regions of the Site. Shallow gradients occur southeast of 100-FR and in a broad arc extending from west of 100-BC toward the southeast between Gable Butte and Gable Mountain (Gable Gap), through the 200 East Area and into the central portion of the Site. The reduction of wastewater discharges has caused water levels to drop significantly; however, a residual groundwater mound beneath the 200 West Area is still present today as shown by the curved water table contours near this area. Additionally, small groundwater mounds exist near the 200 Area Treated Effluent Disposal Facility (TEDF) and State-Approved Land Disposal Site wastewater disposal sites.

Comparing the approximate rate of water table decline in the 200 East Area with that in the 200 West Area shows that the rate of decline is three to four times faster in the 200 West Area. This is probably due, in part, to the greater increase in water level at U Pond than at B Pond. Also, the water table gradient is extremely flat in the 200 East Area, whereas the gradient is steeper beneath the 200 West Area. This indicates that a small increment of water table decline must be spread out over a much larger area in the 200 East Area than in the 200 West Area (Figure 2-11).

Figure 2-11. Water Table Elevations at Groundwater Monitoring Wells Close to U-Pond (200 West Area) and B-Pond (200 East Area).

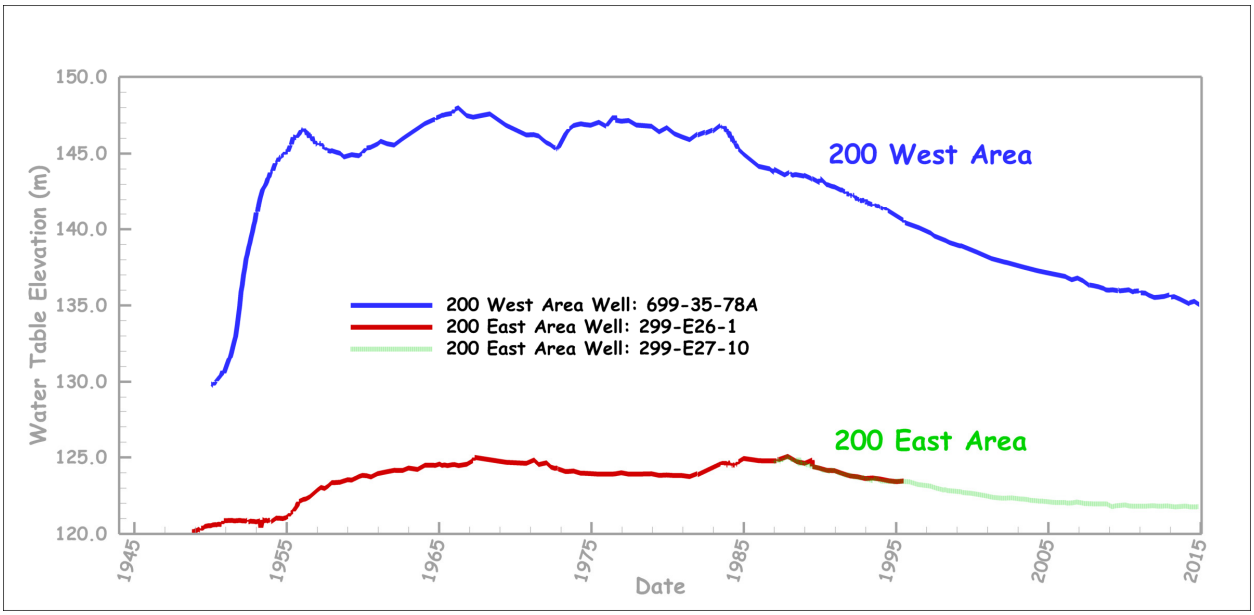

With cessation of discharges to B Pond, the northward migration of contaminated groundwater from the 200 East Area slowed as the gradient decreased. By 2009, the unconfined aquifer presented a broad relatively flat water table, with the groundwater divide moving near the northern half of the 200 East Area around WMA C. At the flow divide, groundwater flow bifurcates to the northeast or southeast, essentially travelling on either side of the remnants of the B Pond hydraulic mound. The exact location of this divide is variable and not easily identifiable. The water table in the 200 East Area is nearly flat and measurement uncertainties are greater than

actual water level differences between wells (DOE/RL-2010-11, Hanford Site Groundwater Monitoring and Performance Report for 2009 Volumes 1 and 2). By July 2011, groundwater flow within the unconfined aquifer in the southern portion of the 200-BP-5 OU (south of Gable Mountain) changed direction by 180 degrees compared to 2007. Since July 2011, the flow has maintained a south-southeast direction from the southern portion of Gable Gap into the northwest quarter of the 200 East Area (DOE/RL-2014-32, Hanford Site Groundwater Monitoring Report for 2013).

The dominant source of water in the unconfined aquifer beneath the 200 East Area and vicinity is inflow from the west. Formerly, the direction of groundwater flow diverged beneath the 200 East Area, with some water flowing toward the north through Gable Gap and some flowing southeast. The flow direction changed during 2011; since then flow has been toward the south and southeast across much of the 200 East Area. This change in flow directions is important because contaminant plumes located in the northwest corner of the 200 East Area located near and under the B Complex (WMA B-BX-BY and nearby Cribs) could flow under WMA C.

The distribution of hydrogeologic units within the unconfined aquifer is a result of Miocene-Pliocene Age geologic uplift and subsequent ancestral Columbia River and Pleistocene cataclysmic flooding and erosion. Highly turbulent floodwaters eroded channels into the basalt flow tops that typically filled with coarse-grained highly permeable channel fill. One such high-permeability channel exists below the water table at WMA C (Figure 2-12). These channel fill structures are often the location of preferential groundwater flow and contaminant migration when the orientation of the channel feature and the direction of groundwater flow align. This allows significant groundwater movement through the unconfined aquifer.

Groundwater velocity in the unconfined aquifer is dependent upon the hydraulic conductivity and effective porosity of the aquifer sediments and the gradient of the water table. In those areas where both Hanford formation and Ringold Formation occur in the unconfined aquifer, the hydraulic conductivity of the Hanford formation gravel-dominated facies (HSU 1) is generally a couple of orders of magnitude higher than the Ringold Formation unit E gravel-dominated facies (HSU 5) (Figure 2-7), and several orders of magnitude higher than that of the RLM (HSU 8). Groundwater in the southern part of 200-BP-5 Groundwater OU flows south and then east around the HSU 8 low-permeability barrier as it moves toward the Columbia River.

The 200-BP-5 groundwater and concurrent contaminant plumes (Figure 2-13) have migrated toward the Columbia River in two general directions. The groundwater divide beneath the 200 East Area bifurcated contaminant plume movement either northwest through Gable Gap or southeast toward the Columbia River:

- Plumes in the northwestern portion of the 200 East Area generally moved northwest toward Gable Gap in the past, but now may be moving to the southeast

- Plumes further south in the 200 East Area moved southeast toward the Columbia River.

Figure 2-12. 200-BP-5 Operable Unit Pleistocene Paleo-Erosional Surface Topography.

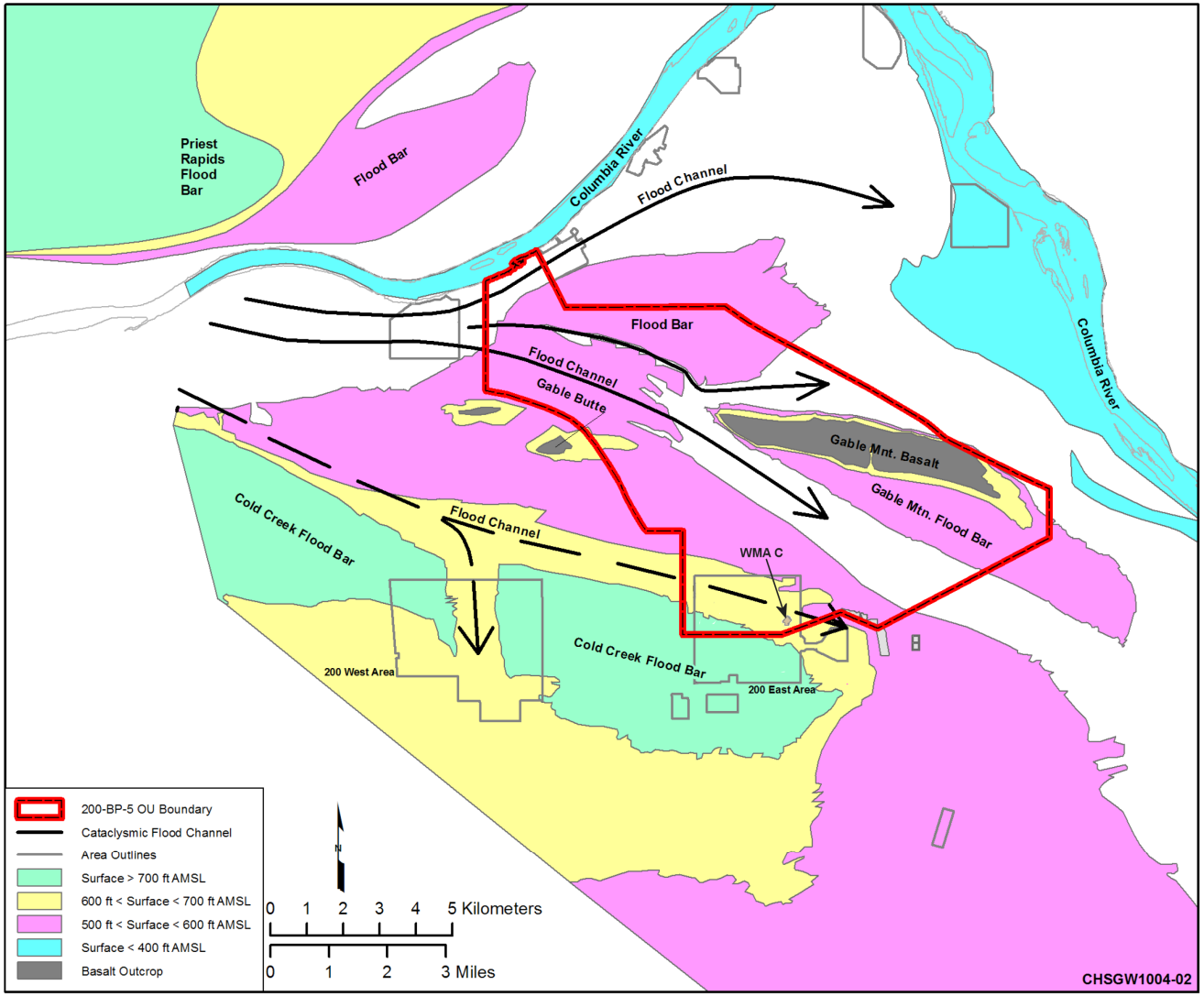

AMSL = above mean sea level OU = operable unit WMA = Waste Management Area

Reference: PNNL-12261, "Revised Hydrogeology for the Suprabasalt Aquifer System, 200-East Area and Vicinity, Hanford Site, Washington."

Figure 2-13. Groundwater Contamination for 2013 which Originated within the Central Plateau along with Central Plateau Groundwater Interest Areas.

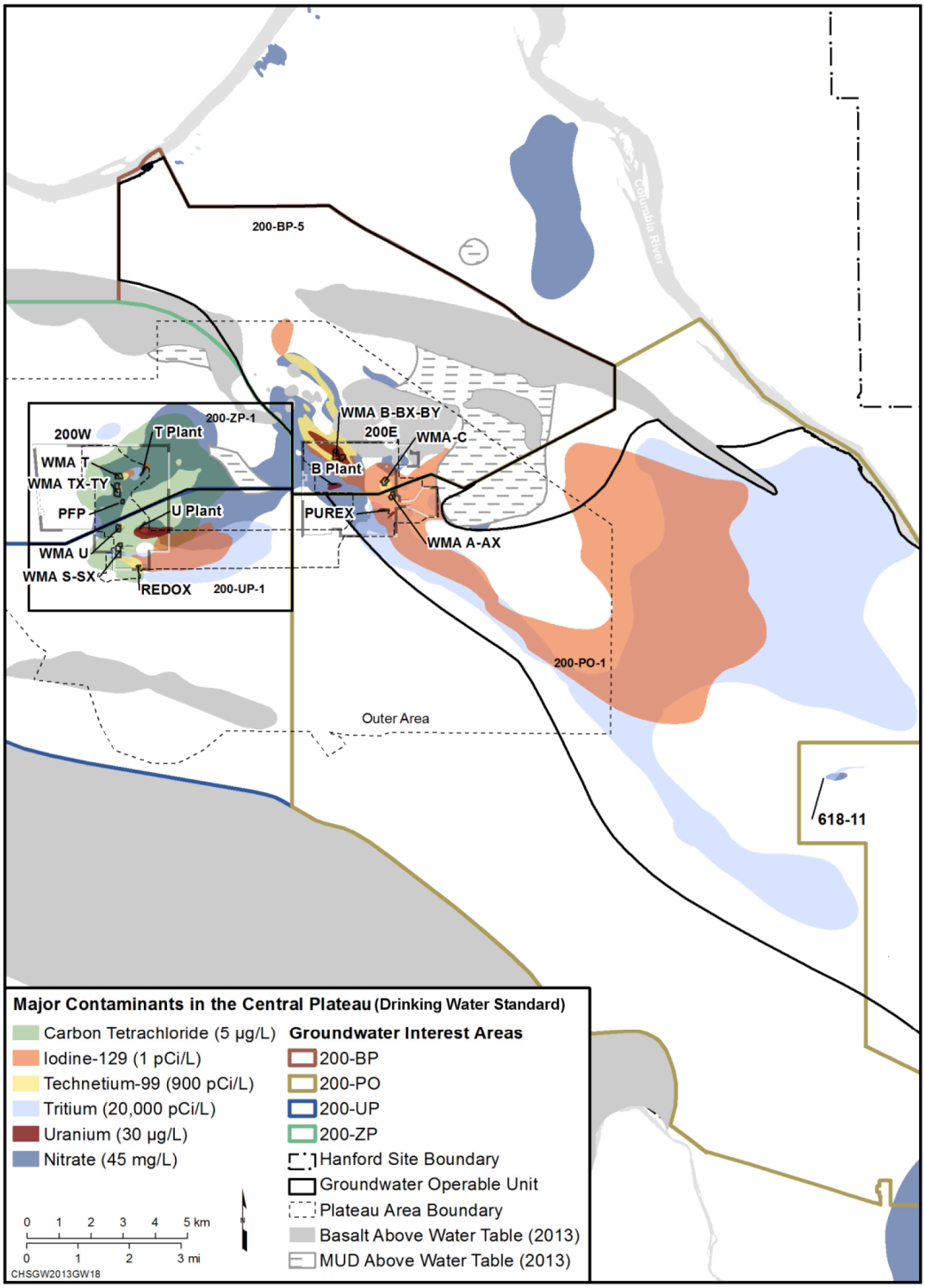

Source: DOE/RL-2014-32, Hanford Site Groundwater Monitoring Report for 2013.

PFP = Plutonium Finishing Plant
PUREX = Plutonium Uranium Extraction (facility)
REDOX = Reduction-Oxidation (facility)
WMA = Waste Management Area

The geometries of most of the contaminant plumes were first established when gradients were steeper and more groundwater flow occurred to the northwest toward the Gable Gap. In 2007 and 2008, stage fluctuations on the Columbia River appeared to cause flow reversals within the unconfined aquifer beyond the Gable Gap. These temporary groundwater flow reversals, and the current nearly-flat water table beneath the 200 East Area, strongly suggest that 200 East Area groundwater and contaminant plumes may move very slowly, stagnate or even reverse seasonally. The flat horizontal gradient measured in 2009 indicates a significant slowing or stalling of the movement of 200-BP-5 contaminant plumes compared to movement in the mid-1990s.

The velocity of groundwater is proportional to the horizontal gradient, and the decline in the horizontal gradients to nearly zero in the aquifer around WMA C indicates significantly lower groundwater velocities during recent years. After cessation of non-permitted liquid disposal to cribs, ponds, and ditches in the mid-1990s, the artificially elevated water table rapidly declined. The water table throughout most of the 200-BP-5 Groundwater OU continues to decline at present, but shows indications of stabilization in recent years. The current horizontal gradient is so small that scientists can barely detect differences in groundwater elevation in the unconfined aquifer around WMA C. For example, the regional gradient to the southeast from the 200 East Area (across the 200-BP-5 and 200-PO-1 Groundwater OUs) has been estimated to be 1.8×10^{-5} m/m, which translates to a difference of less than 2 cm across a kilometer (DOE/RL-2008-66, Hanford Site Groundwater Monitoring for Fiscal Year 2008).

2.3 WASTE MANAGEMENT AREA C SITE CHARACTERIZATION

This section provides a brief summary of the characterization of the vadose zone and unconfined aquifer in and around WMA C, including contamination in both the vadose zone and unconfined aquifer. Since the late 1990s there has been an extensive effort to characterize the vadose zone and unconfined aquifer around WMA C. These efforts are described in numerous documents including, but not limited to, DOE/ORP-2008-01, RCRA Facility Investigation Report for Hanford Single-Shell Tank Waste Management Areas, Appendix L; DOE/RL-2014-32; GJO-98-39-TAR/GJO-HAN-18, “Hanford Tank Farms Vadose Zone: C Tank Farm Report”; GJO-98-39-TARA/GJO-HAN-18, “Hanford Tank Farms Vadose Zone: Addendum to the C Tank Farm Report”; RPP-PLAN-39114, “Phase 2 RCRA Facility Investigation/Corrective Measures Study Work Plan for Waste Management Area C”; RPP-RPT-56356, “Development of Alternative Digital Geologic Models of Waste Management Area C”; and RPP-RPT-58339. For more detailed information, please refer to the characterization documents.

The principal driver for site characterization at WMA C is a number of confirmed or suspected waste loss events which occurred in WMA C (labeled as UPRs in Figure 2-14) during its operational history. These included suspected tank leaks and known waste losses from waste transfer piping systems. The current understanding of contaminant occurrences and environmental conditions at WMA C is described in RPP-ENV-33418 and DOE/ORP-2008-01 and summarized in Section 2.1 of this document. The primary contamination zones currently identified in WMA C include a localized high ^{137}Cs activity zone near the bottom of the southwest part of tank C-105 and three UPRs near waste transfer pipelines and diversion boxes

in the southwest part of WMA C. Sampling at groundwater wells 299-E27-21 and 299-E27-23 along the southern boundary of WMA C (Figure 2-14) had results for ^{99}Tc at concentrations greater than 25 times the drinking water standard (DWS) of 900 pCi/L.

Figure 2-14. Waste Management Area C Tanks, Infrastructure, and Associated Unplanned Releases.

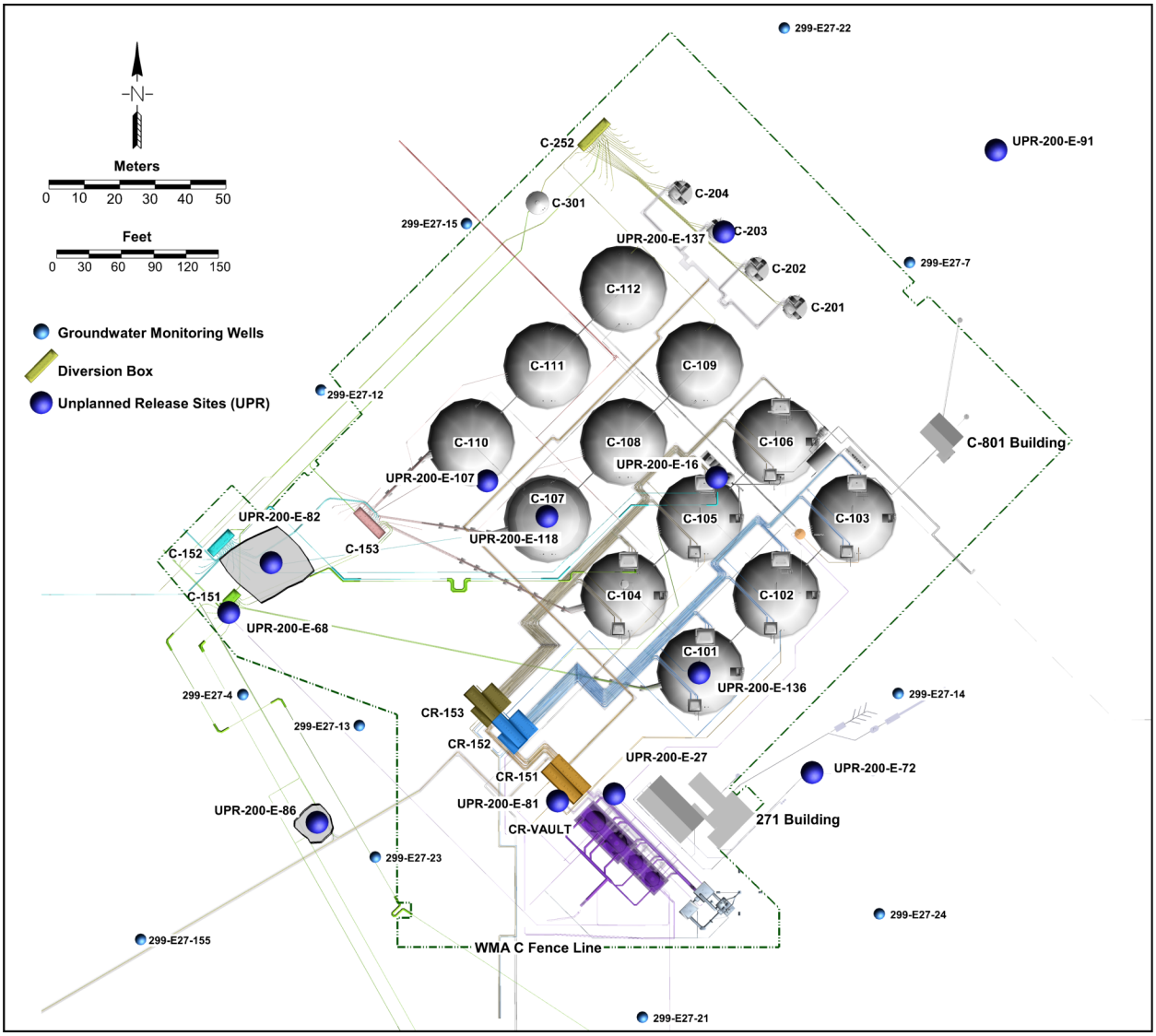

WMA = Waste Management Area

2.3.1 Geology of Waste Management Area C

The geology of WMA C is summarized from the information provided in DOE/ORP-2008-01; DOE/RL-2009-127 Draft A; RPP-RPT-46088, "Flow and Transport in the Natural System at Waste Management Area C"; and RPP-RPT-56356. A generalized fence diagram through WMAs A-AX and C is shown in Figure 2-15.

Figure 2-15. Fence Diagram Showing Cross-Sections through Waste Management Areas A-AX and C.

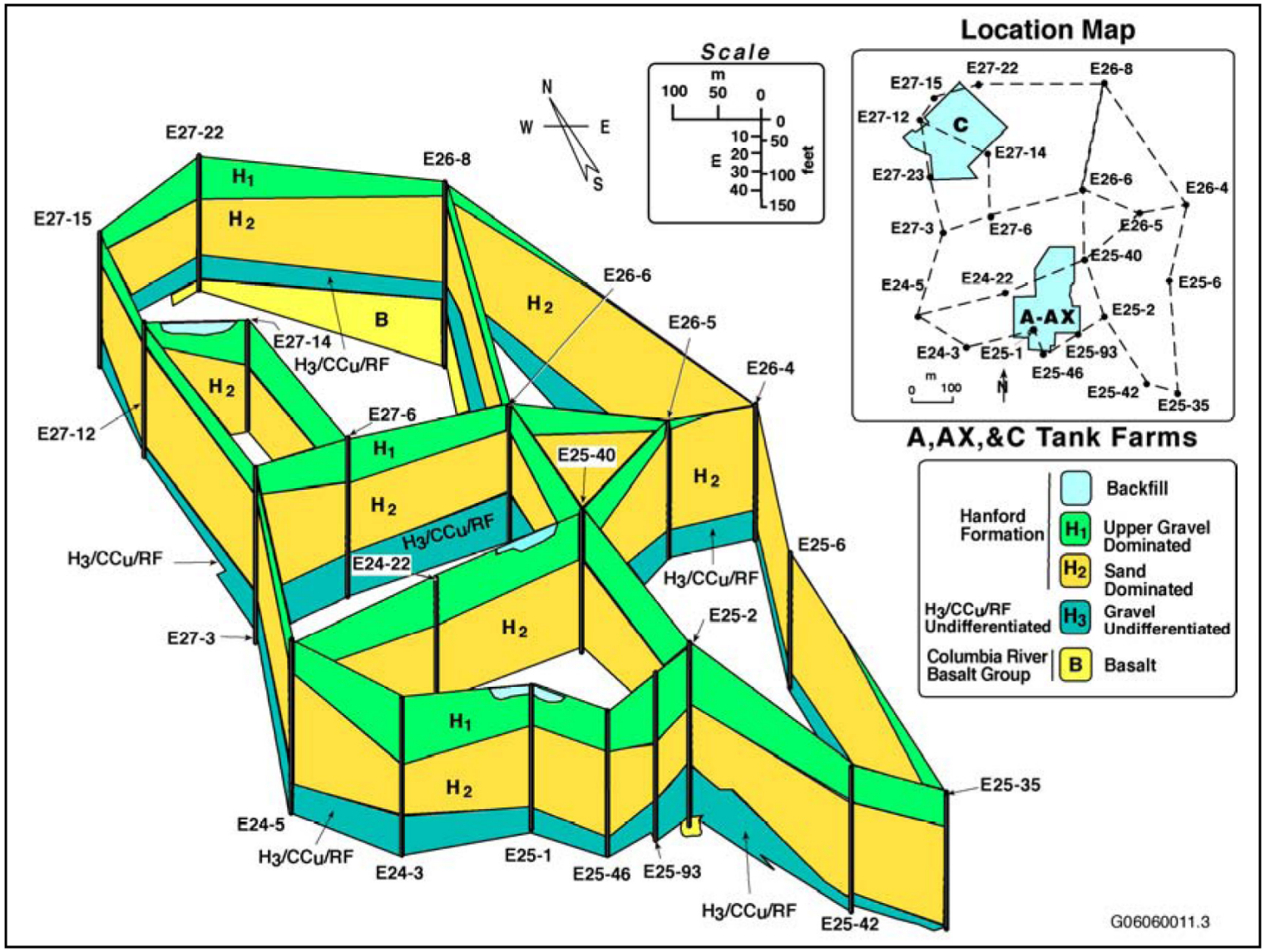

$H_3/CC_u/RF$ = undifferentiated Hanford Formation, Cold Creek unit and Ringold Formation

Six stratigraphic units lie within WMAs A-AX and C. From oldest to youngest, the primary geologic units are:

- Columbia River Basalt Group
- Undifferentiated Hanford lower gravelly sequence (H3 unit)/Cold Creek/Ringold formations
- Hanford formation – sand sequence (H2 unit)
- Hanford formation – upper gravelly sequence (H1 unit)
- Backfill
- Recent deposits.

The general characteristics of these units are described in more detail in RPP-RPT-46088 and RPP-RPT-56356. At WMA C, it is not possible to separate out the Ringold Formation, CCu and the lower gravely sequence of the Hanford formation (H3). In the vicinity of WMA C, this unit is referred to as undifferentiated H3, CCu and Ringold Formation ($H_3/CC_u/RF$) because of the scouring within the paleochannel underlying WMA C (Figure 2-12). The SSTs at WMA C were emplaced in an excavation of the Hanford formation sediments of the upper, gravel-dominated (H1) unit. This excavation may also locally intercept the upper portions of the sand-dominated Hanford (H2) unit. Once the tanks were built, the excavation was backfilled with reworked sediments of the upper, gravel-dominated (H1) unit. The water table or the unconfined aquifer's surface lies ~60 m (~200 ft) below the bottom of the tank farms excavations within the undifferentiated $H_3/CC_u/RF$.

The geologic strata underlying WMA C was characterized in conjunction with soil sampling and borehole logging for radionuclides and hazardous waste constituents as part of the Phase 1 and 2 RCRA Facility Investigations at WMA C. The borehole and geologic logging was used to identify the elevations of tops of the geologic units in the vicinity of WMA C. Specifically potassium, uranium, thorium (K-U-T) data from geophysical logs were used to map the tops of the different geologic units at WMA C (RPP-RPT-56356). Two alternative geologic models were developed based on this data.

Additional conceptual models are being developed with detailed heterogeneous representations of the geologic framework at WMA C. One is a facies-based model based primarily on a geostatistical analysis of the K-U-T data collected in selected direct push boreholes within WMA C; the other is based on geostatistical evaluations of volumetric moisture content measured in multiple direct push boreholes and drywells within WMA C.

The major difference between the two existing developed alternative models is whether or not a sandy gravel facies is to include a silt layer identified at the bottom of the H2 subunit in the vicinity of WMA C. The K-U-T data (i.e., a lower gross gamma and potassium count) indicates that there is a coarsening of the sand at the bottom of the H2 unit turning more into a sandy

gravel. Underlying this sandy gravel facies is a silt unit with a strong potassium peak and occasional strong natural uranium peak. The difficulty in making this determination is that there are few direct pushes or drywells that are at a sufficient depth to obtain both good geophysical logs and geologic logs (with drill cuttings). The drill cuttings from some of the nearby groundwater wells indicated that there was definite fining of the sands along with some silt found at the vertical location as indicated by the K-U-T data in the geophysical logs, but a competent silt layer was not observed. Alternative Geologic Model I does not include the sandy gravel and underlying silt unit with the H2 unit, while Alternative Geologic Model II does include them. The existence of these layers could cause increased lateral movement in the vadose zone. A series of fence diagrams showing the differences between the two models within WMA C is given in RPP-RPT-56356. The fence diagram for both these models running southwest to northeast through the center of WMA C is given in Figure 2-16.

2.3.2 Vadose Zone Characterization at Waste Management Area C

Since the late 1990s, there have been the following three major campaigns to characterize the vadose zone at WMA C:

1) Log the existing drywells around each of the 100-series SSTs to provide baseline characterization, which took place in the late 1990s

2) Phase 1 RCRA Facility Investigation, which took soil samples close to the high ^{137}Cs activity found near SST 241-C-105 and to probe underneath the gunite cap at UPR-200-E-82 where a pipeline failure lead to the loss of PSN waste (4.3 Ci/gal of ^{137}Cs)

3) Phase 2 RCRA Facility Investigation, in which site characterization data was collected at the 23 sites across the farm.

The results of these characterization efforts are summarized in the following sections.

2.3.2.1 Drywell Monitoring at Waste Management Area C. Waste Management Area C has 70 drywell monitoring boreholes (see Figure 2-17) available for leak detection monitoring and to provide access for limited vadose zone characterization (e.g., geophysical logging). These drywells were drilled from 1944 to 1982. In 1997, C Farm drywells were logged using a high-resolution spectral gamma logging system. This effort was part of the baseline characterization for WMA C. Results are documented in GJO-98-39-TAR/GJO-HAN-18 and its associated addendum GJO-98-39-TARA/GJO-HAN-18. The depth ranges for most of these drywells is between 30.5 and 45.7 m bgs (100 and 150 ft bgs). The deepest drywell in WMA C is 47.2 m bgs (155 ft bgs) (30-00-03), and the maximum logged depth is 43.6 m bgs (143 ft bgs) (30-04-08).

The major gamma-emitting contaminants associated with WMA C are ^{137}Cs and ^{60}Co with lesser amounts of ^{154}Eu. These contaminants are located mostly in and around areas of confirmed or suspected tank and pipeline leaks. Although most of the drywells are deeper than the surrounding contamination, some zones of contamination extend deeper than nearby drywells. Consequently, the maximum depth of vadose zone contamination is not known in some areas of WMA C.

Figure 2-16. Fence Diagram of Alternative Geologic Models for Waste Management Area C.

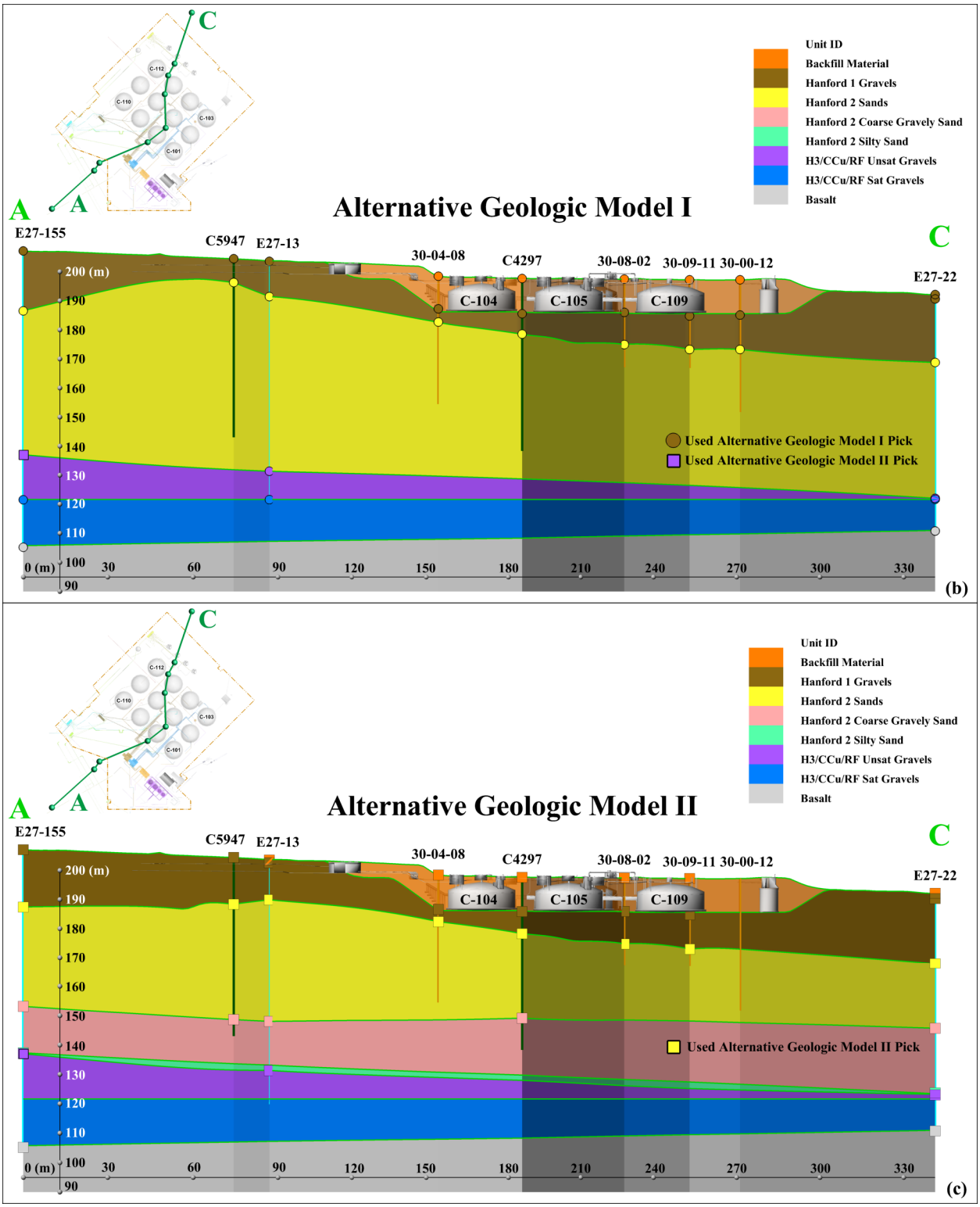

H3/CCu/RF = undifferentiated Hanford Formation, Cold Creek unit and Ringold Formation

Figure 2-17. Vadose Zone and Groundwater Monitoring Network for Waste Management Area C.

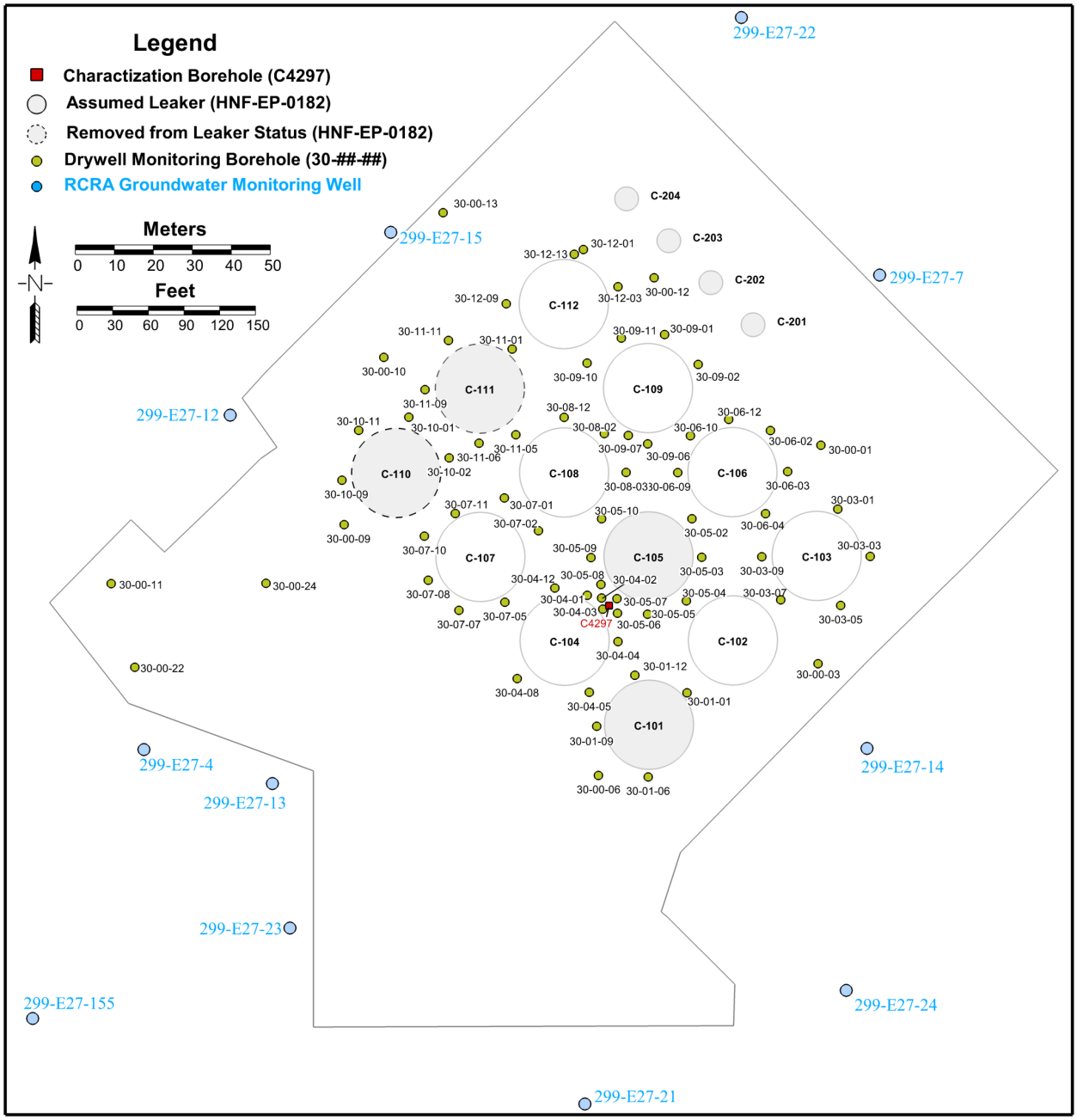

Reference: HNF-EP-0182, "Waste Tank Summary Report for Month Ending September 30, 2013," Rev. 306.

RCRA = Resource Conservation and Recovery Act of 1976

Figure 2-18 provides a visualization of the vadose zone contamination beneath WMA C as represented by ^{137}Cs data and the ^{99}Tc at borehole C4297. This figure is a three-dimensional (3-D) perspective of WMA C providing locations of tanks and associated drywells. Tanks are considered to be leakers based on information in HNF-EP-0182, "Waste Tank Summary Report for Month Ending February 28, 2015," Rev. 326. For ^{137}Cs each drywell is represented with a

single vertical line. Shaded rings around the drywells indicate the level of vadose zone contamination based on spectral gamma logging results. Only the more significant soil contamination zones (i.e., ^{137}Cs contamination levels greater than 10 pCi/g) are shown.

Spectral gamma logging data provided in Figure 2-18 indicate the presence of contamination in the region between tanks C-104 and C-105. The most concentrated contamination occurs at drywell 30-05-07 on the southwest side of tank C-105 (Figure 2-18), where two high ^{137}Cs concentration zones occur at and below the tank bottom (DOE/ORP-2008-01).

2.3.2.2 Phase 1 RCRA Facility Investigation Characterization Activities and Results. In 2004, vadose characterization activities were conducted at WMA C in support of the RCRA corrective action. The first phase concentrated on characterizing an area of high ^{137}Cs concentrations observed in drywells at the depth of the base of tank C-105 below the cascade line running between tanks C-104 and C-105 and the pipeline leak known as UPR-200-E-82 close to the 241-C-152 diversion box. The characterization borehole drilled next to tank C-105 was the deepest characterization within WMA C at 59.9 m (196.5 ft) bgs at the time. Results from soil sampling show the greatest concentration of ^{99}Tc (8.4 pCi/g) and nitrate (20 µg/g) at 41.1 to 47.2 m bgs (~135 to 155 ft bgs). Also shown on Figure 2-18 are sample locations showing where the more mobile ^{99}Tc was found in characterization borehole C4297.

Slant direct pushes underneath the gunite cap at UPR-200-E-82 found ^{99}Tc (28.6 pCi/g) and nitrate (19.7 µg/g) centered below the pipeline leak at 23.5 m bgs (77 ft bgs). Complete results of the first phase of characterization are documented in DOE/ORP-2008-01 Appendix L and in RPP-35484, "Field Investigation Report for Waste Management Areas C and A-AX."

2.3.2.3 Phase 2 RCRA Facility Investigation Characterization Activities. The second phase started in 2008 and characterization data was collected per the work plan (RPP-PLAN-39114). For Phase 2, site characterization data was collected at the 23 sites identified in Figure 2-19. Each characterization site was given a letter map designation. The site characterization activities for Phase 2 included the following:

a. Soil collection and analysis through direct push boreholes technology

b. Geophysical logging at drywell boreholes and groundwater monitoring wells

c. Surface Geophysical Exploration

d. Tissue sampling for ecological risk assessment

e. Possible sampling of vadose zone during the installation of any new groundwater wells within ~30 m (~100 ft) of WMA C.

RPP-PLAN-39114 provides a complete description of what was to be collected at each of these sites. During the preparation of the work plan for the Phase 2 characterization, a transitional characterization (Phase 1.5) effort was undertaken and vadose zone characterization took place at two past UPR sites (UPR-200-E-81 and UPR-200-E-86) (Figure 2-20). This transitional characterization effort was called "near-term characterization" and focused on the deployment of

hydraulically-driven direct push technology to push boreholes (i.e., Phase 1.5) for geophysical logging, placement of deep electrodes, and to collect soil samples. The results of both the transitional characterization and the Phase 2 vadose zone characterization efforts are given in RPP-RPT-58339 and are summarized in the following section.

2.3.2.4 Overview of Characterization Results from RCRA Facility Investigations. As a part of the Phase 2 RCRA facility investigation (RFI)/corrective measures study (CMS), a significant amount of work has been performed to characterize contamination in the vadose zone within and around WMA C. The area shows evidence of widespread shallow and deep contamination and a discontinuity between soil constituents and groundwater contamination, and there continues to be a limited understanding of the linkage between sources and contaminants at WMA C. In general, contamination has been found from the surface to depths of ~73 m (240 ft) bgs. It is difficult to make specific correlations because the various waste releases have occurred in near proximity and in an area of up to 7 hectares (16 acres).

Several observations could be made from the Phase 2 RFI characterization efforts. For instance, gamma logging showed higher gamma spectra near the soil surface and near locations of suspected waste losses, confirming that waste had entered the soil and that many gamma-emitting radionuclides did not show significant mobility. Moisture logging showed layers of higher moisture interspersed with lower moisture. These observations were consistent with expectation of high moisture content with finer grain size. Although the SGE campaign did not determine conclusively whether individual 200-series tanks leaked, it did identify that soil anomalies in the area suggested the possible presence of elevated moisture and/or possible contamination (e.g., UPR-200-E-81).

As identified, Phase 2 sampling efforts did not represent a random statistical sampling scheme at WMA C. The Phase 2 investigation targeted locations where contamination was expected to be found based on historic records of waste losses. Table 2-4 provides an overview of the areas investigated at WMA C.

For the most part, sampling did not show high concentrations of mobile constituents in any specific depth range. The following observations should be noted.

- Many sampling locations showed concentrations of mobile constituents somewhat above background (37 out of 45 constituents), suggesting for the most part that mobile constituents had migrated through the region, to greater depths.

- Increased concentrations of some mobile contaminants above background were found in samples from all depths.

- As the Phase 2 RFI characterization was proceeding, the groundwater monitoring program was finding additional evidence that waste from the WMA C facilities had reached groundwater (see Section 2 of RPP-RPT-58339).

- Information collected in and near other tank farms suggested that geologic layers in the soil have the potential to provide lateral movement of water and mobile contaminants.

Figure 2-18. Three-Dimensional Perspective of Waste Management Area C Tanks and Drywells Showing Occurrence of Significant (>10 pCi/g) Cesium-137 Contamination in the Vadose Zone along with Technetium-99 at Borehole C4297.

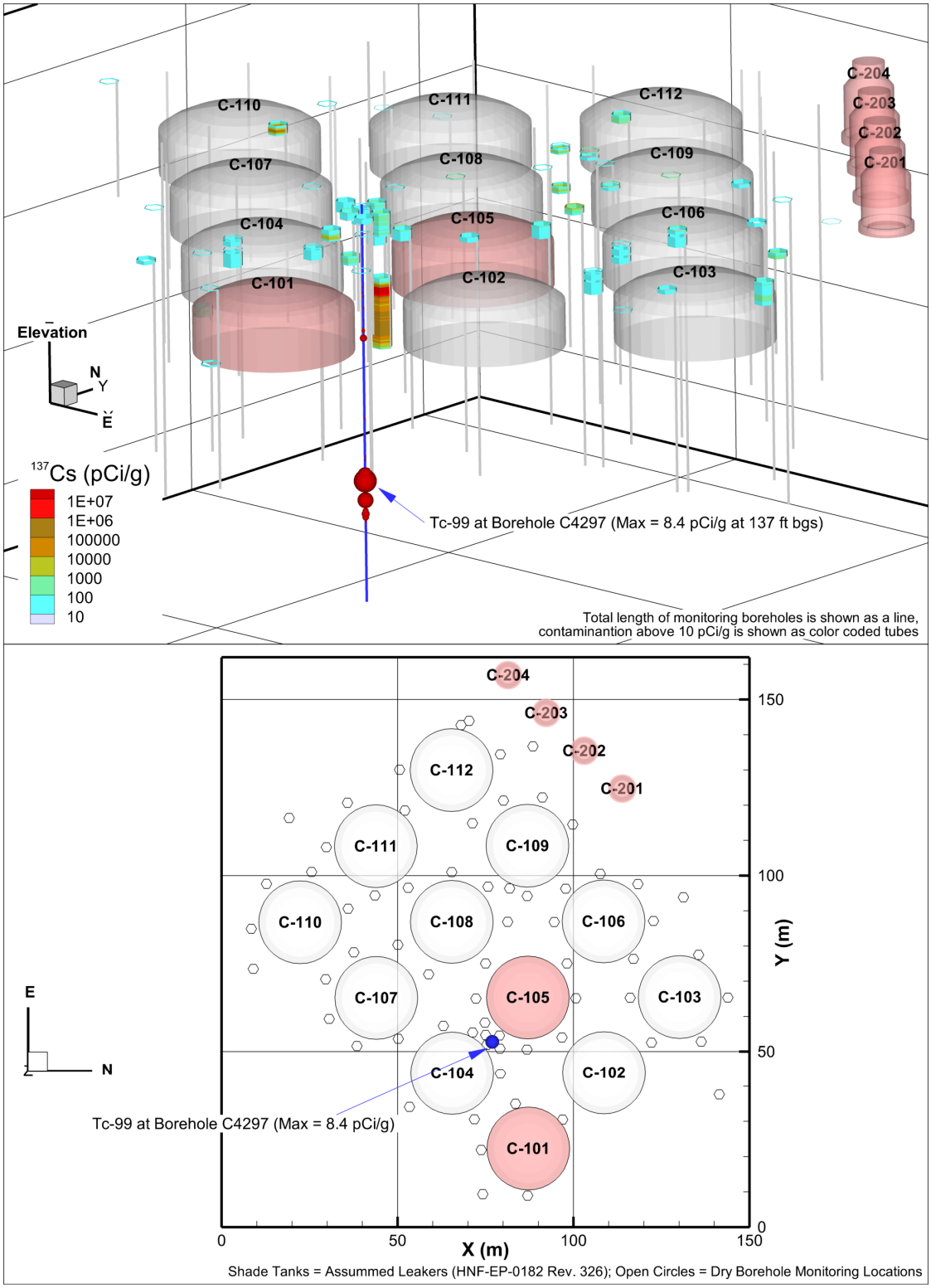

Reference: HNF-EP-0182, "Waste Tank Summary Report for Month Ending February 28, 2015," Rev. 326.

Figure 2-19. Completed Phase 2 RCRA Facility Investigation Characterization Locations.

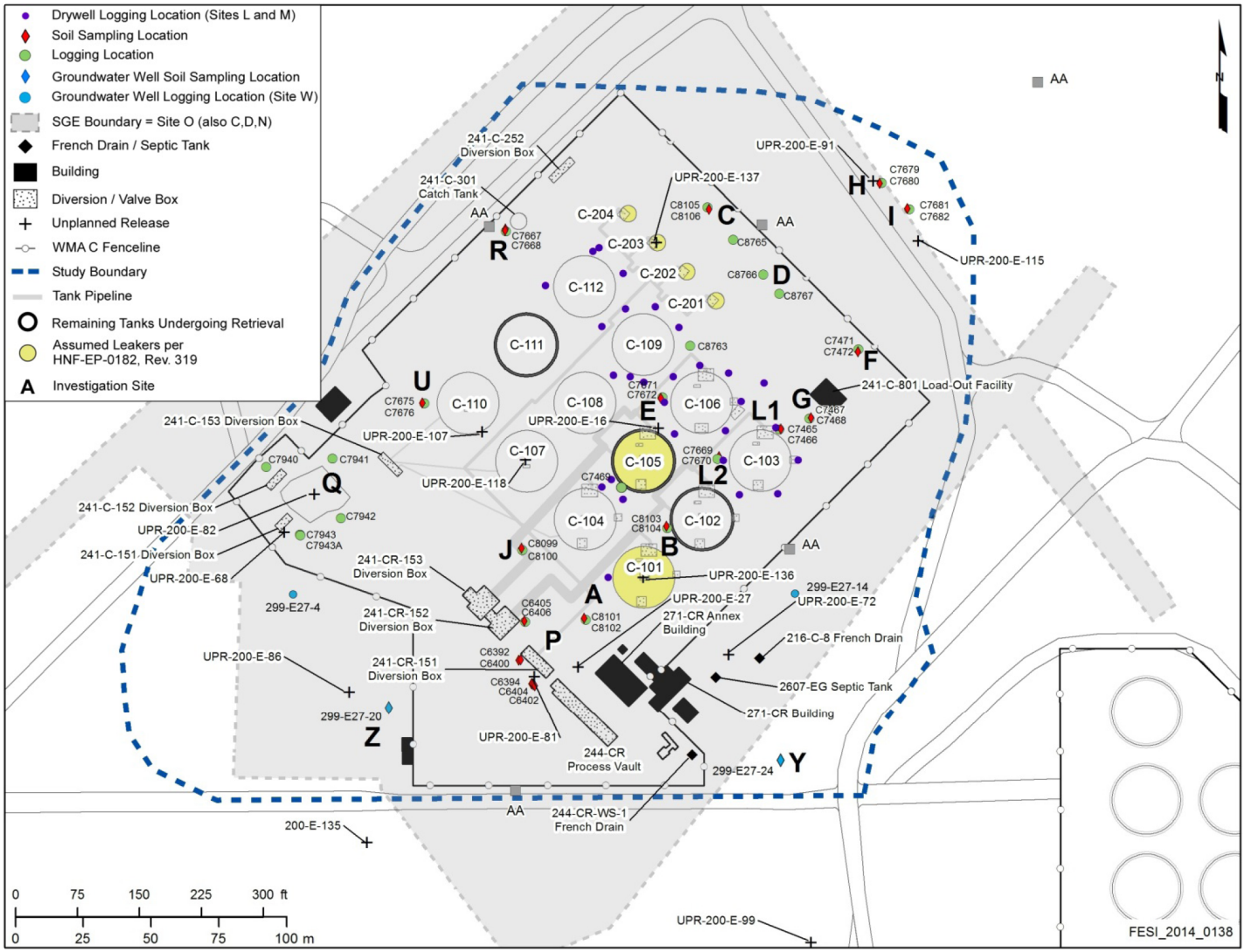

RCRA = Resource Conservation and Recovery Act of 1976 SGE = Surface Geophysical Exploration WMA = Waste Management Area

Reference: HNF-EP-0182, "Waste Tank Summary Report for Month Ending July 31, 2014," Rev. 319.

Figure 2-20. Completed Transitional (Phase 1.5) Characterization Locations.

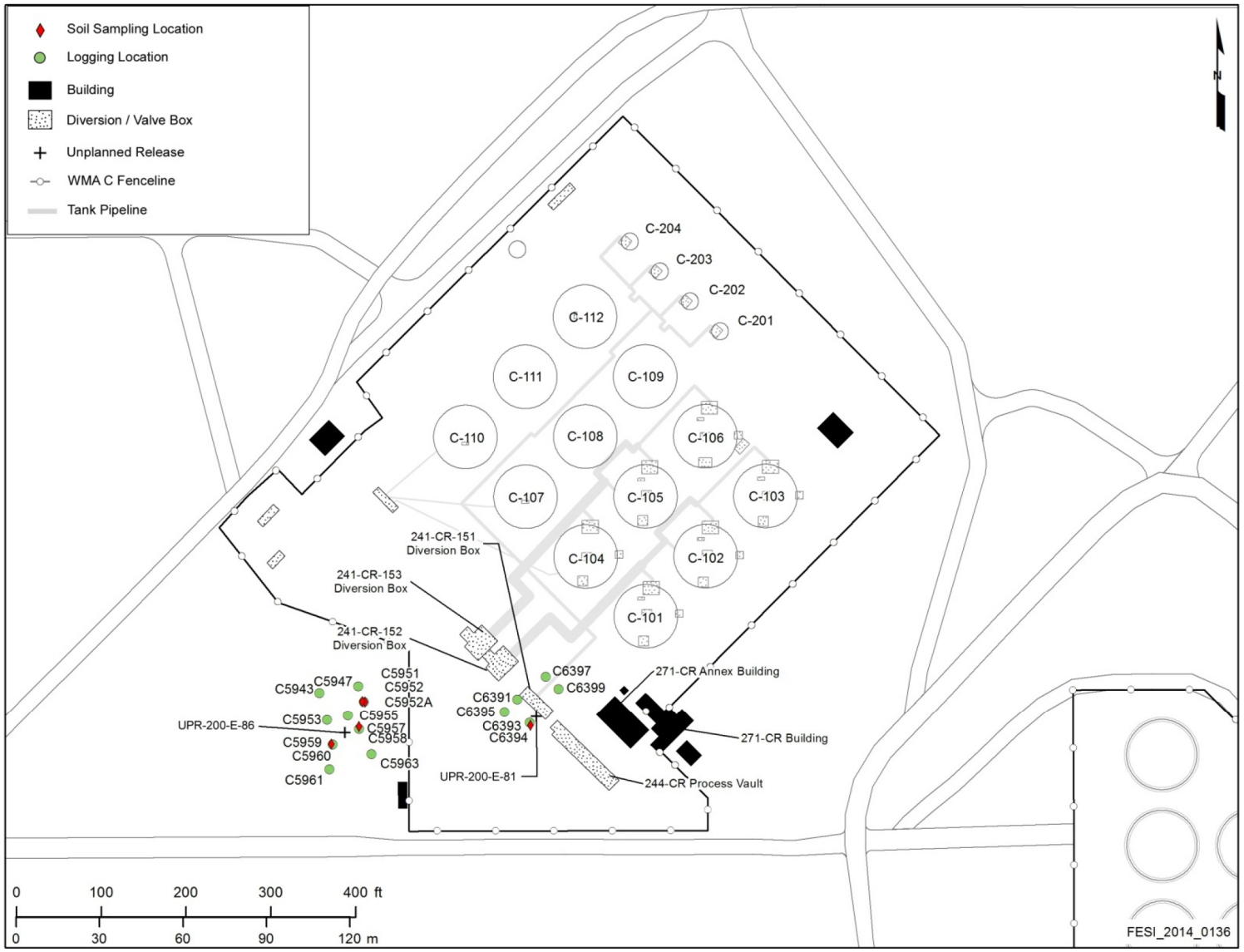

WMA = Waste Management Area

Table 2-4. Summary of Field Efforts Related to Areas Investigated in Waste Management Area C RCRA Facility Investigation. (2 sheets)

Area Investigated	Field Efforts[1]
Tank 241-C-101	• Group A + B Direct Push Logging • Group A + B Analytical • Drywell Logging (30-01-01, 30-01-01, 30-01-06, and 30-01-09) • Site O Surface Geophysical Exploration
Area between Tanks 241-C-103 (C-103) and 241-C-106 (C-106)	• Group L1 + L2 Direct Push Logging • Group L1 + L2 Analytical • Drywell Logging (30-00-01, 30-03-01, 30-03-03, 30-03-05, 30-03-07, 30-03-09, 30-06-02, 30-06-03, 30-06-04, 30-06-09, 30-06-10, and 30-06-12) • Site O Surface Geophysical Exploration
Tank C-103 and Building C-801 and the building's chemical drain	• Group F + G Direct Push Logging • Group F + G Analytical • Drywells Logging (30-03-01, 30-03-03, 30-03-05, 30-03-07, and 30-03-09) • Site O Surface Geophysical Exploration
Tank 241-C-104	• Site J Direct Push Logging • Site J Analytical • Site M Drywell Logging (30-04-01, 30-04-02, 30-04-03, 30-04-04, 30-04-05, 30-04-08, 30-04-12, and 30-05-06) • Site O Surface Geophysical Exploration
Tank 241-C-105	• C4297 Analytical and Logging • C7469 Direct Push Logging • Drywell Logging (30-05-02, 30-05-07, and 30-05-08)
Area between Tanks C-106 and 241-C-109	• Site E Direct Push Logging • Site E Analytical • Site M Drywell Logging (30-00-01, 30-06-02, 30-06-03, 30-06-04, 30-06-09, 30-06-10, 30-06-12, 30-09-01 ,30-09-02, 30-09-06, 30-09-10, and 30-09-11) • Site O Surface Geophysical Exploration
Tank 241-C-108	• Drywell Logging (30-05-10, 30-07-01, 30-07-02, 30-08-02, 30-08-03, 30-08-12, and 30-09-07)
Tank 241-C-110	• Site U Direct Push Logging • Site U Analytical • Site M Drywell Logging (30-00-09, 30-10-01, 30-10-02, 30-10-09, and 30-10-11) • Site O Surface Geophysical Exploration
Tank 241-C-111	• Drywell Logging (30-11-01, 30-11-05, 30-11-06, 30-11-09, and 30-11-11)
Tank 241-C-112	• Drywell Logging (30-00-12, 30-12-01, 30-12-03, 30-12-09, and 30-12-13)
C-200s tanks	• Group C + D Direct Push Logging • Site C Analytical • Group C + D Surface Geophysical Exploration
UPR-81	• Phase 1.5 and Phase 2 Site P Direct Push Logging • Phase 1.5 and Phase 2 Site P Analytical • Site N Surface Geophysical Exploration

Table 2-4. Summary of Field Efforts Related to Areas Investigated in Waste Management Area C RCRA Facility Investigation. (2 sheets)

Area Investigated	Field Efforts[1]
UPR-82	• Pre-RFI Analytical Locations 5 and 10 identified in ARH-1945[2] • Phase 1 Direct Push Logging • Phase 1 Analytical • Site Q Direct Push Logging • Site N Surface Geophysical Exploration
UPR-86	• Phase 1.5 Direct Push Logging • Phase 1.5 Analytical • 299-E27-20 (Site Z) Analytical • Site N Surface Geophysical Exploration
URP-91 and URP-115	• Group H + I Direct Push Logging • Group H + I Analytical • Site O Surface Geophysical Exploration
Area near C-301 catch tank	• Site R Direct Push Logging • Site R Analytical • Site O Surface Geophysical Exploration

[1] Investigation groups and sites and associated direct push borehole locations are provided in Figure 2-19. Approximately 70 drywells were logged in Waste Management Area C, not all are listed in this table. Location of these drywells are provided in Figure 2-17.

[2] ARH-1945, "B Plant Ion Exchange Feed Leak" summarizes the results of a historical investigation performed at UPR-200-E-82-27 in the early1970s to evaluate an unplanned release of liquid waste containing ^{137}Cs.

RCRA = Resource Conservation and Recovery Act of 1976

Results of the Phase 2 investigation confirm the expectation that a number of immobile waste constituents remain near sources of waste releases. Mobile constituents have moved into the vadose zone to varying depths as a result of the waste release and geochemical processes. In addition to vertical movement of the contamination, lateral migration is also suspected. Although there may be a preferential direction in some parts of the tank farm, spreading in other directions due to smaller lenses of less permeable soil cannot be ruled out.

With respect to data gaps, only Site X could not be accessed during the field investigation. Specifically, Site X, which was to be located near tank C-105, was added to Revision 2 of the work plan to better define the area of contamination associated with a historic waste loss from tank C-105. The goal of the investigation was to gain information about a contamination under the tank, which was thought to be accomplished with an angled direct push under the tank. However, based on the available information already collected from WMA C, it is not certain if this additional field information is needed, or if it will be of value. The area continues to be difficult to access and it is thought that model analysis of past leaks may provide any additional information, if needed. Therefore, no further field characterization is recommended at this site.

Additionally, as identified, direct pushes at Site R were completed to assess a potential waste release from the catch tank. Characterization data obtained through the field effort yielded less

than expected contamination levels (i.e., minimal soil background exceedances). It is understood that additional information may be required to make retrieval and closure decisions for C-301 catch tank, beyond the scope of the characterization covered in the Phase 2 RFI; however, it is believed that no further soil characterization around the C-301 catch tank is needed.

2.3.2.5 General Observations of Phase 1 and 2 Vadose Zone Characterization Results for Selected Contaminants of Potential Concern. Following is a summary of general observations of selected constituents of potential concern (COPCs) in different investigation areas at WMA C. The selected COPCs represent three classes of constituent mobility:

- Mobile constituents (K_d = 0 mL/g which include ^{99}Tc, nitrate, sulfate, and chromium)
- Slightly sorbed constituents (K_ds between 0.2 to 0.6 mL/g including ^{129}I, ^{60}Co, and uranium)
- Sorbed constituents (K_ds > 0.6 mL/g including ^{137}Cs, ^{90}Sr, and tributyl phosphate).

2.3.2.5.1 Mobile Constituents (K_d = 0 mL/g).

Technetium-99: In the Phase 2 RFI/CMS investigation, ^{99}Tc was detected in 16 samples from six Investigation Sites/Groups. The maximum reported value was a non-detect result of 76 [BYUJ][1] pCi/g from Investigation Group L1+L2 at a depth of 35 m (115 ft) bgs (deep); however, the highest detected value was 53.5 [Y] pCi/g from Site U at a depth of 39 m (129 ft) bgs (deep).

Technetium-99 was detected in Phase 2 WMA C shallow and deep soil samples as follows.

- Shallow (≤ 5 m [15 ft] bgs) depths only: none.
- Deep (>5 m [15 ft] bgs) depths only: Investigation Groups A+B, F+G, L1+L2 and Sites R and U.

Both shallow (≤ 5 m [15 ft] bgs) and deep (> 5 m [15 ft] bgs) depths: Investigation Group P.

Technetium-99 was below detection at all other Investigation Sites/Groups and depths. At borehole C4297 (Phase 1 Characterization), ^{99}Tc was reported for 98 of 110 soil samples analyzed for radionuclides. All detectable results for ^{99}Tc were found at depths below 5 m (17 ft) bgs. Concentrations ranged from -8.48 pCi/g to 8.42 pCi/g, with the maximum concentration occurring at depth of 41.68 m (136.75 ft) bgs. Enriched or elevated concentrations of ^{99}Tc were found at depths between 12.4 and 20.9 m (40.8 and 66.2 ft) bgs and between 40.77 and 49 m (133.75 and 159 ft) bgs. At depths between 12.4 and 20.2 m (40.8 and 66.2 ft) bgs, ^{99}Tc was coincident with elevated concentrations of ^{238}U and ^{60}Co. Co-occurrence of maximum concentrations of ^{99}Tc and nitrate were observed between 41 and 46 m (135 and 150 ft) bgs.

[1] Flag(s) for laboratory qualifier on the results will be enclosed in []; please see Table 2-5 and HNF-38155, "HEIS Sample, Result, and Sampling Site Data Dictionary" for meaning on the laboratory qualifiers.

Table 2-5. Hanford Environmental Information System Laboratory Qualifier Table. (2 sheets)

A laboratory-generated character string containing codes in combinations that qualify the associated result. Different forms have different permitted combinations of valid qualifiers; however, B and U are mutually exclusive qualifiers on all forms. The valid qualifier codes and their translations are as follows.	
CODE	TRANSLATION
*	INORGANICS – Duplicate analysis not within control limits.
+	INORGANICS – Correlation coefficient for Method of Standard Additions is < 0.995.
>	WETCHEM – Result greater than quantifiable range or greater than upper limit of the analysis range.
A	ORGANICS – Valid for tentatively identified compounds (TICs) only: The TIC is a suspected aldol-condensation product.
B	INORGANICS and WETCHEM – The analyte was detected at a value less than the contract required detection limit, but greater than or equal to the instrument detection limit (IDL)/minimum detection limit (MDL) (as appropriate). ORGANICS – The analyte was detected in both the associated quality control (QC) blank and in the sample. RATIONUCLIDES (HEISPROD/PNLGW) – The associated QC sample blank has a result >= 2X the minimum detectable activity (MDA) and, after corrections, result is >= MDA for this sample. Surface Environmental Surveillance Project (SESP) – The associated QC sample blank has a result >= MDA and, after corrections, result is >= MDA for this sample.
C	INORGANICS/WETCHEM: The analyte was detected in both the sample and the associated QC blank, and the sample concentration was <= 5X the blank concentration. ORGANICS (PESTICIDE only) – The identification of a pesticide confirmed by gas chromatograph/mass spectrometer (GC/MS).
D	ORGANICS/WETCHEM – Analyte was identified in an analysis at a secondary dilution factor (i.e., dilution factor different than 1.0).
E	INORGANICS – Reported value is estimated because of interference. See comment on cover page, hardcopy case narrative, or specific FORM I. ORGANICS – Concentration exceeds the calibration range of the GC/MS. Not applicable for PESTICIDES/PCBs.
J	ALL – The reported value is an estimate. Analyte was analyzed for and detected, but has potentially larger associated error factors in the result. If this qualifier is applied for any reason other than results reported close to the analytical detection limit, an explanation must be provided in the associated hardcopy Sample Data Summary Package and/or case narrative.
L	MDL <= value < contract required quantitation limit (CRQL) [RETIRED]
M	INORGANICS – Duplicate precision criteria not met.
N	ALL (except GC/MS based analysis) – Spike sample recovery is outside control limits. ORGANICS (GC/MS only) – Presumptive evidence of compound based on mass spectral library search.
P	ORGANICS (PCB only) – Aroclor target analyte with greater than 25% difference between column analyses.
Q	ORGANICS (Dioxins only) – Estimated maximum concentration. Used if one of the qualitative identification criteria is not met (e.g., Cl isotopic rations outside theoretical range.)
S	INORGANICS – Reported value determined by the Method of Standard Additions.

Table 2-5. Hanford Environmental Information System Laboratory Qualifier Table. (2 sheets)

CODE	TRANSLATION
U	ALL – Analyzed for but not detected above limiting criteria. NOTE: Limiting criteria may be any of the following: value reported < 0; value reported < counting error; value reported < total analytical error; value_rptd <=contract MDL/IDL/MDA/practical quantitation limit (PQL).
W	INORGANICS – Post-digestion spike recovery for graphite furnace atomic absorption (GFAA) out of control limit. Sample absorbency < 50% of spike absorbency.
X	ALL – Other specific flags and notes required to properly qualify the result are described in the hardcopy Sample Data Summary Package and/or Case narrative. Additional information may be found in the RESULT_COMMENT field for this record.
Y	Same as X if more than one flag is required.
Z	Same as X and Y if more than two flags are required.
NOTE: If no qualifier code is reported with the analytical result, then the value reported is believed to be reliable without qualification.	
This Field is in the RESULT Table	

Nitrate: In the Phase 2 RFI/CMS investigation, nitrate was reported above background in eight samples at WMA C. The maximum concentration (198,000 µg/kg) was reported at Investigation Area Group F+G at a depth of 38 m (126 ft) bgs.

The distribution of concentrations above background for shallow and deep soils is as follows.

- Shallow (≤ 5 m [15 ft] bgs) depths only: Investigation Group H+I.
- Deep (>5 m [15 ft] bgs) depths only: Investigation Groups A+B, F+G, L1+L2, P, and Site U.
- Both shallow (≤ 5 m [15 ft] bgs) and deep (> 5 m [15 ft] bgs) depths: none.

Nitrate results for all other locations were less than background or were below detection.

At borehole C-4297 (Phase 1 Characterization), nitrate was detected in 51 of 72 soil samples with concentrations ranging from below detection to 19.5 µg/g (RPP-35484). The greatest number of nitrate detections were reported at depths below 18 m (60 ft) bgs. Only one of the 51 detected concentrations of nitrate (0.52 µg/g) was reported in shallow (≤5 m [15 ft] bgs) soil samples. The maximum nitrate concentration of 19.5 µg/g was reported at a depth of 41.68 m (136.75 ft) bgs. The highest concentrations of nitrate were reported between two depth intervals; between 40.77 and 41.68 m (133.75 and 136.75 ft) bgs, and between 46.2 and 49.15 m (151.6 and 161.25 ft) bgs. Elevated nitrate concentrations in the 40.77 and 41.68 m (133.75 and 136.75 ft) bgs interval were co-located with maximum concentrations of sulfate and calcium.

Sulfate: In the Phase 2 RFI/CMS investigation, sulfate was reported above background in three samples collected during Phase 2. The maximum concentration was 592,000 µg/kg from Investigation Group A+B at a depth of 4.3 m (14.2 ft) bgs (shallow).

Sulfate exceeded background in Phase 2 WMA C soils as follows.

- Shallow (≤ 5 m [15 ft] bgs) depths only: Investigation Group H+I.
- Deep (>5 m [15 ft] bgs) depths only: none.
- Both shallow (≤ 5 m [15 ft] bgs) and deep (> 5 m [15 ft] bgs) depths: Investigation Groups A+B.

Results for all other locations were less than background or were below detection.

At borehole C-4297 (Phase 1 Characterization), sulfate concentrations were reported for 72 soil samples. The highest concentrations of sulfate (80.9 µg/g to 104 µg/g) were reported at depths ranging from 40.77 to 41.68 m (133.75 and 136.75 ft) bgs, coincident with elevated concentrations of nitrate and calcium.

Chromium: Chromium, a dangerous waste constituent, was reported above background in 29 samples from nine Investigation Sites/Groups. The maximum concentration of chromium was 44,500 µg/kg from Site U at a depth of 48 m (158 ft) bgs (deep).

Chromium exceeded background in Phase 2 WMA C soils as follows.

- Shallow (≤ 5 m [15 ft] bgs) depths only: none.
- Deep (>5 m [15 ft] bgs) depths only: Investigation Groups A+B, F+G, H+I, L1+L2, and Sites C, E, and J.
- Both shallow (≤ 5 m [15 ft] bgs) and deep (> 5 m [15 ft] bgs) depths: Investigation Groups H+I, P, and Site U.

Chromium was not reported above background at Site R.

Cyanide: Cyanide was not detected or was detected below background at all locations during the Phase 2 soil investigation.

2.3.2.5.2 Slightly Sorbed Constituents (K_ds between 0.2 to 0.6 mL/g).

Iodine-129: In the Phase 2 RFI/CMS investigation, ^{129}I was detected in one sample at a concentration of 0.808 [B] pCi/g from Investigation Group P at a depth of 2 m (6 ft) bgs (shallow). Iodine-129 results for all other locations and depths were below detection. Note that ^{129}I contamination in groundwater is present throughout the east half of the 200 East Area and are believed to be from liquid waste facilities in the northern portion of the 200-PO-1 OU (DOE/RL-2011-01, Hanford Site Groundwater Monitoring Report for 2010).

Cobalt-60: Cobalt-60 was reported above background in 138 samples across all locations and depths. However, all results were reported as non-detects. The maximum reported concentration was 3.13 [U] pCi/g from Investigation Group P at a depth of 2 m (7 ft) bgs (shallow).

In borehole C-4297 (Phase 1 Characterization), low levels of ^{60}Co (<1 pCi/g) were found at depths from 12 to 20 m (40 to 65 ft) bgs.

Cobalt-60 is one of the key constituents indicative of tank waste contamination identified in gross gamma and spectral gamma logging in drywells and direct push boreholes. A summary of results for gross gamma and spectral gamma logging results relevant to ^{60}Co in drywells and direct push boreholes in each of the investigation areas of the RFI are discussed in Section 5.2 of the RFI (RPP-RPT-58339, Rev. A). All logs used in the RFI are provided in Appendix T of the RFI (RPP-RPT-58339, Rev. A).

Uranium: Uranium was reported above background in 44 samples from three Investigation Sites/Groups. All results were reported as non-detects. The maximum concentration was 101,000 U at Investigation Group P from a depth of 5 m (15 ft) bgs (shallow).

Uranium exceeded background in Phase 2 WMA C soil samples as follows.

- Shallow (≤ 5 m [15 ft] bgs) depths only: none.
- Deep (> 5 m [15 ft] bgs) depths only: none.
- Both shallow (≤ 5 m [15 ft] bgs) and deep (> 5 m [15 ft] bgs) depths: Investigation Groups F+G, L1+L2, P.

Uranium results for all other locations were less than background or were below detection.

2.3.2.5.3 Sorbed Constituents (K_d > 0.6 mL/g).

Cesium-137: Cesium-137 was reported above background in 34 samples from eight Investigation Sites/Groups. The maximum concentration was 73.1 pCi/g from Investigation Group P at a depth of 5 m (15 ft) bgs (shallow).

Cesium-137 exceeded background in Phase 2 WMA C soil samples as follows.

- Shallow (≤ 5 m [15 ft] bgs) depths only: Investigation Groups A+B, L1+L2, and Sites C, E, J, and U.
- Deep (> 5 m [15 ft] bgs) depths only: none.
- Both shallow (≤ 5 m [15 ft] bgs) and deep (> 5 m [15 ft] bgs) depths: Investigation Groups F+G and P.

Cesium-137 results for Investigation Group H+I and Site R were less than background or below detection.

In borehole C-4297 (Phase 1 Characterization), detailed characterization showed that ^{137}Cs was detected between the ground surface and 6 m (19 ft) in depth at concentrations up to 1,700 pCi/g. The log report states that the profile of the gamma log between 3 and 5 m (11 and 16 ft) bgs is suggestive of a point source of contamination such as a pipeline and may be waste inside a nearby pipeline. No significant ^{137}Cs activity was observed below the base of the tank.

Cesium-137 is one of the key constituents identified in spectral gamma logging in drywells and direct push boreholes. A summary of results for these logging results relevant to ^{137}Cs in drywells and direct push boreholes in each of the investigation areas of the RFI are discussed in Section 5.2 of the RFI (RPP-RPT-58339, Rev. A). All logs used in the RFI are provided in Appendix T of the RFI (RPP-RPT-58339, Rev. A).

Strontium-90: Strontium-90 was reported above background in 141 samples from all Investigation Sites/Groups. The maximum concentration was 141 pCi/g from Investigation Group P at a depth of 3 m (11 ft) bgs (shallow). Some results exceeding background were reported as non-detects.

Strontium-90 exceeded background in Phase 2 WMA C soil samples as follows.

- Shallow (≤ 5 m [15 ft] bgs) depths only: none.
- Deep (> 5 m [15 ft] bgs) depths only: Investigation Sites R, and U.
- Both shallow (≤ 5 m [15 ft] bgs) and deep (>5 m [15 ft] bgs) depths: Investigation Groups A+B, E, F+G, H+I, P, and Site J.

Tributyl Phosphate: Tributyl phosphate was not detected or was detected below background at all locations during the Phase 2 RFI/CMS investigation.

2.3.2.6 Moisture Content Results. Moisture content data from both neutron logging and laboratory analyses were collected during both Phase 1 and 2 characterization efforts of the RCRA facility investigation. A statistical summary of this moisture content data is provided here. The reader is referred to Appendix B for additional detailed information about this moisture content data and its use in the PA model development process.

The neutron logging data came from two drywells and 63 direct push boreholes. Laboratory measured moisture content (weight % converted to volumetric moisture content) came from one groundwater well (299-E27-22) and one characterization borehole (C4297).

The spacing for the neutron logging of moisture content varied from 0.05 m to 0.15 m (~0.15 ft to 0.5 ft). The spacing on the laboratory samples was greater. A total of 32,912 measurements were made and moisture content ranged from 0.11 to 30.64 volumetric percent, with a mean of 5.69 and a median of 5.09. Furthermore, the formations were identified in each

well/borehole/direct push and a statistical analysis of volumetric moisture content data was run for each formation (Table 2-6). The locations for the moisture content measurements are shown in Figure 2-21.

2.3.3 Unconfined Aquifer at Waste Management Area C

The unconfined aquifer underlying WMA C has been monitored on a quarterly basis since 1992. This section provides a summary of the flow conditions underlying WMA C, a brief description of the monitoring network, a summary of the contamination observed in the unconfined aquifer, and a brief interpretation of the results.

2.3.3.1 Groundwater Flow Conditions. The water table or potentiometric surface lies ~60 m (~200 ft) below the bottom of the tank farm excavations within the undifferentiated H_3/CC_u/RF located in the paleochannel (Figure 2-6 and Figure 2-12). The aquifer materials consist dominantly of sandy gravel or silty sandy gravel. The water table elevation beneath WMA C is ~122 m (400 ft) North American Vertical Datum of 1988 (NAVD88) with ~77 m (255 ft) of vadose zone. The aquifer thickness, based on the top of basalt at 108 m (355 ft), is ~13.4 m (44 ft).

Scouring of suprabasalt sediments in the paleochannels is evident in that, along much of its path, only the Hanford formation overlies the top of the basalt (Figure 2-6). Hanford formation material makes up almost entirely the material within the paleochannels in general, as well as all of the material within the paleochannel at the WMA C water table. Removal of pre-Hanford formation suprabasalt sediments, with the possible exception of a thin layer of CCu beneath the eastern half of WMA C, is apparent. This suggests that the width of the paleochannel beneath WMA C is over 500 m. Wells 299-E27-14 and 299-E27-15 penetrate the Hanford formation within the paleochannel beneath WMA C.

Hydraulic conductivity values reported for the aquifer in this area vary considerably, ranging from 0.04 (silt lenses within the sandy gravel) to 6,900 m/day (0.13 to 22,640 ft/day). Additional hydraulic property data from aquifer testing at wells near WMA C is provided in RPP-RPT-46088. More recently, additional large-scale hydraulic property data are derived from The Central Plateau Groundwater Model (CPGWM) (CP-47631, "Model Package Report: Central Plateau Groundwater Model Version 3.3," Rev. 0) incorporates the large-scale geologic and hydrogeologic features, and provides estimates of water levels, hydraulic gradients, and groundwater flows throughout the 200 West and 200 East Areas for current and expected future groundwater conditions. The CPGWM provides calibrated hydraulic conductivity estimates for the model layers and HSUs present within the aquifer in the vicinity of WMA C. The thicknesses of the different aquifer HSUs are mapped from the CPGWM onto the WMA C RCRA closure analysis model flow domain. An averaging scheme weighted according to HSU thickness provides estimates of the equivalent homogeneous medium (EHM) effective saturated hydraulic conductivity and the hydraulic gradient. The weighted average of hydraulic conductivity of the CPGWM HSUs mapped onto the WMA C flow domain indicates that the effective saturated hydraulic conductivity is ~11,000 m/day.

Table 2-6. Summary Statistics for Volumetric Moisture Content in the Lithologic Units Underlying Waste Management Area C.

Unit	Count of Wells	Count of Measurements	Minimum (Vol %)	Maximum (Vol %)	Average (Vol %)	Median (Vol %)	Mode (Vol %)	Standard Deviation	Variance
Backfill	52	4,052	0.11	30.61	8.09	7.48	6.20	3.71	13.75
H1	66	7,977	0.13	30.64	5.88	4.72	3.26	3.67	13.47
H2	64	20,876	1.06	26.32	5.15	4.96	4.89	1.82	3.30
H3	1	7	5.54	7.09	6.18	6.01	Too Few	0.65	0.43
Waste Management Area C	67	32,912	0.11	30.64	5.69	5.09	4.89	2.82	7.95

Figure 2-21. Moisture Content (% Vol) Measurements in Vadose Zone at Waste Management Area C.

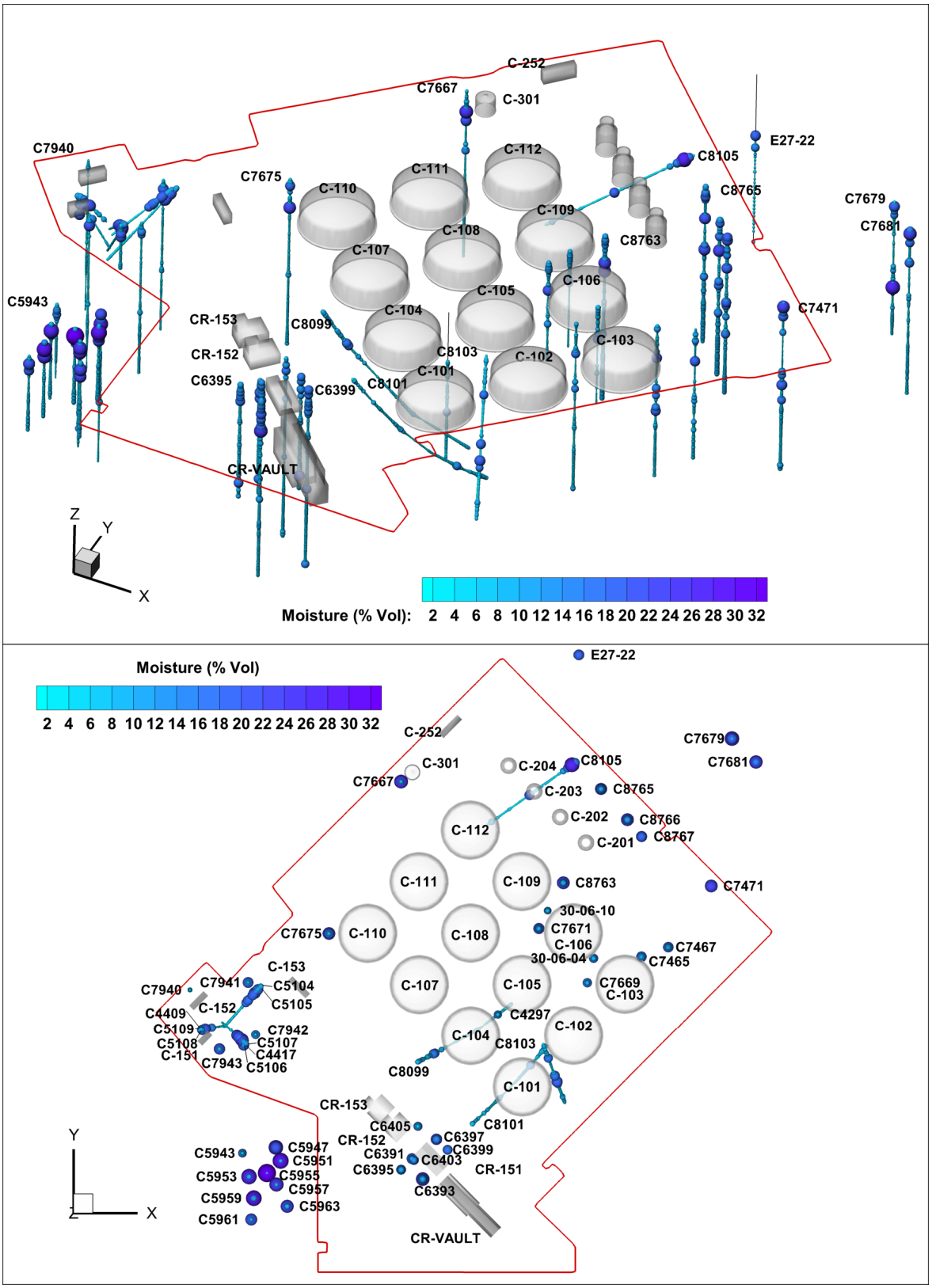

Currently, the general groundwater flow direction in the unconfined aquifer beneath WMA C is to the south/southeast. The water table is very flat overall, with an estimated hydraulic gradient between 1×10^{-5} to 2×10^{-5} m/m; the estimated groundwater flow velocity ranges from 0.2 to 0.4 m/day (0.7 to 1.3 ft/day) (RPP-RPT-46088). Those hydraulic gradient estimates are also consistent with those recently reported in SGW-54165, "Evaluation of the Unconfined Aquifer Hydraulic Gradient Beneath the 200 East Area, Hanford Site" for the unconfined aquifer near the Integrated Disposal Facility (IDF) and PUREX cribs. Also coincident with the flow change are decreasing concentrations of other contaminants in monitoring wells west of C Farm, indicating a change in flow direction. These observations and other interpretations discussed in SGW-58561, "WMA C Quarterly October through December 2014 Quarterly Groundwater Monitoring Report" provide sufficient evidence for the determination of a south to southeast flow direction at WMA C. These estimates are also consistent with the CPGWM.

The discharge of large volumes of wastewater in the early 1950s to B Pond (Figure 2-8) raised the water table in the vicinity of WMAs C and A-AX as much as 4.9 m (16 ft) above the pre-Hanford Site operations level (PNNL-14548, "Hanford Site Groundwater Monitoring for Fiscal Year 2003"). The corresponding flow direction underneath WMA C at this time was toward the southwest (DOE/ORP-2008-01 Appendix H). Water levels began to decline in the late 1980s when wastewater discharges were reduced. The decline has become even more pronounced since other effluent discharges throughout the 200 Areas ceased in 1995 (Figure 2-11). Water levels are expected to continue declining within the region surrounding WMAs A-AX and C, with the flow direction changing to the southeast. With the change in flow direction, contamination originating in the B Complex in the northwest corner of 200 East may flow underneath WMA C in the not too distant future.

The recent gradual northward shift of the groundwater divide has important implications for the direction and rate of groundwater flow and contaminant transport. The divide and its movement are significant because it has changed the direction in which contaminants migrate in the 200-BP-5 Groundwater OU in the vicinity of WMA C. The exact location of the current groundwater divide is uncertain because of the extremely flat surface of the water table. As artificial recharge has been significantly reduced in recent years, groundwater levels have declined, though the rate of decline has slowed in recent years. Declining water levels and changes in discharge practices are certainly affecting contaminant concentrations and contaminant migration patterns in the 200-BP-5 Groundwater OU (DOE/RL-2008-66).

2.3.3.2 Groundwater Monitoring. Quarterly groundwater monitoring was initiated at WMA C in 1992 in accordance with WHC-SD-EN-AP-012, "Interim-Status Groundwater Monitoring Plan for the Single-Shell Tanks." The initial well network consisted of five wells: 299-E27-7, 299-E27-12, 299-E27-13, 299-E27-14, and 299-E27-15 (see Figure 2-17). These wells were used for quarterly groundwater monitoring beginning in March 1992 and continued until the Fall of 1993. In the Spring of 1994, semi-annual sampling began for indicator parameter evaluation. Monthly sampling began in June 1998 to prepare for sluicing at tank C-106. The monthly sampling was scaled back to bi-monthly in 2000 and then returned to quarterly sampling in 2001. In 2001, a new monitoring plan, PNNL-13024, "RCRA Groundwater Monitoring Plan for Single-Shell Tank Waste Management Area C at the Hanford Site," was initiated and required additional wells to ensure adequate monitoring network

coverage for WMA C. Wells 299-E27-4, 299-E27-21, 299-E27-22, and 299-E27-23 (Figure 2-17) were subsequently added to the network.

In 2009, WMA C was placed in assessment monitoring because of the exceedance of the critical mean for the indicator parameter specific conductance. In addition, the dangerous constituent cyanide has been found in groundwater beneath WMA C, albeit at levels much lower than the DWS. To meet quarterly RCRA assessment requirements, a new monitoring plan (DOE/RL-2009-77, Groundwater Quality Assessment Plan for the Single-Shell Tank Waste Management Area C) was developed which superseded PNNL-13024. Currently, assessment monitoring is being completed in accordance with DOE/RL-2009-77. Three wells (299-E27-24, 299-E27-25, and 299-E27-155; see Figure 2-17) were added to the network per DOE/RL-2009-77. Well 299-E27-25 is not shown on Figure 2-17; it is located ~170 m (~550 ft) northeast of the northeast fenceline of WMA C. The WMA C groundwater monitoring network now is composed of the following 12 wells:

299-E27-4	299-E27-7	299-E27-12	299-E27-13	299-E27-14	299-E27-15
299-E27-21	299-E27-22	299-E27-23	299-E27-24	299-E27-25	299-E27-155

In addition to meeting the quarterly assessment requirements, quarterly monitoring is also done to meet the requirements of External letter 04-TPD-083, "Agreement on Content of Tank Waste Retrieval Work Plans," in which quarterly groundwater monitoring sample results are to be provided to Ecology during tank retrievals. To meet the sampling requirements, the groundwater monitoring analyses include RCRA and AEA constituents from the following: anions, cyanide, metals ^{99}Tc, gross beta, total uranium, and low-level gamma scan. The most recent quarterly monitoring report is SGW-59669, "WMA C Quarterly October Through December 2015 Quarterly Groundwater Monitoring Report."

2.3.3.3 Groundwater Contamination. In SGW-59669, the results of sampling for 129 constituents across the WMA C monitoring network are provided. In that report, six analytes (cyanide, nickel, nitrate, sulfate, ^{99}Tc, and uranium) are discussed in detail.

Table 2-7 provides summary statistics for these analytes for the past ten years. It also identifies the date at which the maximum for a particular analyte was collected and in which monitoring well the maximum was collected.

Observations of elevated concentrations of nitrate, sulfate, and ^{99}Tc appear to be associated with past releases from WMA C because these constituents are much higher in the downgradient wells compared to upgradient wells, and they exceed their respective groundwater DWSs/maximum contaminant levels (MCLs). Additionally, cyanide, which is a dangerous waste constituent, is also found in the aquifer at levels above detection limit, but well below the DWS of 200 µg/L. The measured cyanide concentration was 14.9 µg/L in December 2015 at well 299-E27-14. Only ^{99}Tc, nitrate, sulfate, and cyanide are discussed further in this section. Technetium-99 exceeded the DWS by a factor of almost 30 and cyanide is a dangerous waste constituent. For discussions and interpretations of the overall trends of other constituents in monitoring wells in the vicinity of WMA C, the reader is referred to SGW-59669.

Technetium-99: In December 2015, ^{99}Tc had concentrations exceeding the 900 pCi/L DWS in 7 of the 11 monitoring wells surrounding WMA C (Figure 2-22). However, in 2006 only 4 of the 11 wells exceeded the DWS. Three of these wells (299-E27-4, 299-E27-13, and 299-E27-23) are located just outside the south central region of WMA C (Figure 2-17). The other well that exceeded the DWS is 299-E27-14, located east of WMA C. Two new wells (299-E27-155 and 299-E27-4) placed to the south and east of WMA C after 2006 also showed ^{99}Tc concentrations above the DWS when they were installed. The ^{99}Tc in the groundwater in that region appears to be centered on well 299-E27-23 with the trend in that well increasing from ~5,000 pCi/L in late 2006 to ~26,000 pCi/L by April 2012. Since then, the trend at the well has been decreasing, falling to ~3,400 pCi/L by December 2014. This decline is associated with changes in the flow direction to the east and southeast. The resulting change in flow direction and sampling in downgradient wells (299-E27-21) from 299-E27-23 show ^{99}Tc increasing in this well, indicating plume movement to the east-southeast. The highest ^{99}Tc found in WMA C was in December of 2015 with a value of 26,700 pCi/L at well 299-E27-21. At well 299-E27-14, ^{99}Tc values ranged between 1,500 and 2,600 pCi/L from 2006 to late 2012. However, in early 2013 they started increasing, peaking in June of 2013 at 10,700 pCi/L and decreasing since then; they had decreased to 2,620 pCi/L by December 2015. Finally, well 299-E27-24 (installed in 2010) shows an initial ^{99}Tc concentration of 2,100 pCi/L that raises to a peak of 5,100 pCi/L in September of 2013, with it slowly dropping to 3,800 pCi/L in December 2015. It is believed the ^{99}Tc found at wells 299-E27-14 and 299-E27-24 is from a different source than ^{99}Tc found in the south central region of WMA C (299-E27-4, 299-E27-21, and 299-E27-23). The specific sources (i.e., tank and/or pipeline) of ^{99}Tc in the groundwater at WMA C has not been identified.

Wells 299-E27-24 and 299-E27-155, which are screened along the bottom of the unconfined aquifer, indicate that ^{99}Tc has migrated throughout the unconfined aquifer. Contamination has also reached the bottom of the aquifer. Depth-discrete samples were taken from wells 299-E27-4, 299-E27-21, and 299-E27-23 in 2010. Like well 299-E27-155, which had depth-discrete samples taken during drilling, the samples taken at wells 299-E27-4 and 299-E27-21 showed increasing contamination with depth. Well 299-E27-23 generally had steady concentrations of around 20,000 pCi/L throughout its depth profile.

Nitrate: General trends for nitrate in wells in the vicinity of WMA C are provided in Figure 2-23. Nitrate concentrations at eight WMA C wells have exceeded 45 mg/L MCL over the past 10 years. Two of the three wells, 299-E27-14 and 299-E27-24, are downgradient of WMA C. The greatest nitrate concentration (118 mg/L) was at well 299-E27-14 in 2012, located on the southeast side of WMA C. Based on concentrations at well 299-E27-24, which was installed in the lower portion of the unconfined aquifer ~66 m (216.5 ft) south of well 299-E27-14 in 2010, the plume extends throughout the 15.5-m (50.9-ft)-thick aquifer. The nitrate concentrations in well 299-E27-24 have been stable, ranging between 65.5 and 73.5 mg/L since sample collection began in 2010. Wells slightly in the southern part of the WMA C farm, (299-E27-4, 299-E27-21, and 299-E27-21) only slightly exceed the MCL ranging between ~35 to 50 mg/L. Well 299-E27-155 was installed in the last quarter of 2007. Nitrate values from this well stayed at ~50 mg/L from 2008 to the beginning of 2014 before dipping 24 mg/L in late 2013, then raising to 66 mg/L at the end of 2015. In addition to these wells, an upgradient monitoring well (off the map to the north of WMA C) was installed in 2010. The nitrate trend in this well has shown a steady increase from 36 mg/L (April 6, 2010) to over 57 mg/L

(December 10, 2015). This well is cross gradient of WMA C and is affected by migrating contaminant plumes to the north.

Currently, nitrate concentrations do not exceed the DWSs in upgradient wells (299-E27-7, 299-E27-22, and 299-E27-25), suggesting a source within C Farm. Furthermore, nitrate concentrations at well 299-E27-14 are more than double past and present upgradient well concentrations.

Sulfate: General trends for sulfate in wells in the vicinity of WMA C are provided in Figure 2-24. Over the past 10 years, sulfate concentration exceeded the secondary MCL for sulfate of 250 mg/L in only three wells (299-E27-7, 299-E27-14, and 299-E27-24). For well 299-E27-7, it was a one-time occurrence in February 2016. From June 2010 to December 2015, sulfate concentrations do not exceed the DWSs in upgradient wells 299-E27-7 and 299-E27-14 which suggests a source of sulfate within C Farm. However, in upgradient well 299-E27-25, sulfate starting exceeding the secondary MCL for sulfate of 250 mg/L in December 2010 with a value of 259 mg/L, and by December 2015 has gradually increased 320 mg/L. This upstream sulfate plume may impact WMA C sometime in the future.

Cyanide: The dangerous waste constituent cyanide was detected at four WMA C wells in December 2014 at concentrations far below the 200 µg/L DWS. A possible reason for the increased number of wells with detectable cyanide between June and December 2014 is that the detection limit for cyanide decreased from 4 to 1.67 µg/L. In December of 2015, two wells (299-E27-14 and 299-E27-24) had concentrations approaching 15 µg/L, while two wells (299-E27-4 and 299-E27-23) had concentrations at or below 5 µg/L (Figure 2-25). The other well (299-E27-7) had historically the highest value (40.7 µg/L) in 2009, but levels had fallen in that well to less than 5 µg/L by 2012. Concentrations at well 299-E27-4 are generally near the detection level but were higher in December of 2009, 2011, and 2014 (10.4, 7.98, and 7.9 µg/L, respectively). Remnant levels of low cyanide concentrations appear to be present sporadically beneath the eastern and western portions of the C Farm facility, while more persistent concentrations exist to the southeast (wells 299-E27-14 and 299-E27-24) as can be seen in Figure 2-25. As discussed in DOE/RL-2009-77, the source is likely be related to past releases from WMA C, but a specific tank/leak source within WMA C has not been identified.

2.3.4 Recent Interpretations of Waste Management Area C Groundwater Chemistry

This section summarizes results of evaluation of ~10 years of analytical groundwater data as part of an effort by the BP-5 Remedial Investigation (RI) that examined recent impacts to groundwater at WMA C. This specific evaluation was used to support one of two approaches in the BP-5 RI to estimate the magnitude of potential fluxes from the vadose zone at WMA C to groundwater based on the evaluation of recent data and information collected at wells located in the vicinity of WMA C. The estimates of contaminant fluxes developed as a part of these efforts were used in the BP-5 RI as a basis for source term estimated used in contaminant fate and transport model simulations that examine the potential for future impacts to groundwater from continuing sources within the vadose zone resulting from past tank waste releases at WMA C. The specific evaluation of groundwater data and information provided in this subsection is described in ECF-Hanford-13-0037, “Development of Source Terms for Inclusion in Fate and

Transport Modeling for Remedial Investigation/Feasibility Studies of the 200-BP-5 and 200-PO-1 Groundwater Operable Units." The results of the contaminant fate and transport modeling are described in detail in ECF-Hanford-13-0031, "Fate and Transport Modeling for Baseline Conditions for Remedial Investigation/Feasibility Studies of the 200-BP-5 and 200-PO-1 Groundwater Operable Units."

2.3.4.1 Technical Approach. The concentration trends used in this evaluation were based on the last 10 years of concentrations in groundwater monitoring wells in the vicinity of WMA C. The focus of this approach was on large changes in concentrations for selected analytes—^{99}Tc, nitrate, sulfate, and chloride—that provide insight into relative contribution from past releases from WMA C. The following steps were undertaken in this calculation approach.

- Year 2008, 2010, and 2012 datasets were selected for this calculation. The groundwater concentrations of ^{99}Tc, nitrate, sulfate, and chloride were analyzed for these years. Time histories for the first three analytes are presented in Figure 2-22. Trends for chloride are not provided here but can be found in ECF-Hanford-13-0037. These trends are described as part of the groundwater contamination section.

- Identified possible plume source areas for ^{99}Tc within the WMA C aquifer.

- The median concentration values were calculated for each analyte for each year and bivariate plots were drawn for the analytes. The bivariate plots with median concentrations were developed and evaluated to identify overall trends in chemistry and calculate mixing lines between the end-member waters and upgradient water types.

- Used information based on bivariate plots and dilution lines along with the long-term observed concentration trends to identify different plume source zones that could be influencing concentration trends seen in monitoring wells in the vicinity of WMA C.

- Provided estimates of ^{99}Tc fluxes to the unconfined aquifer.

2.3.4.2 Technetium-99 Source Areas within the Groundwater at Waste Management Area C. Well data suggest two sources for the contamination: one on the western side of WMA C, which appears to be migrating to the southeast as of 2012, and one in the southeast of WMA C. The wells which can be associated with the southeastern plume are 299-E27-14, 299-E27-24, and 299-E27-7. The wells associated with the western plume are 299-E27-13, 299-E27-23, and 299-E27-4. The data suggest that the contamination in the southeast comes from a different source than the contamination in the west. The three major lines of evidence for this are as follows.

- The concentration trends are different: the southeastern wells 299-E27-14 and 299-E27-24 display a nearly stable ^{99}Tc trend (Figure 2-26), while the western wells 299-E27-13 and 299-E27-23 show increasing values from approximately 2000 to 2010, then decreasing from approximately 2010 to 2015 (Figure 2-27).

- The ^{99}Tc-to-nitrate ratios are different: the southeastern wells 299-E27-14 and 299-E27-24 display a nearly stable ^{99}Tc-to-nitrate ratio of ~50 through 2012. Wells beneath the BY crib display a similar ratio, suggesting a similar source material. The western wells 299-E27-13 and 299-E27-23 show a five-fold increase in the ^{99}Tc-to-nitrate ratio after 2008 (Figure 2-28).

- There is more cyanide present in the southeast than the west: wells 299-E27-14 and 299-E27-24 are impacted by a ferrocyanide-derived waste, while analysis of the contamination in the western wells is more representative of a PUREX-derived liquid waste (Figure 2-25).

A change in groundwater flow appears to have shifted the center of the western plume. From 2012 to 2013, the center of the western plume seems to have shifted from well 299-E27-23 to 299-E27-21 (Figure 2-13). The ^{99}Tc concentration increases at well 299-E27-21 as it decreases in well 299-E27-23. Furthermore, the technetium-to-nitrate ratio at the presumed new center of the plume in well 299-E27-21 was, in December 2013, nearly identical to the technetium-to-nitrate ratio at well 299-E27-23 near its peak in 2010, indicating a change in groundwater flow direction sometime in mid-2011.

Technetium-99, the contamination to the southeast of WMA C appears to be sourced from ferrocyanide-derived waste. The highest concentrations of nitrate occur in the southeast as well, near well 299-E27-14. From a measurement of 12.4 mg/L in Fall 1998, the concentrations at well 299-E27-14 increased until finally reaching the DWS in 2003, with peaks occurring in the Fall after 2006 (Figure 2-23). Nitrate concentrations at well 299-E27-24, which is ~60 m south of well 299-E27-14, average ~70 mg/L, ~20 to 30 mg/L less than those at well 299-E27-14. The cyanide-to-nitrate ratio indicates these wells are contaminated from a local, similar source (Figure 2-29).

2.3.4.3 Evaluation of Bivariate Plots and Mixing Lines Using Selected Chemical Concentration Ratios. Following is a brief discussion of results of the bivariate plot and mixing line evaluation for ^{99}Tc/nitrate versus nitrate and ^{99}Tc/sulfate versus sulfate summarized in ECF-Hanford-13-0037. An evaluation of bivariate and mixing lines for nitrate/chloride versus chloride was also done as a part of the ECF-Hanford-13-0037 analysis but is not provided in the section. The reader is referred to ECF-Hanford-13-0037 for more information on the latter analysis.

2.3.4.3.1 Evaluation of Technetium-99/Nitrate Ratio Versus Nitrate. Bivariate plots of ^{99}Tc/nitrate ratio versus nitrate by year, provided in Figure 2-30, were used to examine overall trends in these specific constituents and evaluate mixing lines between the end-member waters and upgradient water types.

From the bivariate plots of ^{99}Tc/nitrate versus nitrate, three different end-member waters (reflecting varying sources) were identified and mixing lines were calculated between the end-member waters and the upgradient water type characterized in this case by chemical concentrations found in well 299-E27-12.

In 2008, the characteristics of the end-member waters were associated with wells 299-E27-23, 299-E27-155, and 299-E27-14. The concentrations from wells that fall along the mixing lines can be explained by dilution of the end-member water with the uncontaminated upgradient water.

By 2010, bivariate plots show end-member waters were still associated with wells 299-E27-23, 299-E27-155, and 299-E27-14. However, because of large increases in ^{99}Tc observed in well 299-E27-23 and associated with well 299-E27-13, the magnitude of the ratios for these two wells are much larger than seen in 2008.

By 2012, bivariate plots show end-member waters were still associated with wells 299-E27-23, 299-E27-155, and 299-E27-14. However, some shifting of the position of two wells, 299-E27-13 and 299-E27-21, is observed. With the decline in ^{99}Tc concentrations in 299-E27-13, the position of this well shifts to come closer to the mixing line between 200-E27-12 and 299-E27-155. As ^{99}Tc concentrations begin to increase in well 299-E27-21, its position on the plot shifts from the mixing line between 299-E27-12 to 299-E27-14 to a location just above the mixing line between 200-E27-12 and 299-E27-155.

By 2013, bivariate plots show some shifts in some of the wells in response to changing ^{99}Tc concentration levels in wells 299-E27-23 and 299-E27-21 that result from changing groundwater conditions from a southwesterly flow to a more south-southeast direction. By 2013, end-member waters are associated with wells 299-E27-21, 299-E27-155 and 299-E27-4, and 299-E27-14. At this time, well 299-E27-23 fell on the mixing line between 299-E27-12 and 299-E27-21. The increase in ^{99}Tc/nitrate ratios in wells 299-E27-14 and 299-E27-24 seems to correlate with corresponding increasing ^{99}Tc concentrations in these wells in 2013.

2.3.4.3.2 Evaluation of Technetium-99/Sulfate Ratio Versus Sulfate. To complement the bivariate plots of ^{99}Tc/nitrate versus nitrate presented in the previous section, the BP-5 RI evaluation also examined bivariate plots of ^{99}Tc/sulfate versus sulfate. The resulting bivariate plots of these constituents are provided in Figure 2-31.

From the bivariate plots of ^{99}Tc/sulfate versus sulfate, three different end-member waters (reflecting varying sources) were also identified and mixing lines were calculated between the end-member waters and the upgradient water type characterized by chemical concentrations found in well 299-E27-12. The identification of three different end members and the shifting of the relative positions of wells among the mixing lines were nearly identical to those found using the ^{99}Tc/nitrate versus nitrate plots. This is supporting evidence in the strong correlation of nitrate and sulfate in this evaluation.

2.3.4.3.3 Nitrate/Chloride Ratio Versus Chloride. The BP-5 RI also examined bivariate plots of nitrate/choride versus chloride to evaluate overall trends in these specific constituents. Results of these bivariate plots by year are provided in Figure 2-32.

Table 2-7. Summary Statistics from January 1, 2006 to January 1, 2016 for Constituents Discussed in SGW-59669*.

Constituent	Maximum	Minimum	Average	Standard Deviation	Unit	Maximum Collected on	Maximum Found at Well	Filtered	Location Count	Location Count Detect	Count	Rejects	Detects
Cyanide	41	1.8	9.5	7.2	µg/L	6/11/2009	299-E27-7	N	12	12	488	7	185
Nickel	191	0.47	12	16	µg/L	9/4/2015	299-E27-4	Y	12	12	476	5	191
Nickel	293	0.23	16	24	µg/L	9/4/2015	299-E27-4	N	12	12	426	6	212
Nitrate	118,000	8,280	37,771	21,262	µg/L	9/7/2012	299-E27-14	N	12	12	509	4	505
Sulfate	345,000	45,600	162,980	75,535	µg/L	5/14/2010	299-E27-24	N	12	12	509	5	504
Tc-99	26,700	7.0	3,854	5,496	pCi/L	12/8/2015	299-E27-21	N	12	11	498	3	460
Uranium	9.9	3.4	5.5	2.3	µg/L	12/10/2013	299-E27-155	Y	12	12	18	1	17
Uranium	10.8	1.8	3.8	1.6	µg/L	9/7/2012 & 3/6/2013	299-E27-14	N	12	12	445	11	434

* Values reported do include those that are suspect or have been rejected by user.

Reference: SGW-59669, "WMA C Quarterly October Through December 2015 Quarterly Groundwater Monitoring Report."

Figure 2-22. Technetium-99 Concentrations above the Drinking Water Standard at Waste Management Area C Wells from January 2006 through December 2015.

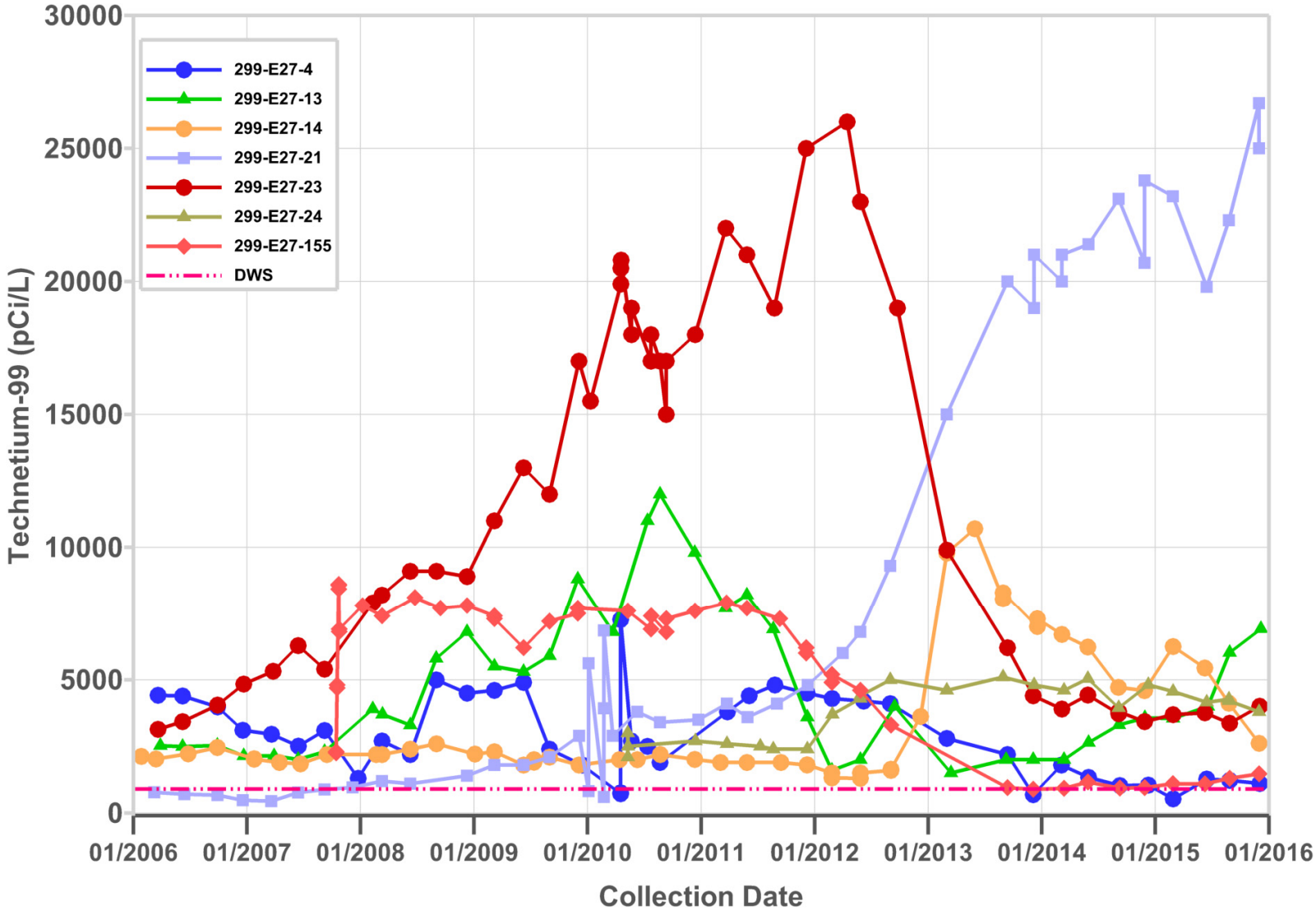

DWS = drinking water standard

Figure 2-23. Nitrate Concentrations above the Maximum Contaminant Level at Waste Management Area C Wells from January 2006 through December 2015.

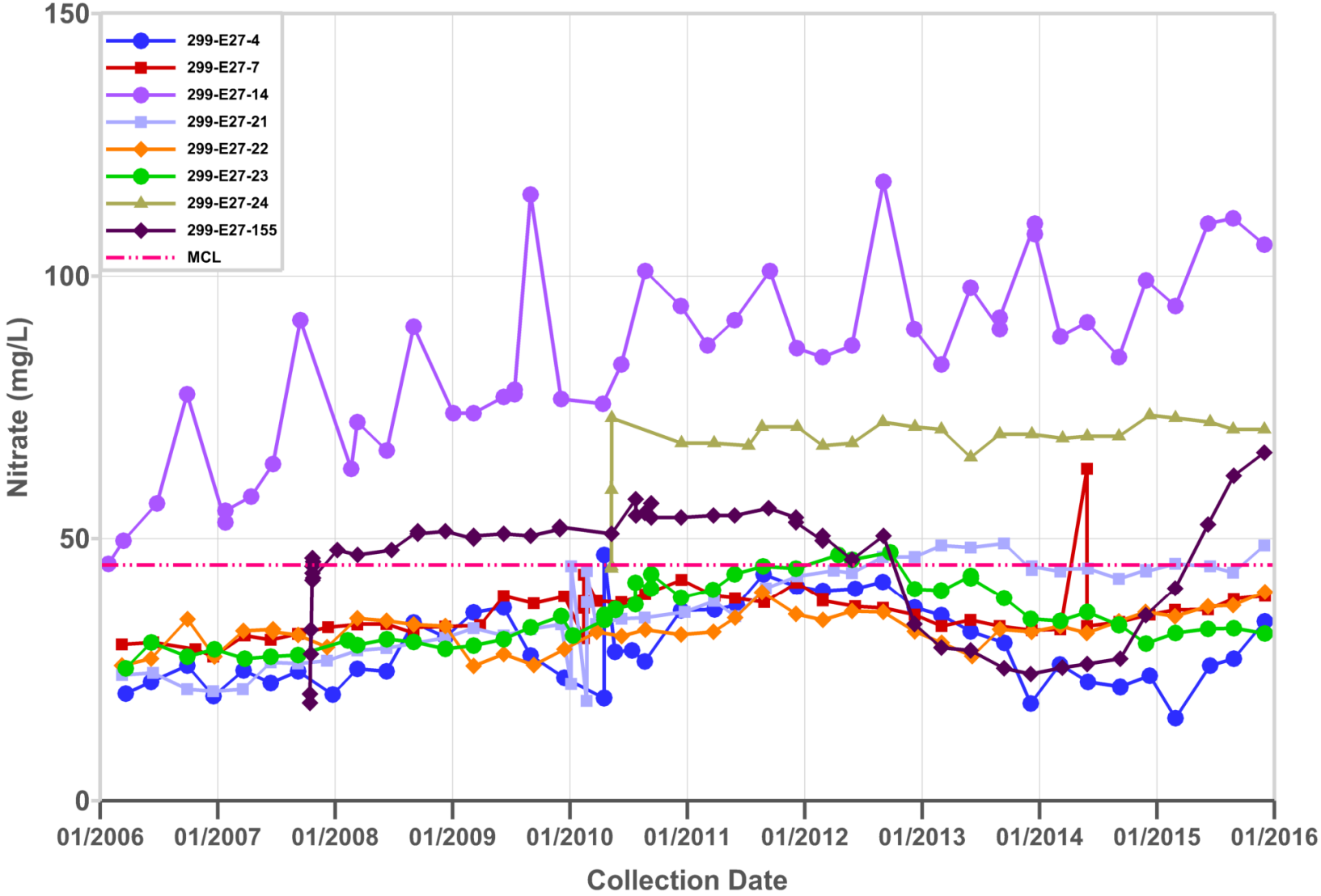

MCL = maximum contaminant level

Figure 2-24. Sulfate Concentrations above the Secondary Maximum Contaminant Level at Waste Management Area C Wells from January 2006 through December 2015.

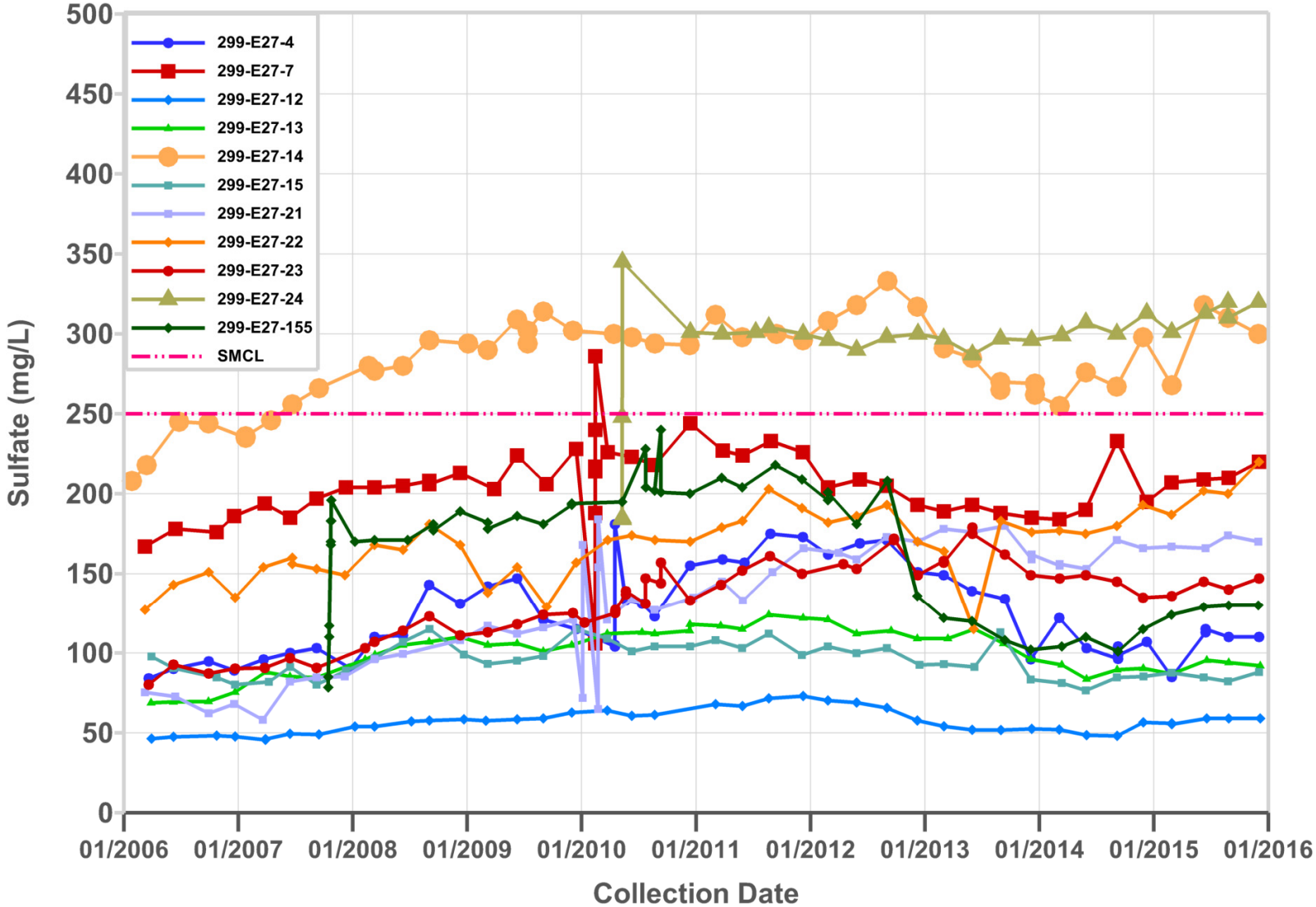

SMCL = Secondary maximum containment level

Figure 2-25. Cyanide Concentrations in Waste Management Area C Wells from January 2006 through December 2015.

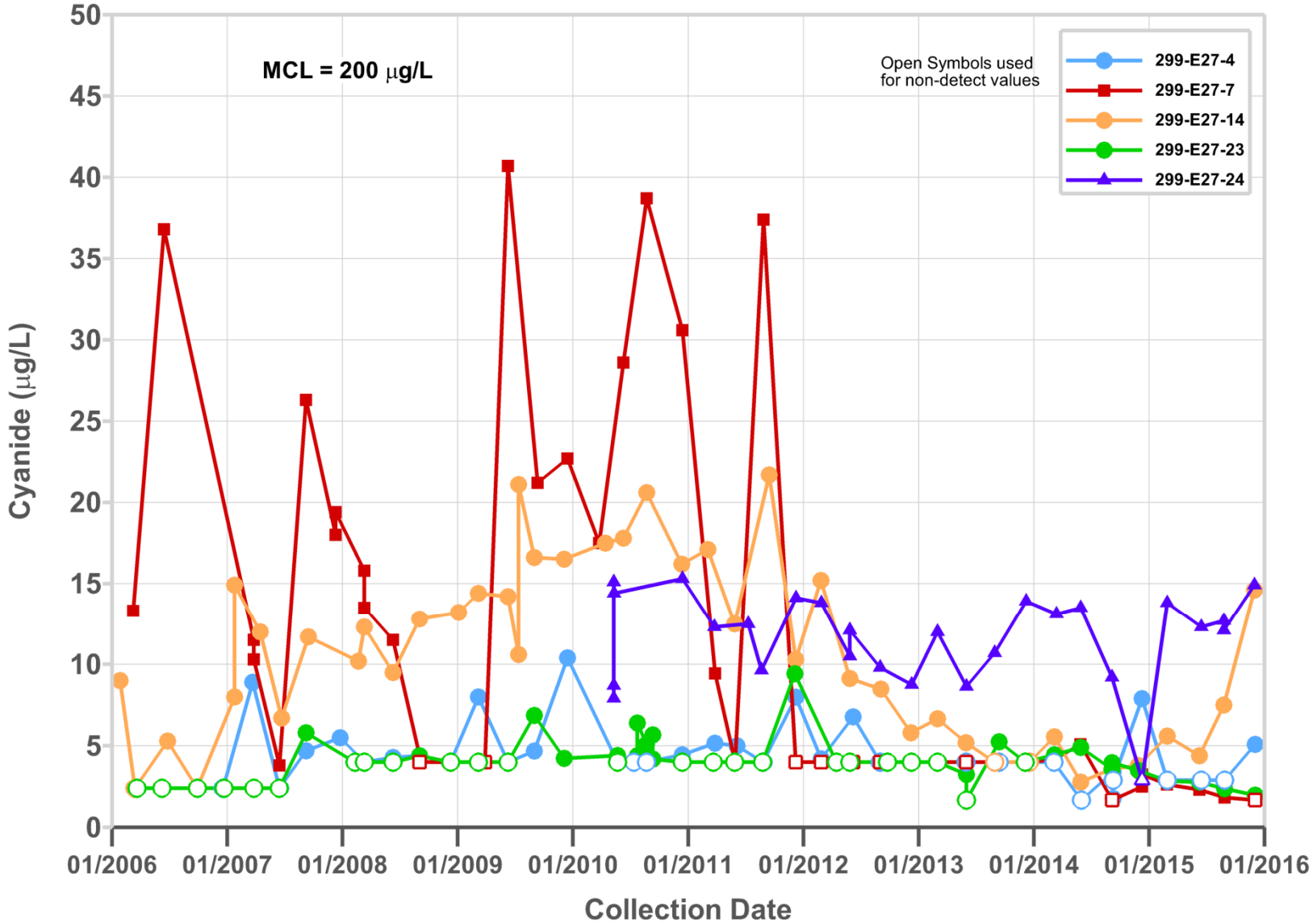

MCL = maximum contaminant level

Figure 2-26. Technetium-99 Activity in Wells 299-E27-7, 299-E27-14, and 299-E27-24 on East and Southeast Side of Waste Management Area C.

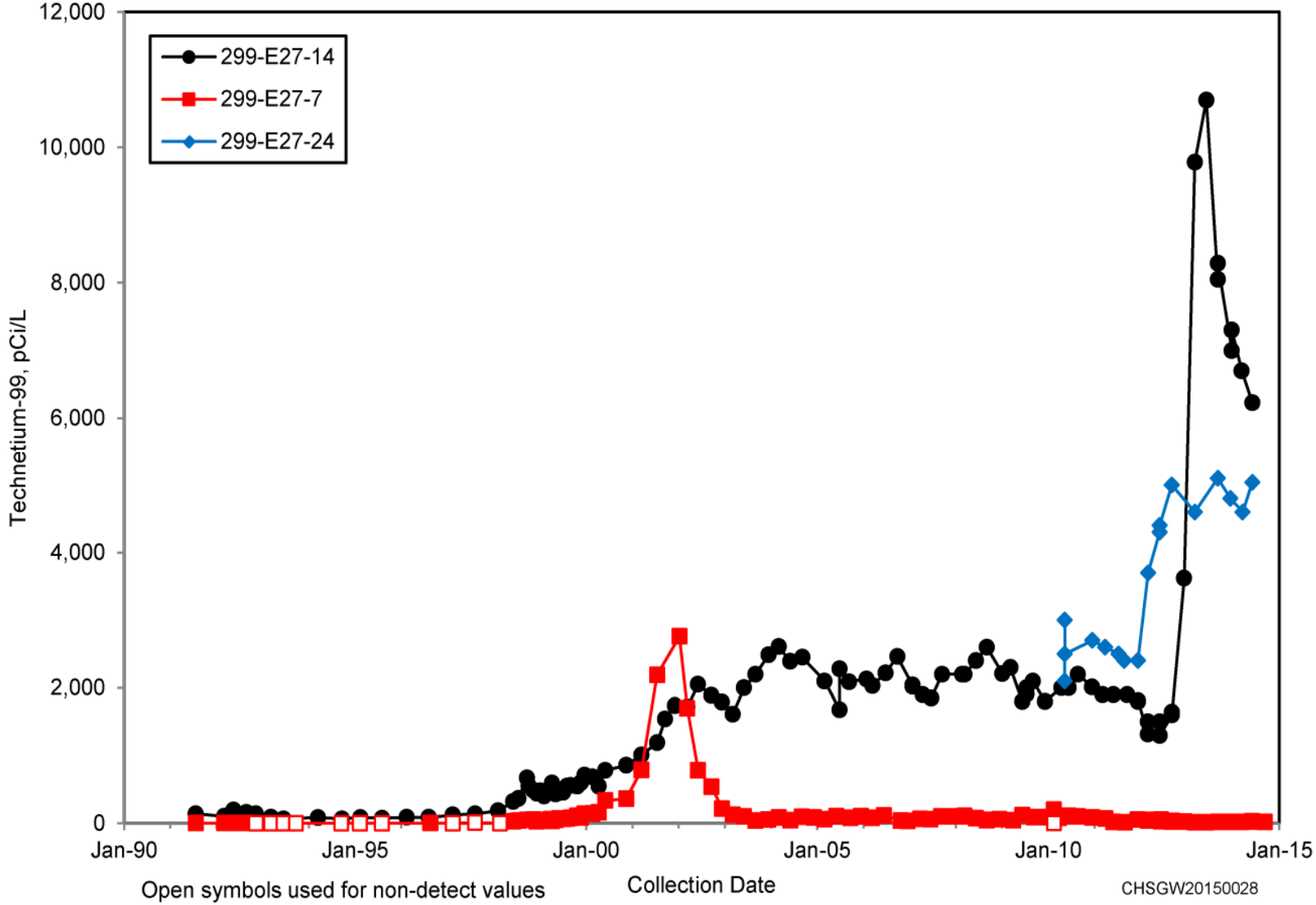

Source: DOE/RL-2009-127, Remedial Investigation Report for the 200-BP-5 Groundwater Operable Unit, Draft A.

Figure 2-27. Technetium-99 Activity in Wells 299-E27-4, 299-E24-13, and 299-E27-23 on West Side of Waste Management Area C.

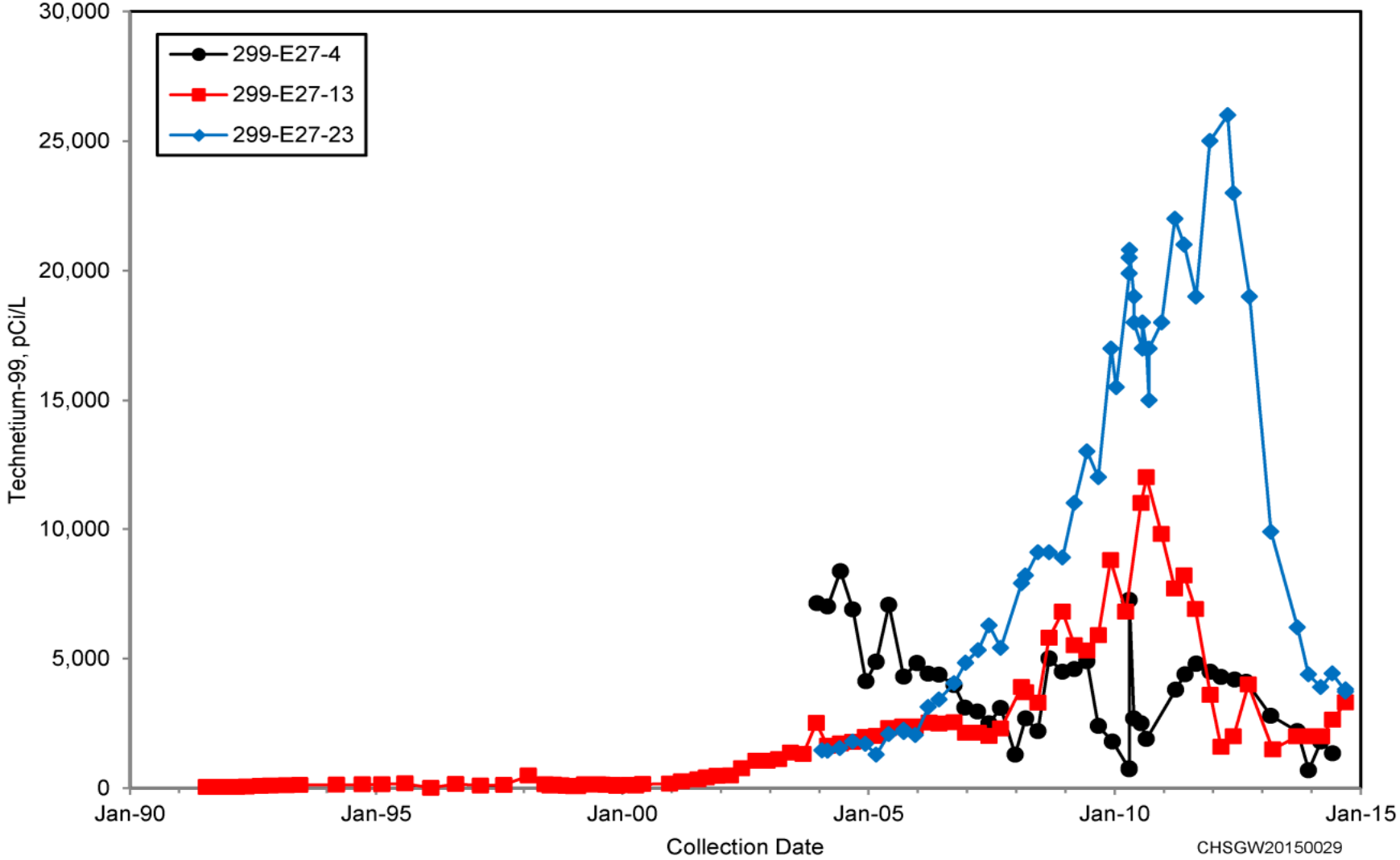

Source: DOE/RL-2009-127, Remedial Investigation Report for the 200-BP-5 Groundwater Operable Unit, Draft A.

Figure 2-28. Technetium-99-to-Nitrate Ratio Comparisons for Wells on West Side (299-E27-21 and 299-E27-23) and Southeast Side (299-E27-14 and 299-E27-23) of Waste Management Area C.

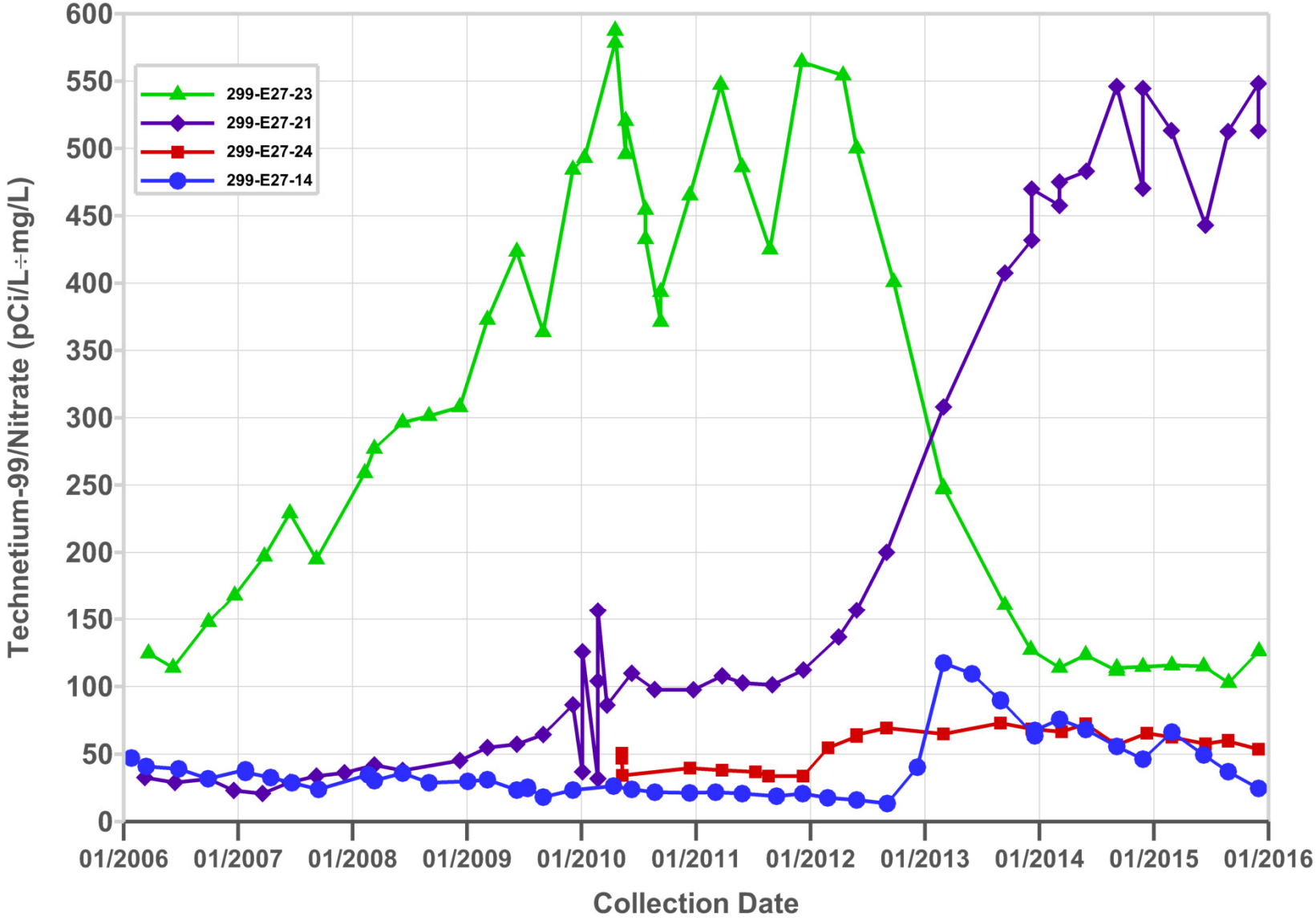

Figure 2-29. Cyanide-to-Nitrate Ratio Comparisons for Well 299-E27-14.

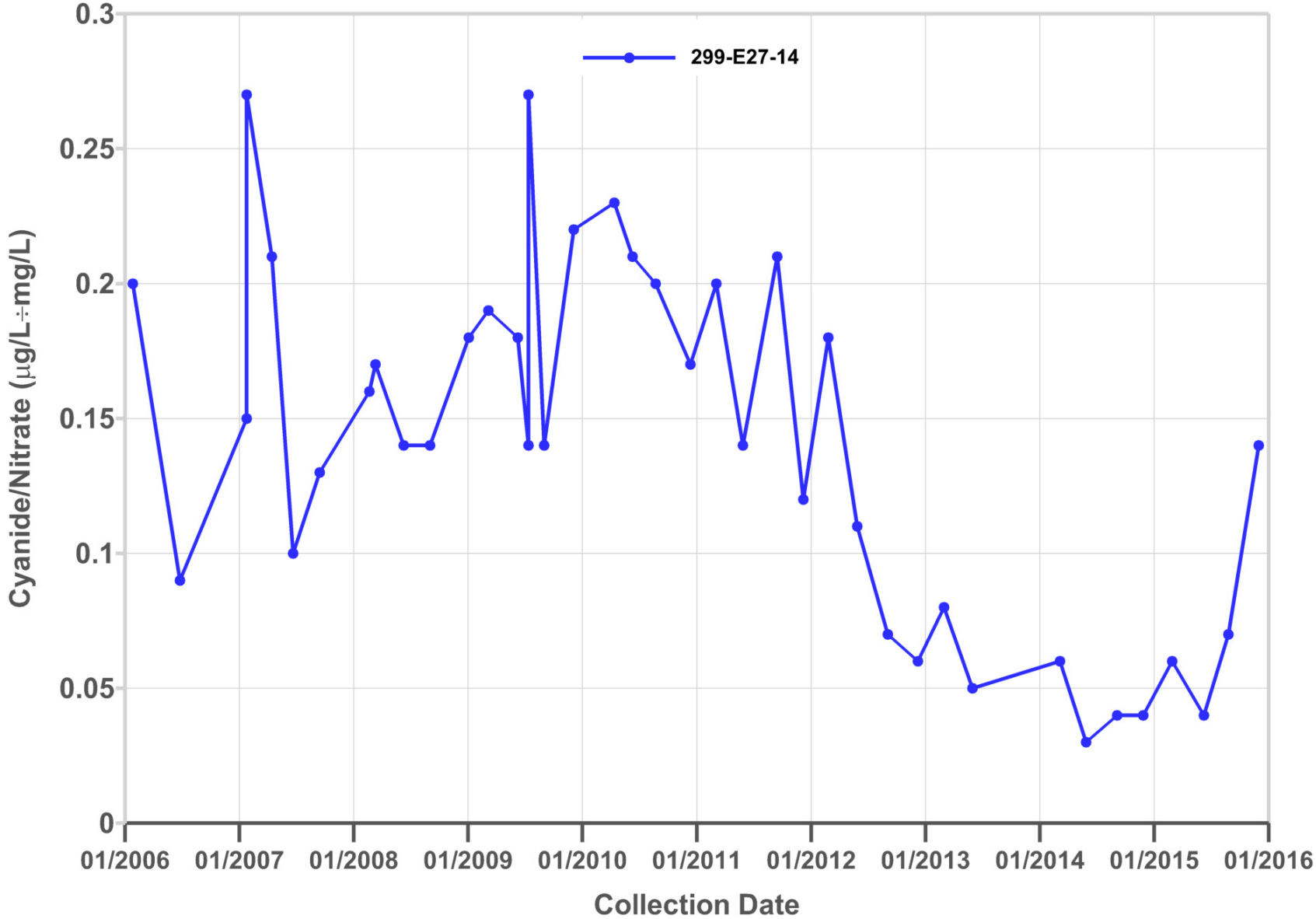

Figure 2-30. Bivariate Plots of Technetium-99/Nitrate Ratio Versus Nitrate by Year.

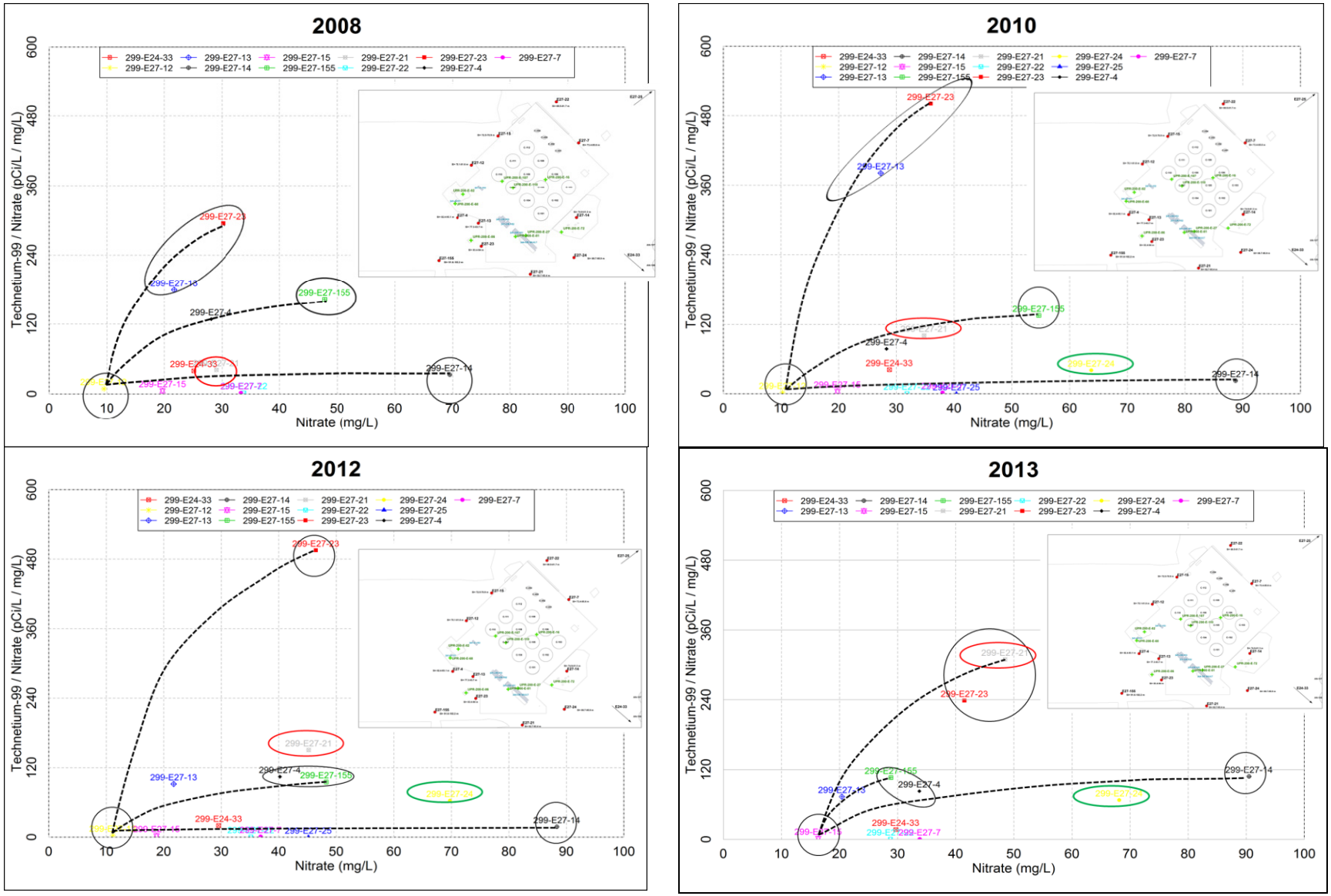

Figure 2-31. Bivariate Plots of Technetium-99/Sulfate Ratio Versus Sulfate by Year.

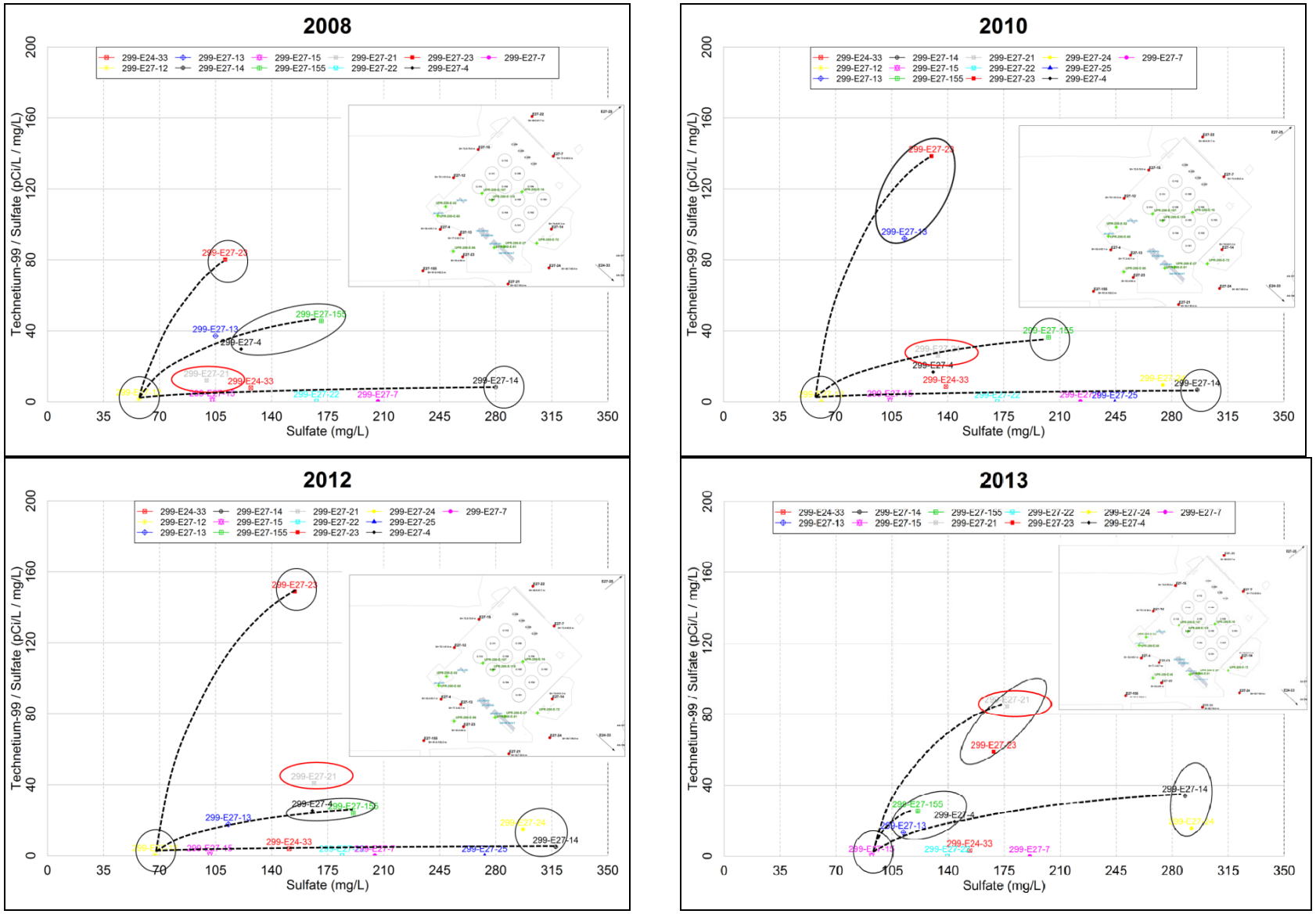

Figure 2-32. Bivariate Plots of Technetium-99/Chloride Ratio Versus Chloride by Year.

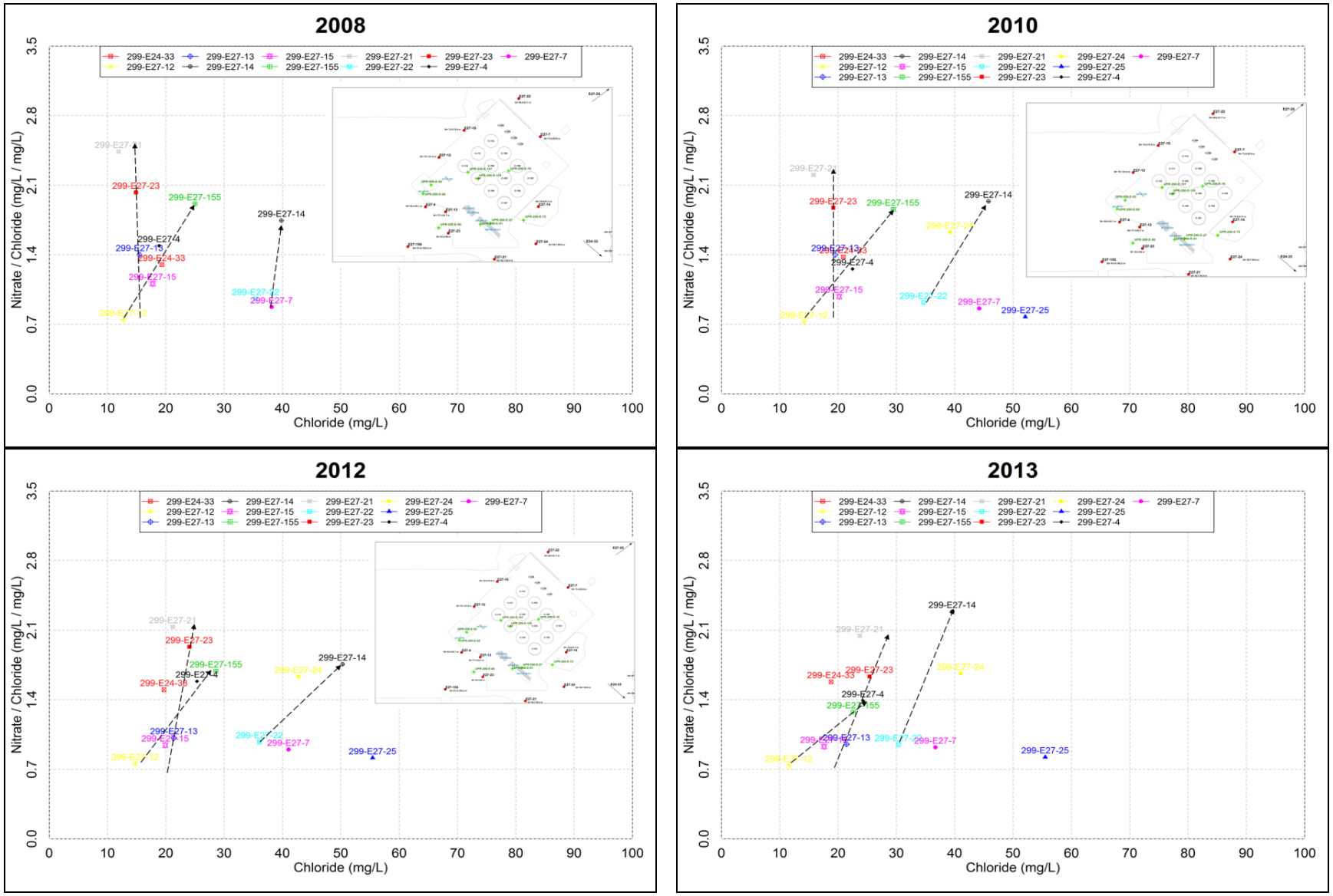

From the bivariate plots of nitrate/chloride versus chloride, three different end-member waters (reflecting varying sources) were identified and mixing lines were calculated between the end-member waters and the upgradient water type. The identification of three different end members and the shifting of the relative positions of wells among the mixing lines were different to those found using the other bivariate plots of ^{99}Tc/nitrate versus nitrate and ^{99}Tc/sulfate versus sulfate.

2.3.4.4 Estimates of Technetium-99 Flux from the Vadose Zone. Two independent methods have been used for estimating ^{99}Tc flux from the vadose zone to the saturated zone in the WMA C vicinity (ECF-Hanford-13-0037; DOE/RL-2009-127, Draft A).

2.3.4.4.1 Method 1: Plume Volume from Annual Groundwater Monitoring Reports. This approach takes the plume shapes defined by the Annual Groundwater Monitoring Reports of the past five years and assumes they are correct and uniform through the saturated thickness. The activity and mass are calculated for each year, and then the difference in activity and mass between each year is the amount added or reduced each year.

This approach is relatively simple and quick. It uses data and interpretations that have been published. The possibility of combining subplumes into one large plume, as well as the bias towards increased plume areas where data are scarce, mean this approach is more likely to over-estimate plume volume (ECF-Hanford-13-0037).

2.3.4.4.2 Method 2: Interpreted Plume Approach. The interpreted plume method uses data from at least the past ten years to create site conceptual models that take account of flow paths and major ion chemistry in order to determine the plume extent. This approach acknowledges that the lower-concentration parts of the plume are not as easily constrained or understood as the zone of high concentration. The more easily understood zone of high concentration is then used as the control volume, and the mass flux is derived based on the flow rate through the control volume, which causes changes in the dissolved concentration. The observed changes in the dissolved concentration define the mass flux.

This approach is more complex than the first estimation method, but can be distilled to a simple conceptual model as seen in Figure 2-33. Mass flux in the saturated zone is controlled by the inflow of water as well as the mass coming in from the vadose zone. The basis of this conceptual model is that the persistence of some plumes is due to continued mass coming in from the vadose zone, as the water flowing through the system would tend to move the contamination out of the control volume, so any mass output would have to be replaced by mass input from the vadose zone to maintain concentrations in the control volume.

This approach assumes Dupuit conditions in an unconfined aquifer, which assumes (ECF-Hanford-13-0037):

- The water table or free surface is only slightly inclined
- Streamlines may be considered horizontal and equipotential lines are vertical
- Slopes of the free surface and hydraulic gradient are equal.

Figure 2-33. Conceptual Model for the Vadose Zone Flux Calculation.

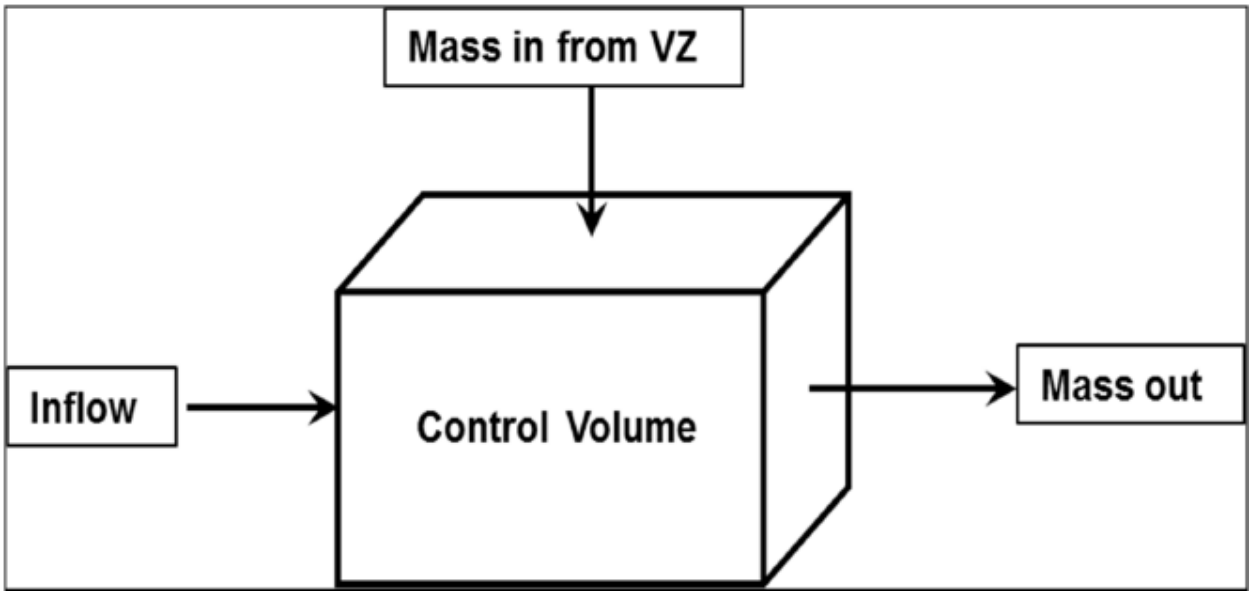

VZ = vadose zone

The groundwater flow equation of continuity is used:

$$\frac{\partial^2 h_x}{\partial x^2} + \frac{\partial^2 h_y}{\partial y^2} + \frac{\partial^2 h_z}{\partial z^2} = 0$$

where h_x, h_y, and h_z are the hydraulic head in the x, y, and z directions. The mass balance equation is also used:

$$\left(\frac{M}{\Delta t}\right)_{UZ} = (Q_s \Delta C)_{SZ}$$

where the left side is the mass flux from the vadose zone (g/yr or Ci/yr) and the right side is the saturated zone mass flux defined by flow rate (Q_x) times the change in concentration (ΔC). Further discussion of the appropriate application of the above equations can be found in ECF-Hanford-13-0037, Section 2.

2.3.4.4.3 Flux Estimation. In the first method, using information from the Groundwater Annual Reports, the calculated total activity residing in the saturated zone is estimated to be ~1 Ci, and it shows an increasing trend (see Figure 2-34). It has been concluded that this value is an overestimate, owing to the extrapolation of the plume area to regions where information is not available (ECF-Hanford-13-0037). Using this method, the average increase in ^{99}Tc activity from year 2008 to year 2012 is calculated to be ~0.17 Ci per year. It was assumed that 6 Ci of ^{99}Tc remains in the vadose zone (ECF-Hanford-13-0037 based this estimate on the data provided in RPP-ENV-33418). It was concluded from these values that it will take about 35 years for the ^{99}Tc in the vadose zone to be released into the saturated zone, assuming uniform flux (ECF-Hanford-13-0037).

Figure 2-34. Estimates of the Activity of Technetium-99 by Two Alternative Methods.

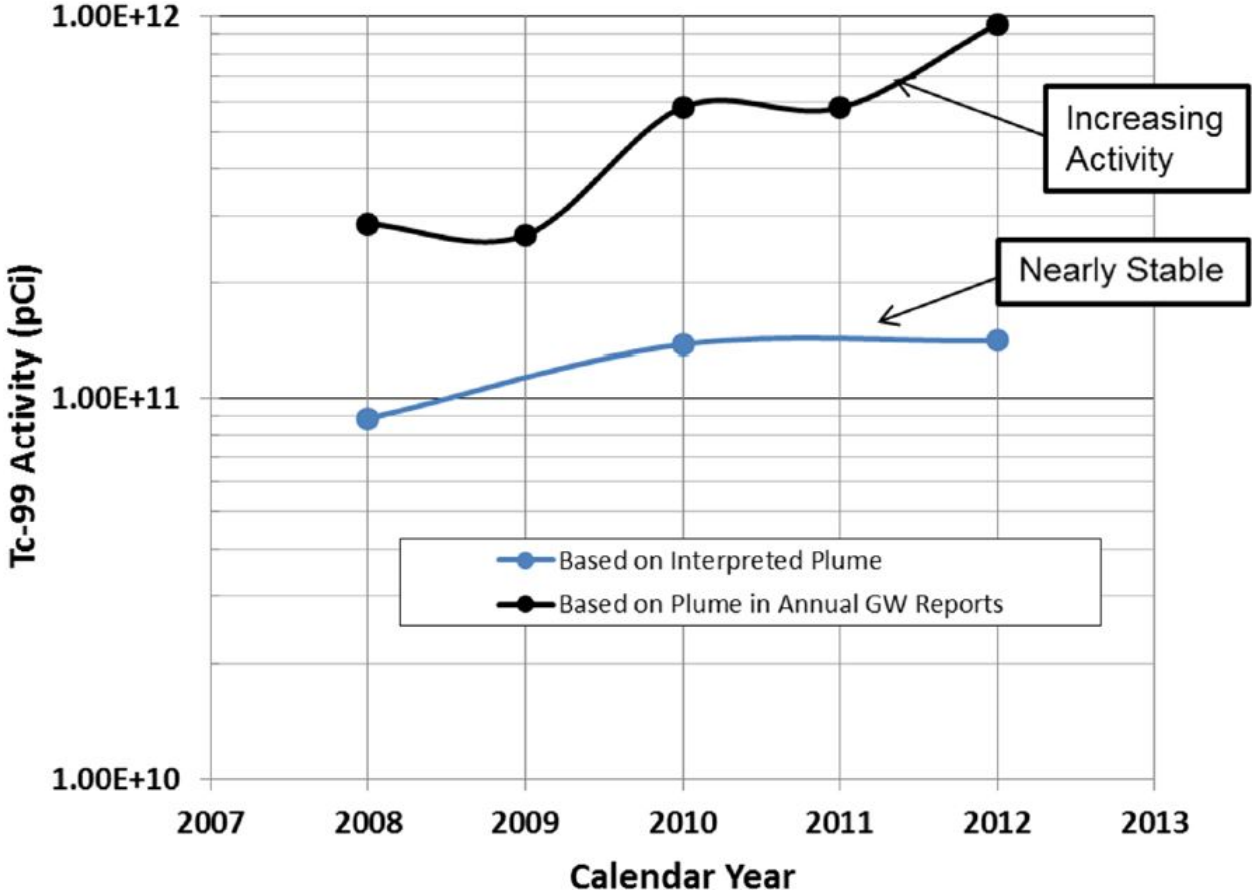

Reference: ECF-Hanford-13-0037, "Development of Source Terms for Inclusion in Fate and Transport Modeling for Remedial Investigation/Feasibility Studies of the 200-BP-5 and 200-PO-1 Groundwater Operable Units."

In the second method, which combined site-specific conceptual models to evaluate a mass balance for ^{99}Tc, the current total activity residing in the saturated zone was estimated to be ~0.14 Ci. Using this method, the activity in the control volume is calculated to have reached a steady state, meaning that the rate at which ^{99}Tc is being transported downgradient is approximately equal to the rate at which it is being transported from the vadose zone to the saturated zone (see Figure 2-34). This rate was estimated to be 0.1 Ci per year (ECF-Hanford-13-0037). Using the estimate of 6 Ci of ^{99}Tc remaining in the vadose zone (see above), it will take ~60 years to be released to the saturated zone.

3.0 FEATURES FOR ANALYSIS

The analysis of past leaks has been structured to meet several goals. First, the analysis is intended to be responsive to ideas and concerns expressed in the 2009 – 2011 PA scoping sessions (see Section 1.1.1), in which specific features of WMA C were identified as requiring particular attention because of their potential to influence the migration of contaminants from WMA C. Second, the analysis is intended to be consistent, to the extent possible, with the PA (RPP-ENV-58782) and RCA (RPP-ENV-58806) for disposal of residual wastes in WMA C. Third, the goal is to provide an understanding of the key features and processes discussed in in the data packages produced for the scoping sessions (Section 1.1.1) that influence the migration of contaminants. Fourth, the goal is to use the understanding gained by the analysis to provide a projection of the future evolution of the contamination beneath WMA C.

This section provides an overview of the model interpretation of the site description and data presented in Sections 1 and 2. This section describes the conceptual models of WMA C relevant to the assessment of past leaks, and the implementation of associated mathematical models. The information related to the analysis and modeling approach is presented in the following subsections:

- Overview of analysis
- Adaptation of the PA conceptual and numerical models used in the evaluation of waste residual impacts
- Conceptual model of source term releases
- Aquifer considerations
- Mathematical models.

3.1 OVERVIEW OF ANALYSIS

The strategy for this analysis of leaks at WMA C is to define and analyze a suite of scoping cases to evaluate the uncertainties associated with past leaks. These uncertainties can be broadly considered to originate from one of the following sources.

- Uncertainties exist in the timing, inventory, and volumes of leaks. These uncertainties have been discussed at length in Revision 4 of RPP-ENV-33418.
- Uncertainties exist in past actions taken to mitigate the surface manifestations of past leaks. In particular, for several UPRs, water was added via firehose to surface contamination to wash it down into the soil column.

- Uncertainties exist in interpreting the groundwater monitoring and vadose zone characterization data on current contamination levels resulting from the past leaks since data represent specific locations,

- Uncertainties exist in the hydrogeological representation of the stratigraphy below WMA C (RPP-RPT-56356). These uncertainties have been addressed in RPP-ENV-58782 and RPP-ENV-58806 by evaluating the consequences of alternative interpretations of the hydrogeology. This approach has continued to be used in the current report.

- Uncertainties exist in the effective values of parameters used in modeling groundwater flow and contaminant transport. These uncertainties are discussed in detail in RPP-ENV-58782 and RPP-ENV-58806.

- Uncertainties exist regarding the evolution of the groundwater system at WMA C over the past several decades, as discussed in Section 2. Anthropogenic water introduced south of WMA C created a gradient generally to the north, which has transitions over recent decades to a gradient generally southward. The transition between these two states occurred approximately coincident with the arrival of the first contaminants at the water table. The feature of the groundwater system evolution introduces additional uncertainties about the trajectory of plumes moving in the aquifer.

The analyses of potential releases of contaminants in residual wastes presented in RPP-ENV-58782 and RPP-ENV-58806 were focused on future site conditions, and as a result did not directly address several of these sources of uncertainty; specifically, those associated with the UPRs at WMA C and those associated with the past evolution of the water table as water was discharge in both the 200 East and 200 West areas. However, in RPP-ENV-58782 and RPP-ENV-58806, a number of approaches to developing confidence in the data, assumptions, and methods were used, as follows.

- Many data were based on WMA C-specific site characterization, sampling, measurements and interpretations, including those for contaminant inventory, geology, hydrology and geochemistry. When data specific to WMA C were not available, data from nearby sites or comparable conditions, as well as data reported in the literature, were used.

- Data were upscaled to represent field-scale processes using scientifically-accepted approaches that have been published in peer-reviewed journals. Upscaling techniques use information from small, core-scale measurements to develop parameters that are applicable to large, field-scale models.

- The process-based modeling software, Subsurface Transport Over Multiple Phases (STOMP)©[1] code (PNNL-12030, "STOMP Subsurface Transport Over Multiple Phases Version 2.0 Theory Guide"; Pacific Northwest National Laboratory, Queried 12/18/2015,

[1] Subsurface Transport Over Multiple Phases (STOMP)© is copyrighted by Battelle Memorial Institute, 1996.

[STOMP User Guide], http://stomp.pnnl.gov/user_guide/STOMP_guide.stm; PNNL-11216, "STOMP Subsurface Transport Over Multiple Phases Application Guide"), has been benchmarked and deemed suitable for use in this PA. The STOMP© code is the pre-authorized modeling software at the Hanford Site for vadose zone and near-field groundwater modeling (Internal memorandum 1301789, "Modeling to Support Regulatory Decisionmaking at Hanford"). The STOMP© code has previously been qualified for simulation use at Hanford by CHPRC (CHPRC-00269, "STOMP Requirements Traceability Matrix CHPRC Build 4"). Sensitivity and uncertainty analyses were conducted to evaluate the effect of parameter uncertainties and alternative conceptual models on the overall performance of the system.

These approaches specifically address uncertainties in model conceptualizations and input parameters for groundwater flow and transport, but do not address uncertainties in past leaks and in past evolution of the groundwater table.

Consequently, the model used in RPP-ENV-58782 and RPP-ENV-58806 was adapted for the past leaks scoping analyses so that the water table was reflective of conditions at WMA C when first arrival of contaminants at the water table was observed. Two approaches were used. In the first approach, the water table was assumed to be fixed or at steady state, and directed in the same way as the prospective water table used for future analyses, but at a higher level, which allows the analysis to represent the shorter travel time in the vadose zone that would have existed when the plumes initially arrived. This approach is intended to represent the time of first arrival and the peak of the groundwater plume, but is not necessarily to represent the spatial distribution of contamination in the groundwater. The second approach was to introduce a time-varying or transient water table to represent the likely evolution of the aquifer gradient over the simulation period. Both of these approaches are described in more detail in Section 4.

The model has been initially compared to ^{99}Tc concentrations in groundwater, since ^{99}Tc is a key risk driver and the contamination levels observed in groundwater monitoring wells are considered to be the result of WMA C past leaks. The ^{99}Tc concentration data observed in groundwater monitoring wells have been used to evaluate the input conditions that are consistent with the arrival times and concentration levels of ^{99}Tc observed historically in the vicinity of WMA C. The resulting constrained model is then also compared with other contaminant data as appropriate.

3.2 ADAPTATION OF THE PERFORMANCE ASSESSMENT CONCEPTUAL AND NUMERICAL MODELS USED IN THE EVALUATION OF WASTE RESIDUAL IMPACTS

The foundation of the conceptual models used in this report is the model(s) developed for the analysis of releases associated with residual wastes as described in RPP-ENV-58782 and RPP-ENV-58806. The basis for that model is reviewed in this section as it is applied to the past leaks analysis. The initial basis for the model has been the Base Case model in RPP-ENV-58782 and RPP-ENV-58806, with appropriate changes to the depth to the water table to reflect the conditions that existed when data showed the leaks arriving at the water table. This change was

made to improve the correlation of the calculated and observed first arrival of contaminants at the water table. This initial basis forms the first analysis case to be evaluated (see Section 4); additional scoping analysis cases have been carried out to explore the effects of alternative conceptual models and input assumptions. These alternative analysis cases have also been described in Section 4.

The WMA C PA methodology (RPP-ENV-58782 and RPP-ENV-58806) uses conceptual models that are based on the physical system and expected contaminant migration pathways. Figure 3-1 provides a schematic representation of both WMA C at closure and the contaminant migration into the environment along the various pathways evaluated in the PA. The WMA C site is composed of both man-made and natural components that are represented in the model. The man-made components of the system that influence contaminant migration include a closure surface barrier, the WMA C tanks, pipelines, and infrastructure, and the distribution of waste in those components. The natural components of the system that influence contaminant migration are a number of mostly horizontal to slightly dipping (to the northeast) stratigraphic layers within the saturated and unsaturated zones, net infiltration resulting from rainfall, and any antecedent moisture conditions (and contaminants) within WMA C or from adjacent sites. Figure 3-2 illustrates the major stratigraphic units for the thick vadose zone at WMA C.

The water table at WMA C is located within the undifferentiated Hanford formation and Cold Creek gravels, and, during Hanford operations, was strongly influenced by large volumes of liquids that were discharged to the subsurface at major waste water discharge facilities located in and around 200 East Area, raising the groundwater elevation in the 200 East Area and vicinity (Figures 2-10 and 2-11). Since the termination of processing operations, the groundwater mounds in the 200 East Area have been dissipating and groundwater flow velocities have slowed. Since the groundwater gradient in the area is so flat, the groundwater monitoring network at WMA C does not have sufficient resolution to use data to directly show the timing and magnitude of the groundwater gradient at WMA C. However, the effect can be illustrated using the nearby low-gradient Low-Level Waste Management Area (LLWMA)-1 monitoring network shown in Figure 3-3. In the period prior to about 2007 to 2008, the gradient orientation at LLWMA is approximately north. Then comes a period between 2008 and mid-2011 when the gradient is ambiguous, variable, and for the most part statistically indeterminate. Since that time the gradient has been approximately south as it returns to its natural gradient as the water mounds dissipate.

A similar pattern of behavior is believed to have occurred at WMA C, with minor differences in the timing of changes, and in the magnitude and orientation of the gradient. As noted above, reliable determination of the gradients at WMA C is not possible because they are so flat that gradient determination requires special methods. Consequently, analysis of the behavior of the aquifer during this time period is best undertaken using modeling.

Figure 3-4 shows an aerial view of WMA C, and surrounding disturbed, undisturbed, and resurfaced areas.

Figure 3-1. Schematic Conceptual Representation of Waste Management Area C and Contaminant Migration into the Environment along the Various Pathways Evaluated in the Performance Assessment.

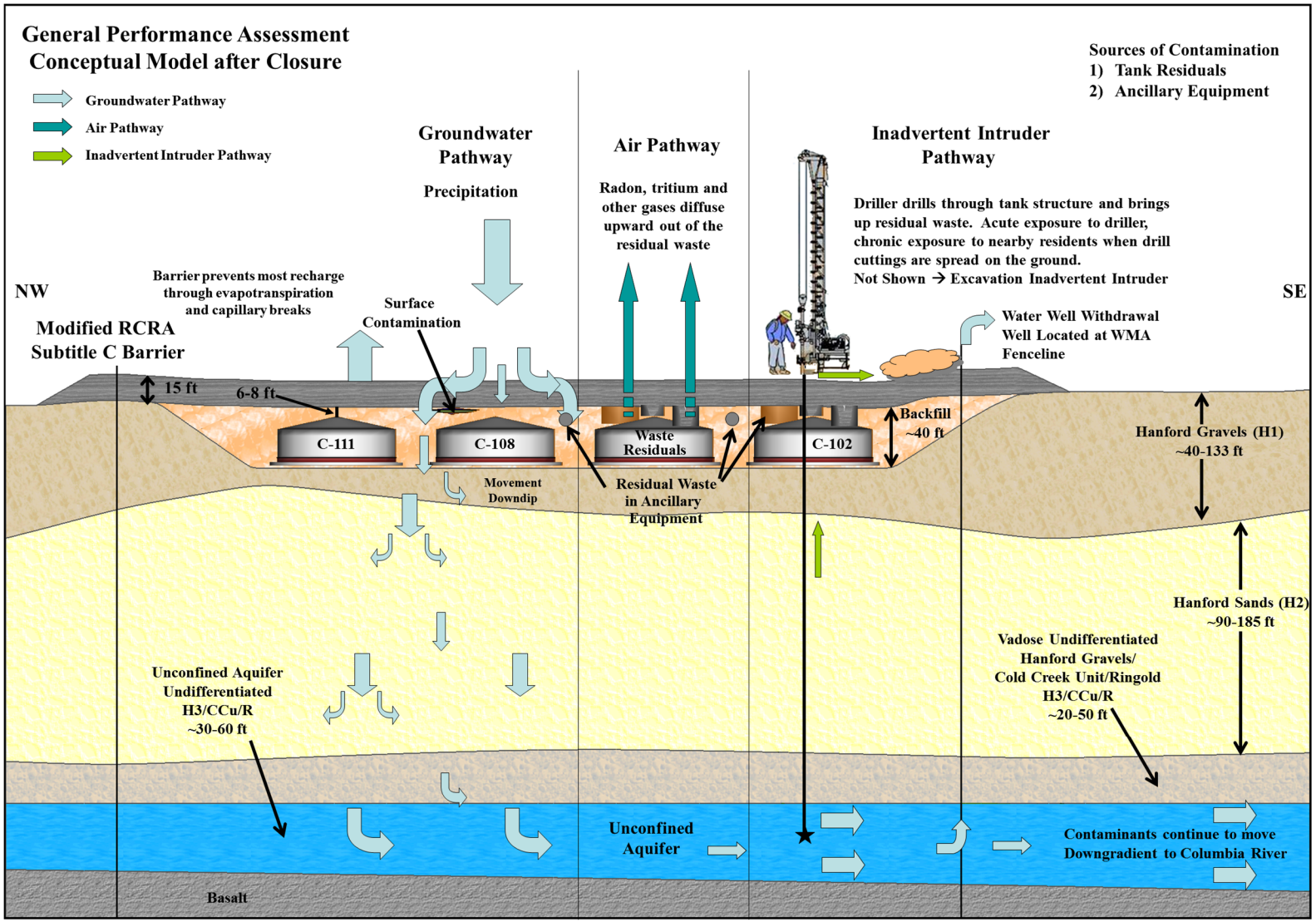

RCRA = Resource Conservation and Recovery Act of 1976 WMA = Waste Management Area

Figure 3-2. Conceptual Model of the Waste Management Area C Site Showing Stratigraphy.

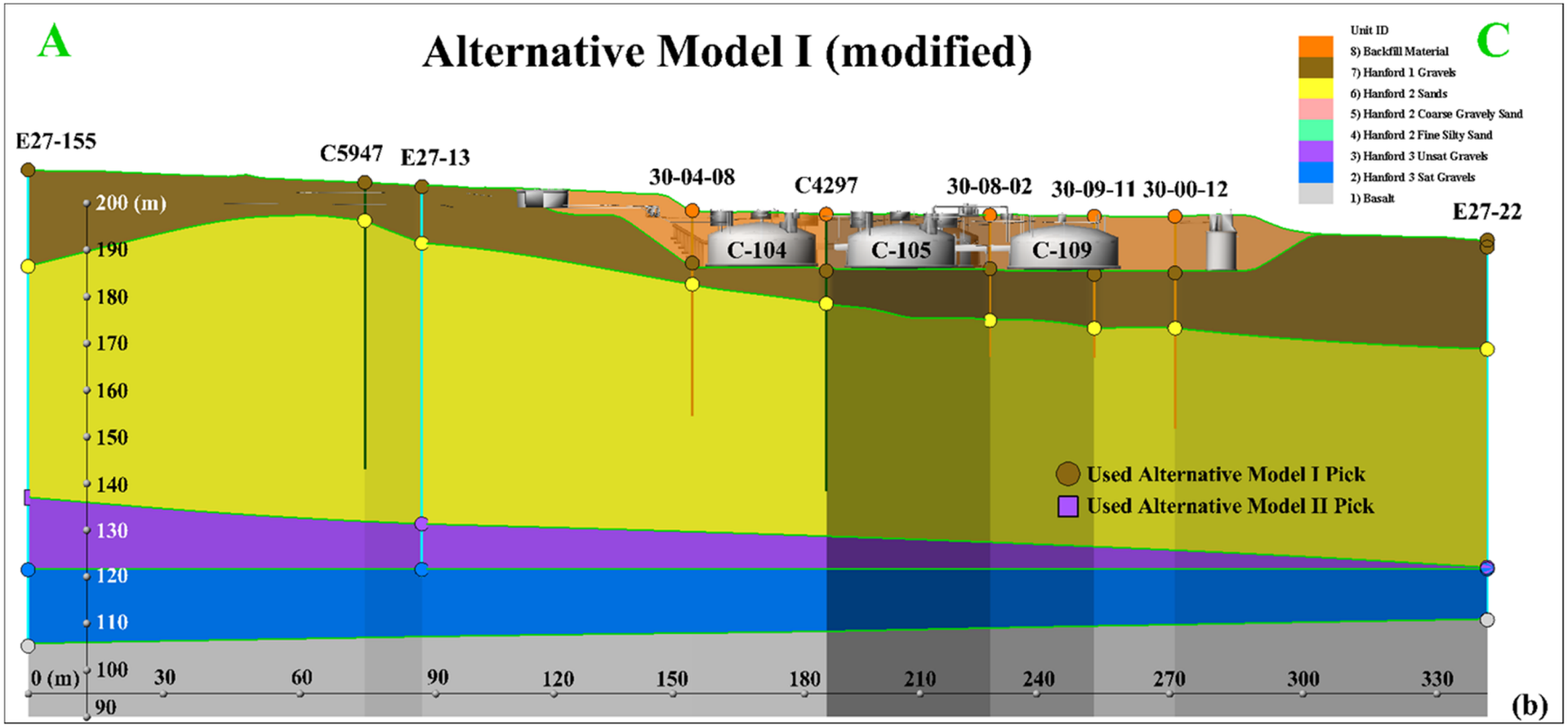

Figure 3-3. Evolution of the Groundwater Gradient In the Low-Level Waste Management Area-1 Monitoring Network. The gradient at the nearby Waste Management Area C evolved in a similar manner and timescale.

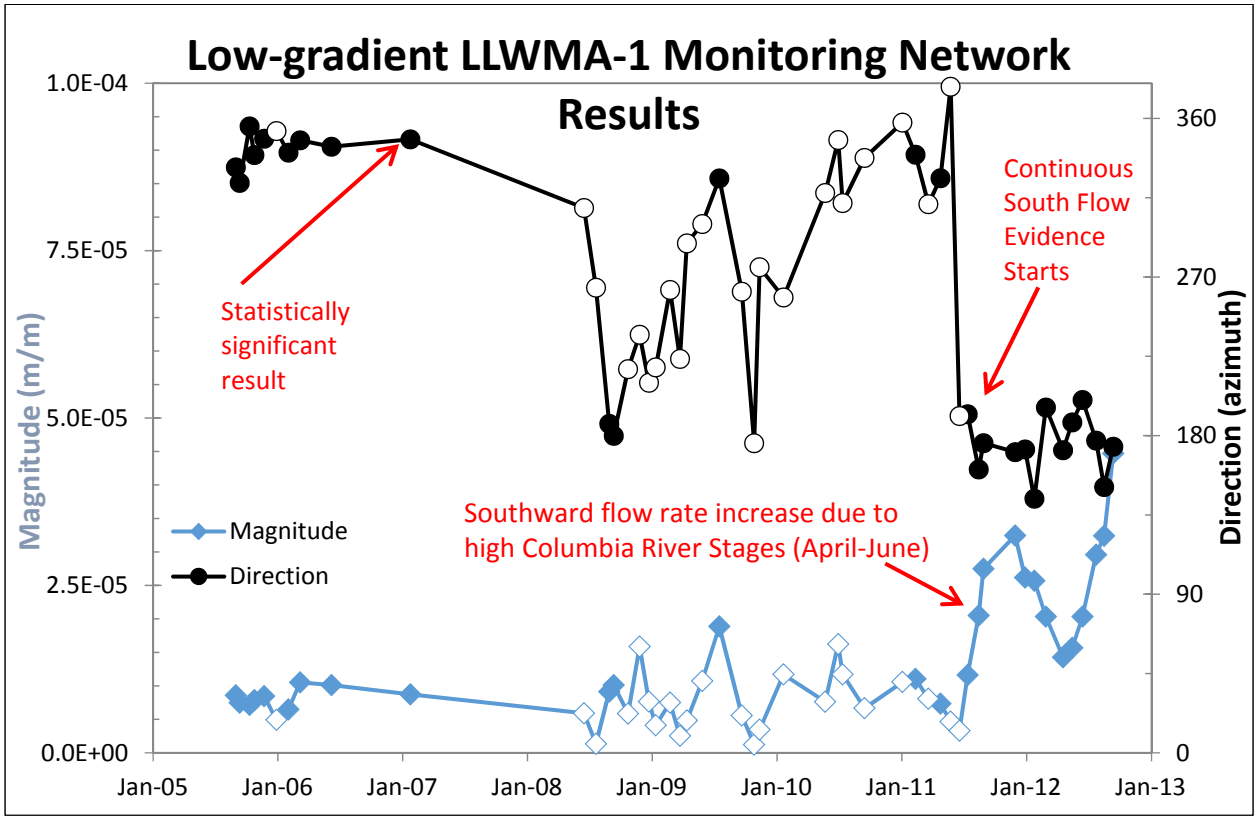

Excerpted from SGW-54165, "Evaluation of the Unconfined Aquifer Hydraulic Gradient Beneath the 200 East Area, Hanford Site."

LLWMA-1 = Low-Level Waste Management Area 1

As discussed in RPP-ENV-58782 and RPP-ENV-58806, the conceptual models and relevant parameters for fate and transport modeling have been developed for the following four time periods:

- Pre-operations and initial construction period (before 1945) representing the time when the tank farm ground remained undisturbed from the Hanford Manhattan Project mission

- Operations period representing tank farm construction, current, and immediate future conditions of the tank farm (1945 to 2020)

- Closure and post-closure period during the assumed design life of the intact surface barrier (2020 to 2520) when the tanks become grouted and radionuclides begin to diffuse out of the grout

- Post-closure period beyond assumed design life of the surface barrier (2520 to 12120) when the performance of the surface barrier is assumed to degrade.

Figure 3-4. Surface Conditions In and Around Waste Management Area C during the Construction and Operations Period.

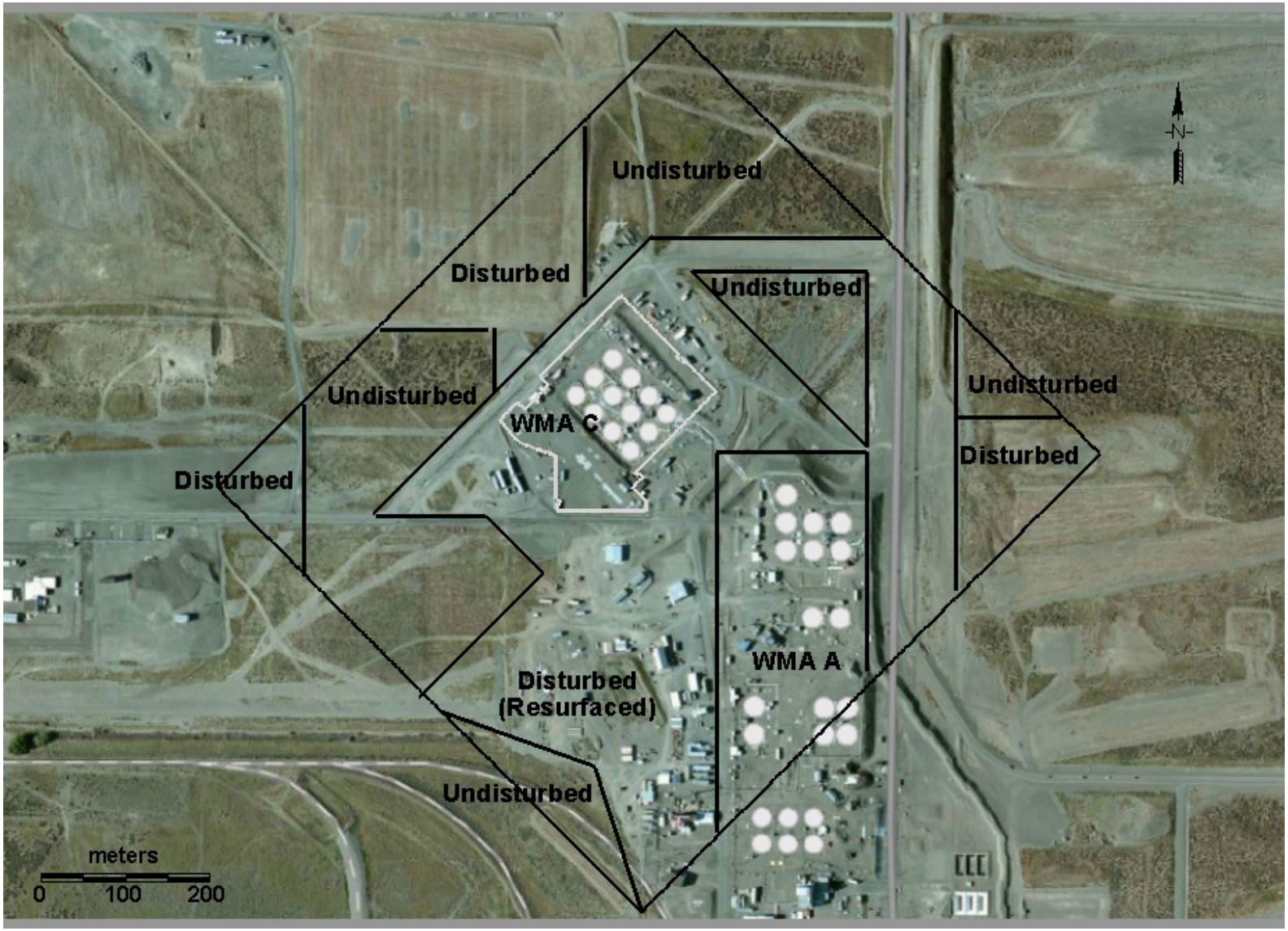

WMA = Waste Management Area

The second of these time periods is most relevant for the analysis of past leaks. The third and fourth time periods are relevant to the future projection of leak contamination into the future.

For WMA C vadose zone modeling, small-scale laboratory measurements provide the basis for hydraulic properties used to predict the large, field-scale flow behavior (Appendix B of RPP-ENV-58782 and RPP-ENV-58806). Each heterogeneous geologic unit is replaced by an EHM with macroscopic flow properties. With each heterogeneous unit assigned its upscaled or effective hydraulic properties, the simulated flow fields predict the bulk or mean flow behavior at the field scale. Upscaling, in effect, accounts for the differences in scale between small, core-scale measurements and large, field-scale modeling. The radionuclides travel through the vadose zone until they reach the water table and the unconfined aquifer. The unconfined aquifer is also treated as an EHM, and an equivalent saturated hydraulic conductivity is estimated for the undifferentiated Hanford gravels and CCu sediments (Appendix C of RPP-ENV-58782 and RPP-ENV-58806) through the use of a calibrated large-scale model.

3.3 CONCEPTUAL MODEL OF SOURCE TERM RELEASES

The source term for the leaks analysis is derived from current estimates of past leaks in Revision 4 of RPP-ENV-33418. A summary of these current estimates is provided in Section 2.1. For the purpose of carrying out calculations, it is necessary to make specific assumptions on inventory, volume, and timing that can be input into STOMP© as the source term for the analysis. As discussed in Section 2.1, there is substantial uncertainty in leak estimates, but the current estimates for ^{99}Tc releases have been used as the basis for a nominal abstracted leak inventory used in the initial calculations. This abstracted inventory is presented in Table 3-1. Scoping analyses presented in Section 4.0 have been used to evaluate alternative assumptions about, specifically, the C-105 leak.

3.4 VADOSE ZONE CONSIDERATIONS

The vadose zone underlying WMA C consists of heterogeneous layers of sediments that vary in thickness at different locations. Alternative conceptual models described in RPP-ENV-58782 and RPP-ENV-58806 present results from several alternative representations of the spatial variability of these sedimentary units to evaluate the consequences of these alternative representations. These alternative representations have been carried forward into the current report.

Features such as clastic dikes and man-made structures (i.e., monitoring wells) can allow water and contaminants to bypass vadose zone continuum fate and transport processes. Clastic dikes (anomalous, subvertical linear features composed of layers of differing particle size distributions) occur in the vadose zone, extend up to tens of meters in length, and crosscut the major layers. At the Hanford Site, there is little evidence of enhanced transport in these preferential pathways in arid and semiarid climates with low-water flux in the vadose zone, particularly where soils are coarse-grained such as in Hanford formation sediments ("Influence of Clastic Dikes on Vertical Migration of Contaminants at the Hanford Site" [Murray et al. 2007]).

Table 3-1. Abstracted Inventory of Technetium-99 Used for the Initial Analysis Cases.

Tank/Unplanned Release	Waste Release Volume, gal*	^{99}Tc, Ci	Time of release
241-C-101	37,000	0.25	Continuous release 1965 – 1969
241-C-104	28,000	0.03	Acute release 1965
241-C-105	2,000 to 20,500	10	Continuous release 1963 – 1967
241-C-108	18,000	0.02	Acute release 1965
241-C-110	2,000	3.4	Continuous release 1971 – 1972
241-C-112	7,000	0.0075	"prior to 1972" taken as acute release 1965
UPR-200-E-81	36,000	0.1	Acute release 1969
UPR-200-E-82	2,600	1.3	Acute release 1969
UPR-200-E-86	17,000	2.7	Acute release 1971
Surface Releases	1,000	0.001	"Unknown" taken as acute release 1965
216-C-8	32,000	0.0	Continuous release 1960 – 1965
Total	169,100	17.5	

* Conversion 1 gallon = 3.78541 liters

However, these features may form preferentially faster flow pathways under conditions closer to saturation, such as may have potentially occurred following leak releases. As a result, a specific analysis case has been set up to evaluate the potential effect of a clastic dike on transport of contaminants from past leaks through the vadose zone (see Section 4.4).

Similarly, the presence of man-made features such as exploratory boreholes and drywells has been speculated to provide a potential fast path for contamination from past leaks. Consequently, an alternative modeling case has been established to evaluate these effects (see Section 4.4).

3.5 AQUIFER CONSIDERATIONS

3.5.1 Flow Considerations

As discussed in RPP-ENV-58782 and RPP-ENV-58806, estimates of hydraulic properties are based on the groundwater flux in the aquifer around WMA C according to the CPGWM calibration reported in CP-47631, "Model Package Report: Central Plateau Groundwater Model Version 6.3.3."

3.5.2 Transport Considerations

The effective transport parameter (i.e., macrodispersivity, bulk density, and diffusivity) estimates used in the base case associated with the WMA C PA (RPP-ENV-58782) and the RCA (RPP-ENV-58806) provide the basis for transport parameters used in this analysis. The basis for the distribution coefficients (K_d) values used to approximate the transport of the radionuclides and chemical contaminants in this analysis (see Table 3-2) also rely on the same estimates for these parameters used in the base case from the PA and RCA.

Table 3-2. Distribution Coefficients (K_d) Values Used to Approximate the Transport of the Radionuclides in the Base Case. (2 sheets)

Element or Contaminant	Base Case K_d (mL/g)				
	< 2mm Material	Backfill	Hanford H1/H3	Hanford H2	Reference
Ac	350	NM	NM	NM	PNNL-16663
Al	1,500	NM	NM	NM	RPP-RPT-46088
Am	600	NM	NM	NM	PNNL-17154
B	3	NM	NM	NM	RPP-RPT-46088
C	1	0.46	0.58	0.8	PNNL-17154
Cm	350	NM	NM	NM	PNNL-16663
CN	0	NM	NM	NM	RPP-RPT-46088
Co	0	0	0	0	PNNL-17154
Cr	0	0	0	0	PNNL-17154
Cs	100	NM	NM	NM	PNNL-17154
Eu	10	NM	NM	NM	PNNL-17154
F	0	0	0	0	PNNL-17154
Fe	25	NM	NM	NM	RPP-RPT-46088
H	0	0	0	0	PNNL-17154
Hg	52	NM	NM	NM	RPP-RPT-46088
I	0.2	0.09	0.12	0.16	PNNL-17154
Mn	65	NM	NM	NM	RPP-RPT-46088
Nb	0	0	0	0	PNNL-16663
Ni	3	1.4	1.7	2.4	PNNL-17154
NO_2	0	0	0	0	PNNL-17154
NO_3	0	0	0	0	PNNL-17154
Np	10	NM	NM	NM	PNNL-17154

Table 3-2. Distribution Coefficients (K_d) Values Used to Approximate the Transport of the Radionuclides in the Base Case. (2 sheets)

Element or Contaminant	Base Case K_d (mL/g)				
	< 2mm Material	Backfill	Hanford H1/H3	Hanford H2	Reference
Pa	300	NM	NM	NM	PNNL-17154
Pb	10	NM	NM	NM	PNNL-17154
Pu	600	NM	NM	NM	PNNL-17154
Ra	10	NM	NM	NM	PNNL-17154
Rn	0	0	0	0	No relevant information available
Se	0.1	0.05	0.06	0.08	PNNL-17154
Sm	10	NM	NM	NM	PNNL-17154
Sn	0.5	0.23	0.29	0.4	PNNL-17154
Sr	10	NM	NM	NM	PNNL-17154
Tributyl Phosphate	1.89	NM	NM	NM	RPP-RPT-46088
Tc	0	0	0	0	PNNL-16663
Th	300	NM	NM	NM	PNNL-16663
U	0.6	0.28	0.35	0.48	RPP-RPT-46088
Zr	300	NM	NM	NM	PNNL-16663

NM = not included in the 3-D modeling because the results of screening indicated the element or contaminant does not arrive at the water table within 10,000 years.

References:
PNNL-16663, "Geochemical Processes Data Package for the Vadose Zone in the Single-Shell Tank Waste Management Areas at the Hanford Site."
PNNL-17154, "Geochemical Characterization Data Package for the Vadose Zone in the Single-Shell Tank Waste Management Areas at the Hanford Site."
RPP-RPT-46088, "Flow and Transport in the Natural System at Waste Management Area C."

3.6 MATHEMATICAL MODELS

This section presents development and implementation of mathematical models that are used to evaluate flow and radionuclide transport. The mathematical models and their implementation are described in RPP-ENV-58782 and RPP-ENV-58806. There is no difference between the STOMP© mathematical models implemented in those reports and the one used here. However, given the additional complexity (i.e., release from the tank structure) of the residual waste PA, in which additional models and features in STOMP© were described, the additional mathematical models specific to the leaks analysis have been added to this section, along with a description of the mathematical implementation of the leak source term.

3.6.1 Source Term

The source term is input directly as a mass of contamination and associated water volume into the STOMP© model at nodes representing the estimated location and duration of the occurrence of the leak. The masses and volumes of the leaks are discussed in Section 2.1.

3.6.2 Groundwater Flow and Contaminant Transport Equations

Analyses were conducted using the STOMP© code, which was used to simulate 3-D flow and contaminant transport through the vadose zone and unconfined aquifer system. To calculate water flow, STOMP© includes the assumption that the vadose zone and unconfined aquifer system can be represented and approximated by an equivalent porous continuum. STOMP© solves the conservation of mass equation using a finite difference approximation to Richards' equation (Soil Physics, 6th edition [Jury and Horton 2004]) that calculates fluid flow entering, exiting, and accumulating within the finite numerical volumes as follows:

$$\frac{\partial\theta}{\partial t} = \sum \frac{\partial}{\partial x}\left[K(\theta)\frac{dh}{d\theta}\frac{\partial\theta}{\partial x}\right] + \frac{\partial}{\partial y}\left[K(\theta)\frac{dh}{d\theta}\frac{\partial\theta}{\partial y}\right] + \frac{\partial}{\partial z}\left[K(\theta)(\frac{dh}{d\theta}\frac{\partial\theta}{\partial z} + 1)\right] \pm S \qquad (3\text{-}1)$$

Where:

$\partial\theta/\partial t$	=	the change in soil moisture content through time
$dh/d\theta$	=	the slope of the soil matric potential-moisture retention relationship curve (cm)
$\partial\theta/\partial\{x, y, z\}$	=	the changes in soil moisture content through space in each direction (1/cm)
$K(\theta)$	=	the hydraulic conductivity (cm/s), which may be anisotropic and is, as expressed, dependent on moisture content
S	=	the amount of water added (source) or subtracted (sink) per unit volume through time (1/s).

Moisture content is a function of soil matric potential, and the soil matric potential-moisture retention relationship is described for each HSU using the following empirical relationship ("A Closed-form Equation for Predicting the Hydraulic Conductivity of Unsaturated Soils" [van Genuchten 1980]; EPA/600/2-91/065, The RETC Code for Quantifying the Hydraulic Functions of Unsaturated Soils):

$$\theta(h) = \theta_r + (\theta_s - \theta_r)\{1 + [\alpha h]^n\}^{-m} \qquad (3\text{-}2)$$

Where $\theta(h)$ is the moisture content, here expressed explicitly as a function of the soil matric potential, and the other terms are defined as follows:

θ_r	=	residual moisture content (dimensionless)
θ_s	=	saturated moisture content (dimensionless)
α	=	a fitting parameter (cm^{-1})
n	=	a fitting parameter (dimensionless)
m	=	$1 - 1/n$.

Combining the van Genuchten model with Mualem's (1976) model ("A New Model for Predicting the Hydraulic Conductivity of Unsaturated Porous Media") for unsaturated conductivity produces the following relationship for hydraulic conductivity and soil matric potential:

$$K(h) = \frac{K_s\{1-(\alpha h)^{mn}[1+(\alpha h)^n]^{-m}\}^2}{[1+(\alpha h)^n]^{ml}} \quad (3\text{-}3)$$

Where *K(h)* is the hydraulic conductivity (cm/s), which is, as expressed, dependent on the soil matric potential; K_s is the saturated hydraulic conductivity (cm/s); and *l* is a pore-connectivity parameter (dimensionless) that Mualem (1976) estimates to be ~0.5 for many soils and is assumed to equal 0.5 in this analysis.

Within STOMP©, tension-dependent anisotropy provides a framework for upscaling small-scale measurements to the effective (upscaled) properties for the large-scale vadose zone (Section 6.4 and Appendix B of RPP-ENV-58782 and RPP-ENV-58806). Each heterogeneous geologic unit is represented in the model by an EHM with macroscopic flow and transport properties. With each heterogeneous unit assigned its upscaled or effective hydraulic properties, the simulated flow fields predict the bulk or mean flow behavior at the field scale. Upscaling, in effect, accounts for the differences in scale between small, core-scale measurements and large, field-scale modeling. Tension-dependent anisotropy provides a framework for upscaling small-scale measurements to the effective (upscaled) properties for the large-scale, macroscopic vadose zone. The stochastic model developed in "Application of Stochastic Methods to Transient Flow and Transport in Heterogeneous Unsaturated Soils" (Polmann 1990) is used to evaluate and apply tension-dependent anisotropy for the HSUs at WMA C. Details about the development of the Polmann stochastic tension-dependent anisotropy model and its application to the HSUs at WMA C are presented in Appendix B, Section B.3.2 of RPP-ENV-58782 and RPP-ENV-58806.

Contaminant transport in STOMP© is described by the conventional advective-dispersive transport solution to the conservation of mass equation described in Soil Physics (5th edition [Jury et al. 1991]) and applied to finite difference volumes:

$$\frac{\partial}{\partial t} M_c = \frac{\partial}{\partial x}(J_x C_l) + \frac{\partial}{\partial y}(J_y C_l) + \frac{\partial}{\partial z}(J_z C_l) + \frac{\partial}{\partial x}\left(D_e \frac{\partial C_l}{\partial x}\right) + \frac{\partial}{\partial y}\left(D_e \frac{\partial C_l}{\partial y}\right) + \frac{\partial}{\partial z}\left(D_e \frac{\partial C_l}{\partial z}\right) - M_c \frac{ln(2)}{t^{1/2}} \quad (3\text{-}4)$$

Where:

$\frac{\partial}{\partial t} M_c$ = the change in contaminant mass or activity present in the finite volume (g or Ci) through time and the mass or activity is calculated according to the equation ($\rho_b C_a + \theta C_l$)

ρ_b = soil bulk density (g/cm^3)

C_a = adsorbed solute concentration (g or Ci per g soil)

θ = moisture content (dimensionless), and as discussed previously, dependent on the soil matric potential

C_l = dissolved solute concentration (g or Ci per mL water)

$J_{x,y,z}$ = fluxes of water carrying contaminants into or out of the finite volume (cm/s) that cross the planes normal to the x, y, and z directions, respectively

D_e = effective dispersion/diffusion coefficient (cm^2/s); note that the entire terms represent the flux of solutes that crosses the planes normal to the x, y, and z directions, respectively, because of diffusion and dispersion

$\frac{\partial c_l}{\partial\{x,y,z\}}$ = the change in dissolved solute concentration through space in the x, y, and z directions, respectively; note that the entire terms represent the flux of solutes that crosses the planes normal to the x, y, and z directions, respectively, because of diffusion and dispersion

$t^{1/2}$ = radioactive half-life(s), the entire term represents the mass of solute lost to radioactive decay.

In Equation 3-4, positive is used to indicate solute entering the finite volume, and negative is used to indicate what is exiting or lost to decay. The adsorbed and dissolved solute concentrations are related through an equilibrium linear sorption coefficient (K_d mL water per g soil) formulation: $C_a = K_d C_l$. No temperature effects are considered for the vadose zone model (i.e., the model used is isothermal).

3.6.3 Implementation of the Groundwater Pathway in STOMP©

This section describes the implementation of STOMP© in the WMA C PA for evaluation of the groundwater pathway. The description presented in this section primarily addresses the development of the conceptual model components and input parameters for flow and transport. The discussion includes the alternative geologic interpretations, which have been carried forward as part of the scoping analysis. Parameter uncertainties are addressed in Section 8 of RPP-ENV-58782 and RPP-ENV-58806. In the current analysis, only limited treatment of parameter uncertainty has been possible because of the large simulation times associated with running the numerical representation of the vadose zone and aquifer systems.

DOE/RL-2011-50, Regulatory Basis and Implementation of a Graded Approach to Evaluation of Groundwater Protection contains the description of the generalized models, conditions, and parameters applicable to the Hanford Site vadose zone, which were refined and augmented for the WMA C PA evaluation, and used here.

The site-specific STOMP© model components for the WMA C PA evaluation are:

- Model domain and boundary conditions
- Hydrogeologic model
- Source term
- Recharge
- Vadose zone hydrogeology and fluid transport
- Groundwater domain and characteristics
- Geochemistry.

The model domain and boundary conditions are included in the list above to emphasize the fundamental nature of boundary conditions used in the modeling.

The following subsections for the individual conceptual model components provide the basis, rationale, and references for the base case values. These base case values have been used as the initial input parameters for the current report, with alternative assumptions and input parameters used as appropriate to show the range of possible outcomes for the range of input uncertainties identified in RPP-ENV-58782 and RPP-ENV-58806. The base case parameters represent single representative values selected for use in deterministic runs of the model, selected from the ranges of plausible parameter values identified in RPP-ENV-58782 and RPP-ENV-58806. These values may differ from parameter estimates for other Hanford Site modeling performed for different purposes or areas of the Hanford Site, or at different scales.

3.6.3.1 Model Domain and Boundary Conditions. The model domain and boundary conditions establish both a framework and limiting conditions for the numerical model. The model domain for flow and transport in the vadose zone is represented numerically in 3-D space, with one of the horizontal axes aligned in the general direction of groundwater flow. Aligning an axis with the general direction of groundwater flow allows concentrations to be calculated more easily downgradient of the waste sites. The numerical model adapts the physical elements of the conceptual model to a Cartesian grid, and also assigns numerical values to the parameters used in algorithms to represent the physical and geochemical systems and processes.

The WMA C model domain is 737.9 m (2,421 ft) northwest to southeast by 795.3 m (2,609 ft) southwest to northeast by 116 m (381 ft), vertically, extending ~12 m (39 ft) below the water table (Figure 3-5 shows the extent of the model domain). The southwestern and northwestern boundaries of the model are 574656.09 m, 136454.41 m, and 575218.45 m, 137016.78 m, respectively (Lambert Coordinate system easting, NOAA Manual NOS NGS 5, “State Plane Coordinate System of 1983”). The southeastern and northeastern boundaries are 575177.86 m, 135932.64 m, and 575740.22 m, 136495.00 m, respectively. The vertical base elevation of the model is nominally 95 m (312 ft) (NAVD88), although the bottom and top of the model domain vary spatially according to the top of basalt elevation and surface relief, respectively (RPP-RPT-56356).

The horizontal node spacing varies between 3.0 and 20 m (9.8 and 65.6 ft) to optimize the discretization in the areas attempting to approximate the slopes associated with construction of WMA C and the 100-series tanks without overwhelming the available computational resources. Figure 3-6 shows the plan view distribution of the calculation nodes. The vertical spacing in the vadose zone ranged between 1 and 1.25 m (3.28 and 4.10 ft) except around the water table, where the spacing decreased to 0.5 m (1.6 ft) to capture the impact of the capillary fringe above the water table. The total number of nodes in the modeled rectangular prism equals 736,653. During the pre-operational phase, the number of active nodes equals 640,565 with 96,088 inactive. Inactive nodes represent space where no flow occurs, e.g., above ground surface, within basalt, or within intact tanks. During the operational and post-closure phases, the number of active nodes equals 637,543 with 99,110 inactive, the increase in inactive nodes attributed to the inactivation of the tank and ancillary equipment nodes within the WMA C excavation.

Figure 3-5. Interpolated Numerical Three-Dimensional Post-Closure Alternative I Hydrogeologic Model.

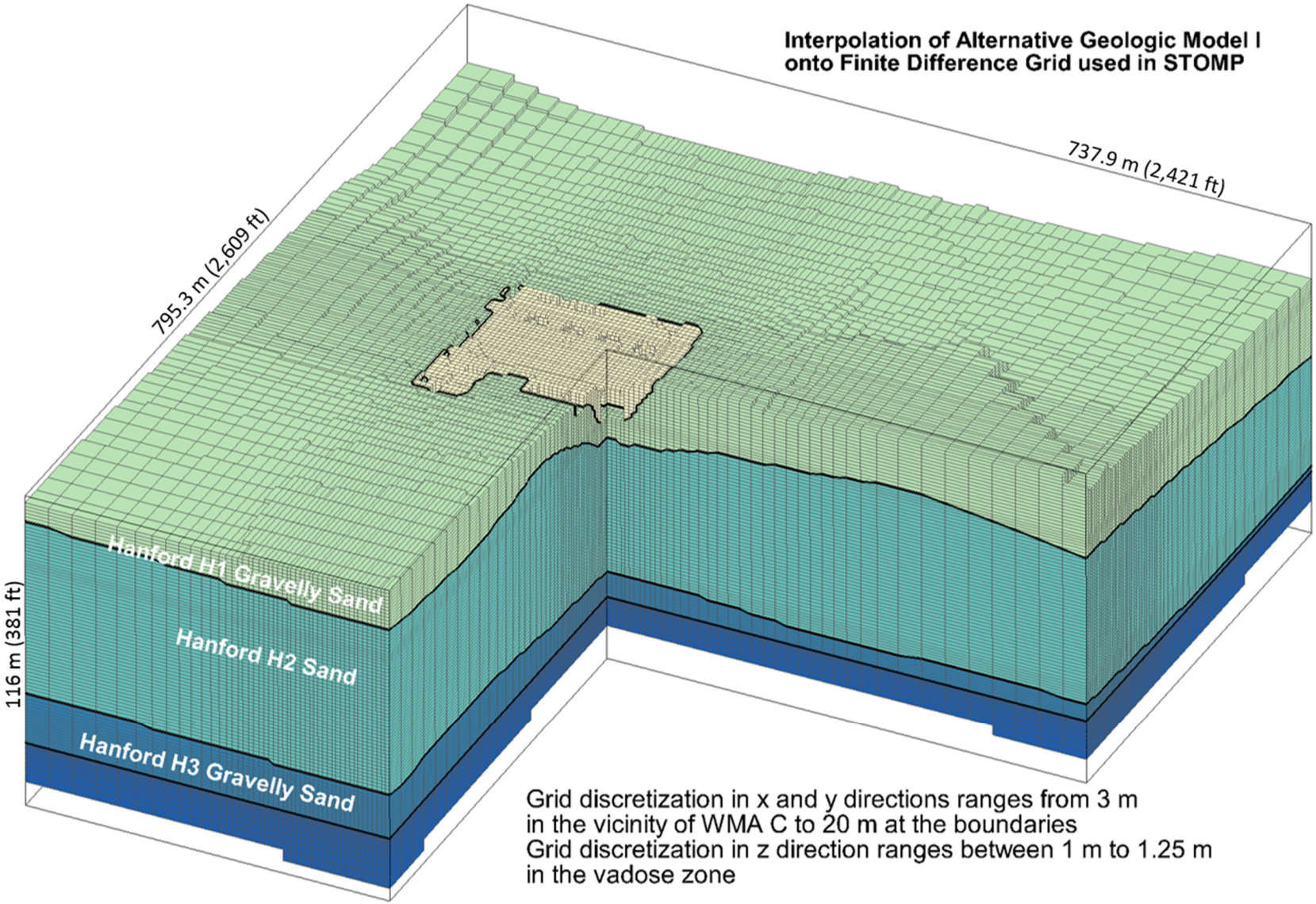

STOMP = Subsurface Transport Over Multiple Phases (computer code) WMA = Waste Management Area

A specified-flux boundary condition was applied at the surface to simulate recharge. Recharge rates varied spatially and temporally along the upper boundary, depending on surface conditions, the presence of WMA C and other facilities, and the time of WMA C operations and surface conditions simulated (RPP-RPT-44042, "Recharge and Waste Release within Engineered System in Waste Management Area C"). The bottom boundary of the unsaturated (vadose) zone is the water table, and the bottom of the model (aquifer) was defined as a no-low boundary condition. Boundary conditions at the sides of the model domain were assumed to be no flow in the vadose zone and prescribed flux and prescribed head in the aquifer on the upgradient and downgradient boundaries, respectively. The boundary condition in the aquifer on the upgradient boundary was assumed to be prescribed flux, calculated on the basis of the hydraulic conductivity and gradient, and independent of recharge. The prescribed flux boundary condition value includes a factor to account for the varying thickness of the unconfined aquifer and uneven surface of the underlying basalt. To account for the non-uniform aquifer thickness from the underlying basalt boundary, the nominal flux rate was calculated as the product of the hydraulic conductivity and gradient (base case values of 11,000 m/day [6.8 mi/day] and 2×10^{-5} m/m [6.6×10^{-5} ft/m], respectively), and was proportioned according to the ratio of the average aquifer cross-sectional area throughout the model domain (9,440 m^2 [2.3 acres]) and the aquifer area along the upgradient boundary (6,151 m^2 [1.5 acres]) where the prescribed flux is applied. The aquifer cross-sectional area refers to the area perpendicular to the direction of groundwater flow. The aquifer cross-sectional area varies from the northwest to southeast boundaries because of the uneven top of the basalt.

3.6.3.2 Hydrogeologic Model. The hydrogeologic conceptual model developed for the WMA C PA (RPP-RPT-46088 and RPP-RPT-56356) provides the information basis and data necessary to prepare the 3-D geologic inputs used in the 3-D numerical model. Each node in the numerical model represents a unique set of horizontal (x and y) coordinates and vertical (z) elevation. A node is assigned the hydrogeologic properties associated with the HSU identified in the RPP-RPT-56356 geologic models as existing in the space represented by the node coordinates and elevation.

Figure 3-5 shows the geologic interpretation prepared by Washington River Protection Solutions, LLC (WRPS) staff and identified as Alternative Model I as interpolated onto the numerical grid used in the fate and transport model. The fence diagram, given in Figure 3-7, shows some internal cross-sections of the geology to illustrate the shape and layering of the hydrogeologic units. Figures 3-8 and 3-9 show the geologic interpretation prepared with input from technical staff of the Nez Perce and identified as Alternative Model II. Alternative Model II includes the separation of the Hanford H2 sand unit into three distinct subunits: the Hanford H2 sand, the Hanford H2 gravelly sand, and the Hanford H2 fine or silty sand. Explanation of the basis and the development of the two geologic interpretations is presented in RPP-RPT-56356. The scoping analysis includes evaluation of an additional alternative geologic model that is identical to Alternative Model I, except that a clastic dike is assumed to exist under tanks C-102, C-105, C-108, and C-111, and another is assumed to exist under tanks C-110, C-111, and C-112. These clastic dikes extend the length and width, respectively, of WMA C, and extend from the bottom of the WMA C excavation to the capillary fringe of the aquifer.

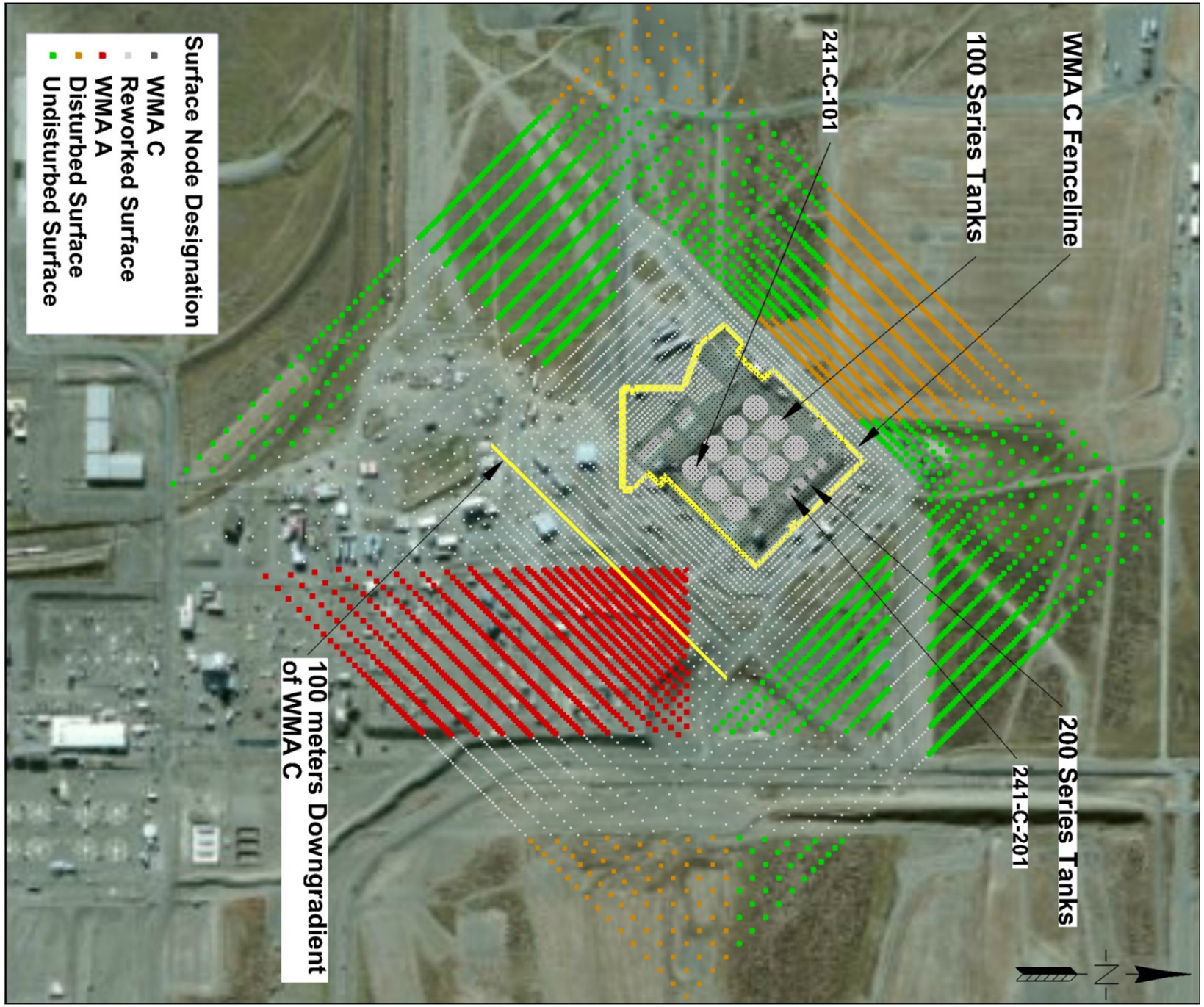

Figure 3-6. Plan View of Waste Management Area C Performance Assessment Model Domain Showing the Horizontal Distribution and Surface Type of the Irregularly-Spaced Calculation Nodes. The resolution increases in the area of Waste Management Area C.

WMA = Waste Management Area

Figure 3-7. Fence Diagram of Interpolated Numerical Three-Dimensional Post-Closure Alternative I Hydrogeologic Model.

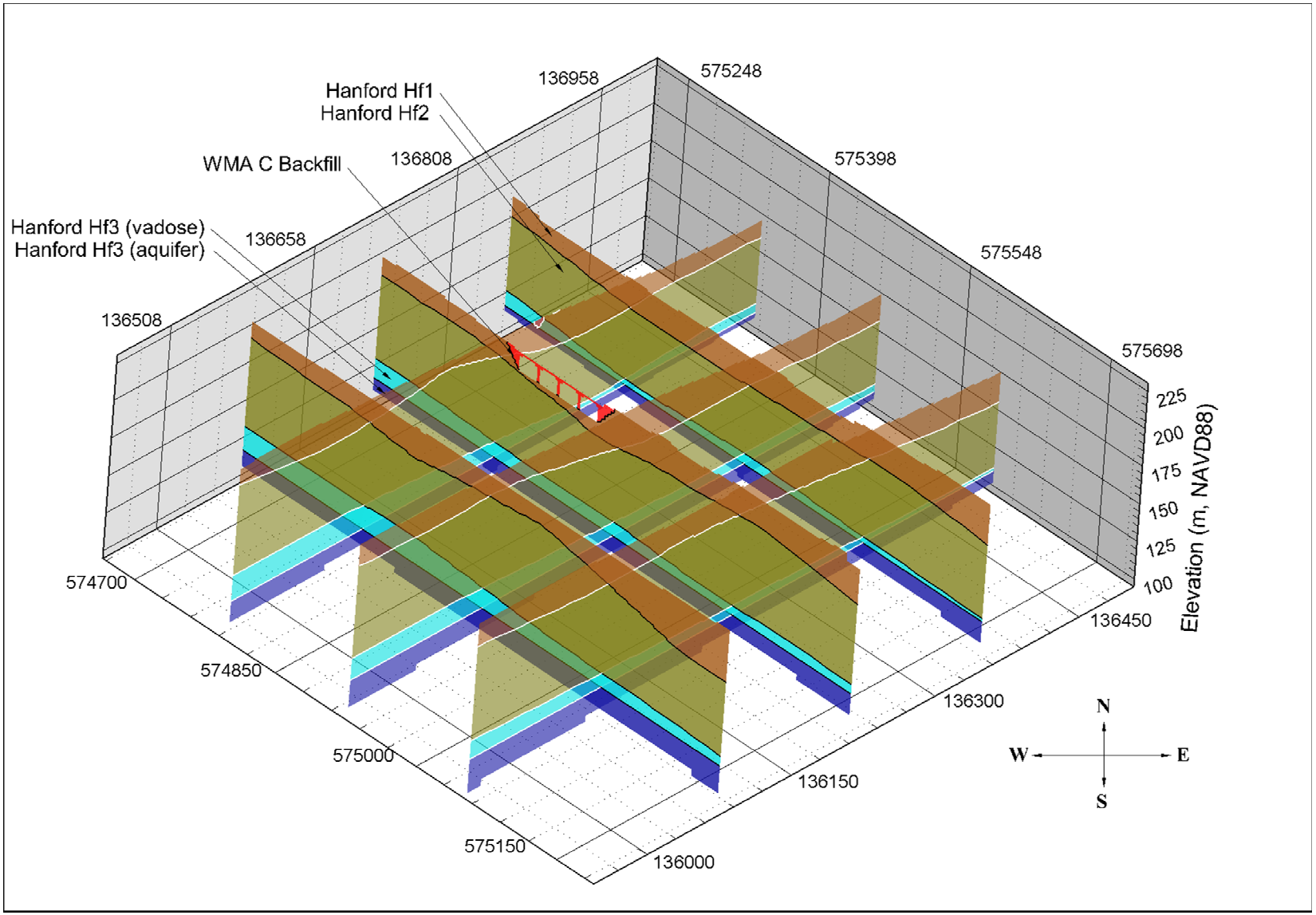

NAVD88 = North American Vertical Datum of 1988, WMA = Waste Management Area, Hf = Hanford formation

Figure 3-8. Interpolated Numerical Three-Dimensional Post-Closure Alternative II Hydrogeologic Model.

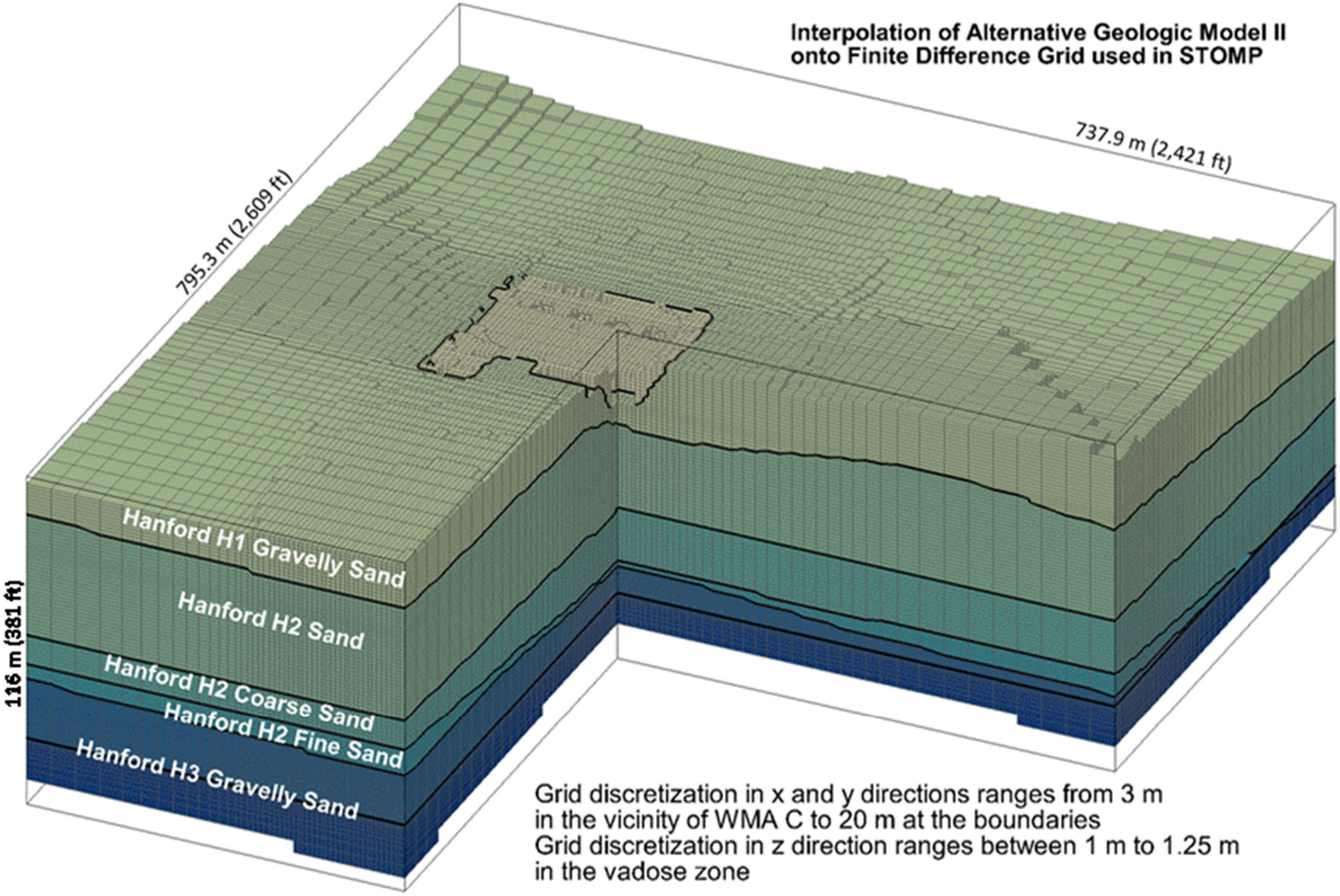

STOMP = Subsurface Transport Over Multiple Phases (computer code) WMA = Waste Management Area

Figure 3-9. Fence Diagram of Interpolated Numerical Three-Dimensional Post-Closure Alternative II Hydrogeologic Model.

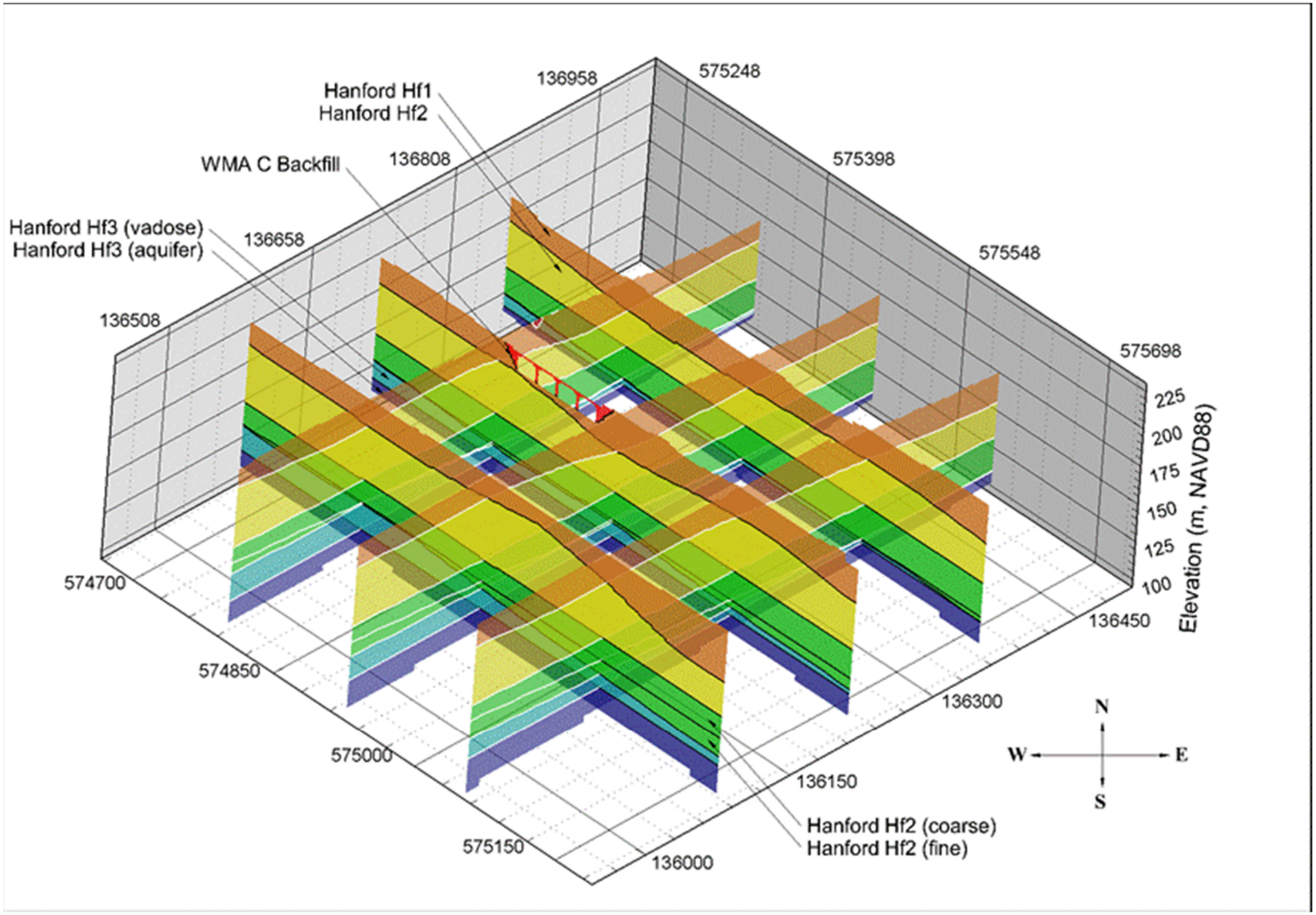

Hf = Hanford formation VD88 = North American Vertical Datum of 1988 WMA = Waste Management Area

3.6.3.3 Recharge. The magnitude of recharge for soils at the Hanford Site varies as a function of the soil type, condition of the vegetation cover, and soil integrity (e.g., disturbed versus undisturbed). The range of recharge values reported in RPP-RPT-44042 represents distinct populations of data based on lysimetry and isotopic measurements, and interpretation—and, in some instances, extrapolation—by Hanford Site subject matter experts. The natural background recharge rates represent a population for natural vegetated conditions. The range of values for operational conditions represents a population of recharge rates for vegetation-free disturbed soil.

The final design for the surface barrier for WMA C at closure has not been developed. The surface barrier is expected to function comparably to a modified RCRA Subtitle C barrier (Section 3.2.1.2.2), which PNNL-16688, "Recharge Data Package for Hanford Single-Shell Tank Waste Management Areas" indicates should function similarly to the Prototype Hanford Barrier. Summary of data collected over 13 years at the Prototype Hanford Barrier (PNNL-17176, "200-BP-1 Prototype Hanford Barrier Annual Monitoring Report for Fiscal Years 2005 Through 2007"; DOE/RL-93-33, Focused Feasibility Study of Engineered Barriers for Waste Management Units in the 200 Areas) indicates that infiltration through the prototype is much less than 0.1 mm/yr (0.004 in./yr), and evaluations of the design using lysimeter data indicate that the barrier is capable of limiting recharge to this amount even with a complete lack of vegetation ("Multiple-Year Water Balance of Soil Covers in a Semiarid Setting" [Fayer and Gee 2006]). However, for base case simulations involving WMA C PA with a functioning surface barrier, a base case recharge rate of 0.5 mm/yr (0.02 in./yr) is assumed, which is consistent with the drainage design specification in DOE/RL-93-33.

At the end of 500 years, the surface barrier performance is assumed to degrade to permit an infiltration rate of 3.5 mm/yr (0.14 in./yr) and maintain that infiltration rate for the remainder of the simulation for the base case. No quantifying data are available for specifying the performance of the barrier top after its design life, but the performance of the surface barrier in limiting recharge is not expected to diminish appreciably (PNNL-16688). According to PNNL-13033, "Recharge Data Package for the Immobilized Low-Activity Waste 2001 Performance Assessment," not even the erosion of the silt loam layer and deposition of dune sand on the barrier is likely to alter the barrier performance significantly. The value of 3.5 mm/yr (0.14 in./yr) corresponds to the recharge in an undisturbed area, which indicates that native vegetation is assumed to reclaim the land.

Although the side slopes and berm are likely to function and perform differently than the surface of the barrier, they are included as part of the barrier surface. The impact of the side slopes on the overall recharge rate is expected to be relatively negligible. The sandy gravel/gravelly sand barrier side slope and berm are assumed eventually to resemble a Burbank loamy sand, and if that assumption is valid, then PNNL-16688 indicates that the long-term recharge rate for that soil type is 1.9 mm/yr (0.07 in./yr), which is less than the 3.5 mm/yr (0.14 in./yr) used in the analysis for the degraded barrier surface. Table 3-3 presents a summary of the base case recharge rates applied to the different surface types present within the WMA C model domain.

3.6.3.4 Vadose Zone Hydrogeology and Transport. The vadose zone hydrogeology and transport information presented here is a brief summary of the information presented in RPP-ENV-58782 and RPP-ENV-58806. Those reports include detailed discussion and

description of the data available and the methods used to develop the base case parameters, and sensitivity and uncertainty distributions and percentile values.

Table 3-3. Base Case Recharge Rate (Net Infiltration) Estimates for Surface Conditions during the Pre-Construction, Operational, and Post-Closure Periods.

Period	Waste Management Area (WMA) C Region and Surface Condition	Base Case Value of Recharge Rate (mm/yr)
Pre-construction (before 1944)	Undisturbed region (Rupert sand with vegetation)	3.5
Operational period (1945 to 2020)	Undisturbed region (Rupert sand with vegetation)	3.5
	WMA C Surface region (Gravel without vegetation)	100
	WMA A Surface region (Gravel without vegetation)	100
	Disturbed revegetated region (Rupert sand with vegetation)	22
	Disturbed unrevegetated region (Rupert sand with no vegetation)	63
Early post-closure (2020 to 2520)	Undisturbed region (Rupert sand with vegetation)	3.5
	WMA C Surface region (Surface barrier with vegetation)	0.5
	WMA A Surface region (Surface barrier with vegetation beginning in 2050)	0.5
	Disturbed revegetated region (Rupert sand with vegetation beginning in 2050 with vegetation recovery completed in 2080)	3.5
	Disturbed unrevegetated region (Rupert sand with no vegetation until vegetation recovery begins in 2050 and completes in 2080)	3.5
Late post-closure (2520 to 3020 and beyond)	Undisturbed region (Rupert sand with vegetation)	3.5
	WMA C Surface region (Surface barrier with vegetation)	3.5
	WMA A Surface region (Degraded surface barrier with vegetation begins in 2550)	3.5
	Disturbed revegetated region (Rupert sand with vegetation recovery completed in 2080)	3.5
	Disturbed unrevegetated region (Rupert sand with vegetation recovery completed in 2080)	3.5

The flow and transport pathway process used for the WMA C vadose zone modeling is porous media continuum flow. The porous media continuum assumption and the soil relative permeability/saturation/capillary pressure relations provide the basis for vadose zone flow and transport modeling (PNNL-11216, PNNL-12030). The vadose zone at the Hanford Site is composed of sediments ranging in particle size associated with gravels to silts or clays. In the model domain, the hydraulic properties describing fluid transport characteristics associated with each geologic layer (also referred to as HSUs) are approximated by average upscaled values, with each unit having different flow and transport parameter values (hydraulic conductivity, bulk

density, and dispersivity). The model describes bulk (or mean) flow and radionuclide transport behavior in the vadose zone, limiting the evaluation to estimating overall and eventual radionuclide impacts to groundwater. Porous media continuum transport in unsaturated media of this type is regarded as the fundamental process and feature for modeling contaminant fate and transport behavior in the vadose zone at the Hanford Site (DOE/RL-2011-50).

Table 3-4 lists the upscaled composite-fitted van Genuchten-Mualem (van Genuchten 1980, Mualem 1976, EPA/600/2-91/065) base case parameters for the various strata at the WMA C site. A stochastic model of variable moisture or tension-dependent anisotropy provides the framework for upscaling small-scale measurements to the effective (upscaled) properties for the large-scale vadose zone (Polmann 1990). The upscaling processes factor the inherent spatial variability that occurs on different scales in heterogeneous media into the field scale parameter estimates ("Stochastic analysis of moisture plume dynamics of a field injection experiment" [Ye et al. 2005], "Estimation of effective unsaturated hydraulic conductivity tensor using spatial moments of observed moisture plume" [Yeh et al. 2005]). Specific upscaled flow parameters include moisture retention, and saturated and unsaturated hydraulic conductivity. Upscaled transport parameters include bulk density, diffusivity, sorption coefficients, and macrodispersivity.

Table 3-4. Composite van Genuchten-Mualem Parameters for Various Strata at the Waste Management Area C Site Used in the Base Case Evaluations of Alternative Geologic Models I and II.

Strata	Number of Samples	θ_s	θ_r	α (1/cm)	n	ℓ^c	Fitted K_s (cm/s)
Backfill (Gravelly)	10	0.138	0.010	0.021	1.374	0.5	5.60E-04
Hanford H1/H3 (Gravel-dominated)	15	0.171	0.011	0.036	1.491	0.5	7.70E-04
Hanford H2 (Sand-dominated)	44	0.315	0.039	0.063	2.047	0.5	4.15E-03
Hanford H2 –Gravel/coarse sand subunit*	not applicable	0.265	0.002	0.108	1.724	0.5	1.68E-02
Hanford H2 – Silty-sand subunit*	not applicable	0.354	0.029	0.040	1.633	0.5	1.79E-03

*Hydraulic properties of these units are only used in numerical model simulation of Alternative Geologic Model II. As an initial estimate of these properties, the hydraulic properties associated with the 5th and 95th percentile realizations of unsaturated hydraulic conductivity curves developed in the Uncertainty and Sensitivity Analysis for the Hanford H2 sand unit were considered to be representative of the Hanford H2 silty sand and the Hanford H2 gravel/coarse sand subunits, respectively.

Estimated unsaturated conductivities, based on saturated conductivity and the van Genuchten retention model, can differ by up to several orders of magnitude with measured conductivities at the dry end (e.g., "Evaluation of van Genuchten-Mualem Relationships to Estimate Unsaturated Hydraulic Conductivity at Low Water Contents" [Khaleel et al. 1995]). Therefore, unlike the conventional approach, the unsaturated conductivities are not based on predictions using the measured retention curve and the measured saturated conductivity. Rather, the soil hydraulic properties are based on a simultaneous fit of moisture retention and unsaturated conductivity

data, and all five unknown parameters θ_r, θ_s, α, n, and K_s, with m=1-1/n (van Genuchten 1980) were fitted to the data via a code named RETention Curve (RETC) (EPA/600/2-91/065). Thus, in order to obtain a better agreement with experimental data for the region of interest (i.e., relatively dry moisture regime), K_s is treated as a fitted parameter during the curve fitting process. This is considered appropriate because the WMA C PA predictions are needed for the relatively dry moisture regime observed in the field, rather than for the saturated or near-saturated regime. The pore size distribution factor, ℓ, was kept fixed at 0.5 during the simultaneous fitting.

For the Alternative Geologic Model II evaluation, the Hanford H2 gravel/coarse sand subunit was assumed to be more transmissive, and the Hanford H2 silty sand less transmissive, than the Hanford H2 sand. Therefore, as an initial estimate of these properties, the hydraulic properties associated with the 5th and 95th percentile realizations of unsaturated hydraulic conductivity curves developed for the Hanford H2 sand unit were considered representative of the Hanford H2 gravel/coarse sand and the Hanford H2 silty sand subunits, respectively.

The effective transport parameter (i.e., macrodispersivity, bulk density, and diffusivity) estimates used in the base case and sensitivity cases are presented. Because of natural variability, the transport parameters are all spatially variable. The purpose is similar to the upscaled flow parameters, to evaluate the effect of such variability on the large-scale transport process. Effective bulk density (ρ_b) estimates are needed to calculate retardation factors for different species. The average ρ_b, E[ρ_b] estimates for various strata at WMA C are presented in Table 3-5. These estimates are derived from bulk density sample values listed in RPP-ENV-58782 and RPP-ENV-58806, Appendix B. The values of macrodispersivity applicable to the scale of the WMA C PA model for the base case evaluation are shown in Table 3-6.

It is assumed that the effective, large-scale diffusion coefficients for all strata in the vadose zone at the WMA C site are a function of volumetric moisture content, θ, and can be expressed using the Millington-Quirk ("Permeability of Porous Solids" [Millington and Quirk 1961]) empirical relation:

$$D_e(\theta) = D_0 \frac{\theta^{10/3}}{\theta_s^2} \tag{6-15}$$

Where:

$D_e(\theta)$ = the effective diffusion coefficient of an ionic species
D_0 = the effective diffusion coefficient for the same species in free water
θ = the localized volumetric moisture content
θ_s = the localized volumetric moisture content at saturation.

The tortuosity formulation in the Millington-Quirk model is based on theoretical considerations absent from other empirical models, and accounts for the ranges of moisture contents present in the vadose zone around WMA C. The molecular diffusion coefficient for all species in pore water is assumed to be 2.5×10^{-5} cm^2/sec (6.98×10^{-4} in.^{2}/sec) (WHC-SD-WM-EE-004, "Performance Assessment of Grouted Double-Shell Tank Waste Disposal at Hanford"), which is

consistent with, and representative of, values used in other Hanford PAs (WHC-EP-0645, "Performance Assessment for the Disposal of Low-Level Waste in the 200 West Area Burial Grounds"; BHI-00169, "Environmental Restoration Disposal Facility Performance Assessment"; WHC-SD-WM-TI-730, "Performance Assessment for the Disposal of Low-Level Waste in the 200 East Area Burial Grounds"; WHC-SD-WM-EE-004, and DOE/ORP-2000-24, Hanford Immobilized Low-Activity Waste Performance Assessment: 2001 Version).

Table 3-5. Effective Bulk Density ($E[\rho_b]$, g/cm^3) Estimates for Various Strata at Waste Management Area C Used in the Base Case Evaluations of Alternative Geologic Models I and II.

Strata	$E[\rho_b]$
Backfill (Gravelly)	2.13
Hanford H1/H3 (Gravel-dominated)	2.05
Hanford H2 (Sand-dominated)	1.71
Hanford H2 – Gravel/coarse sand subunit*	1.88
Hanford H2 – Silty-sand subunit*	1.94

*Effective bulk densities of these units are only used in numerical model simulation of Alternative Geologic Model II.

Table 3-6. Macrodispersity Estimates for Various Strata at Waste Management Area C Used in the Base Case Evaluations of Alternative Geologic Models I and II.

Strata	A_L (cm)	A_T (cm)
Backfill (Gravelly)	~20	2.0
Hanford H1/H3 (Gravel-dominated)	~20	2.0
Hanford H2 (Sand-dominated)	~25	2.5
Hanford H2 –Gravel/coarse sand subunit*	~25	2.5
Hanford H2 – Silty-sand subunit*	~25	2.5

*Macrodisperisivities of these units are only used in numerical model simulation of Alternative Geologic Model II.

3.6.3.5 Groundwater Domain and Characteristics. The groundwater in the aquifer system in the vicinity of WMA C has been studied extensively as part of the site characterization that is discussed in RPP-RPT-46088 and Section 2 of this report. The groundwater conceptual model for WMA C includes the uppermost unconfined aquifer system that exists within a channel eroded by the cataclysmic floods of the Pleistocene age. The base of the aquifer is the underlying basalt surface. The undifferentiated lower sands and gravels associated with the Hanford formation, CCu, and the Ringold Formation (Unit A) that comprise the aquifer sediments are simply categorized as saturated Hanford H3 sediments in the model. The thickness of the uppermost aquifer beneath WMA C is ~12 m (39 ft).

Groundwater flow beneath WMA C has been historically difficult to measure because the hydraulic gradient is very small and the hydraulic conductivity is very high in this region of the Hanford Site. In addition, the water table continues to recover from the operational liquid discharges at 216-B-3 Pond system and other large discharge sites in 200 East Area. The projected equilibrium state is expected to be similar to its pre-Hanford behavior described in Section 3.1.9.2 and Appendix C of RPP-ENV-58782 and RPP-ENV-58806). As a result, the post-closure position of the water table and associated hydraulic gradient can only be evaluated through modeling. Consequently, the groundwater flux in the aquifer beneath WMA C is calculated on the basis of the aquifer hydraulic properties, and the hydraulic gradient projected to exist in the future.

The hydraulic heads around WMA C are expected to continue declining slowly (Figure 2-11) until they stabilize around 119.5 m (392 ft) within 100 years in the future (CP-47631). The gradient is generally expected to slope from northwest to southeast with a value of ~0.00002 m/m, which is close to the one observed prior to start of Hanford operations (Figure 3-10). Appreciable changes in hydraulic gradient are not expected in the future once the hydraulic heads stabilize.

These changing conditions lead to considerable challenges in modeling the past leaks. The hydraulic heads, head gradients, and gradient orientations are significantly uncertain and change on the time scales as the arrival of the plumes from the vadose zone. This means that at any particular point in time in the analysis it is uncertain how the model results correspond to the reality reflected by observed groundwater monitoring data. In the face of these uncertainties, the aquifer representation has been undertaken in the following two ways.

- A scoping case has been implemented that approximates the best understanding of the changes in the water table as a function of time (see Section 5.0). A calibrated CPGWM (CP-47631) serves as the basis for the model and the time-dependent evolution of the unconfined aquifer at WMA C. The development of CPGWM incorporates over 30 years of experience on development and application of groundwater models for the Central Plateau [PNL-10886, "Development of a Three-Dimensional Ground-Water Model of the Hanford Site Unconfined Aquifer System: FY 1995 Status Report"; PNNL-13641, "Uncertainty Analysis Framework – Hanford Site-Wide Groundwater Flow and Transport Model"; PNNL-14398, "Transient Inverse Calibration of the Site-Wide Groundwater Flow Model (ACM-2): FY 2003 Progress Report"; PNNL-14753, "Groundwater Data Package for Hanford Assessments"; PNNL-12261, "Revised Hydrogeology for the Suprabasalt Aquifer System, 200-East Area and Vicinity, Hanford Site, Washington"]. The CPGWM incorporates the large-scale geologic and hydrogeologic features and provides estimates of water levels, hydraulic gradients, and groundwater flows throughout the 200 West and 200 East Areas, for past, current, and expected future groundwater conditions. Simulated water levels have been compared to observed values for wells located upgradient (well 299-E27-15) and downgradient (well 299-E27-14) of WMA C (Figure 3-11). The observed heads and CPGWM-simulated heads, representing a time span of over 20 years, compare well providing confidence in the predictive capabilities of the CPGWM.

- All other scoping analyses have assumed a constant steady-state aquifer gradient magnitude and orientation. These have been chosen to be consistent with the long-term gradient assumed in RPP-ENV-58782 and RPP-ENV-58806 with hydraulic heads representative of past conditions to take account of the shorter travel distance in the vadose zone compared to the post-closure period. Since the orientation of this gradient does not correspond to the reality of the past, the concentrations calculated in these analysis cases will not correctly calculate concentrations at any point in space. So, for instance, direct comparison of the concentrations at well 299-E27-23 with model concentrations at the location of 299-E27-23 do not give meaningful comparisons. However, they do permit evaluation of peak concentrations as a function of distance from the source.

Within the WMA C flow domain, the weighted average of hydraulic conductivity derived from the CPGWM is ~11,000 m/day (33,000 ft/day). Thus, the base case horizontal saturated hydraulic conductivity for the aquifer is estimated to be 11,000 m/day (33,000 ft/day). The CPGWM estimate of vertical anisotropy ratio of 0.1 is also incorporated in the WMA C base case. Table 3-7 presents a summary of the aquifer base case hydraulic parameters for the Hanford H3 – aquifer. The aquifer, identified as Hanford H3 – aquifer, is separated from that portion of the Hanford H3 above the water table, reflecting the distinctly different saturation conditions.

3.6.3.6 Sorption Characteristics. The scoping analysis cases presented in Section 4 focus on ^{99}Tc, for which an assumption of zero sorption is appropriate. For forward calculations, base-case K_d values for other contaminants described in RPP-ENV-58782 and RPP-ENV-58806 are used.

3.7 SUMMARY OF FEATURES AND DEFINITION OF SCOPING ANALYSIS CASES

As discussed in Section 3.1, uncertainties exist in a number of the features associated with modeling past leaks at WMA C. As part of the scoping sessions held in 2009 through 2011, a set of topics were identified that need to be explored through scoping analysis cases. These issues can be broadly thought of belonging to one of the following three categories.

- Topics associated with the leaks themselves: their inventory, volume, timing, and location.

- Topics associated with the vadose zone: the effects of soil heterogeneity, the effects of alternative conceptualizations of the geological media, the effects of man-made features such as dry wells, and the potential effects of unknown features such as a clastic dike under WMA C.

- Topics associated with the saturated zone evolution in time during the operational period and its effect on the observed changes in patterns of contamination at the monitoring wells.

Figure 3-10. Hindcast Water Table Map of the Hanford Site, January 1944.

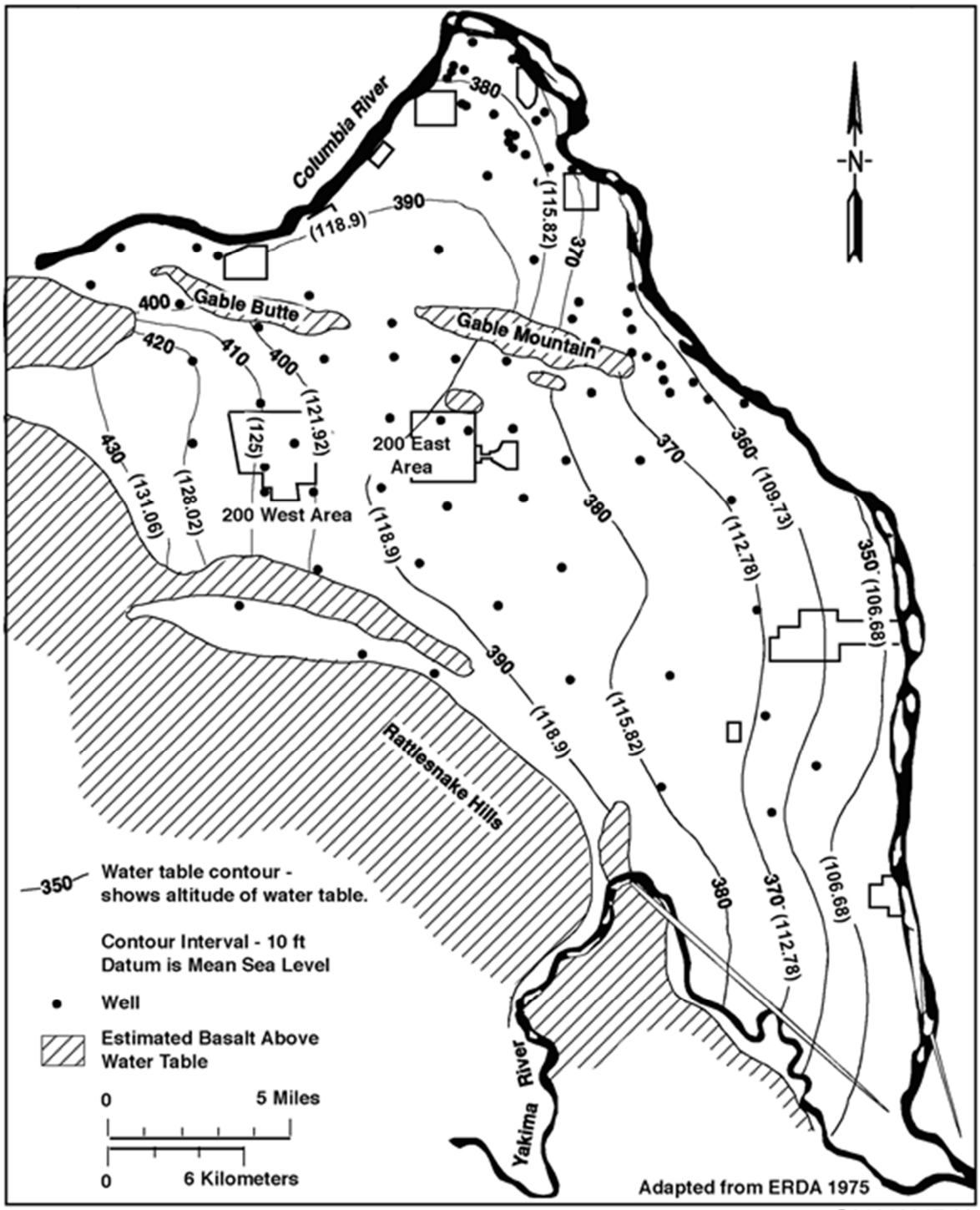

ERDA 1975 = ERDA-1538, "Final Environmental Statement, Waste Management Operations, Hanford Reservation, Richland, Washington."

Source: WHC-SD-ER-TI-003, "Geology and Hydrology of the Hanford Site: A Standardized Text for Use in Westinghouse Hanford Company Documents and Reports."

Figure 3-11. Central Plateau Groundwater Model Calibration Results in the Vicinity of Waste Management Area C.

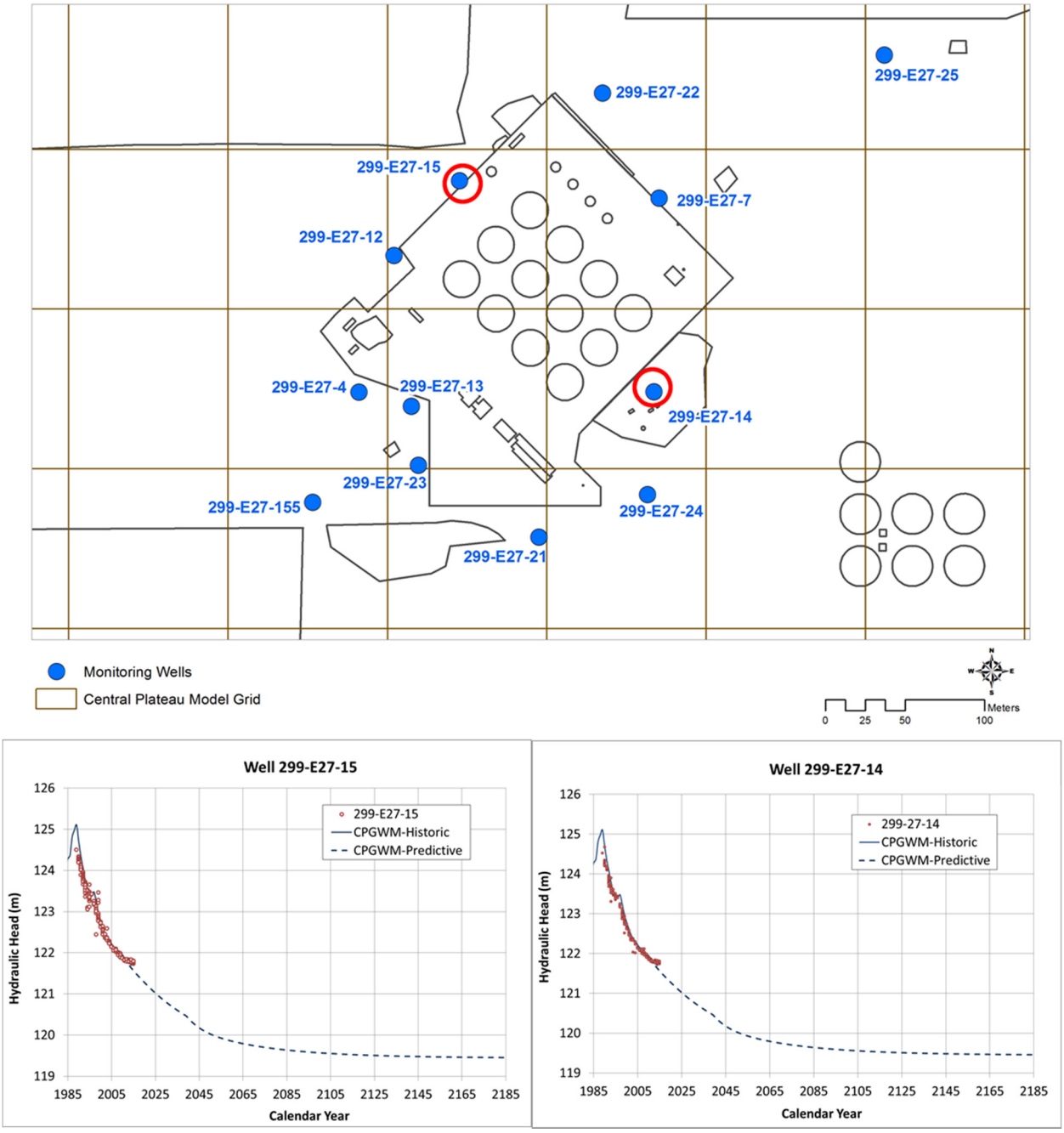

CPGWM = Central Plateau Groundwater Model

Reference: CP-47631, "Model Package Report: Central Plateau Groundwater Model Version 6.3.3."

To address these topics, a suite of scoping analysis cases have been identified and are described in Section 4.0.

Table 3-7. Base Case Soil Hydraulic Properties for Aquifer Soil Type Used for Base Case at Waste Management Area C.

Aquifer Soil Type	Total Porosity	Saturated Moisture Content	Horizontal Saturated Hydraulic Conductivity[a] (m/day)	Longitudinal Dispersivity[b] (m)	Aquifer Hydraulic Gradient (m/m)	Average Aquifer Water Flux ($m^3/day/m^2$)
Hanford H3 (aquifer)	0.20	0.20	11,000	10.5	0.00002	0.22

[a] Vertical Saturated Hydraulic Conductivity assumed equal to 1/10 of the Horizontal Saturated Hydraulic Conductivity.
[b] Transverse dispersivity assumed to be equal to 1/10 of the longitudinal dispersivity.

Reference: RPP-RPT-46088, "Flow and Transport in the Natural System at Waste Management Area C."

This page intentionally left blank.

4.0 SCOPING ANALYSES OF PAST WASTE RELEASES

In this section, a series of scoping analysis cases are described that use the PA model developed for the assessment of potential future releases from residual wastes, documented in RPP-ENV-58782 and RPP-ENV-58806, with appropriate adaptations to represent past conditions at WMA C. Sources of contamination have been introduced into the model to represent the occurrence of the past leaks at the times at which they are believed to have occurred. It is worth noting that the input parameters for vadose zone flow used in the residual waste model were selected to be representative of the dry (volumetric moisture < 6%) conditions expected under WMA C in the future in the post-closure period. These parameters are not necessarily representative of past conditions when recharge through the farm was higher and additional anthropogenic water was added with the leaks. Therefore, one of the uncertainties to be addressed is the role of vadose zone parameter selection in evaluating the behavior of past leaks.

The focus of the analysis cases presented in this section is to provide improved understanding of the phenomena and parameters that have led to the current state of contamination below and near WMA C. The focus of the analysis cases reported in this section is on ^{99}Tc contamination, which is unambiguously the result of past UPRs from WMA C. Groundwater in the vicinity of WMA C has also seen impacts by other COPCs (e.g., nitrate, sulfate, for example), but ^{99}Tc is the contaminant that accounts for the majority of the past and current dose and risk impacts to groundwater at WMA C.

The goal of the scoping analyses is to match, to the extent possible, the arrival times of the contamination at the water table and general concentration levels observed in monitoring wells. These two indicators are regarded as the most reliable and reproducible aspects of the groundwater monitoring data. Given the uncertainties in the estimates and timing of past leaks and complexities of the behavior of the site, it is unrealistic to hope to achieve exact matches with data. Instead, the goal is to provide a reasonable match with data, in a way that provides information and insight into the processes and parameter values that are consistent with observed contamination in monitoring wells at WMA C. The general shapes of the breakthrough curves observed in data (sharp rises and falls in concentration) are believed to be associated with shifts in the direction of the groundwater flow. This aspect of the breakthrough curves is not well represented by the scoping cases presented in this section, since they all assume a constant groundwater flow rate and direction. Analyses that take account of the changing water table are presented in Section 5, and those analyses are intended to provide insight into the rapid rise and fall of observed data.

The scoping analyses presented in this chapter evaluate changes in calculated groundwater impacts that result from changes in input parameter estimates or changes to a conceptual model, such as the interpretation of the hydrogeologic units. The range of analysis cases are generally intended to evaluate changes in parameters and modeling assumptions, to demonstrate the effect that alternative assumptions and estimates have on the groundwater arrival times and concentrations in and around the tank farm.

Primary sources of alternative modeling assumptions are natural system heterogeneities; heterogeneities introduced by tank farm and infrastructure construction; the timing, volume and inventory of the leaks; and appropriate values for input parameters that affect arrival times and groundwater concentrations. These analyses are run as deterministic analyses, without assigning a likelihood of occurrence to a particular result other than (in some cases) a qualitative evaluation of its likelihood.

The scoping analyses quantify the ranges of calculated groundwater concentration outcomes due to single-parameter or multiple-parameter changes that represent an underlying shift in the conceptual model. The analyses quantify the impact that alternative views of the engineered and natural systems may have on groundwater concentrations to better understand the evolution of the existing concentrations observed in groundwater around WMA C; this improved understanding may then be used to provide estimates of future impacts associated with the past UPRs (see Section 7). These estimates of future impacts are intended to support potential remedial decisions for WMA C.

The set of scoping analyses are presented in Table 4-1. The table includes a brief explanation of each scoping analysis to provide insight into the alternative assumptions it is intended to evaluate. Because these scoping cases involve changes to the underlying flow field, the analysis was best done using a process model and STOMP© to perform the calculations.

In Table 4-1, the scoping analyses represent categories of uncertainty. The scoping cases can be grouped in four categories: (1) changes to estimates of UPR volume and inventory, (2) changes in groundwater flow rate (hence dilution) in the saturated zone, (3) changes in recharge, and (4) changes in vadose zone geology and hydrologic parameters. The first set of scoping simulations (Cases 1a and 1b) addresses the range of estimated ^{99}Tc inventory and the leak volume. The set of groundwater flux cases (Case 2a and 2b) correspond to altered aquifer flow rates that produce lower and upper confidence limits of aquifer dilution. The set of recharge-related scoping analyses (Cases 3a –3c) address elements associated with the magnitude of the net infiltration through the tank farm surface and surrounding disturbed ground. The set of vadose zone cases (Cases 4a-4f) examine the impacts of changes in the hydrologic parameters and spatial heterogeneity in the vadose zone. This set of cases considers evaluations of a range of cases that include Case 4a – a case to represent Alternative Geologic Model II; Case 4b – a case to represent a heterogeneous representation of the vadose zone; Cases 4c and 4d – cases to represent upper and lower confidence limits for vadose zone hydraulic properties; Case 4e – a case to represent a hypothesized presence of a clastic dike within the WMA C fenceline, and Case 4f – a case to represent a hypothesized existence of an unsealed or poorly sealed borehole in the tank farm.

For this analysis case, the STOMP©-based model developed for the PA and RCA of residual wastes has been modified to match the approximate water table elevation that currently exists. This modification was made to approximate the depth to the water table that existed when the plumes arrived at the water table, so that this model will represent the time of first arrival at the water table of past leaks better than the base-case PA and RCA model. The decline in the water table and its effect on the gradient and orientation of the flow have been discussed in Section 2.5.

In the scoping analyses these changes are not evaluated; instead, the water table is assumed to be static, at its current level, for the duration of the analysis.

Table 4-1. Description of Past Tank Waste Release Scoping Cases. (2 sheets)

Scoping Case (Abbreviation)	Scoping Case Description and Purpose
Case 1a (Hi_inv)	Assumes prescribed invariant aquifer boundary conditions, similar to the base case of the DOE 435.1 PA and RCRA Closure Analysis, with a modification to account for the increased water table elevation in the WMA C area under current conditions. The water table has been set to approximate current conditions of ~122.25 m above Mean Sea Level. The hydrogeologic framework, vadose zone, and groundwater flow and transport parameters remain unchanged from the base case of the DOE 435.1 PA and RCRA Closure Analysis. This case also assumes current estimates of leak inventories and volumes that includes the upper bound inventory (9.8 Ci) and volume 77,600 L (20,500 gals) developed for tank 241-C-105 (C-105).
Case 1b (Lo_inv)	This case is similar to Case 1a but assumes current estimates of leak inventories and volumes that includes the lower bound inventory (1 Ci) and volume 7,570 L (2,000 gals) developed for tank C-105.
Cases Related to Changes in Groundwater Flux Rates	
Case 2a (GWflux_10%)	Assumes same parameterization and past leak volumes and inventories as Case 1a but with the aquifer flux set at 10th percentile values used in the uncertainty analysis developed for the DOE 435.1 PA. This case corresponds to altered aquifer flow producing minimal aquifer dilution compared to Hi_inv.
Case 2b (GWflux_90%)	Assumes same parameterization and past leak volumes and inventories as Case 1a but with the aquifer flux set at 90th percentile values used in the uncertainty analysis developed the DOE 435.1 PA. This case corresponds to altered aquifer flow producing a higher level of aquifer dilution compared to Hi_inv.
Cases Related to Changes in Recharge Rates	
Case 3a (EnhanceRech_150)	Assumes same parameterization and past leak volumes and inventories as Case 1a but with a recharge rate of 150 mm/yr applied for the tank farm area within the WMA C model domain to evaluate effect of increased recharge inside of the tank farm area on past releases.
Case 3b (EnhanceRech_100)	Assumes same parameterization and past leak volumes and inventories as Case 1a but with a recharge rate of 100 mm/yr for all areas within the WMA C model domain to evaluate effect of increased anthropogenic recharge outside of the tank farm area on past releases.
Case 3c (Gunite_Cap)	Assumes same parameterization and past leak volumes and inventories as Case 1a but some local changes at UPRs-E-81, -82, and -86. These changes include an additional 1,135 Lpm (300 gpm) of wash water for 4 hours at the time of release (a one-time addition of 272,550 L [72,000 gal]). Twenty years after UPRs-E-82, and -86, a gunite cap was applied to those two surfaces which is assumed to change the infiltration at those UPRs to 1 mm/y (UPR-E-81 includes does not have a gunite cap). The case investigates the effects of potential localized water use and caps at selected UPRs on those past releases.

Table 4-1. Description of Past Tank Waste Release Scoping Cases. (2 sheets)

Scoping Case (Abbreviation)	Scoping Case Description and Purpose
Cases Related to Changes in Vadose Zone Parameters/Conceptualizations	
Case 4a (ACM_II)	Assumes the same parameterization and past leak volumes and inventories as Case 1a but with the geologic interpretation using the picks for the top of the units supplied by Nez Perce staff for Alternative Geologic Model II. This case examines the effect of a finer alternative treatment of major hydrogeologic units in the vadose zone on past releases.
Case 4b (ACM_hetero)	Assumes vadose zone parameterization in the heterogeneous (i.e., based on moisture contents in the vadose zone underlying WMA C) hydrogeologic model interpretation developed for use in DOE 435.1 PA and RCRA Closure Analysis with Case 1a leak volumes and inventories. This case examines the effect of heterogeneous treatment of sediments in the vadose zone on past releases.
Case 4c (vzprop_50%)	Assumes same parameterization and past leak volumes and inventories as Case 1a but with vadose zone hydraulic properties at the 50th percentile values as set in the uncertainty analysis developed for the DOE 435.1 PA. This case evaluates the effect on past releases of higher vadose zone hydraulic properties than used in Case 1a.
Case 4d (vzprop_95%)	Assumes same parameterization and past leak volumes and inventories as Case 1a but with vadose zone hydraulic properties at the 95th percentile values as set in the uncertainty analysis developed for the DOE 435.1 PA. This case evaluates the effect on past releases of lower vadose zone hydraulic properties than used in Case 1a.
Case 4e (ACM_dike)	Assumes same parameterization and past leak volumes and inventories as Case 1a but with a hypothetical clastic dike placed below tank C-105. This case evaluates the effect on past releases of a possible preferential pathway for contaminants in the vicinity of tank C-105.
Case 4f (ACM_borehole)	Assumes same parameterization and past leak volumes and inventories as Case 1a but with the additional assumption of an inadequately sealed borehole at well 299-E27-70 (drywell 30-05-02), located near the past tank leak near C-105. This case evaluates the effect on past releases for another possible type of preferential pathway for contaminants in the vicinity of tank C-105.

PA = performance assessment
RCRA = Resource Conservation and Recovery Act of 1976
UPR = unplanned release
WMA = Waste Management Area

Reference: DOE 435.1, Radioactive Waste Management.

The hydraulic heads around WMA C are expected to continue declining slowly, as shown in Figure 4-1, until they stabilize around year 2030 at 119.5 m (392 ft) above Mean Sea Level. The stable projected long-term aquifer conditions were evaluated in the radiological PA of residual contamination (RPP-ENV-58782) and the RCA for WMA C (RPP-ENV-58806).

For the scoping analyses, the water table elevation in the WMA C area has been set to approximate current conditions, around 122 m (Figure 4-1); the boundary condition of the 3-D STOMP© model developed for the PA/RCA has been changed to 122.50 m (401.9 ft) above Mean Sea Level. This change in the model was implemented by updating the model boundary conditions. The updated water table location resulted an average 14-m-thick saturated zone in

this analysis case. Everything else in the model has been kept the same as the PA/RCA model (RPP-ENV-58782, RPP-ENV-58806).

The scoping analyses discussed in this section do not attempt to include the effects that the changes in hydraulic gradient magnitude and direction have introduced to the groundwater flow field since Hanford began discharging large quantities of liquid. The direction has rotated 180 degrees since the startup of operations, and the gradient has been highly variable and very difficult to measure. Instead, the scoping analysis only evaluates the relative change in the results that each change in input produces in the aquifer with a static gradient magnitude and direction.

As a result of the complicating effect of the variable water table on monitoring data, it is not appropriate to compare the model results at the location of the monitoring wells. The static gradient applied in the model is not necessarily oriented in the same direction as the real water table at any given time in the analysis. Instead, the model is used to calculate concentrations as fixed distances from the releases, and this is used as an indicator of the effect of distance from the leak on groundwater concentrations. Since the tank C-105 leak is the predominant source in the tank farm, a distance of 60 m was selected as one distance used in the scoping analyses. This represents both the approximate distance from the tank C-105 leak to the fenceline in a southeasterly direction, and also the approximate distance to monitoring well 299-E27-14 (see Figure 4-2). Concentrations were also calculated at 60 m downgradient from the WMA C fenceline, representing the approximate distance to monitoring well 299-E27-24 (see Figure 4-2), and at 20 m, which provides an upper bound concentration for the calculation taking account of the dilution that occurs as the plume moves downgradient in the aquifer. The 60-m distance from tank C-105 to the fenceline and the additional 60 m downgradient from the WMA C fenceline, represent the approximate distance to monitoring wells 299-E27-23 and 299-E27-21, two other locations where significant concentrations of ^{99}Tc have been observed.

These points of calculation (PoCals) primarily focus on the tank C-105 leak, and the calculated concentrations largely represent the contribution of the tank C-105 leak. However, in all scoping analysis cases the entire inventory of all leaks is implemented.

4.1 CASE 1: EFFECT OF LEAK INVENTORIES AND VOLUMES

4.1.1 Case Description

The purpose of Case 1 is to evaluate the effect of leak inventory and volume on peak concentrations and arrival time at the aquifer. Given the dominance of the tank C-105 leak in terms of total ^{99}Tc released, the focus of this case is on the inventory and volume of the tank C-105 leak. Case 1a uses upper bound leak inventories and volumes based on an assumed upper bound inventory for the tank C-105 waste loss of 9.8 Ci and an upper bound leak volume of 77,600 L (20,500 gal). Case 1b uses the lower bound leak inventories and volumes based on an assumed lower bound inventory for the tank C-105 waste loss of 1.0 Ci and a lower bound leak volume of 7,570 L (2,000 gal).

Figure 4-1. Decreases in Water Table Level with Time at Waste Management Area C, with a Projection to Future Conditions.

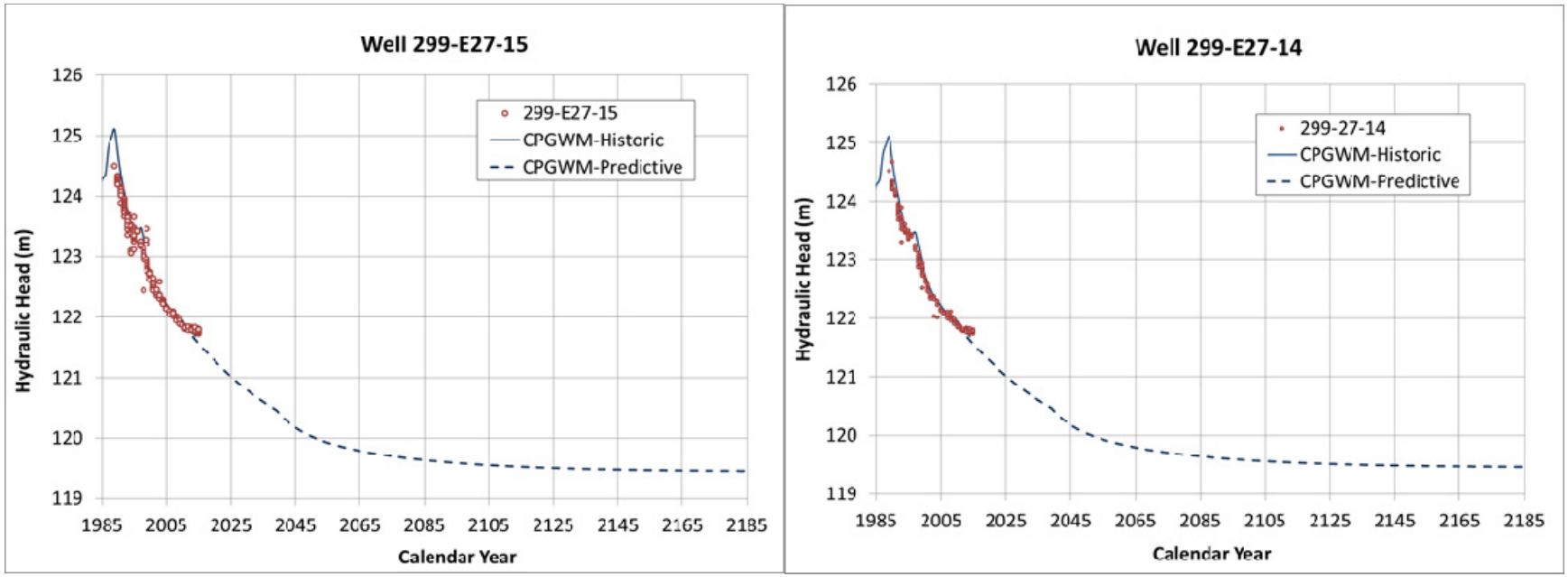

CPGWM = Central Plateau Groundwater Model

References:

RPP-ENV-58782, "Performance Assessment of Waste Management Area C, Hanford Site, Washington," Appendix C – Technical Basis for Waste Management Area C Unconfined Aquifer Conceptual Model: Field Data and Related Investigations.

CP-47631, "Model Package Report: Central Plateau Groundwater Model Version 6.3.3."

Figure 4-2. Points of Calculation for the Scoping Analyses.

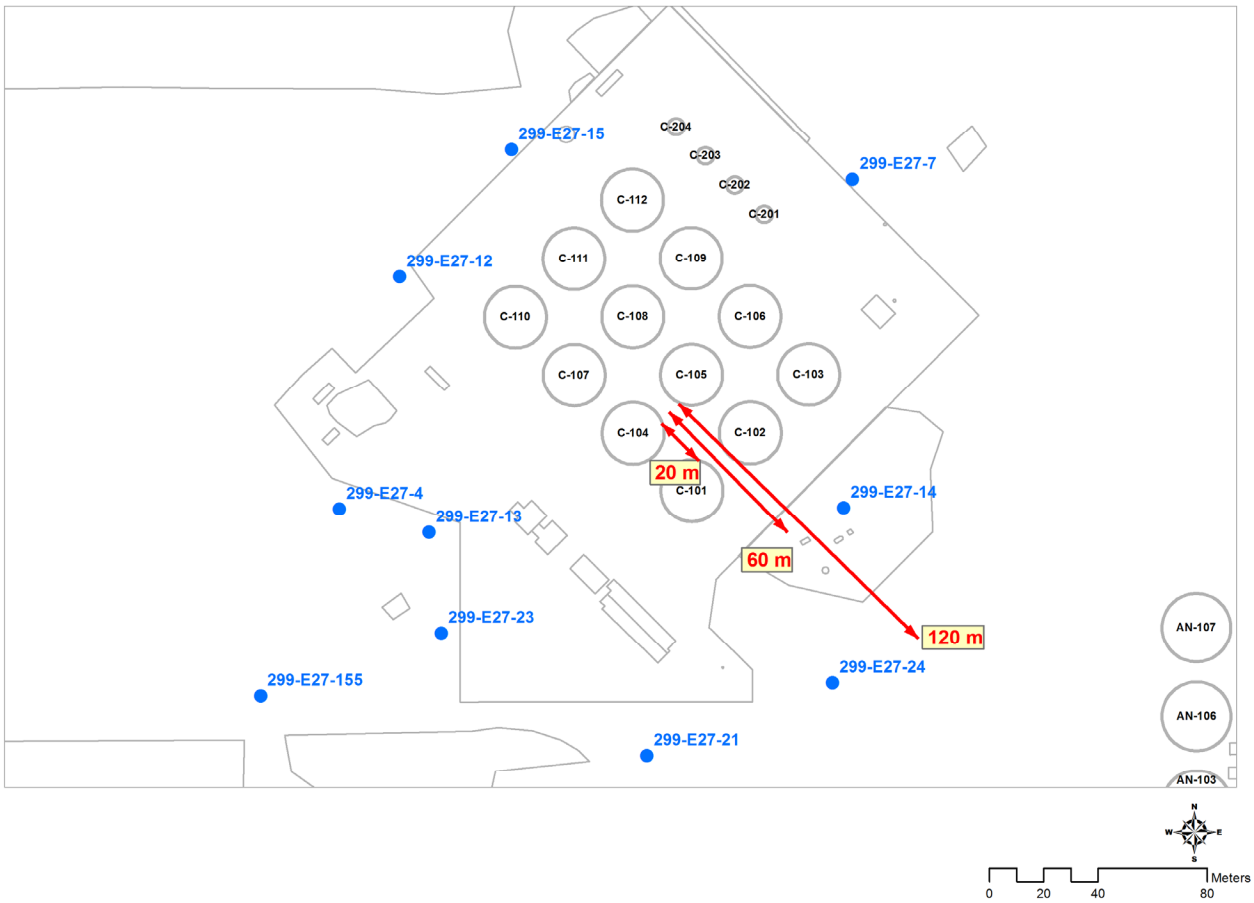

4.1.2 Case Results

Results of Case 1a are shown in Figures 4-3 and 4-4 and summarized at selected PoCals in Table 4-2. In Figure 4-3, the development of the plumes is shown between the year 2000 and the year 2030. The peak concentrations in the aquifer are seen to reach a maximum around the year 2016, after which concentrations are generally seen to fall. The dominant impacts originate for past releases simulated at tank C-105. Impacts at the water table from UPR-86—which is located in an area of slightly lower recharge (63 mm/yr) than assumed within the tank area (100 mm/yr)—are delayed relative to the impacts from other sources within the tank farm proper.

The ^{99}Tc concentrations versus time for the 20-m, 60-m, and 120-m calculation points downgradient of tank C-105, which represent the highest concentrations within the domain, are shown in Figure 4-4. These figures illustrate the drop-off in ^{99}Tc concentration levels with distance from this source and confirm that the peak calculated concentrations occur around 2015 to 2020 followed by falling concentrations. The calculated peak concentrations for Case 1a are in the range 6,000 to 23,000 pCi/L over the downgradient distances evaluated. Owing to the high hydraulic conductivity and associated groundwater flux considered in the scoping case, these results also confirm how quickly elevated concentrations realized near the source release

area, once the simulated releases reach the water table, can migrate in the direction of flow to the tank farm fenceline and other downgradient locations.

A comparison of simulated results with ^{99}Tc concentration levels historically observed at wells 299-E27-14 and 299-E27-23 is also shown in Figure 4-4. The 60-m and 120-m calculated breakthrough curves provide a reasonable match of the first arrival time of the plumes. However, the peak calculated concentrations at 60 m and 120 m are somewhat below the measured peak concentrations. The calculated curve for 20 m produces a better match for the peak concentration observed at well 299-E27-23, but produces a poorer match of the arrival time of the plume than the 60 m and 120 m breakthrough curves.

Results for Case 1b are shown in Figures 4-5 and 4-6 and summarized at selected PoCals in Table 4-2. The timing of the development of the plumes is very similar to Case 1a, but the resulting plume is significantly lower in concentration than Case 1a, and significantly lower than measured groundwater concentrations. As a result of this observation, all other scoping cases were evaluated using the volumes and inventories used in Case 1a. The lower bound inventory and volume for the tank C-105 leak has been judged to be inconsistent with groundwater concentrations in monitoring wells.

4.2 CASE 2: EFFECT OF CHANGES IN GROUNDWATER FLUX RATES

4.2.1 Case Descriptions

The set of two analysis cases described in this section both make use of the Case 1a analysis with input modifications to allow for examination of the effect of changed groundwater flux rates. The parameters that determine the groundwater flux and the amount of dilution that occurs in the aquifer are the hydraulic conductivity and hydraulic gradient. In a natural system, the two parameters offset one another. If the groundwater flux through an aquifer volume remains constant, then in areas with high hydraulic conductivity, the hydraulic gradient will be less, and vice versa. They are considered to be coupled parameters because changes to the flux term caused by changes made to one term are inseparable from changes made to the other term. These parameters act inversely proportional to one another, and the same change in the flux can be made by making the same proportional change to either parameter. Therefore, only one of the parameters needs to be varied to produce the variability in the flux necessary to conduct the sensitivity analysis.

The scoping analysis includes two cases evaluating different values of groundwater flux:

- **Case 2a**: This case assumes the 10th percentile value for aquifer flux (0.11 m/day)

- **Case 2b**: This case assumes the 90th percentile value (0.33 m/day).

The underlying distribution of this specific hydraulic property parameter used in these cases was developed as a part of the uncertainty analysis performed to support the WMA C DOE 435.1 PA (see Section 8.1.3.6 in RPP-ENV-58782).

Figure 4-3. Development of Technetium-99 Plumes over Selected Time Periods for Case 1a (Upper Bound Inventory for the Tank 241-C-105 Leak).

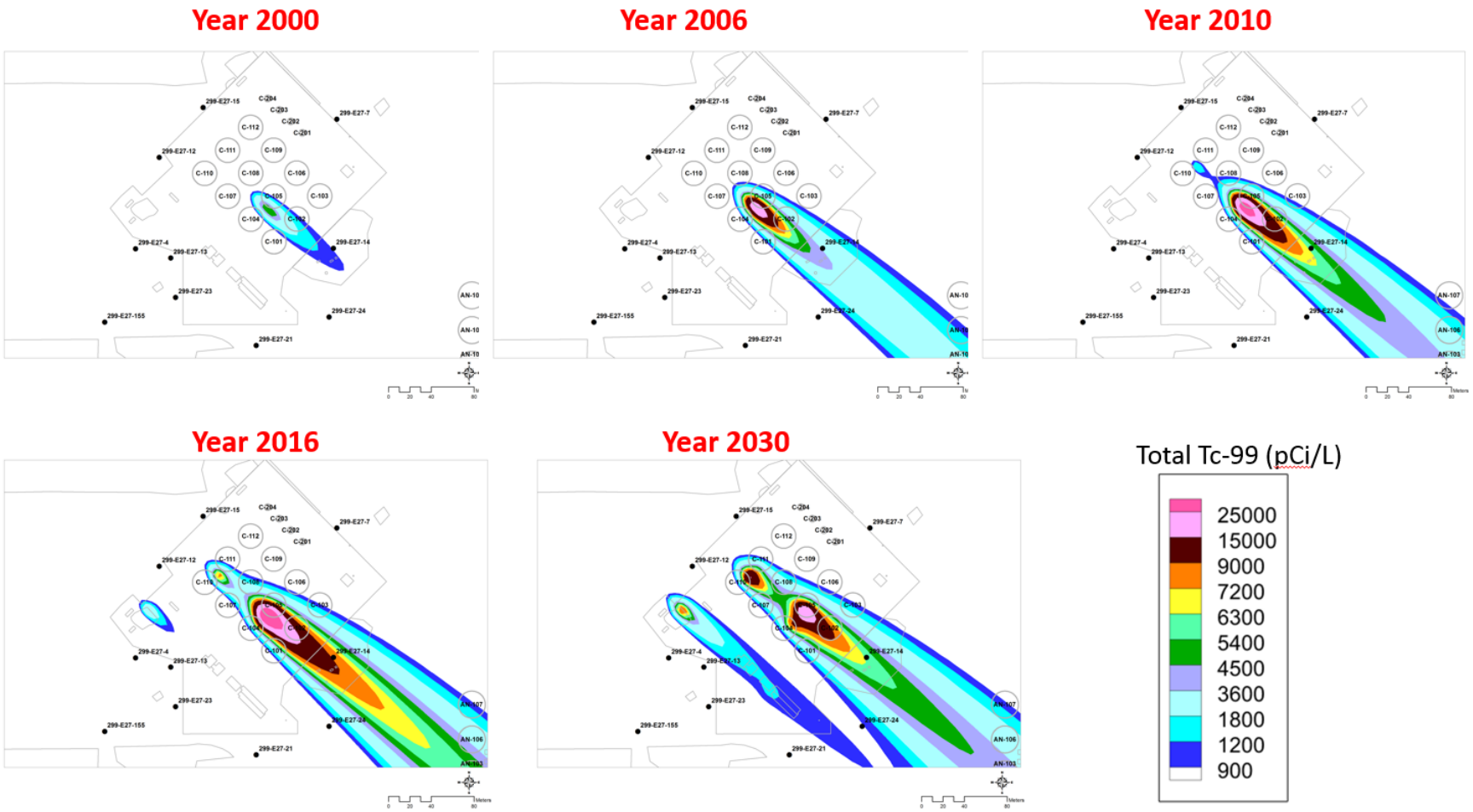

Figure 4-4. Concentrations at the Selected Points of Calculation for Case 1a (Upper Bound Inventory for the Tank 241-C-105 Leak). Also shown on the figure are measured technetium-99 concentration data from wells 299-E27-14 and 299-E27-23.

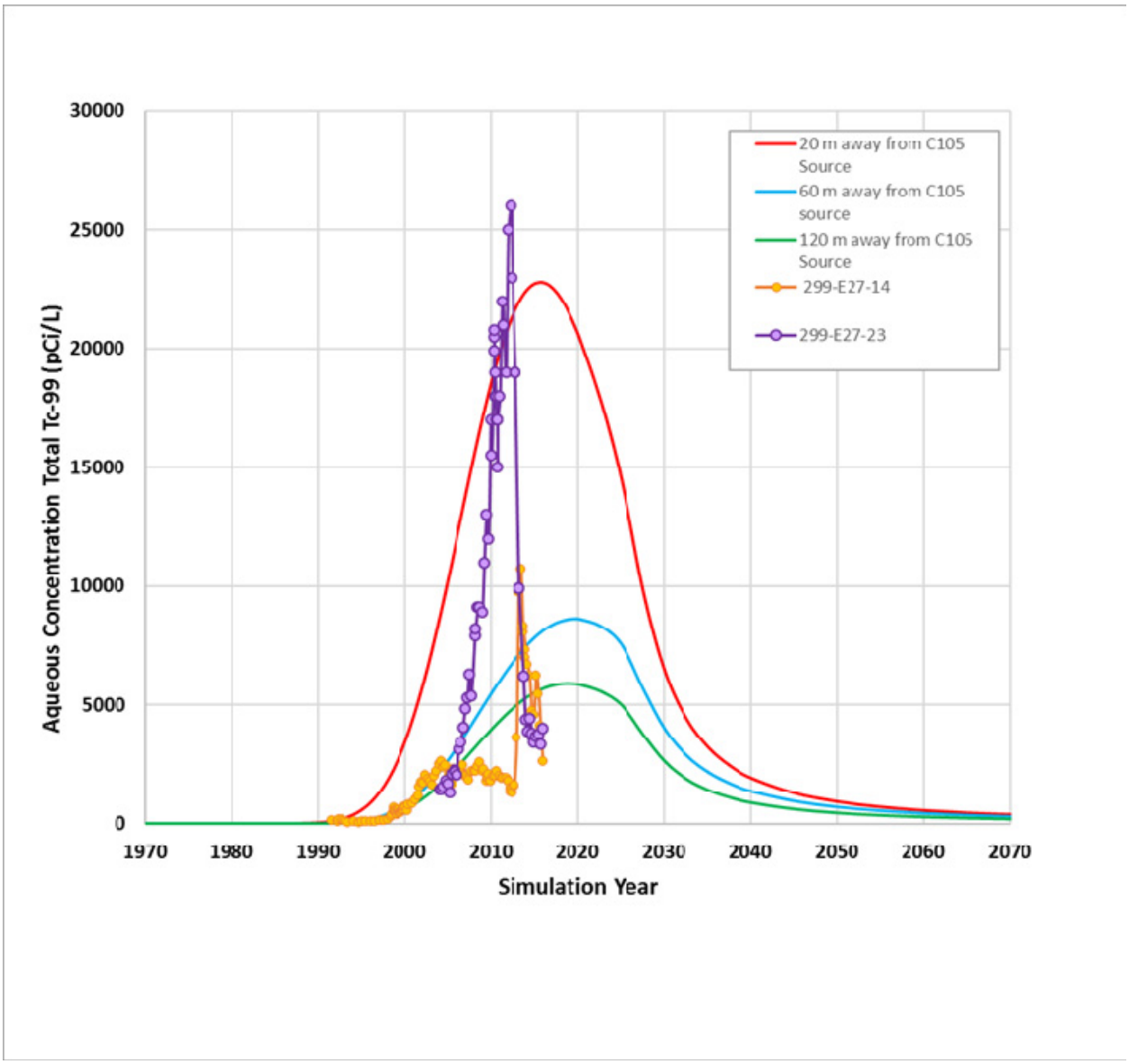

4.2.2 Case Results

Results of Case 2a (10th percentile groundwater flux) are presented in Figures 4-7 and 4-8 and summarized at selected PoCals in Table 4-3. The time of arrival of the plume is identical to Case 1, and provides a reasonable match to the monitoring data. In addition, the peak concentrations at 60 m and 120 m are in reasonable agreement with the data from the monitoring wells, and the calculated concentrations at 20 m exceed the measured values.

Table 4-2. Comparison of the Technetium-99 Concentration Results at Selected Points of Calculation for Scoping Cases 1a and 1b.

	Model Results at 20 Meters Downgradient of Tank 241-C-105 Waste Release Location		Model Results at 60 Meters Downgradient of Tank 241-C-105 Waste Release Location		Model Results at 120 Meters Downgradient of Tank 241-C-105 Waste Release Location	
Case Number	**Time of Maximum Concentration (Calendar Year)**	**Maximum Concentration (pCi/L)**	**Time of Maximum Concentration (Calendar Year)**	**Maximum Concentration (pCi/L)**	**Time of Maximum Concentration (Calendar Year)**	**Maximum Concentration (pCi/L)**
Case 1a	2015	22,800	2017	9,800	2018	5,900
Case 1b	2023	4,200	2023	2,700	2023	1,900

Figure 4-5. Development of the Technetium-99 Plumes over Selected Time Periods for Case 1b (Lower Bound Inventory for the Tank 241-C-105 Leak).

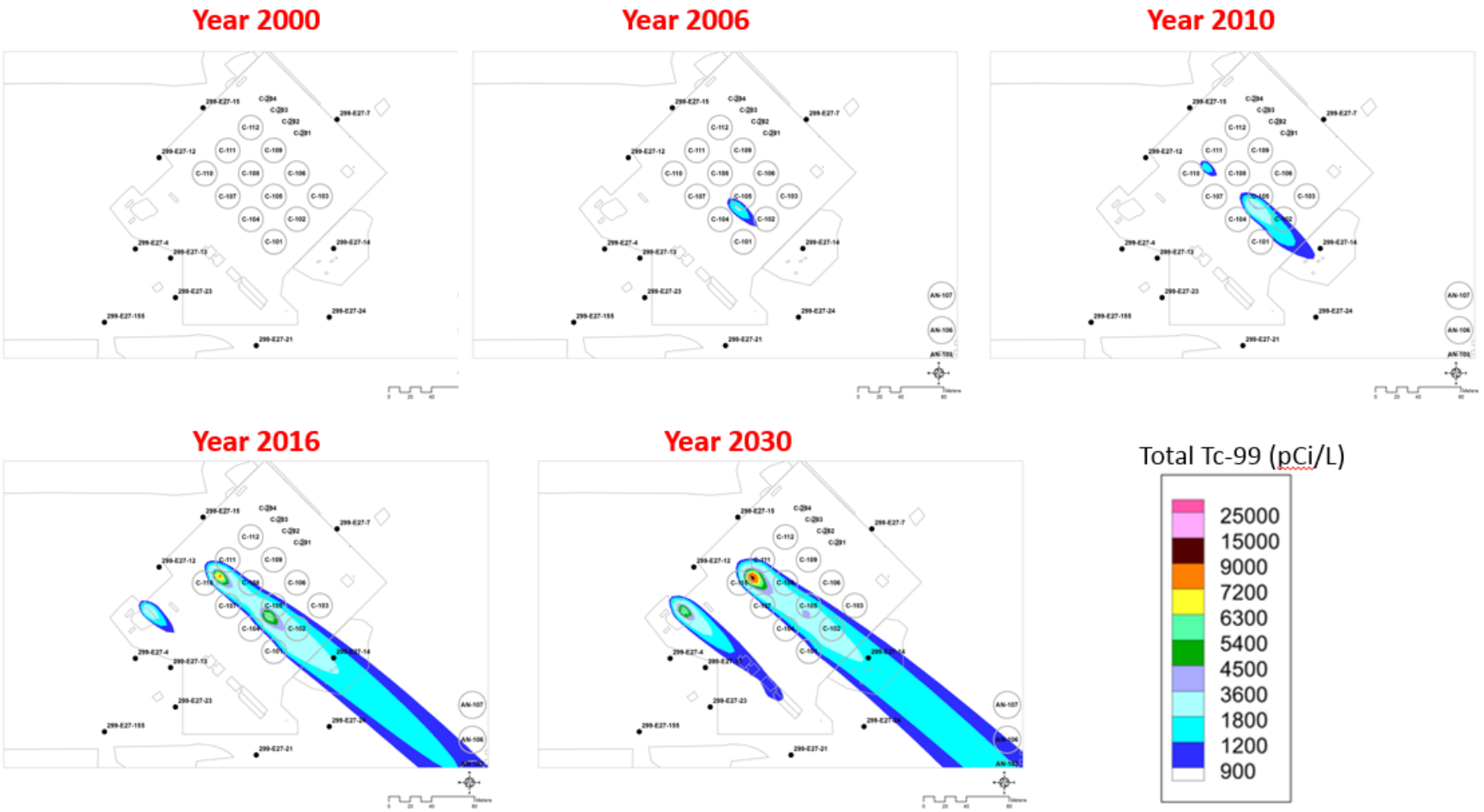

Figure 4-6. Concentrations at the Selected Points of Calculation for Case 1b (Lower Bound Inventory for the Tank 241-C-105 Leak). Also shown on the figure are measured technetium-99 concentration data from wells 299-E27-14 and 299-E27-23.

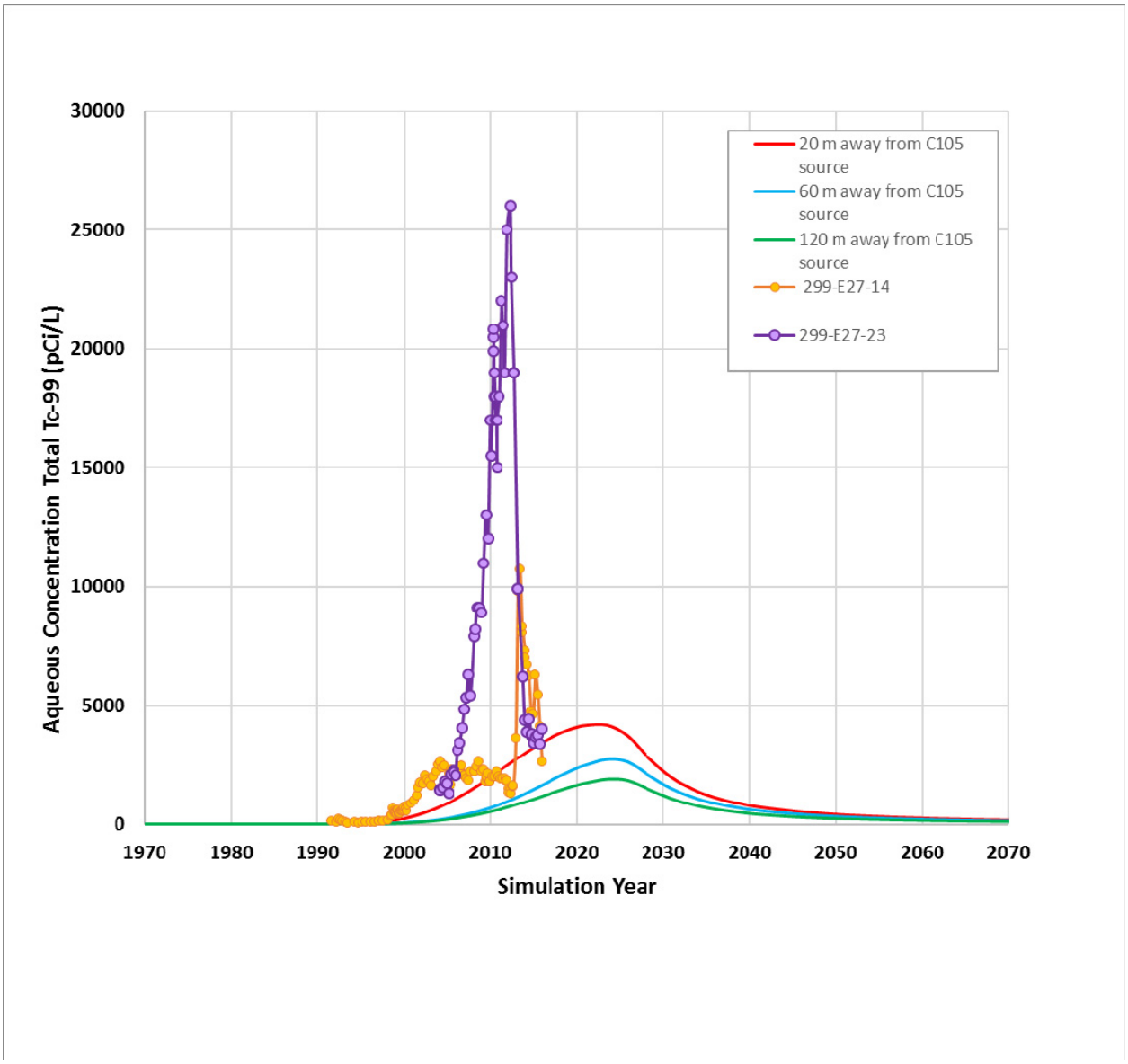

Results of Case 2b (90th percentile groundwater flux) are presented in Figures 4-9 and 4-10 and also summarized at selected PoCals in Table 4-3. The time of arrival of the plume is identical to Case 1 and Case 2a, and provides a reasonable match to the first arrival times seen in monitoring data. However, the peak concentrations at 60 m and 120 m are significantly below the monitoring data, and even the calculated 20 m values are less than the measured values.

Figure 4-7. Development of the Technetium-99 Plumes at Selected Time Periods for Case 2a (10th Percentile Groundwater Flux).

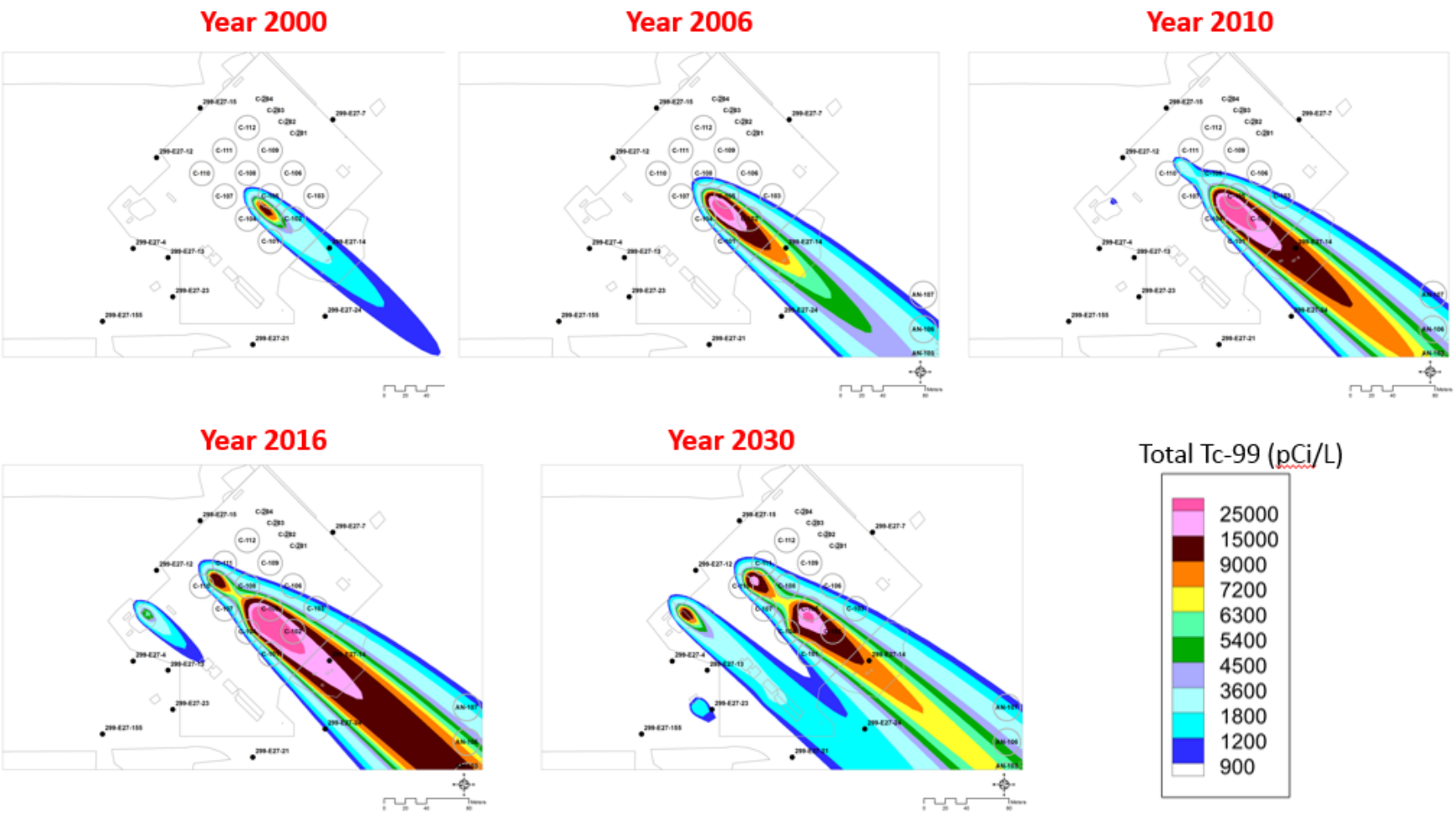

Figure 4-8. Concentrations at the Selected Points of Calculation for Case 2a (10th Percentile Groundwater Flux). Also shown on the figure are measured technetium-99 concentration data from wells 299-E27-14 and 299-E27-23.

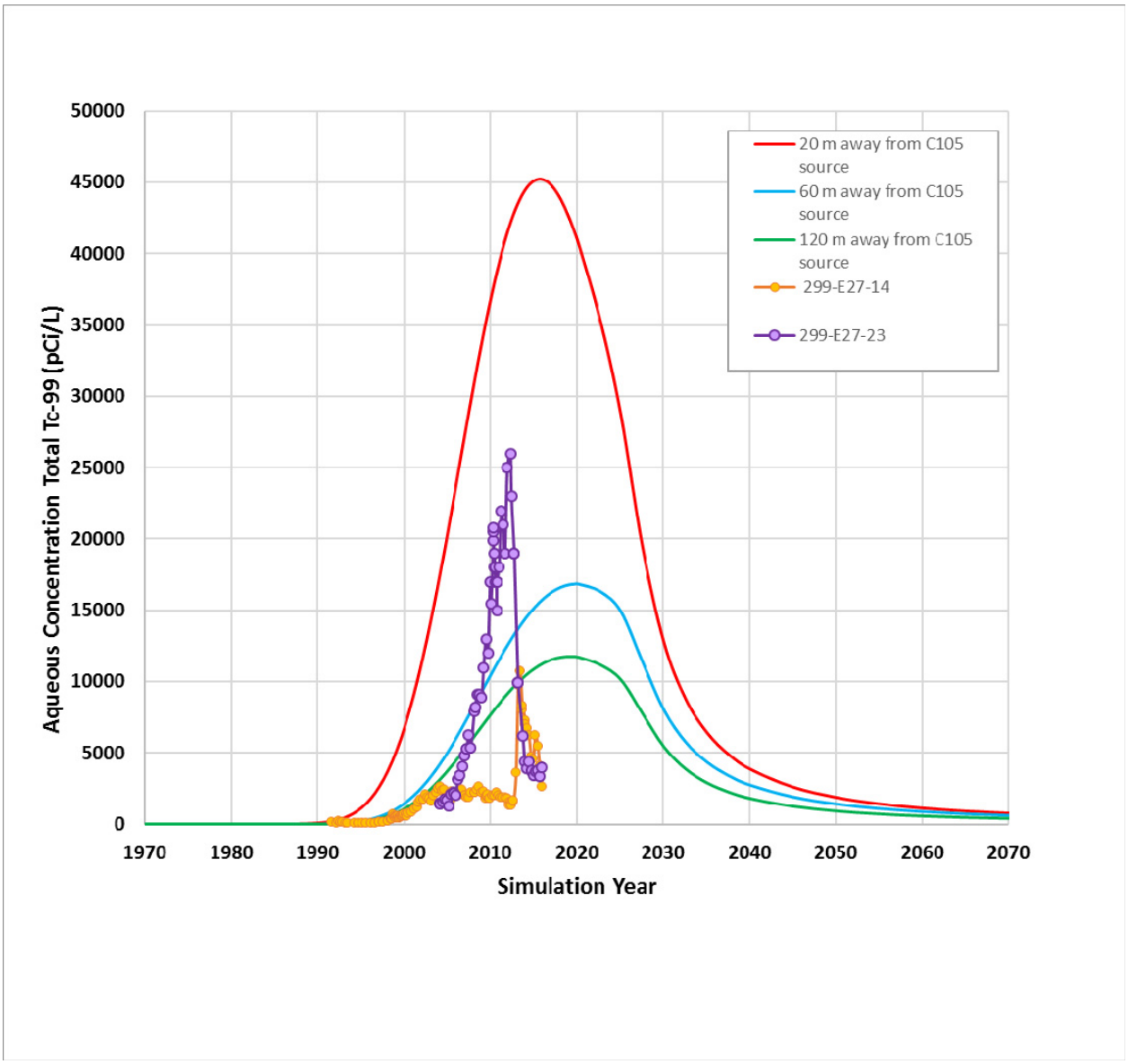

4.3 CASE 3: EFFECT OF CHANGES IN RECHARGE CONDITIONS

4.3.1 Case Descriptions

In this evaluation, recharge-related parameters were varied to examine the impact of recharge affecting events on the maximum concentration estimated at the fenceline PoCal. The recharge scoping evaluations address the variability related to surface conditions that affect recharge. Because of the spatial component of this analysis, it was conducted using STOMP©. For this

analysis, the vadose zone and aquifer hydraulic properties remain unchanged from their base case values.

A total of three recharge scoping cases were evaluated.

- **Case 3a**: This case assumes higher recharge of 150 mm/yr everywhere in the vicinity of WMA C where disturbed soil conditions exist (see Figure 4-11) to reflect the effect of increased but uniform anthropogenic recharge during operations on past leak migration inside the tank farm area (see Table 4-4).

- **Case 3b**: This case assumes higher recharge of 100 mm/yr everywhere in the vicinity of WMA C where disturbed soil conditions exist (see Figure 4-11) to reflect the effect of uniform recharge inside and outside of the farm during operations on past leak migration in the general area of the tank farm (see Table 4-4).

- **Case 3c:** This case examines the effect of gunite caps emplaced at UPR-82, and UPR-86 and local use of water at UPR-81, UPR-82, and UPR-86 to force contamination downward into the vadose zone shortly after identification of waste release.

4.3.2 Case Results

Results of Case 3a (150 mm/y recharge) are presented in Figures 4-12 and 4-13 and summarized at selected PoCals in Table 4-5. The time of arrival of the plume is earlier than Case 1, and is substantially earlier than indicated by the monitoring data. In addition, the peak concentrations at 60 m and 120 m are somewhat lower than the data from the monitoring wells, and only the peak calculated concentrations at 20 m are close to the data for well 299-E27-23.

Results of Case 3b (100 mm/y recharge) are presented in Figures 4-14 and 4-15 and summarized at selected PoCals in Table 4-5. The time of arrival, peak concentrations, and shape of the plume are very similar to Case 1, with the arrival time providing a reasonable match to the first arrivial of ^{99}Tc in monitoring data. However, peak concentrations are somewhat lower than seen for these other scoping cases.

Results of Case 3c (treatment of UPRs-82 and -86 with a firehose followed by installation of a gunite cap) are presented in Figures 4-16 and 4-17 and also summarized at selected PoCals in Table 4-5. The time of arrival, peak concentrations, and shape of the plume are very similar to Case 1, with the arrival time providing a reasonable match to the monitoring data and the peak concentrations somewhat lower.

Table 4-3. Comparison of the Technetium-99 Concentration Results at Selected Points of Calculation for Scoping Cases 2a and 2b.

	Model Results at 20 Meters Downgradient of Tank 241-C-105 Waste Release Location		Model Results at 60 Meters Downgradient of Tank 241-C-105 Waste Release Location		Model Results at 120 Meters Downgradient of Tank 241-C-105 Waste Release Location	
Case Number	**Time of Maximum Concentration (Calendar Year)**	**Maximum Concentration (pCi/L)**	**Time of Maximum Concentration (Calendar Year)**	**Maximum Concentration (pCi/L)**	**Time of Maximum Concentration (Calendar Year)**	**Maximum Concentration (pCi/L)**
Case 2a	2015	45,200	2019	16,800	2019	11,800
Case 2b	2015	15,200	2019	5,800	2019	3,900

Figure 4-9. Development of the Technetium-99 Plumes for Selected Time Periods for Case 2b (90th Percentile Groundwater Flux).

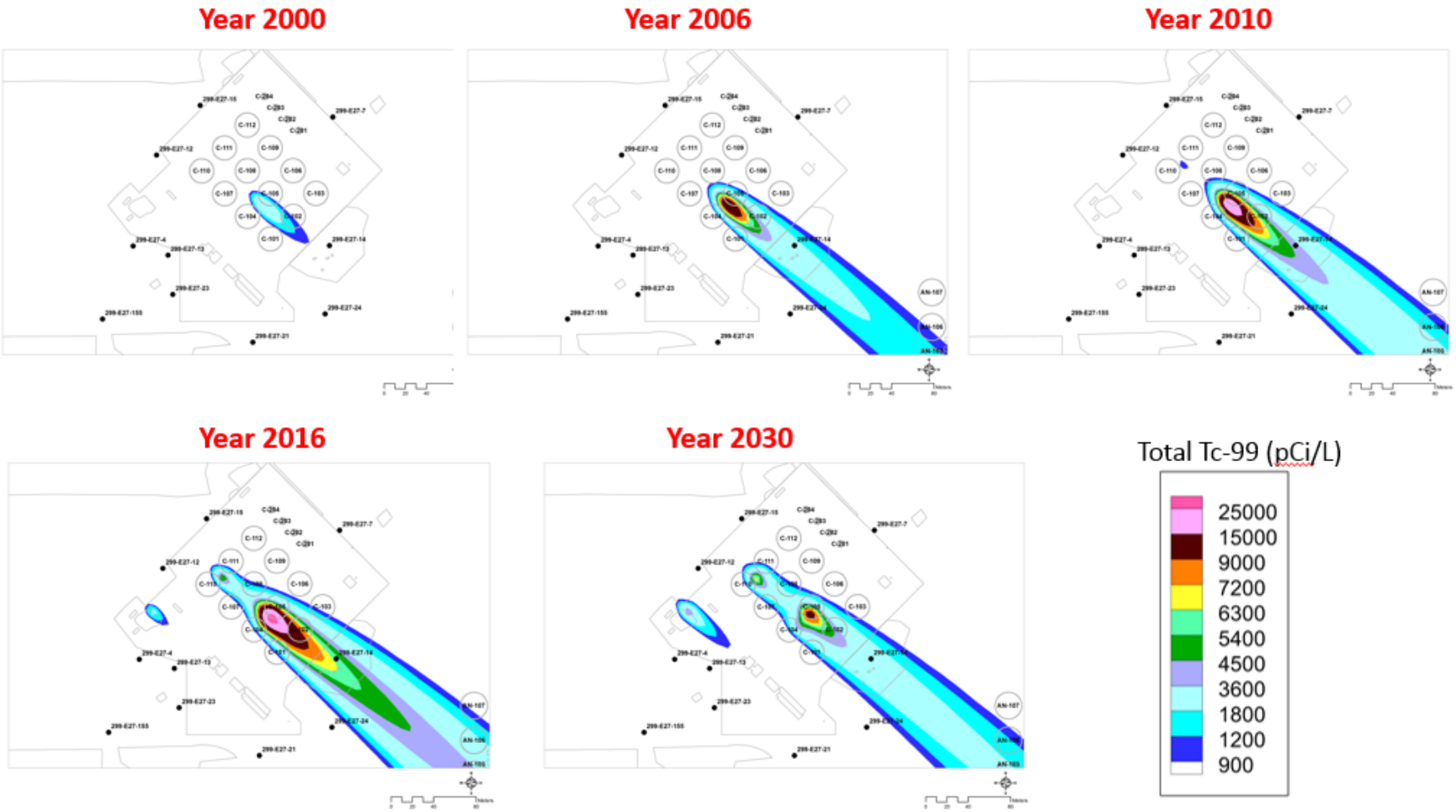

Figure 4-10. Concentrations at the Selected Points of Calculation for Case 2b (90th Percentile Groundwater Flux). Also shown on the figure are measured technetium-99 concentration data from wells 299-E27-14 and 299-E27-23.

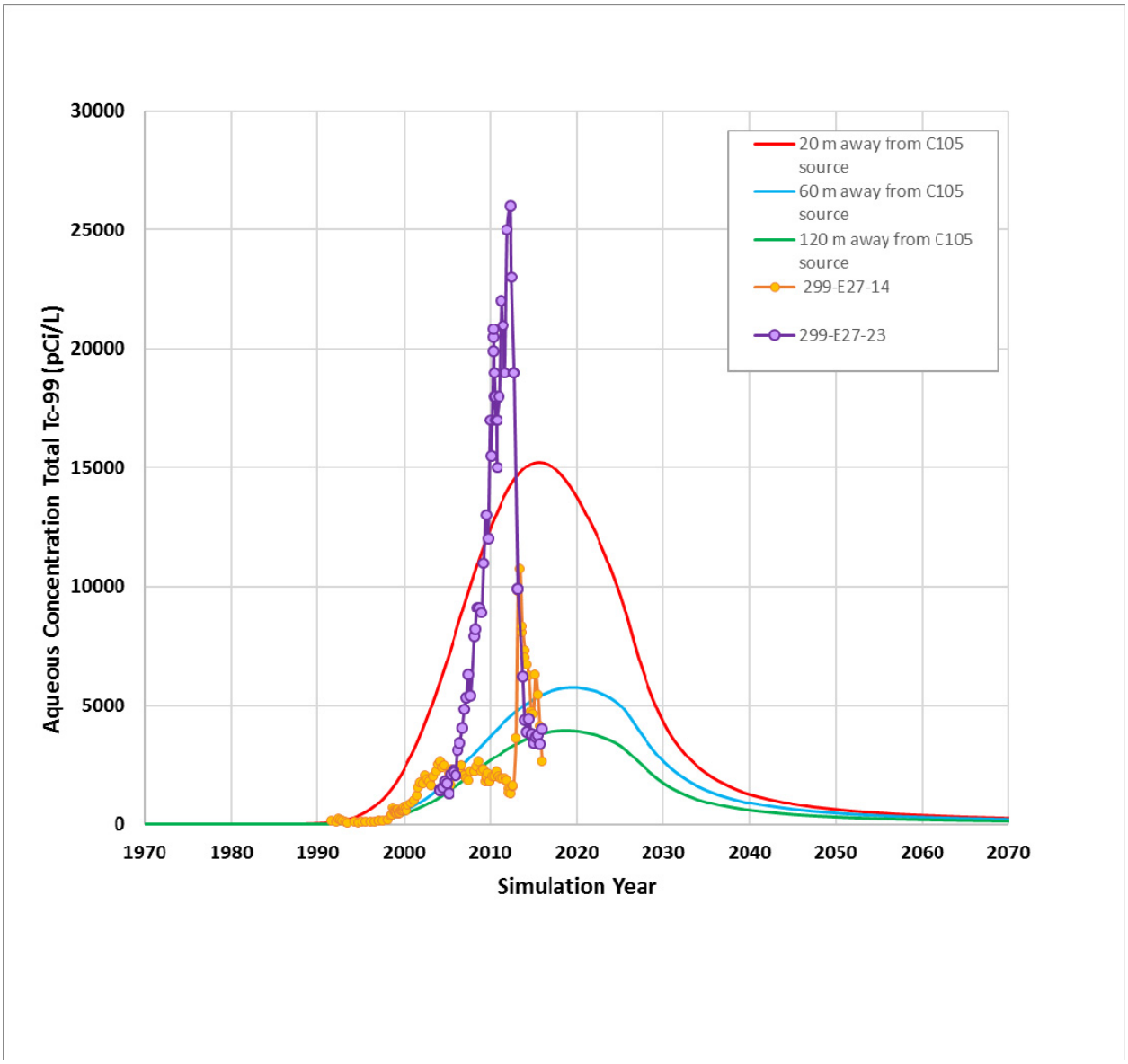

Figure 4-11. Surface Conditions In and Around Waste Management Area C during the Construction and Operations Period.

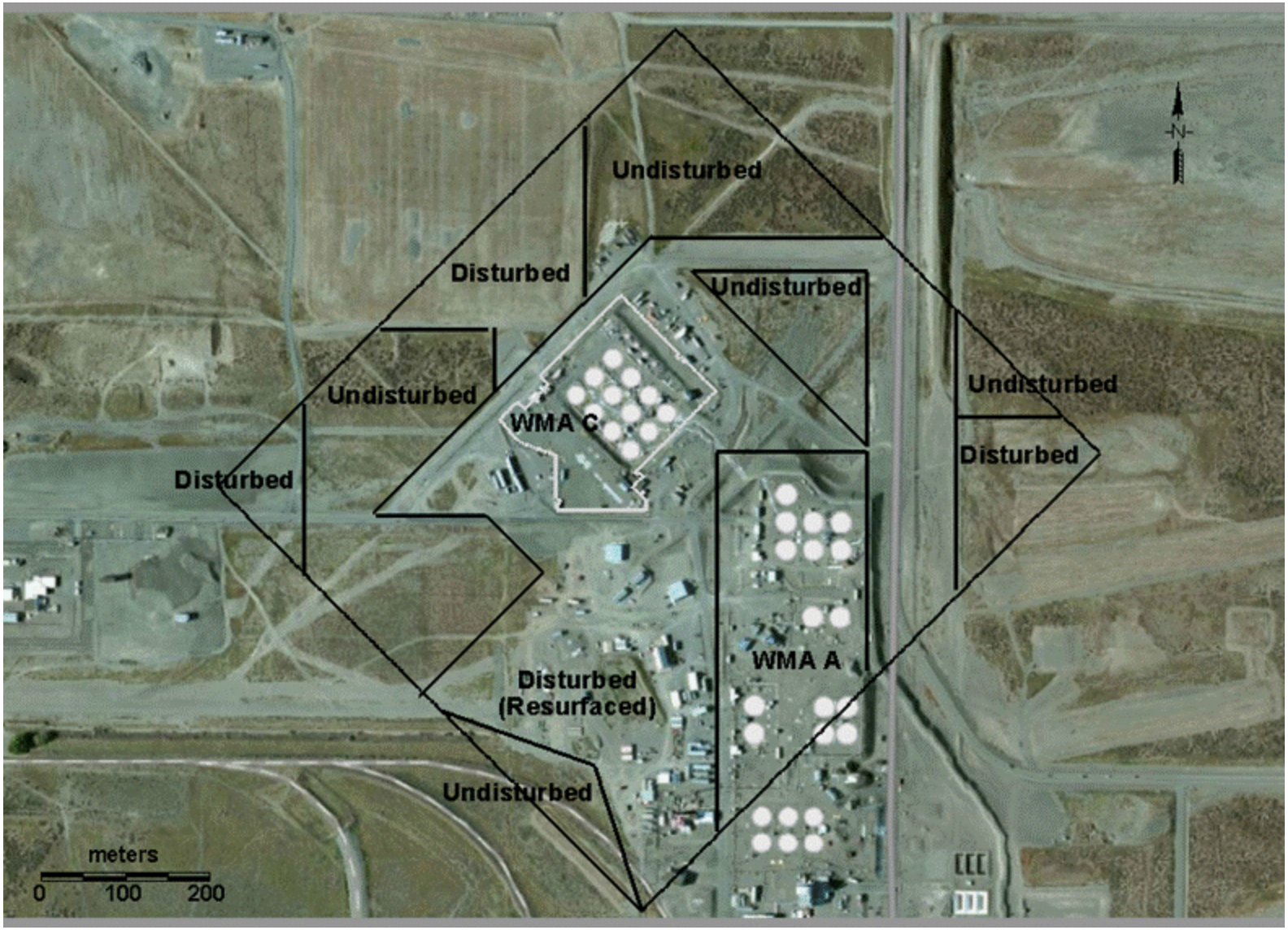

WMA = Waste Management Area

Table 4-4. Assumed Recharge Rates (Net Infiltration) for Surface Conditions during the Pre-Construction, Operational Periods Used in Cases 1a, 1b, 3a, and 3b.

Period	Waste Management Area (WMA) C Region and Surface Condition*	Case 1a and 1b Recharge Rate (mm/yr)	Case 3a	Case 3b
Pre-construction (before 1944)	Undisturbed region (Rupert sand with vegetation)	3.5	3.5	3.5
Operational period (1945 to 2020)	Undisturbed region (Rupert sand with vegetation)	3.5	3.5	3.5
	WMA C Surface region (Gravel without vegetation)	100	150	100
	WMA A Surface region (Gravel without vegetation)	100	150	100
	Disturbed revegetated region (Rupert sand with vegetation)	22	150	100
	Disturbed unrevegetated region (Rupert sand with no vegetation)	63	150	100

* Areas described are shown in Figure 4-11.

4.4 CASE 4: EFFECT OF CHANGING VADOZE ZONE PARAMETERS AND CONCEPTUALIZATION

4.4.1 Case Description and Model Implementation

The vadose zone evaluation includes a number of different alternate conceptualizations of the geology and vadose parameters.

- **Case 4a**: This case evaluates Alternative Geologic Model II that was developed in the DOE 435.1 PA and the RCA effort. This conceptual model considers the Hanford H2 Sand unit to consist of three subunits that each possess different hydraulic characteristics (Figure 4-18). Most of the formation remains identified as H2 Sand and the hydraulic properties for it remain unchanged from the base case analysis. Near the base of the Hanford H2 Sand unit in Alternative Geologic Model II are fine and coarse sand subunits. For this scoping evaluation, these subunits are assigned the Hanford H2 Sand 5th and 95th percentile hydraulic property sets, respectively.

- **Case 4b**: This case evaluates an alternative conceptual model of a heterogeneous representation of the vadose zone that was developed in the DOE 435.1 PA and the RCA effort. The development of this model is described in detail in Appendix F of RPP-ENV-58782. A depiction of the numerical implementation is provided in Figure 4-19.

Figure 4-12. Development of the Technetium-99 Plumes for Selected Time Periods for Case 3a (150 mm/y Recharge).

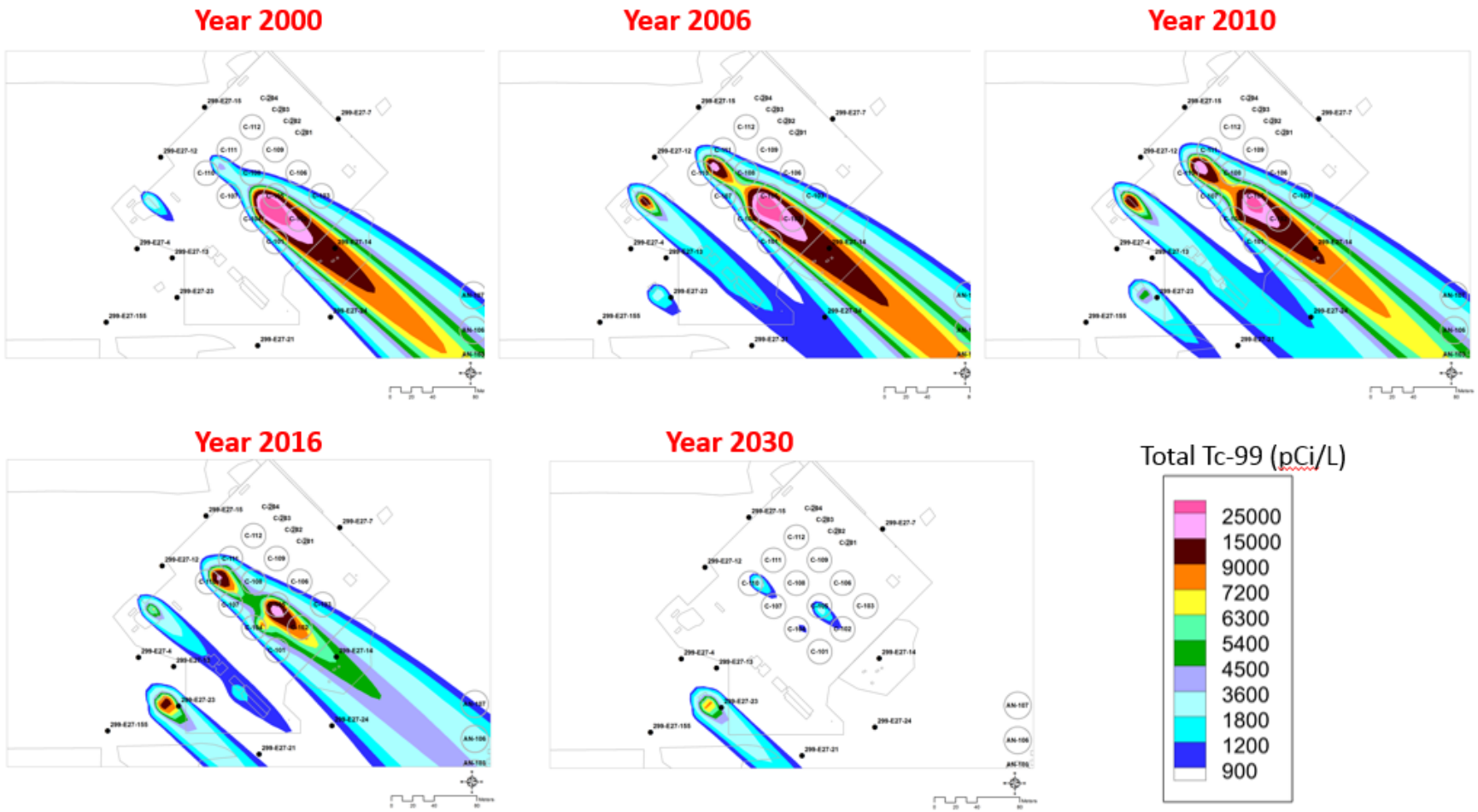

Figure 4-13. Concentrations at Selected Points of Calculation for Case 3a (150 mm/y Recharge). Also shown on the figure are measured technetium-99 concentration data from wells 299-E27-14 and 299-E27-23.

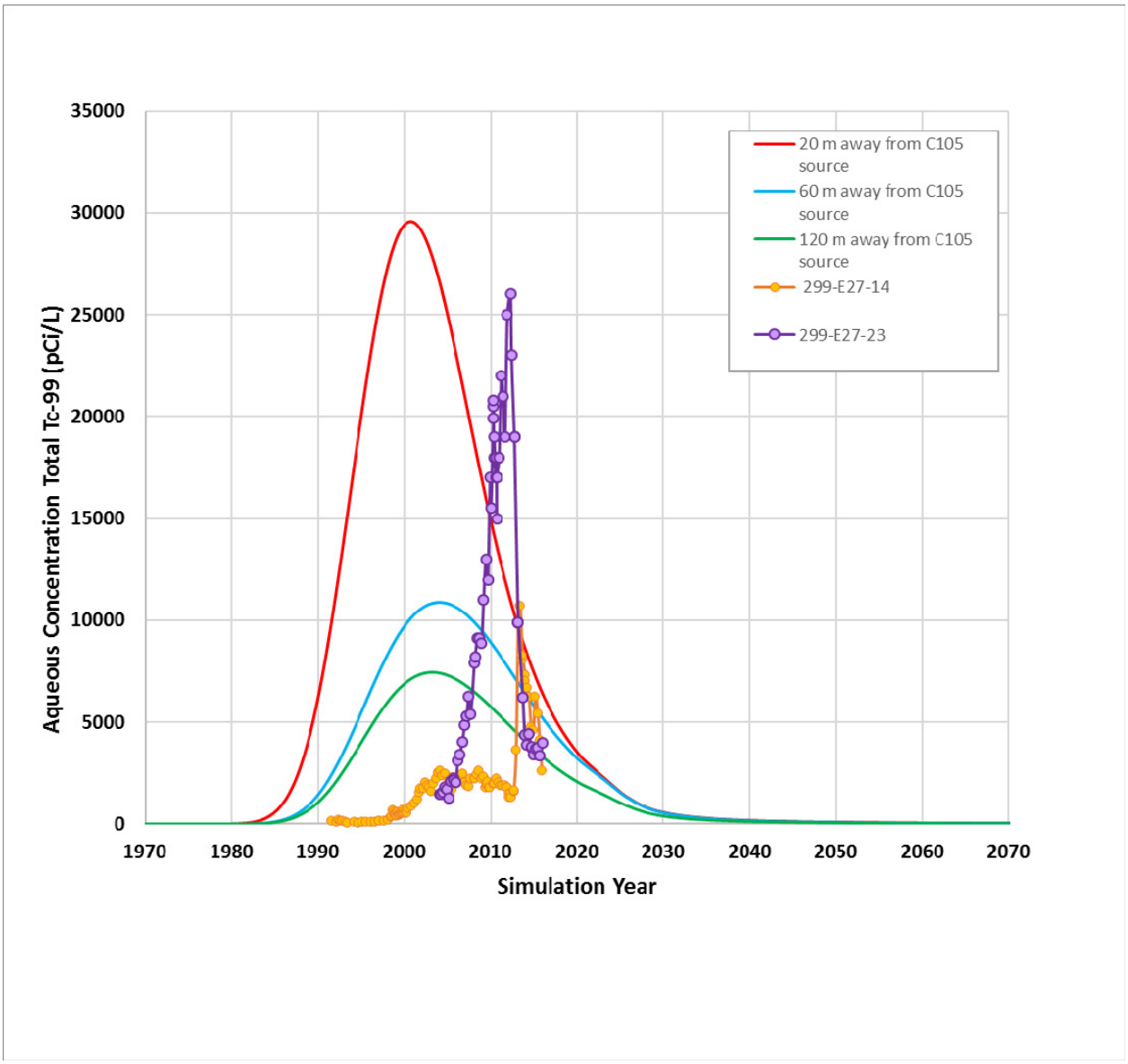

- **<u>Case 4c and 4d:</u>** These two cases evaluate the effect of changing vadose zone hydraulic properties associated with flow and dispersion in the vadose zone. Four vadose zone parameters were varied: van Genuchten α and n (coupled), saturated moisture content (θ_s), residual moisture content (θ_r), and fitted saturated hydraulic conductivity (K_s). The parameters were varied in accordance with the percentile relationships determined in the uncertainty analysis. It is important to note that the percentiles refer to sets of parameter values and not to the properties individually (as discussed in Appendix B of RPP-ENV-58782). Thus, the maximum van Genuchten residual saturation parameter

does not necessarily represent the largest value of θ_r, but instead represents the value associated with the fitted unsaturated hydraulic conductivity curve and corresponding set of hydraulic properties that produces the highest flow velocity at the pre-Hanford operations recharge rate. The values of four vadose zone parameters, van Genuchten α and n (coupled), θ_s, θ_r, and fitted saturated hydraulic conductivity (K_s) varied for the median [vzp02], and 95th [vzp03]) percentile sets of parameters are presented in Section 8.1.4 of RPP-ENV-58782 (see Table 4-6). These evaluations used the Case 1 recharge values and time sequence and other model parameters.

- **Case 4e**: This case evaluates one representation of a preferential pathway, a clastic dike, hypothetically located underneath tank C-105. Clastic dikes are discrete polygonal (plan view) features, and typically range in width from 3 cm to 1 m (1.2 in. to 3.3 ft), from 1.5 m to 100 m (4.9 ft to 328 ft) in segment length, and from 2 m (6.6 ft) to greater than 20 m (65.6 ft) in depth (BHI-01103). An especially long clastic dike segment does not appear to exist in the vicinity of WMA C tank area because, if one did, then drywell moisture measurements would reflect localized evidence of a continuous band of high moisture. Localized measurements of relatively high moisture like that have not been observed in drywell moisture logs within WMA C.

  For the scoping case, the length of the dike is assumed to extend for 7.6 m (25 ft), and 3-D model discretization imposes a minimum width of 3.8 m (12 ft) for the dike. Although a width of 3.8 m (12 ft) is more representative of a planar feature than a dike, finer resolution of the model grid is not practicable with the available computational resources (see Figure 4-20). The planar area of the dike is 29 m^2 (312 ft^2), which is comparable to a 1-m (3.3-ft)-wide dike that extends the entire diameter of the tank (23 m^2 [246 ft^2]). Clastic dikes of this size typically occur in sand, silt, and only occasionally in gravel (BHI-01103); therefore, the model representation of the dike extends throughout the depth of the Hanford H2 Sand (Figure 4-20 shows the location of tank C-105; the clastic dike is centered beneath the tank in the Hanford H2 Sand shown in the figure). The hydraulic parameters assigned to the clastic dike material were selected to determine whether the flux conditions exist at WMA C such that the clastic dikes provide a preferential flow path for the residual waste. Thus, the set of clastic dike hydraulic parameters from among the samples listed in PNNL-23711, "Physical, Hydraulic, and Transport Properties of Sediments and Engineered Materials Associated with Hanford Immobilized Low-Activity Waste" that produced the highest pore water velocity at the undisturbed recharge rate of 3.5 mm/yr (0.14 in./yr) were assigned to the clastic dike material.

- **Case 4f:** This case evaluates another representation of a preferential pathway, which in this case is a poorly sealed or unsealed borehole, hypothetically located adjacent to tank C-105. For this evaluation, the borehole is assumed to be 299-E27-70 (30-05-02). For the scoping case, the depth of the borehole is assumed to extend in length the extent of the drill depth of 299-E27-70, 40 m (130 ft), and 3-D model discretization imposes minimum length and width surface dimensions of 3.8 m (12 ft) each for the borehole (see Figure 4-21). Finer resolution of the model grid is not practicable with the available computational resources.

Figure 4-14. Development of the Technetium-99 Plumes for Selected Time Periods for Case 3b (100 mm/y Recharge).

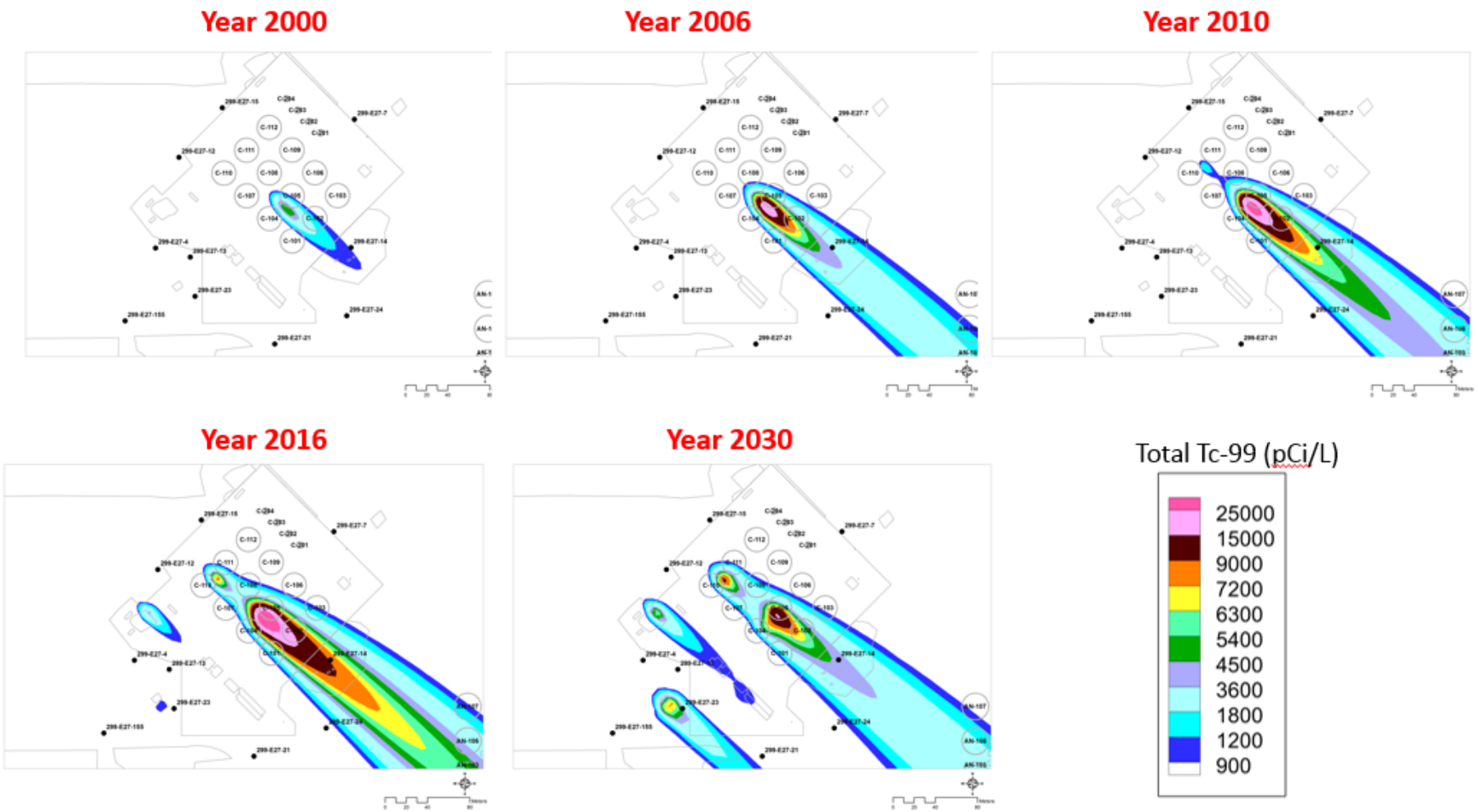

Figure 4-15. Concentrations at Selected Points of Calculation for Case 3b (100 mm/y Recharge). Also shown on the figure are measured technetium-99 concentration data from wells 299-E27-14 and 299-E27-23.

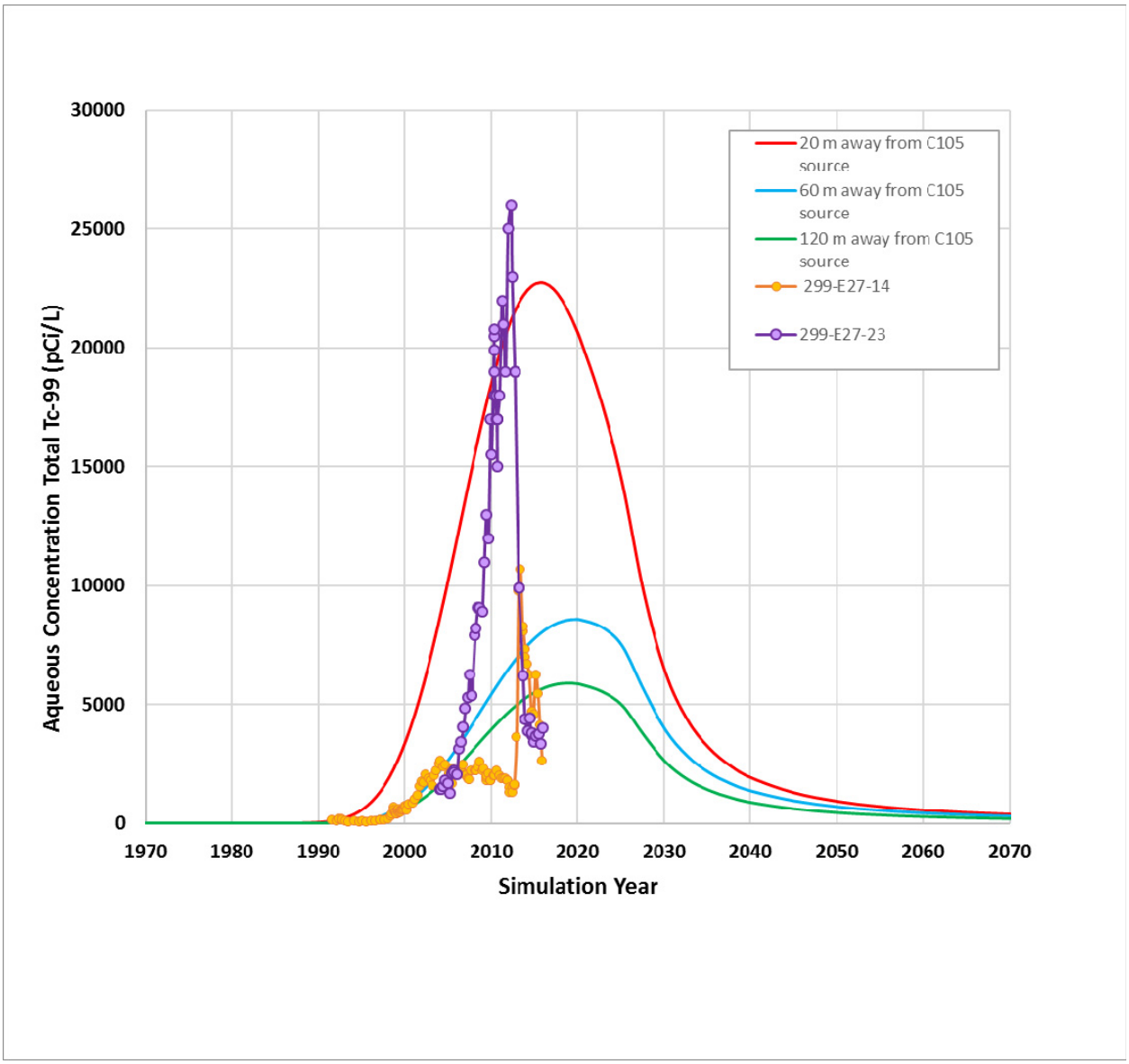

4.4.2 Case Results

Results of Case 4a (Alternative Geologic Model II) are presented in Figures 4-22 and 4-23 and summarized at selected PoCals in Table 4-7. The time of arrival, peak concentrations, and shape of the plume are very similar to Case 1, with the arrival time providing a reasonable match to the monitoring data and the peak concentrations somewhat lower.

Table 4-5. Comparison of the Technetium-99 Concentration Results at Selected Points of Calculation for Scoping Cases 3a through 3d.

	Model Results at 20 Meters Downgradient of Tank 241-C-105 Waste Release Location		Model Results at 60 Meters Downgradient of Tank 241-C-105 Waste Release Location		Model Results at 120 Meters Downgradient of Tank 241-C-105 Waste Release Location	
Case Number	**Time of Maximum Concentration (Calendar Year)**	**Maximum Concentration (pCi/L)**	**Time of Maximum Concentration (Calendar Year)**	**Maximum Concentration (pCi/L)**	**Time of Maximum Concentration (Calendar Year)**	**Maximum Concentration (pCi/L)**
Case 3a	2000	29,500	2002	12,500	2003	7,500
Case 3b	2015	22,700	2017	9,800	2018	5,900
Case 3c	2015	22,800	2017	9,800	2018	5,900

Figure 4-16. Development of Technetium-99 Plumes for Selected Time Periods for Case 3c (Firehose Water Addition Followed by Gunite Cover).

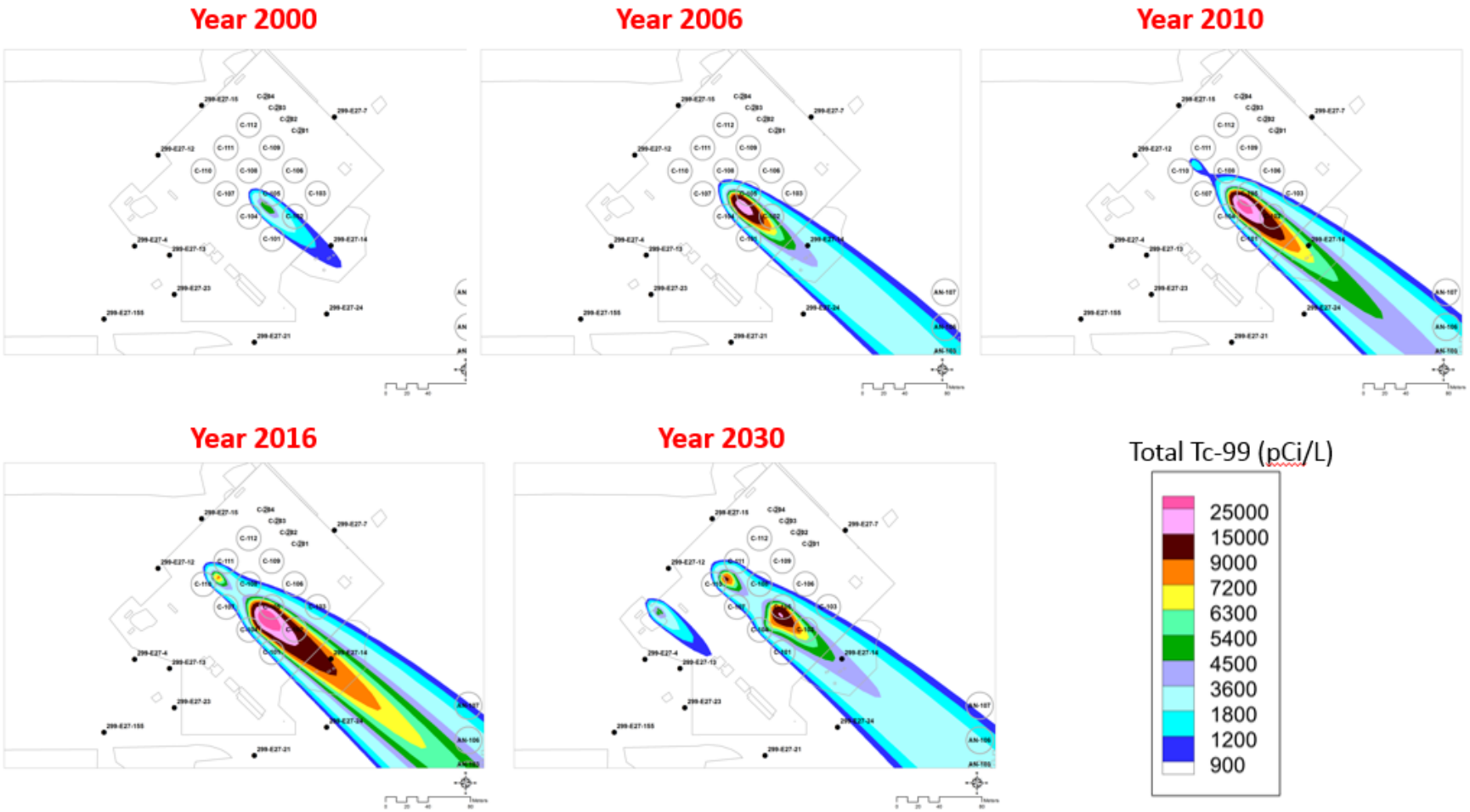

Figure 4-17. Concentrations at Selected Points of Calculation for Case 3c (Firehose Water Addition followed by Gunite Cover). Also shown on the figure are measured technetium-99 concentration data from wells 299-E27-14 and 299-E27-23.

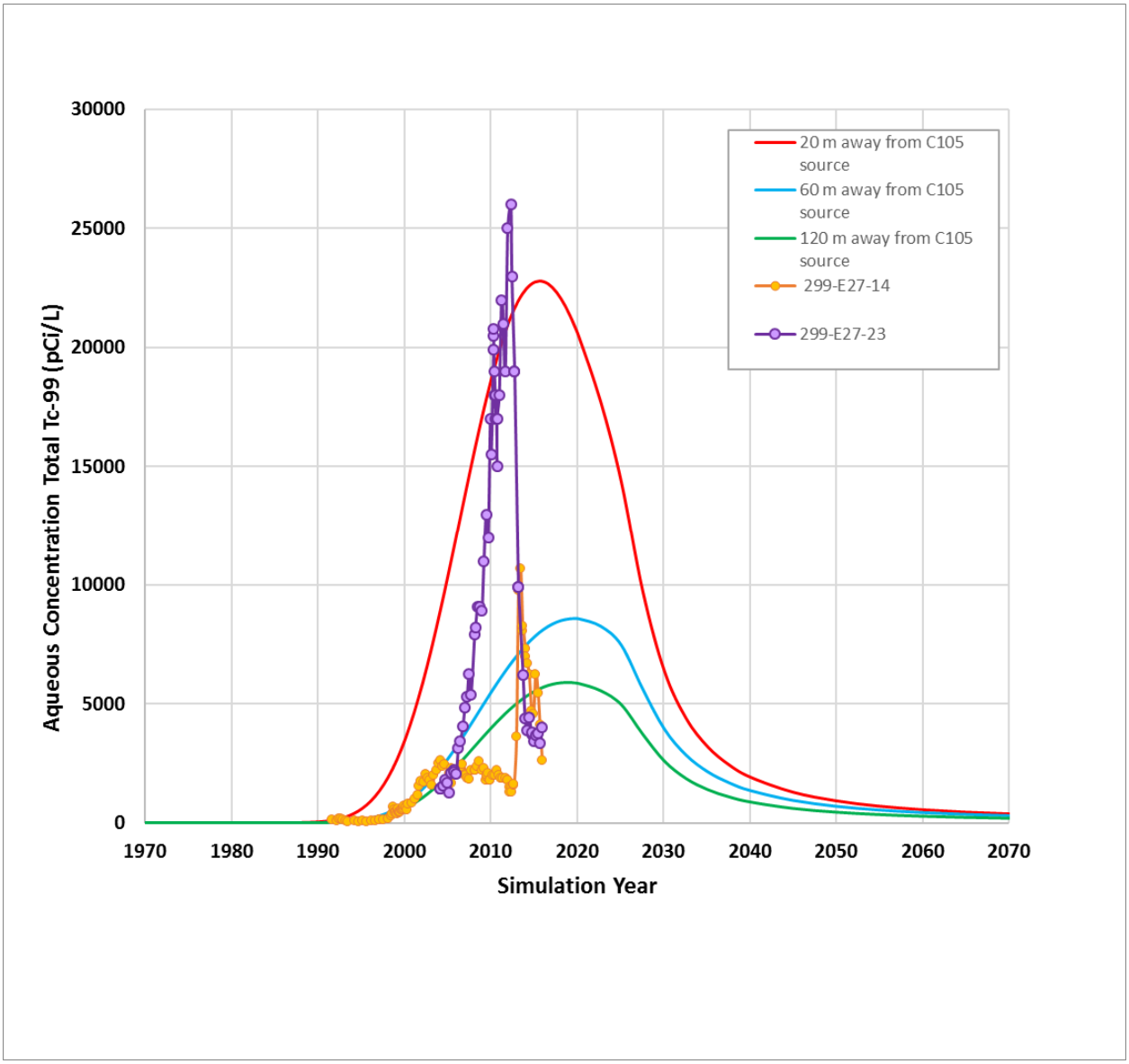

Results of Case 4b (heterogeneous model) are presented in Figures 4-24 and 4-25 and summarized at selected PoCals in Table 4-7. The time of arrival of the plume is earlier than Case 1, and is substantially earlier than indicated by the monitoring data. In addition, the peak concentrations at 60 m and 120 m are somewhat lower than the data from the monitoring wells, and only the peak calculated concentrations at 20 m are close to the data for well 299-E27-23.

Figure 4-18. Depiction of Interpolated Numerical Three-Dimensional Model of Alternative Conceptual Model II for Scoping Case 4a.

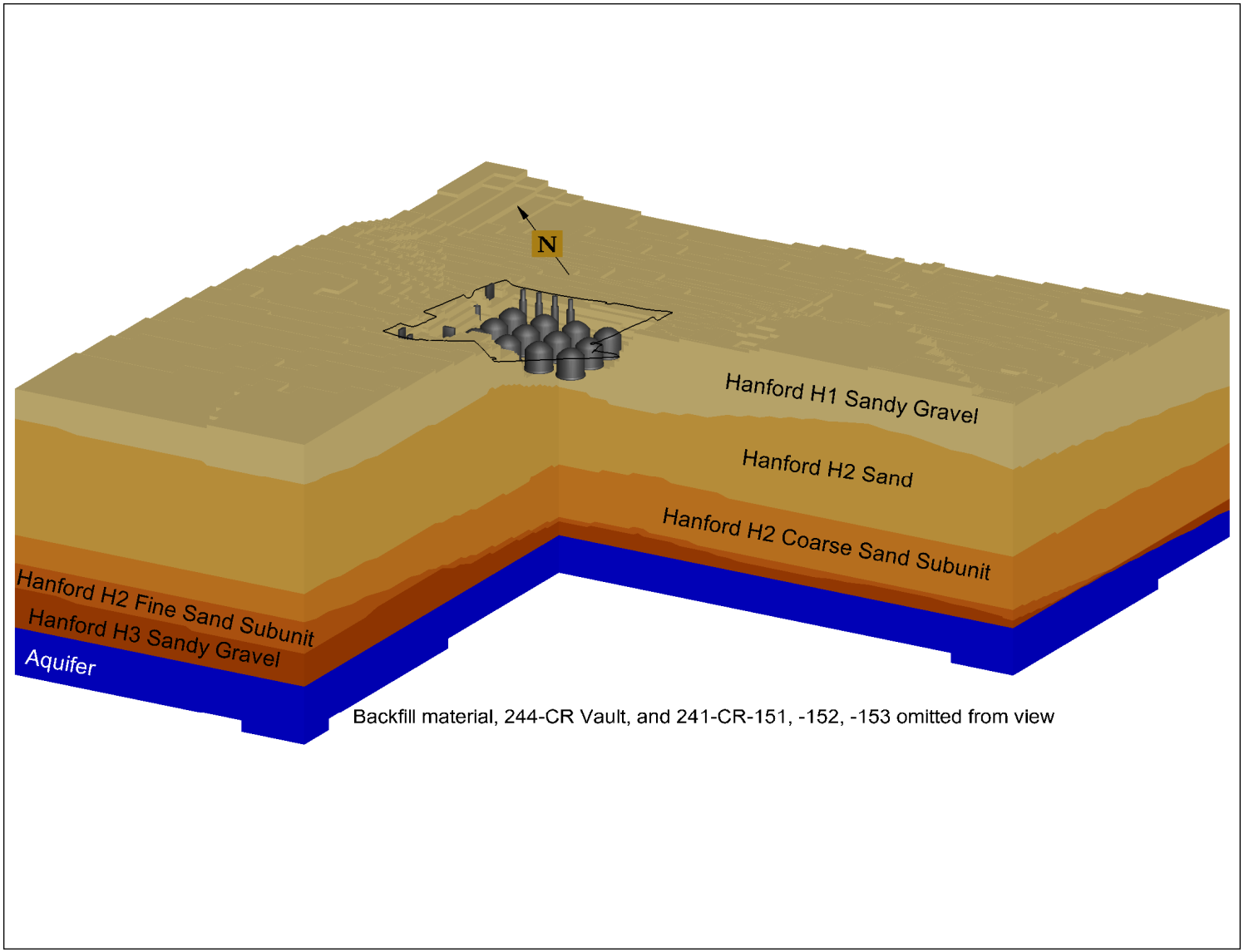

Figure 4-19. Depiction of Interpolated Numerical Three-Dimensional Model of Heterogeneous Alternative Conceptual Model for Scoping Case 4b.

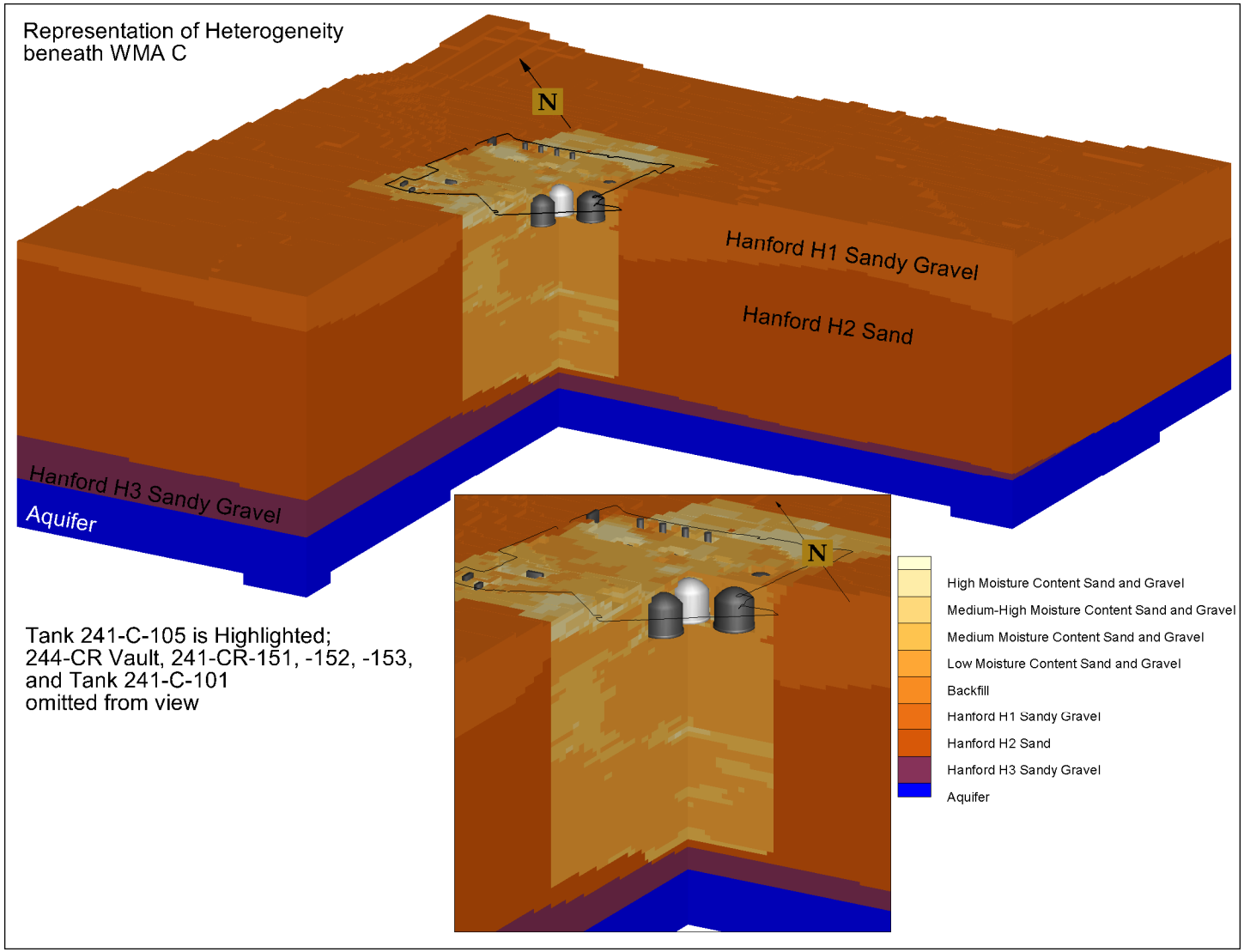

WMA = Waste Management Area

Table 4-6. van Genuchten-Mualem Parameters Corresponding to the Percentiles Selected for Cases 1a, 1b, 4c, and 4d from the Vertical Pore Water Velocity Cumulative Distribution Functions.

Strata (tension)	Percentile	K_s (cm/s)	θ_s	θ_r	α (1/cm)	n
Backfill	5th Percentile	7.91E-06	0.2217	1.23E-02	0.0026	1.441
	25th Percentile	1.08E-05	0.1319	1.57E-02	0.0031	1.310
	Case 4c – 50th Percentile	7.31E-05	0.203	5.94E-03	0.0086	1.577
	75th Percentile	1.98E-04	0.1409	1.42E-02	0.0123	1.470
	Case 4d – 95th Percentile	3.13E-04	0.1287	1.35E-02	0.0298	1.635
	Case 1a and 1b	5.60E-04	0.138	1.10E-02	0.021	1.374
Hanford H1/H3	5th Percentile	7.78E-05	0.2887	3.24E-02	0.0121	1.335
	25th Percentile	5.14E-06	0.2118	2.08E-02	0.0062	1.733
	Case 4c – 50th Percentile	1.49E-04	0.1735	3.06E-02	0.0124	1.603
	75th Percentile	1.58E-03	0.309	7.01E-03	0.0238	1.717
	Case 4d – 95th Percentile	2.99E-04	0.102	1.45E-02	0.0152	1.760
	Case 1a and 1b	7.70E-04	0.171	1.11E-02	0.036	1.491
Hanford H2	5th Percentile	1.79E-03	0.3541	2.89E-02	0.0402	1.633
	25th Percentile	1.15E-03	0.2893	2.99E-02	0.0266	1.971
	Case 4c – 50th Percentile	2.20E-02	0.3304	2.72E-02	0.1253	1.889
	75th Percentile	3.79E-02	0.3474	2.05E-02	0.0966	1.966
	Case 4d – 95th Percentile	1.68E-02	0.2652	2.11E-03	0.1076	1.724
	Case 1a and 1b	4.15E-03	0.315	3.92E-02	0.063	2.047

Table adapted from Table 8-7 in Section 8 of RPP-ENV-58782, "Performance Assessment of Waste Management Area C, Hanford Site, Washington."

Note: The connectivity parameter ℓ is assumed to be 0.5 for all strata and all percentile values.

Results of Case 4c (median hydraulic properties) are presented in Figures 4-26 and 4-27 and summarized at selected PoCals in Table 4-7. The time of arrival, peak concentrations, and shape of the plume are very similar to Case 1, with the arrival time providing a reasonable match to the monitoring data and the peak concentrations somewhat lower.

Results of Case 4d (95th percentile hydraulic properties) are presented in Figures 4-28 and 4-29 and summarized at selected PoCals in Table 4-7. The time of arrival is substantially earlier than the monitoring data, with peak concentrations similar to Case 1, somewhat lower than the peak concentration in monitoring data.

Figure 4-20. Depiction of Hypothetical Clastic Dike near Tank 241-C-105 Conceptualized for Scoping Case 4e.

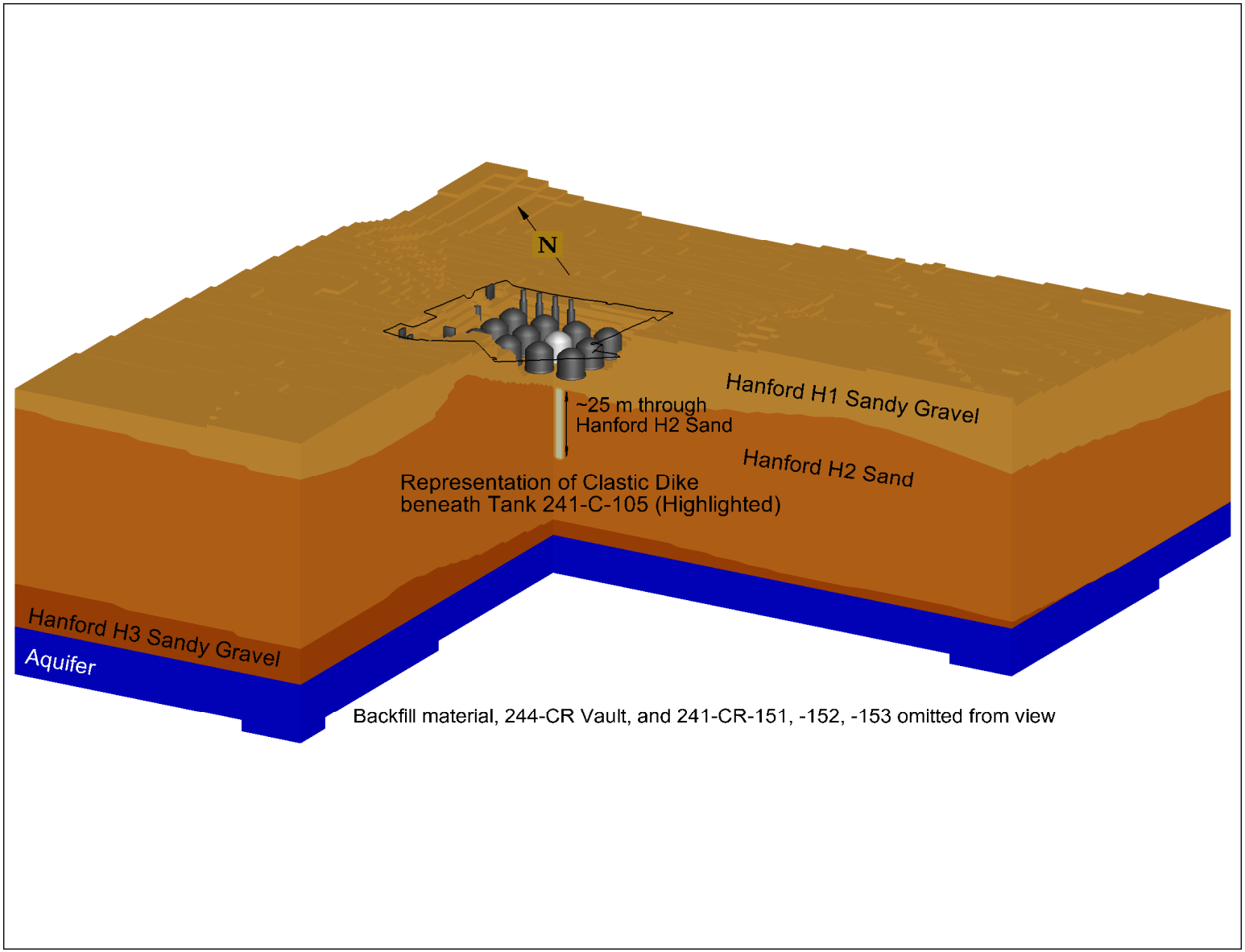

Figure 4-21. Depiction of Hypothetical Unsealed Borehole Near Tank 241-C-105 Conceptualized for Scoping Case 4f.

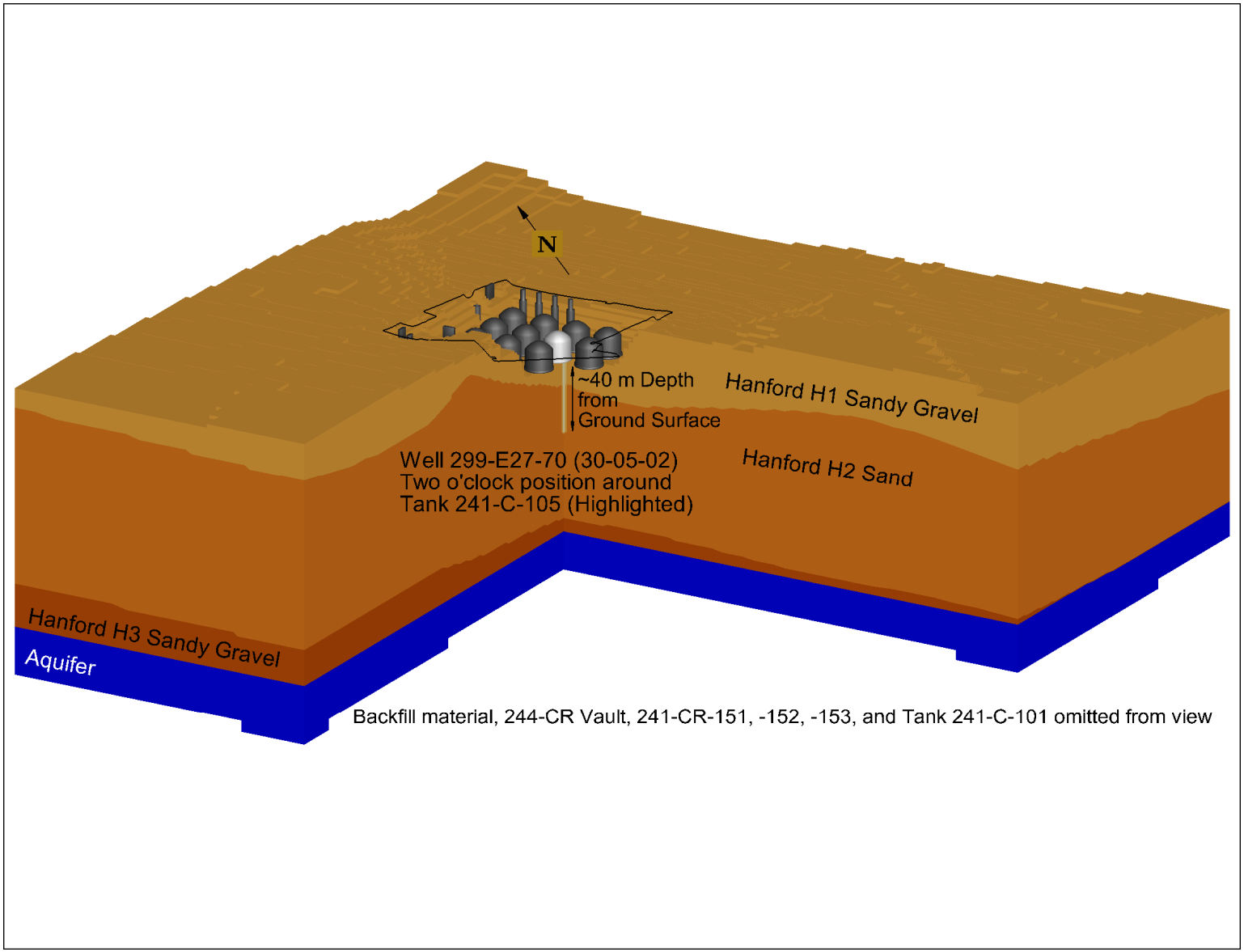

Figure 4-22. Development of Technetium-99 Plumes for Selected Time Periods for Case 4a (Alternative Geologic Model II).

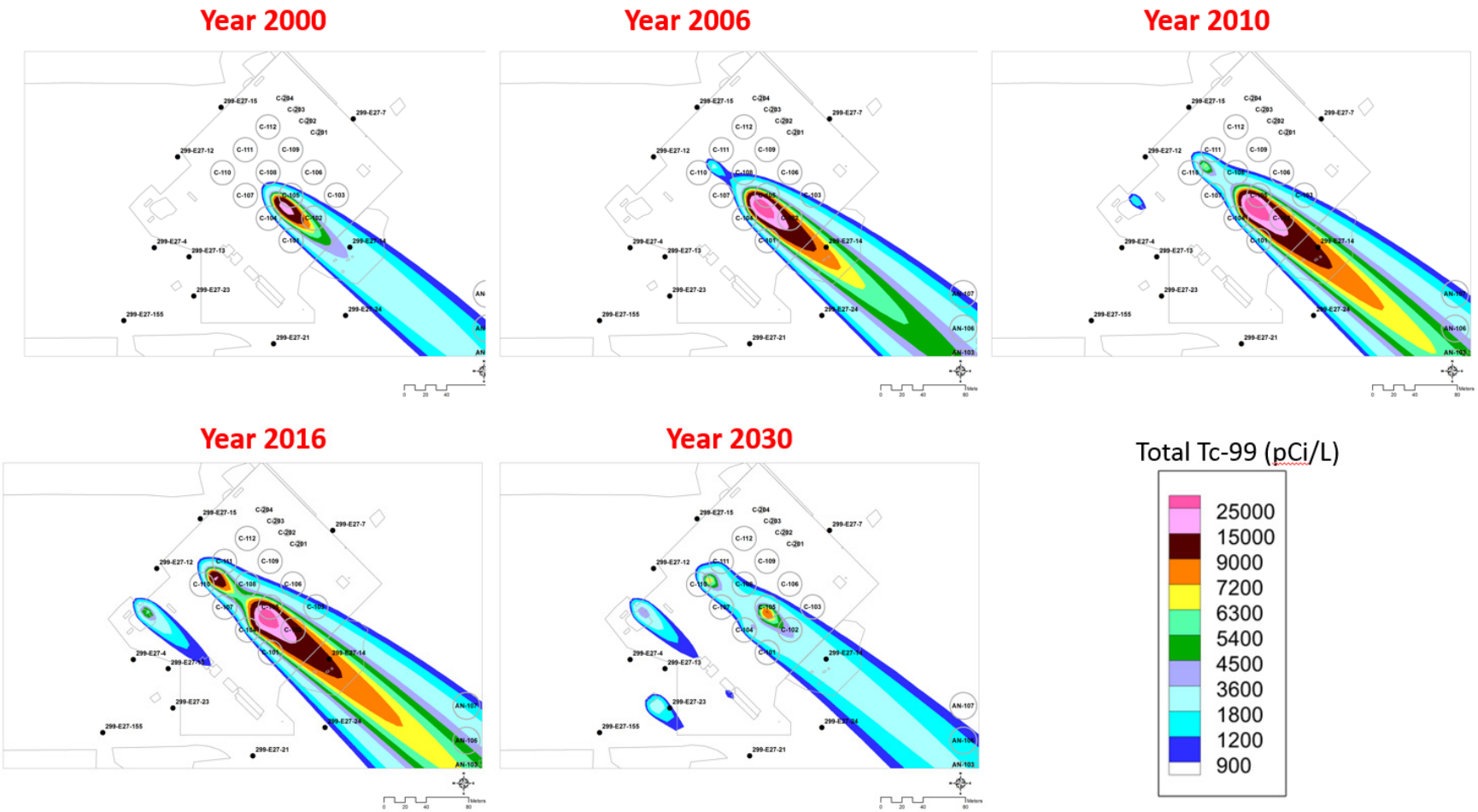

Figure 4-23. Concentrations at Selected Points of Calculation for Case 4a (Alternative Geologic Model II). Also shown on the figure are measured technetium-99 concentration data from wells 299-E27-14 and 299-E27-23.

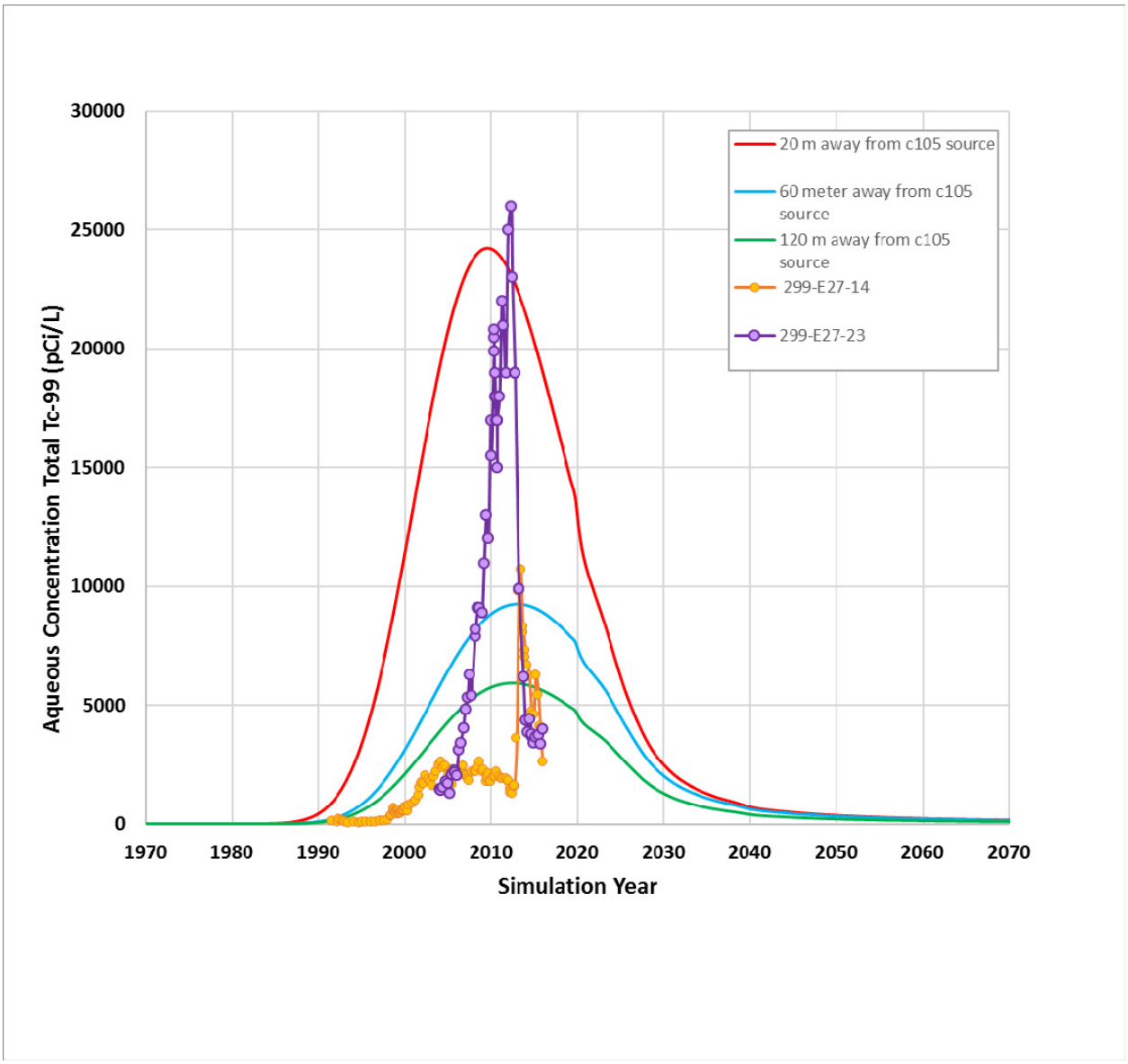

Results of Case 4e (clastic dike) are presented in Figures 4-30 and 4-31 and summarized at selected PoCals in Table 4-7. The peak concentrations and shape of the plume are very similar to Case 1, with the arrival time slightly earlier than Case 1.

Results of Case 4f (borehole preferential pathway) are presented in Figures 4-32 and 4-33. The peak concentrations and shape of the plume are very similar to Case 1, with the arrival time slightly earlier than Case 1.

Table 4-7. Comparison of the Simulated Technetium-99 Concentration Results at Selected Points of Calculation for Scoping Cases 4a through 4f.

	Model Results at 20 Meters Downgradient of Tank 241-C-105 Waste Release Location		Model Results at 60 Meters Downgradient of Tank 241-C-105 Waste Release Location		Model Results at 120 Meters Downgradient of Tank 241-C-105 Waste Release Location	
Case Number	**Time of Maximum Concentration (Calendar Year)**	**Maximum Concentration (pCi/L)**	**Time of Maximum Concentration (Calendar Year)**	**Maximum Concentration (pCi/L)**	**Time of Maximum Concentration (Calendar Year)**	**Maximum Concentration (pCi/L)**
Case 4a	2010	24,200	2011	10,200	2012	5,900
Case 4b	2002	23,700	2004	9,300	2004	6,200
Case 4c	2010	25,300	2013	12,100	2012	7,400
Case 4d	1995	30,700	1998	12,600	1997	7,900
Case 4e	2016	21,000	2018	9,300	2019	5,700
Case 4f	2016	22,400	2018	9,700	2019	5,900

Figure 4-24. Development of Technetium-99 Plumes for Selected Time Periods for Case 4b (Alternative Heterogeneous Model).

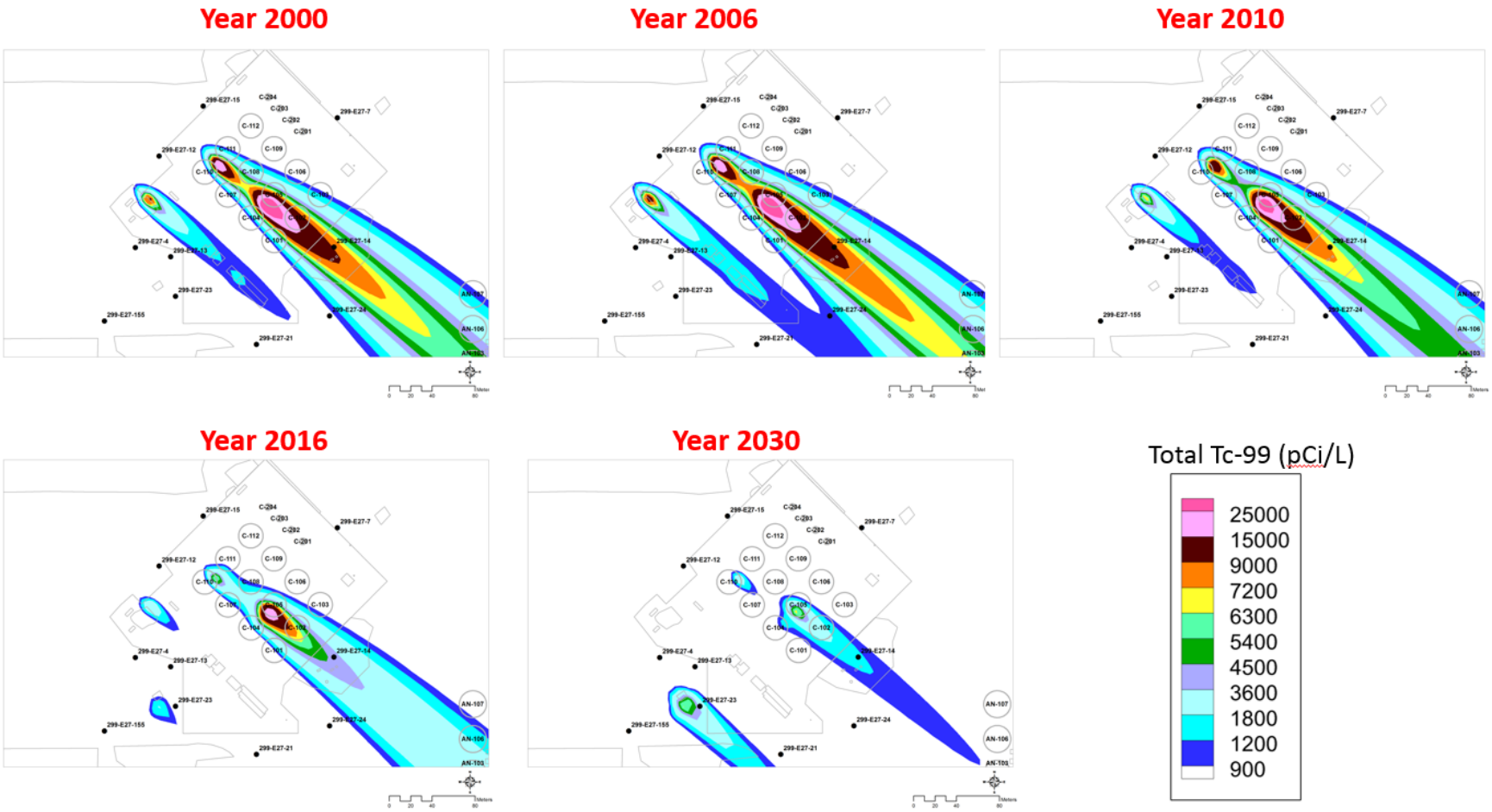

Figure 4-25. Concentrations at Selected Points of Calculation for Case 4b (Alternative Heterogeneous Model). Also shown on the figure are measured technetium-99 concentration data from wells 299-E27-14 and 299-E27-23.

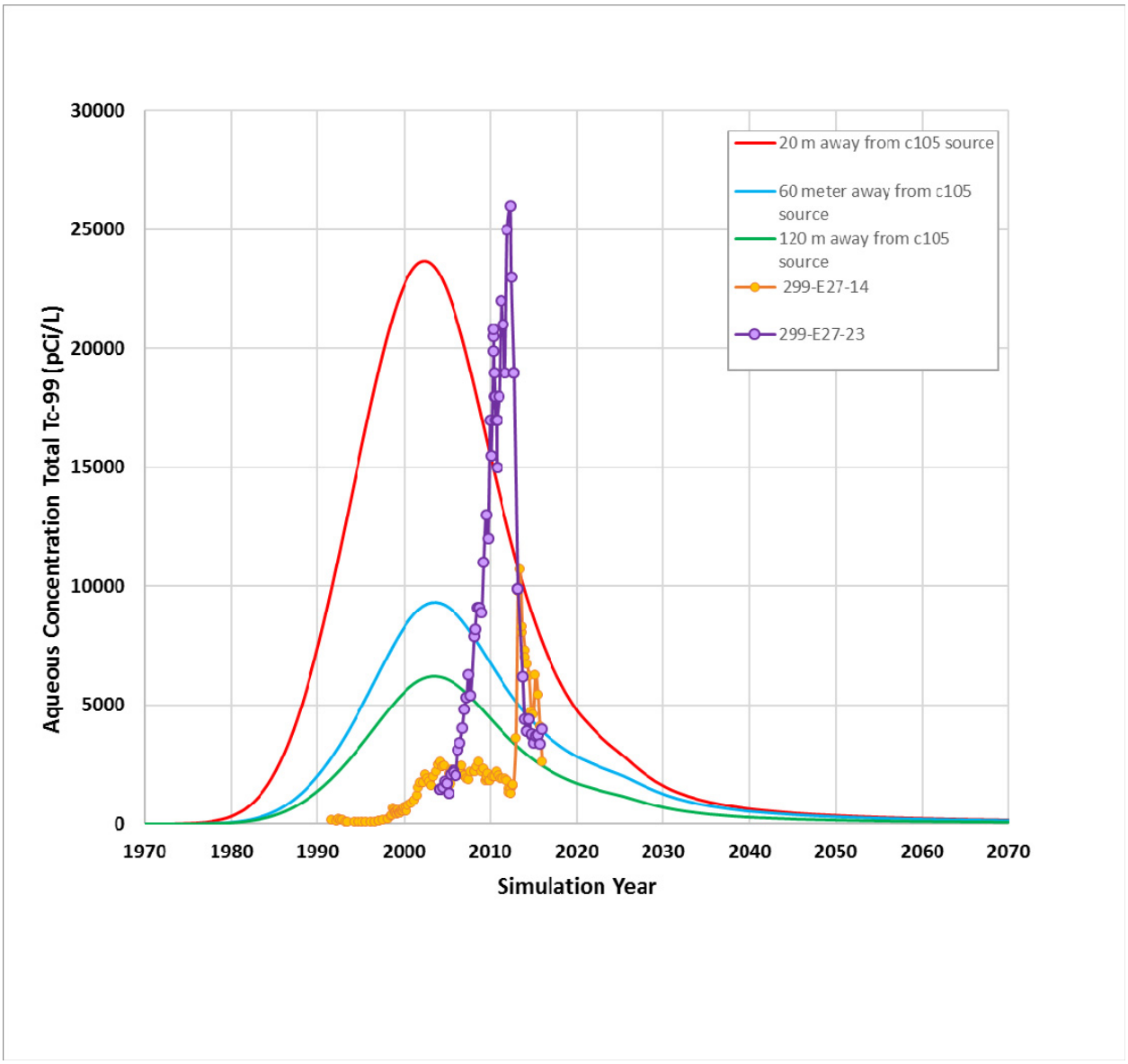

4.5 SUMMARY OF ANALYSIS CASES AND ASSOCIATED OBSERVATIONS

The analysis cases presented in this section have had the goal to match, to the extent possible, the arrival times of the contamination at the water table and the general concentration levels observed in monitoring wells downgradient of the tank farms. The intention is to explore the modeling assumptions and input parameter values that are consistent with the observed arrival times and concentration values.

Figure 4-26. Development of Technetium-99 Plumes for Selected Time Periods for Case 4c (Median Hydraulic Properties).

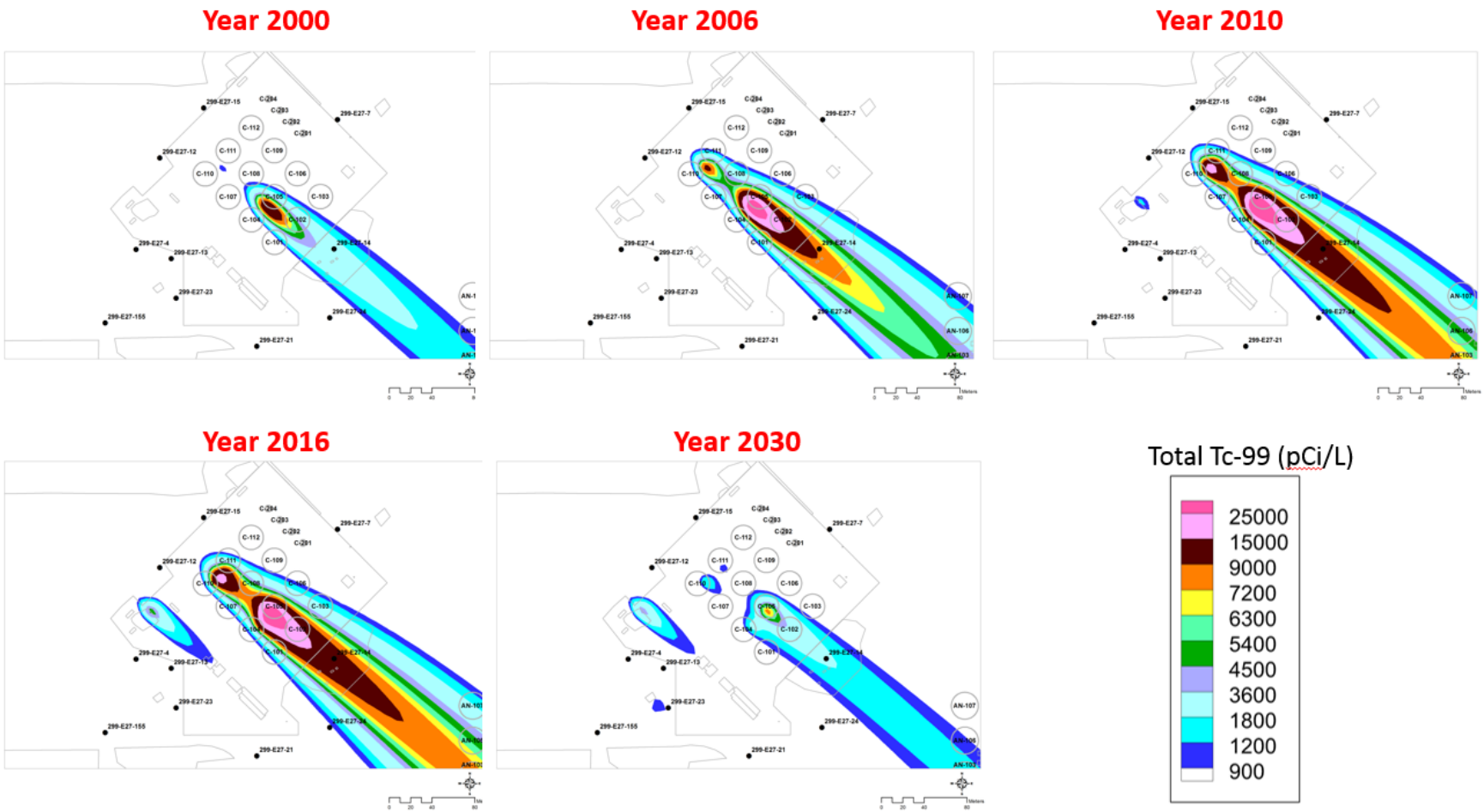

Figure 4-27. Concentrations at Selected Points of Calculation for Case 4c (Median Hydraulic Properties). Also shown on the figure are measured technetium-99 concentration data from wells 299-E27-14 and 299-E27-23.

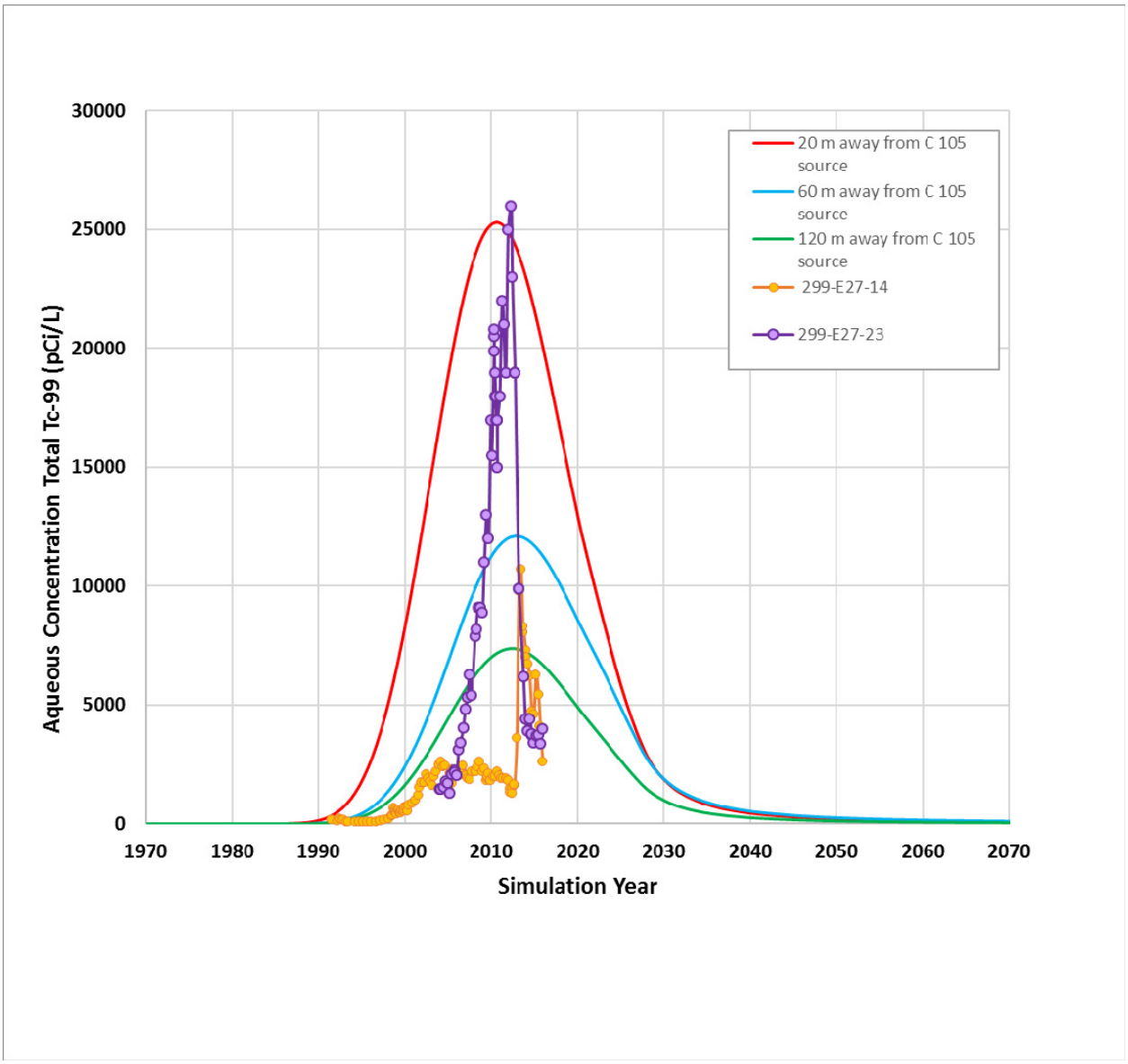

The shapes of the curves presented in this section generally do not provide good matches to the rapid rise and fall of the measured data. This occurs because the data are influenced by the changing orientation of the water table during the period when the plumes arrived at the wells. The steady-state aquifer implemented in the scoping analyses presented in this section do not represent the changes that lead to the sharp changes in the observed data. This feature of the data is explored in greater depth in Section 5.0.

Figure 4-28. Development of Technetium-99 Plumes for Selected Time Periods for Case 4d (95th Percentile Hydraulic Properties).

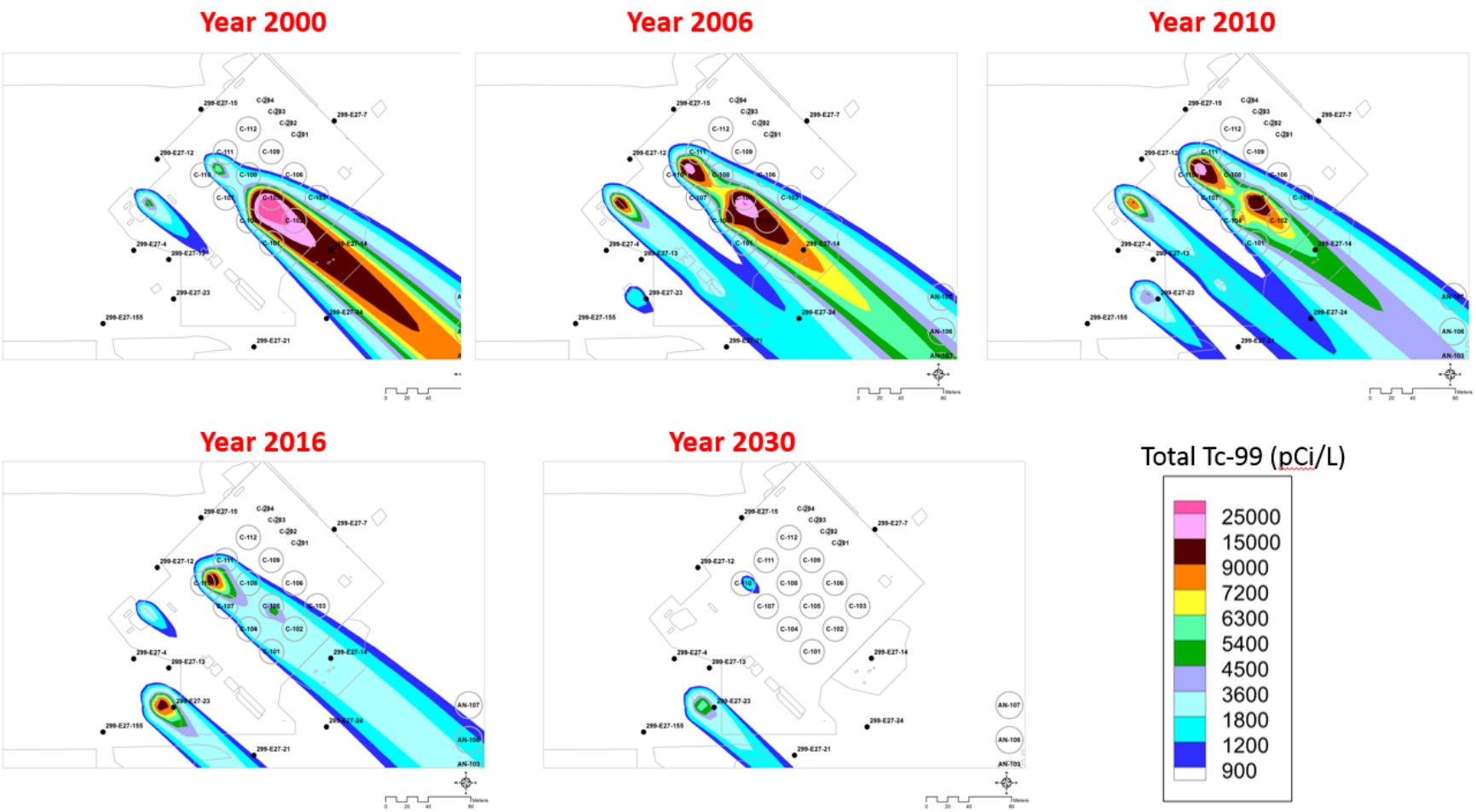

Figure 4-29. Concentrations at Selected Points of Calculation for Case 4d (95th Percentile Hydraulic Properties). Also shown on the figure are measured technetium-99 concentration data from wells 299-E27-14 and 299-E27-23.

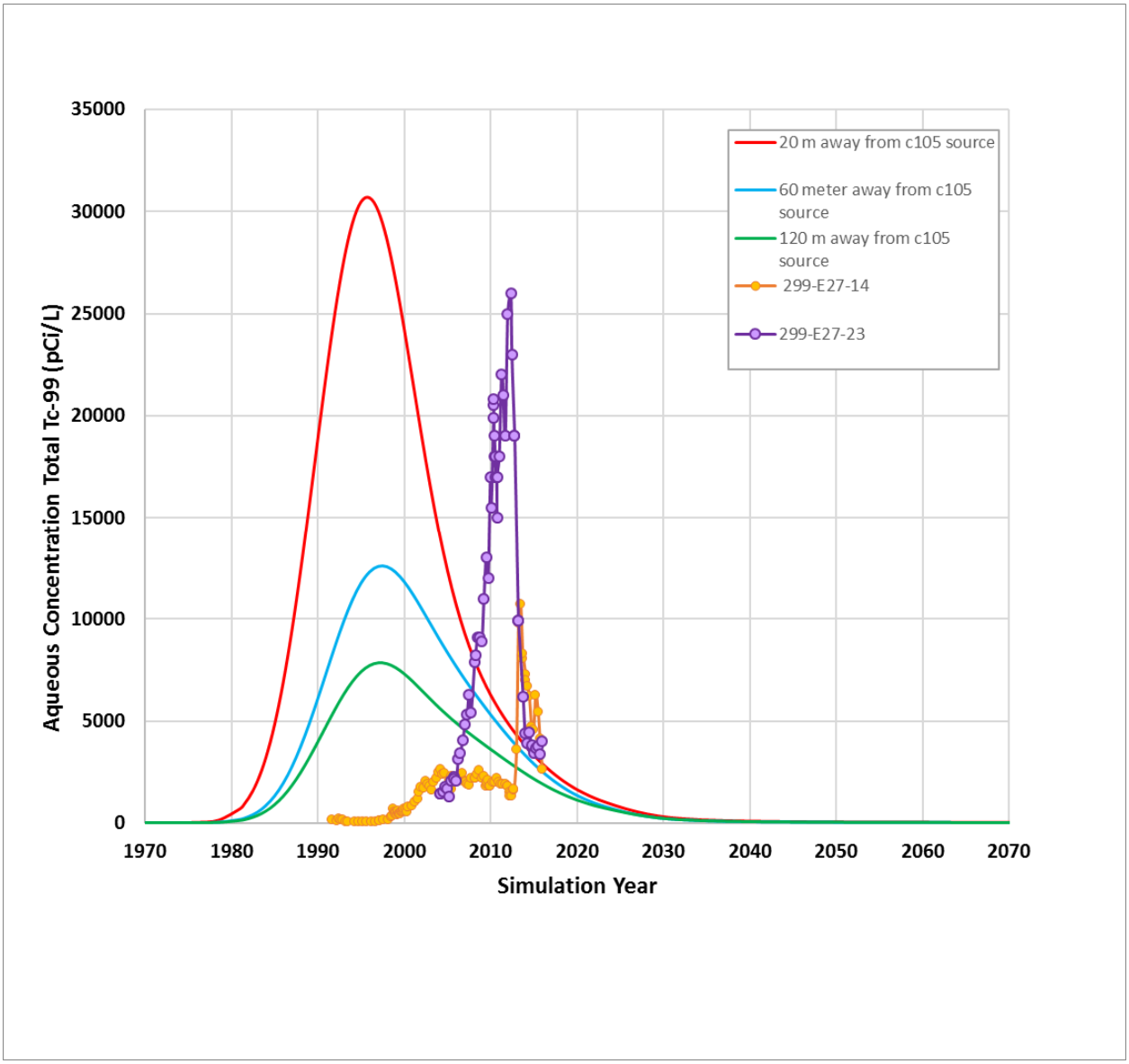

A comparison of all scoping case modeling results at 60 m and at 120 m against ^{99}Tc concentrations observed in wells 299-E27-14 and 299-E27-23 is provided in Figures 4-34 and 4-35 and summarized at selected points of calculation in Table 4-8. It is observed that three scoping analysis cases produced results in which the arrival time of the calculated plume appears to be substantially earlier than the observations in the wells. These scoping analysis cases are

- Case 3a, in which the recharge was increased to 150 mm/y;

- Case 4b, in which the spatial variability of the vadose zone properties was represented by an alternative heterogeneous representation; and

- Case 4d, in which the flow properties of the vadose zone soil were set to their 95th percentile values.

Cases 1a and 1b represents a minimal change from the PA/RCA model for residual wastes presented in RPP-ENV-58782 and RPP-ENV-58806, with the level of the water table elevated to represent an appropriate travel distance to the water table for the leaks. Case 1a uses upper bound leak inventories and volumes based on an assumed upper bound inventory for the tank C-105 waste loss of 9.8 Ci and an upper bound leak volume of 75,600 L (20,500 gal). Case 1b uses the lower bound leak inventories and volumes based on an assumed lower bound inventory for the tank C-105 waste loss of 1.0 Ci and a lower bound leak volume of 7,570 L (2,000 gal).

Case 1 investigated alternative leak inventories for ^{99}Tc in the tank C-105 leak. It was found that the lower bound estimate of a 1 Ci leak is inconsistent with maximum concentration levels of ^{99}Tc observed in the monitoring data at key monitoring well locations (see Figure 4-6). Using this observation, the inventory for the tank C-105 leak was therefore established at 10 Ci for the other analysis cases.

Cases 2a and 2b investigated the effect of changing groundwater fluxes on the model results. It was found that the higher flux rates led to a greater dilution of plume concentrations at the water table, and it is concluded that the lower groundwater flux rate provides concentration levels of ^{99}Tc that are more consistent with monitoring data observed in key monitoring well locations (see Figures 4-34 and 4-35).

Cases 3a through 3b investigated the general effect of a higher recharge rate than used in the other scoping analysis cases. Generally it was found that the higher recharge rates led to early arrival of the plume at the water table. At a rate of 100 mm/y the difference is negligible, but at 150 mm/y the higher recharge rate generated earlier arrival times that are not consistent with monitoring data observed in key monitoring well locations (see Figure 4-34 and 4-35).

Case 3c investigated the effect of a localized addition of water using a firehose to mitigate the operational hazard of leaks at UPRs -82 and -86, followed by the addition of gunite caps on the UPRs. The results of the analysis case are very similar to Case 1, indicating that this past practice has had little effect on the waste releases from the three UPRs at WMA C (see Figure 4-34 and 4-35).

Cases 4a through 4f investigated a number of vadose zone parameters and conceptual models of potential interest, to evaluate the potential for heterogeneities in the vadose zone to affect the plume development migration.

Figure 4-30. Development of Technetium-99 Plumes for Selected Time Periods for Case 4e (Clastic Dike).

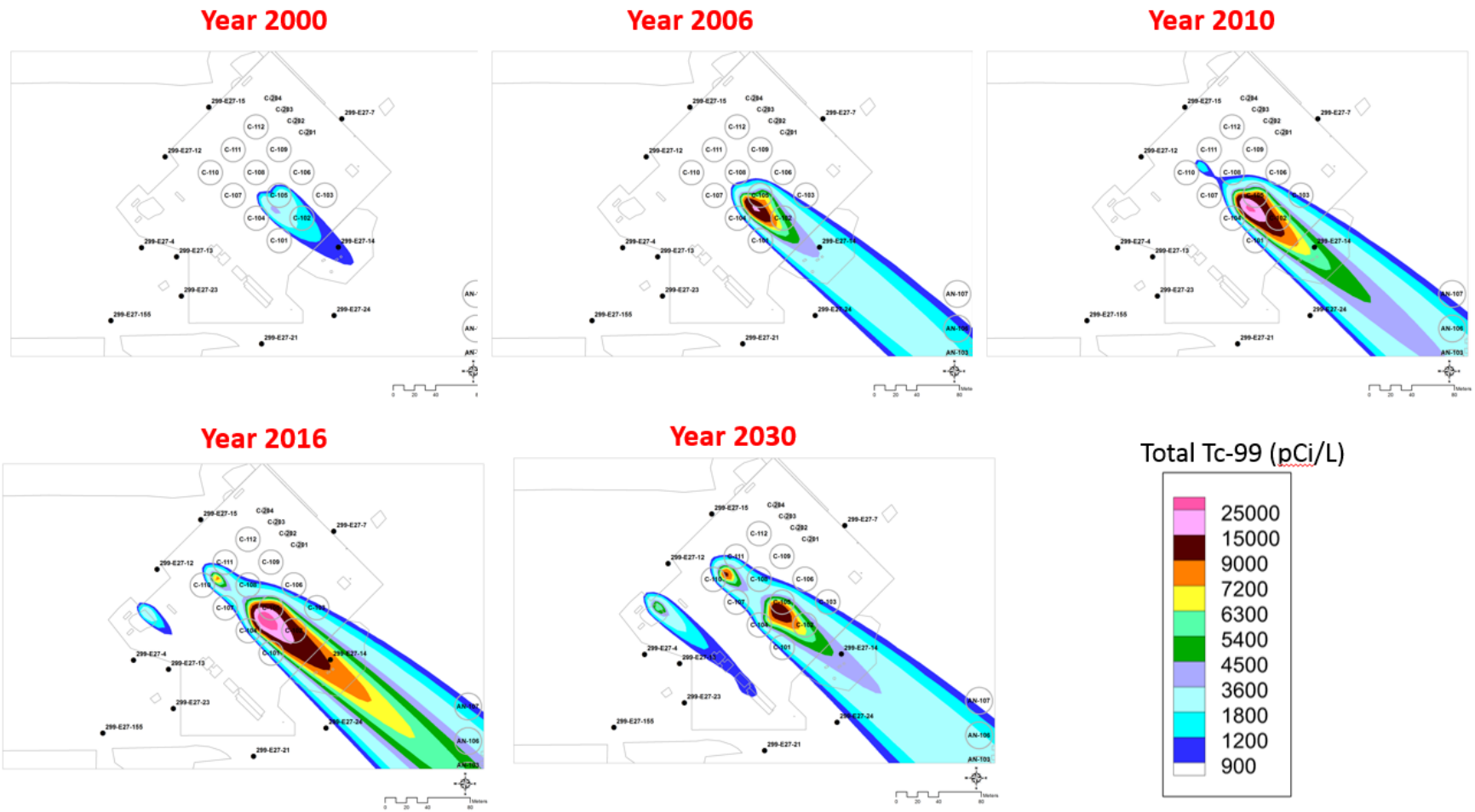

Figure 4-31. Concentrations at Selected Points of Calculation for Case 4e (Clastic Dike). Also shown on the figure are measured technetium-99 concentration data from wells 299-E27-14 and 299-E27-23.

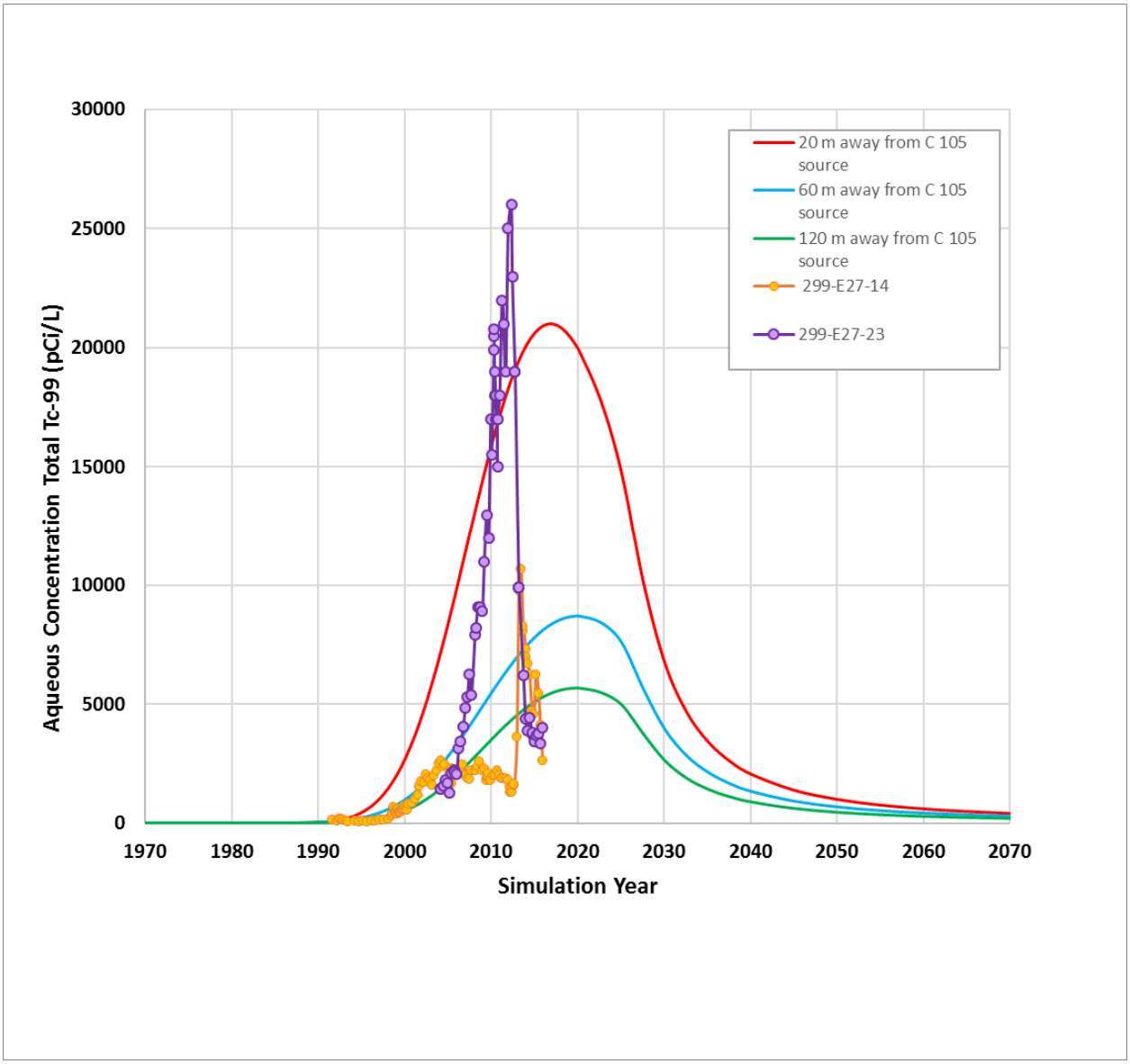

The results of these analysis cases compared to available monitoring data (see Figure 4-34 and 4-35) indicate the following:

- The evaluation of ACM-II in Case 4a showed that adding refinement in the Hanford H2 Sand unit does not strongly affect the results of the analysis. Neither alternative model represented in Case 4a and Case 1a is clearly superior to the other in terms of explaining the monitoring well data.

- The evaluation in Case 4b of ACM using a heterogeneous representation of the vadose zone showed that adding heterogeneity resulted in an earlier arrival that has been observed in monitoring wells and concentrations levels that were lower than those shown for Case 1a. This alternative model appears to be inconsistent with data and is not preferred for further analyses.

- The evaluation of median values of vadose zone hydraulic properties in Case 4c showed arrival time and concentration results that were not significantly different than those for Case 1a. However, the evaluation of 95th percentile values of vadose zone hydraulic properties in Case 4d showed arrival time results that were significantly different than those for Case 1a and the arrival times and concentration levels of ^{99}Tc concentrations from key monitoring wells. Therefore, the use of 95th percentile properties is not preferred for use in further analyses.

- The evaluation of a hypothetical clastic dike and a poorly sealed borehole located near the assumed waste release near tank C-105 in Cases 4e and 4f showed a slightly earlier arrival time at the water and only a small effect of estimated peak concentrations. Since these scoping analysis cases produce results that are similar to cases in which these features are absent, they are not preferred for use in further analyses.

At the outset, it was unclear whether the vadose zone properties, developed for dry post-closure conditions, would be appropriate for the wetter conditions associated with past leaks. Based on the agreement in arrival times between scoping cases that use the dry-calibrated properties and measured data, it is concluded that this is not a significant concern for modeling of the past leaks.

Figure 4-32. Development of Technetium-99 Plumes for Selected Time Periods for Case 4f (Borehole Preferential Pathway).

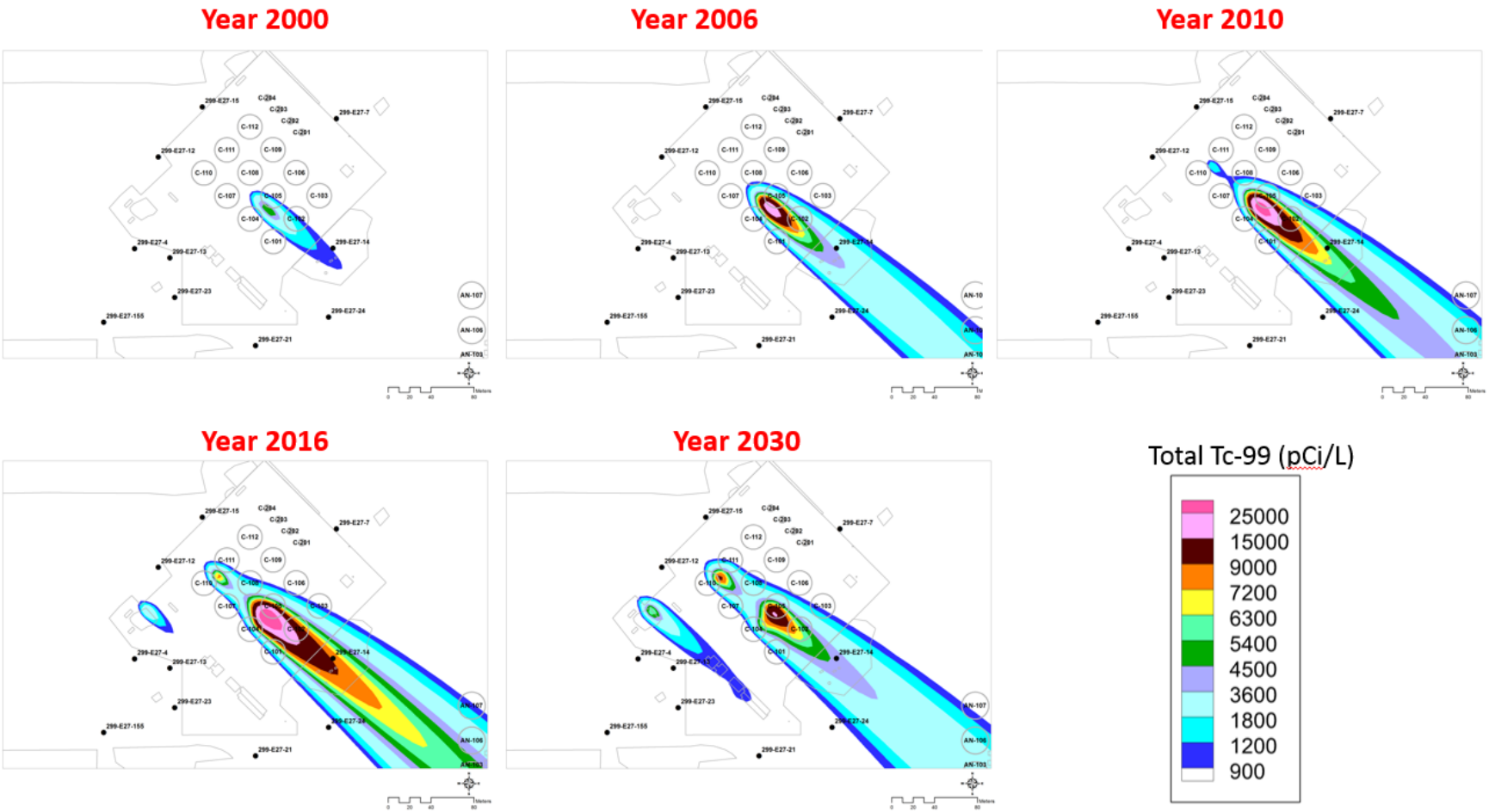

Figure 4-33. Concentrations at Selected Points of Calculation for Case 4f (Borehole Preferential Pathway). Also shown on the figure are measured technetium-99 concentration data from wells 299-E27-14 and 299-E27-23.

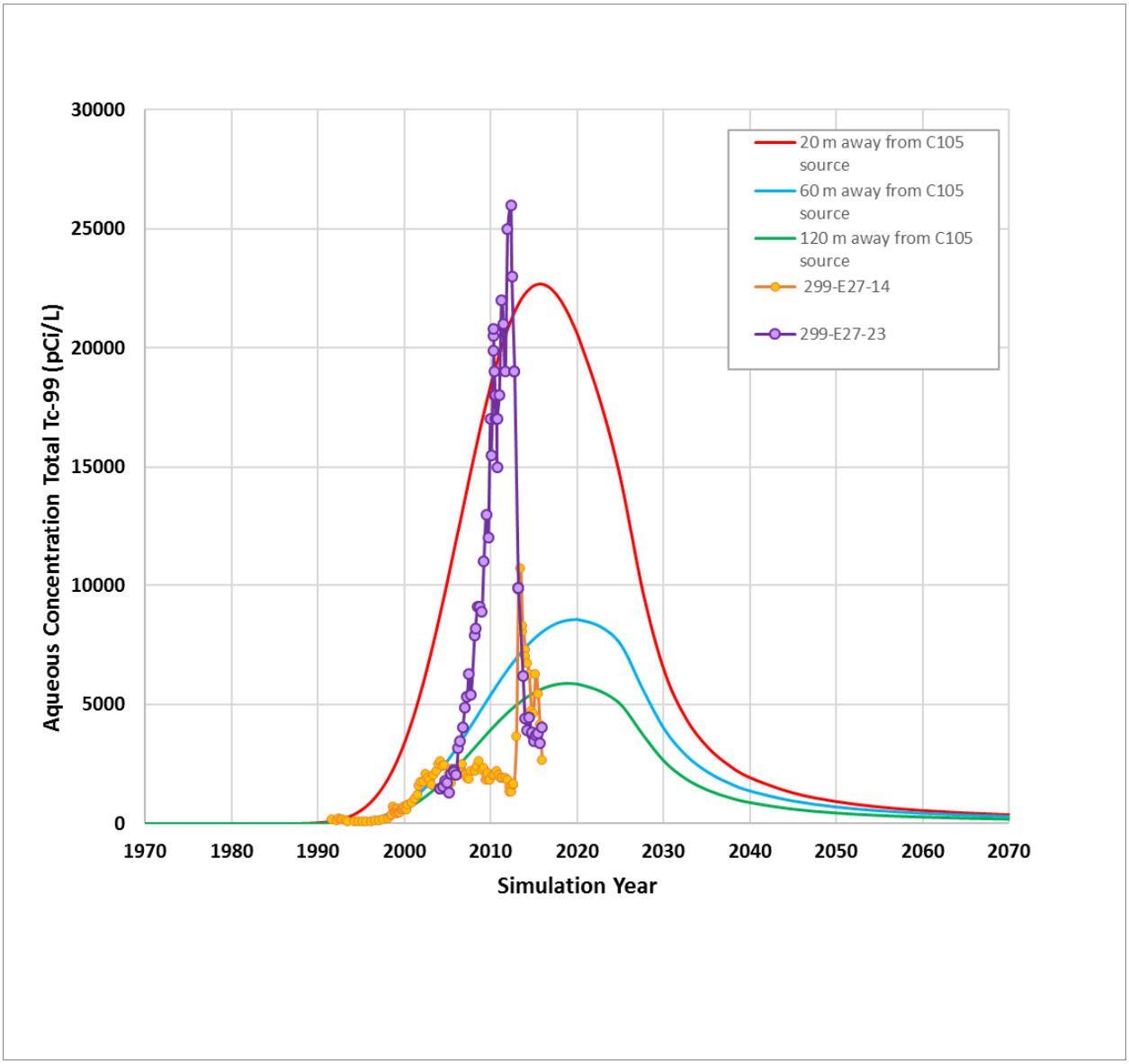

Figure 4-34. Comparison of All Scoping Analysis Cases at 60 Meters Downgradient for the Tank 241-C-105 Past Release Location. Also shown on the figure are measured technetium-99 concentration data from wells 299-E-27-14 and 299-E27-23.

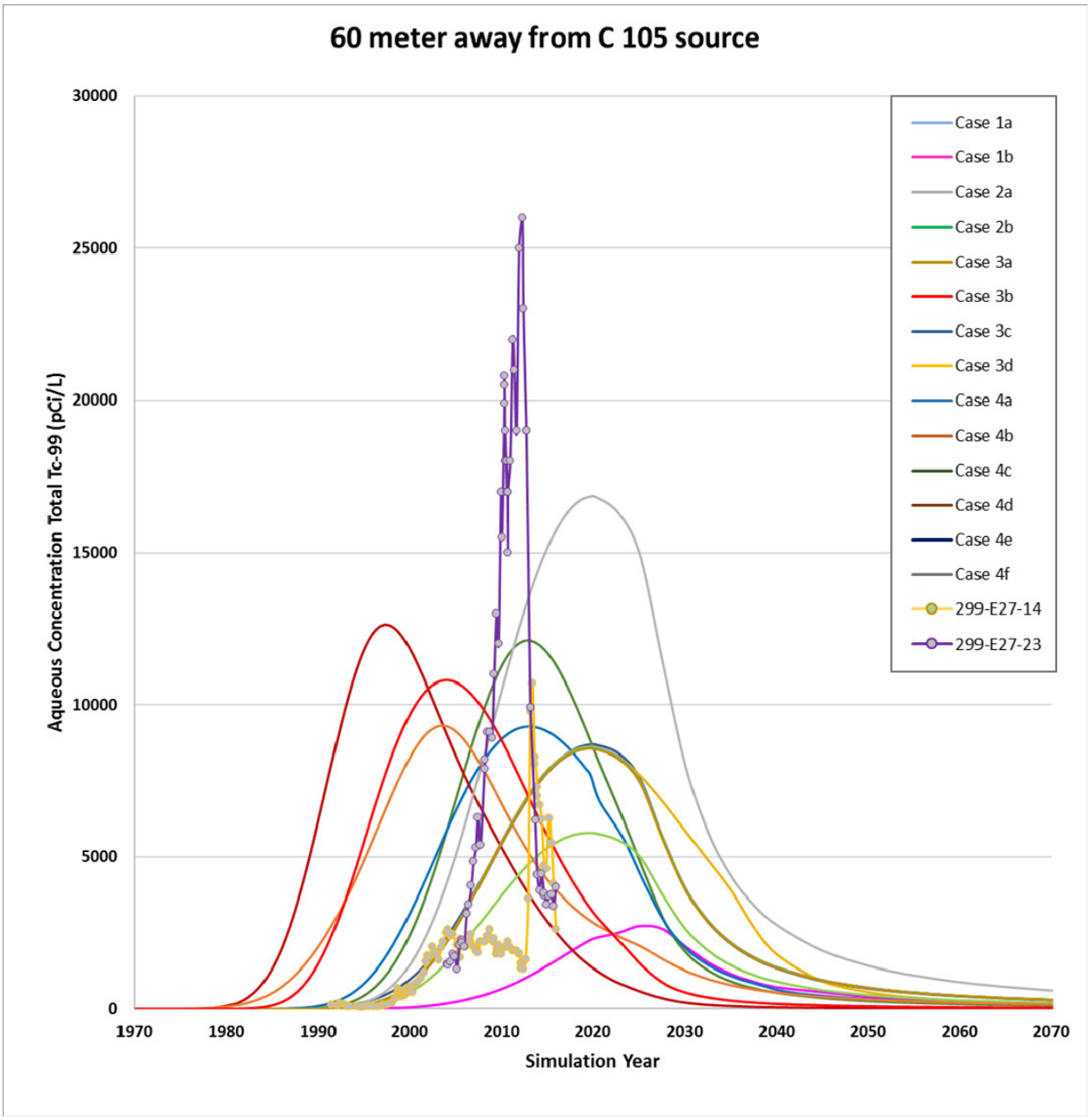

Figure 4-35. Comparison of All Scoping Analysis Cases at 120 Meters Downgradient for the Tank 241-C-105 Past Release Location. Also shown on the figure are measured technetium-99 concentration data from wells 299-E27-14 and 299-E27-23.

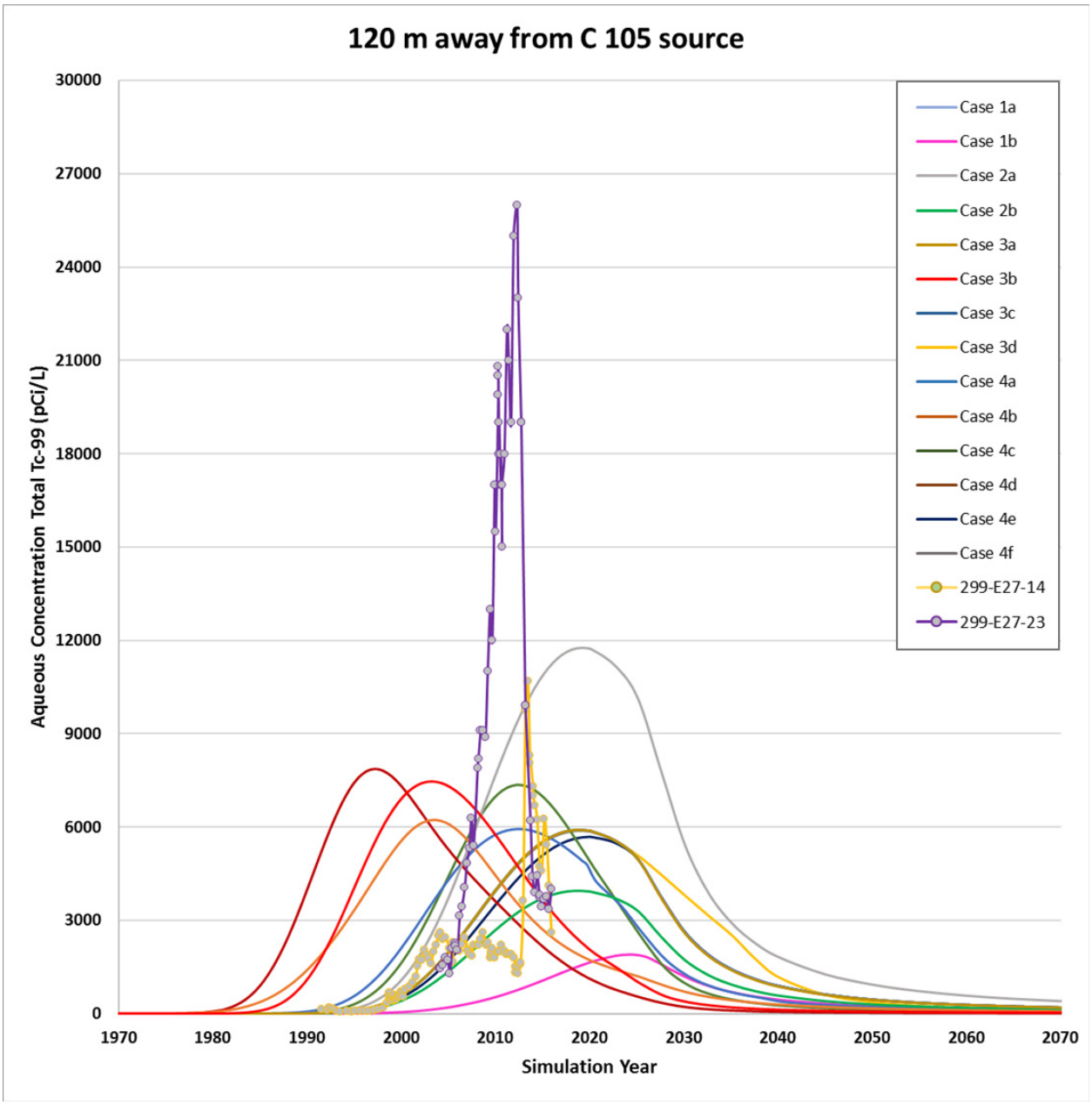

Table 4-8. Comparison of the Technetium-99 Concentration Results at Selected Points of Calculation for All Scoping Analysis Cases.

	Model Results at 20 Meters Downgradient of Tank 241-C-105 Waste Release Location		Model Results at 60 Meters Downgradient of Tank 241-C-105 Waste Release Location		Model Results at 120 Meters Downgradient of Tank 241-C-105 Waste Release Location	
Case Number	**Time of Maximum Concentration (Calendar Year)**	**Maximum Concentration (pCi/L)**	**Time of Maximum Concentration (Calendar Year)**	**Maximum Concentration (pCi/L)**	**Time of Maximum Concentration (Calendar Year)**	**Maximum Concentration (pCi/L)**
Case 1a	2015	22,800	2017	9,800	2018	5,900
Case 1b	2023	4,200	2023	2,700	2023	1,900
Case 2a	2015	45,200	2019	16,800	2019	11,800
Case 2b	2015	15,200	2019	5,800	2019	3,900
Case 3a	2000	29,500	2002	12,500	2003	7,500
Case 3b	2015	22,700	2017	9,800	2018	5,900
Case 3c	2015	22,800	2017	9,800	2018	5,900
Case 3d	2015	22,800	2017	9,800	2018	5,900
Case 4a	2010	24,200	2011	10,200	2012	5,900
Case 4b	2002	23,700	2004	9,300	2004	6,200
Case 4c	2010	25,300	2013	12,100	2012	7,400
Case 4d	1995	30,700	1998	12,600	1997	7,900
Case 4e	2016	21,000	2018	9,300	2019	5,700
Case 4f	2016	22,400	2018	9,700	2019	5,900

5.0 EVALUATION OF THE EFFECTS OF TRANSIENT WATER TABLE

In this section, results of a set of transient model cases of past leak behavior are presented. These transient model analysis cases attempt to approximate the flow conditions in the unconfined aquifer that have existed at WMA C from its construction in 1944 to present day (Figures 2-10 and 2-11). The analysis intends to provide some insight into and basis for the timing, size, and inventory of the past leaks, and the changing hydraulic conditions (i.e., hydraulic gradient [direction and magnitude]) responsible for producing the concentrations levels observed in the monitoring wells. Existing data do not provide a sufficient basis to determine a complete or definitive description of the orientation and magnitude of the hydraulic gradient during most of the operations period. The gradient appears to have shifted direction several times, and the timing of the shifts is highly uncertain, particularly after discharge to 216-B-3 (B Pond) ceased in 1994. Consequently, the model implements modeled and subjective approximations of the gradient direction and magnitude between 1944 and 2020. The combination of the available but limited (especially sparse groundwater monitoring measurements made from 1944 through the early 1990s) field data and the model results manages to provide some basis for developing model assumptions and determining bounded estimates of model input parameters. The transient evaluation also provides some element of confidence that the model parameters and equations can adequately represent the physical conditions and past events of WMA C. This assurance improves the confidence in the model's ability to evaluate and estimate future impacts from the past leaks and other sources.

5.1 TRANSIENT MODEL DESCRIPTION AND IMPLEMENTATION

The transient model scope is to approximate the flow conditions that have existed at WMA C from its construction in 1944 to present day, with a focus on the period of time when past waste releases were potentially impacting groundwater at WMA C. During the time, referred to as the operations period, the hydraulic gradient, both in direction and magnitude, appears to have been highly variable, and flow appears to have occurred in several directions. Although the focus of the modeling analysis is the time after the leaks arrive at the water table in the late 1990s through the present, the analysis period begins in 1944 to account for the changed conditions caused by construction and operation of the tank farm. Construction altered the ground surface which impacted the net infiltration as early as 1960.

Between the introduction of the WMA C infrastructure and backfill material in the farm, the change in recharge at the surface, and the variations in the water table boundary conditions, STOMP© required an impractical amount of time to solve the flow equations for the 1944 to 1960 time period. As a simplification and expedient for the model, the pre-Hanford steady-state conditioning includes the tank farm backfill and structures, but the operations period ignores water table fluctuations prior to 1981. Although the first documented leak occurred in 1960, the groundwater monitoring results indicate that ^{99}Tc does not reach the water table until after 1981, so the water table fluctuations before then are essentially irrelevant. Therefore, model analyses ignore the water table fluctuations prior to 1981, and the period from 1944 to 1981 is simply simulated with the 1981 water table boundary conditions in the aquifer. This assumption to ignore water table fluctuations prior to 1981 is further supported by groundwater monitoring

measurements for ^{99}Tc and nitrate. Although both of these contaminants are reported in low levels in monitoring wells in the early 1990s, rising trends for these contaminants in WMA C wells were not observed until the late 1990s.

5.1.1 Central Plateau Groundwater Model

The initial basis of the flow conditions included in these analysis cases was derived from the CPGWM calibration results (CP-47631, Rev. 0) for the period of interest. The CPGWM provides calibrated output that approximates the water table during the operations period. The CPGWM represents the most recent culmination of understanding of the unconfined aquifer under the Central Plateau and, given the rigorous nature of the development effort, is deemed to be the most suitable for estimating and predicting flow.

The CPGWM represents the best current understanding of groundwater flow conditions under the Central Plateau. The CPGWM represents the product of ongoing development and continued improvement that began in fiscal year 2009, and has undergone several revisions (currently at Revision 6.3.3) to improve its performance with respect to calibration. CPGWM 6.3.3 takes account of the historical development of understanding the unconfined aquifer, along with current interpretations of the geology (including the extent of the paleochannel beneath WMA C), and up-to-date measurements of the recovery of the water table from operational discharges (CP-47631). The CPGWM incorporates the large-scale geologic and hydrogeologic features, and provides estimates of water levels, hydraulic gradients, and groundwater flows throughout the 200 West and 200 East Areas for past, current, and expected future groundwater conditions (CP-47631).

The CPGWM calibration places emphasis on matching water level data from the 1940s, early 1950s, and first decade of the 21st century to estimate hydraulic properties using flow conditions relatively unperturbed by site operations (CP-47631). The observed heads in wells located upgradient and downgradient of the WMA C and corresponding CPGWM-simulated heads, representing a time span of over 20 years, compare well as indicated in Figure 5-1, providing confidence in the estimative and predictive capabilities of the CPGWM.

5.1.2 Application of the Central Plateau Groundwater Model to Waste Management Area C

The CPGWM provides an estimate of the water table on an approximately annual basis for the operations period. The grid spacing of the CPGWM is 100 m by 100 m, which is much coarser than the grid spacing used in the WMA C model, but provides adequate output to establish boundary conditions to the WMA C model for the operations period. Hydraulic head values calculated by the CPGWM are interpolated onto the boundary nodes of the WMA C model. Figure 5-2 shows an example of the alignment of the two grids and the values interpolated from the CPGWM representing the year 2000. Each WMA C model node is contained by the triangle formed by the three closest CPGWM nodes, and the value interpolated is the distance-weighted average of those three CPGWM node values. The figure also illustrates the difficulty in evaluating the hydraulic head and gradient in the area around WMA C. The difference between the maximum value (122.791) and minimum value (122.781) across the entire domain of the

WMA C model domain is only 10 mm. The interpolation repeats for each year between 1944 and 2040 that the CPGWM provides hydraulic head values. These boundary conditions provide the basis for the WMA C model's attempt to approximate the flow conditions during the time from 1944 to present day.

The boundary condition type, either prescribed head or prescribed flux, is defined according to the hydraulic head elevation along each boundary. Nine values representing the span of each boundary are averaged, and the average values rounded to three significant digits are ranked highest to lowest. Boundaries ranked 1 or 2 are designated as prescribed flux, and boundaries ranked 3 or 4 are designated as prescribed head. Figure 5-3 shows nodes used to calculate each boundary's average, the average values, and the ranking of the boundaries representing the year 2000. The overall simulation period is broken into discrete segments according to changes in the boundary condition types. Whenever a boundary condition changes from prescribed head to prescribed flux, or vice-versa, the existing segment ends and a new one begins. Table 5-1 shows the rankings segments for the period 1944 to 2040.

The prescribed head boundary condition values are based on the interpolated values, converted to aqueous pressure. The calculation of the prescribed flux boundary condition values involves some intermediate steps. The flux for a particular node is calculated according to the gradient between the hydraulic head values of that node and the corresponding node on the opposite boundary. For example, for any node located along the first column of nodes (i.e., i =1, j = 1, …, jmax), the flux is calculated according to the following equation:

$$q_{1,j} = -K_{sat}\left(\frac{h_{imax,j} - h_{1,j}}{737.9\ m}\right)$$

where $q_{1,j}$ is the flux at node j along the first column of nodes, K_{sat} is the aquifer hydraulic conductivity (m/yr), $h_{1,j}$ and $h_{max,j}$ are the hydraulic head values (m) at node j along the first and last columns of nodes, respectively, and 737.9 m is the distance across the model domain from the first to the last column of nodes. To calculate flux at node j along the last column of nodes, the equation becomes

$$q_{imax,j} = -K_{sat}\left(\frac{h_{1,j} - h_{imax,j}}{737.9\ m}\right)$$

For fluxes along the first or last row of nodes, the equations become, respectively,

$$q_{i,1} = -K_{sat}\left(\frac{h_{i,jmax} - h_{i,1}}{795.3\ m}\right) \quad and \quad q_{i,jmax} = -K_{sat}\left(\frac{h_{i,1} - h_{i,jmax}}{795.3\ m}\right)$$

where the distance equals 795.3 m. If the flux equals a negative value, then the flux is assigned a value of 0.

Figure 5-1. Central Plateau Groundwater Model Calibration Results in the Vicinity of Waste Management Area C.

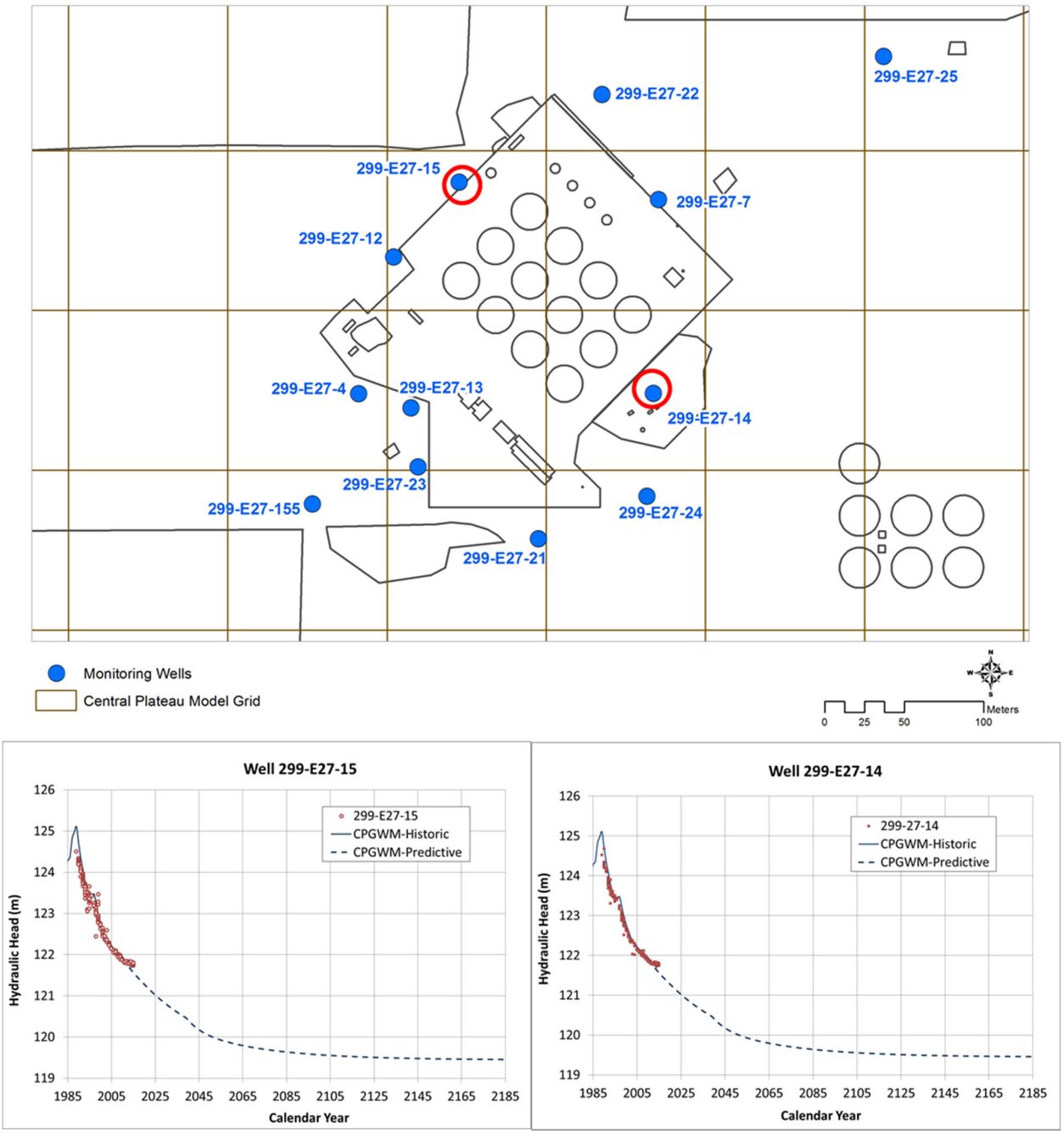

CPGWM = Central Plateau Groundwater Model

Figure 5-2. Alignment of the Central Plateau Groundwater Model and Waste Management Area C Unplanned Release Model Grids and Central Plateau Groundwater Model Hydraulic Head Interpolation Values Representing Calendar Year 2000 on a Triangular Mesh.

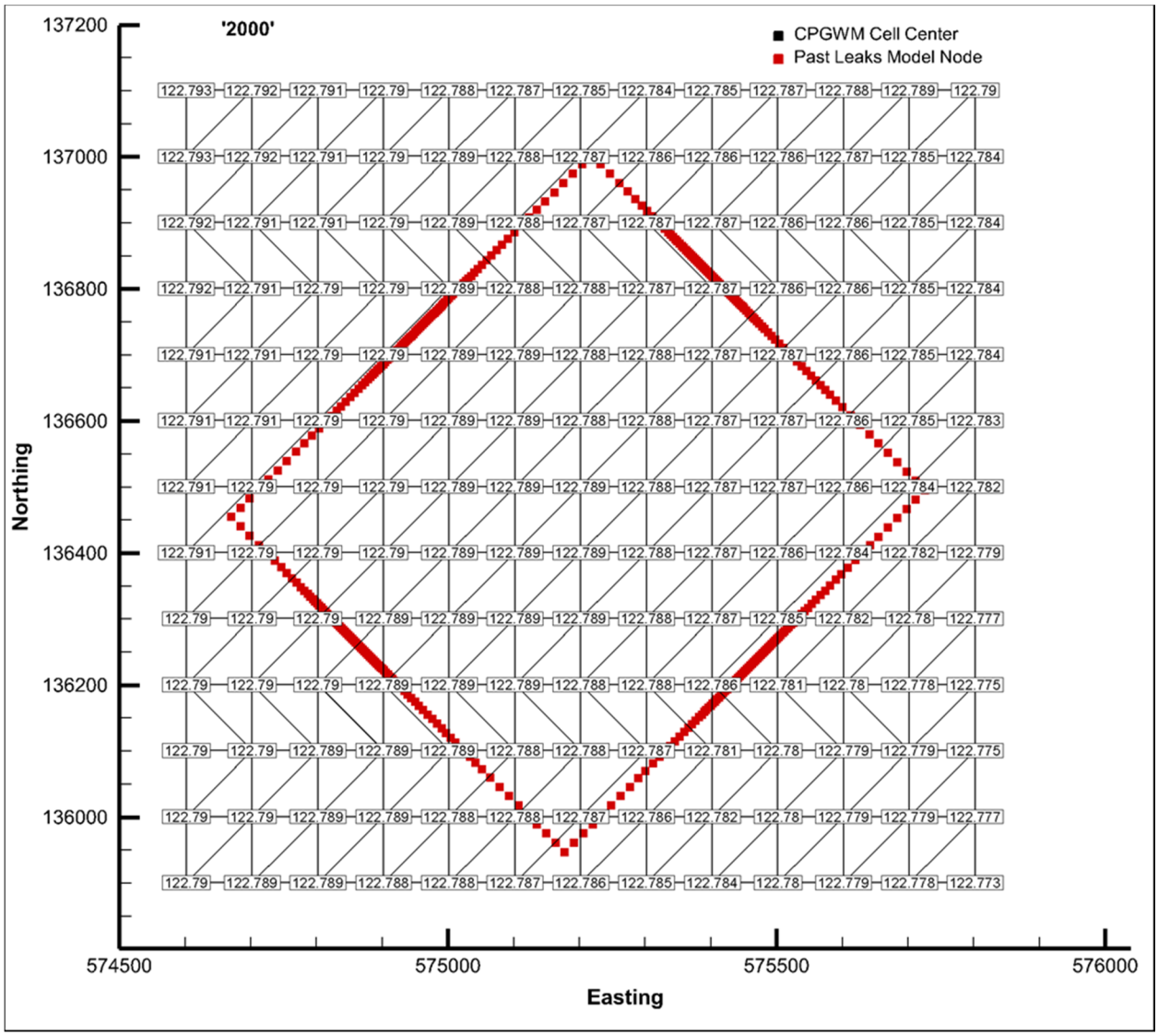

CPGWM = Central Plateau Groundwater Model

5.2 EVALUATION OF THE TRANSIENT WATER TABLE HYDRAULIC GRADIENT

The magnitude and direction of the hydraulic gradient in the 200 East Area is very low and very difficult to measure accurately. Further compounding the problem of determining the magnitude and direction of the hydraulic gradient in the 200 East Area during the operations period is that the water table increased ~9 m because of the volume of wastewater disposal occurring in the ponds near the 200 East Area (DOE/RL-2014-32). The presence of the groundwater mounds

also affected the direction of groundwater movement, having caused radial flow to occur from around the discharge areas while those facilities operated (Figure 5-4). Water levels have declined since the cessation of wastewater discharges to 216-B-3 (B Pond) and 216-A-25 (Gable Mountain Pond), but the water table remains ~2 to 3 m above the projected steady-state conditions (CP-47631). In the vicinity of WMA C, direction of groundwater flow and magnitude of the hydraulic gradient have been inferred from water-level measurements made around LLWMA-1, which is located ~2,300 m northwest of WMA C (SGW-54165).

Figure 5-3. Waste Management Area C Unplanned Release Model Grid Hydraulic Head Boundary Averaging Values Representing Calendar Year 2000.

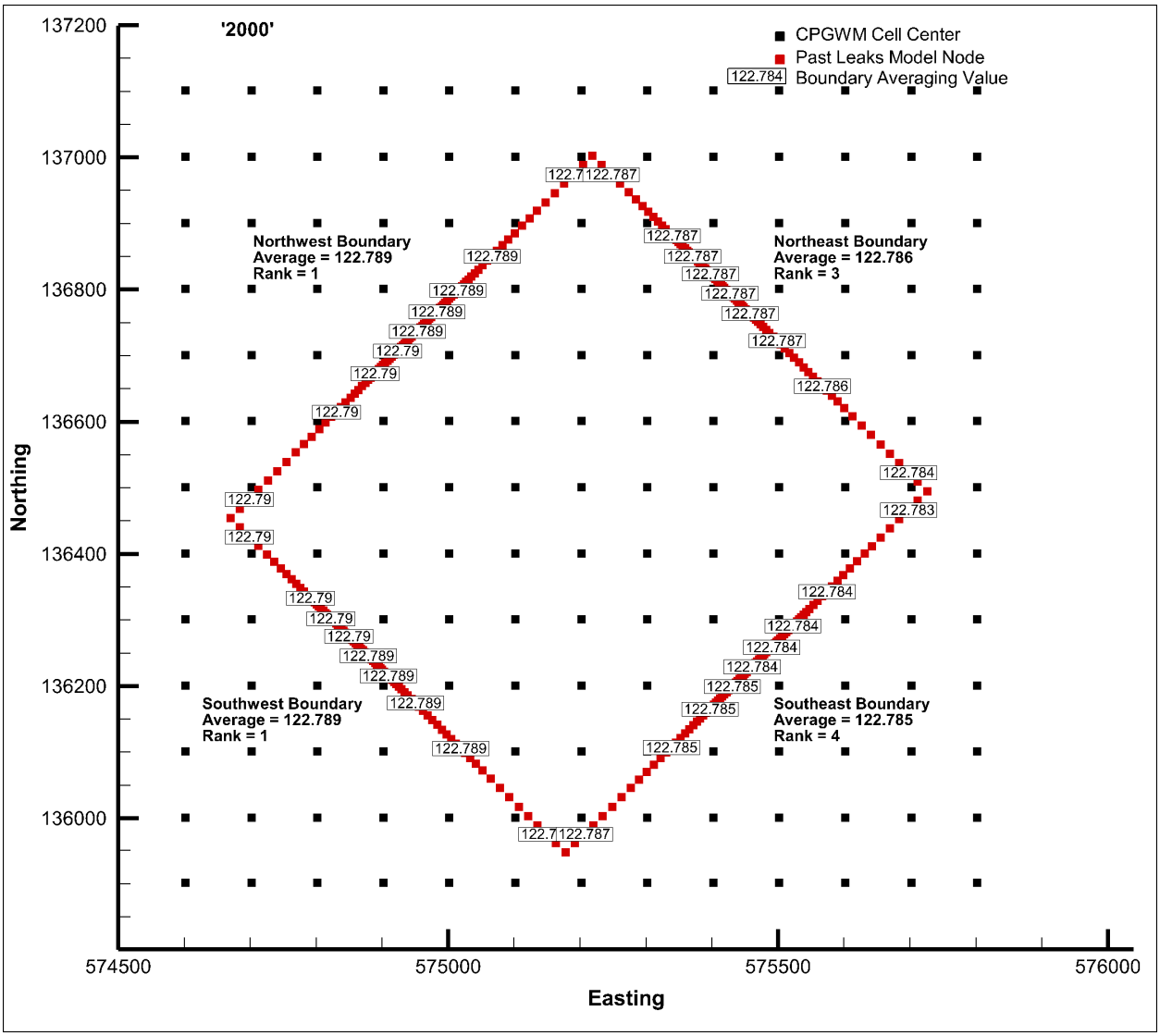

CPGWM = Central Plateau Groundwater Model

Table 5-1. Central Plateau Groundwater Model Hydraulic Head Interpolation Values and Waste Management Area C Unplanned Release Model Grid Boundary Rankings. (3 sheets)

Year	Interpolated Hydraulic Head (m)				Boundary Ranking			
	Southwest	Northwest	Southeast	Northeast	Southwest	Northwest	Southeast	Northeast
1969	125.018	125.026	125.017	125.029	3	2	4	1
1970	124.694	124.695	124.697	124.698	4	3	2	1
1971	124.609	124.615	124.608	124.616	3	2	4	1
1972	124.545	124.549	124.547	124.552	4	2	3	1
1973	124.326	124.326	124.332	124.331	4	3	1	2
1974	124.097	124.096	124.102	124.100	3	4	1	2
1975	123.945	123.946	123.949	123.948	4	3	1	2
1976	123.860	123.861	123.863	123.864	4	3	2	1
1977	123.827	123.830	123.827	123.831	4	2	3	1
1978	123.806	123.809	123.808	123.811	4	2	3	1
1979	123.820	123.822	123.823	123.825	4	3	2	1
1980	123.645	123.643	123.649	123.645	2	4	1	3
1981	123.649	123.650	123.653	123.654	4	3	2	1
1982	123.668	123.666	123.680	123.673	3	4	1	2
1983	123.779	123.783	123.785	123.788	4	3	2	1
1983.5	123.866	123.873	123.864	123.873	3	2	4	1
1984	124.002	124.010	123.998	124.010	3	2	4	1
1985	124.274	124.280	124.274	124.281	3	2	4	1
1986	124.367	124.370	124.368	124.372	4	2	3	1
1987	124.816	124.807	124.858	124.833	3	4	1	2
1988	124.983	124.971	125.029	125.000	3	4	1	2
1989	125.111	125.094	125.169	125.131	3	4	1	2
1990	124.701	124.687	124.738	124.706	3	4	1	2
1991	124.339	124.328	124.361	124.338	2	4	1	3

Table 5-1. Central Plateau Groundwater Model Hydraulic Head Interpolation Values and Waste Management Area C Unplanned Release Model Grid Boundary Rankings. (3 sheets)

Year	Interpolated Hydraulic Head (m)				Boundary Ranking			
	Southwest	Northwest	Southeast	Northeast	Southwest	Northwest	Southeast	Northeast
1992	124.062	124.051	124.082	124.059	2	4	1	3
1993	123.764	123.756	123.775	123.759	2	4	1	3
1994	123.566	123.559	123.574	123.561	2	4	1	3
1995	123.483	123.477	123.494	123.481	2	4	1	3
1996	123.416	123.412	123.424	123.415	2	4	1	3
1997	123.478	123.474	123.493	123.482	3	4	1	2
1998	123.234	123.231	123.239	123.232	2	4	1	3
1999	122.976	122.973	122.974	122.972	1	3	2	4
2000	122.789	122.789	122.785	122.786	2	1	4	3
2001	122.622	122.622	122.617	122.619	1	2	4	3
2002	122.472	122.472	122.466	122.468	2	1	4	3
2003	122.371	122.372	122.365	122.368	2	1	4	3
2004	122.304	122.304	122.298	122.301	2	1	4	3
2005	122.218	122.219	122.212	122.216	2	1	4	3
2006	122.145	122.147	122.138	122.144	2	1	4	3
2007	122.090	122.092	122.083	122.089	2	1	4	3
2008	122.048	122.050	122.040	122.046	2	1	4	3
2009	122.000	122.002	121.992	121.999	2	1	4	3
2010	121.948	121.950	121.940	121.947	2	1	4	3
2011	121.860	121.862	121.852	121.859	2	1	4	3
2012	121.790	121.793	121.781	121.789	2	1	4	3
2013	121.740	121.743	121.730	121.739	2	1	4	3
2015	121.625	121.628	121.614	121.624	2	1	4	3
2016.2	121.549	121.552	121.538	121.548	2	1	4	3

Table 5-1. Central Plateau Groundwater Model Hydraulic Head Interpolation Values and Waste Management Area C Unplanned Release Model Grid Boundary Rankings. (3 sheets)

Year	Interpolated Hydraulic Head (m)				Boundary Ranking			
	Southwest	Northwest	Southeast	Northeast	Southwest	Northwest	Southeast	Northeast
2017.4	121.477	121.481	121.467	121.477	2	1	4	3
2018.7	121.405	121.408	121.394	121.404	2	1	4	3
2020	121.330	121.334	121.320	121.330	2	1	4	3
2021.2	121.267	121.271	121.257	121.267	2	1	4	3
2022.4	121.201	121.205	121.191	121.201	2	1	4	3
2023.7	121.134	121.137	121.124	121.133	2	1	4	3
2025	121.066	121.070	121.056	121.066	2	1	4	3
2026.2	121.010	121.013	121.000	121.009	2	1	4	3
2027.4	120.952	120.955	120.942	120.951	2	1	4	3
2028.7	120.894	120.897	120.884	120.893	2	1	4	3
2030	120.836	120.839	120.826	120.835	2	1	4	3
2031.2	120.787	120.790	120.777	120.786	2	1	4	3
2032.4	120.737	120.740	120.727	120.737	2	1	4	3
2033.7	120.687	120.690	120.677	120.687	2	1	4	3
2035	120.637	120.640	120.627	120.637	2	1	4	3
2036.2	120.595	120.598	120.586	120.595	2	1	4	3
2037.4	120.552	120.555	120.543	120.552	2	1	4	3
2038.7	120.509	120.512	120.499	120.508	2	1	4	3
2040	120.465	120.469	120.456	120.465	2	1	4	3

Figure 5-4. Inferred Direction of Flow During the Operations Period When the High Volume Discharge Facilities Operated.

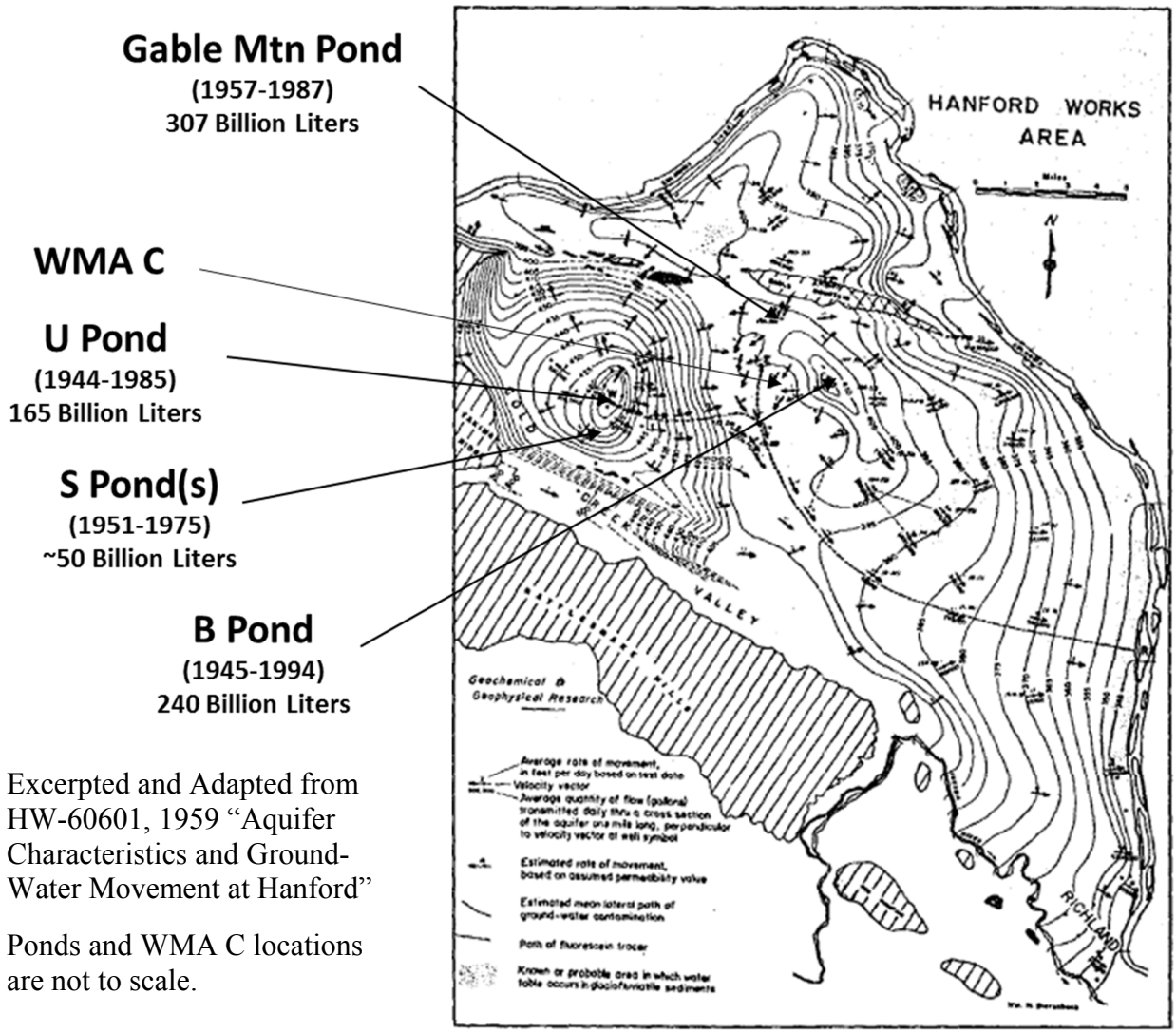

Excerpted and Adapted from HW-60601, 1959 "Aquifer Characteristics and Ground-Water Movement at Hanford"

Ponds and WMA C locations are not to scale.

WMA = Waste Management Area

Large seasonal changes in Columbia River stage and discharges to the TEDF, located 3 km (1.9 mi) east of the 200 East Area, also appear to affect water levels within the highly transmissive paleochannel beneath WMA C (SGW-54165). For example, the hydraulic gradient aligned toward the north-northwest between September 2005 and January 2007, but during August and September 2008 the hydraulic gradient temporarily reversed toward the south, presumably because of the high Columbia River stage during the summer of 2008 (SGW-54165). From October 2008 through June 2011, the hydraulic gradient remained indeterminate, although the flow appeared to reverse slowly back to a north. Beginning in the summer of 2011, the hydraulic gradient direction reversed again and remained toward the south through the end of September 2012 (SGW-54165). During the time between 2005 and 2012, the magnitude of the gradient remained less than 5×10^{-5} m/m. Since 2012, the gradient appears to have acquired a relatively stable south-southeastern direction with a magnitude of ~ 2×10^{-5} m/m.

During the times when the gradient reverses direction, both the magnitude and direction become indeterminate and how the direction reverses, either in a clockwise or counterclockwise manner, is unknown. To address uncertainty in the gradient reversal, the UPR evaluation includes conceptual models of both rotation directions. The boundary conditions adapted directly from the CPGWM (Table 5-1) indicate that the gradient rotates clockwise from the northwest to the southeast. The UPR evaluation implementing a counterclockwise from the northwest to the southeast modifies the boundary conditions by imposing an assumed rotation and magnitude to the gradient between 1999 and 2015 (Table 5-2). The average hydraulic head of the four interpolated boundaries (Table 5-1) is then projected to the four boundaries according to the assumed gradient, and the new boundary values are ranked (Table 5-3) from the highest water table elevation (1) to the lowest water table elevation (4). The ranking indicates direction of groundwater flow across WMA C for that particular year.

5.3 RESULTS OF SELECTED TRANSIENT WATER TABLE MODELS

The results of the modeling provide a basis to evaluate the assumptions and uncertainties associated with the flow direction and magnitude during the operations period. The results also provide a basis to evaluate the estimates regarding inventory and volumes of past leaks for the purpose of better constraining estimates of the existing contamination. These aspects of the modeling analysis help provide some insight into the events and hydraulic conditions responsible for producing the measured concentrations levels and observed changes in the individual wells (e.g., locations and timing of source releases, the timing of changes in flow direction, and the varying magnitude of the hydraulic gradient during the gradual changes in flow directions).

5.3.1 Results of the Assumed Clockwise Rotation of the Transient Hydraulic Gradient Model

The CPGWM boundary conditions (Table 5-1) and results of the clockwise gradient rotation simulation indicate that the gradient reverses direction rather abruptly between 1998 and 2002, as indicated by the ranking numbers. Figure 5-5 shows the model results of the plume development using the CPGWM boundary conditions and associated changes in groundwater flow conditions as it evolves in the aquifer from 1998 to 2005. According to the figures, the plume appears to be headed in a northwestern direction in 1998, and the direction rotates clockwise to the southeast by 2002. The model results involving this manner of gradient rotation do not match the observed concentrations of ^{99}Tc in the monitoring wells surrounding WMA C. Although the modeling results of the timing of the peak concentration at well 299-E27-7 coincide with the timing of the peak concentration observed in the monitoring data, the magnitude of the peak concentration values differ by an order of magnitude (Figure 5-6).

The monitoring data indicate that ^{99}Tc arrived southwest of the tank farm in wells 299-E27-4, 299-E27-13, and 299-E27-23 around 2000, first reaching a peak concentration in well 299-E27-4 by 2004, and then reaching peak concentrations in the other two wells around 2011 and 2012. The modeling results representing these wells exhibit little response to the ^{99}Tc releases (Figure 5-6). This lack of response is a likely consequence of the rapid change and almost complete reversal in the direction of the gradient between 1998 and 2000 included in the

CPGWM-based boundary conditions (Table 5-2). According to the CPGWM boundary conditions, the gradient switches direction by almost 180 degrees almost immediately, and does not become oriented toward the southwest. None of the results representing the three wells exceeds 150 pCi/L until after 2020 in the simulations. This is almost two orders of magnitude less than the peak concentrations measured in the three wells (Figure 5-6).

Table 5-2. Comparison of Central Plateau Groundwater Model Hydraulic Gradient Results (Magnitude and Direction) and Central Plateau Groundwater Model Results Modified to Rotate the Hydraulic Gradient Counterclockwise at Waste Management Area C.

Year	Interpolated Hydraulic Gradient (m)				
	Central Plateau Groundwater Model		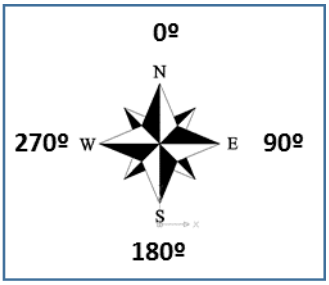	Modified Central Plateau Groundwater Model	
	Magnitude	Degrees Clockwise from North		Magnitude	Degrees Clockwise from North
1996	1.6E-05	319		1.6E-05	319
1997	2.6E-05	304		2.6E-05	304
1998	1.1E-05	328		1.1E-05	328
1999	5.2E-06	30		5.1E-06	33
2000	6.6E-06	100		3.5E-06	31
2001	7.8E-06	106		1.7E-06	29
2002	9.6E-06	103		0	27
2003	1.0E-05	113		0	327
2004	9.0E-06	110		1.7E-06	267
2005	9.8E-06	120		3.5E-06	262
2006	1.2E-05	129		5.2E-06	257
2007	1.2E-05	129		5.1E-06	252
2008	1.4E-05	124		5.1E-06	247
2009	1.4E-05	130		5.3E-06	242
2010	1.4E-05	130		5.1E-06	236
2011	1.4E-05	130		5.2E-06	230
2012	1.6E-05	131		5.3E-06	224
2013	1.8E-05	131		5.2E-06	184
2015	1.9E-05	131		5.1E-06	144

The modeling results representing the three wells south and southeast of the tank farm, 299-E27-21, 299-E27-24, and 299-E27-14, do not fit the monitoring data very well. The modeling results indicate that ^{99}Tc arrives in well 299-E27-14 in 2000, and that the concentration jumps to 9,000 pCi/L almost immediately (Figure 5-7). The concentration increases to a peak

value of 14,200 pCi/L in 2011, and remains relatively stable at that level thereafter. The monitoring data indicate that the concentration in the well measured around 100 pCi/L as early as 1991 when sampling and analysis for ^{99}Tc began at the well. From 1997 to 2003, the concentration increased from 100 pCi/L to 2,600 pCi/L. The concentration remained relatively stable at that level until 2012 when it began increasing and reached its peak value of 10,700 pCi/L in 2013. The concentration has steadily declined since then, measuring 2,620 pCi/L in 2016. While the peak concentration of the modeling results is comparable to the peak measured value, the trend exhibited by the modeling results does not agree with the trend observed in the monitoring data. The modeling results representing wells 299-E27-21 and 299-E27-24 also do not agree with the monitoring data. Concentrations in excess of 25,000 pCi/L and 5,000 pCi/L have been measured in those wells, but the modeling results for the wells are each more than an order of magnitude less than the measured values. Because sampling did not begin in the wells until 2003 and 2010, respectively, it is difficult to evaluate the timing of arrival. Overall, the comparison of the simulated concentrations at the locations in the model representing the monitoring wells and the data collected from the monitoring wells do not corroborate the clockwise conceptualization of the gradient movement.

Table 5-3. Central Plateau Groundwater Model Hydraulic Head Interpolation Values Modified to Rotate the Hydraulic Gradient Counterclockwise at Waste Management Area C, and Revised Model Grid Boundary Rankings.

Year	Interpolated Hydraulic Head (m)				Boundary Ranking			
	Southwest	Northwest	Southeast	Northeast	Southwest	Northwest	Southeast	Northeast
1999	122.976	122.973	122.974	122.972	1	3	2	4
2000	122.789	122.787	122.788	122.786	1	3	2	4
2001	122.62	122.62	122.62	122.619	1	3	2	4
2002	122.469	122.469	122.469	122.469	1	1	1	1
2003	122.369	122.369	122.369	122.369	1	1	1	1
2004	122.301	122.301	122.302	122.302	4	3	2	1
2005	122.215	122.216	122.217	122.217	4	3	2	1
2006	122.142	122.143	122.145	122.145	4	3	2	1
2007	122.087	122.088	122.09	122.091	4	3	2	1
2008	122.044	122.045	122.047	122.048	4	3	2	1
2009	121.996	121.998	121.999	122	4	3	2	1
2010	121.944	121.946	121.946	121.948	4	3	2	1
2011	121.856	121.858	121.858	121.86	4	3	2	1
2012	121.786	121.788	121.788	121.79	4	2	3	1
2013	121.736	121.739	121.737	121.739	4	2	3	1
2015	121.622	121.625	121.621	121.623	3	1	4	2

5.3.2 Results of the Assumed Counter-Clockwise Rotation of the Transient Hydraulic Gradient Model

The results of the simulation with the revised boundary conditions indicating gradient changing in a counterclockwise motion corroborate much better with the data collected from the monitoring wells than did the results of the initial simulation. Figure 5-8 shows the model results of the plume as it evolves in the aquifer from 1998 to 2016. The simulated concentrations at the locations in the model representing the monitoring wells appear to coincide reasonably well in both timing and magnitude with data collected from the monitoring wells (Figures 5-9 and 5-10).

The modeling results of the timing of the peak concentration at well 299-E27-7 coincide with the timing of the peak concentration observed in the monitoring data, and the magnitude of the peak concentration values differ by less than an a factor of 2 (Figure 5-8). The modeling results representing well 299-E27-15 are more problematic and less consistent with the measured data. The modeled concentration exhibits three distinct peaks in response to the ^{99}Tc releases, and the modeled peak value exceeds the maximum measured value by approximately an order of magnitude. This well is located upgradient of WMA C relative to the long-term groundwater hydraulic gradient. The imposed rotation appears to include more of an upgradient component than the data indicate existed during the late 1990s and middle 2000s, but this discrepancy appears to be relatively minor compared to the overall performance of the model in representing the data collected from the other monitoring wells.

The modeling results approximate reasonably well the timing of arrival and magnitude of concentration of the ^{99}Tc in groundwater southwest of the tank farm (Figure 5-8). The modeling results indicate a peak concentration occurring in 2006 at well 299-E27-4, where the data reach their peak in 2004. The magnitude of the modeled and measured peak values are nearly identical. The model results indicate the peak concentration occurred in well 299-E27-13 about five years before the data reach their peak in that well, but the magnitude of the modeled and measured peak values differs by less than 50%. The magnitude of the modeled and measured peak values of well 299-E27-23 are very comparable, 31,000 pCi/L and 26,000 pCi/L, respectively, with the modeled peak arriving in the well about one year before the data indicate the peak arrived. Similarly, the magnitude of the modeled and measured peak values of well 299-E27-21 are comparable, 19,600 pCi/L and 26,700 pCi/L, respectively, although the concentration present in well 299-E27-21 may not yet have reached a peak. The model indicates that the peak occurred in 2014, but the data continue to increase in concentration from that time to present day.

The modeling results representing the arrival of the peak concentration of ^{99}Tc in wells-299-E27-24 and 299-E27-14 appear to lag the actual peak arrival by a few years (Figure 5-9). The modeling results indicate that ^{99}Tc concentration peaked in well 299-E27-24 in late 2015 whereas the monitoring data peaked in 2013. The modeling results indicate that ^{99}Tc concentration will not peak in well 299-E27-14 until late 2016, but the monitoring data peaked in 2013. The magnitude of the modeled concentration levels and measured peak concentration values observed at these wells differs but are within the same order of magnitude. This difference is less than 50% for well 299-E27-14, and the modeled peak value for well 299-E27-24 is within a factor of 3 of the measured peak in that well.

Figure 5-5. Simulated Technetium-99 Plume in Groundwater Calendar Years 1998, 2000, 2002, 2005, 2010 and 2016 and Resulting from Waste Management Area C Unplanned Releases (Clockwise Rotation of the Hydraulic Gradient Based on Central Plateau Groundwater Model Boundary Conditions).

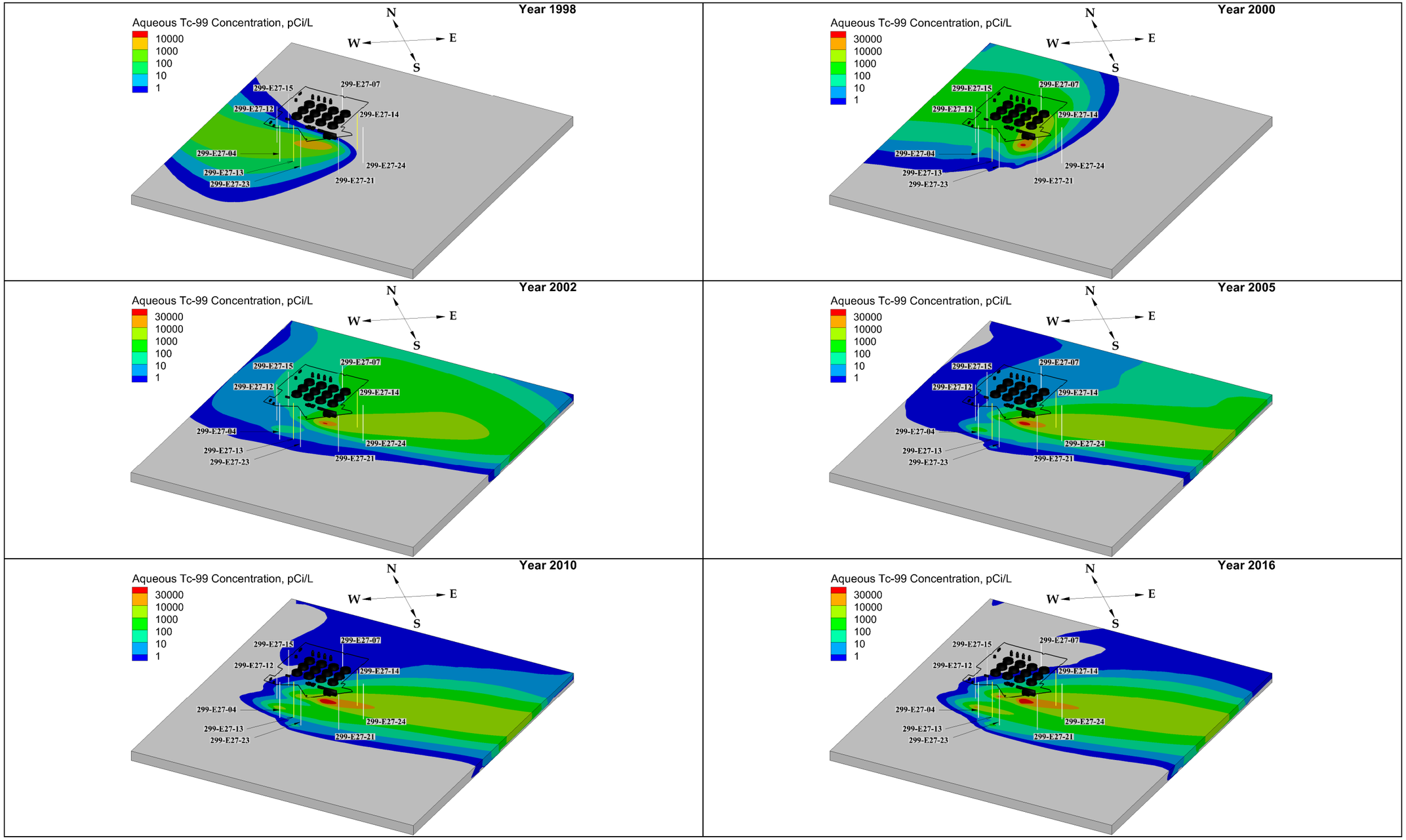

Figure 5-6. Comparison of Simulated Technetium-99 Concentrations in Groundwater to Measured Concentrations around the Northeast, Northwest, and Southwest of Waste Management Area C. Using Initial Conceptual Model with Clockwise Rotation of the Hydraulic Gradient.

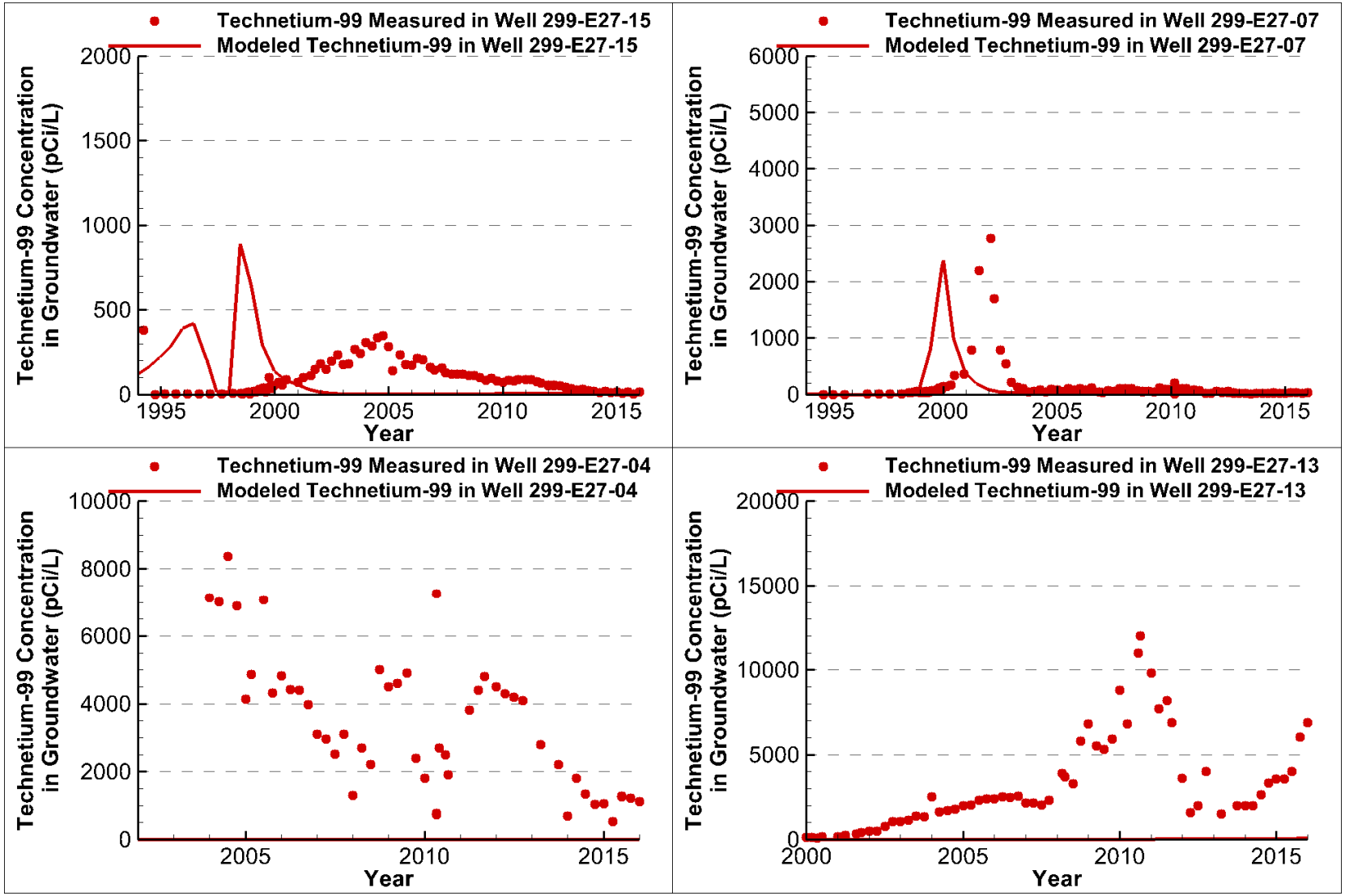

Figure 5-7. Comparison of Simulated Technetium-99 Concentrations in Groundwater to Measured Concentrations around the Southwest and Southeast of Waste Management Area C. Using Initial Conceptual Model with Clockwise Rotation of the Hydraulic Gradient.

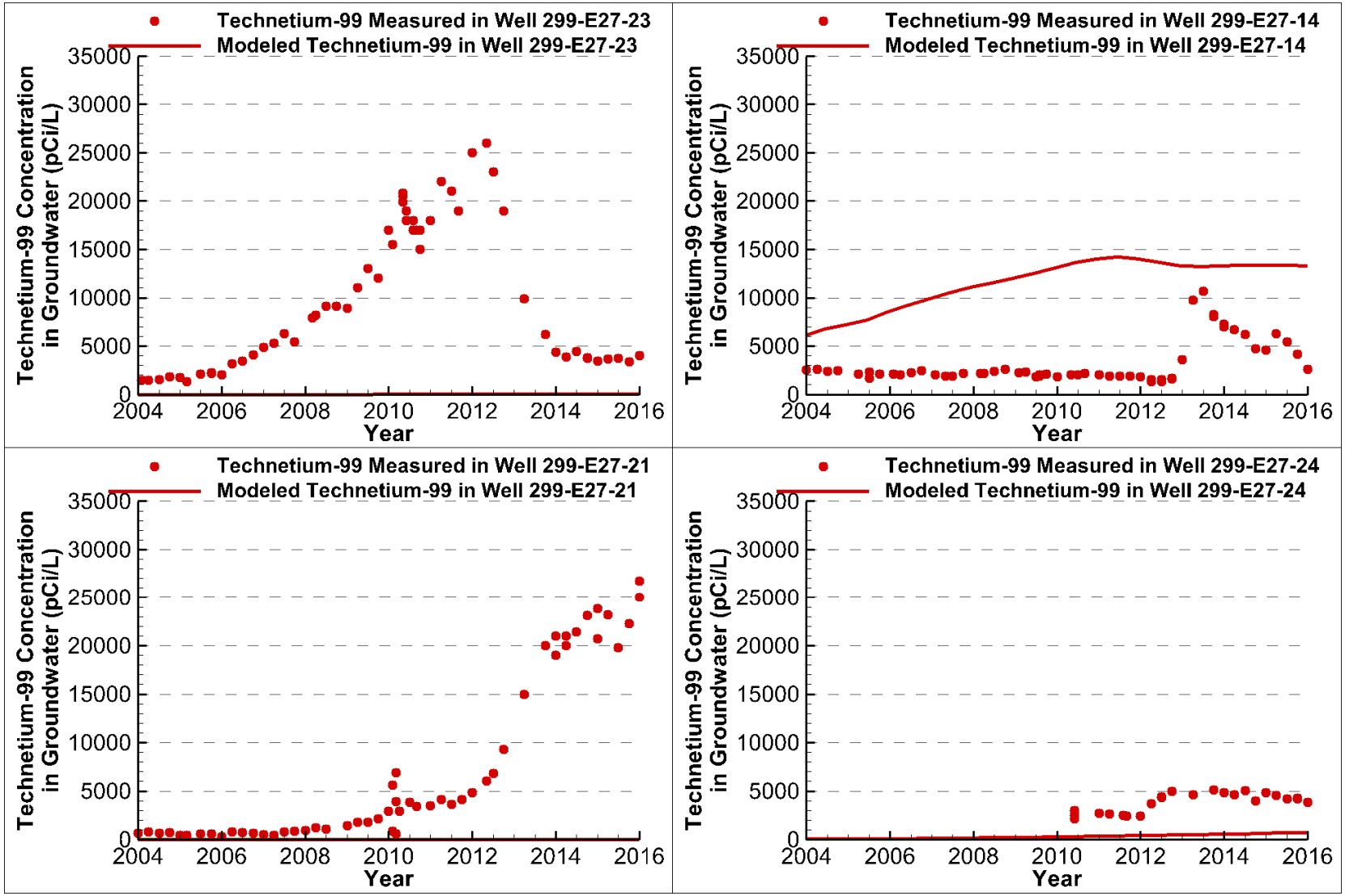

Figure 5-8. Simulated Technetium-99 Plume in Groundwater Calendar Years 1998, 2002, 2004, 2008, 2012 and 2016 and Resulting from Waste Management Area C Unplanned Releases (Counterclockwise Rotation of the Hydraulic Gradient).

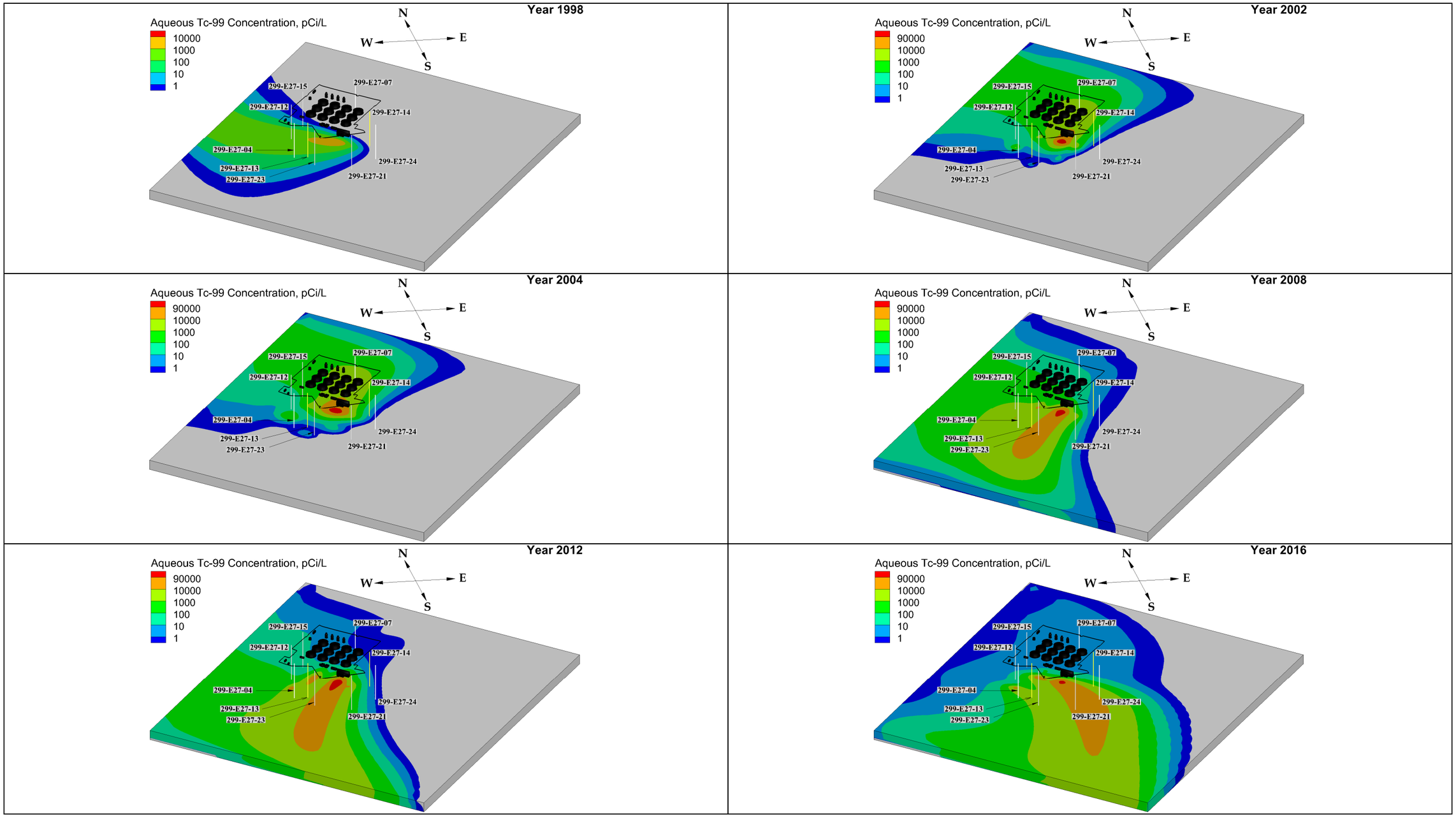

Figure 5-9. Comparison of Simulated Technetium-99 Concentrations in Groundwater to Measured Concentrations around the Northeast, Northwest, and Southwest of Waste Management Area C. Conceptual Model with Counterclockwise Rotation of the Hydraulic Gradient.

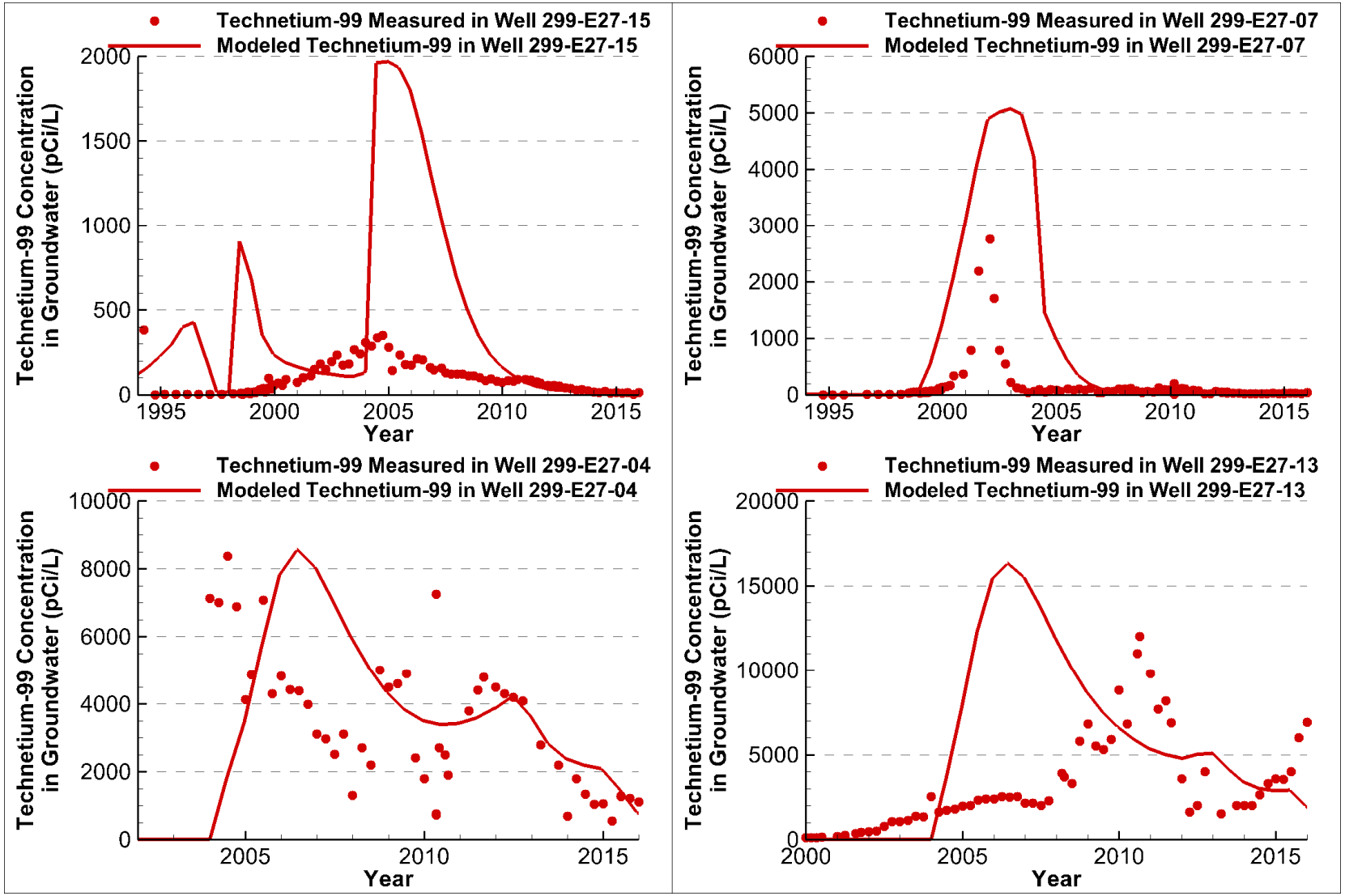

Figure 5-10. Comparison of Simulated Technetium-99 Concentrations in Groundwater to Measured Concentrations around the Southwest and Southeast of Waste Management Area C. Using Conceptual Model with Counterclockwise Rotation of the Hydraulic Gradient.

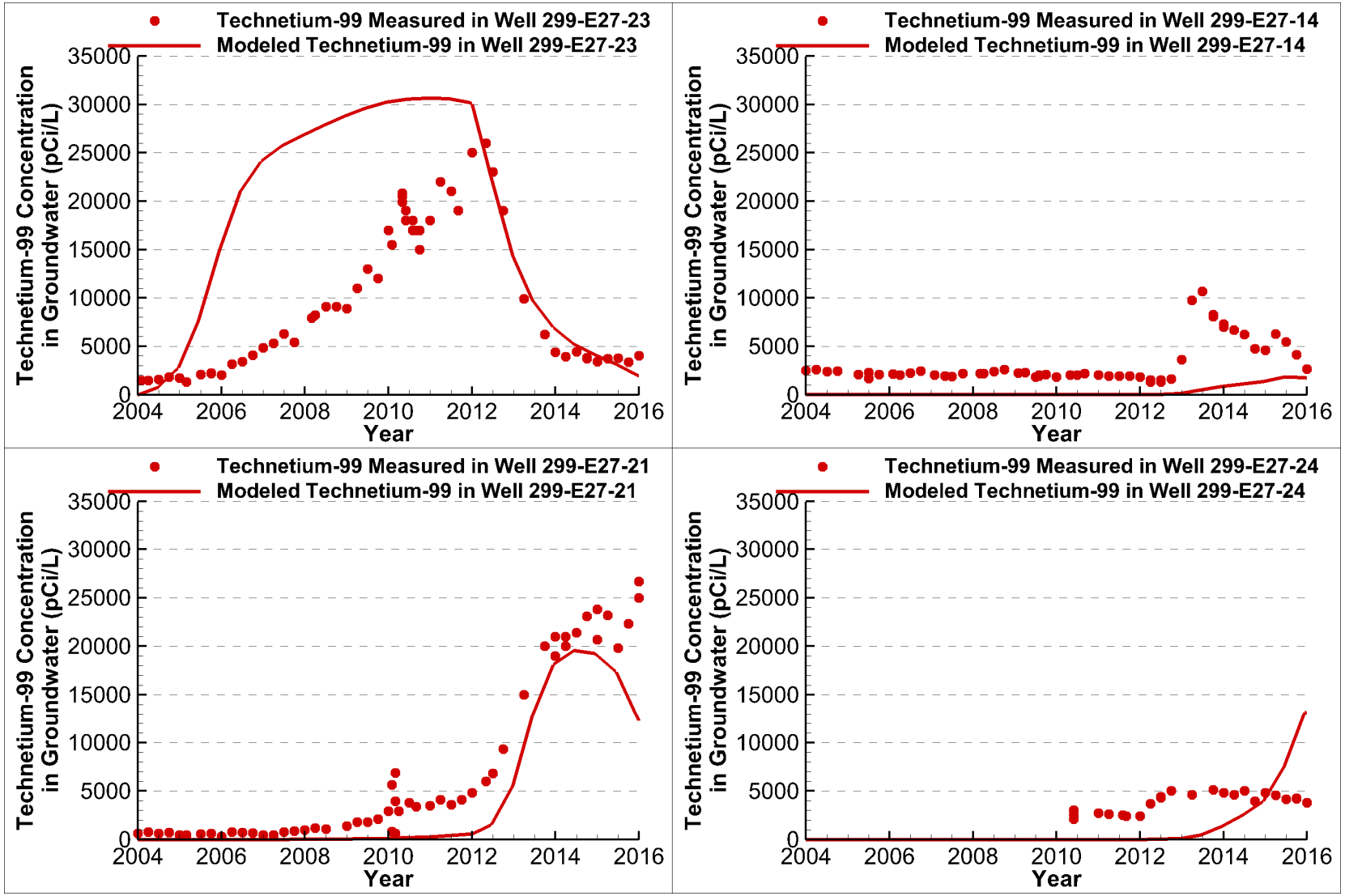

5.3.3 Summary

The conceptual model involving the counterclockwise rotation of the hydraulic gradient from northwest to southeast, and the associated numerical model results, appear capable of approximating observed field data for the time of arrival of ^{99}Tc to groundwater and concentration levels of ^{99}Tc in groundwater. The model results include several assumptions regarding the timing and inventory of the past releases, and direction and magnitude of the hydraulic gradient during the time it could not be measured. Because of these assumptions, it is unknown how accurately the model calculations represent the actual release of ^{99}Tc and its transport in the vadose zone and groundwater. The results do, however, provide some insight into the concentration levels observed in monitoring wells, and the changes in concentration that have occurred in those wells since 2000. The concentration of ^{99}Tc observed in most of the monitoring wells appears to change too abruptly to represent the one-dimensional passing of a contaminant front. The modeling results indicate that the concentration in the wells changes so abruptly because the direction and the magnitude of the groundwater hydraulic gradient changes. The rotation of the gradient continually changes the orientation of the groundwater plumes relative to the wells. The high concentrations measured in wells 299-E27-23 and 299-E27-13 between 2010 and 2012 likely correspond to the time when those wells were located downgradient of the sources. By 2014, the concentration in those two wells dropped markedly, while the concentration in well 299-E27-21 began increasing quickly around that same time. According to the modeling results, this pattern in the data can be explained by, and corresponds to, the further rotation of gradient from the south to the southeast.

The release from tank C-105 appears to be the dominant source of ^{99}Tc observed in groundwater in the monitoring wells. According to the inventory estimates in RPP-RPT-42294, it is the only release large enough and that occurred early enough to bring about the concentration levels observed in the monitoring wells. Whether or not the release from tank C-105 is truly the dominant source of ^{99}Tc observed at the monitoring wells is unknown. However, the modeling results do indicate that most of the ^{99}Tc observed in the monitoring wells located southwest of the farm originated from the sources inside the farm, and not from the UPRs that occurred away from the tanks. These three UPRs occurred later than the release from tank C-105, and the modeling results exhibit the implications of this. The concentration of ^{99}Tc in the wells located nearest the UPRs is dominated by the ^{99}Tc contained in the release from tank C-105. The concentration of ^{99}Tc attributed to the ^{99}Tc contained in three UPRs peaks a few years after the concentration of ^{99}Tc peaks because of the tank C-105 release. This is later than the data indicate that the peaks occurred in the wells.

5.3.4 Conclusion

The modeling results indicate that as the water table returns to more natural conditions, the rotation of the gradient will continue to alter the primary movement of the plumes from primarily a southerly direction to a more southeasterly direction in the near future. The very high concentration levels of ^{99}Tc observed in wells 299-E27-23 and 299-E27-21, southwest and south of WMA C, respectively, are likely to be observed in wells 299-E27-24 and 299-E27-14, which are located to the southeast of WMA C.

The combination of the field data and the model results provide a reasonable basis for developing model assumptions and determining bounded estimates of input parameters. The model provides a basis to evaluate the uncertainties in the inventory and volumes of past leaks for the purpose of better constraining estimates of the existing contamination. The transient evaluation also provides an element of confidence that the model parameters and equations can adequately represent the physical conditions and past events of WMA C. This assurance improves the confidence in the model's ability to evaluate and estimate future impacts from the past leaks.

6.0 FUTURE IMPACTS OF PAST WASTE LEAKS AND RELEASES

In this section, results for a set of forward calculations to evaluate the future consequences of the past waste leaks and releases are presented to evaluate how the groundwater concentrations may change in the future based on the constraints on the scoping modeling analysis cases established in Section 4.0 and 5.0.

Included in this section are:

- Results of a screening analysis used to identify key constituents to evaluate in this analysis
- Results of transport analysis of past waste releases both before and after the time of assumed site closure in year 2020.

6.1 APPROACH TO THE FORWARD PROJECTION

The scoping analyses presented in Section 4 of this report provide comparisons of the STOMP© model to groundwater monitoring data to evaluate the credibility of alternative assumptions for the migration of the leaks from the time of their occurrence to today. As discussed in Section 4.8, several analysis cases were inconsistent with data and additional analysis cases produced comparable results to each other. Of the steady-state aquifer cases that were consistent with the arrival time at the aquifer, none were obviously superior to others in terms of explaining the observed groundwater monitoring well data.

The analysis that showed the best representation of most groundwater monitoring well data was the transient water table analysis presented in Section 5. However, the conditions evaluated in that case are not relevant for projections into the future, as the current water table orientation is expected to be similar to the projected future water table, with only the height and gradient changing as it relaxes to its long-term state.

Scoping Analysis Case 1a (Table 4-1) was selected to project concentrations into the future. This selection has several advantages. Case 1a has the fewest alterations from the residual waste PA (RPP-ENV-58782) and RCA (RPP-ENV-58806) model, differing only in the height of the aquifer, allowing the effects of residual wastes and leaks to be considered on a common basis. It approximates the arrival times at the aquifer and aquifer concentrations as that observed in the 299-E27-14 monitoring well evaluated in the scoping analysis. It therefore has been judged to be the most appropriate analysis case to use for projecting future consequences of the leaks. While Case 1a provides useful insights on projected contaminant concentrations, the results should be interpreted with understanding of uncertainties inherent in evaluating transport processes in the natural system. The effect on arrival times and magnitude of contaminant concentrations resulting from some of these uncertain parameters was evaluated in Section 4 (see Table 4-1). The linear relationship of potential increases or decreases in estimated groundwater flux to corresponding decreases or increases on predicted concentrations levels is of particular importance.

To implement the forward projection, a distinction must be made between the behavior of sorbing and nonsorbing contaminants. The analysis cases presented in Section 4 were established to evaluate nonsorbing contaminants, with ^{99}Tc being the indicator contaminant of concern used in the cases. Nonsorbing contaminants such as ^{99}Tc arrive at the water table during the time period between the occurrence of the leaks and today, as indicated by both monitoring data and model results. During that time, the water table was elevated, as discussed extensively in previous sections, and as a result the scoping analysis cases were implemented with an elevated water table. By contrast, sorbing contaminants are expected to arrive at the water table in the future, in some cases the distant future, when the water table will have recovered its long-term steady level. Appropriate modeling of the arrival at the water table for sorbing contaminants should therefore use the expected future water table level. This is the assumption used in the PA/RCA model documented in RPP-ENV-58782 and RPP-ENV-58806.

Therefore, the forward modeling of leaks has been undertaken using slightly different models for the sorbing and nonsorbing contaminants. For sorbing contaminants the PA/RCA model was used, while for nonsorbing contaminants Case 1a was used. The two models are compared in Figure 6-1. In both cases the leaks were introduced into the model in the same manner as described in Section 4. The inventories of the contaminants considered in the analysis are shown in Table 6-1.

6.2 IDENTIFICATION OF CONTAMINANTS OF POTENTIAL CONCERN

The STOMP© 3-D groundwater flow and transport model was used to identify those COPCs that are not sufficiently mobile to impact groundwater until more than 10,000 years. This step helps to streamline the past release analysis, and to focus attention on the contaminants that may impact the environment within a plausible time frame of evaluation.

The criterion chosen for screening is the first-arrival time of the contaminant. Hydraulic property selection was carried out to yield maximum transport rates. Maximum net infiltration rates were also assumed in this analysis. An incremental range of K_d values was evaluated between 0.25 mL/g and 2.5 mL/g (prior to gravel correction) to determine threshold values that reached the water table in 1,000 and 10,000 years. The use of such approaches is accepted by the EPA, and appropriate methods are outlined in EPA guidance (EPA/540/F-95/041, Soil Screening Guidance: Fact Sheet). This approach minimizes the number of contaminants eliminated from analysis. As a result, some contaminants may only arrive at the water table for particular sensitivity and uncertainty evaluations (i.e., evaluations that minimize the time of transport through the vadose zone). For the conditions of analysis used in many of the scoping analysis cases, a number of the radionuclide contaminants may have no impact on the past leaks analyses results because their transport to the water table requires more than 10,000 years.

Results of the screening analysis are presented in Figure 6-. The results show that the time of first arrival is a strong linear function of the K_d value. From this relationship, the first-arrival time for any radionuclide can be estimated accurately by using the trend equation shown on the figure. According to the screening model results, the minimum K_d values that produce an impact to groundwater within 1,000 years and 10,000 years are less than 0.5 mL/g (without any gravel correction), and less than 2 mL/g (without any gravel correction), respectively.

Figure 6-1. Case 1a Past Leak Model Used for Nonsorbing Contaminants for the Forward Projection Compared to the Performance Assessment/RCRA Closure Analysis Model Used for the Sorbing Contaminants.

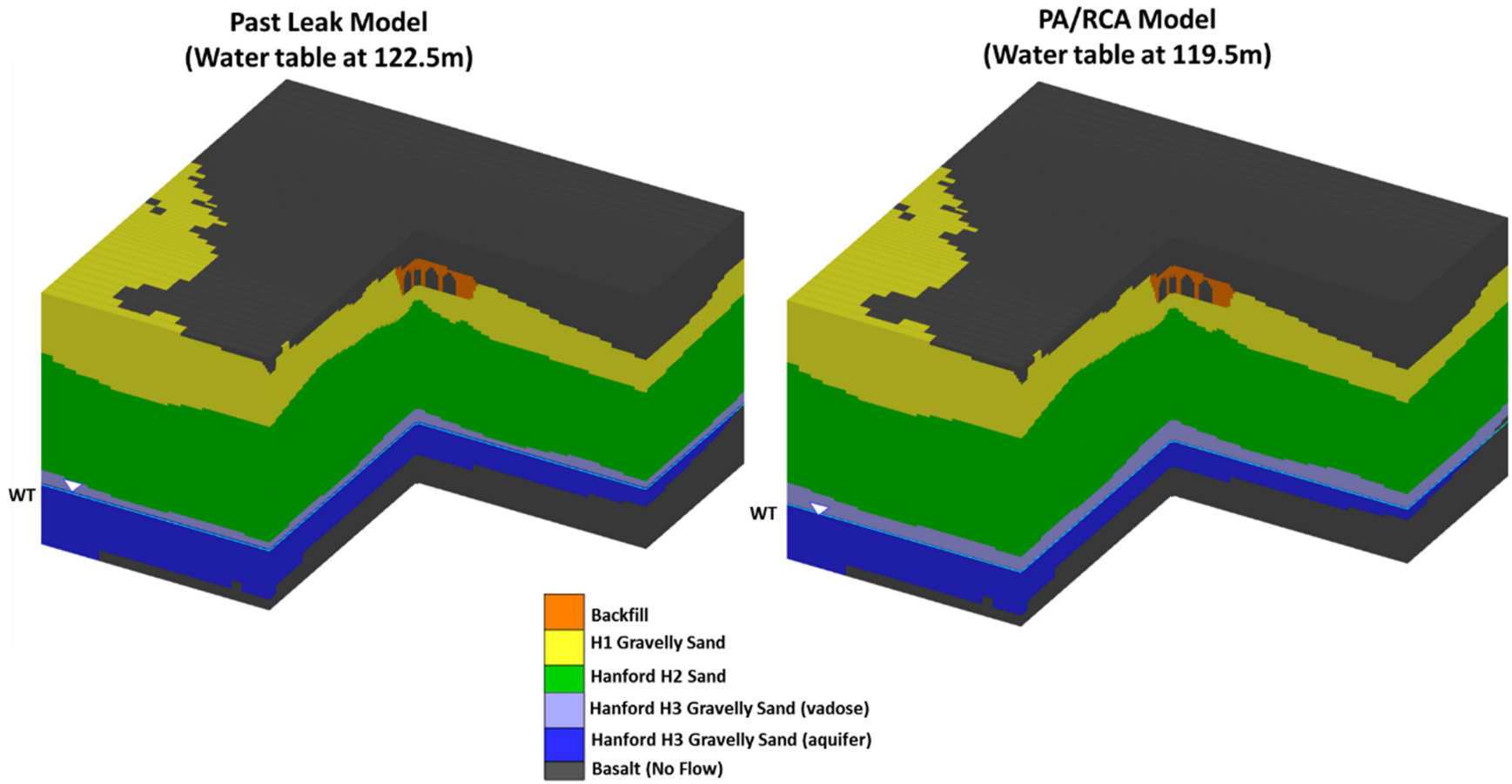

PA = performance assessment
RCA = RCRA Closure Analysis
RCRA = Resource Conservation and Recovery Act of 1976

References:
RPP-ENV-58782, "Performance Assessment of Waste Management Area C, Hanford Site, Washington."
RPP-ENV-58806, "RCRA Closure Analysis of Tank Waste Residuals Impacts at Waste Management Area C, Hanford Site, Washington."

The first-arrival times for each of the representative K_d values used in the COPC calculations are summarized in Table 6-2. The results of the COPC analysis indicate that even when using parameter estimates biased to produce the greatest pore water velocity in the vadose zone: (1) contaminants with a $K_d > 0.50$ mL/g do not reach groundwater within 1,000 years, and (2) radionuclides with a $K_d \geq 2.0$ mL/g do not reach groundwater within 10,000 years (Table 6-2). While the actual 10,000-year K_d cutoff is likely only slightly greater than 2.0 mL/g, the COPC evaluation did not include a representative contaminant with a K_d value between 2 mL/g and 2.5 mL/g (Table 6-2).

Of the list of radionuclides and non-radiological contaminants considered (Table 6-1), some are modeled as nonsorbing contaminants ($K_d = 0$ mL/g). These are ^{99}Tc, ^{3}H, ^{60}Co, SO_4, NO_3, and Cr. The remaining contaminants (^{79}Se, ^{129}I, ^{126}Sn, ^{238}U, and total uranium) are modeled with small retardation (K_d values between 0.1 and 0.6 mL/g). Other radionuclides and non-radiological contaminants that are part of the WMA C past release inventory are not included in further groundwater impact analysis due to either larger retardation or small inventories.

6.3 FUTURE PROJECTIONS OF PAST WASTE LEAKS AND RELEASES

This analysis of future impacts of past release includes calculations of the highest calculated concentration, with an allowance for some volume averaging based on projected groundwater use, at the WMA C fenceline. To determine the highest groundwater concentration, the modeling results indicate the average concentration in the aquifer within nine segments along a hypothetical line parallel to the southeast edge of WMA C (Figure 6-3). Most of the nine segments are ~30 m (98 ft) long (Table 6-3), and aligned such that the centerlines of the plumes in the groundwater resulting from the past releases from a single line of 100-series tanks parallel to the direction of groundwater flow (e.g., the centerline of the plumes resulting from the past releases from tanks C-105 and C-108) intersect the fenceline within the same PoCal segment. Two of the three segments substantially different than 30 m (98 ft) long align with the more irregularly spaced centerlines of the plumes resulting from the UPRs that are not associated with a particular tank. The third segment, PoCal 5, represents a gap between adjacent centerlines.

EPA/540/R-95/128, Soil Screening Guidance: Technical Background Document and WAC 173-340-747, "Deriving Soil Concentrations for Groundwater Protection," imply that the aquifer mixing width ought to equal the width of contamination entering the aquifer. Other PAs conducted at Hanford and other DOE facilities have used an aquifer mixing width equal to the width of the facility (e.g., WCH-520, "Performance Assessment for the Environmental Restoration Disposal Facility, Hanford Site, Washington"; WSRC-MS-2003-00582, "Performance Assessment/Composite Analysis Modeling to Support a Holistic Strategy for the Closure of F Area, a Large Nuclear Complex at the Savannah River Site"). As indicated previously, the width of the PoCal segments is sufficient to intercept the centerline of the plumes resulting from the tank residuals from a single line of 100-series tanks, which appears consistent with the intent of EPA/540/R-95/128 and WAC 173-340-747. The aquifer mixing zone extends into the upper 5 m (16.4 ft) of the aquifer on the basis of the 4.5 m (15 ft) well screen length (and

mixing zone dimension) associated with state monitoring well descriptions (e.g., see Equation 747-4 in WAC 173-340-747).

6.3.1 Results of Groundwater Pathway Evaluation: Time before Assumed Closure of Waste Management Area C in 2020

The results of modeling Case 1a indicate that only contaminants with K_d values less than or equal to 0.1 mL/g arrive in groundwater at the fenceline PoCals within 1,000 years (Table 6-4). Among radionuclides, the only ones producing concentrations computed by the STOMP© software that exceed zero in groundwater at the WMA C fenceline before closure are ^{99}Tc, tritium, ^{60}Co, and ^{79}Se. The concentrations in groundwater of ^{99}Tc, tritium, and ^{60}Co reach a peak during this period. The maximum concentration of ^{99}Tc in groundwater at the fenceline during this period is 9,400 pCi/L in 2018, which is over a factor of 10 greater than its DWS of 900 pCi/L (Figure 6-4). The maximum concentration attenuates by almost one-third to 6,700 pCi/L after traveling 100 m through the aquifer (Figure 6-5). The predicted maximum concentration of tritium in groundwater at the fenceline during this period is about 22,000 pCi/L in 2012, which is slightly over its DWS of 20,000 pCi/L (Figure 6-6). The tritium concentrations predicted at the 100-m downgradient location (Figure 6-7) undergo comparable attenuation as ^{99}Tc does between the fenceline and the 100-m downgradient location. The predicted peak concentration of ^{60}Co at the 100 m boundary is about 860 pCi/L that occurs in 2009 (Figure 6-8) and exceeds the DWS of 100 pCi/L by a factor of 8. Selenium-79 arrives at the fenceline and 100 m downgradient of it shortly before closure; however, the maximum concentration at any of the PoCals is less than 0.001 pCi/L (Figure 6-9). The peak concentrations for ^{79}Se occur much later (Table 6-4).

The predicted high concentrations of tritium are inconsistent with the observed concentrations in groundwater wells around WMA C, which have remained significantly below the predicted values throughout the monitoring record. Recent concentrations of tritium in wells in the vicinity of WMA C are generally found to be between 1,000 and 2,000 pCi/L. The current results are conservative in that they do not account for the fact that tritium partitions into the vapor phase and a significant mass depletion can occur in the vadose zone from vapor phase transport towards the surface. This mass depletion is conservatively ignored in the transport model, where all of the mass is assumed to remain within the aqueous phase and transported for evaluating the groundwater impacts.

The predicted high concentrations of ^{60}Co are also inconsistent with the observed concentrations in groundwater wells around WMA C. Concentrations of ^{60}Co have remained significantly below the predicted values throughout the monitoring record. Recent concentrations of ^{60}Co in wells in the vicinity of WMA C have been below detection limits for a number of years.

For ^{60}Co, the choice of applying K_d of 0 mL/g throughout the vadose zone and saturated zone leads to an overestimation of ^{60}Co concentrations in the groundwater. Sorption characteristics of ^{60}Co can vary widely and are discussed in Appendix A of PNNL-16663, "Geochemical Processes Data Package for the Vadose Zone in the Single-Shell Tank Waste Management Areas at the Hanford Site." Based on review of literature in PNNL-16663 and available data for adsorption of cobalt on Hanford sediments, the following conclusions can be drawn: (a) Co(II)

is the stable valence state in water under oxidizing and moderately reducing conditions, (b) Co(II) is highly immobile (K_d > 1,000 mL/g) for typical Hanford groundwater and vadose zone conditions in the absence of organic chelating agents such as EDTA (ethylenediaminetetraacetic acid), and (c) moderate-to-high concentrations of CN^- and EDTA reduce Co(II) adsorption on sediments. Although Co-EDTA anionic complex can form initially, over time it undergoes dissociation via a complex series of reactions with iron and aluminum oxides in the sediments. These dissolution-exchange reactions generate a suite of adsorbates that compete for EDTA and oxidize Co(II) to a stable and weakly reactive complex. The adsorption behavior of cobalt therefore varies greatly and is a function of pH, oxidation state, sediment interactions, and environmental availability of organic complexants.

Based on this information, it is conceptualized that near the source locations of past leaks and UPRs, the mobility of Co(II) could be high due to possible availability of chelating agents and organic complexants in the waste stream. But with increasing transport distance away from the source location and with increasing dissolution-exchange reactions with the sediments in the vadose zone, the sorption behavior will change towards a gradually increasing K_d value. PNNL-17154, "Geochemical Characterization Data Package for the Vadose Zone in the Single-Shell Tank Waste Management Areas at the Hanford Site" recommends a best-estimate K_d value of 0 mL/g for ^{60}Co (II, III) for high and intermediate impact zones influenced by waste streams and a best-estimate K_d value of 10 mL/g for minimally impacted zones. Since the exact depths of these impact zones are not available within WMA C, it is not possible to precisely apply the variable K_d values. Instead, a uniform small K_d value is considered for ^{60}Co in the transport model to evaluate the impact of imposing minor retardation along the transport pathway.

To evaluate the sensitivity to minor amounts of retardation, an additonal simulation was made with selected K_d of 0.1 mL/g. The results of this simulation on peak flux of ^{60}Co at the water table indicate that by just considering a small change in sorption behavior, the flux of ^{60}Co is reduced dramatically. With its short half-life (5.27 years) and small amount of assumed adsorption which delays the arrival of ^{60}Co at the water table, the ^{60}Co inventory associated with the simulated leaks decays away during its transport through the vadose zone and no impacts are seen at the water table during the period of analysis. The transport modeling results based on the use of a small K_d value (e.g., 0.1 mL/g) are consistent with the observations of non-detects in the recent monitoring record of groundwater wells surrounding WMA C.

The only non-radiological contaminants arriving in groundwater at the WMA C fenceline before closure are nitrate, sulfate, and hexavalent chromium. The concentrations in groundwater of nitrate, sulfate, and hexavalent chromium (if all chromium is assumed to be hexavalent) reach a peak during this period. None of these exceed a regulatory standard unless all of the chromium is assumed to be hexavalent. The maximum concentration of nitrate in groundwater at any of the PoCals during this period is 9 mg/L in 2017 at PoCal 6 (Figure 6-10). The concentration of nitrate reaches a peak during this period at PoCal 6, but is still increasing at PoCal 3 in 2020. The sulfate reaches a peak concentration of 0.6 mL/g in 2018 at PoCal 6 (Figure 6-11). The maximum concentration of hexavalent chromium is 0.06 mg/L at PoCal 6 in 2019, if all chromium is assumed to be hexavalent (Figure 6-12). Any of the hexavalent chromium that reduces to trivalent chromium fails to reach the water table within 10,000 years because the K_d of trivalent chromium exceeds the K_d screening criterion.

Table 6-1. Leak Inventories of Contaminants of Concern Used in the Forward Projection Analyses.

Leak Site	Tank 241-C-101	Tank 241-C-104	Tank 241-C-105 (high estimate)	Tank 241-C-108	Tank 241-C-110	Tank 241-C-112	UPR-81	UPR-82	UPR-86	Surface Contamination	French Drain 216-C-8
Estimated Leak Time	**Late 1965 through 1969**	**~1965**	**Multiple releases between 1963 and 1967; another possible in first quarter of 1968**	**~1965**	**Sometime between 1971 and 1972**	**Sometime between 1946 and 1974**	**October, 1969**	**December, 1969**	**December, 1969 (discovered)**	**Unknown (Assumed to be 1965)**	**January 1960 through March 1965**
Modeled Leak Beginning Time	**1965**	**1965**	**1963**	**1965**	**1971**	**1965**	**1969**	**1969**	**1971**	**1965**	**1960**
Leak Volume (gal)*	37,000	28,000	20,500	18,000	2,000	7,000	36,000	2,600	17,000	1,000	32,000
Tc-99 (Ci)	2.49E-01	3.01E-02	9.84E+00	1.94E-02	3.36E+00	7.53E-03	1.10E-01	1.25E+00	2.68E+00	1.08E-03	0
I-129 (Ci)	3.84E-02	2.97E-02	5.91E-04	1.91E-02	1.99E-03	7.42E-03	9.53E-02	7.49E-05	1.61E-04	1.06E-03	0
Co-60 (Ci)	1.96E+02	1.48E+02	2.06E+02	9.52E+01	2.91E+01	3.70E+01	7.60E+02	1.19E+01	1.96E+01	5.29E+00	0
H-3 (Ci)	1.74E+02	1.34E+02	5.81E+00	8.62E+01	2.50E+00	3.35E+01	5.55E+02	5.26E-01	1.01E+00	4.79E+00	0
U-238 (Ci)	1.45E-03	1.10E-03	6.00E-04	7.05E-04	2.42E-04	2.74E-04	5.64E-03	7.61E-05	1.64E-04	3.92E-05	2.00E-05
Se-79 (Ci)	7.59E-04	6.91E-05	3.15E-02	4.44E-05	1.05E-02	1.73E-05	2.64E-04	3.99E-03	8.59E-03	2.47E-06	0
Sn-126 (Ci)	3.14E-03	2.85E-04	1.31E-01	1.83E-04	4.39E-02	7.11E-05	1.09E-03	1.67E-02	3.58E-02	1.02E-05	0
NO3 (kg)	5.90E+03	4.53E+03	4.32E+02	2.91E+03	1.82E+03	1.13E+03	2.32E+04	5.48E+01	1.18E+02	1.62E+02	1.46E-01
SO4 (kg)	1.29E+02	9.03E+01	6.91E+02	5.81E+01	2.12E+02	2.26E+01	3.53E+02	8.76E+01	1.88E+02	3.23E+00	1.37E-01
Cr (kg)	2.32E+01	1.70E+01	2.46E+01	1.09E+01	3.86E+01	4.25E+00	8.68E+01	3.12E+00	6.70E+00	6.07E-01	0
Utot (kg)	4.34E+00	3.29E+00	1.80E+00	2.11E+00	7.27E-01	8.21E-01	1.69E+01	2.28E-01	4.90E-01	1.17E-01	6.00E-05

Source : RPP-RPT-42294, "Hanford Waste Management Area C Soil Contamination Inventory Estimates," Rev. 2.

Note: The inventory estimates have been radioactive decay corrected to the beginning of the leak or unplanned release modeled year.

* Conversion 1 gallon = 3.78541 liters

Leak time sources	
C-101	Section 4.1.3.3 "Timing of the Release", RPP-ENV-33418, "Hanford C-Farm Leak Inventory Assessments Report," Rev. 4
C-104	Section 4.7.2 "Leak Assessment Considerations", Section 4.7.3.3 "Timing of the Release", RPP-ENV-33418, Rev. 4
C-105 (low estimate)	
C-105 (high estimate)	Section 4.2.3.1 "Release type", Section 4.2.1 "Leak Status of Tank 241-C-105", and Section 4.2.3.3 "Timing of the Release", RPP-ENV-33418, Rev. 4
C-108	Section 4.8.2 "Leak Assessment Considerations" and Section 4.8.3.3 "Timing of the Release", RPP-ENV-33418, Rev. 4
C-110	Section 4.3.2 "Leak Assessment Considerations", and Section 4.3.3.3 "Timing of the Release", RPP-ENV-33418, Rev. 4.
C-112	Section 4.9.2 "Leak Assessment Considerations", and Section 4.9.3.3 "Timing of the Release", RPP-ENV-33418, Rev. 4
UPR-81	Section 5.2.3.3 "Timing of Release" and Table 5-1, Section 5.2.1 "UPR-200-E-81 Data and information", RPP-ENV-33418, Rev. 4
UPR-82	Section 5.3.3.3 "Timing of Release" and Table 5-1, Section 5.3.1 "UPR-200-E-82 Data and information", RPP-ENV-33418, Rev. 4
UPR-86	Section 5.4.3.3 "Timing of Release" and Section 5.4.3.1, and Table 5-1, RPP-ENV-33418, Rev. 4
Surface	RPP-RPT-42294, "Hanford Waste Management Area C Soil Contamination Inventory Estimates," Rev. 2
French Drain 216-C-8	Section 6.4 "216-C-8 French Drain", RPP-ENV-33418, Rev. 4. Not cited, but also a good source of information is RPP-RPT-42294, Rev. 2

Figure 6-2. First-Arrival Time (in Calendar Year) of Radionuclides for Various K_d Values Based on Screening Analysis Using Subsurface Transport Over Multiple Phases.

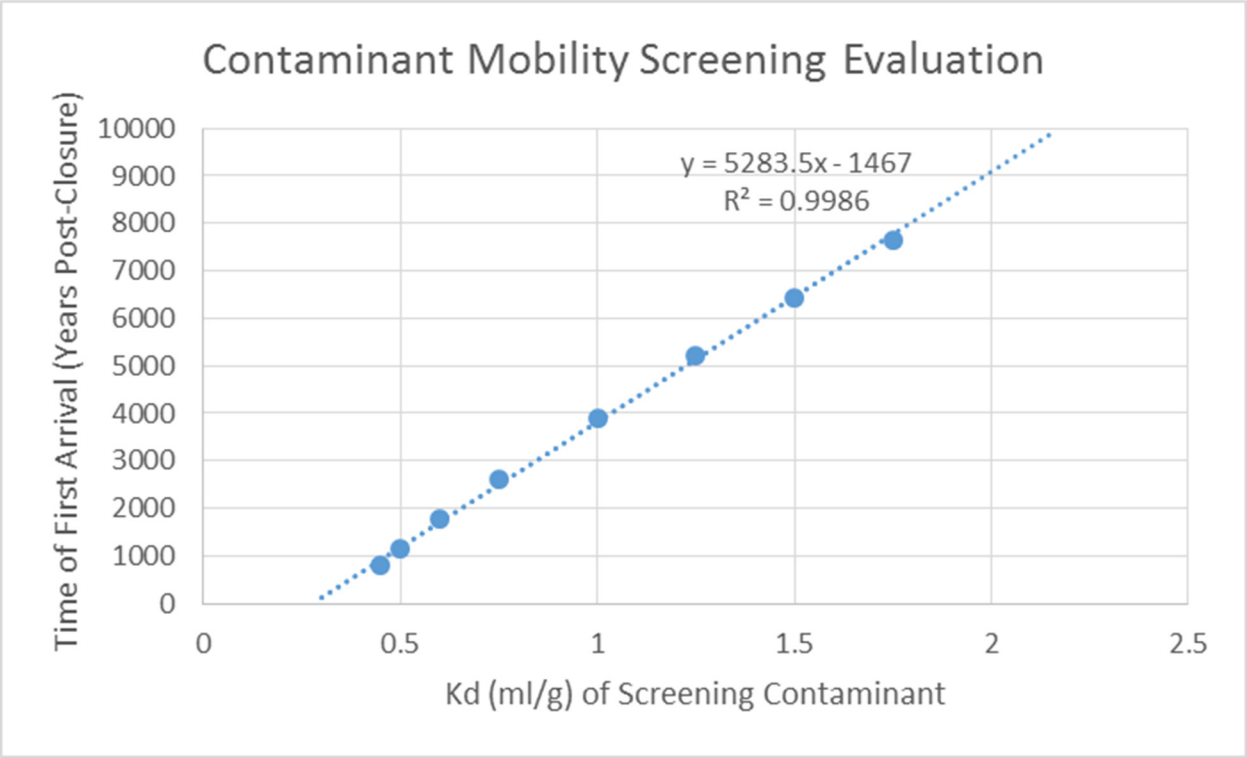

Table 6-2. First-Arrival Time (in Calendar Year) of Radionuclides for Various K_d Values Based on Screening Analysis Using Subsurface Transport Over Multiple Phases.

Contaminant K_d (Material < 2 mm) (mL/g)	Calendar Year of First Arrival at Water Table	Time of Arrival, Post-Closure (Closure Occurring in 2020) Years
0.25	1997	-23
0.3	2006	-14
0.45	2842.5	822.5
0.5	3170	1,150
0.6	3815	1,795
0.75	4640	2,620
1	5930	3,910
1.25	7240	5,220
1.5	8460	6,440
1.75	9670	7,650
2	> 12020	> 10,000

Figure 6-3. Points of Calculation 100 Meters Downgradient of Waste Management Area C.

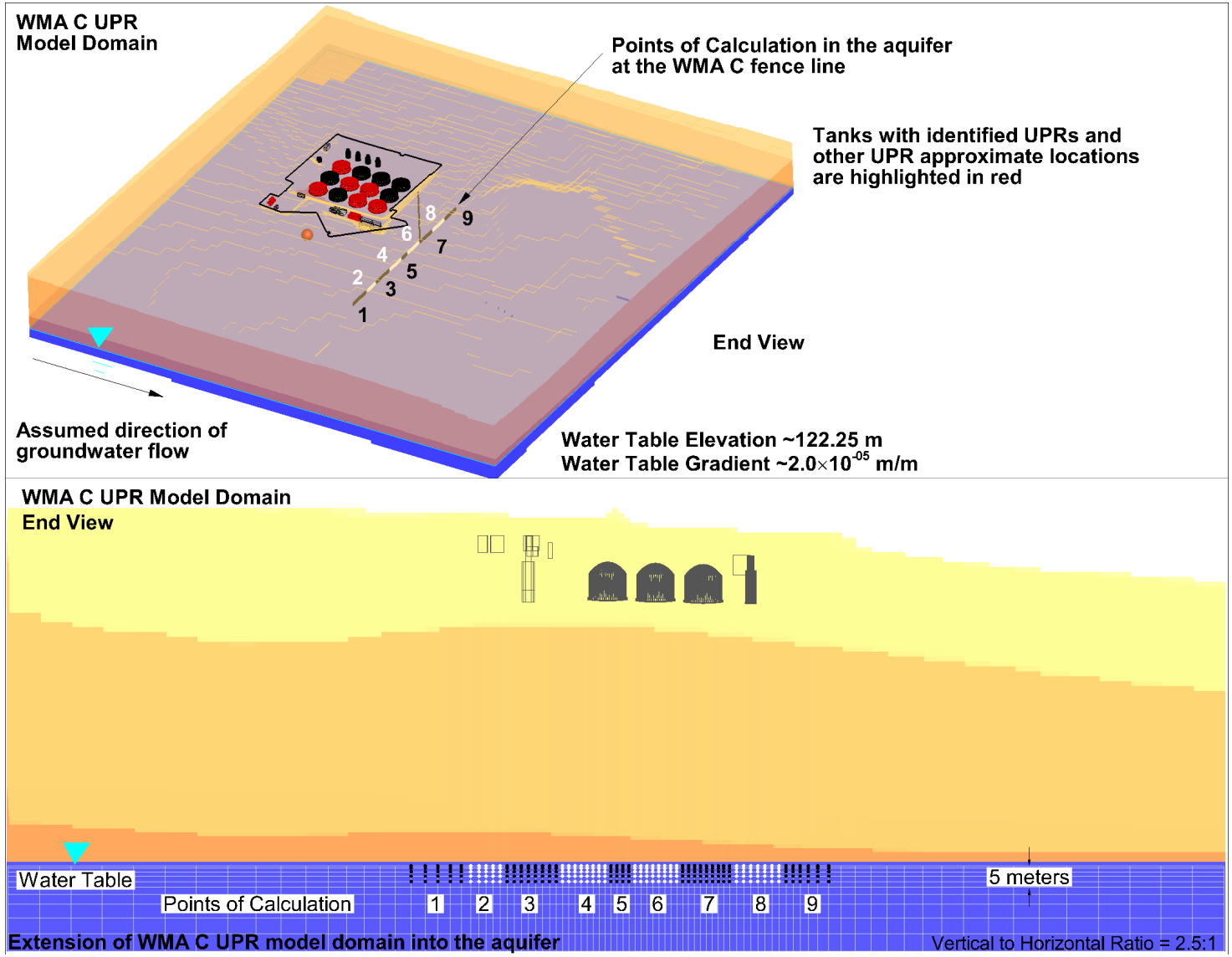

PA = Performance Assessment WMA = Waste Management Area

Table 6-3. Width of the Nine Points of Calculation at the Waste Management Area C Fenceline.

Points of Calculation								
1	2	3	4	5	6	7	8	9
Width (m)	Width (m)	Width (m)	Width (m)	Width (m)	Width (m)	Width (m)	Width (m)	Width (m)
40	24	35.5	31	15.3	30.4	34.1	31.5	33.5

Concentration contours of ^{99}Tc and nitrate in the vadose zone corresponding to years 2000 and 2016 are shown in Figures 6-13 through 6-16, respectively. Technetium-99 and nitrate contained in the past leaks have reached the water table by 2000, but the center of the ^{99}Tc and nitrate mass remains above the water table. By 2016, the center of the ^{99}Tc mass has reached the water table, while the center of the nitrate mass remains just above the water table. Table 6-4 provides a summary of results for those radionuclides and non-radiological contaminants arriving in groundwater at the WMA C fenceline before closure.

6.3.2 Results of Groundwater Pathway Evaluation: Time after Assumed Closure of Waste Management Area C in 2020

Except for nitrate, the concentration all of the radionuclides and non-radiological contaminants with a K_d of 0 mL/g decreases markedly 100 m downgradient of the fenceline after the assumed closure of WMA C in 2020. The concentration of nitrate at PoCal 3 reaches a peak value of 7 mg/L in 2030 and then begins to decline steadily and reaches a value of less than 1 mg/L by 2120 (refer to Figure 6-10). The concentrations in groundwater of ^{99}Tc, sulfate, and hexavalent chromium, if all chromium is assumed to be hexavalent, also (refer to Figures 6-4, 6-11, and 6-12, respectively) decline steadily from the peak value reached during the period before the assumed closure of WMA C in 2020. By 2120, the maximum concentrations of ^{99}Tc, sulfate, and hexavalent chromium 100 m downgradient of the fenceline decrease to less than 100 pCi/L, 0.01 mg/L (10 µg/L), and 0.001 mg/L (1 µg/L), respectively.

The concentration of ^{79}Se increases after 2020 and reaches a peak value of 0.5 pCi/L in 4040 (refer to Figure 6-8). The concentration decreases after that until reaching an effective zero value by year 9000. The concentration of ^{129}I at the WMA C fenceline reaches a peak value of slightly greater than 1.0 pCi/L in year 5920 at PoCal 6, with a second relative peak value of 0.9 pCi/L occurring at PoCal 3 in 8380 (Figure 6-17). The former value slightly exceeds the MCL for ^{129}I, which is 1 pCi/L, and the latter value is slightly less than the MCL. One hundred meters downgradient of the fenceline, the maximum concentration values at the two aforementioned PoCals are 0.8 and 0.6 pCi/L, respectively (Figure 6-18). The ^{129}I decreases from the peak values but persists at the PoCals through the end of the simulation period. The maximum concentration at PoCal 3 100 m downgradient of the fenceline in year 12020 is less than 0.02 pCi/L.

Table 6-4. Summary Results of Radionuclides and Non-Radiological Contaminants that Arrive in Groundwater at the Waste Management Area C Fenceline before Closure. (3 sheets)

	Cobalt-60				Hydrogen-3 (Tritium)			
	Fenceline		100 Meters Downgradient		Fenceline		100 Meters Downgradient	
	Year of Peak	Peak Concentration (pCi/L)	Year of Peak	Peak Concentration (pCi/L)	Year of Peak	Peak Concentration (pCi/L)	Year of Peak	Peak Concentration (pCi/L)
PoCal 1	2036	0.6	2025	1	2030	11	2028	66
PoCal 2	2024	24	2024	34	2028	1,300	2028	1,700
PoCal 3	2024	200	2024	120	2027	10,000	2028	6,000
PoCal 4	2010	59	2011	97	2016	1,300	2025	2,500
PoCal 5	2009	990	2009	490	2013	20,000	2013	9,600
PoCal 6	2008	1,200	2009	860	2012	22,000	2013	16,000
PoCal 7	2009	200	2009	420	2013	3,800	2013	7,600
PoCal 8	2010	33	2010	92	2015	890	2014	2,000
PoCal 9	2011	5	2011	18	2015	140	2015	490
	Selenium-79				Technetium-99			
	Fenceline		100 Meters Downgradient		Fenceline		100 Meters Downgradient	
Year of Peak	Year of Peak	Peak Concentration (pCi/L)	Year of Peak	Peak Concentration (pCi/L)	Year of Peak	Peak Concentration (pCi/L)	Year of Peak	Peak Concentration (pCi/L)
PoCal 1	4515	0.1	4520	0.06	2055	1,500	2056	980
PoCal 2	4575	0.04	4555	0.06	2055	450	2055	720
PoCal 3	4910	0.04	4830	0.04	2026	910	2026	740
PoCal 4	4640	0.05	4605	0.05	2025	880	2025	1,100
PoCal 5	4045	0.3	4080	0.2	2019	5,000	2020	3,300
PoCal 6	4040	0.7	4045	0.5	2019	9,400	2019	6,600

Table 6-4. Summary Results of Radionuclides and Non-Radiological Contaminants that Arrive in Groundwater at the Waste Management Area C Fenceline before Closure. (3 sheets)

Selenium-79 (continued)					Technetium-99 (continued)			
	Fenceline		100 Meters Downgradient		Fenceline		100 Meters Downgradient	
Year of Peak	Year of Peak	Peak Concentration (pCi/L)	Year of Peak	Peak Concentration (pCi/L)	Year of Peak	Peak Concentration (pCi/L)	Year of Peak	Peak Concentration (pCi/L)
PoCal 7	4090	0.2	4065	0.4	2022	2,200	2021	4,100
PoCal 8	4100	0.05	4085	0.2	2024	240	2023	920
PoCal 9	4100	0.008	4095	0.04	2024	26	2024	150
Hexavalent Chromium					**Nitrate**			
	Fenceline		**100 Meters Downgradient**		**Fenceline**		**100 Meters Downgradient**	
	Year of Peak	**Peak Concentration (mg/L)**	**Year of Peak**	**Peak Concentration (mg/L)**	**Year of Peak**	**Peak Concentration (mg/L)**	**Year of Peak**	**Peak Concentration (mg/L)**
PoCal 1	2055	0.004	2055	0.003	2055	0.07	2052	0.1
PoCal 2	2032	0.006	2031	0.009	2032	2	2031	2
PoCal 3	2030	0.05	2030	0.03	2030	13	2031	7
PoCal 4	2026	0.008	2027	0.01	2026	1	2029	3
PoCal 5	2019	0.06	2020	0.03	2018	11	2018	6
PoCal 6	2020	0.08	2020	0.06	2017	12	2018	9
PoCal 7	2023	0.02	2022	0.03	2019	3	2019	5
PoCal 8	2023	0.004	2023	0.009	2020	0.6	2020	1
PoCal 9	2023	0.0005	2023	0.002	2020	0.1	2021	0.3

Table 6-4. Summary Results of Radionuclides and Non-Radiological Contaminants that Arrive in Groundwater at the Waste Management Area C Fenceline before Closure. (3 sheets)

Sulfate				
	Fenceline		100 Meters Downgradient	
	Year of Peak	Peak Concentration (mg/L)	Year of Peak	Peak Concentration (mg/L)
PoCal 1	2055	0.1	2056	0.07
PoCal 2	2054	0.05	2054	0.07
PoCal 3	2029	0.2	2029	0.2
PoCal 4	2025	0.08	2026	0.1
PoCal 5	2018	0.6	2019	0.3
PoCal 6	2018	0.9	2018	0.6
PoCal 7	2021	0.2	2020	0.4
PoCal 8	2022	0.03	2021	0.08
PoCal 9	2022	0.003	2022	0.02

Figure 6-4. Concentration of Technetium-99 in Groundwater in the Points of Calculation at the Fenceline.

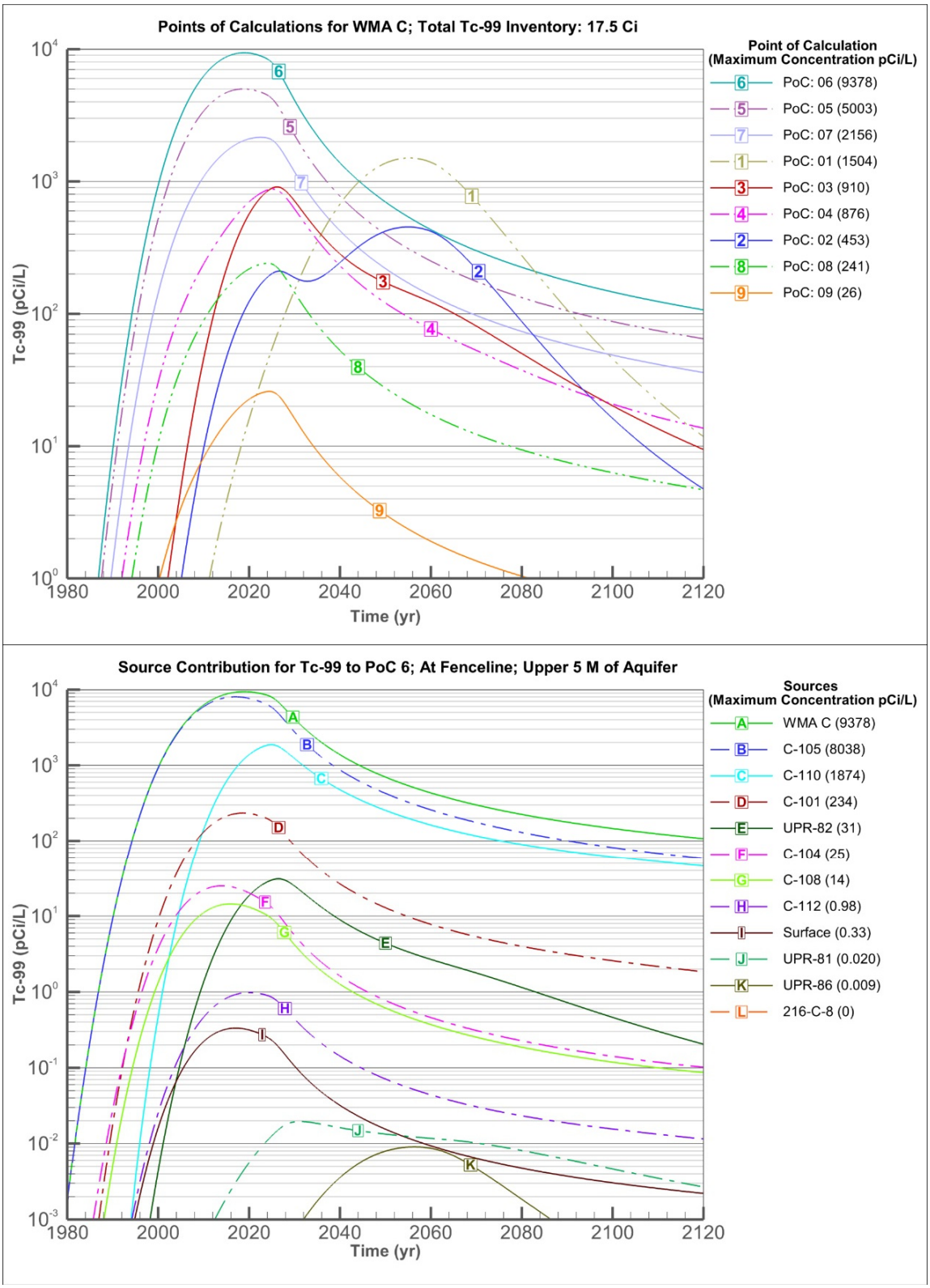

PoC = point of calculation WMA = Waste Management Area

Figure 6-5. Concentration of Technetium-99 in Groundwater in the Points of Calculation 100 Meters Downgradient of the Fenceline.

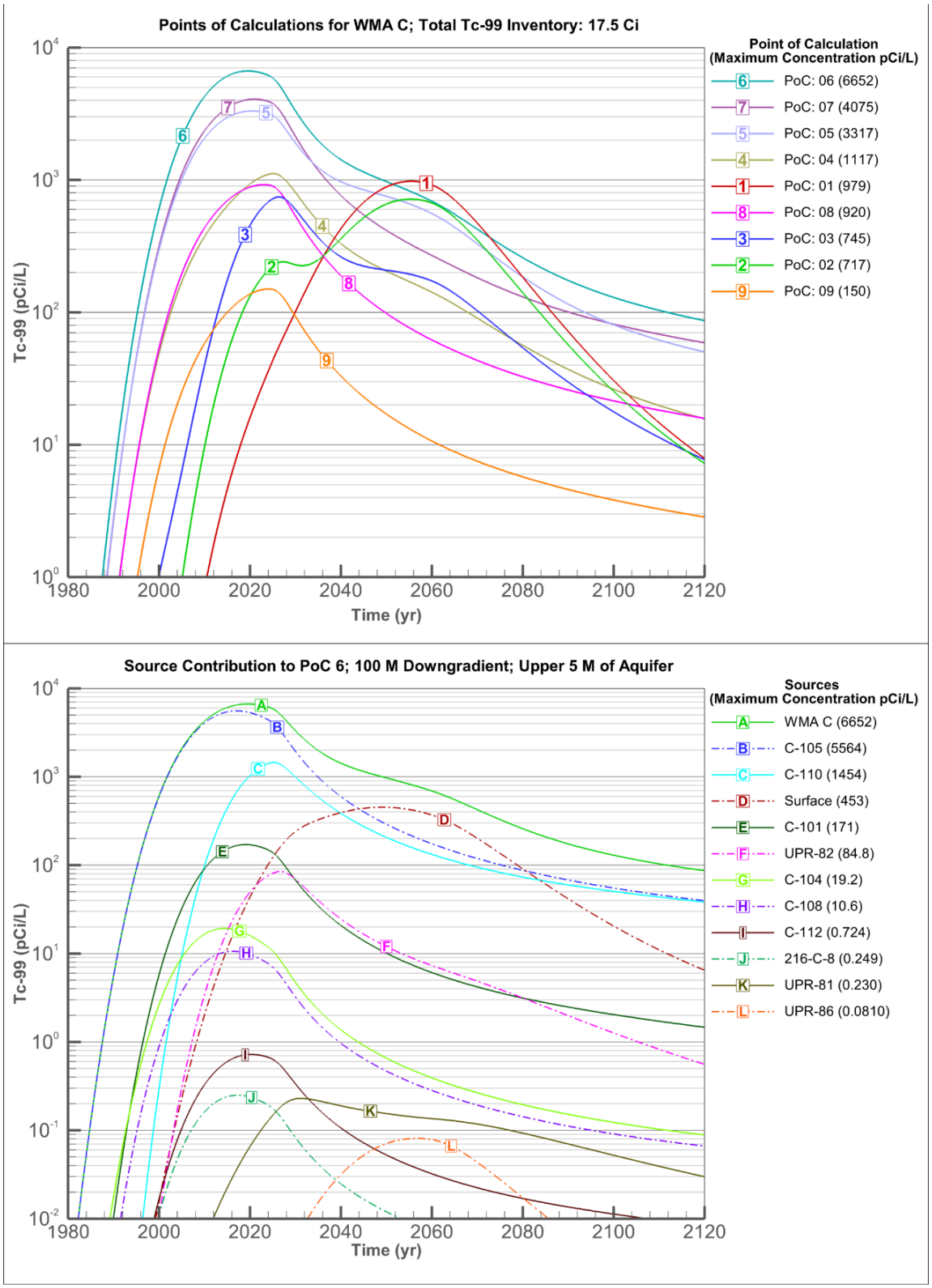

PoC = point of calculation WMA = Waste Management Area

Figure 6-6. Concentration of Tritium in Groundwater in the Points of Calculation at the Fenceline.

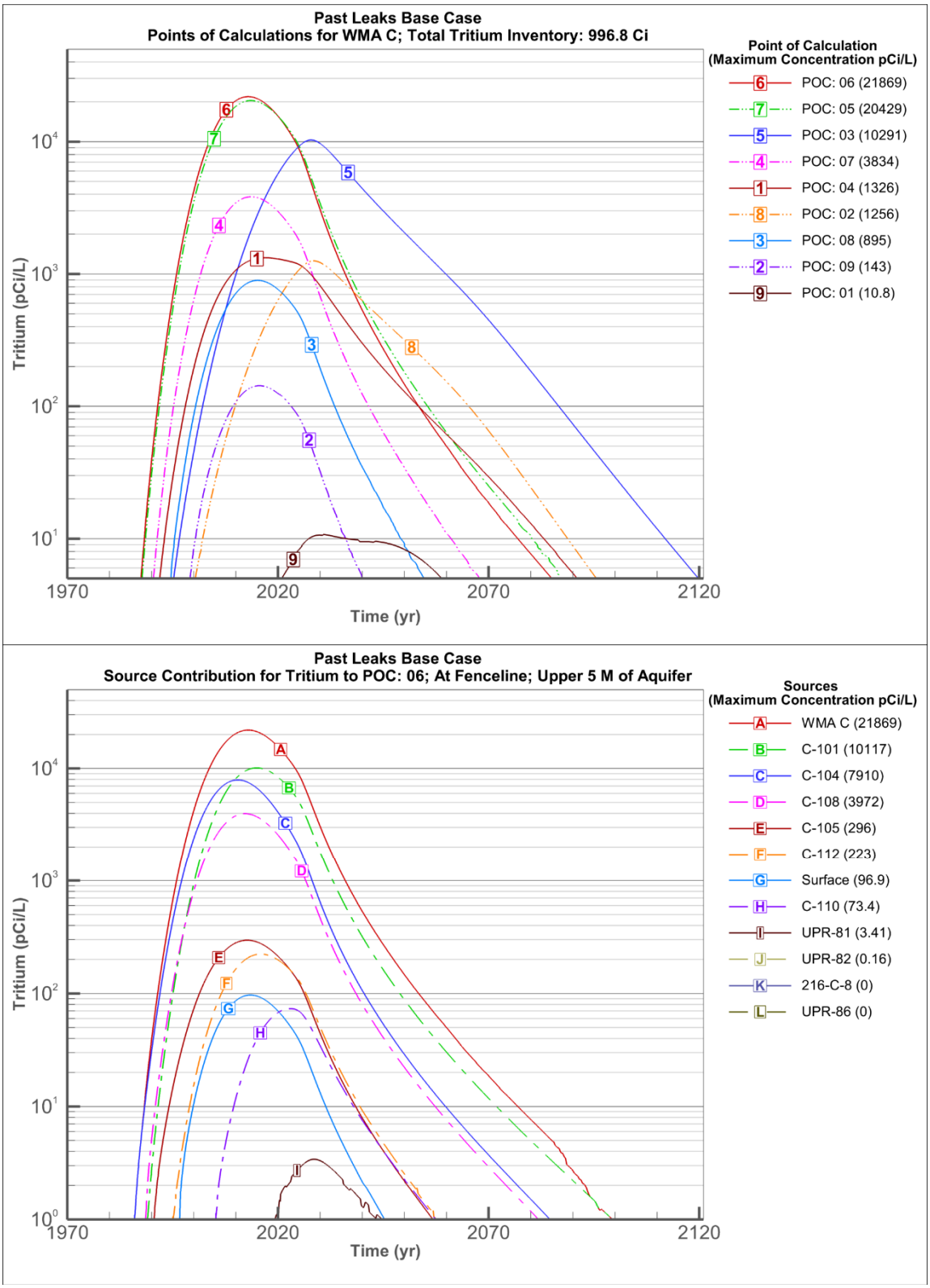

PoC = point of calculation WMA = Waste Management Area

Figure 6-7. Concentration of Tritium in Groundwater in the Points of Calculation 100 Meters Downgradient of the Fenceline.

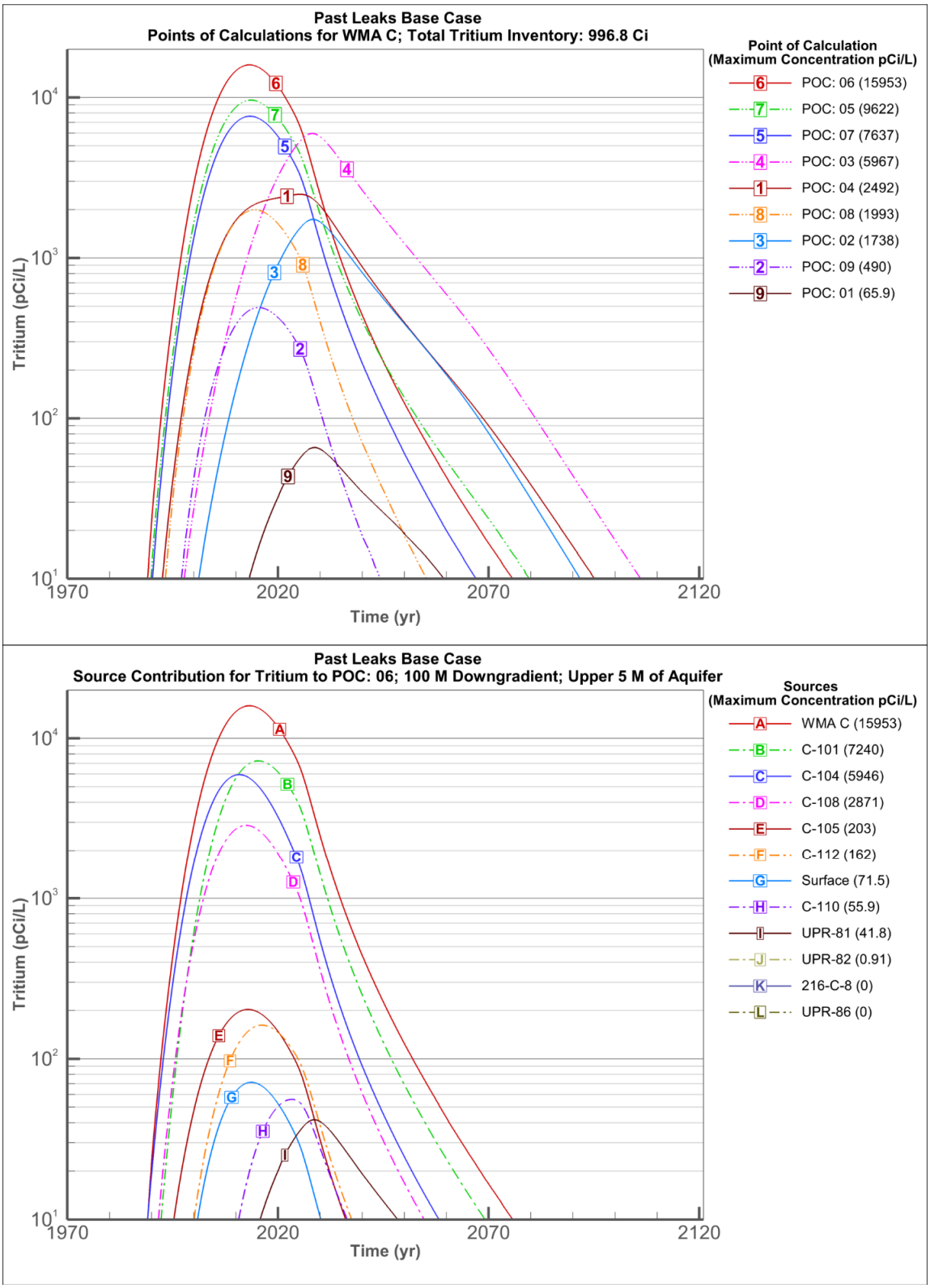

PoC = point of calculation WMA = Waste Management Area

Figure 6-8. Concentration of Cobalt-60 in Groundwater in the Points of Calculation 100 Meters Downgradient of the Fenceline.

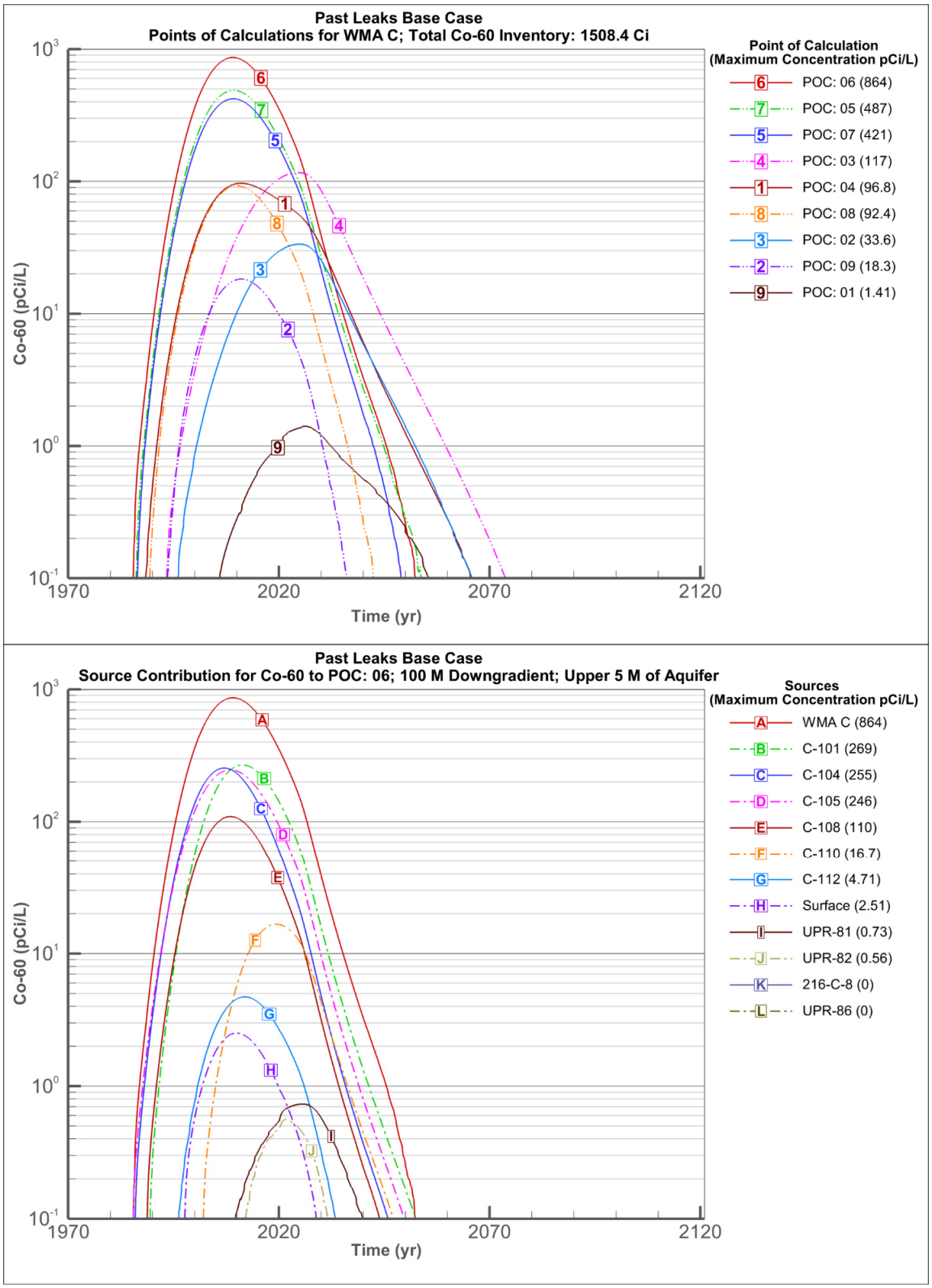

PoC = point of calculation WMA = Waste Management Area

Figure 6-9. Concentration of Selenium-79 in Groundwater in the Points of Calculation 100 Meters Downgradient of the Fenceline.

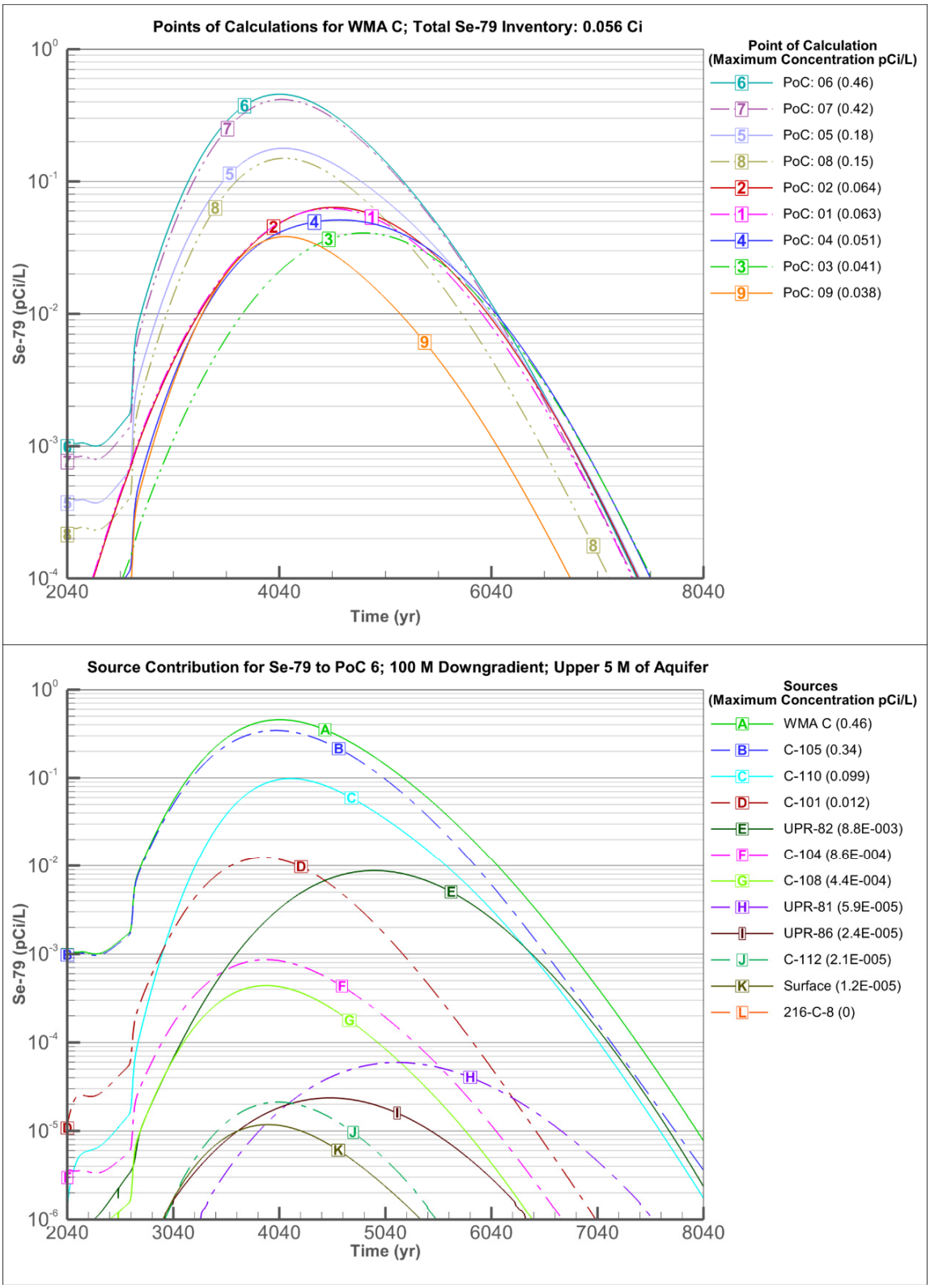

PoC = point of calculation WMA = Waste Management Area

Figure 6-10. Concentration of Nitrate in Groundwater in the Points of Calculation 100 Meters Downgradient of the Fenceline.

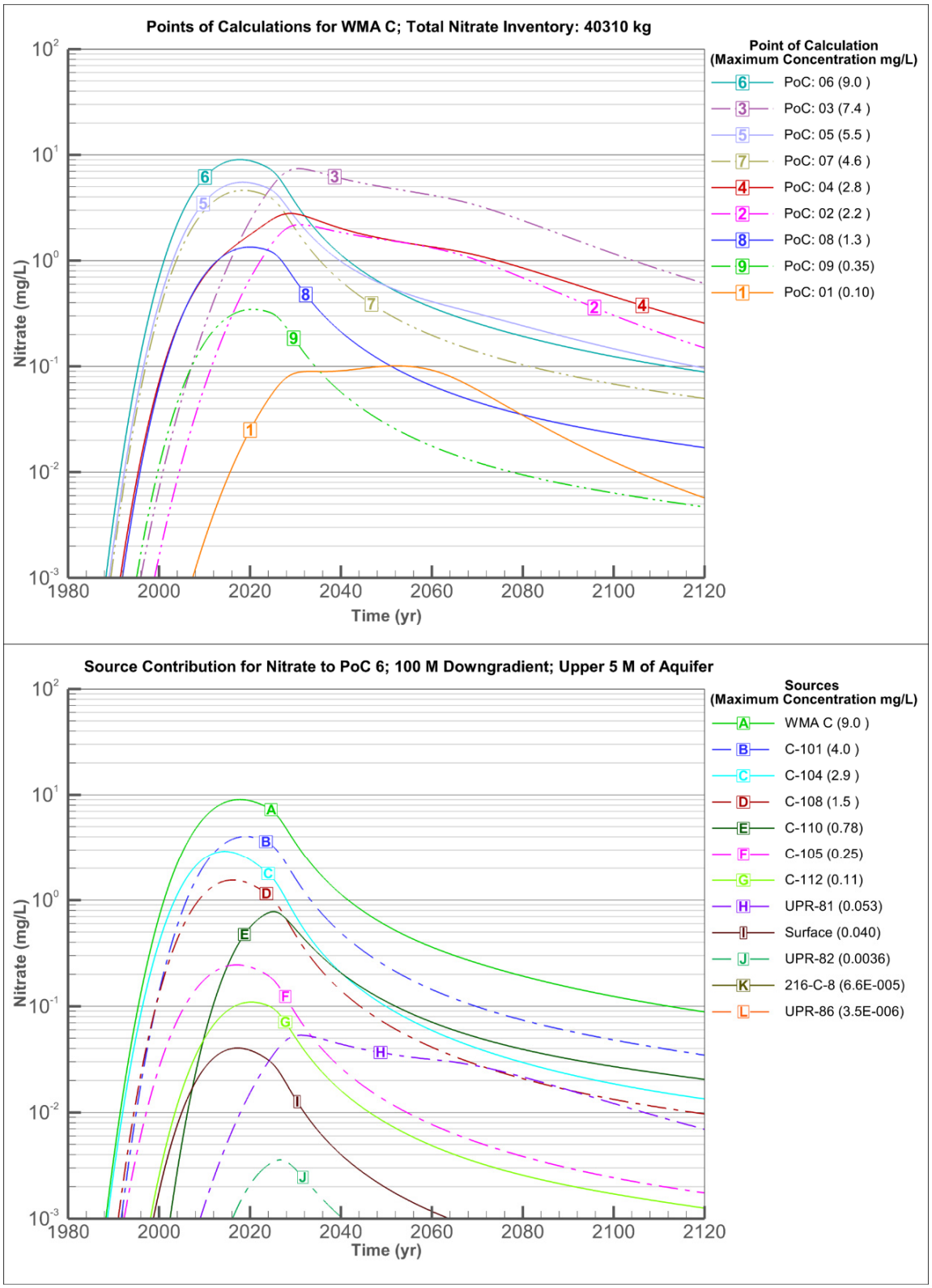

PoC = point of calculation WMA = Waste Management Area

Figure 6-11. Concentration of Sulfate in Groundwater in the Points of Calculation 100 Meters Downgradient of the Fenceline.

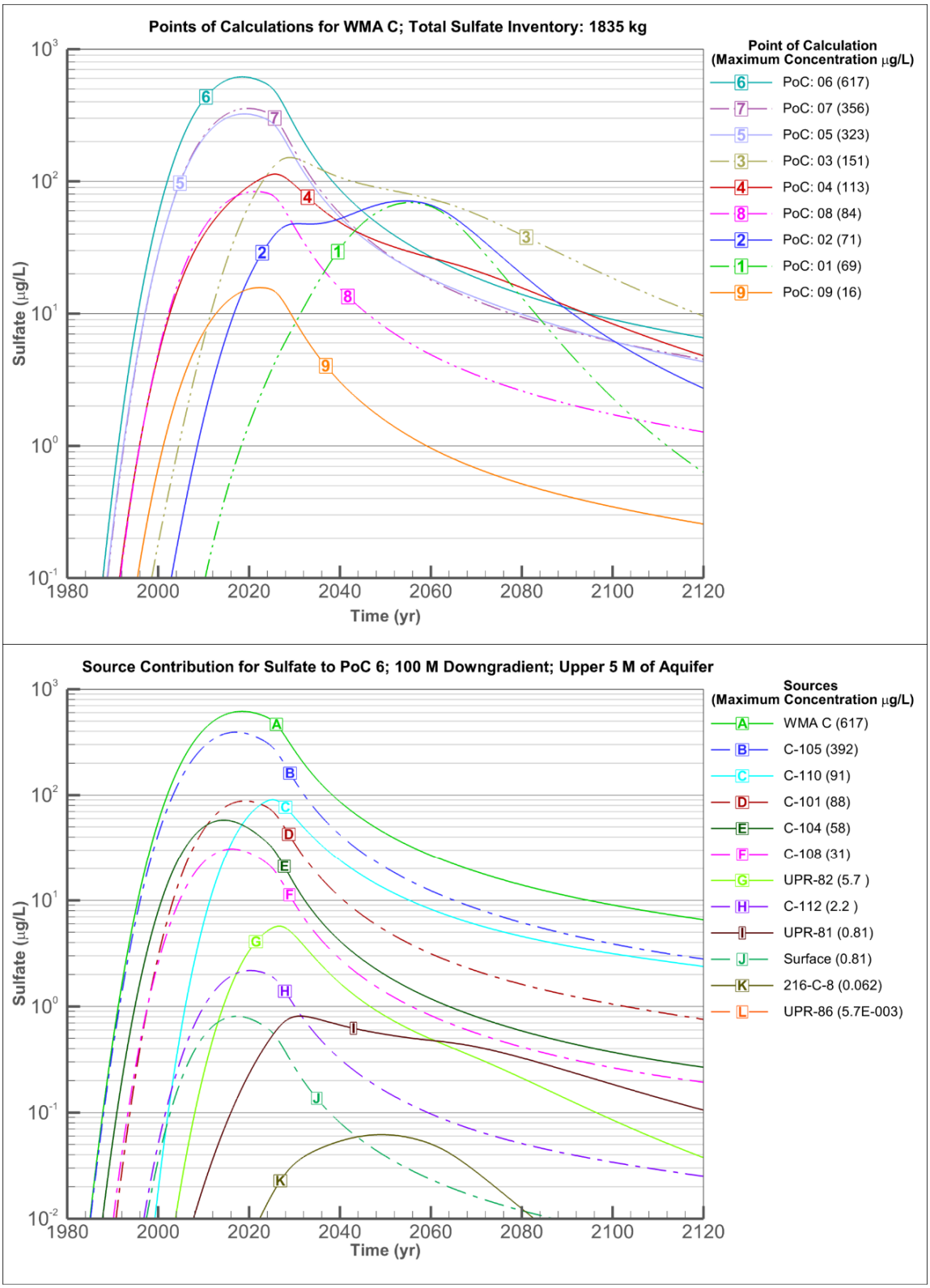

PoC = point of calculation WMA = Waste Management Area

Figure 6-12. Concentration of Chromium (as Cr^{+6}) in Groundwater in the Points of Calculation 100 Meters Downgradient of the Fenceline.

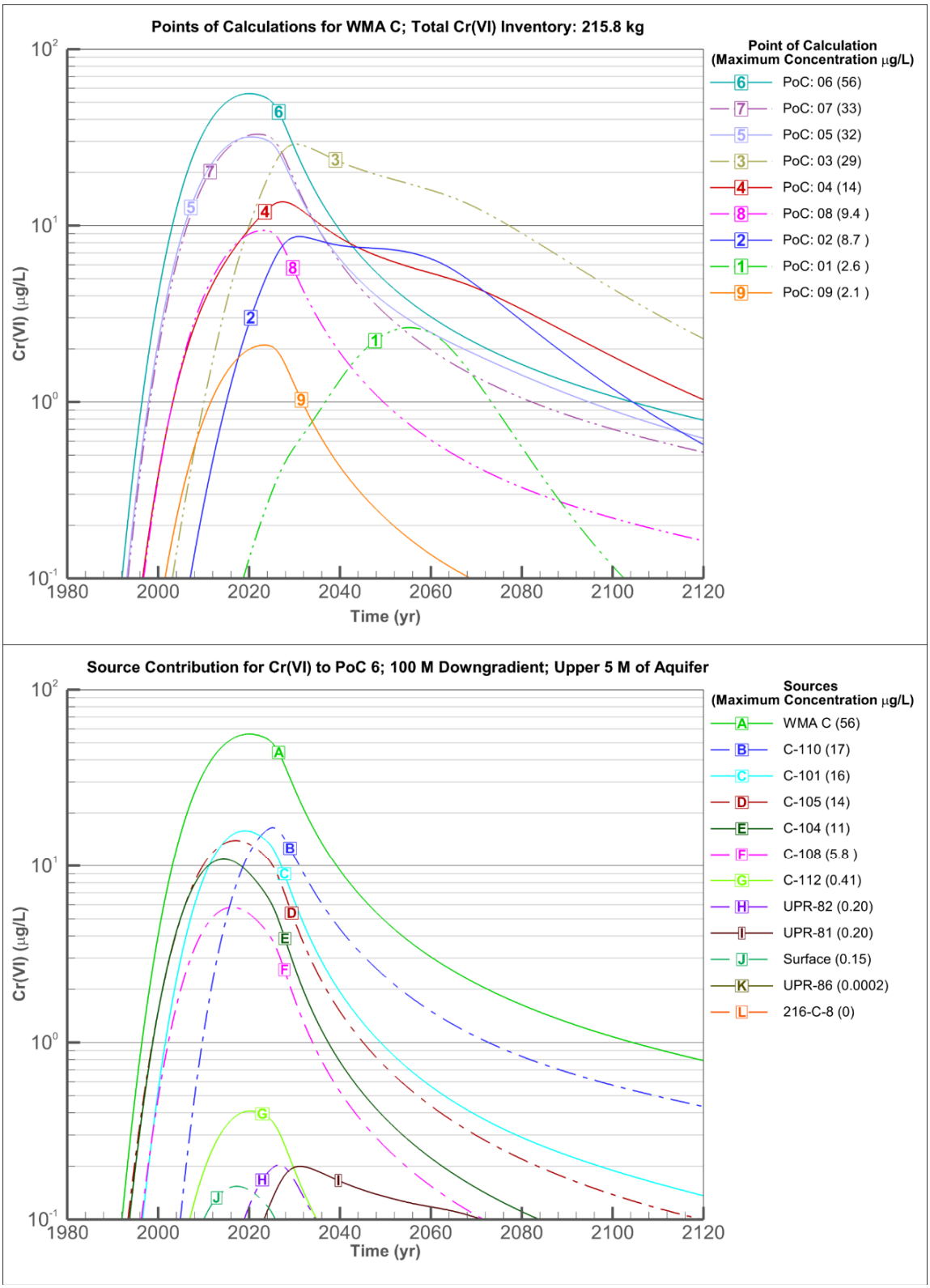

PoC = point of calculation WMA = Waste Management Area

Figure 6-13. Concentration Contours of Technetium-99 along Cross-Section Planes through Unplanned Releases 200-E-81 and 200-E-82 and Tank Row 241-C-110, 241-C-107, 241-C-104 and 241-C-101 Corresponding to Year 2000.

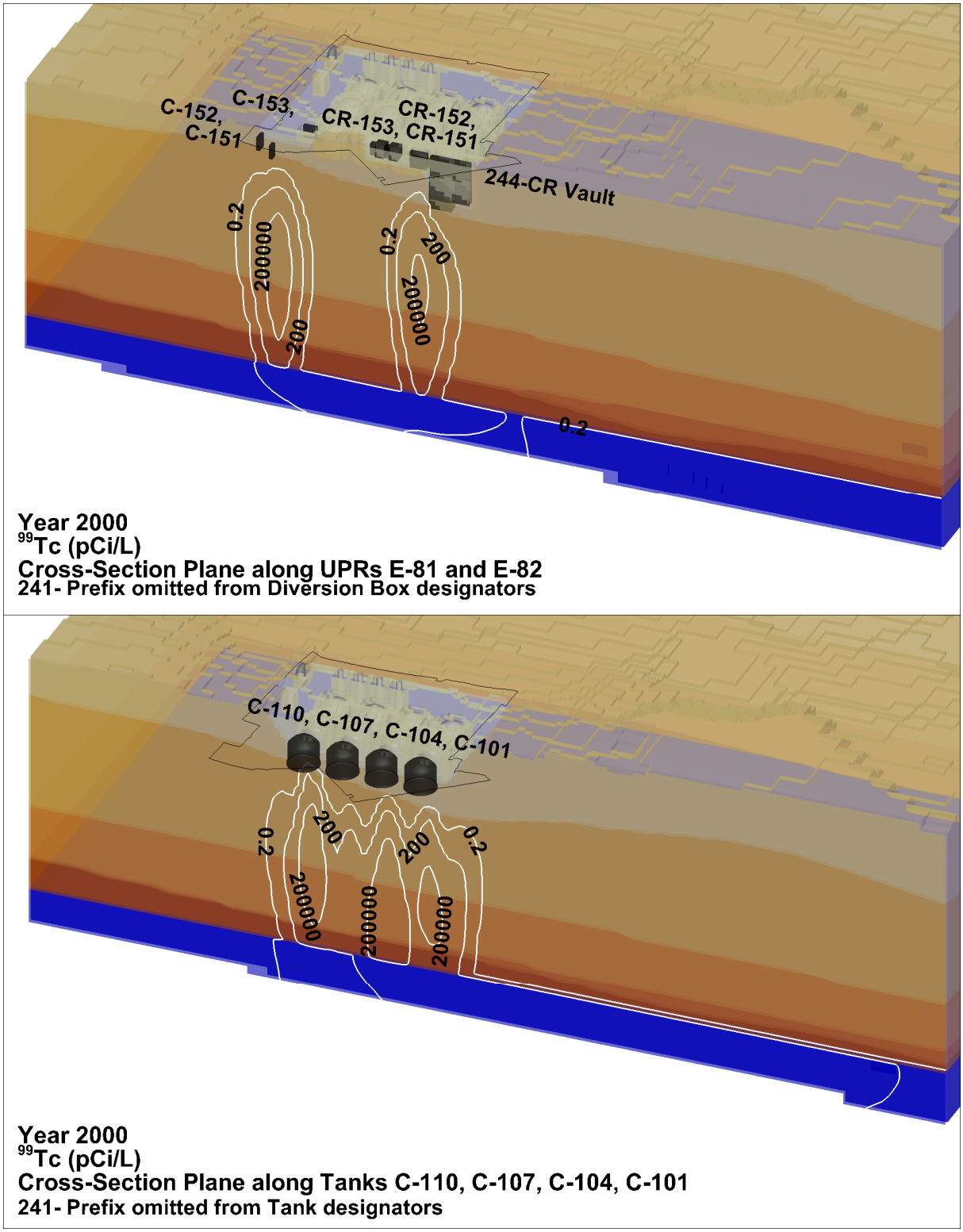

UPR = unplanned release

Figure 6-14. Concentration Contours of Technetium-99 along Cross-Section Planes through Unplanned Releases 200-E-81 and 200-E-82 and Tank Row 241-C-110, 241-C-107, 241-C-104 and 241-C-101 Corresponding to Year 2016.

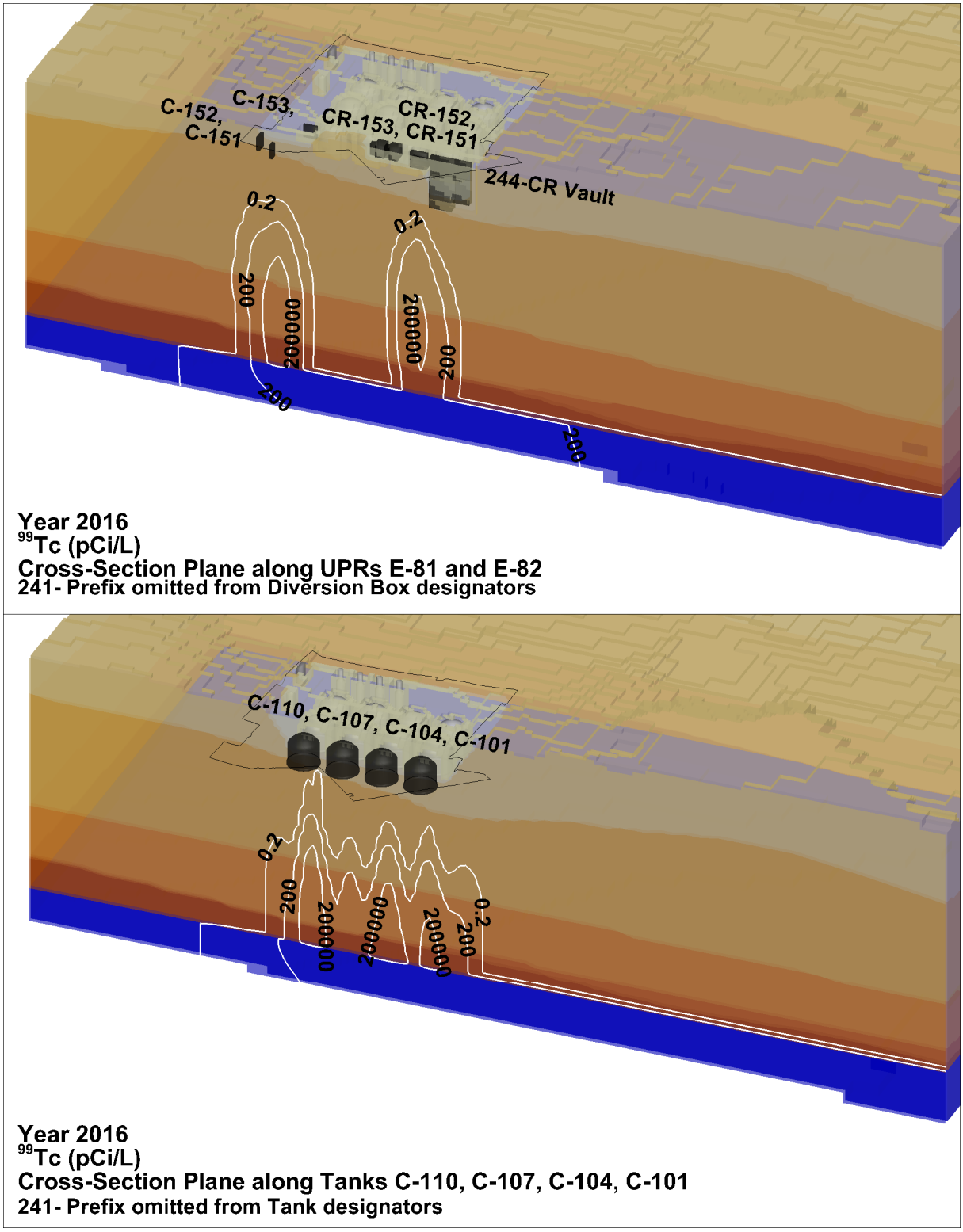

UPR = unplanned release

Figure 6-15. Concentration Contours of Nitrate along Cross-Section Planes through Unplanned Releases 200-E-81 and 200-E-82 and Tank Row 241-C-110, 241-C-107, 241-C-104 and 241-C-101 Corresponding to Year 2000.

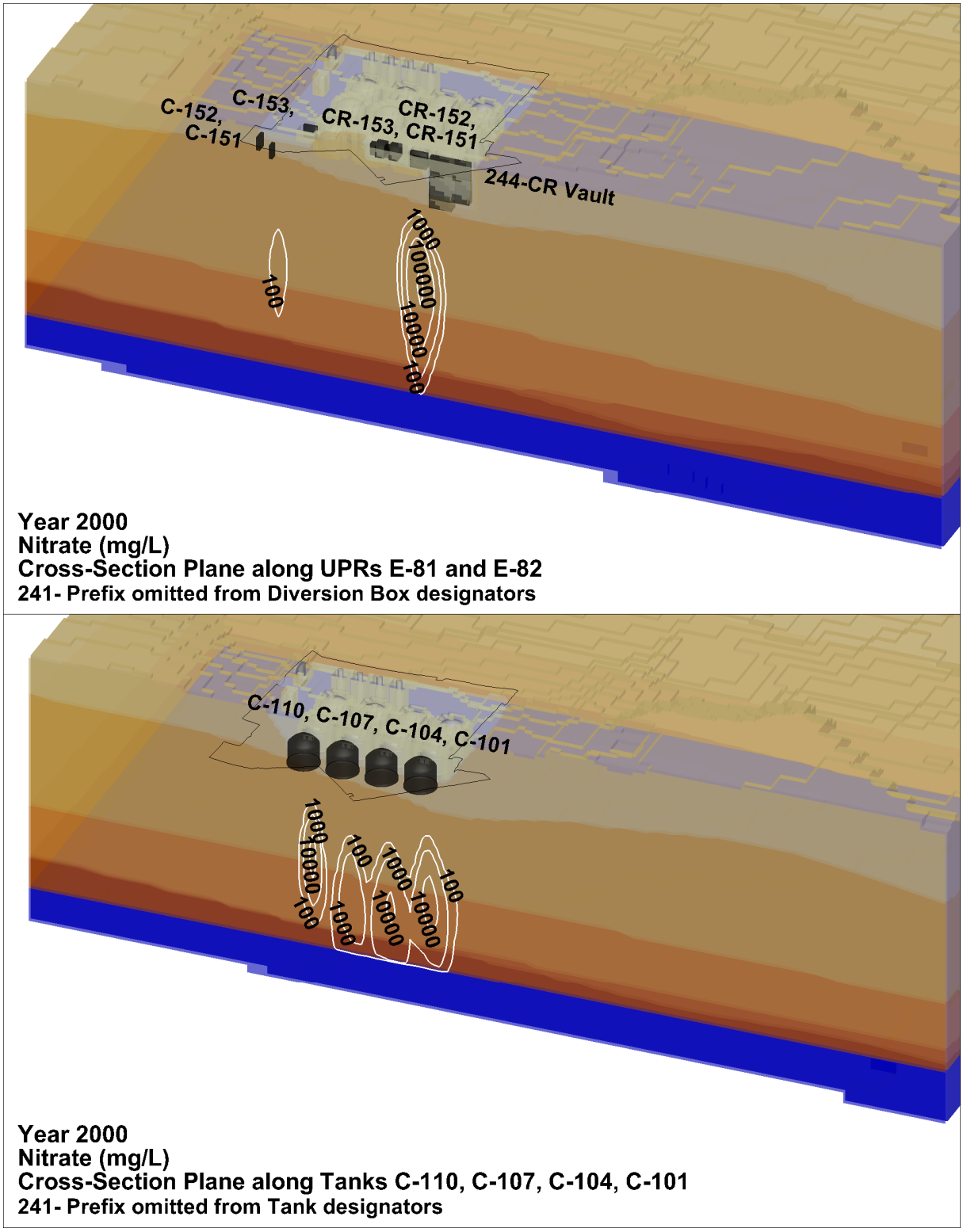

UPR = unplanned release

Figure 6-16. Concentration Contours of Nitrate along Cross-Section Planes through Unplanned Releases 200-E-81 and 200-E-82 and Tank Row 241-C-110, 241-C-107, 241-C-104 and 241-C-101 Corresponding to Year 2016.

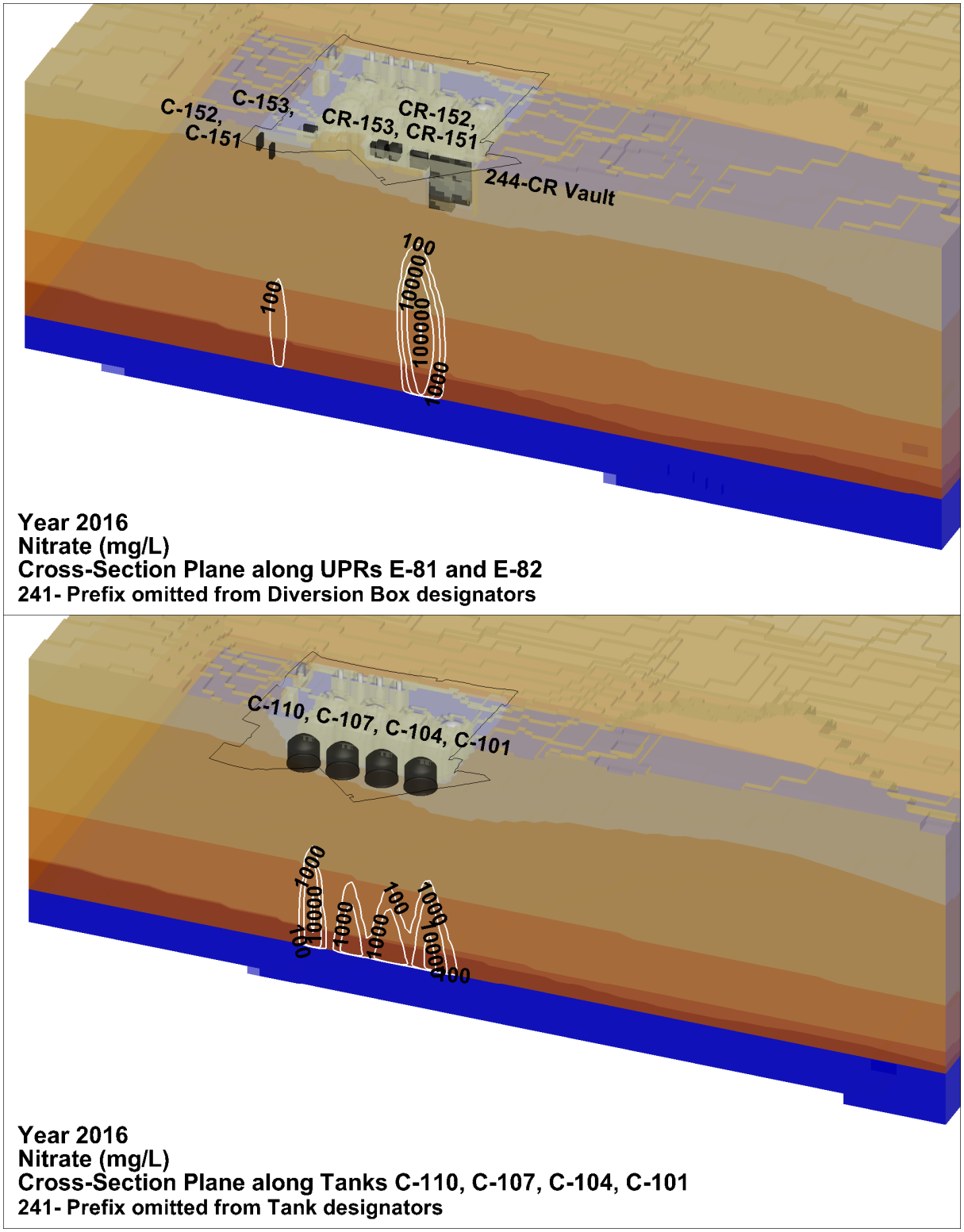

UPR = unplanned release

Figure 6-17. Concentration of Iodine-129 in Groundwater in the Points of Calculation at the Fenceline.

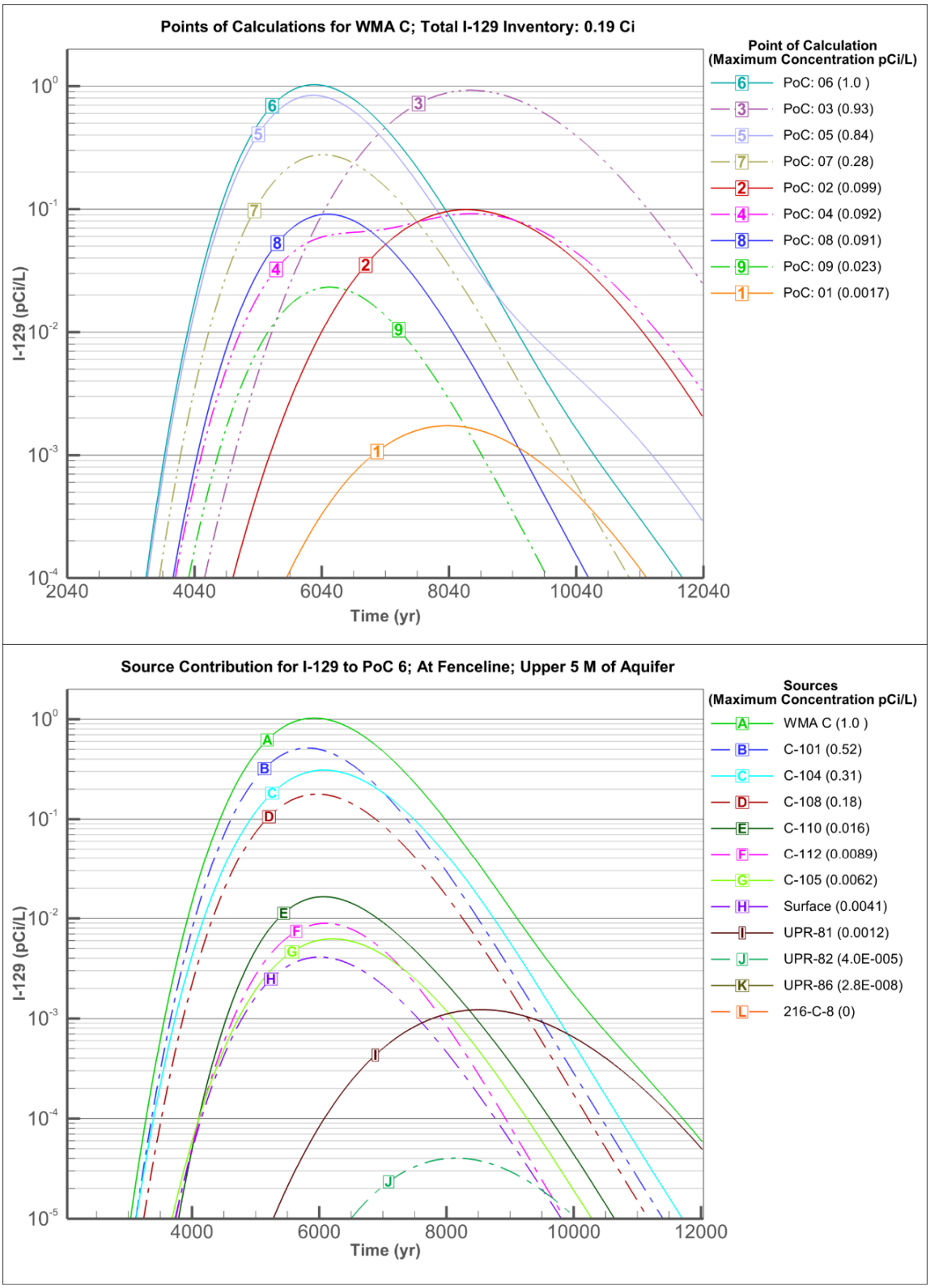

PoC = point of calculation WMA = Waste Management Area

Figure 6-18. Concentration of Iodine-129 in Groundwater in the Points of Calculation 100 Meters Downgradient of the Fenceline.

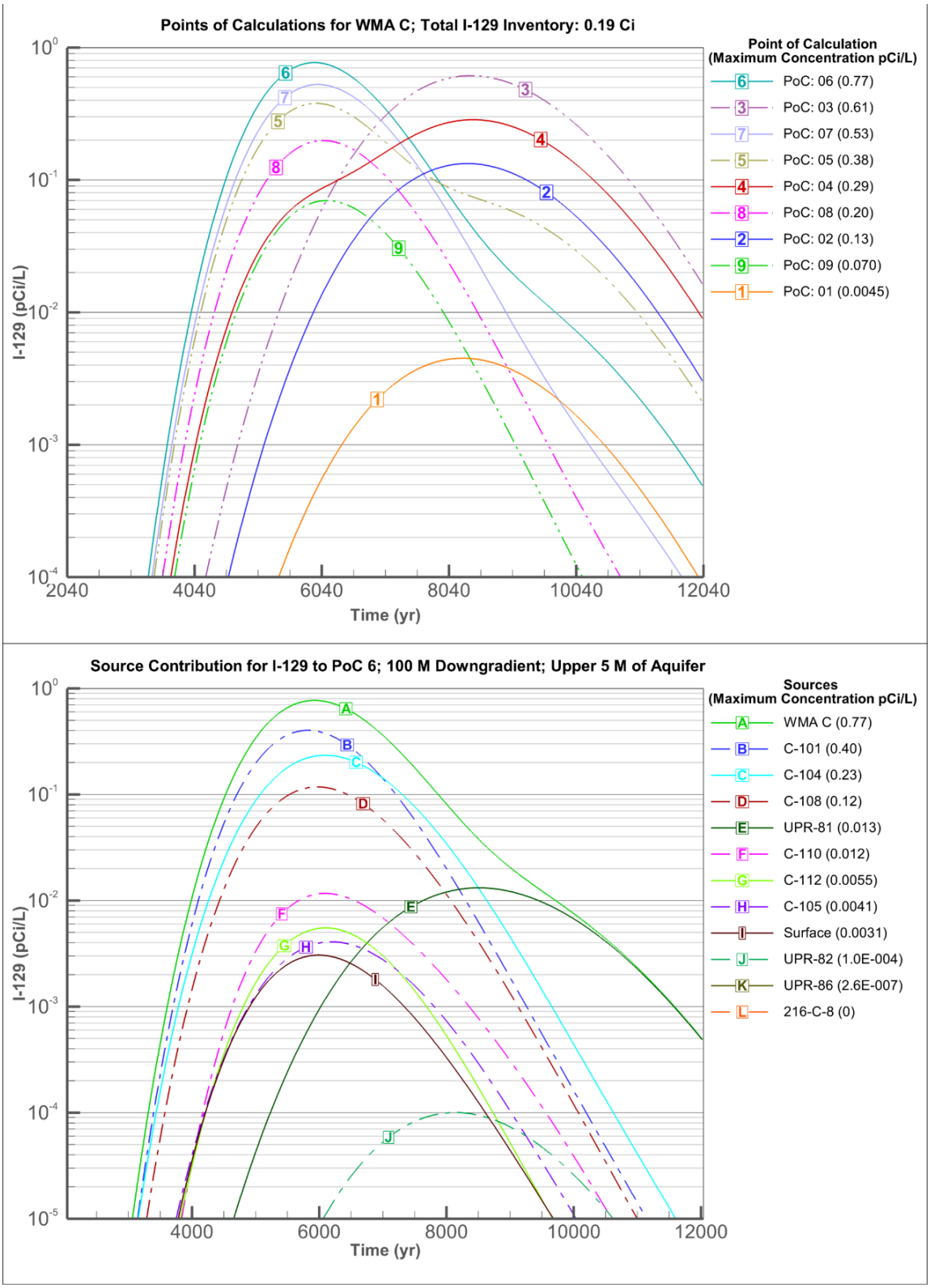

PoC = point of calculation WMA = Waste Management Area

The calculated concentration of ^{126}Sn reaches a peak 10,000 years after the assumed closure of WMA C in 2020. The maximum concentration 100 m downgradient of the fenceline at this time is 0.5 pCi/L at PoCal 6 (Figure 6-19). Neither the concentration of ^{238}U or total uranium reach a peak within 10,000 years after the assumed closure of WMA C. Both of the trends are increasing at the end of the evaluation period. The maximum concentration of ^{238}U remains less than 0.01 pCi/L (Figure 6-20), and the concentration of total uranium reaches a maximum value of ~0.02 µg/L (Figure 6-21). Similar to ^{99}Tc and other non-sorbing radionuclides and non-radiological contaminants, the maximum concentration of ^{238}U and total uranium 100 m downgradient of the WMA C fenceline represent an ~25% reduction in concentration from the fenceline values (Figures 6-22 and 6-23, respectively). Table 6-5 provides a summary of results for those radionuclides and non-radiological contaminants that arrive in groundwater at the WMA C fenceline after the assumed date of closure in 2020.

6.3.3 Results of Groundwater Pathway Evaluation: Contaminant Flux to Groundwater

Figures 6-24 through 6-27 show the calculated fluxes of ^{99}Tc, NO_3, ^{79}Se, and ^{238}U from the vadose zone entering groundwater. The source of ^{99}Tc associated with tank C-105 dominates the ^{99}Tc flux to groundwater, especially during the time that the peak concentrations occur in groundwater at PoCal 6 (Figure 6-24). The source associated with tank C-110 provides the second largest flux and is the second largest component of the absolute peak concentration of ^{99}Tc that occurs at PoCal 6 (refer to Figures 6-4 and 6-5). Although the sources of ^{99}Tc associated with UPRs E-86 and E-82 provide the third and fourth largest fluxes, respectively, the plumes in groundwater resulting from the UPRs are offset from PoCal 6 and do not contribute substantially to the concentration calculated there. Tank C-101 is better aligned with PoCal 6 than the UPRs, so although the flux of ^{99}Tc associated with that tank is less than either of those two UPRs, it is the third largest contributor to the peak concentration of ^{99}Tc that occurs at PoCal 6. The arrival of the ^{99}Tc fluxes at the water table from the three UPRs not ascribed to a particular tank (i.e., UPRs E-81, E-82, and E-86) lags the arrival of the flux from tank C-105 because the three UPRs occur after the tank C-105 release and begin at shallower depths in the vadose zone. In addition, UPR E-86 is located outside the tank farm, where the ground is described as resurfaced and the net infiltration (63 mm/yr) is less than the amount in the tank farm gravel (100 mm/yr).

As indicated back in Figure 6-10, the concentration of nitrate reaches its absolute peak value at PoCal 6 in 2017. The sources of nitrate associated with the six tank-ascribed UPRs are the six largest contributors to the peak concentration, even though the source and flux associated with UPR-81 is larger than any of those associated with the tanks (Figure 6-25). The proximity of the tank-ascribed UPRs to one another and their alignment with PoCal 6 result in comingling of the sources and fluxes. The relative peak that occurs later in 2030 at PoCal 3 is almost solely a consequence of the source associated with UPR-81, and the nitrate flux associated with UPR-81 is almost entirely responsible for producing the concentration calculated at PoCal 3.

Figure 6-19. Concentration of Tin-126 in Groundwater in the Points of Calculation 100 Meters Downgradient of the Fenceline.

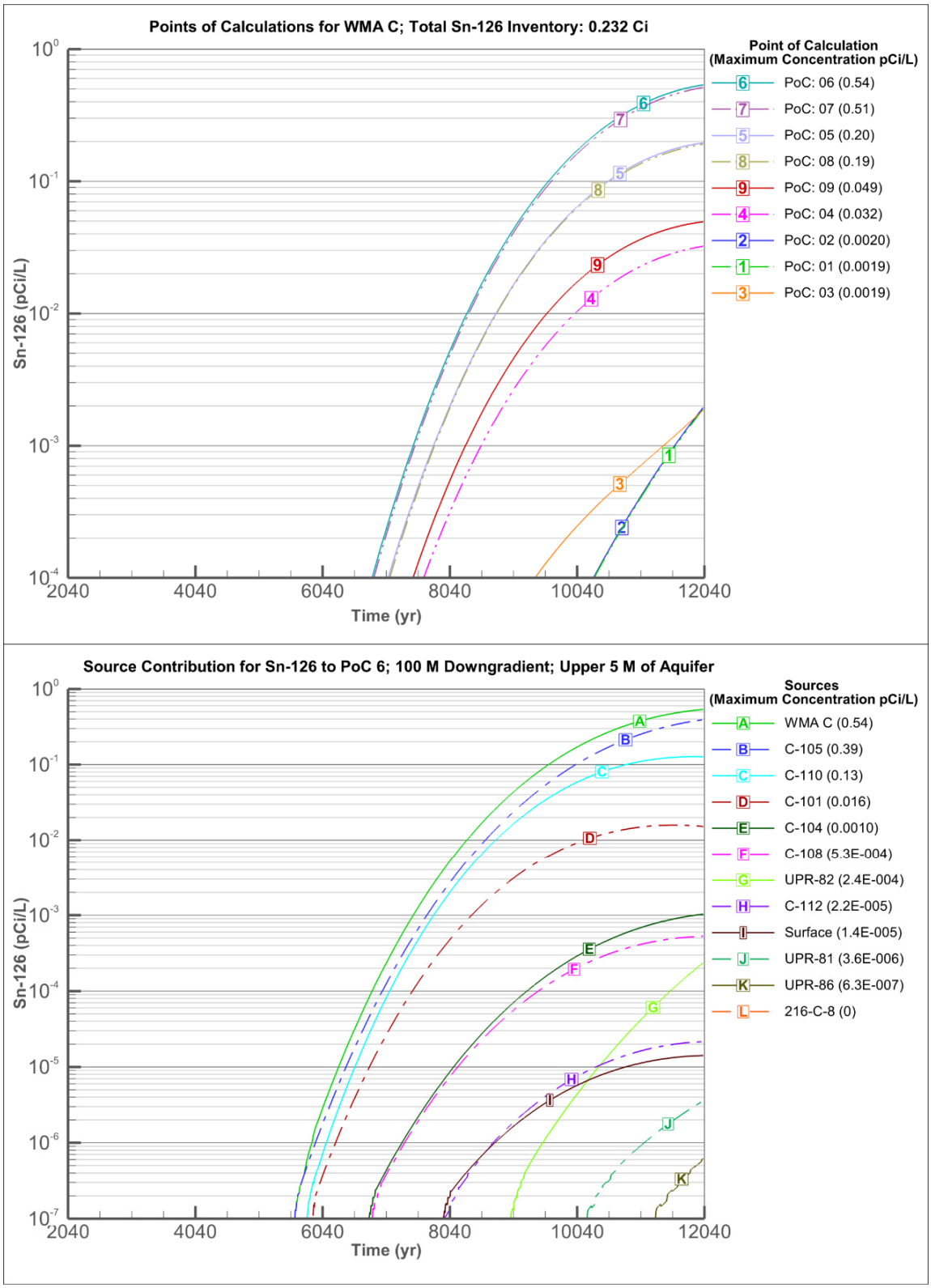

PoC = point of calculation WMA = Waste Management Area

Figure 6-20. Concentration of Uranium-238 in Groundwater in the Points of Calculation 100 Meters Downgradient of the Fenceline.

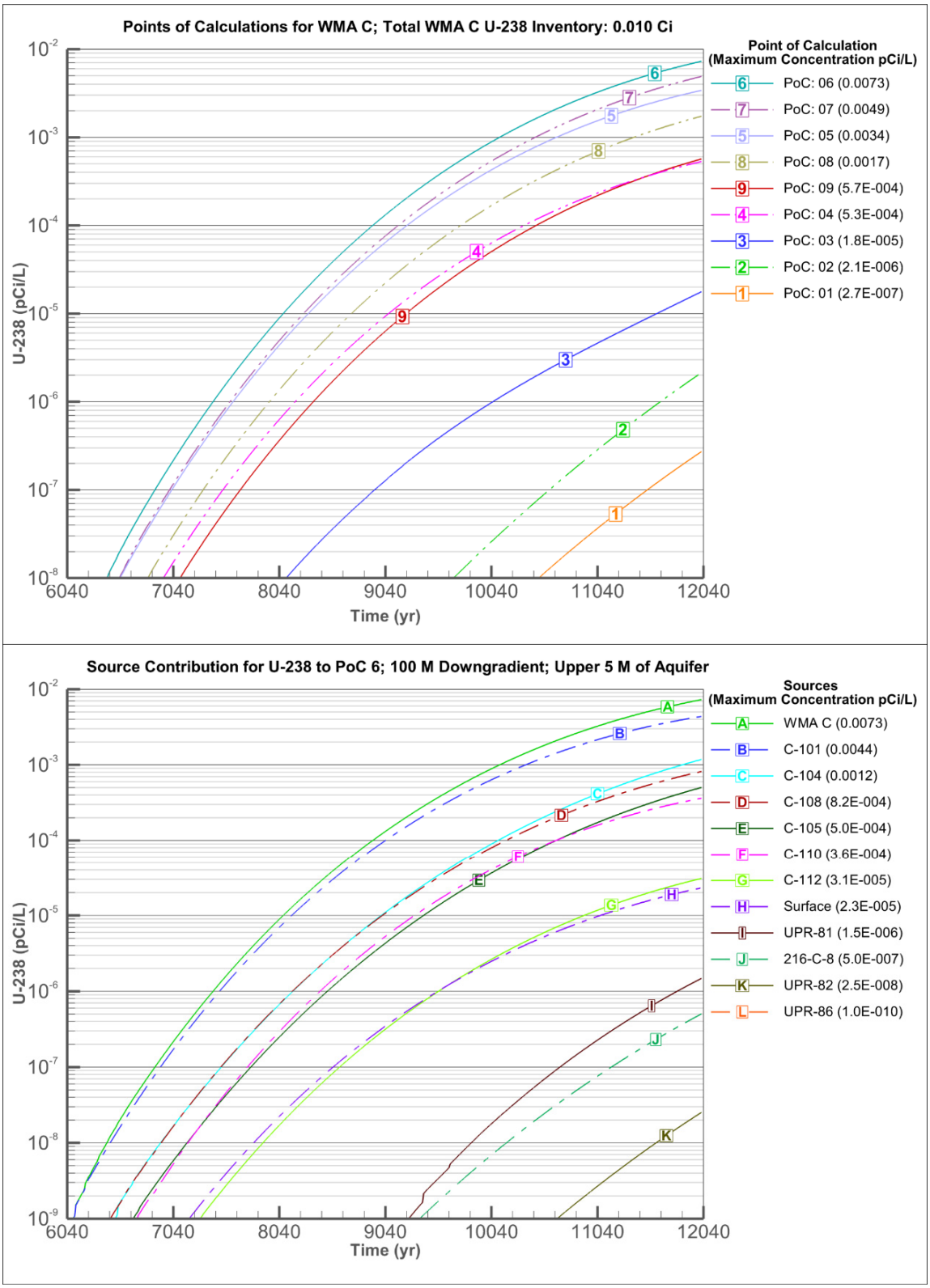

PoC = point of calculation WMA = Waste Management Area

Figure 6-21. Concentration of Total Uranium in Groundwater in the Points of Calculation 100 Meters Downgradient of the Fenceline.

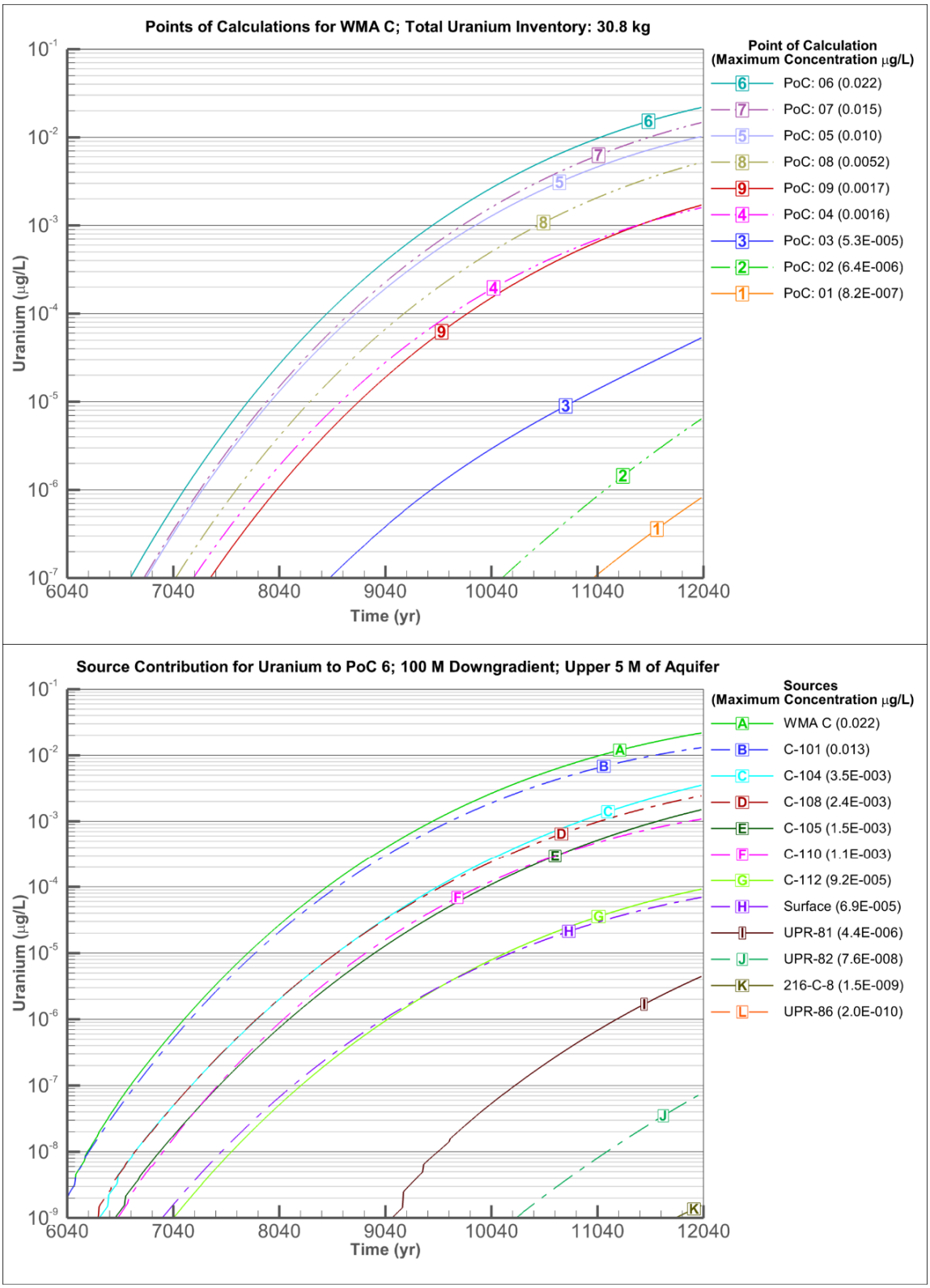

PoC = point of calculation WMA = Waste Management Area

Figure 6-22. Concentration of Uranium-238 in Groundwater in the Points of Calculation at the Fenceline.

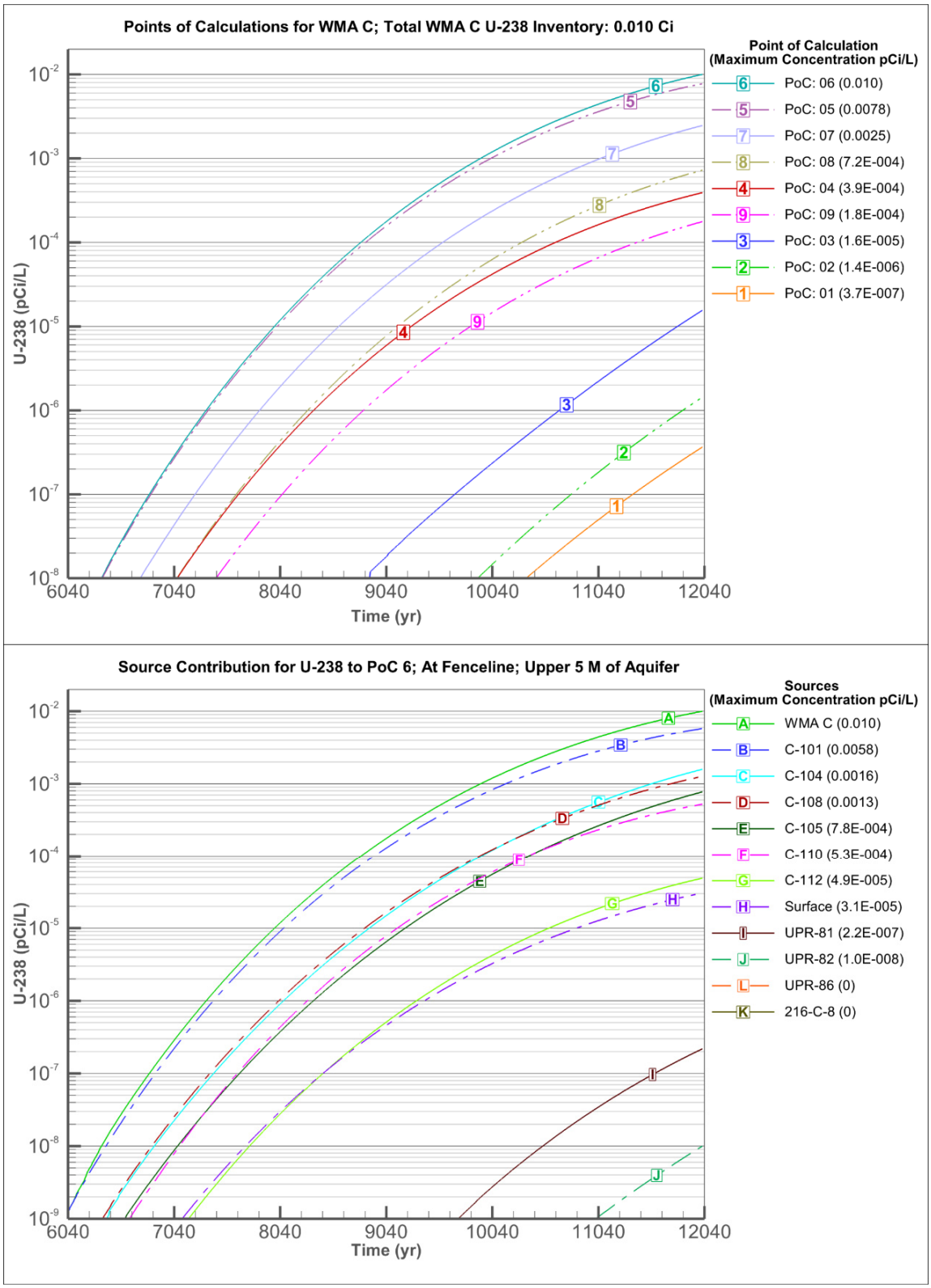

PoC = point of calculation WMA = Waste Management Area

Figure 6-23. Concentration of Total Uranium in Groundwater in the Points of Calculation at the Fenceline.

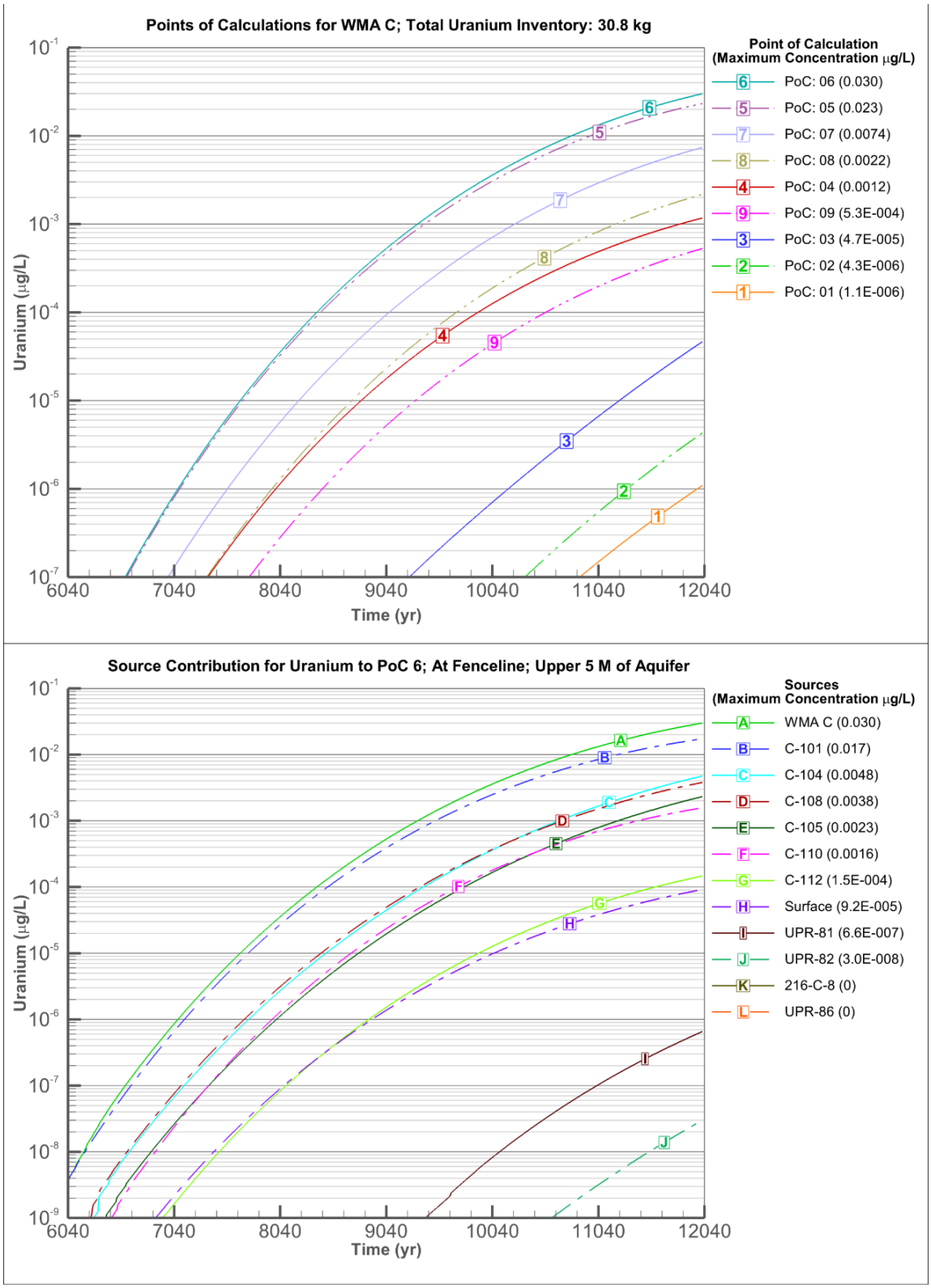

PoC = point of calculation WMA = Waste Management Area

Table 6-5. Summary Results of Radionuclides and Non-Radiological Contaminants that Arrive in Groundwater at the Waste Management Area C Fenceline after Closure.

	Iodine-129				Tin-126			
	Fenceline		100 Meters Downgradient		Fenceline		100 Meters Downgradient	
	Year of Peak	Peak Concentration (pCi/L)	Year of Peak	Peak Concentration (pCi/L)	Year of Peak	Peak Concentration (pCi/L)	Year of Peak	Peak Concentration (pCi/L)
PoCal 1	8020	0.002	8260	0.005	12020	0.003	12020	0.002
PoCal 2	8310	0.1	8330	0.1	12020	0.001	12020	0.002
PoCal 3	8380	0.9	8380	0.6	12020	0.001	12020	0.002
PoCal 4	8400	0.09	8420	0.3	12020	0.03	12020	0.03
PoCal 5	5910	0.8	5950	0.4	12020	0.3	12020	0.2
PoCal 6	5920	1	5920	0.8	12020	0.8	12020	0.5
PoCal 7	6060	0.3	5980	0.5	12020	0.3	12020	0.5
PoCal 8	6130	0.09	6060	0.2	12020	0.06	12020	0.2
PoCal 9	6160	0.02	6120	0.07	12020	0.01	12020	0.05
	Uranium-238				Total Uranium			
	Fenceline		100 Meters Downgradient		Fenceline		100 Meters Downgradient	
Year of Peak	Year of Peak	Peak Concentration (pCi/L)	Year of Peak	Peak Concentration (pCi/L)	Year of Peak	Peak Concentration (mg/L)	Year of Peak	Peak Concentration (pCi/L)
PoCal 1	12020	0.0000004	12020	0.0000003	12020	0.000001	12020	0.0000008
PoCal 2	12020	0.000001	12020	0.000002	12020	0.000004	12020	0.000006
PoCal 3	12020	0.00002	12020	0.00002	12020	0.00005	12020	0.00005
PoCal 4	12020	0.0004	12020	0.0005	12020	0.001	12020	0.002
PoCal 5	12020	0.008	12020	0.003	12020	0.02	12020	0.01
PoCal 6	12020	0.01	12020	0.007	12020	0.03	12020	0.02
PoCal 7	12020	0.002	12020	0.005	12020	0.007	12020	0.01
PoCal 8	12020	0.0007	12020	0.002	12020	0.002	12020	0.005
PoCal 9	12020	0.0002	12020	0.0006	12020	0.0005	12020	0.002

Figure 6-24. Flux of Technetium-99 from the Vadose Zone that Enters Groundwater.

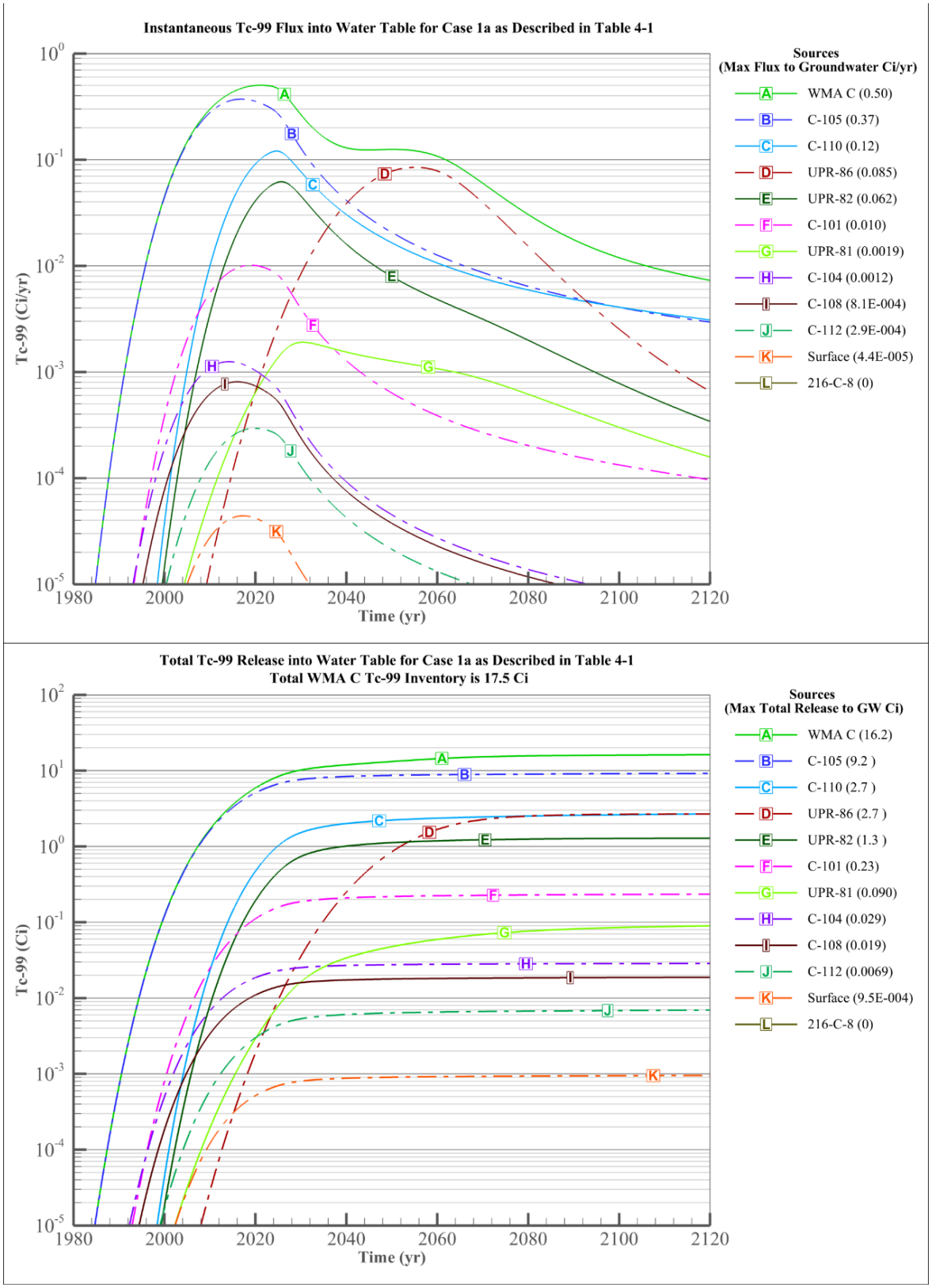

WMA = Waste Management Area

Figure 6-25. Flux of Nitrate from the Vadose Zone that Enters Groundwater.

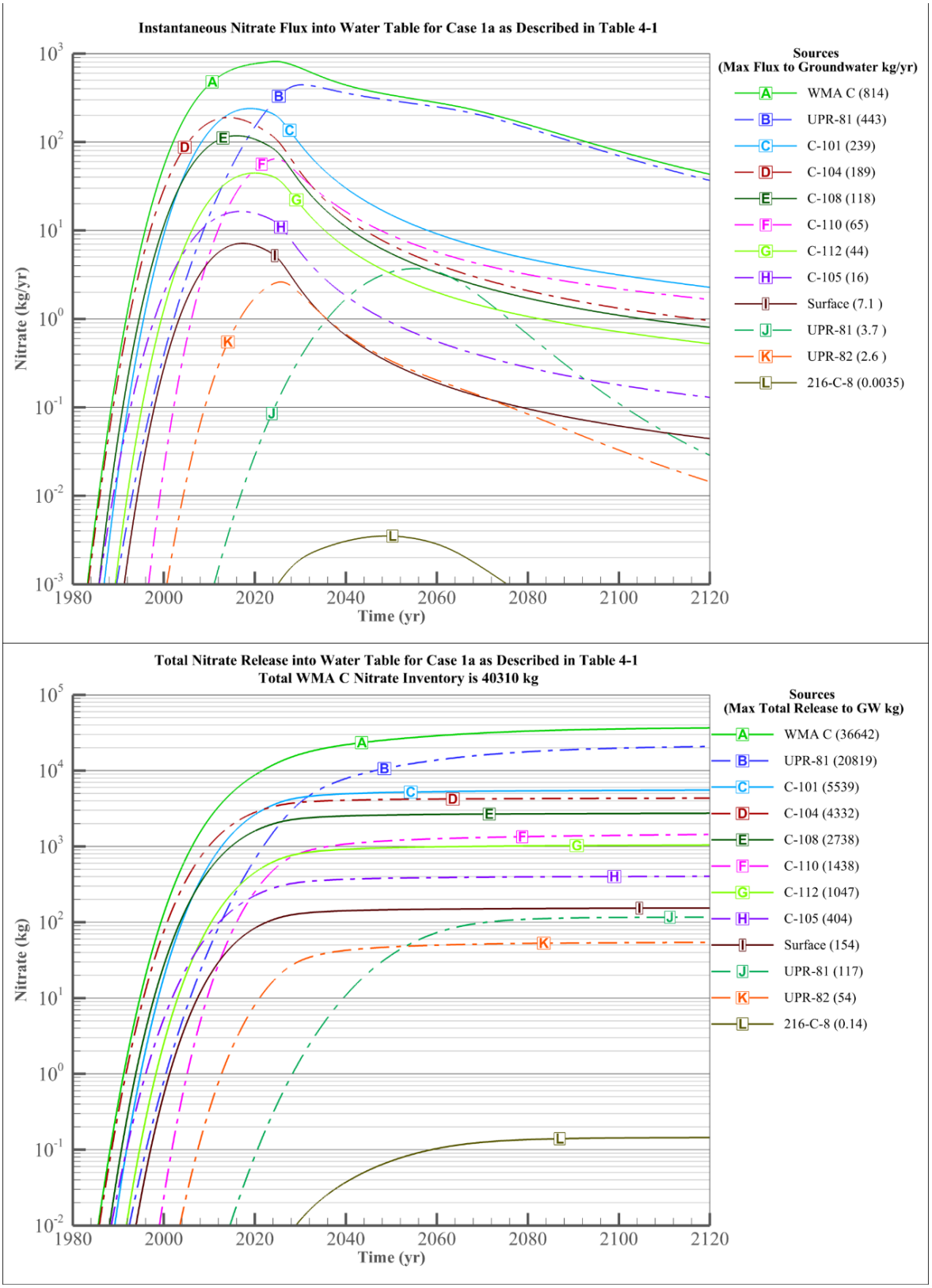

WMA = Waste Management Area

Figure 6-26. Flux of Selenium-79 from the Vadose Zone that Enters Groundwater.

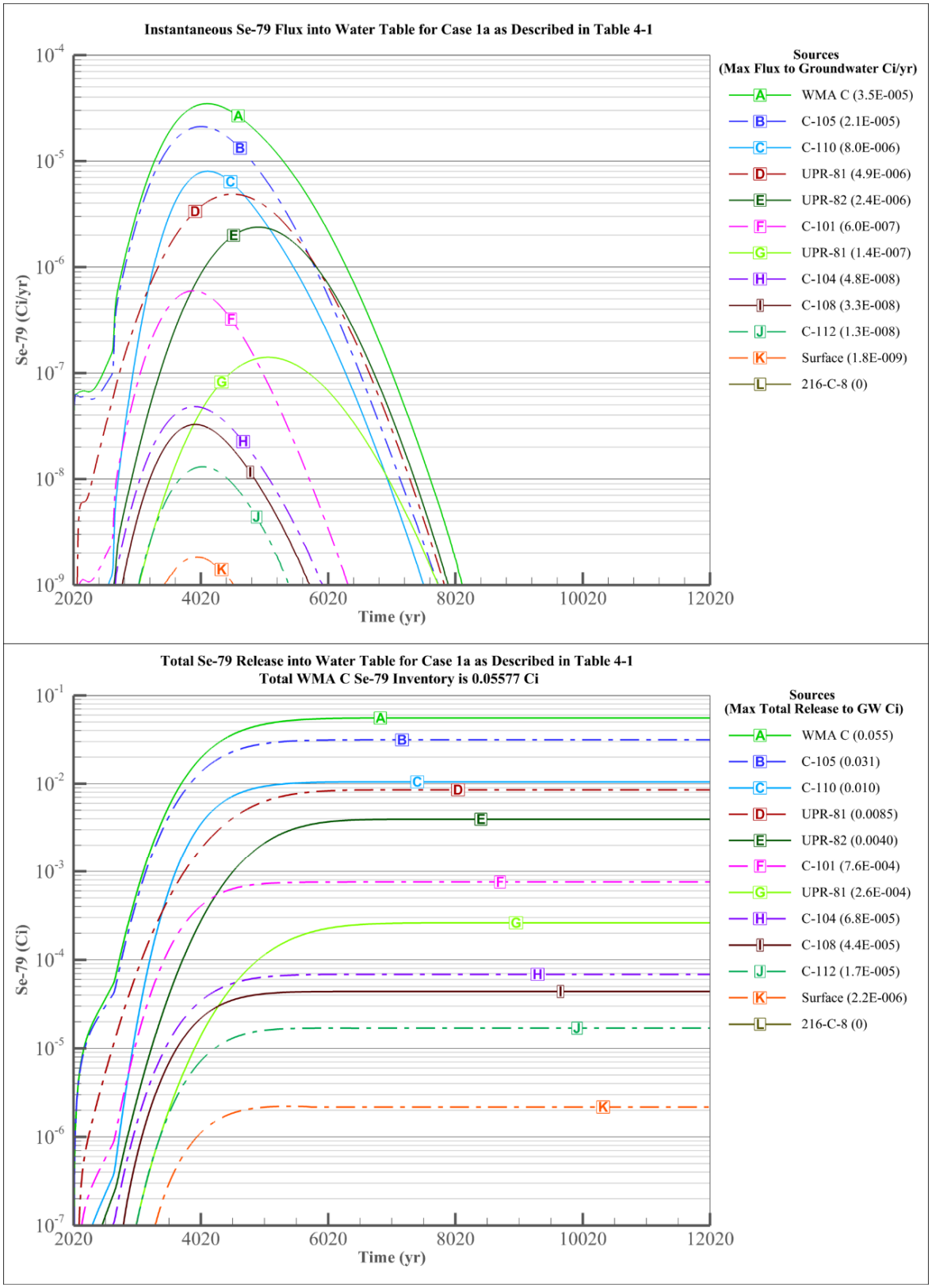

WMA = Waste Management Area

Figure 6-27. Flux of Uranium-238 from the Vadose Zone that Enters Groundwater.

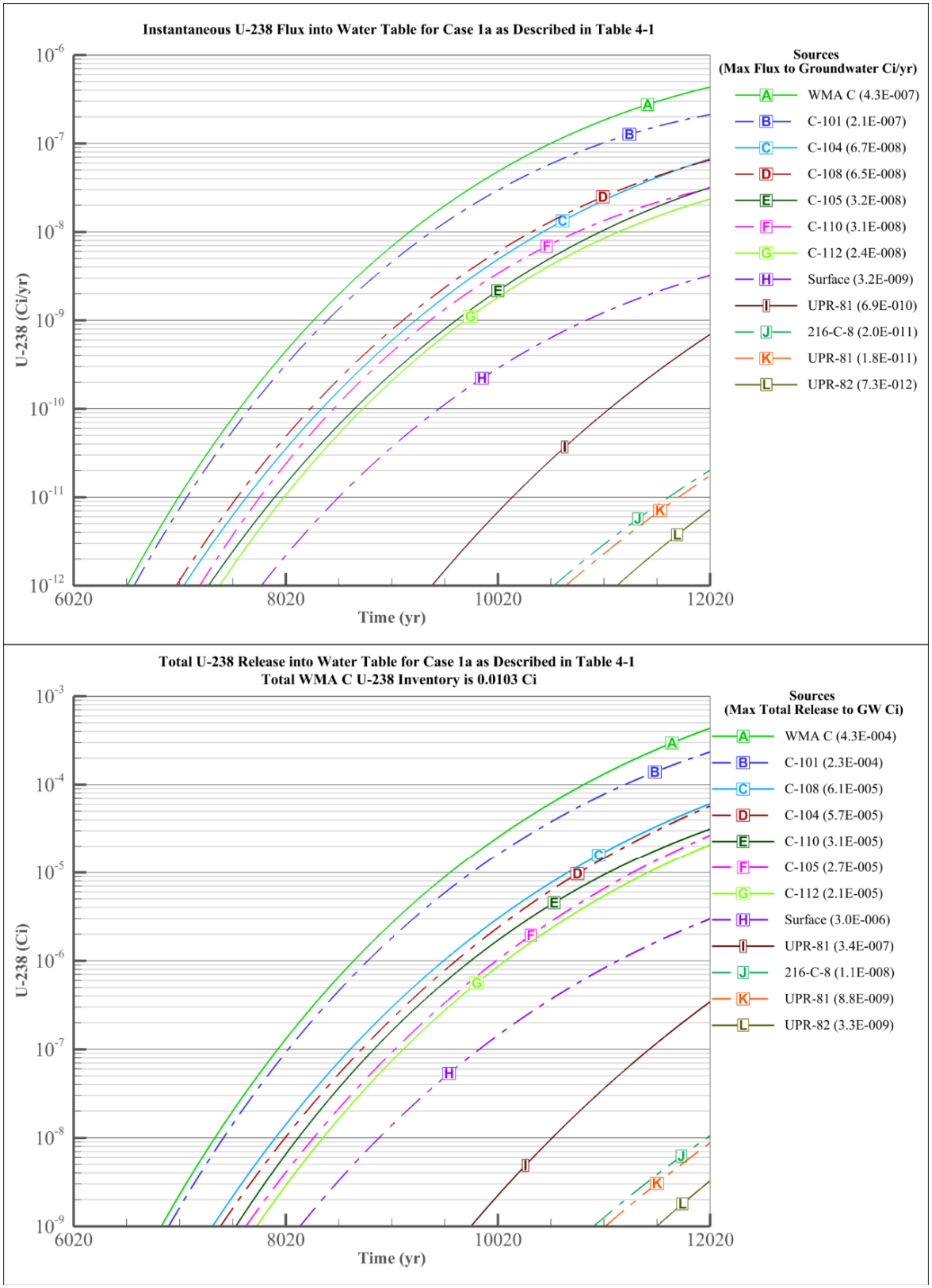

WMA = Waste Management Area

The source of ^{79}Se associated with tank C-105 dominates the ^{79}Se fluxes to groundwater, especially during the time that the peak concentrations occur in groundwater at PoCals 6 and 7 (Figure 6-26). The ^{79}Se breakthrough curves for PoCals 6 and 7 are nearly identical (refer to Figure 6-9). The source associated with tank C-110 provides the second largest flux and is the second largest component of the absolute peak concentration of ^{99}Tc that occurs at both PoCal 6 and PoCal 7. The flux of ^{79}Se associated with tank C-105 is responsible for about 75% of the total flux and resulting concentration at PoCals 6 and 7. Together, the sources of ^{79}Se associated with tanks C-105 and C-110 provide more than 95% of the total flux and resulting concentration at PoCals 6 and 7.

As indicated back in Figure 6-20, the concentration of ^{238}U does not reach its maximum value at any of the PoCals until the end of the simulation period 10,000 years after the assumed closure date of WMA C. The absolute peak concentration likely occurs after this time. Similarly, the flux of ^{238}U to groundwater does not reach its maximum value until the end of the simulation period (Figure 6-27). The source of ^{238}U associated with tank C-101 is the largest component of the flux of ^{238}U to groundwater, and by itself is responsible for approximately half of the ^{238}U that enters groundwater. The next two largest fluxes indicated by Figure 6-27 result from the UPRs associated with tanks C-104 and C-108, but the magnitude of these flux values is approximately one-third that of the maximum flux resulting from the tank C-101 UPR.

6.4 DISCUSSION OF MONITORING RESULTS WITH PROJECTED MODELING RESULTS FOR NITRATE, SULFATE, AND CHROMIUM

Nitrate and sulfate plumes existed in the groundwater around WMA C prior to when the WMA C past releases are estimated to have reached the water table. The nitrate and sulfate contamination in the aquifer likely stems from the regional plume that has many sources away from WMA C. Nitrate and sulfate concentrations measured between 1990 and 1997 (data available from prior to 1990 are sparse) in regional wells where impacts from WMA C are unlikely, e.g., wells 299-E26-8, 299-E24-8, and 299-E27-9, range between 5 and 10 mg/L, and 40 and 96 mg/L, respectively. Because of the apparent regional sources of nitrate and sulfate, it is difficult to quantify the nitrate and sulfate impacts caused by the past releases at WMA C or distinguish them from those originating elsewhere.

According to the monitoring data and the modeling results, nitrate and sulfate contained in the past releases from WMA C do not appear to have reached the water table until after 1997. Trends in the nitrate and sulfate concentrations remain relatively stable until the late 1990s when they begin to increase markedly. Technetium-99 appears to be a distinct signature contaminant in groundwater associated with the WMA C past releases because there are no other known nearby sources of ^{99}Tc. Groundwater monitoring results collected from wells surrounding WMA C—299-E27-7, 299-E27-12, 299-E27-13, 299-E27-14, and 299-E27-15—indicate that ^{99}Tc did not arrive at the water table in substantial quantity until after 1997.

Around WMA C, increases in the nitrate and sulfate concentrations coincide with increases in the ^{99}Tc concentration. However, in most wells the nitrate and sulfate concentrations do not decrease when the ^{99}Tc concentration does, or they remain at relatively elevated levels compared

to where they started prior to the arrival of the ^{99}Tc. Although the shifting hydraulic gradient may have directed a different portion of the pre-existing plume toward the monitoring wells, the sustained elevated concentrations of nitrate and sulfate appear to be more indicative of the arrival of a different plume. This different plume appears to have arrived in the area about the same time as when the WMA C past releases initially reached the water table, and consists of relatively high concentrations of nitrate and sulfate with a relatively low concentration of ^{99}Tc.

The arrival at the water table of the source originating from UPR-200-E-81, and its co-mingling with the ^{99}Tc associated with releases from the 100-series tanks, provides an explanation of the nitrate concentrations that have been observed in wells to the south and southwest of WMA C, e.g., 299-E27-13 and 299-E27-23. UPR-200-E-81 is estimated to contain a relatively small quantity of ^{99}Tc and a relatively large quantity of nitrate (RPP-RPT-42294). According to the modeling results, the groundwater concentration of ^{99}Tc that released from the 100-series tanks peaks around year 2019, but the concentration of nitrate that released in UPR-200-E-81 peaks around year 2030. The initial increase in nitrate concentration observed in the monitoring wells surrounding WMA C appears to be attributable to the releases from the 100-series tanks, with the later elevated concentrations sustained by the nitrate contained in UPR-200-E-81. Similar to the ^{99}Tc modeling results, the application of the long-term steady-state gradient appears to cause the magnitude of the modeled nitrate concentrations at the WMA C fenceline (~12 to 13 mg/L) to underestimate the observed concentrations by factors that range from ~2 (well 299-E27-13) to ~8 (well 299-E27-14). The hydraulic gradient during operations reversed, which indicates that it must have decreased, and measurements made during 2005 through 2011 indicate the gradient measured less than one half of the estimated steady-state value while reestablishing a south or southeasterly direction (SGW-54165). As the gradient provides a proportional indicator of the groundwater flux, and the concentration of contaminants in groundwater is generally inversely proportional to the flux, the application of the estimated steady-state gradient in the model likely contributes to the underestimation of contaminant concentrations in the modeling results.

The trends in the sulfate concentrations measured in the monitoring wells around WMA C tend to track very closely with the trends in the nitrate data. The consistency of the correlation between the sulfate and nitrate concentration data almost assuredly indicates common sources of those contaminants. The difference between the magnitude of the modeled sulfate concentrations at the WMA C fenceline (< 1 mg/L) are orders of magnitude less than the increases observed in the measured data between 2000 and 2010. During this time, for example, the concentration of sulfate increases from ~20 mg/L to 120 mg/L in well 299-E27-13, from ~60 mg/L to 180 mg/L in well 299-E27-21, and from ~70 mg/L to 300 mg/L in well 299-E27-14.

The trends in the chromium concentrations measured in the monitoring wells around WMA C do not track very closely with the trends in the nitrate, sulfate, or ^{99}Tc data. Most wells do show an increase in chromium concentration around 2010 relative to the years around it, but the chromium monitoring data present no discernable trend or correlation with the nitrate, sulfate, or ^{99}Tc data. Compared to the years preceding 2010, the chromium concentration in 2010 is ~8 to 10 µg/L greater in wells 299-E27-13, 299-E27-21, 299-E27-23, and 299-E27-14. According to the modeling results, chromium concentrations would be expected to increase by ~76 µg/L, and that is without factoring in the underestimation observed in the concentrations of nitrate and ^{99}Tc. The disparity between the model results and the monitoring data may be attributed to the

modeling assumption that all chromium inventory is and remains hexavalent chromium. Not all of the chromium inventory in the tanks was hexavalent, and much of the hexavalent chromium that may have been released would have reacted with the oxides of iron, aluminum, and manganese due to waste fluid-sediment interactions and become either relatively immobilized or partially reduced to trivalent chromium. Some surface adsorption is also likely due to formation of reactive surfaces from mineral reactions that would occur during neutralization of the waste stream. Trivalent chromium is relatively immobile in the environment; estimates of its distribution coefficient (K_d) typically exceed the 10,000-year screening threshold value established in Section 4 [Washington State Department of Ecology Cleanup Levels and Risk Calculation (CLARC), Queried 08/30/2016, [CLARC Data Tables – July 2015, Chemical Parameters], https://fortress.wa.gov/ecy/clarc/FocusSheets/CLARC%20Parameters.pdf]. Thus, it appears unlikely that chromium contained in the past releases is responsible for the chromium contamination that exists in groundwater.

This page intentionally left blank.

7.0 OTHER SOURCES OF CONTAMINATION AT WASTE MANAGEMENT AREA C

In this section, the forward projections of groundwater concentrations from past leaks are compared to two additional sources that have the potential to impact groundwater under WMA C. These potential sources of contamination are tank residual waste that will be left in tanks and ancillary equipment at a landfill closed WMA C, as discussed in RPP-ENV-58782 and RPP-ENV-58806; and sources of contamination upgradient to WMA C that are contributing to current groundwater contamination in the general vicinity and could impact groundwater at WMA C in the future. This section is intended to put the forward projections of past leaks in context of the broader groundwater contamination conditions now and into the future at WMA C.

7.1 CONTRIBUTION OF CONTAMINATION ASSOCIATED WITH UPGRADIENT SOURCES

In this section, future projections are discussed of the contribution to contamination under WMA C from upgradient sources. It is emphasized that existing evaluations of upgradient contamination assume that there will be no remedial activities undertaken at B Complex. They therefore likely provide significant overestimations of future contamination discharges. Therefore, the results in this section should only be regarded as a qualitative indication of the relative importance of various sources of contamination at WMA C.

The current understanding of groundwater contamination in the vicinity of WMA C has been described in the RI for the 200-BP-5 Groundwater OU (DOE/RL-2009-127 Draft A). The 200-BP-5 OU extends north-northwest from the 200 East Area, across the Hanford Site, to the Columbia River, and includes WMA C (Figure 2-3). The observed groundwater contamination in the 200-BP-5 OU resulted largely from liquid waste generated during the operational period of B Plant and associated facilities within the northern portion of the 200 East Area (DOE/RL-2009-127 Draft A).

The most recent interpretation (2013) of the groundwater plumes in the 200-BP-5 OU is shown in Figure 7-1. The figure shows the regions in which the plumes exceed their drinking water standard; lower levels of contamination exist in wider regions than shown on the map. The groundwater plumes and data were further implemented (DOE/RL-2009-127 Draft A) in a model designated P2R, which allows the evaluation of the time dependence of plumes arriving at WMA C. A complete description of the P2R model is provided in CP-57037, “Model Package Report: Plateau to River Groundwater Transport Model Version 7.1,” and its application to simulate contaminant fate and transport for the scenarios is detailed in ECF-Hanford-13-0031. A summary of the model and its results is presented in DOE/RL-2009-127 Draft A.

Results of the P2R model have been used to provide estimates of the contribution of upgradient sources at WMA C. The basis for this discussion is the remedial evaluation case described in ECF-Hanford-15-0011, “Evaluation of Contaminant Transport for the 200-BP-5 and 200-PO-1 Operable Units Feasibility Study Evaluation of Remedial Alternatives,” Draft A. The remedial

evaluation case provides a baseline set of simulation results that can be used to compare subsequent simulations in order to assess treatment effectiveness. Key features of the remedial evaluation case for the 200 East Feasibility Study include (ECF-Hanford-15-0011):

- Initial contaminant concentration distributions are based on the average concentrations from the annual report plumes within the boundary of each computational cell
- No continuing source is considered for cyanide and ^{129}I
- A continuing source is considered for NO_3, ^{99}Tc and ^{238}U
- Discharge from TEDF is assumed to occur.

Results of the remedial evaluation case for contaminants of concern are presented in Figures 7-2 to 7-12. The peak values of these curves are summarized in Table 7-1. Depictions of the calculated future plumes from upgradient sources are presented in Appendix B.

7.1.1 Technetium-99

The P2R model (DOE/RL-2009-127 Draft A) was used to simulate the evolution of the ^{99}Tc plume forward in time, beginning at year 2015. The results of the analysis are shown in Figures 7-2 to 7-5. The figures show a high concentration plume of ^{99}Tc under B Complex at the beginning of the simulation, part of which moves in the direction of WMA C, while part discharges through Gable Gap. A second source of ^{99}Tc in the analysis is that associated with leaks from WMA C. Over the next ~20 years the plume moves with groundwater past WMA C, leading to a period of high ^{99}Tc concentration beginning in about 2020 and lasting until about 2035. Following that time the concentrations decrease continuously in time.

The time dependence of the ^{99}Tc contamination from upstream sources is shown in Figure 7-6. The peak concentration of about 1,400 pCi/L is at the present day or the near future with a second lower peak around 2060.

7.1.2 Nitrate

The P2R model was used to simulate the evolution of the nitrate plume forward in time, beginning at year 2015. The results of the analysis are shown in Figures 7-7 to 7-10. The figures show a high concentration plume of nitrate under B Complex at the beginning of the simulation, part of which moves in the direction of WMA C, while part discharges through Gable Gap. Over the next ~20 years the plume moves with groundwater past WMA C, leading to a period of high nitrate concentration beginning in about 2020 and lasting until about 2035. Following that time the nitrate concentrations decrease continuously in time.

The time dependence nitrate contamination from upstream sources is shown in Figure 7-11. The peak concentration of about 130 mg/L is at the present day or the near future.

Figure 7-1. 2013 200-BP-5 Operable Unit Consolidated Plume Map.

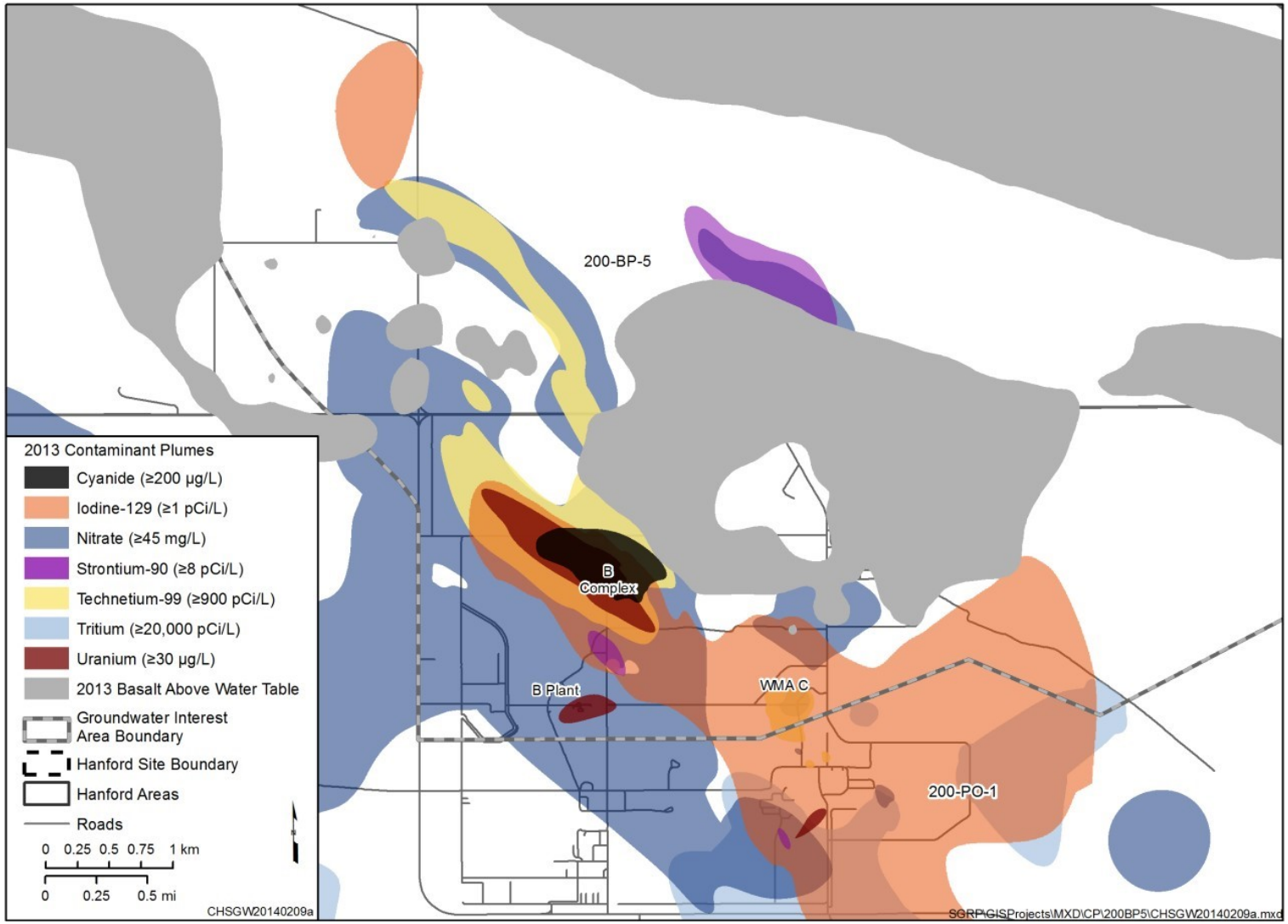

WMA = Waste Management Area

Source: DOE/RL-2009-127, Remedial Investigation Report for the 200-BP-5 Groundwater Operable Unit, Draft A.

Figure 7-2. The Technetium-99 Plume at Year 2015 (Year 0 of the Simulation) for the Remedial Evaluation Case of 200-BP-5.

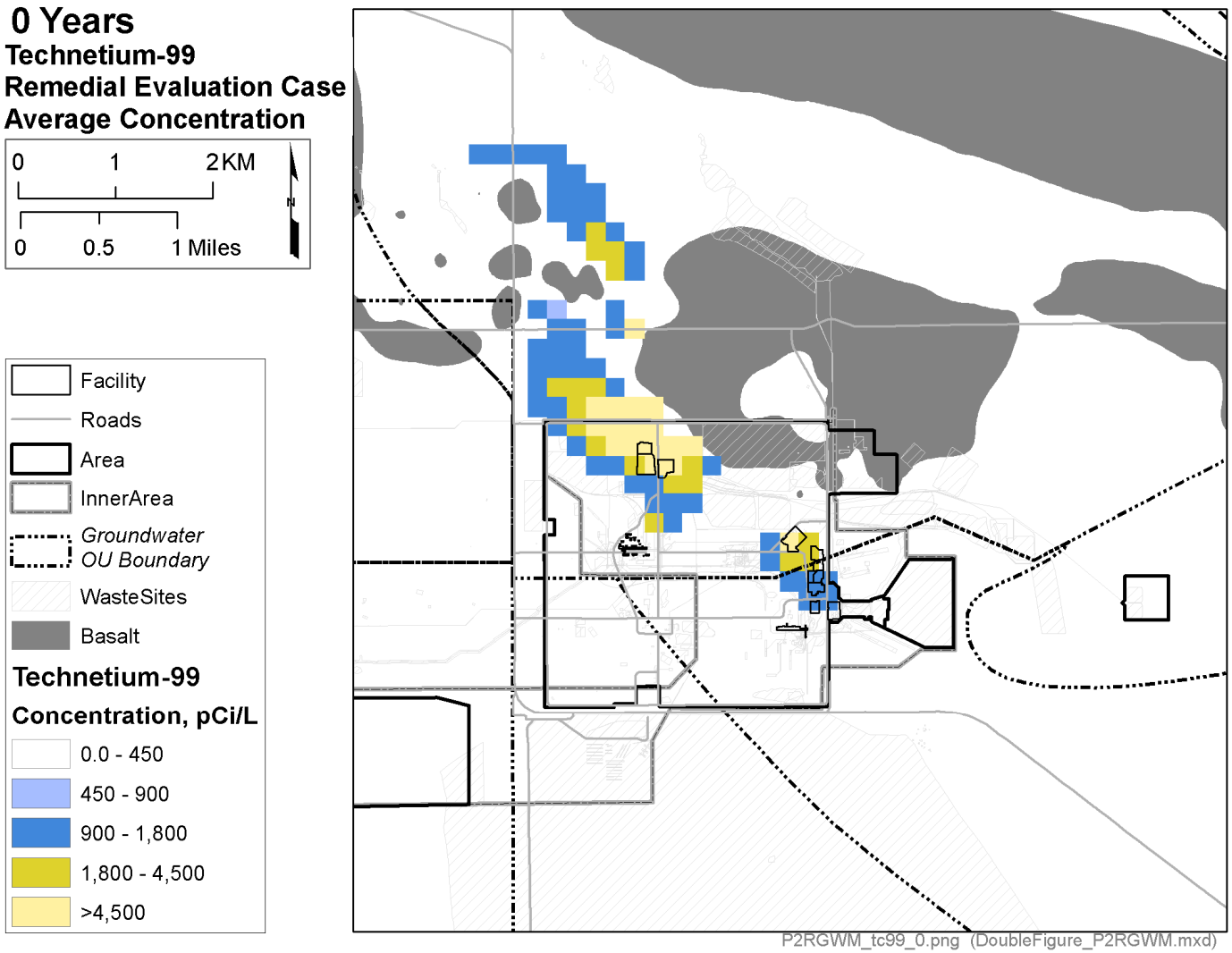

OU = operable unit

Note: The higher concentrations (yellow contours) are both upgradient from Waste Management Area C in the B Complex area and under Waste Management Area C.

Figure 7-3. The Technetium-99 Plume at Year 2020 (Year 5 of the Simulation) for the Remedial Evaluation Case of 200-BP-5.

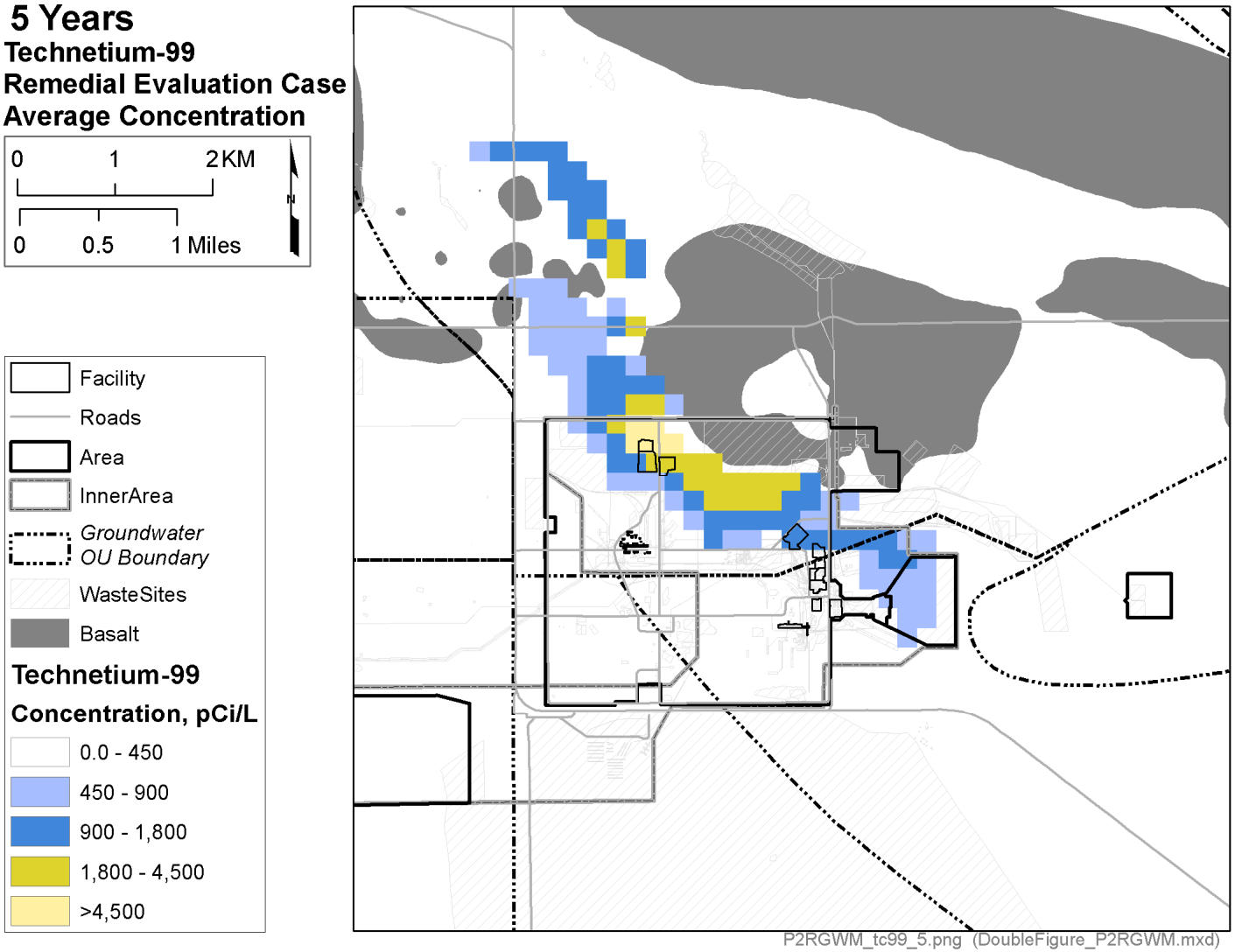

OU = operable unit

Note: The higher concentrations (yellow contours) from B Complex have moved significantly toward Waste Management Area C.

Figure 7-4. The Technetium-99 Plume at Year 2025 (Year 10 of the Simulation) for the Remedial Evaluation Case of 200-BP-5.

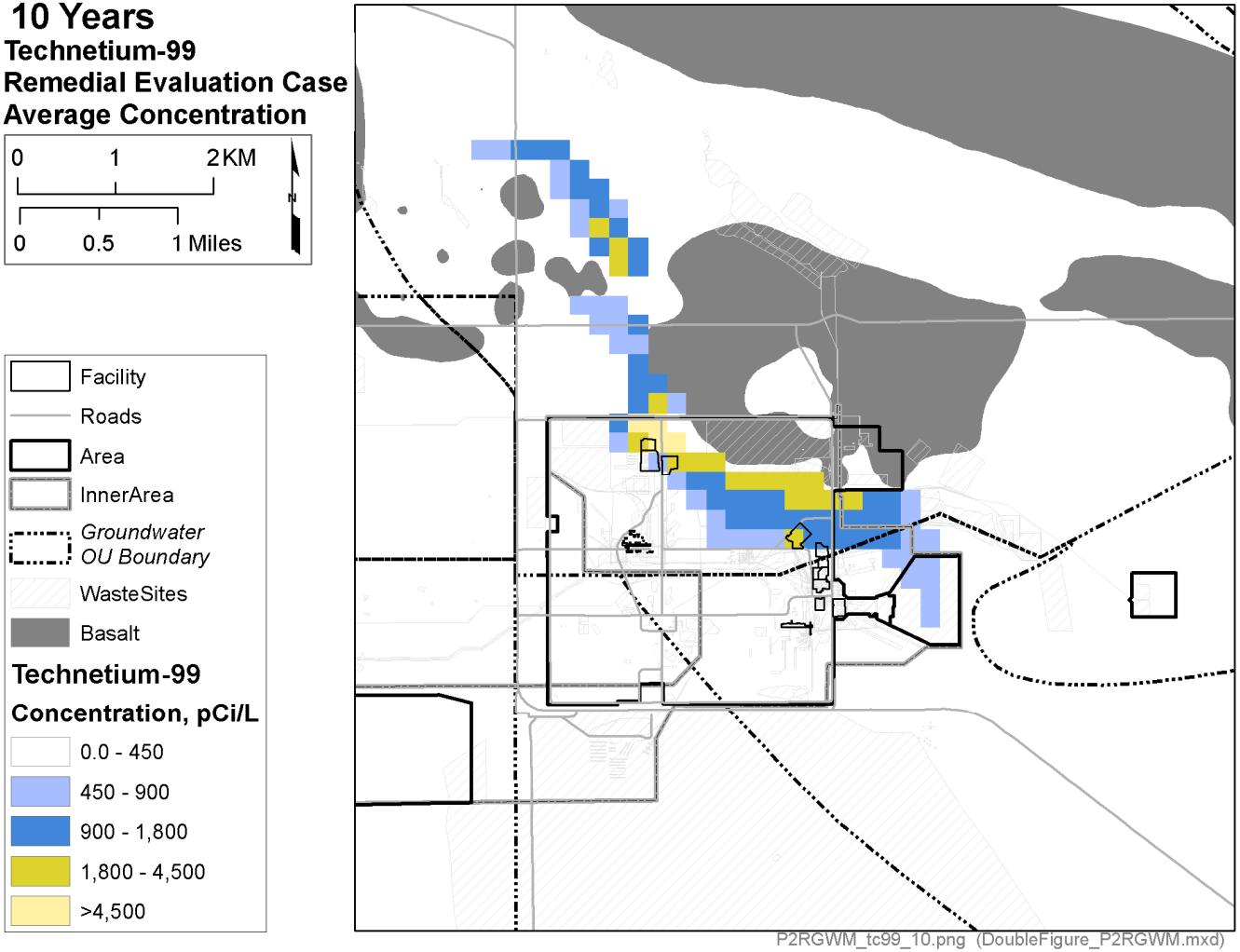

OU = operable unit

Note: Yellow higher concentration contour has moved to the vicinity of Waste Management Area C, but has remained slightly north of Waste Management Area C.

Figure 7-5. The Technetium-99 Plume at Year 2035 (Year 20 of the Simulation) for the Remedial Evaluation Case of 200-BP-5.

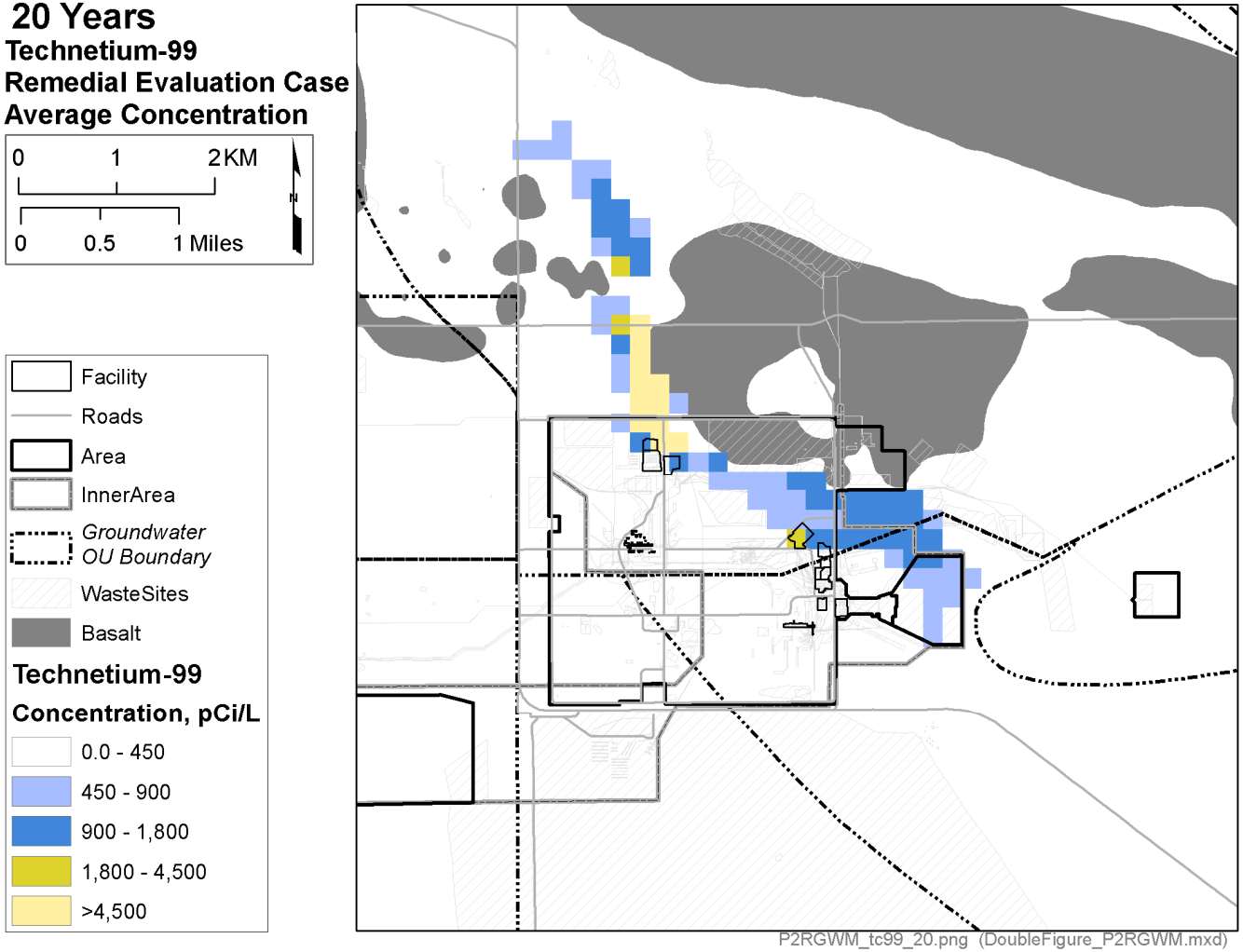

OU = operable unit

Note: The center of mass of the higher concentration contour has moved downgradient from Waste Management Area C and has significantly dispersed to the extent that it no longer shows up as a yellow contour.

Figure 7-6. Remedial Evaluation Case Technetium-99 Concentrations at Waste Management Area C as a Function of Time.

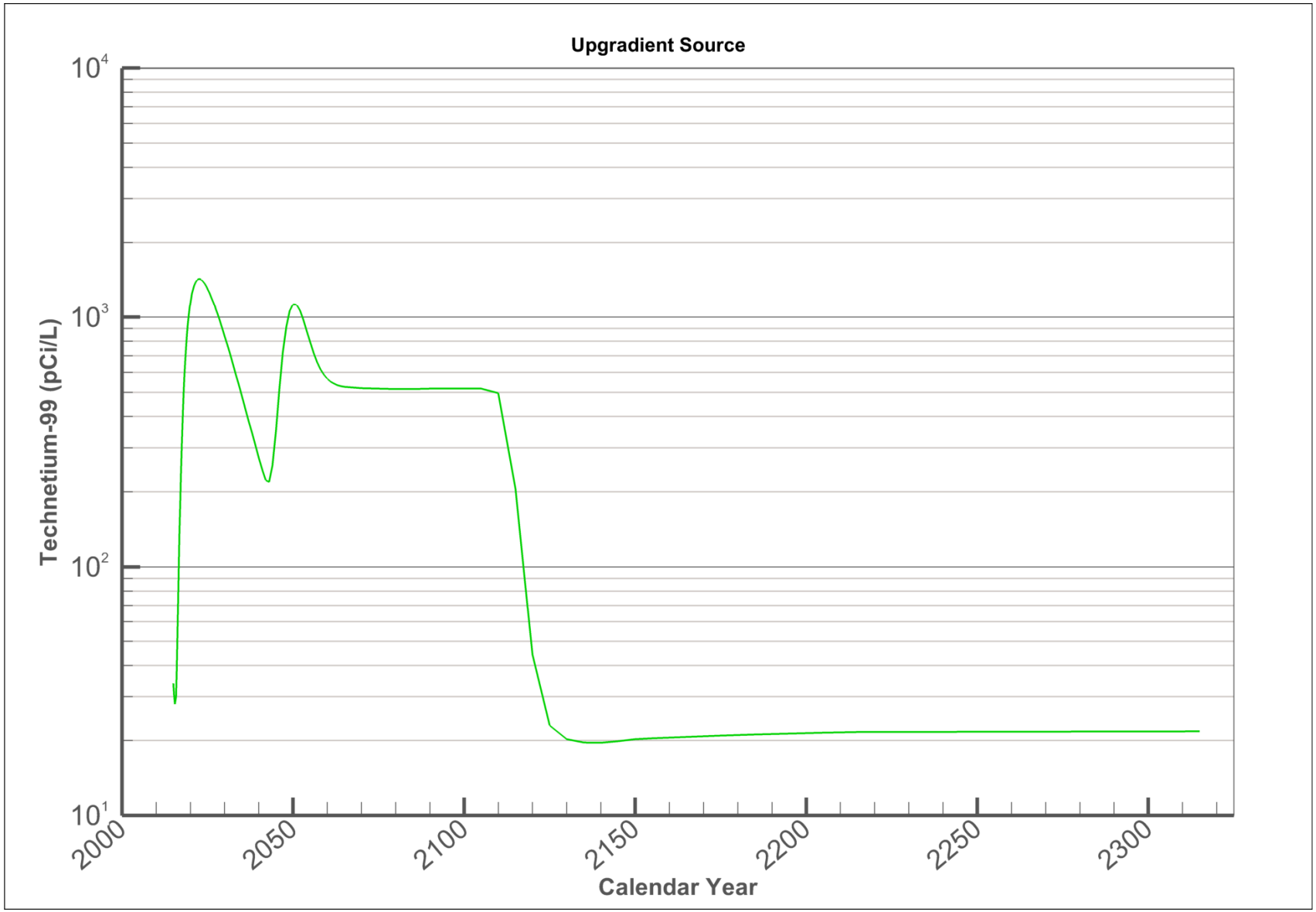

Figure 7-7. The Nitrate Plume at Year 2015 (Year 0 of the Simulation) for the Remedial Evaluation Case of 200-BP-5.

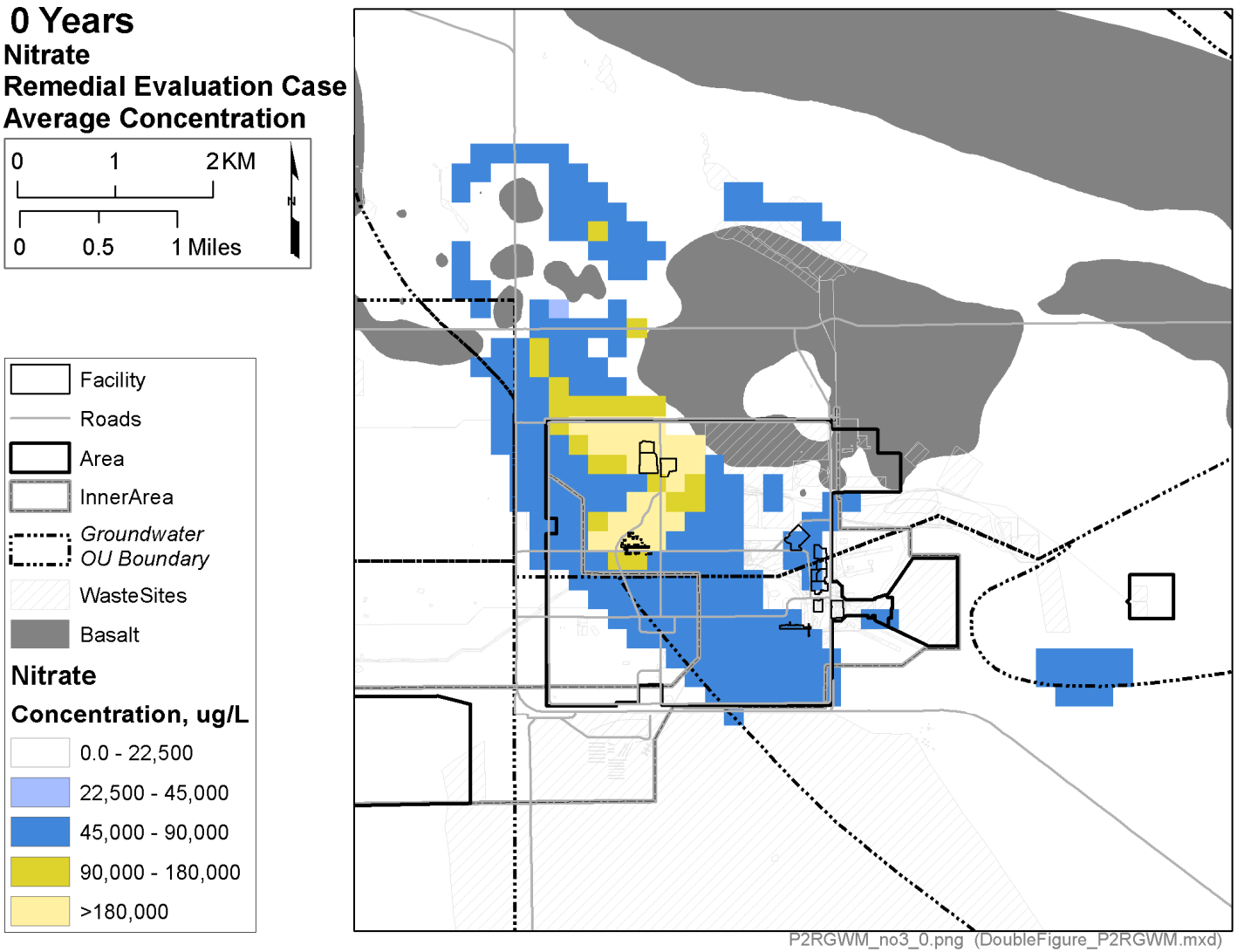

OU = operable unit

Note: The higher concentrations (yellow contours) are entirely upgradient from Waste Management Area C in the B Complex area.

Figure 7-8. The Nitrate Plume at Year 2025 (Year 10 of the Simulation) for the Remedial Evaluation Case of 200-BP-5.

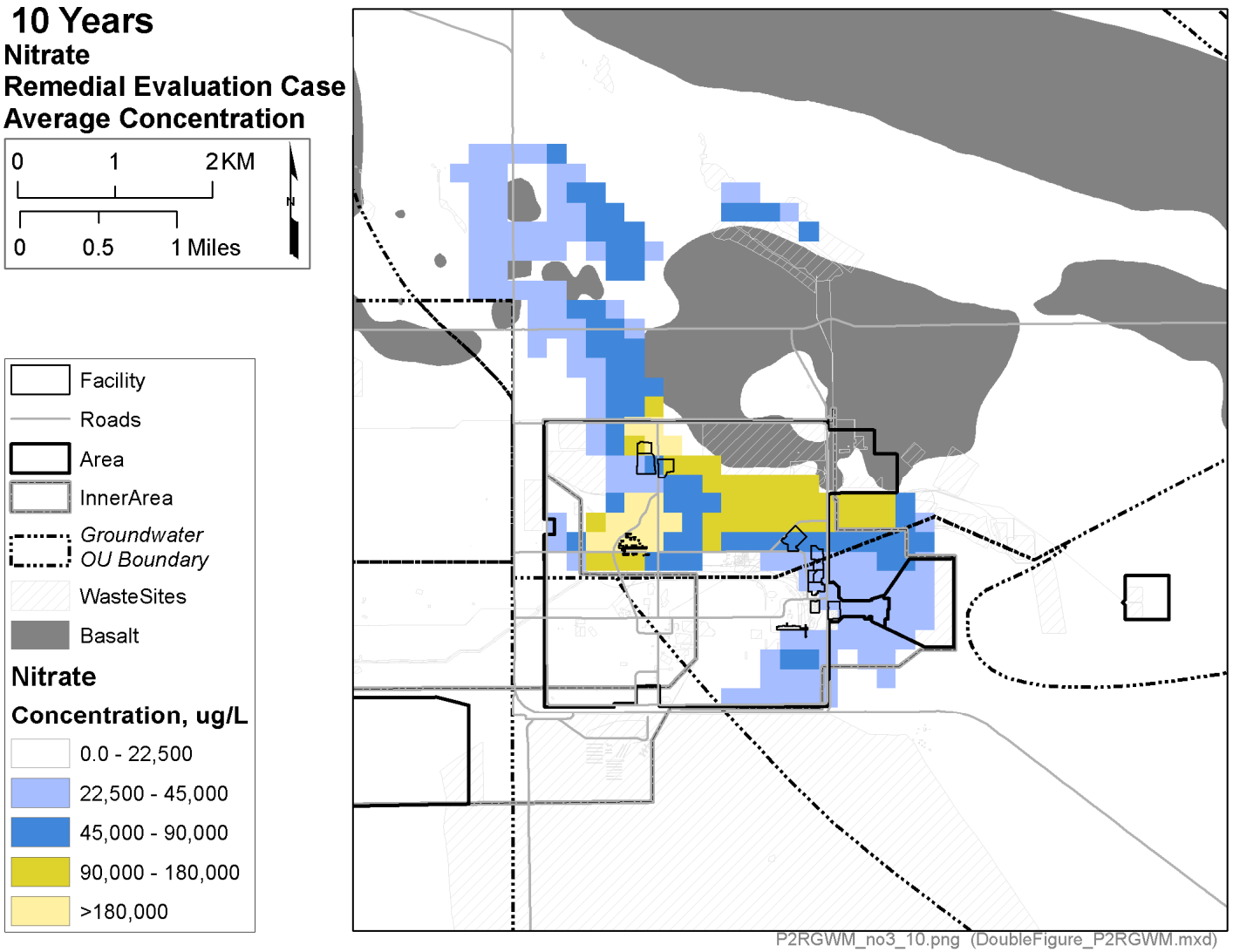

OU = operable unit

Note: The yellow higher concentration contour has moved to the vicinity of Waste Management Area C.

Figure 7-9. The Nitrate Plume at Year 2030 (Year 15 of the Simulation) for the Remedial Evaluation Case of 200-BP-5.

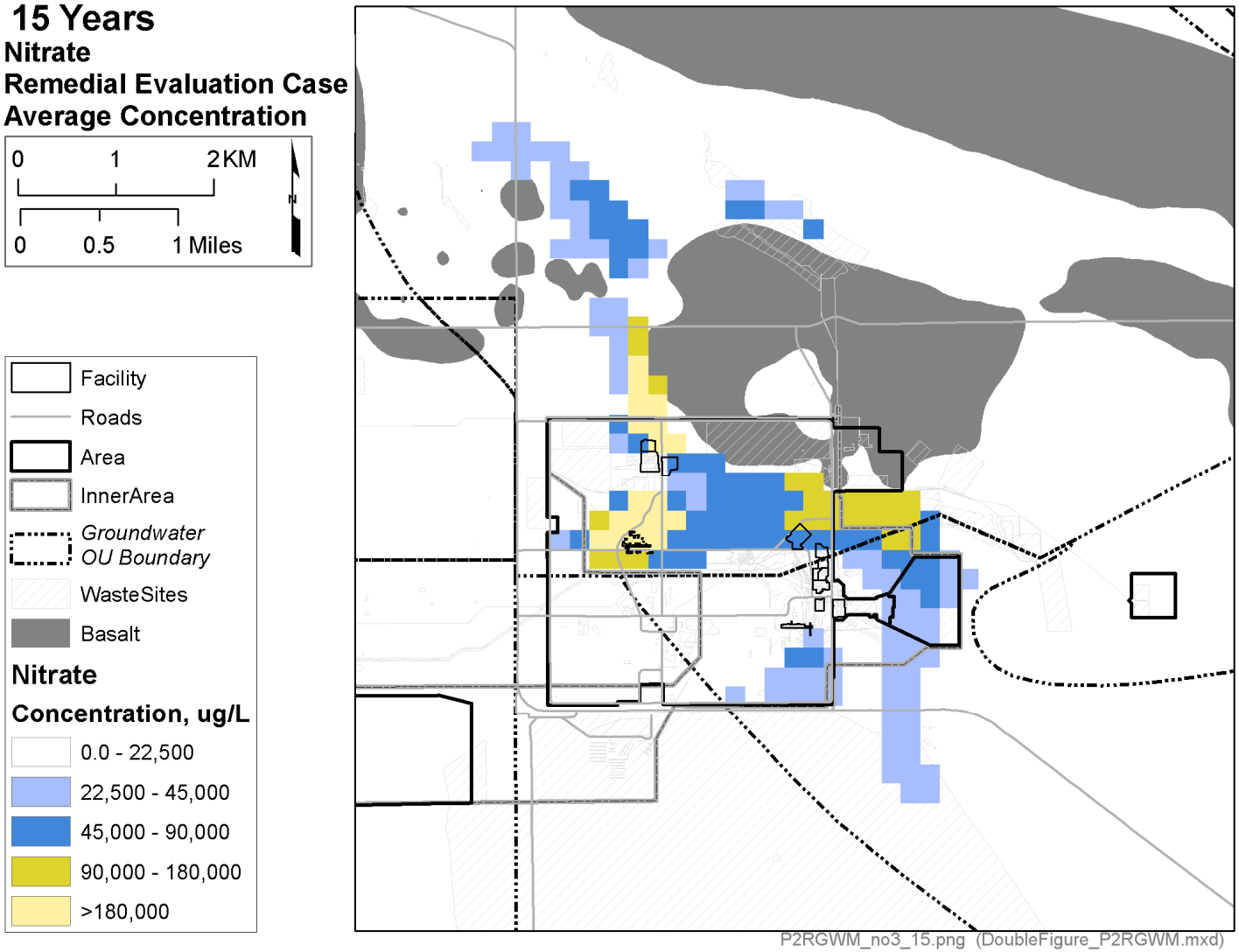

OU = operable unit

Note: The yellow higher concentration contour is predominantly downgradient from Waste Management Area C.

Figure 7-10. The Nitrate Plume at Year 2035 (Year 20 of the Simulation) for the Remedial Evaluation Case of 200-BP-5.

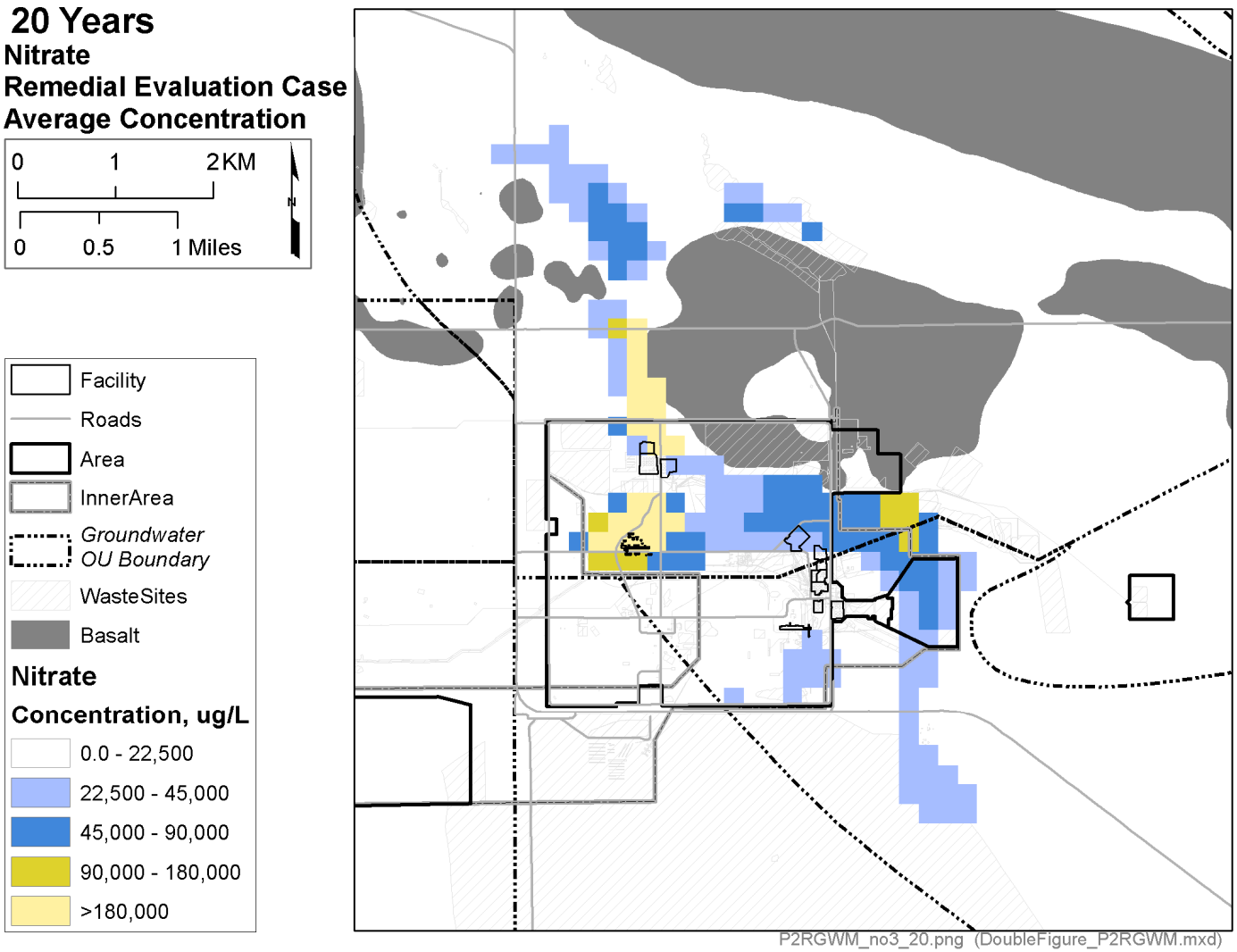

OU = operable unit

Note: The center of mass of the yellow higher concentration contour has moved downgradient from Waste Management Area C and has significantly dispersed.

Figure 7-11. Remedial Evaluation Case Nitrate Concentrations at Waste Management Area C as a Function of Time.

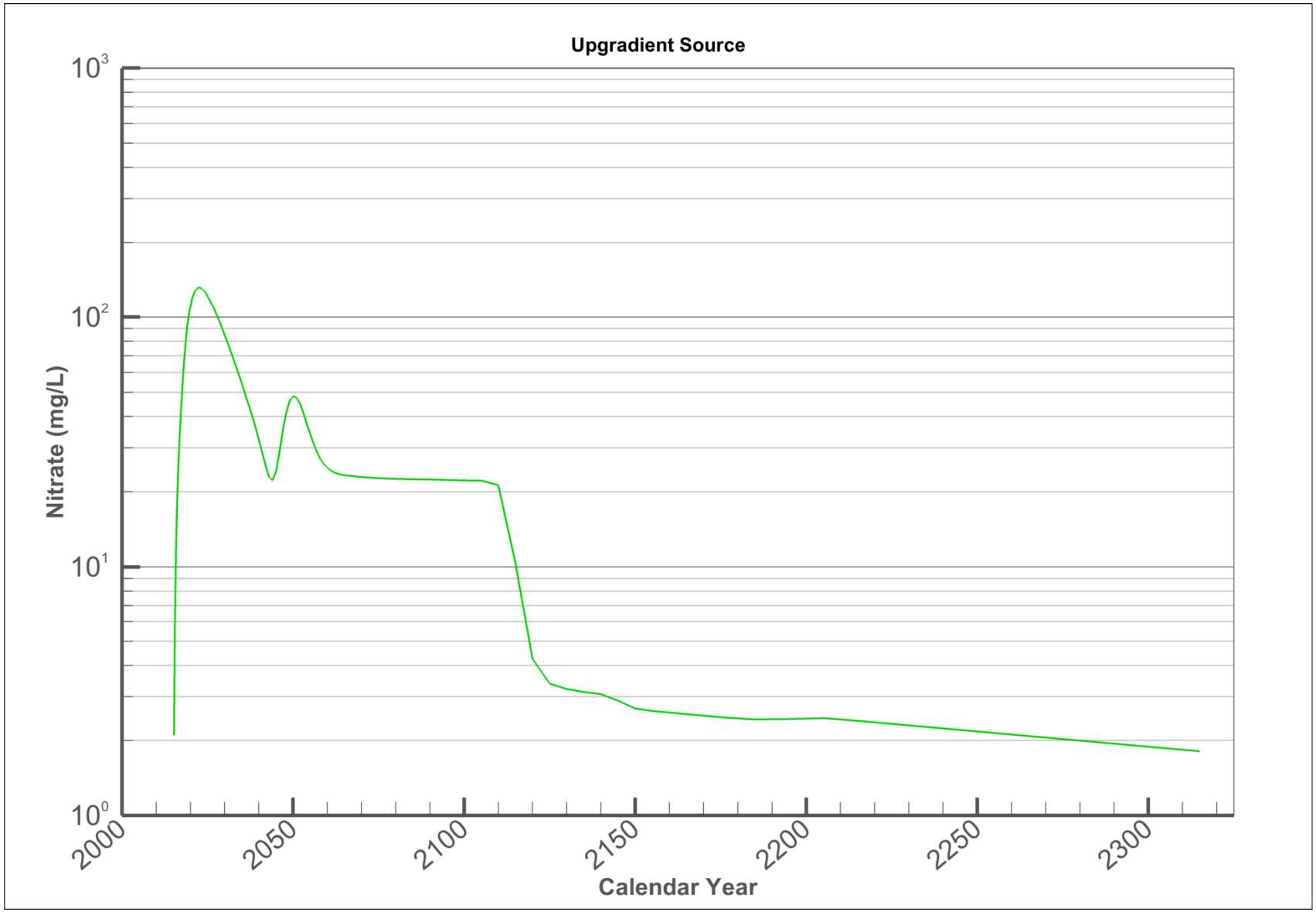

Figure 7-12. The Cyanide Plume at Year 2015 (Year 0 of the Simulation) for the Remedial Evaluation Case of 200-BP-5.

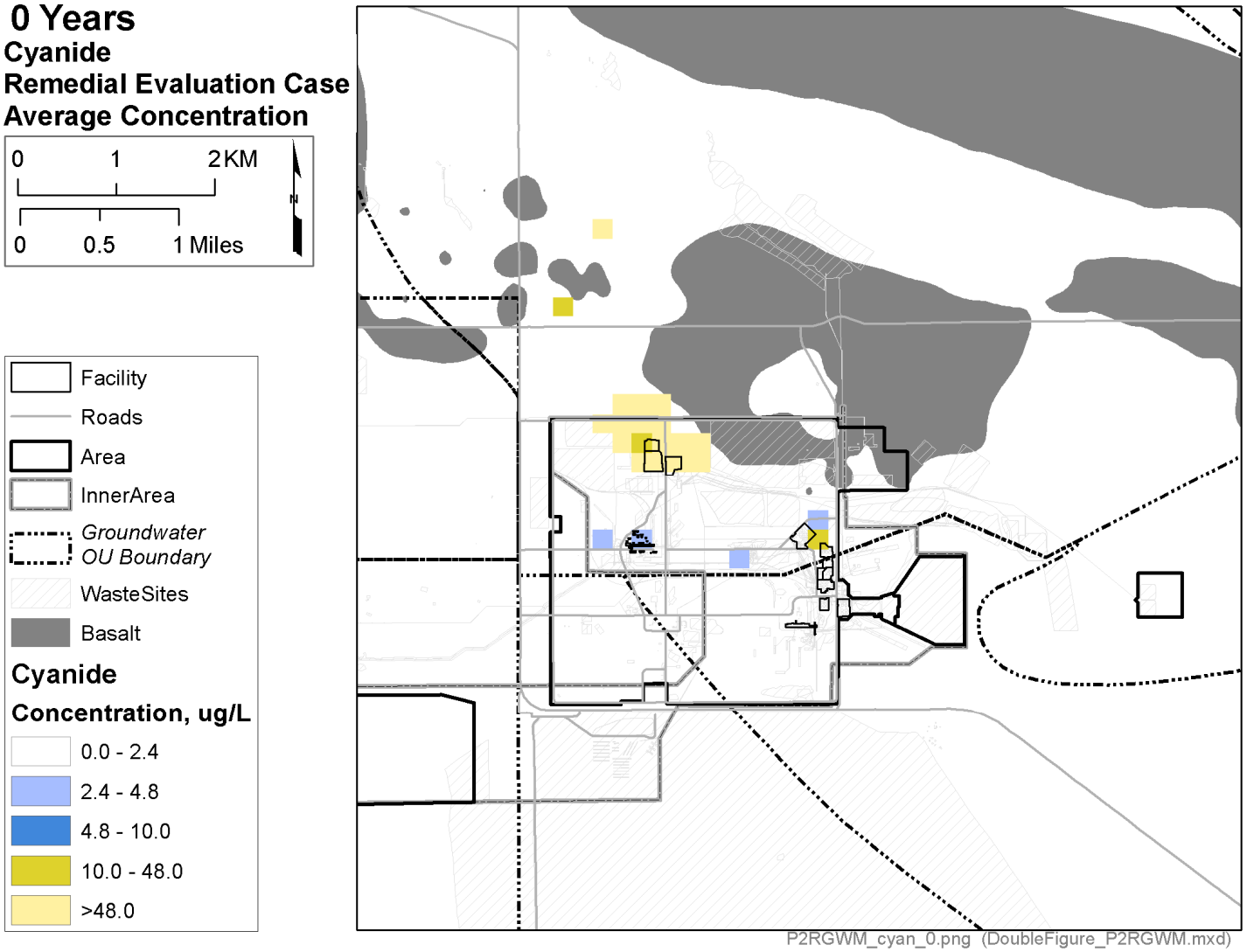

OU = operable unit

Note: The predominant source in the 200-BP-5 Operable Unit is shown under B Complex.

Table 7-1. Peak Concentrations and Time of Peak of Arrival at Waste Management Area C from the Calculated Remedial Evaluation Case for Upgradient Sources.

Contaminant of Concern	Peak Calculated Concentration	Calculated Year of Peak
Tc-99	1,430 pCi/L	2023
NO3	130 mg/L	2022
Uranium	38 µg/L	2059
I-129	4.3 pCi/L	2015
CN	39 µg/L	2023

7.1.3 Cyanide

The P2R model (DOE/RL-2009-127 Draft A) was used to simulate the evolution of the cyanide plume forward in time, beginning at year 2015. Cyanide is not a key contaminant of concern in the WMA C residual waste analyses (RPP-ENV-58806) or the past leak analyses presented in this report, but are included in this discussion of upgradient sources for the sake of completeness. The results of the analysis are shown in Figures 7-12 to 7-15. The figures show elevated concentrations of cyanide in the vicinity of B Complex. By about 2020 the plume has begun to arrive at WMA C. By 2025 the center of mass of the plume is in the vicinity of WMA C, and by 2035 it has moved downgradient from WMA C.

The time dependence of the cyanide contamination from upstream sources is shown in Figure 7-16. The peak concentration of about 38 µg/L is at the present day or the near future.

7.1.4 Iodine-129

The P2R model (DOE/RL-2009-127 Draft A) was used to simulate the evolution of the ^{129}I plume forward in time, beginning at year 2015. The results of the analysis are shown in Figures 7-17 to 7-20. The figures show a ubiquitous high concentration plume of ^{129}I throughout the 200-BP-5 OU. The concentrations near WMA C remain in the higher concentration (dark blue) contour for the first 10 years. By 2035 the concentration has begun to decrease (light blue contour), and by 2045 the area under WMA C shows minimal ^{129}I concentration.

The time dependence of ^{129}I contamination from upstream sources is shown in Figure 7-21. The peak concentration of about 4 pCi/L is at the present day or the near future.

7.1.5 Uranium

The P2R model (DOE/RL-2009-127 Draft A) was used to simulate the evolution of the total uranium plume forward in time, beginning at year 2015. The results of the analysis are shown in Figures 7-22 to 7-26. The figures show a high concentration plume of ^{238}U under B Complex at the beginning of the simulation, which predominantly moves toward WMA C. The uranium plume moves more slowly than ^{99}Tc or nitrate, and over the next ~130 years the plume moves with groundwater past WMA C, leading to a period of higher ^{235}U concentration beginning in about 2050 and lasting until about 2150.

Figure 7-13. The Cyanide Plume at Year 2020 (Year 5 of the Simulation) for the Remedial Evaluation Case of 200-BP-5.

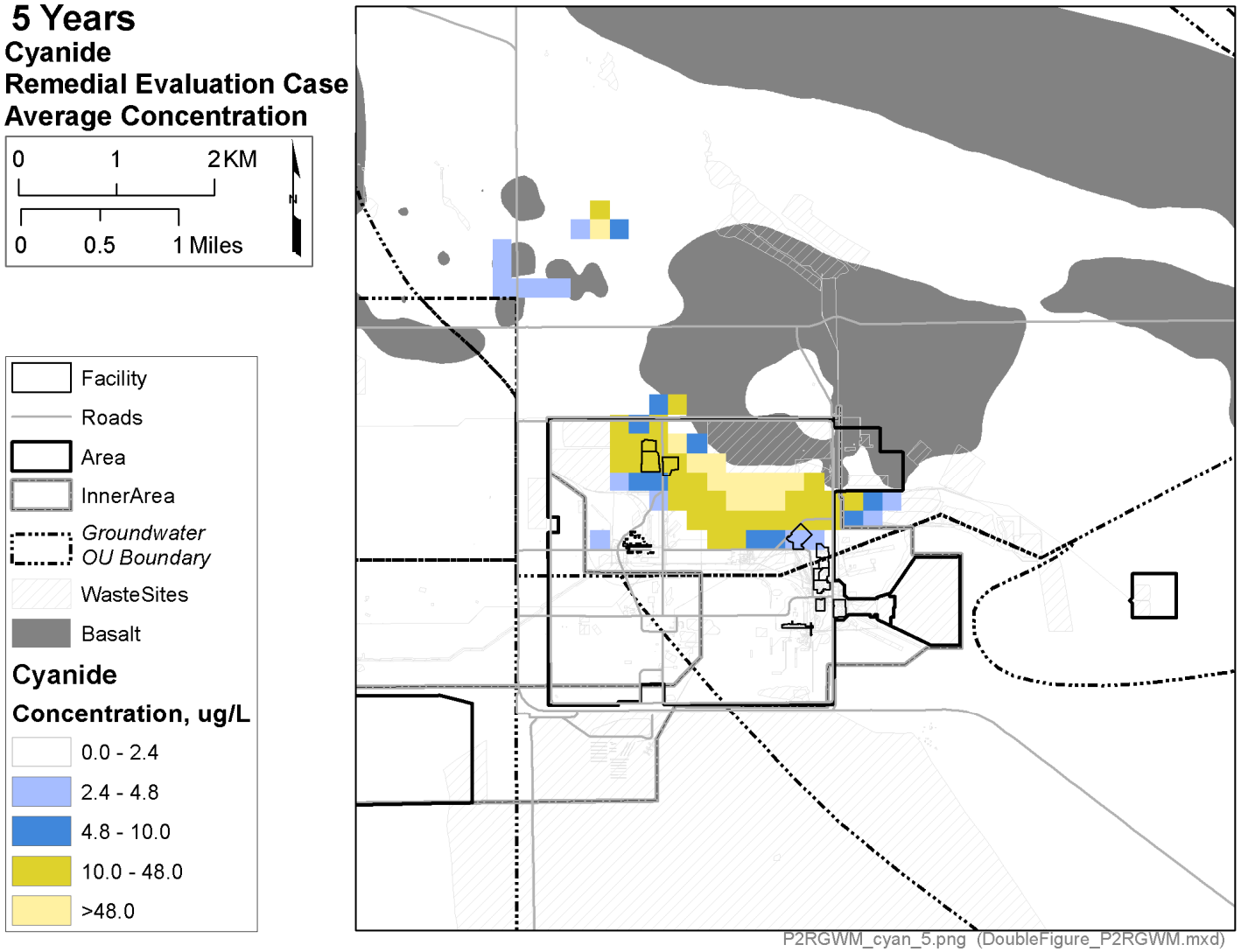

OU = operable unit

Note: The predominant source originating under B Complex has begun to arrive at Waste Management Area C.

Figure 7-14. The Cyanide Plume at Year 2025 (Year 10 of the Simulation) for the Remedial Evaluation Case of 200-BP-5.

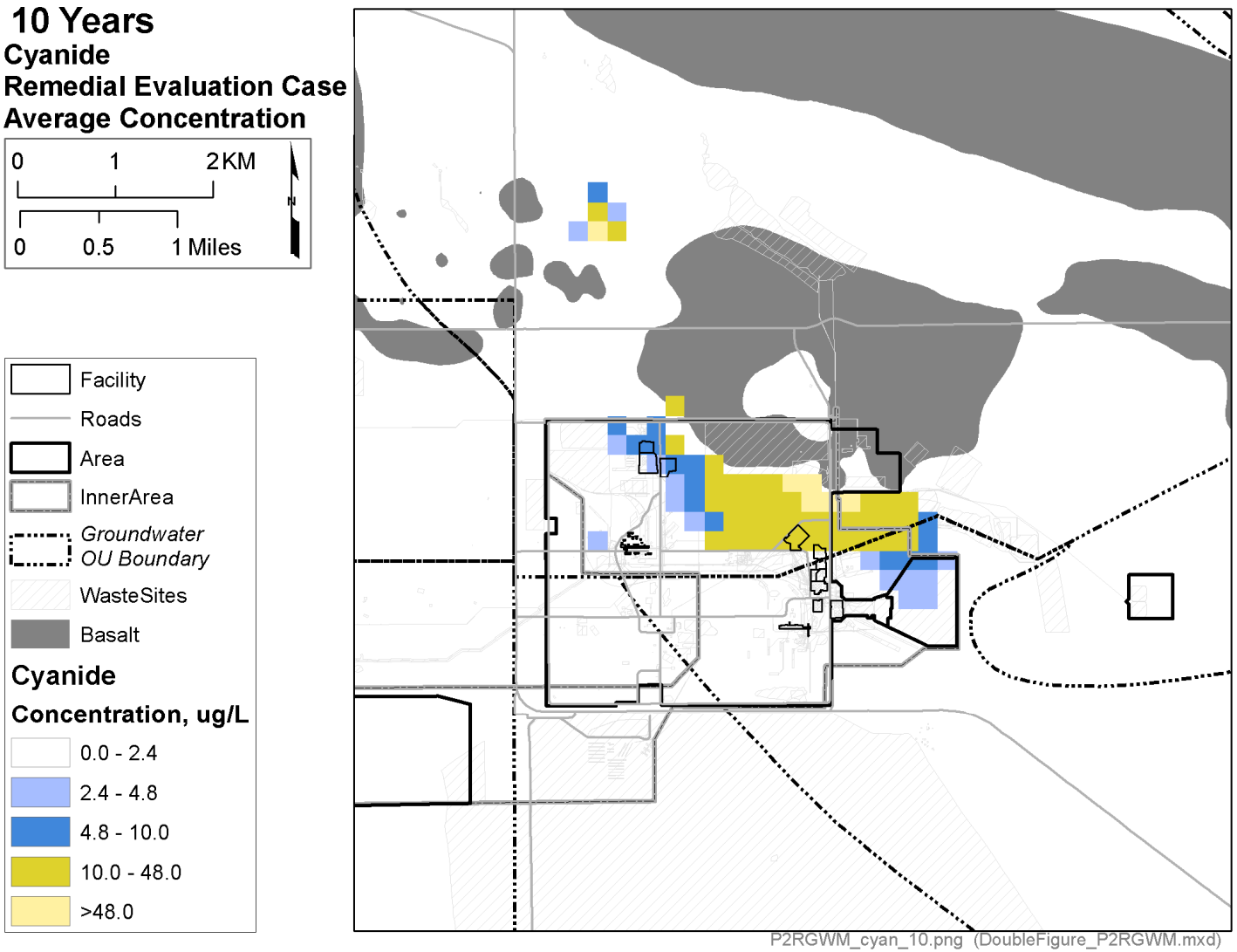

OU = operable unit

Note: The center of mass of the plume is in the vicinity of Waste Management Area C.

Figure 7-15. The Cyanide Plume at Year 2025 (Year 10 of the Simulation) for the Remedial Evaluation Case of 200-BP-5.

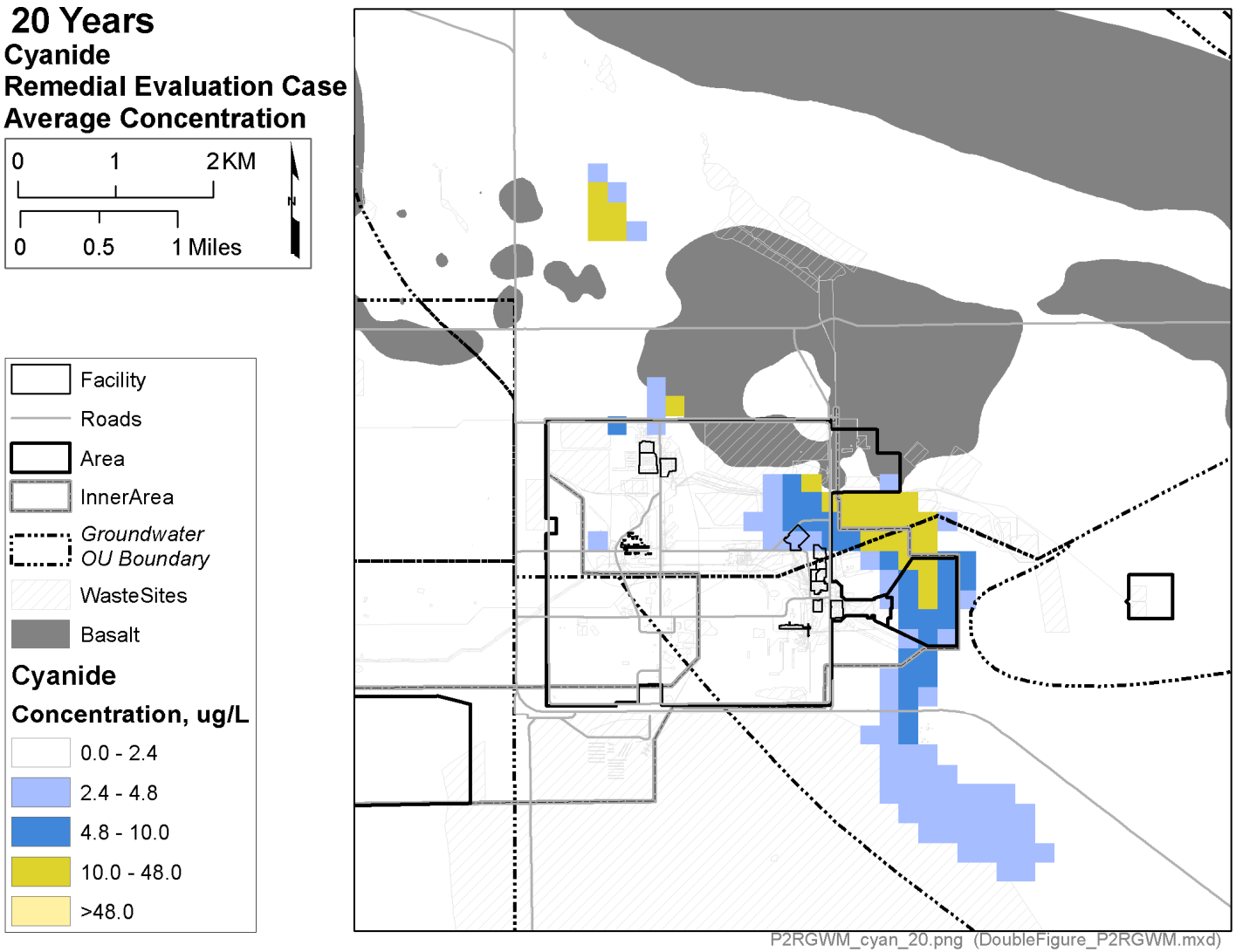

OU = operable unit

Note: The center of mass of the plume has moved downgradient from Waste Management Area C.

Figure 7-16. Remedial Evaluation Case Cyanide Concentrations at Waste Management Area C as a Function of Time.

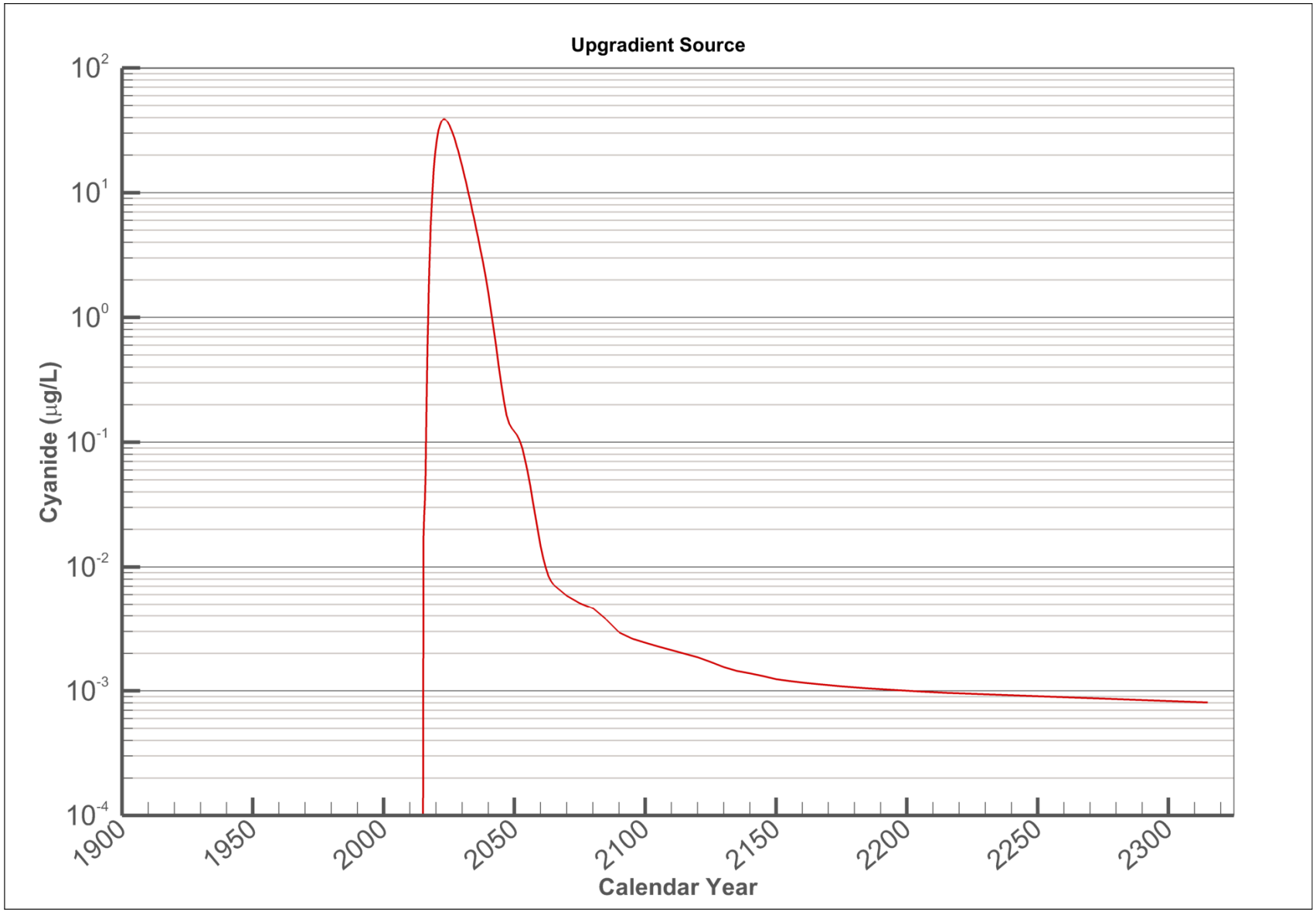

Figure 7-17. The Iodine-129 Plume at Year 2015 (Year 0 of the Simulation) for the Remedial Evaluation Case of 200-BP-5.

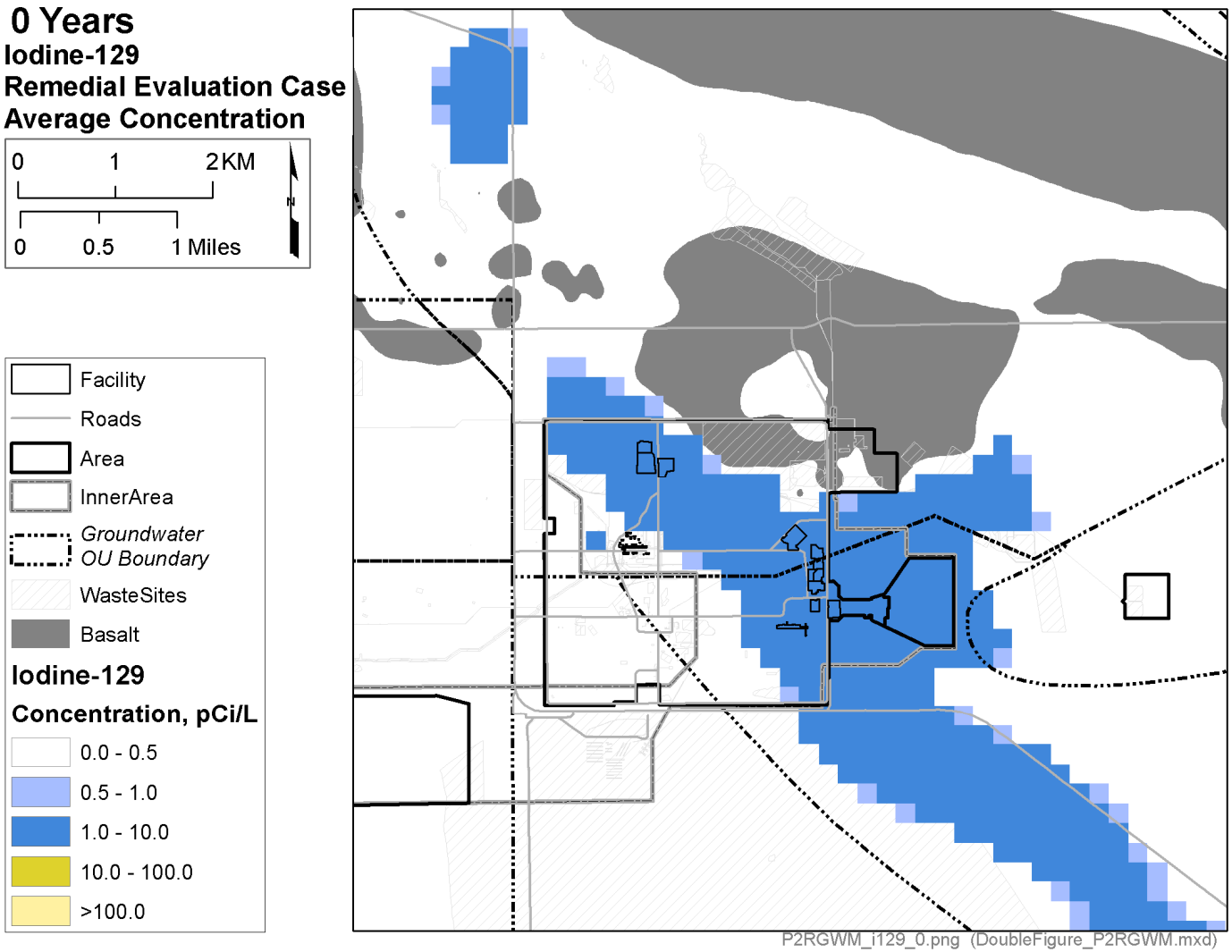

OU = operable unit

Note: The higher concentrations (dark blue contours) are widely distributed in the 200-BP-5 Operable Unit including under Waste Management Area C.

Figure 7-18. The Iodine-129 Plume at Year 2025 (Year 10 of the Simulation) for the Remedial Evaluation Case of 200-BP-5.

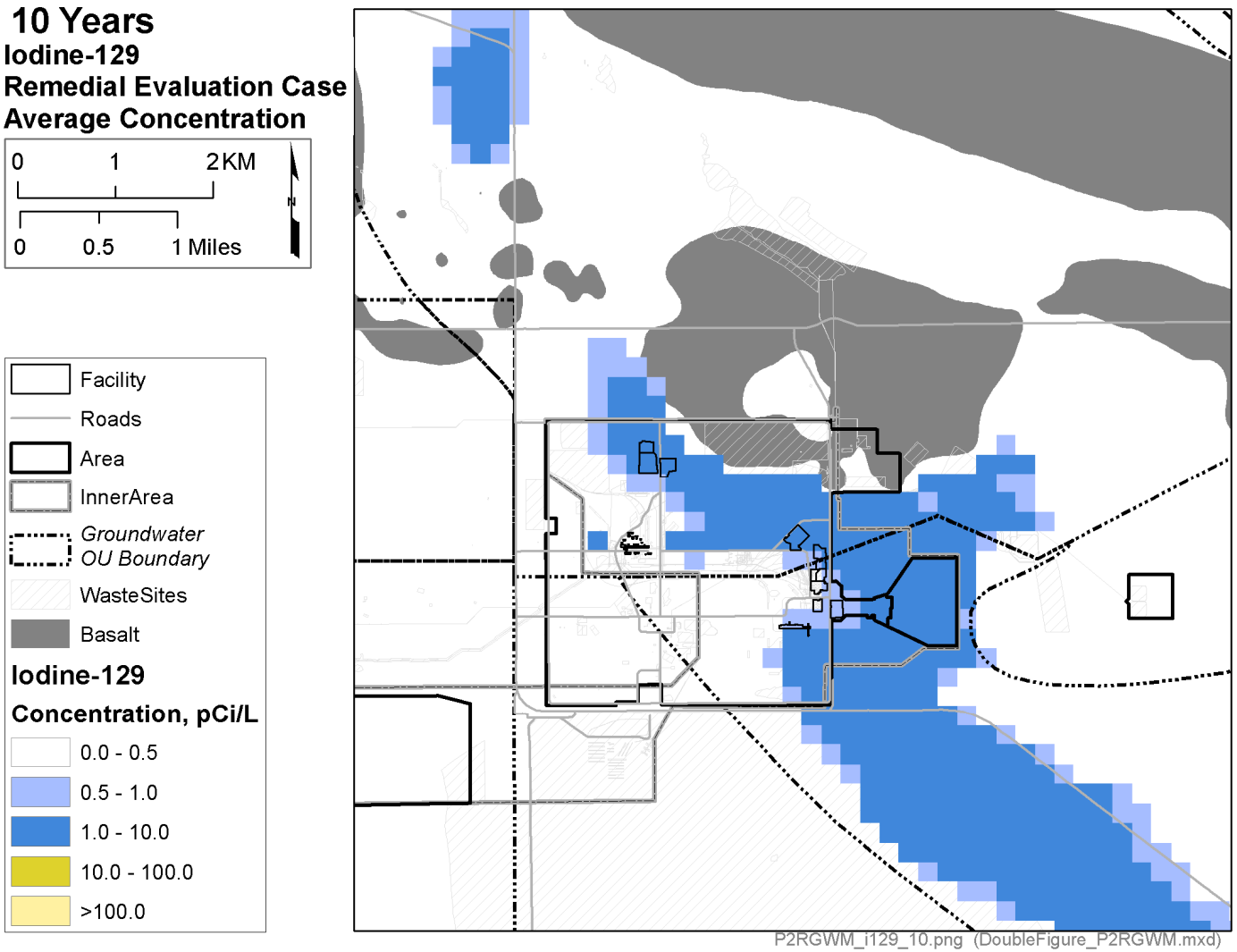

OU = operable unit

Note: The higher concentrations (dark blue contours) remain widely distributed in the 200-BP-5 Operable Unit and near Waste Management Area C.

Figure 7-19. The Iodine-129 Plume at Year 2035 (Year 20 of the Simulation) for the Remedial Evaluation Case of 200-BP-5.

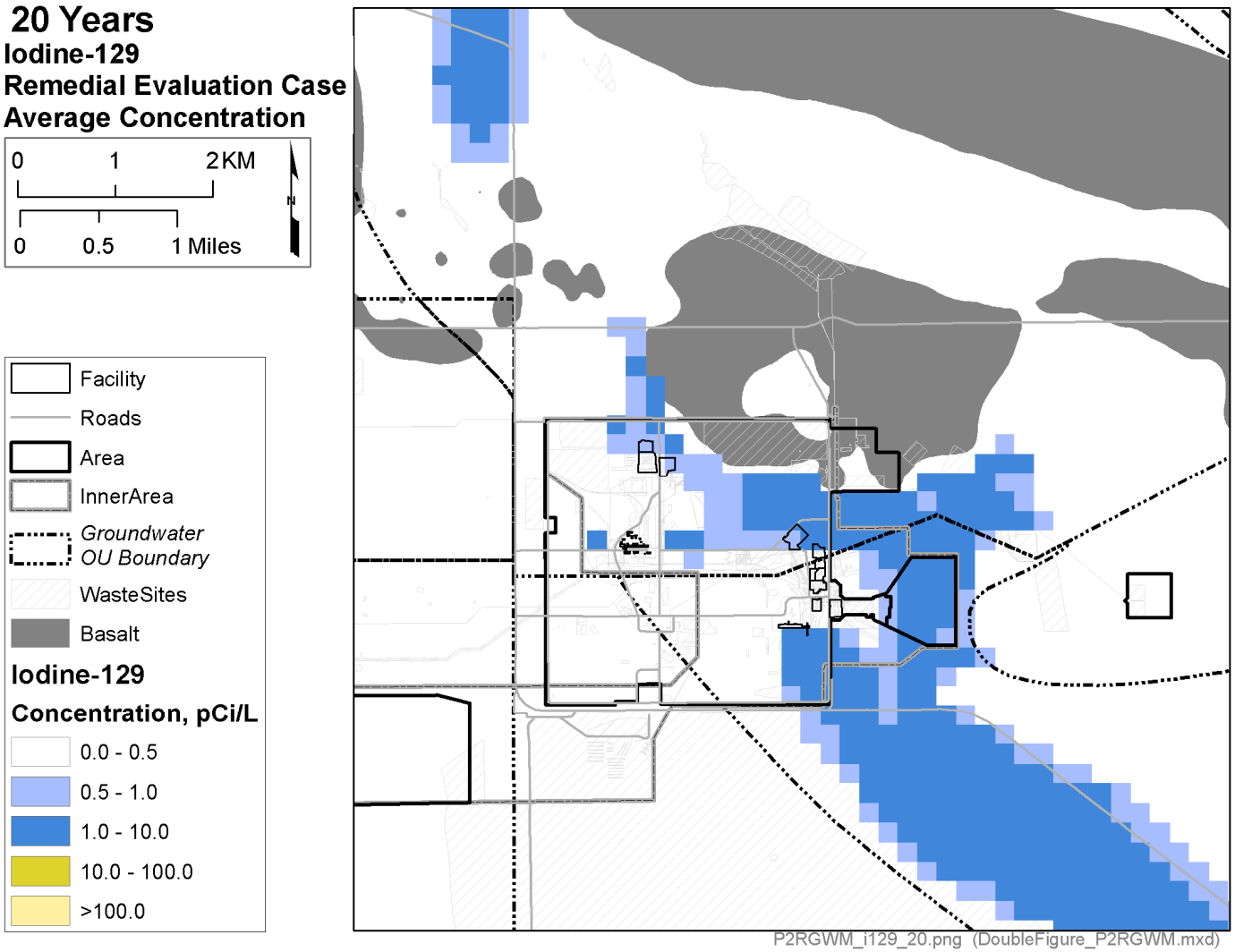

OU = operable unit

Note: The higher concentrations (dark blue contours) remain widely distributed in the 200-BP-5 Operable Unit, but have begun to move downgradient from Waste Management Area C.

Figure 7-20. The Iodine-129 Plume at Year 2045 (Year 30 of the Simulation) for the Remedial Evaluation Case of 200-BP-5.

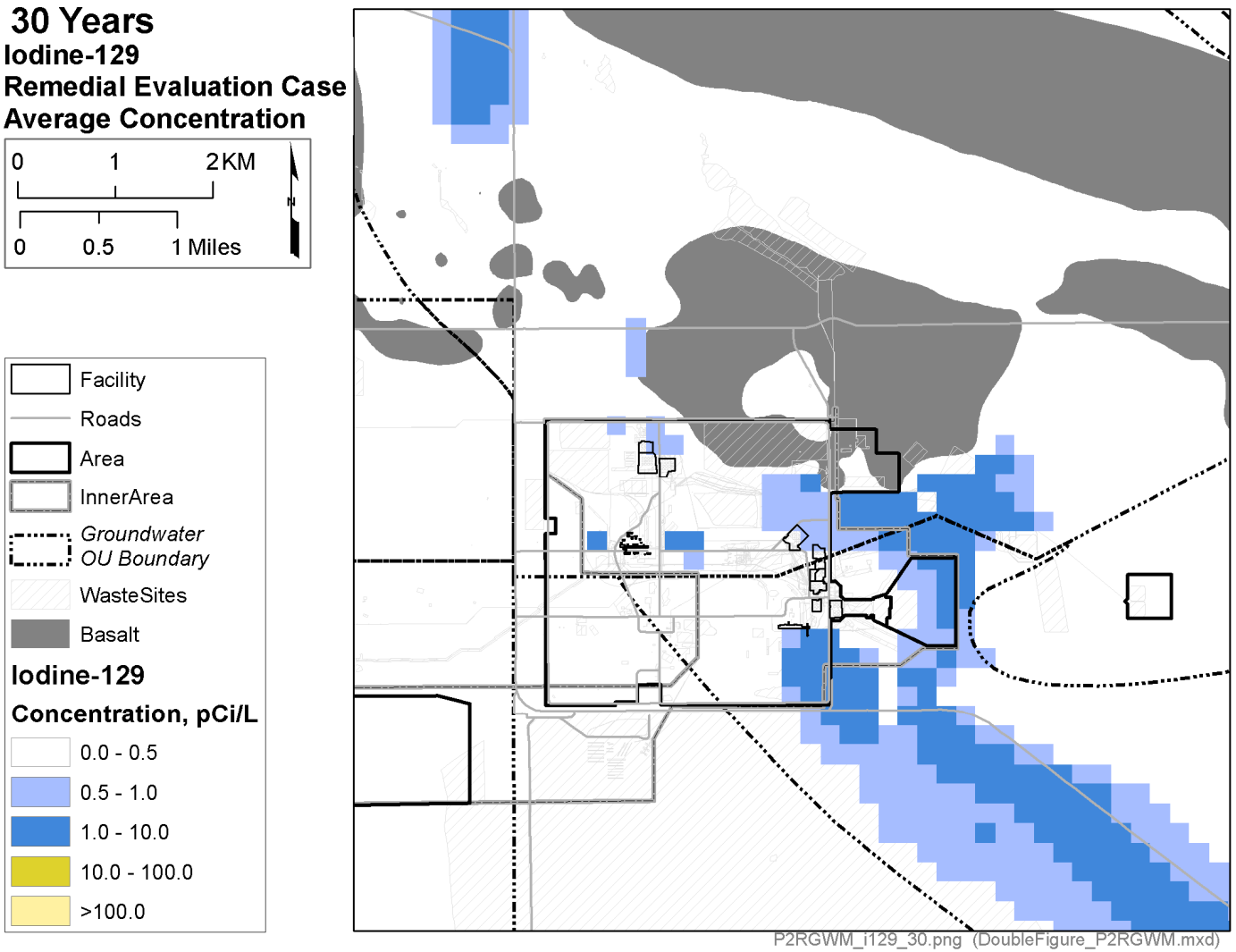

OU = operable unit

Note: Both the higher concentrations (dark blue contours) and lower concentration (light blue contours) have moved downgradient from Waste Management Area C.

Figure 7-21. Remedial Evaluation Case Iodine-129 Concentrations at Waste Management Area C as a Function of Time.

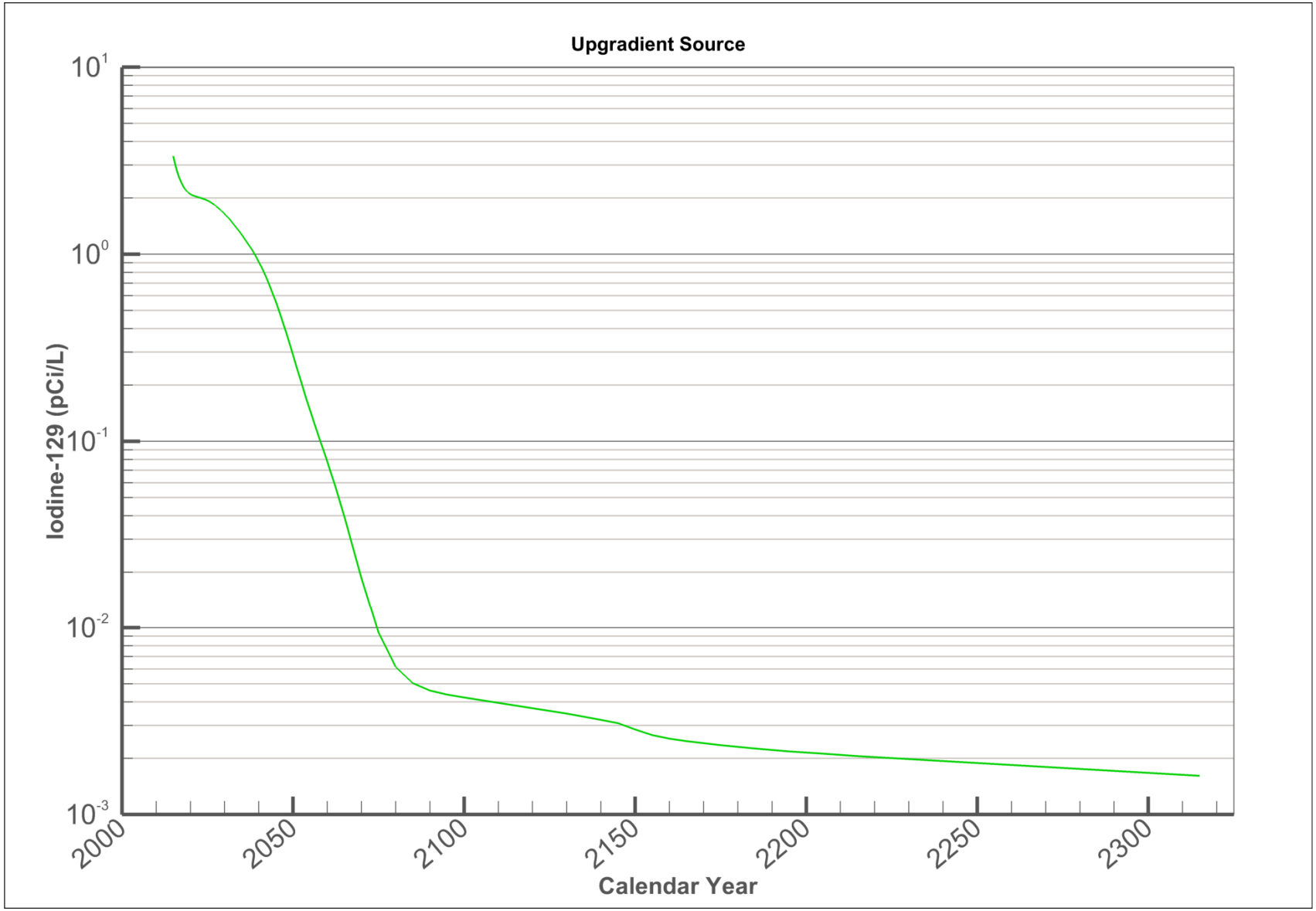

Figure 7-22. The Uranium Plume at Year 2015 (Year 0 of the Simulation) for the Remedial Evaluation Case of 200-BP-5.

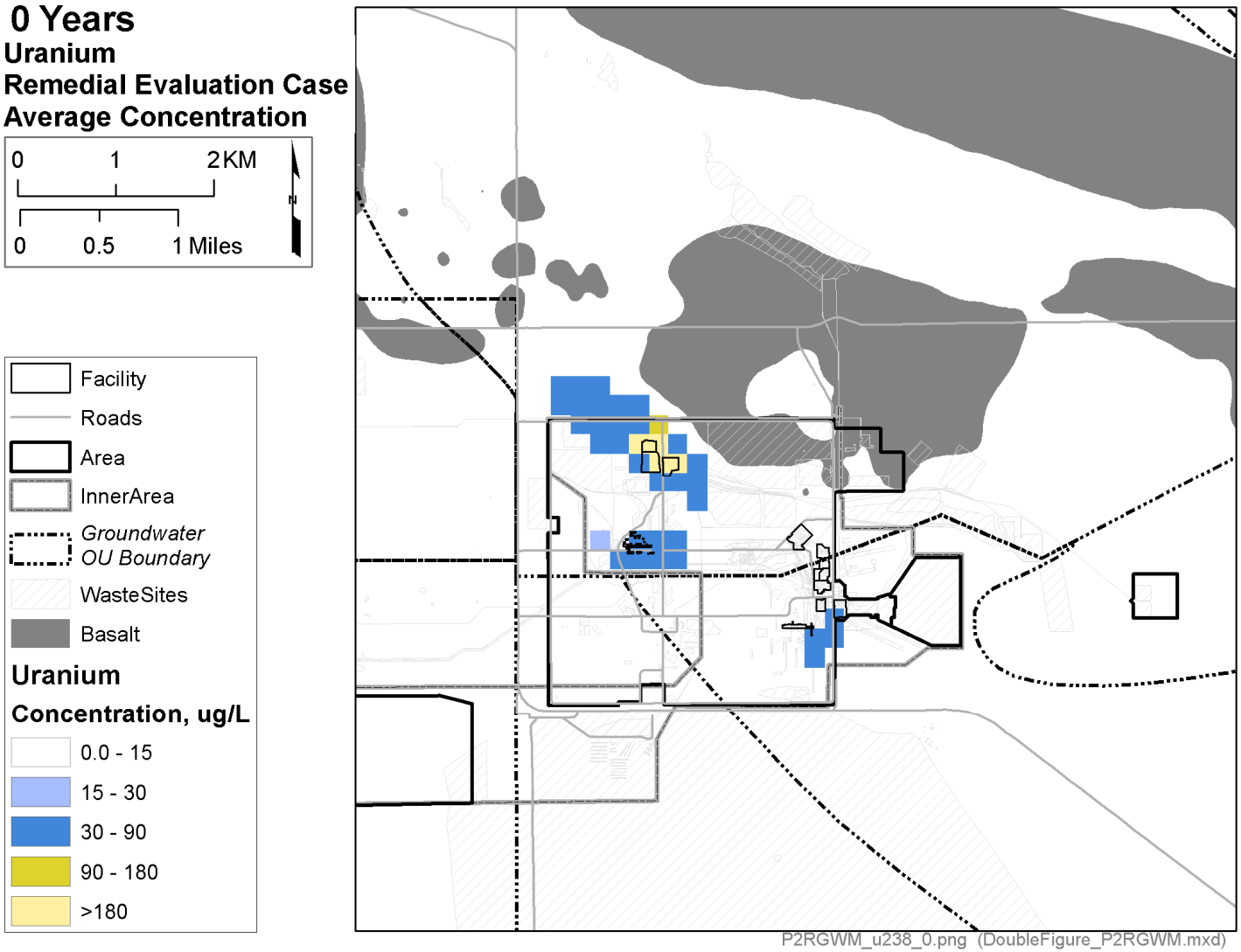

OU = operable unit

Note: Note that the higher concentrations (yellow contours are entirely upgradient from Waste Management Area C in the B Complex area.

Figure 7-23. The Uranium Plume at Year 2035 (Year 20 of the Simulation) for the Remedial Evaluation Case of 200-BP-5.

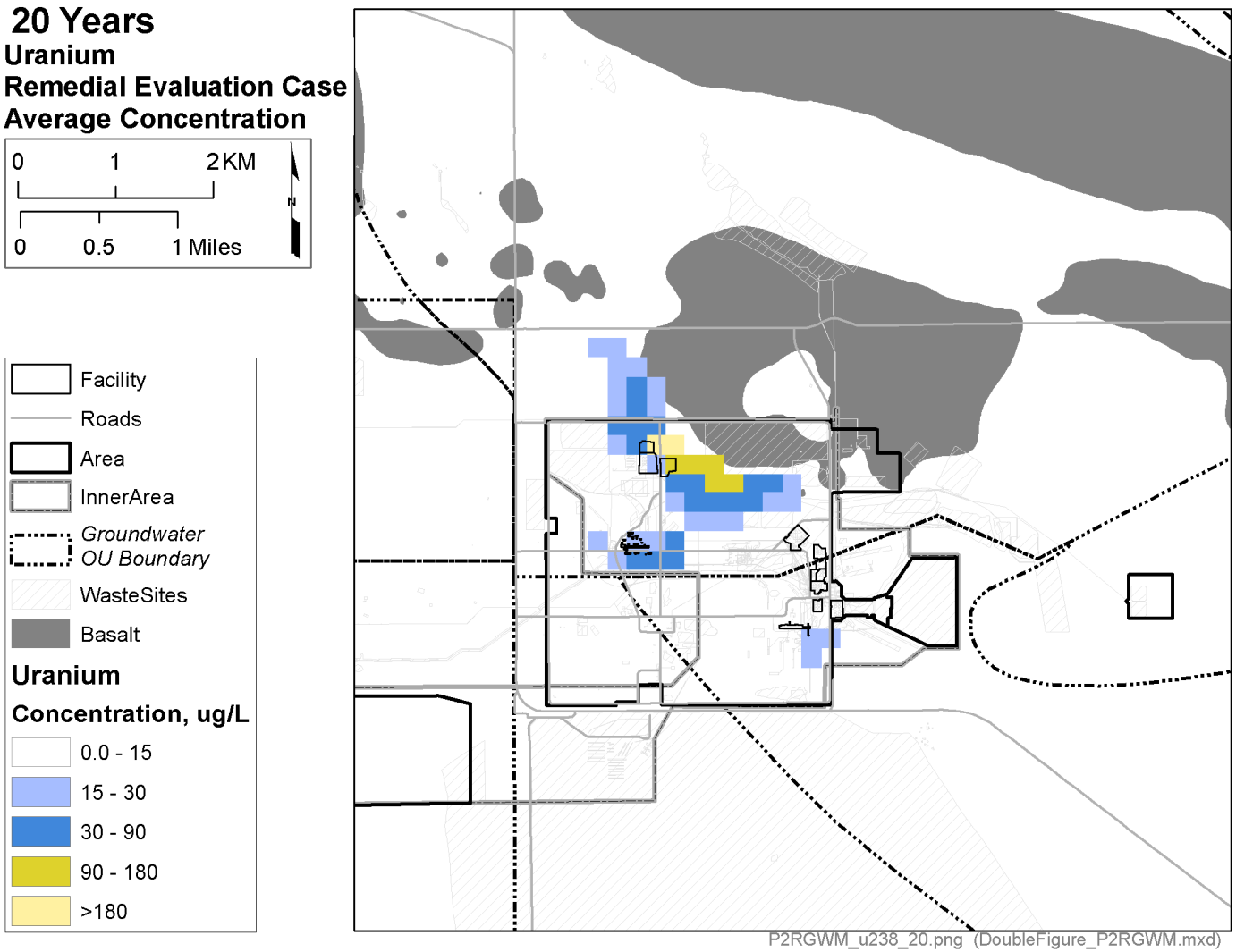

OU = operable unit

Note: The higher concentrations (yellow contours) have moved in the direction of Waste Management Area C but have not yet arrived. At this point in time the conservative species ^{99}Tc and nitrate have already passed Waste Management Area C.

Figure 7-24. The Uranium Plume at Year 2045 (Year 30 of the Simulation) for the Remedial Evaluation Case of 200-BP-5.

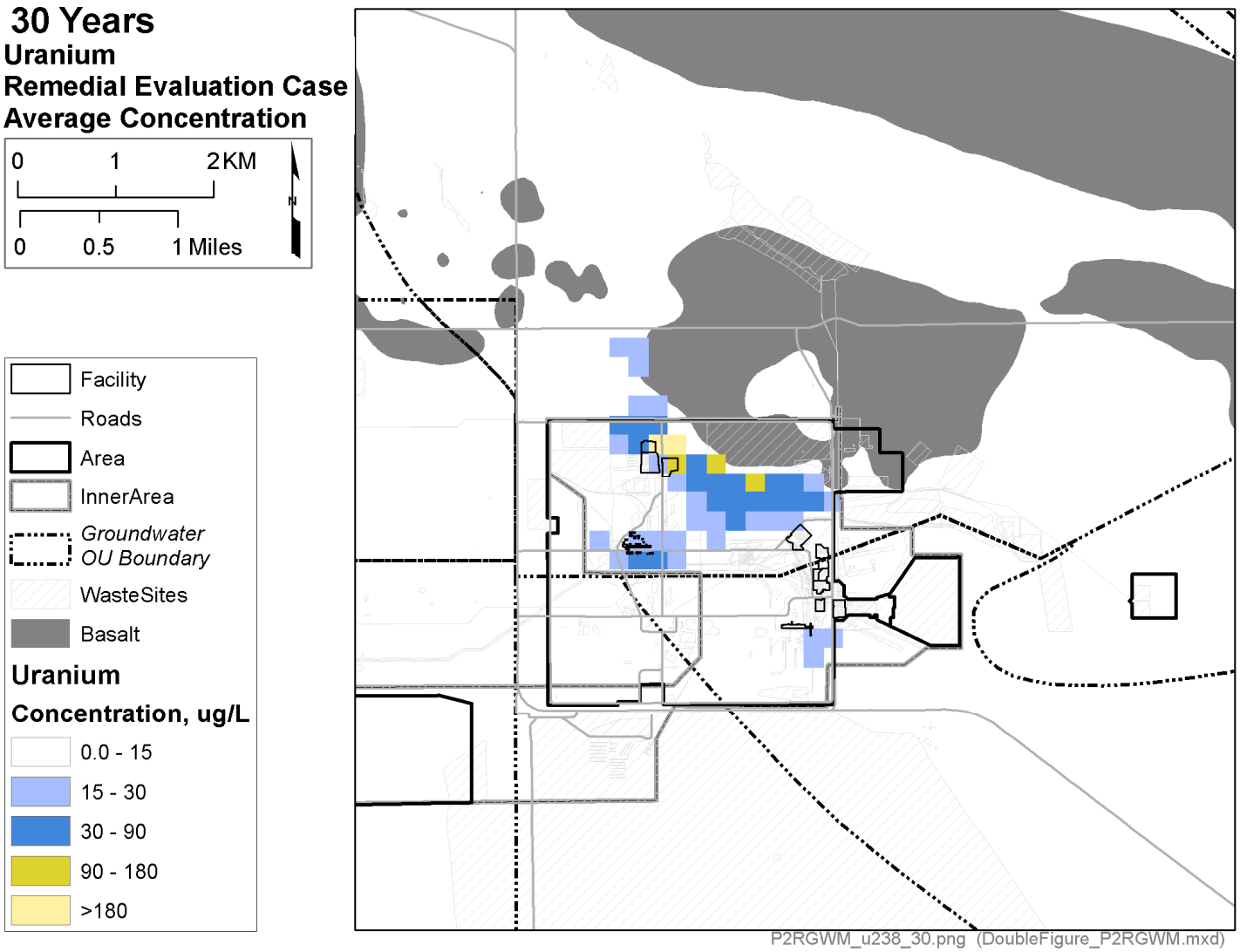

OU = operable unit

Note: Somewhat elevated ^{238}U concentrations have begun to arrive at Waste Management Area C.

Figure 7-25. The Uranium Plume at Year 2065 (Year 50 of the Simulation) for the Remedial Evaluation Case of 200-BP-5.

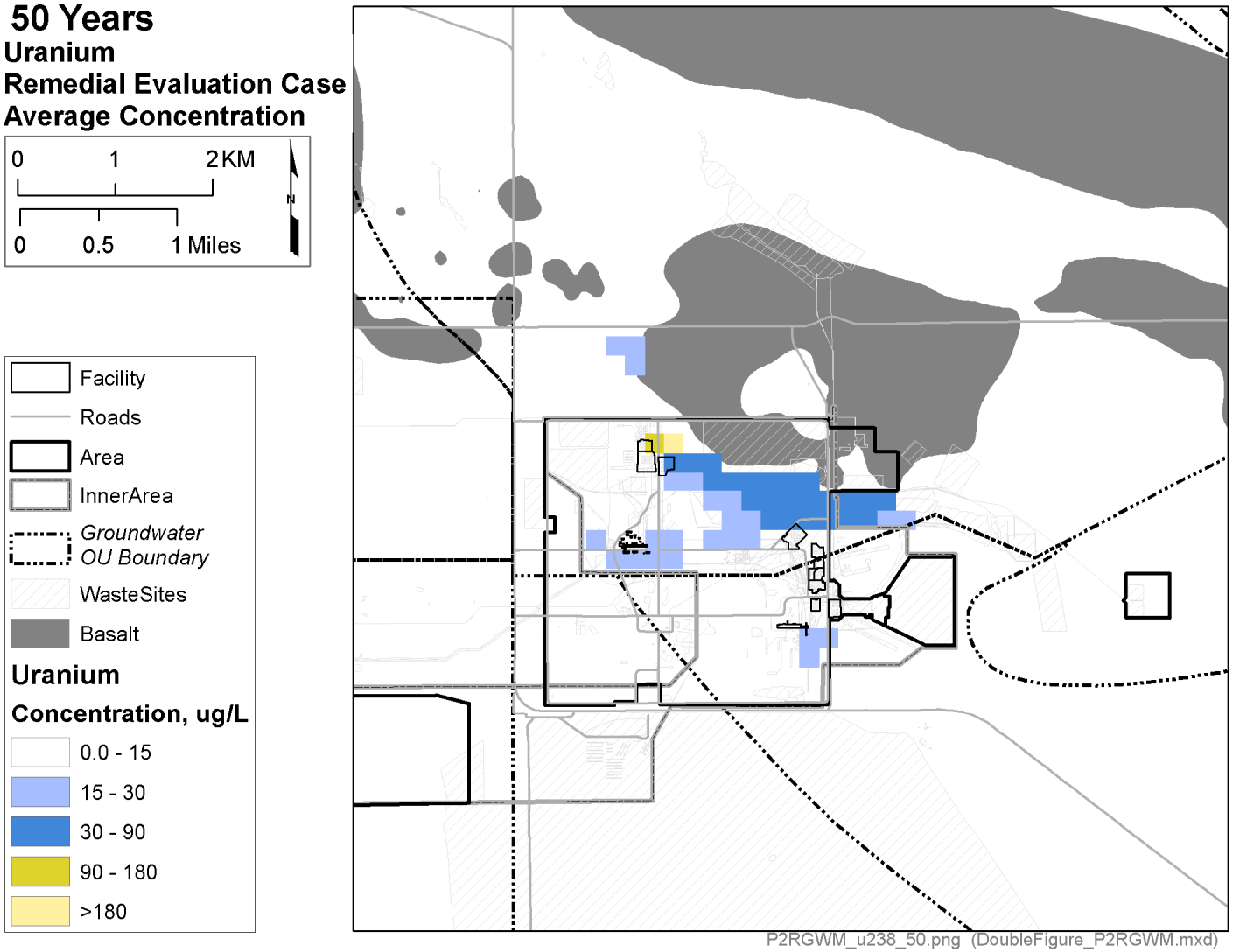

OU = operable unit

Note: The center of mass of the elevated uranium concentrations is in the vicinity of Waste Management Area C, remaining slightly to the north.

Figure 7-26. The Uranium Plume at Year 2150 (Year 135 of the Simulation) for the Remedial Evaluation Case of 200-BP-5.

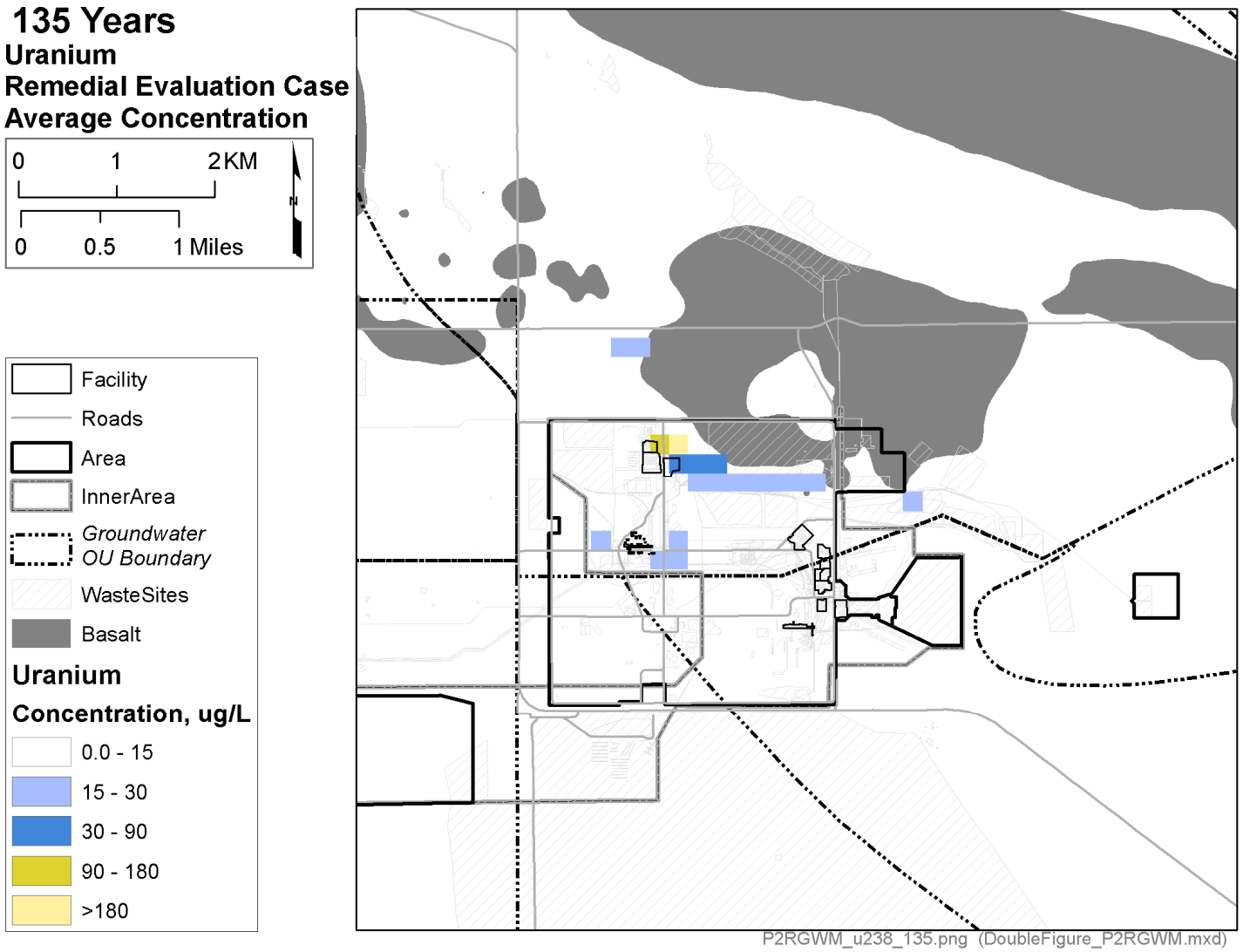

OU = operable unit

Note: The concentrations in the vicinity of Waste Management Area C are no longer significantly elevated.

The time dependence of uranium contamination from upstream sources is shown in Figure 7-27. The peak concentration of ~38 µg/L occurs around 2060.

7.2 CONTRIBUTION OF RESIDUAL WASTES

In this section, future projections of the contributions of groundwater impacts from landfill closure of residual wastes in tanks and ancillary equipment at WMA C are summarized. The details of the analyses and approaches that produced these results are presented in the PA report (RPP-ENV-58782) and RCA report (RPP-ENV-58806).

In each of the sections below, concentrations are reported at a distance 100 m from the boundary of the facility. To find the peak concentration in groundwater at this distance, a set of nine PoCals are used to evaluate the local concentration. Since the points of concentration are affected by different sources in WMA C, they have different peak concentrations. The results presented in this section represent the PoCal with the highest peak concentration, which may differ between contaminants. Results presented in this section are the "base case" results of the PA and RCA; both the PA and the RCA present extensive discussions of sensitivity and uncertainties in the analyses, and the base case results are understood as indicators of performance in the context of the broader treatment of uncertainties presented in RPP-ENV-58782 and RPP-ENV-58806.

7.2.1 Technetium-99

Technetium-99 is a key dose contributor in the residual waste performance assessment (RPP-ENV-58782). It is a mobile contaminant (K_d=0) and is not significantly retained in the residual wastes over performance assessment time scales. Calculated concentrations of ^{99}Tc at the highest point of calculation are presented in Figure 7-28. The peak concentration is 30 pCi/L at 1,570 years after closure. The spatial distribution of ^{99}Tc at the time of the peak concentration is shown in Figure 7-29.

7.2.2 Nitrate

Nitrate is a key contaminant of concern in the RCA (RPP-ENV-58806). It is a mobile contaminant (K_d=0.0). Calculated concentrations of nitrate at the PoCals are presented in Figure 7-30. The peak concentration within 10,000 years is 0.3 mg/L at 1,375 years after closure. The spatial distribution of nitrate at the time of the peak concentration is shown in Figure 7-31. The current MCL for nitrate is 45 mg/L.

7.2.3 Iodine-129

Iodine-129 is a key contaminant of concern in the PA (RPP-ENV-58782). It is a slightly sorbed contaminant (K_d=0.2). Calculated concentrations of ^{129}I at the PoCals are presented in Figure 7-32. The peak concentration within 10,000 years is 0.004 pCi/L at 6,200 years after closure. The current MCL for ^{129}I is 1 pCi/L.

Figure 7-27. Remedial Evaluation Case Total Uranium Concentrations at Waste Management Area C as a Function of Time.

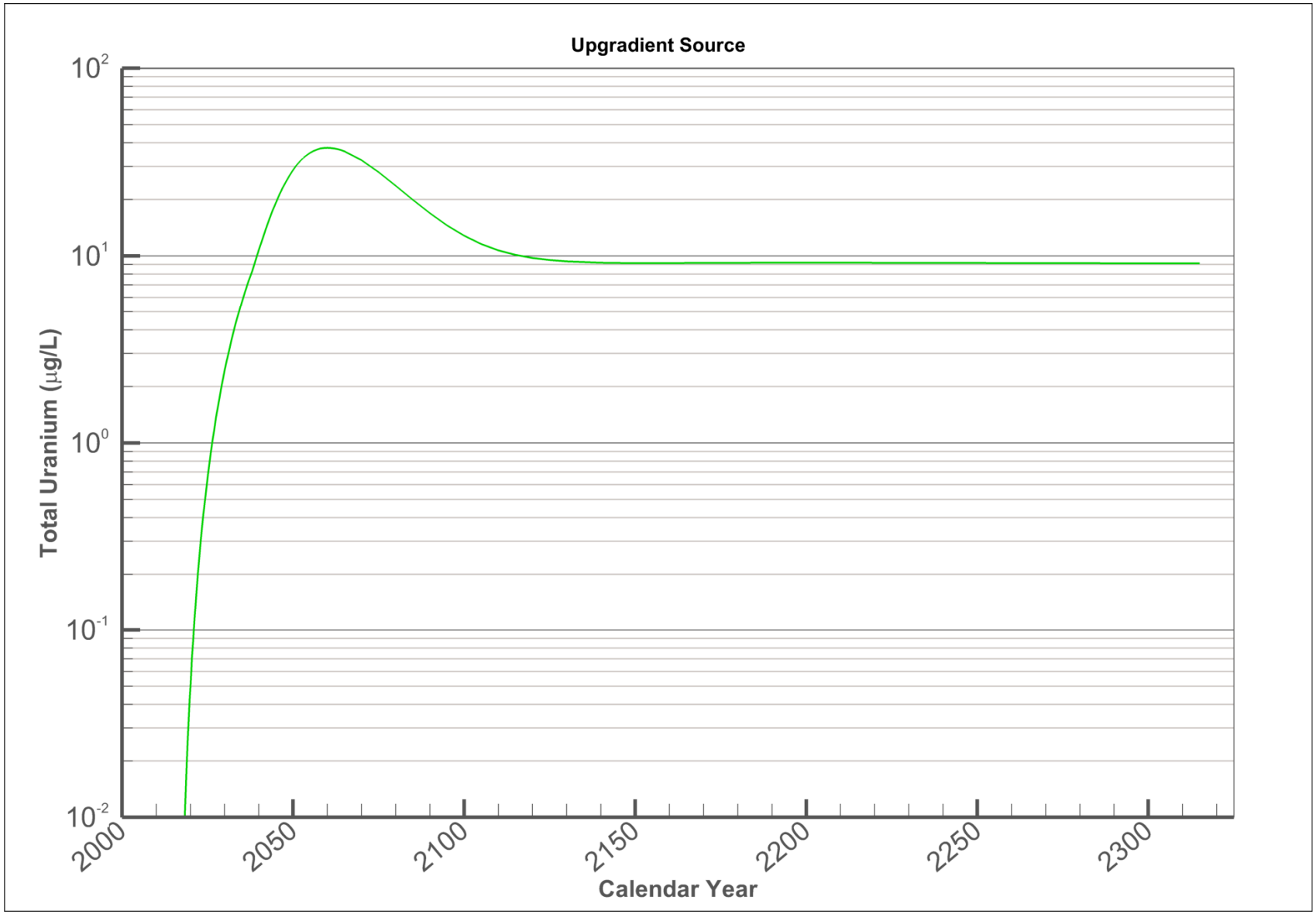

Figure 7-28. Groundwater Concentration of Technetium-99 at the Highest Point of Calculation 100 Meters Downgradient from Waste Management Area C.

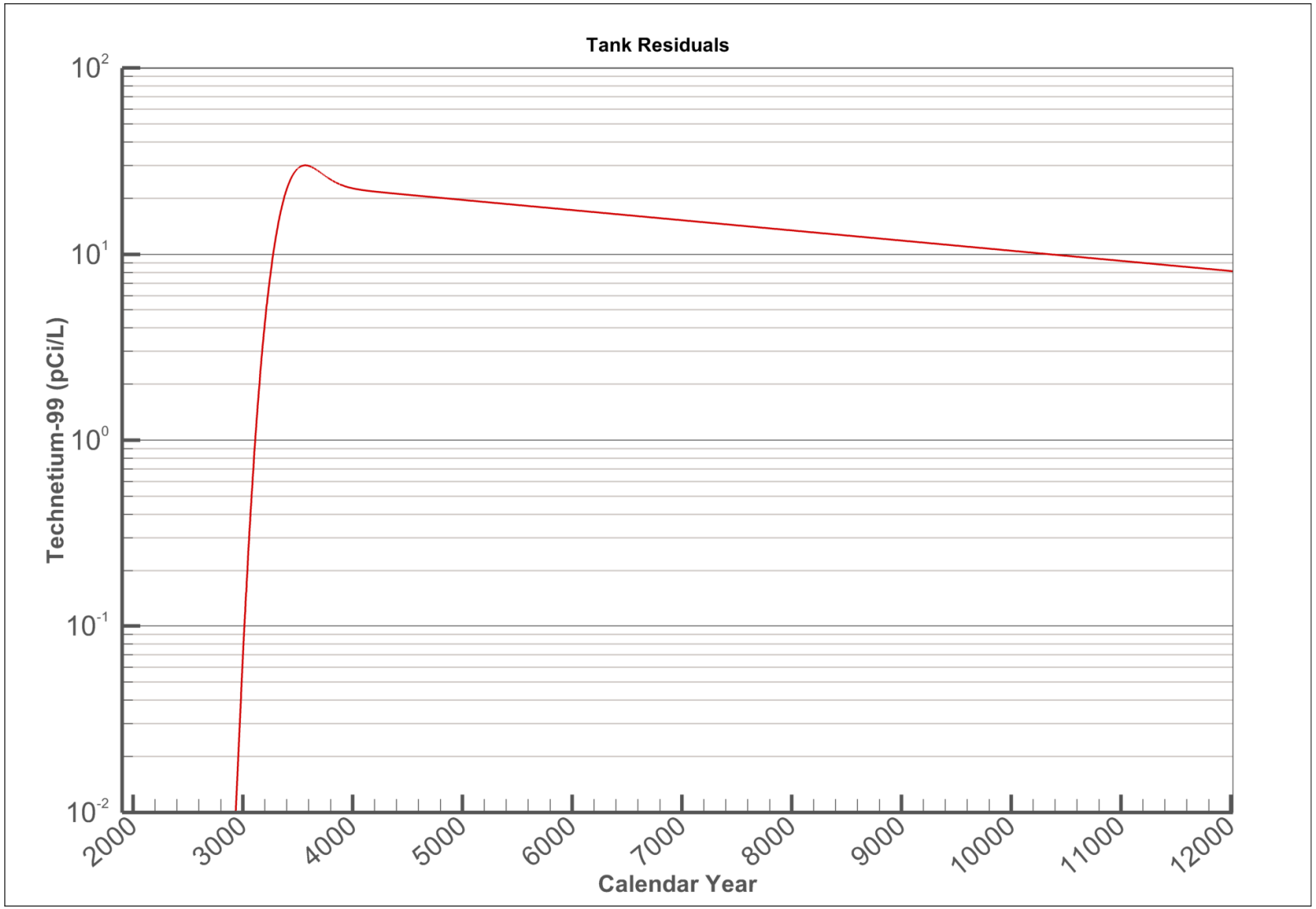

Source: RPP-ENV-58782, "Performance Assessment of Waste Management Area C, Hanford Site, Washington."

Figure 7-29. Extent of Technetium-99 Plume in Groundwater 1,570 Years after Closure at the Time of the Maximum Concentration at the Point of Compliance.

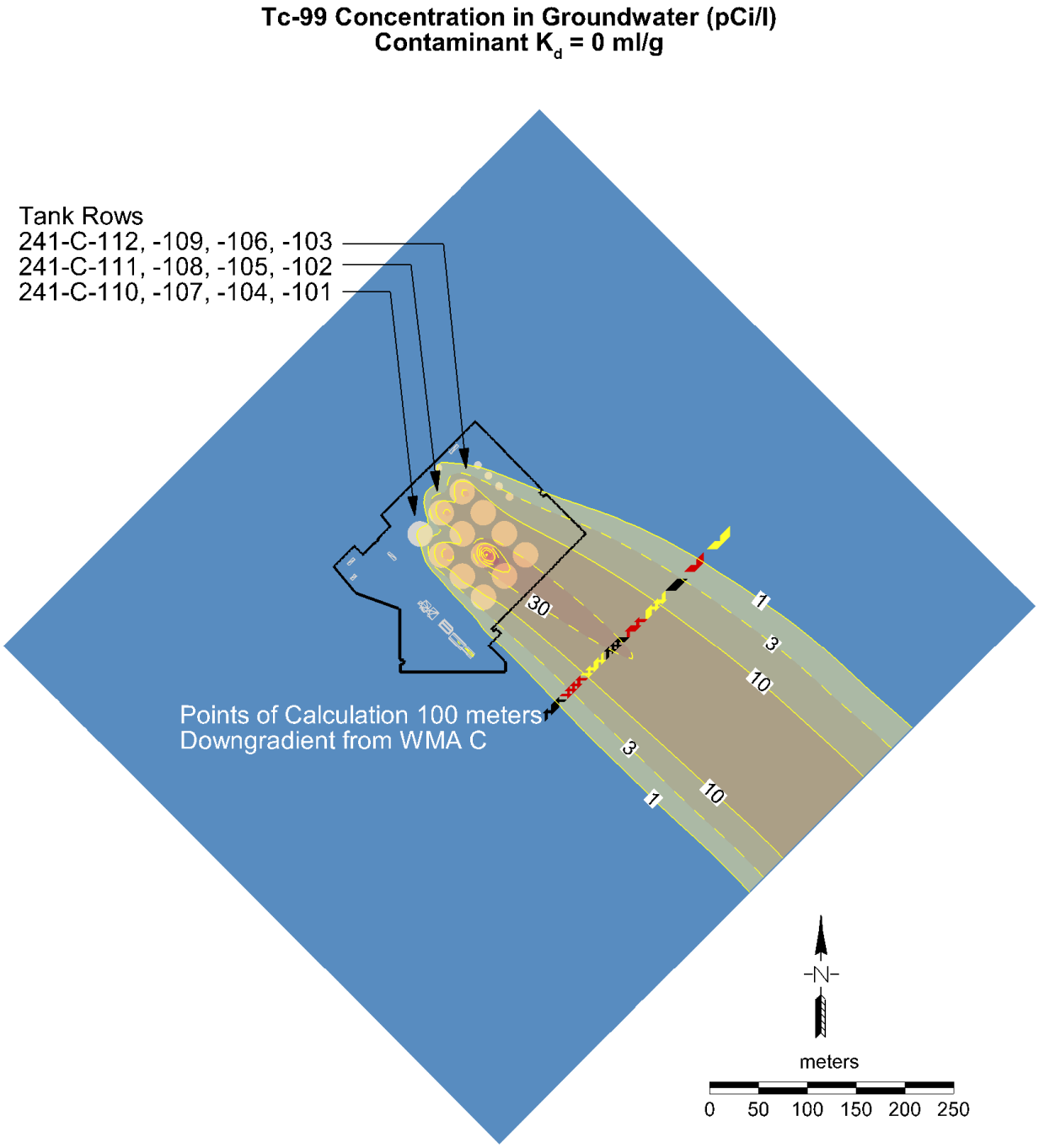

Approximate time of peak concentration at point of calculation

WMA = Waste Management Area

Source: RPP-ENV-58782, "Performance Assessment of Waste Management Area C, Hanford Site, Washington."

Figure 7-30. Maximum Predicted Groundwater Concentration of Nitrate (K_d = 0 mL/g) at All Points of Calculation 100 Meters Downgradient from Waste Management Area C from Residual Wastes.

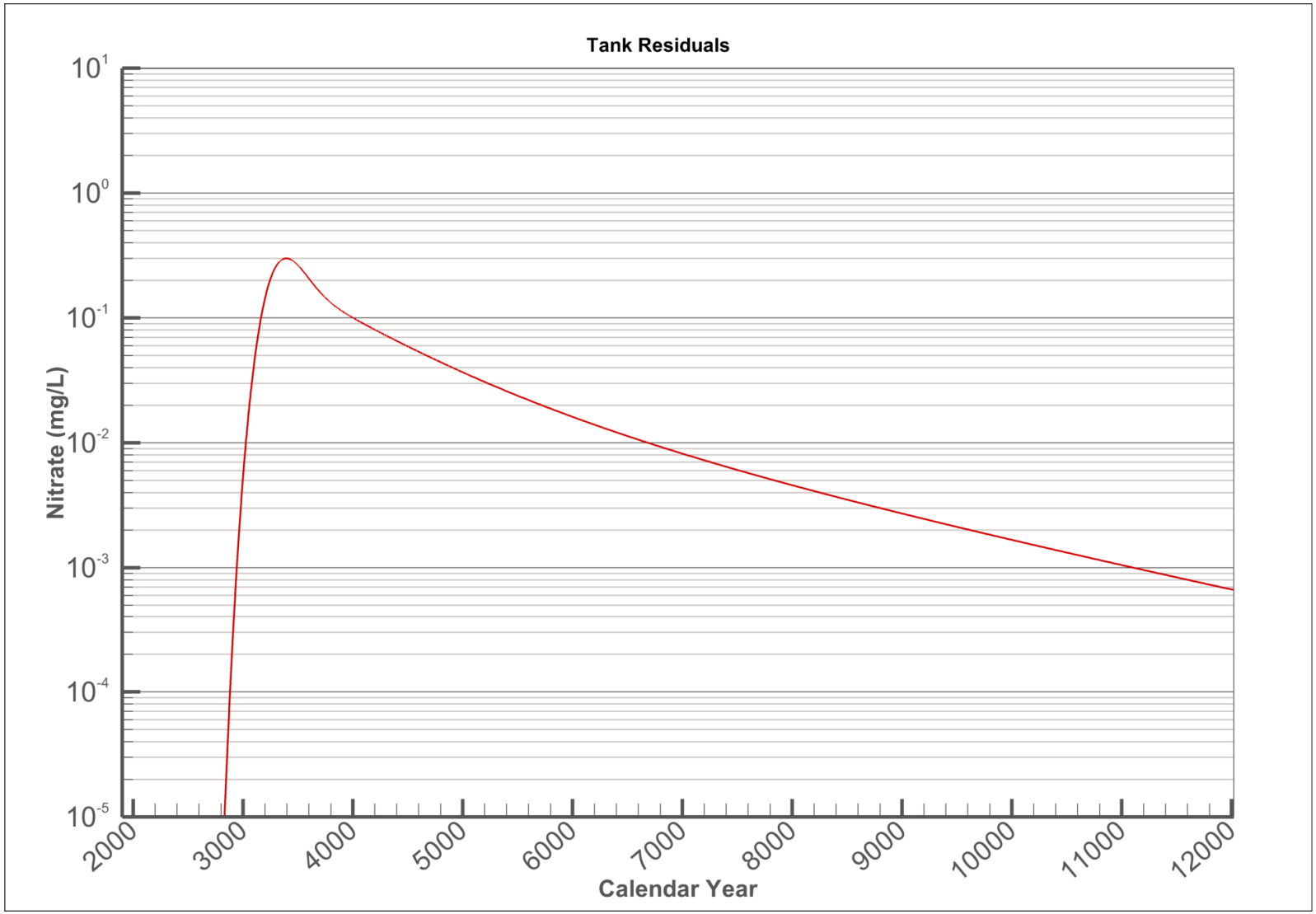

Source: RPP-ENV-58806, "RCRA Closure Analysis of Tank Waste Residuals Impacts at Waste Management Area C, Hanford Site, Washington."

Figure 7-31. Extent of Nitrate Plume in Groundwater 1,375 Years after Closure at the Time of the Maximum Concentration at the 100-meter Point of Calculation.

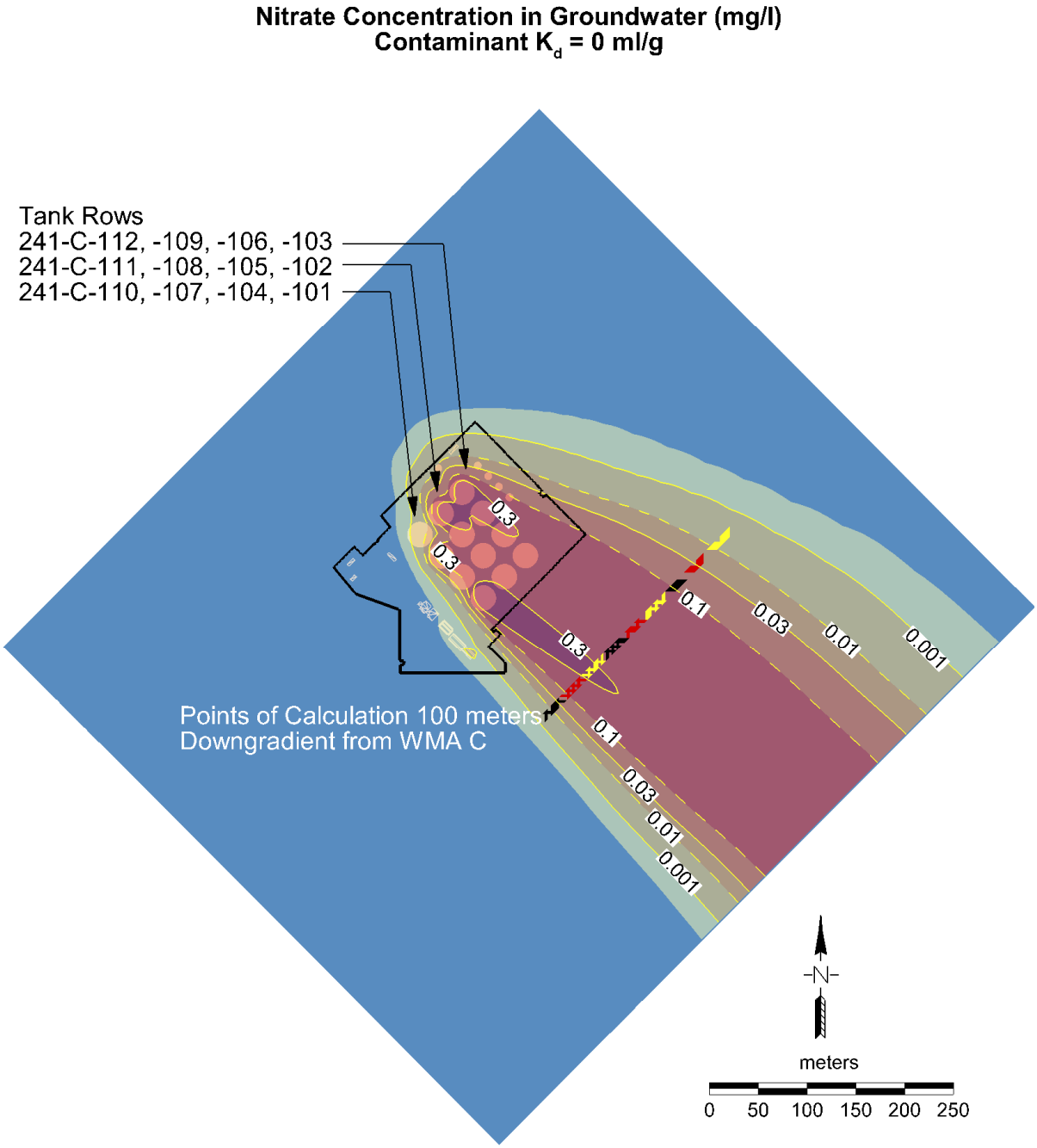

Approximate time of peak concentration at point of calculation

WMA = Waste Management Area

Source: RPP-ENV-58806, "RCRA Closure Analysis of Tank Waste Residuals Impacts at Waste Management Area C, Hanford Site, Washington."

Figure 7-32. Groundwater Concentration of Iodine-129 at All Points of Calculation 100 Meters Downgradient from Waste Management Area C from Residual Wastes.

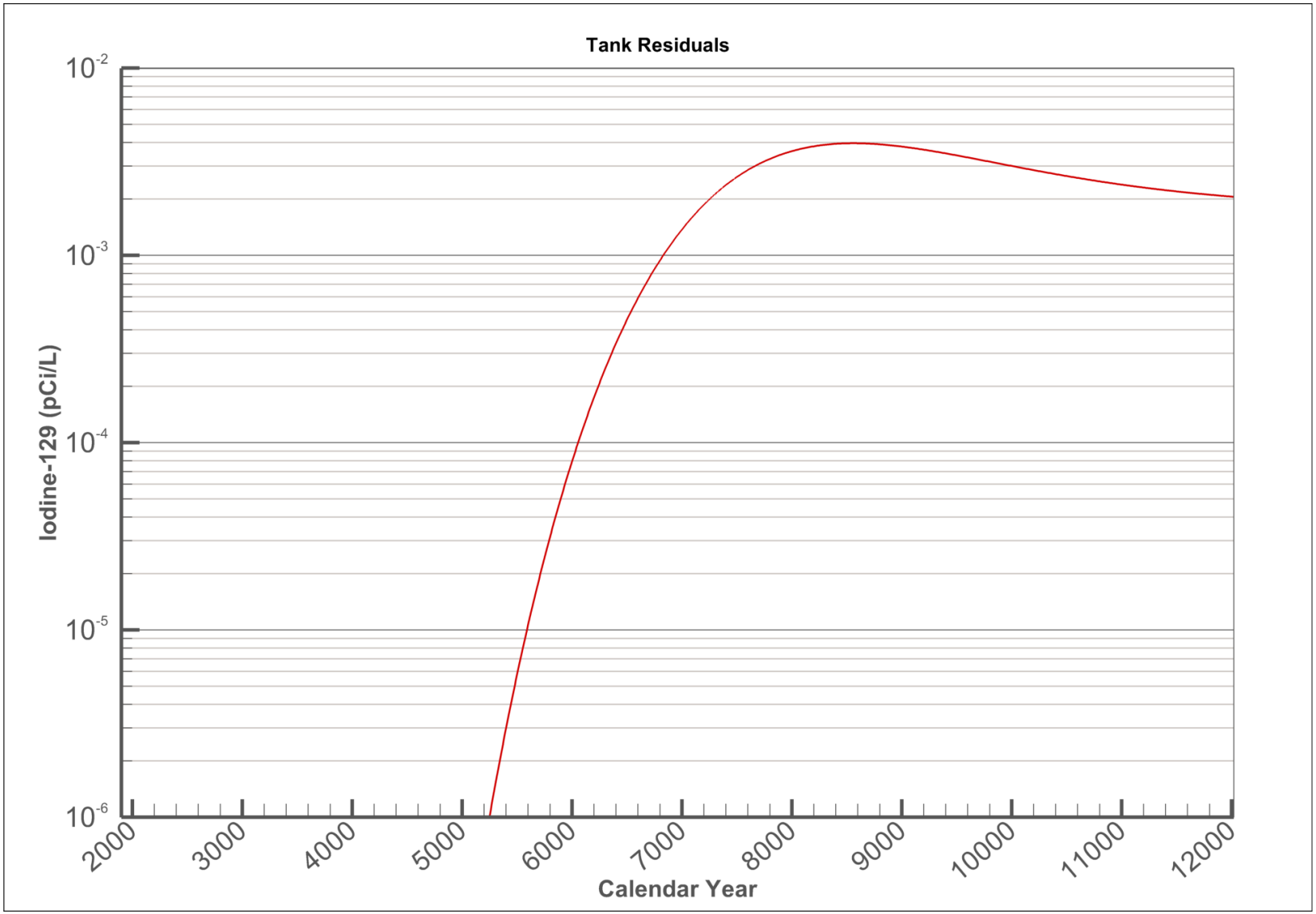

7.2.4 Uranium-238/Total Uranium

Uranium-238 is not a key dose contributor in the residual waste PA (RPP-ENV-58782), but uranium is of broad concern as a contaminant in the Central Plateau, and concentrations of total uranium are presented in the RCA (RPP-ENV-58806). It is a semi-mobile contaminant (K_d=0.6). Calculated concentrations of ^{238}U at the highest point of calculation are presented in Figure 7-33a, and total uranium in Figure 7-33b. The peak concentration for ^{238}U within 10,000 years is 0.02 pCi/L at 10,000 years after closure. The peak concentration for total uranium within 10,000 years is 0.05 µg/L at 10,000 years after closure. The concentrations are still increasing at 10,000 years. The current MCL for total uranium is 30 µg/L.

7.3 COMPARISON OF UPGRADIENT SOURCES, RESIDUAL WASTES, AND PAST LEAKS

In this section, a qualitative comparison is provided between projected concentrations from past leaks, residual wastes, and upgradient sources. Caution must be used in drawing too strong conclusions from this comparison, because the purpose and intent of each is different, and the underlying assumptions differ. Key assumptions in the analyses include the following.

- The projected concentrations for upgradient sources are based on an assumption that no remedial activities will be conducted. Currently-planned remedial actions will likely reduce these concentrations.

- The concentrations calculated for residual wastes are intended for regulatory compliance, and are calculated at a distance 100 m downgradient from WMA C. This location does not correspond to the location of the results presented in Chapter 4.

Consequently, results for the past leaks analysis were calculated at the 100 m PoCals, allowing direct comparisons of results from the assessment of leaks and of residual wastes. Results for the upgradient sources represent the upgradient locations presented in Section 8.2, so caution must be exercised in the comparison with the WMA C sources.

7.3.1 Technetium-99

A comparison of results for ^{99}Tc are presented in Figure 7-34, along with results from the residual waste PA and upgradient sources. The calculation of concentrations from leaks and residual wastes coincide at the same line of analysis at 100 m downgradient, but the upgradient source concentrations are at the PoCals from the P2R model discussed in Section 7.1. The peak concentration of ^{99}Tc associated with the past leaks is ~2 orders of magnitude higher than for residual wastes, and about a factor of 5 higher than upgradient sources. It should be noted that because the peak ^{99}Tc concentration is calculated 100 m downgradient, it does not correspond well to the measured concentrations in monitoring wells, and is about a factor of 4 lower than the highest measured concentration. The peak for past leaks and upgradient contamination is now or in the near future; the peak for residual wastes is ~1,400 years in the future.

Figure 7-33a. Predicted Groundwater Concentration of Uranium-238 at the Highest Point of Calculation 100 Meters Downgradient from Waste Management Area C.

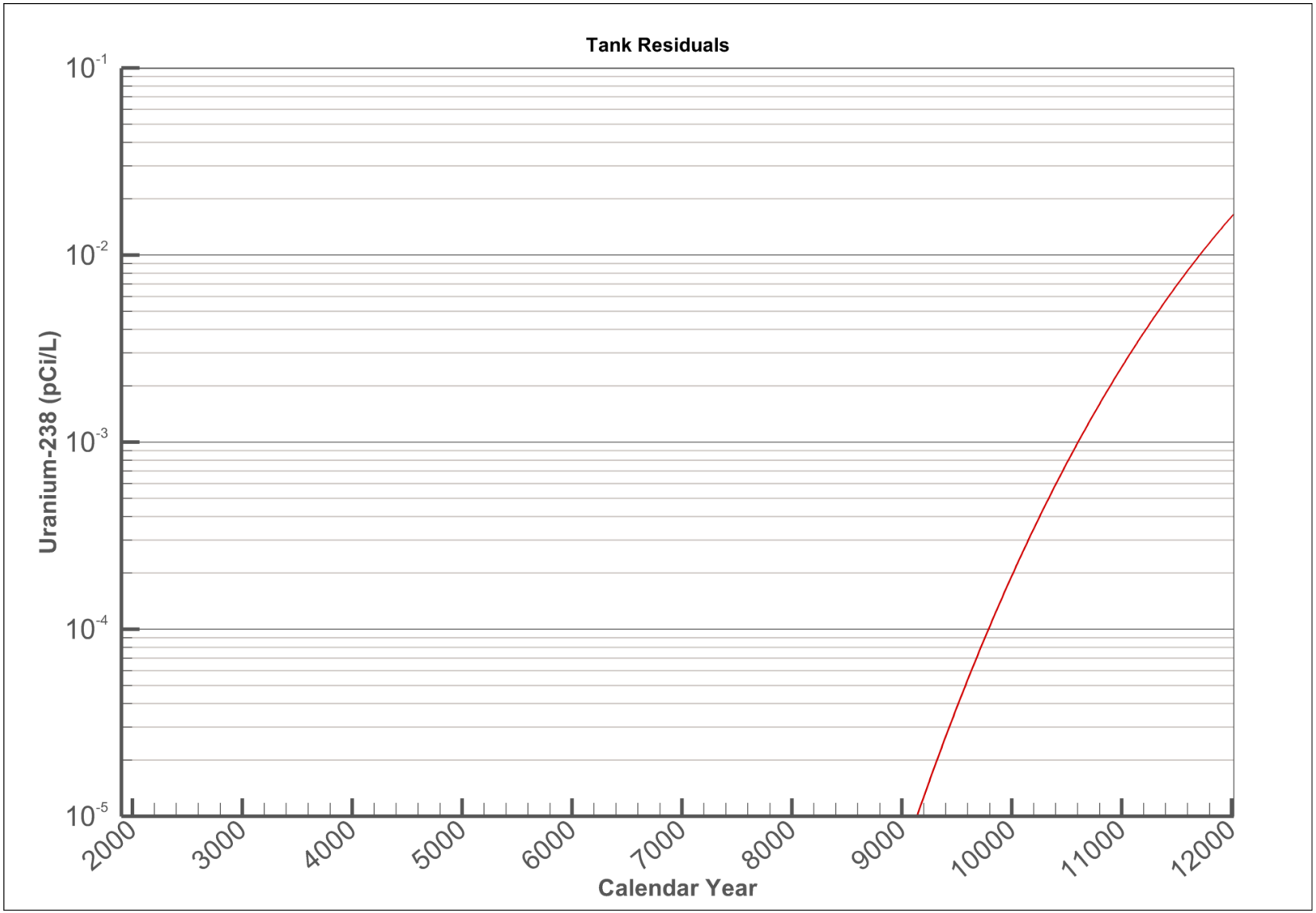

Figure 7-33b. Predicted Groundwater Concentration of Total Uranium at the Highest Point of Calculation 100 Meters Downgradient from Waste Management Area C.

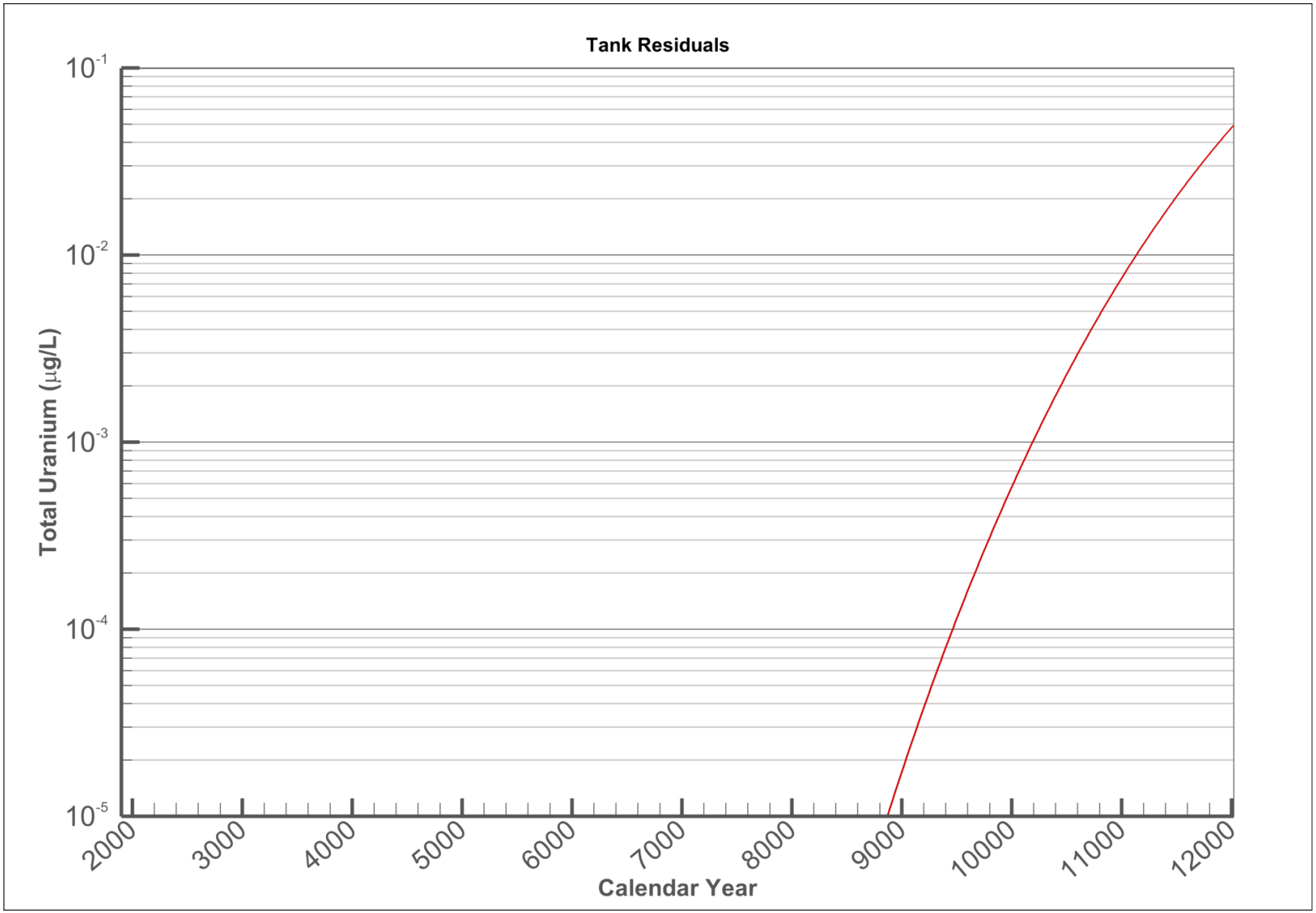

Figure 7-34. Results of the Past Leak Analysis for Technetium-99 at Points of Calculation 100 Meters Downgradient, Compared to Results from the Residual Waste Analysis and Upgradient Sources.

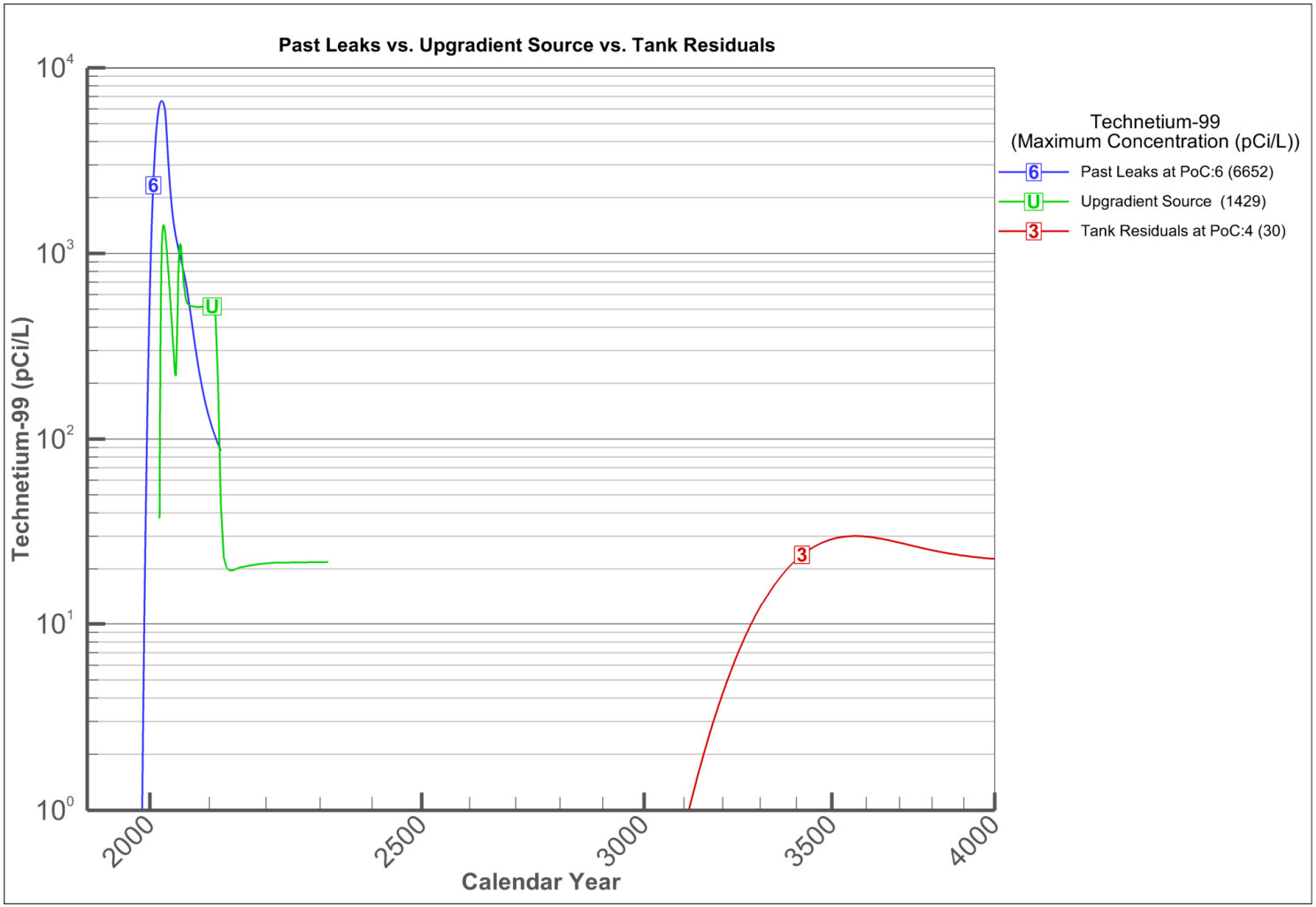

PoC = point of calculation

Note: The peak concentration for each curve is shown in parenthesis in the legend. The plots are on log-log scale to allow comparison of curves at different scales.

7.3.2 Nitrate

A comparison of the results for nitrate are presented in Figure 7-35, along with results from the residual waste PA and upgradient sources. The calculation of concentrations from leaks and residual wastes coincide at the same line of analysis at 100 m downgradient, but the upgradient source concentrations are at the PoCals from the P2R model discussed in Section 7.1. The concentration of nitrate is ~2 orders of magnitude higher than for both residual wastes. The peak concentration for past leaks is now or the near future, whereas the peak concentration from residual wastes is ~1,400 years in the future. Upgradient sources are more than an order of magnitude higher than the peak concentration from past leaks at WMA C.

7.3.3 Iodine-129

A comparison of the results for total uranium are presented in Figure 7-36, along with results from the residual waste PA and upgradient sources. The calculation of concentrations from leaks and residual wastes coincide at the same line of analysis at 100 m downgradient, but the upgradient source concentrations are at the points of calculation from the P2R model discussed in Section 7.1. The concentration of ^{129}I associated with the past leaks is more than 2 orders of magnitude higher than for residual wastes; both peaks occur thousands of years in the future. The peak concentration associated with upgradient sources is the highest among the three, is occurring now or the near future, and does not overlap substantially with the ^{129}I from either sources in WMA C.

7.3.4 Total Uranium

A comparison of the results for total uranium are presented in Figure 7-37, along with results from the residual waste PA and upgradient sources. The calculation of concentrations from leaks and residual wastes coincide at the same line of analysis at 100 m downgradient, but the upgradient source concentrations are at the PoCals from the P2R model discussed in Section 7.1. The concentrations of uranium associated with the past leaks and residual wastes are about the same, and occur at the end of the simulation period (10,000 years). The peak uranium concentration from upgradient sources is ~3 orders of magnitude higher, and occurs in the near future.

7.4 SUMMARY OF PEAK CONCENTRATIONS OF CONTAMINANTS OF POTENTIAL CONCERN

A comparison of the peak concentrations and time of the peaks is shown in Table 7-2. Calculated concentrations from upgradient sources are significantly higher than peak concentrations for all contaminants except ^{99}Tc. However, as discussed in Section 8.3, the evaluations of upgradient contamination assume that there will be no remedial activities undertaken at B Complex. They therefore likely provide significant overestimations of future contamination discharges. Therefore, the results in this section should only be regarded as a qualitative indication of the relative importance of various sources of contamination at WMA C.

Figure 7-35. Results of the Past Leak Analysis for Nitrate at Points of Calculation 100 Meters Downgradient, Compared to Results from the Residual Waste Analysis and Upgradient Sources.

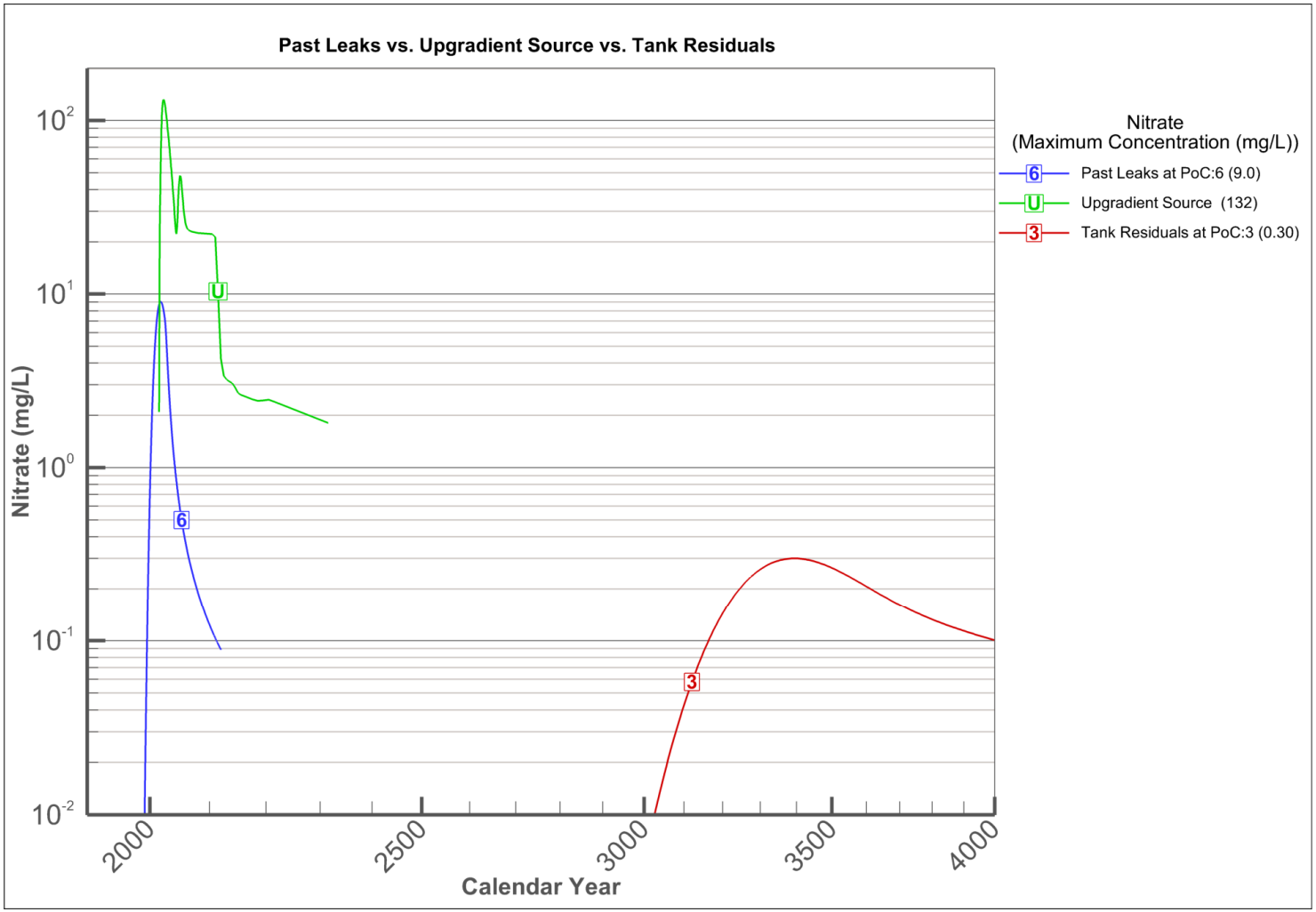

PoC = point of calculation

Note: The peak concentration for each curve is shown in parenthesis in the legend. The plots are on log-log scale to allow comparison of curves at different scales.

Figure 7-36. Results of the Past Leak Analysis for Iodine-129 at Points of Calculation 100 Meters Downgradient, Compared to Results from the Residual Waste Analysis and Upgradient Sources.

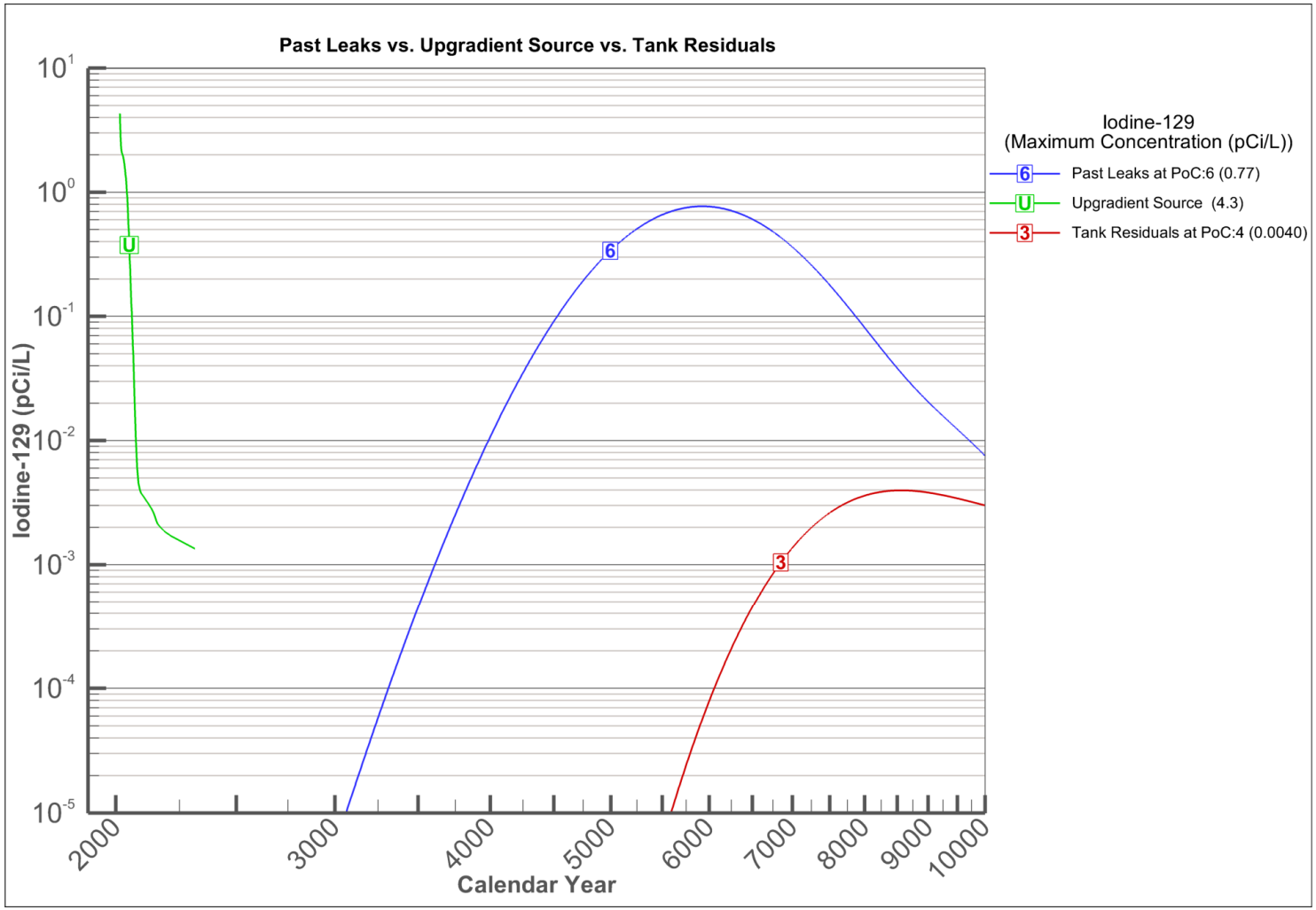

PoC = point of calculation

Note: The peak concentration for each curve is shown in parenthesis in the legend. The plots are on log-log scale to allow comparison of curves at different scales.

Figure 7-37. Results of the Past Leak Analysis for Total Uranium at Points of Calculation 100 Meters Downgradient, Compared to Results from the Residual Waste Analysis and Upgradient Sources.

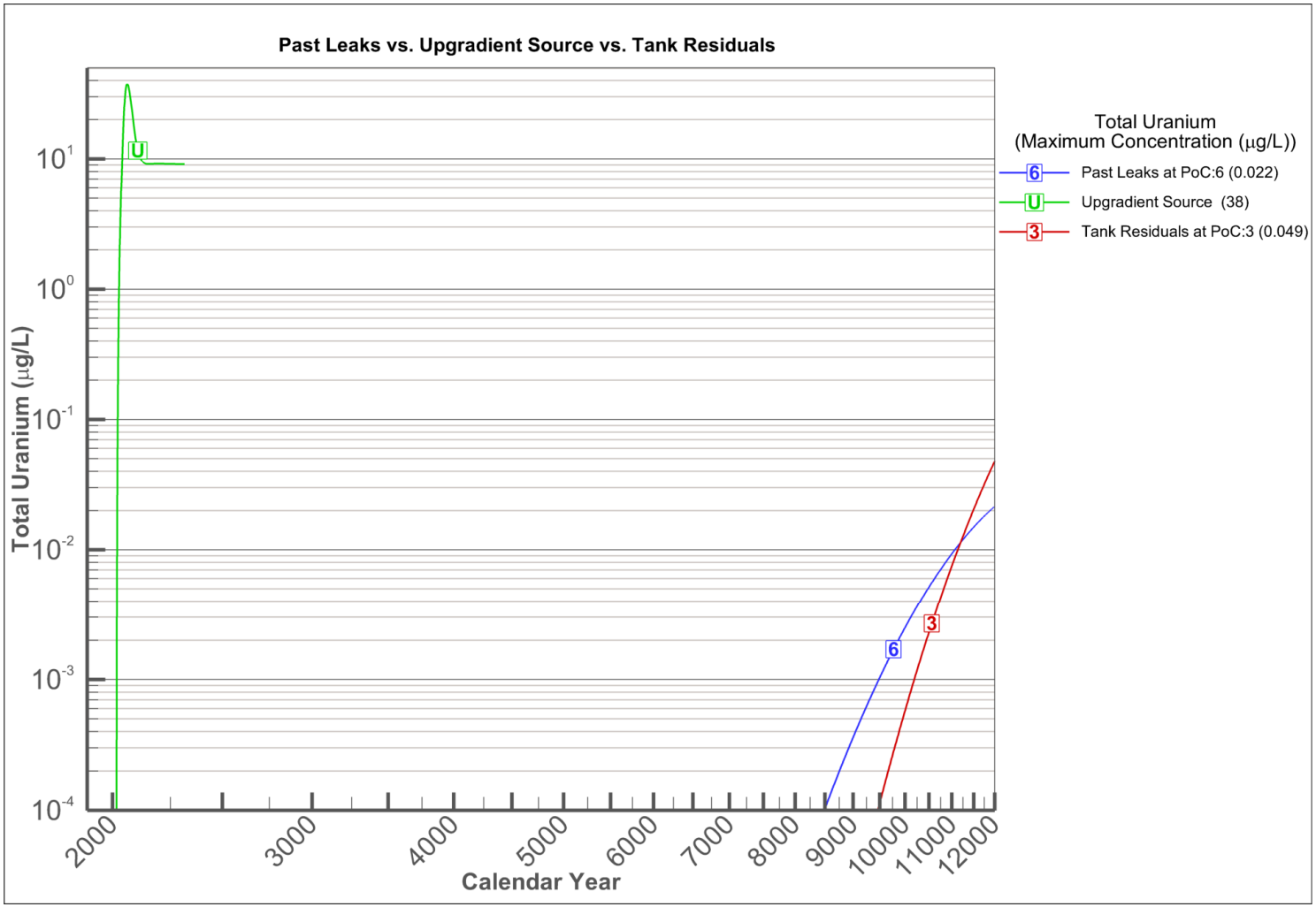

PoC = point of calculation

Note: The peak concentration for each curve is shown in parenthesis in the legend. The plots are on log-log scale to allow comparison of curves at different scales.

Table 7-2. Comparison of Peak Concentrations and Approximate Calendar Year of the Occurrence of the Peak.

Values have been rounded.

Contaminant	Past Leaks		Residual Wastes		Upgradient Sources	
	Year of Peak	Peak Concentration	Year of Peak	Peak Concentration	Year of Peak	Peak Concentration
Tc-99	2020	6,650 pCi/L	3500	30 pCi/L	2020	1,430 pCi/L
Total uranium	12000	0.02 µg/L	12000	0.05 µg/L	2020	38 µg/L
Nitrate	2020	9.0 mg/L	3500	0.3 mg/L	2020	130 mg/L
I-129	6000	0.8 pCi/L	8500	0.004 pCi/L	2020	4.3 pCi/L

This page intentionally left blank.

8.0 SUMMARY AND OBSERVATIONS

The analysis of past leaks has been structured to meet several goals. First, the analysis is intended to be responsive to ideas and concerns expressed in the 2009 – 2011 PA scoping sessions (see Section 1.1.1), in which specific features of WMA C were identified as requiring particular attention because of their potential to influence the migration of contaminants from WMA C. Second, the analysis is intended to be consistent, to the extent possible, with the PA (RPP-ENV-58782) and RCA (RPP-ENV-58806) for disposal of residual wastes in WMA C. Third, the goal is to provide an understanding of the key features and processes discussed in Sections 1 and 2 that influence the migration of contaminants. Fourth, the goal is to use the understanding gained by the analysis to provide a projection of the future evolution of the contamination beneath WMA C.

The scoping analyses presented in Section 4 of this report provide comparisons of alternative conceptual and numerical models of WMA C to groundwater monitoring data to evaluate the credibility of alternative assumptions for the migration of the leaks from the time of their occurrence to today. The alternative models evaluated different assumptions about leak volumes and inventories, groundwater flux, recharge, and vadose zone conceptual models.

Scoping analysis Cases 1a and 1b represent a minimal change from the PA/RCA model for residual wastes presented in RPP-ENV-58782 and RPP-ENV-58806, with the level of the water table elevated to represent an appropriate travel distance to the water table for the leaks. Case 1a uses upper bound leak inventories and volumes based on an assumed upper bound inventory for the tank C-105 waste loss of 9.8 Ci and an upper bound leak volume of 75,600 L (20,500 gal). Case 1b uses the lower bound leak inventories and volumes based on assumed lower bound ^{99}Tc inventory for the tank C-105 waste loss of 1.0 Ci and a lower bound leak volume of 7,570 L (2,000 gal).

Scoping analysis Case 1b produced concentrations substantially below observed concentrations for ^{99}Tc in observation wells. It was concluded that the lower bound estimate is inconsistent with data, and the upper bound estimate of 10 Ci ^{99}Tc in the tank C-105 leak waste was used for all other analyses. The upper bound estimate, when evaluated with the 10th percentile aquifer flux and in the transient water table boundary analysis, produces modeled concentration results comparable to the highest values measured in the monitoring wells around WMA C.

Cases 2a and 2b investigated the effect of changing groundwater fluxes on the model results. It was found that the higher flux rates led to a greater dilution of plume concentrations at the water table, and it is concluded that the lower groundwater flux rate provides concentration levels of ^{99}Tc that are more consistent with monitoring data observed in key monitoring well locations (see Figures 4-34 and 4-35).

Cases 3a and 3b investigated the general effect of a higher recharge rate than used in the other scoping analysis cases. Generally it was found that the higher recharge rates led to early arrival of the plume at the water table. At a rate of 100 mm/y the difference is negligible, but at 150 mm/y the higher recharge rate generated earlier arrival times that are not consistent with monitoring data observed in key monitoring well locations (see Figures 4-34 and 4-35).

Case 3c investigated the effect of a localized addition of water using a firehose to mitigate the operational hazard of leaks at UPRs -82 and -86, followed by the addition of gunite caps on the UPRs. The results of the analysis case are very similar to Case 1, indicating that this past practice had little effect on the downward migration of waste releases from the three UPRs to groundwater at WMA C (see Figures 4-34 and 4-35).

Cases 4a through 4f investigated a number of vadose zone parameters and conceptual models of potential interest, to evaluate the potential for heterogeneities in the vadose zone to affect the plume development migration.

The results of these analysis cases compared to available monitoring data (see Figures 4-34 and 4-35) indicate the following.

- The evaluation of ACM-II in Case 4a showed that adding refinement in the Hanford H2 Sand unit did not strongly affect the results of the analysis. Neither alternative model represented in Case 4a and Case 1a was found to be clearly superior to the other in terms of explaining the monitoring well data.

- The evaluation in Case 4b of ACM using a heterogeneous representation of the vadose zone in Case 4b showed that adding heterogeneity resulted in an earlier arrival time than has been observed in monitoring wells and concentrations levels that were lower than those shown for Case 1a. This alternative model appears to be inconsistent with data and is not preferred for further analyses.

- The evaluation of median values of vadose zone hydraulic properties in Case 4c showed arrival time and concentration results that were not significantly different than those for Case 1a. However, the evaluation of 95th percentile values of vadose zone hydraulic properties in Case 4d showed arrival time results that were significantly different than those for Case 1a and the arrival times and concentration levels of ^{99}Tc concentrations from key monitoring wells. Therefore, the use of 95th percentile properties is not preferred for use in further analyses.

The evaluation of a hypothetical clastic dike and a poorly sealed borehole located near the assumed waste release near tank C-105 in Cases 4e and 4f showed a slightly earlier arrival time at the water table and only a small effect of estimated peak concentrations. Since these scoping analysis cases produce results that are similar to cases in which these features are absent, they are not preferred to use in further analyses.

As discussed in Section 4.8, three scoping analysis cases produced results in which the arrival time of the calculated plume appears to be substantially earlier than the observations in the wells. These scoping analysis cases are

- Case 3a, in which the recharge was increased to 150 mm/y,

- Case 4b, in which the spatial variability of the vadose zone properties was represented by an alternative heterogeneous representation, and

- Case 4d, in which the flow properties of the vadose zone soil were set to their 95th percentile values.

The remaining scoping analysis cases evaluated in Section 4 produced comparable results to each other, and none were obviously superior to others in terms of explaining the observation well data. When uncertainties in groundwater fluxes were taken into account, these scoping analyses were capable of producing both arrival times and concentrations consistent with observed monitoring well data for ^{99}Tc.

The analysis in Section 4 that showed the best representation of the observation well data was made with the transient water table analysis presented in Section 5. However, it was necessary to make alterations to the boundary conditions to achieve the good agreement with data. These alterations are speculative but serve to provide insight into the evolution of the monitoring well data.

The model analysis of transient flow conditions provided in Section 5 showed that the conceptual model involving the counterclockwise rotation of the hydraulic gradient from northwest to southeast provided the best representation of observed conditions in monitoring wells near WMA C. The associated numerical model results appear capable of approximating observed field data for the time of arrival of ^{99}Tc to groundwater and concentration levels of ^{99}Tc in groundwater. The model results include several assumptions regarding the timing and inventory of the past releases, and direction and magnitude of the hydraulic gradient during the time it could not be measured. Because of these assumptions, it is unknown how accurately the model calculations represent the actual release of ^{99}Tc and its transport in the vadose zone and groundwater. The results do, however, provide some insight into the concentration levels observed in monitoring wells, and the changes in concentration that have occurred in those wells since 2000. The concentration of ^{99}Tc observed in most of the monitoring wells appears to change too abruptly to represent the one-dimensional passing of a contaminant front. The modeling results indicate that the concentration in the wells changes so abruptly because of the direction and the magnitude of the groundwater hydraulic gradient changes. The rotation of the gradient continually changes the orientation of the groundwater plumes relative to the wells. The high concentrations measured in wells 299-E27-23 and 299-E27-13 between 2010 and 2012 likely correspond to the time when those wells were located downgradient of the sources. By 2014, the concentration in those two wells dropped markedly, while the concentration in well 299-E27-21 began increasing quickly around that same time. According to the modeling results, this pattern in the data can be explained by, and corresponds to, the further rotation of gradient from the south to the southeast.

The release from tank C-105 appears to be the dominant source of ^{99}Tc observed in groundwater in the monitoring wells. According to the inventory estimates in RPP-RPT-42294, it is the only release large enough and that occurred early enough to bring about the concentration levels observed in the monitoring wells. Whether or not the release from tank C-105 is truly the dominant source of ^{99}Tc observed at the monitoring wells is unknown. However, the modeling results do indicate that most of the ^{99}Tc observed in the monitoring wells located southwest of the farm originated from the sources inside the farm, and not from the UPRs that occurred away from the tanks. These three UPRs occurred later than the release from tank C-105, and the

modeling results exhibit the implications of this. The concentration of ^{99}Tc in the wells located nearest the UPRs is dominated by the ^{99}Tc contained in the release from tank C-105. The concentration of ^{99}Tc attributed to the ^{99}Tc contained in the three UPRs peaks a few years after the concentration of ^{99}Tc peaks because of the tank C-105 release. This is later than the data indicate that the peaks occurred in the wells.

The modeling results indicate that as the water table returns to more natural conditions, the rotation of the gradient will continue to alter the primary movement of the plumes from primarily a southerly direction to a more southeasterly direction in the near future. The very high concentration levels of ^{99}Tc observed in wells 299-E27-23 and 299-E27-21, southwest and south of WMA C, respectively, are likely to be observed in wells 299-E27-24 and 299-E27-14, which are located to the southeast of WMA C.

In the assessment of the impacts of past waste releases into the future, sorbing and nonsorbing contaminants were treated differently, because of the anticipated difference in the height of the water table now and in the future. As a result of this difference, the forward modeling of leaks has been undertaken using models with different water table heights for the sorbing and nonsorbing contaminants. For sorbing contaminants the PA/RCA model was used, while for nonsorbing contaminants, Scoping Case 1a was used.

The forward projection results lead to several observations, as follows.

- Model results indicate that current high concentrations of ^{99}Tc below WMA C are expected to decline over the next several decades as the contamination plume disperses in the aquifer.

- Contaminated groundwater, which is now impacted by releases from past waste leaks and losses at WMA C and, in the future, by upgradient sources in the B Complex area, will continue to migrate downgradient and will impact groundwater in local areas contained within the 200-PO-1 groundwater OU such as the A Complex area.

- There are not significant overlaps between releases from residual wastes in a closed WMA C and the releases from leaks.

- Compared to the releases from WMA C past leaks or residual wastes, the releases from upgradient sources produce more significant groundwater concentrations for all contaminants other than ^{99}Tc. For ^{99}Tc, the concentrations associated with past leaks are the most significant.

9.0 REFERENCES

04-TPD-083, 2004, "Agreement on Content of Tank Waste Retrieval Work Plans" (external letter from R. J. Schepens to M. A. Wilson, Nuclear Waste Program, State of Washington Department of Ecology, August 20), U.S. Department of Energy, Office of River Protection, Richland, Washington.

1301789, 2012, "Modeling to Support Regulatory Decisionmaking at Hanford" (internal memorandum from A. C. Williams to M. S. McCormick [Richland Operations Office] and S. L. Samuelson [Office Of River Protection], October 9), Associate Principal Deputy Assistant Secretary for Environmental Management, U.S. Department of Energy, Washington, D.C.

40 CFR 141, "National Primary Drinking Water Regulations," Code of Federal Regulations, as amended.

ARH-1945, 1971, "B Plant Ion Exchange Feed Line Leak," Atlantic Richfield Hanford Company, Richland, Washington.

BHI-00169, 1995, "Environmental Restoration Disposal Facility Performance Assessment," Revision 00, Bechtel Hanford, Inc., Richland, Washington.

BHI-01103, 1999, "Clastic Injection Dikes of the Pasco Basin and Vicinity – Geologic Atlas Series," Rev. 0, Bechtel Hanford, Inc., Richland, Washington.

BNWL-B-360, 1974, "Selected Water Table Contour Maps and Well Hydrographs for the Hanford Reservation, 1944-1973," Pacific Northwest Laboratory, Richland, Washington.

CHPRC-00269, 2013, "STOMP Requirements Traceability Matrix CHPRC Build 4," Rev. 3, CH2M HILL Plateau Remediation Company, Richland, Washington.

CP-47631, 2011, "Model Package Report: Central Plateau Groundwater Model Version 3.3," Rev. 0, CH2M HILL Plateau Remediation Company, Richland, Washington.

CP-47631, 2015, "Model Package Report: Central Plateau Groundwater Model Version 6.3.3," Rev. 2, INTERA, Inc., Richland, Washington.

CP-57037, 2015, "Model Package Report: Plateau to River Groundwater Transport Model Version 7.1," Rev. 0, CH2M HILL Plateau Remediation Company, Richland, Washington.

DOE/EIS-0391, 2012, "Final Tank Closure and Waste Management Environmental Impact Statement for the Hanford Site, Richland, Washington," U.S. Department of Energy, Washington, D.C.

DOE O 435.1, 2001, Radioactive Waste Management, U.S. Department of Energy, Washington, D.C.

DOE/ORP-2000-24, 2001, Hanford Immobilized Low-Activity Waste Performance Assessment: 2001 Version, Rev. 0, U.S. Department of Energy, Office of River Protection, Richland, Washington.

DOE/ORP-2005-01, 2006, Initial Single-Shell Tank System Performance Assessment for the Hanford Site, Rev. 0, U.S. Department of Energy, Office of River Protection, Richland, Washington.

DOE/ORP-2008-01, 2010, RCRA Facility Investigation Report for Hanford Single-Shell Tank Waste Management Areas, Rev. 1, U.S. Department of Energy, Office of River Protection, Richland, Washington.

DOE/RL-93-33, 1996, Focused Feasibility Study of Engineered Barriers for Waste Management Units in the 200 Areas, Rev. 1, U.S. Department of Energy, Richland Operations Office, Richland, Washington.

DOE/RL-2008-66, 2009, Hanford Site Groundwater Monitoring for Fiscal Year 2008, Rev. 0, U.S. Department of Energy, Richland Operations Office, Richland, Washington.

DOE/RL-2009-77, 2010, Groundwater Quality Assessment Plan for the Single-Shell Tank Waste Management Area C, Rev. 0, U.S. Department of Energy, Richland Operations Office, Richland, Washington.

DOE/RL-2009-127, 2015, Remedial Investigation Report for the 200-BP-5 Groundwater Operable Unit, Draft A, U.S. Department of Energy, Richland Operations Office, Richland, Washington.

DOE/RL-2010-11, 2010, Hanford Site Groundwater Monitoring and Performance Report for 2009 Volumes 1 and 2, Rev. 1, U.S. Department of Energy, Richland Operations Office, Richland, Washington.

DOE/RL-2011-01, 2011, Hanford Site Groundwater Monitoring Report for 2010, Rev. 0, U.S. Department of Energy, Richland Operations Office, Richland, Washington.

DOE/RL-2011-50, 2012, Regulatory Basis and Implementation of a Graded Approach to Evaluation of Groundwater Protection, Rev. 1, U.S. Department of Energy, Richland Operations Office, Richland, Washington.

DOE/RL-2011-118, 2012, Hanford Site Groundwater Monitoring for 2011, Rev. 0, U.S. Department of Energy, Richland Operations Office, Richland, Washington.

DOE/RL-2014-32, 2014, Hanford Site Groundwater Monitoring Report for 2013, Rev. 0, U.S. Department of Energy, Richland Operations Office, Richland, Washington.

DOE/RL-2015-07, 2015, Hanford Site Groundwater Monitoring Report for 2014, Rev. 0, U.S. Department of Energy, Richland Operations Office, Richland, Washington.

ECF-Hanford-13-0031, 2015, "Fate and Transport Modeling for Baseline Conditions for Remedial Investigation/Feasibility Studies of the 200-BP-5 and 200-PO-1 Groundwater Operable Units," Rev. 0, CH2M HILL Plateau Remediation Company, Richland, Washington.

ECF-Hanford-13-0037, 2015, "Development of Source Terms for Inclusion in Fate and Transport Modeling for Remedial Investigation/Feasibility Studies of the 200-BP-5 and 200-PO-1 Groundwater Operable Units," Rev. 0, INTERA, Inc., Richland, Washington.

ECF-Hanford-15-0011, 2015, "Evaluation of Contaminant Transport for the 200-BP-5 and 200-PO-1 Operable Units Feasibility Study Evaluation of Remedial Alternatives," Draft A, Washington River Protection Solutions, LLC, Richland, Washington.

Ecology, EPA, and DOE, 1989, Hanford Federal Facility Agreement and Consent Order – Tri-Party Agreement, 2 vols., as amended, State of Washington Department of Ecology, U.S. Environmental Protection Agency, and U.S. Department of Energy, Olympia, Washington.

EPA/540/F-95/041, 1996, Soil Screening Guidance: Fact Sheet, Publication 9355.4-14FSA, U.S. Environmental Protection Agency, Office of Solid Waste and Emergency Response, Washington, D.C.

EPA/540/R-95/128, 1996, Soil Screening Guidance: Technical Background Document, Second Edition, U.S. Environmental Protection Agency, Washington, D.C.

EPA/600/2-91/065, 1991, The RETC Code for Quantifying the Hydraulic Functions of Unsaturated Soils, Office of Research and Development, U.S. Environmental Protection Agency, Washington, D.C.

ERDA-1538, 1975, "Final Environmental Impact Statement, Waste Management Operations, Hanford Reservation, Richland, Washington," U.S. Energy Research and Development Administration, Richland, Washington.

Fayer, M. J., and G. W. Gee, 2006, "Multiple-Year Water Balance of Soil Covers in a Semiarid Setting," Journal of Environmental Quality, Vol. 35, No. 2, pp. 366–377.

GJO-98-39-TAR/GJO-HAN-18, 1998, "Hanford Tank Farms Vadose Zone: C Tank Farm Report," U.S. Department of Energy, Grand Junction Office, Grand Junction, Colorado.

GJO-98-39-TARA/GJO-HAN-18, 2000, "Hanford Tank Farms Vadose Zone: Addendum to the C Tank Farm Report," U.S. Department of Energy, Grand Junction Office, Grand Junction, Colorado.

HNF-38155, 2013, "HEIS Sample, Result, and Sampling Site Data Dictionary," Rev. 1, CH2M HILL Plateau Remediation Company, Richland, Washington.

HNF-EP-0182, 2013, "Waste Tank Summary Report for Month Ending September 30, 2013," Rev. 306, Washington River Protection Solutions, LLC, Richland, Washington.

HNF-EP-0182, 2015, "Waste Tank Summary Report for Month Ending February 28, 2015," Rev. 326, Washington River Protection Solutions, LLC, Richland, Washington.

HW-60601, 1959, "Aquifer Characteristics and Ground-Water Movement at Hanford," General Electric Company, Richland, Washington.

Jury, W. A., W. R. Gardner, and W. H. Gardner, 1991, Soil Physics, 5th edition, Wiley and Sons, Inc., New York, New York.

Jury, W. A. and R. Horton, 2004, Soil Physics, 6th edition, Wiley and Sons, Inc., New York, New York.

Khaleel, R., J. F. Relyea, and J. L. Conca, 1995, "Evaluation of van Genuchten-Mualem Relationships to Estimate Unsaturated Hydraulic Conductivity at Low Water Contents," Water Resources Research, Vol. 31, Issue 11, pp. 2659–2668.

Millington, R. J. and J. P. Quirk, 1961, "Permeability of Porous Solids," Transactions of the Faraday Society, Vol. 57, pp. 1200–1207.

Mualem, Y., 1976, "A New Model for Predicting the Hydraulic Conductivity of Unsaturated Porous Media," Water Resources Research, Vol. 12, No. 3, pp. 513–522.

Murray, C. J., A. L. Ward, and J. L. Wilson, 2007, "Influence of Clastic Dikes on Vertical Migration of Contaminants at the Hanford Site," Vadose Zone Journal, Vol. 6, No. 4, pp. 959–970.

NOAA Manual NOS NGS 5, 1990, "State Plane Coordinate System of 1983," National Geodetic Survey, U.S. Department of Commerce, National Oceanic and Atmospheric Administration, Rockville, Maryland.

Pacific Northwest National Laboratory, Queried 12/18/2015, [STOMP User Guide], http://stomp.pnnl.gov/user_guide/STOMP_guide.stm.

PNL-6464, 1988, "Environmental Monitoring at Hanford for 1987," Pacific Northwest Laboratory, Richland, Washington.

PNL-10886, 1995, "Development of a Three-Dimensional Ground-Water Model of the Hanford Site Unconfined Aquifer System: FY 1995 Status Report," Pacific Northwest National Laboratory, Richland, Washington.

PNNL-11216, 1997, "STOMP Subsurface Transport Over Multiple Phases Application Guide," Pacific Northwest National Laboratory, Richland, Washington.

PNNL-12030, 2000, "STOMP Subsurface Transport Over Multiple Phases Version 2.0 Theory Guide," Pacific Northwest National Laboratory, Richland, Washington.

PNNL-12261, 2000, "Revised Hydrogeology for the Suprabasalt Aquifer System, 200-East Area and Vicinity, Hanford Site, Washington," Pacific Northwest National Laboratory, Richland, Washington.

PNNL-13024, 2001, "RCRA Groundwater Monitoring Plan for Single-Shell Tank Waste Management Area C at the Hanford Site," as amended, Pacific Northwest National Laboratory, Richland, Washington.

PNNL-13033, 1999, "Recharge Data Package for the Immobilized Low-Activity Waste 2001 Performance Assessment," Pacific Northwest National Laboratory, Richland, Washington.

PNNL-13641, 2001, "Uncertainty Analysis Framework – Hanford Site-Wide Groundwater Flow and Transport Model," Pacific Northwest National Laboratory, Richland, Washington.

PNNL-14224, 2003, "Influence of Clastic Dikes on Vertical Migration of Contaminants in the Vadose Zone at Hanford," Pacific Northwest National Laboratory, Richland, Washington.

PNNL-14398, 2003, "Transient Inverse Calibration of the Site-Wide Groundwater Flow Model (ACM-2): FY 2003 Progress Report," Pacific Northwest National Laboratory, Richland, Washington.

PNNL-14548, 2004, "Hanford Site Groundwater Monitoring for Fiscal Year 2003," Pacific Northwest National Laboratory, Richland, Washington.

PNNL-14753, 2006, "Groundwater Data Package for Hanford Assessments," Rev. 1, Pacific Northwest National Laboratory, Richland, Washington.

PNNL-15837, 2007, "Data Package for Past and Current Groundwater Flow and Contamination Beneath Single-Shell Tank Waste Management Areas," Pacific Northwest National Laboratory, Richland, Washington.

PNNL-16663, 2007, "Geochemical Processes Data Package for the Vadose Zone in the Single-Shell Tank Waste Management Areas at the Hanford Site," Pacific Northwest National Laboratory, Richland, Washington.

PNNL-16688, 2007, "Recharge Data Package for Hanford Single-Shell Tank Waste Management Areas," Pacific Northwest National Laboratory, Richland, Washington.

PNNL-17154, 2008, "Geochemical Characterization Data Package for the Vadose Zone in the Single-Shell Tank Waste Management Areas at the Hanford Site," Pacific Northwest National Laboratory, Richland, Washington.

PNNL-17154, 2008, "Geochemical Characterization Data Package for the Vadose Zone in the Single-Shell Tank Waste Management Areas at the Hanford Site," Pacific Northwest National Laboratory, Richland, Washington.

PNNL-17176, 2007, "200-BP-1 Prototype Hanford Barrier Annual Monitoring Report for Fiscal Years 2005 Through 2007," Pacific Northwest National Laboratory, Richland, Washington.

PNNL-19702, 2010, "Hydrogeologic Model for the Gable Gap Area, Hanford Site," Pacific Northwest National Laboratory, Richland, Washington.

PNNL-23711, 2015, "Physical, Hydraulic, and Transport Properties of Sediments and Engineered Materials Associated with Hanford Immobilized Low-Activity Waste," RPT-IGTP-004, Rev. 0, Pacific Northwest National Laboratory, Richland, Washington.

Resource Conservation and Recovery Act of 1976, 42 USC 6901, et seq.

RHO-CD-673, 1979, "Handbook 200 Areas Waste Sites," Rockwell Hanford Operations, Richland, Washington.

RPP-14430, 2003, "Subsurface Conditions Description of the C and A-AX Waste Management Area," Rev. 0, CH2M HILL Hanford Group, Inc., Richland, Washington.

RPP-19822, 2005, "Hanford Defined Waste Model – Revision 5.0," Rev. 0-A, CH2M HILL Hanford Group, Inc./Technical Resources International, Inc., Richland, Washington.

RPP-23748, 2006, "Geology, Hydrogeology, Geochemistry, and Mineralogy Data Package for the Single-Shell Tank Waste Management Areas at the Hanford Site," Rev. 0, CH2M HILL Hanford Group, Inc., Richland, Washington.

RPP-26744, 2005, "Hanford Soil Inventory Model, Rev. 1," Rev. 0, CH2M HILL Hanford Group, Inc., Richland, Washington.

RPP-32681, 2013, "Process to Assess Tank Farm Leaks in Support of Retrieval and Closure Planning," Rev. 2, Washington River Protection Solutions, LLC, Richland, Washington.

RPP-35484, 2008, "Field Investigation Report for Waste Management Areas C and A-AX," Rev. 1, CH2M HILL Hanford Group, Inc., Richland, Washington.

RPP-ASMT-38219, 2008, "Tank 241-C-110 Leak Assessment Report," Rev. 0, CH2M HILL Hanford Group, Inc., Richland, Washington.

RPP-ASMT-39155, 2008, "Tank 241-C-111 Leak Assessment Report," Rev. 0, CH2M HILL Hanford Group, Inc., Richland, Washington.

RPP-ASMT-46452, 2010, "Tank 241-C-105 Leak Assessment Completion Report," Rev. 0, Washington River Protection Solutions, LLC, Richland, Washington.

RPP-ENV-33418, 2016, "Hanford C-Farm Leak Inventory Assessments Report," Rev. 4, Washington River Protection Solutions, LLC, Richland, Washington.

RPP-ENV-58782, 2016, "Performance Assessment of Waste Management Area C, Hanford Site, Washington," Rev. 0, Washington River Protection Solutions, LLC, Richland, Washington.

RPP-ENV-58806, 2016, "RCRA Closure Analysis of Tank Waste Residuals Impacts at Waste Management Area C, Hanford Site, Washington," Rev. 0, Washington River Protection Solutions, LLC, Richland, Washington.

RPP-PLAN-39114, 2012, "Phase 2 RCRA Facility Investigation/Corrective Measures Study Work Plan for Waste Management Area C," Rev. 2, Washington River Protection Solutions, LLC, Richland, Washington.

RPP-RPT-41918, 2010, "Assessment Context for Performance Assessment for Waste in C Tank Farm Facilities after Closure," Rev. 0, Washington River Protection Solutions, LLC, Richland, Washington.

RPP-RPT-42294, 2016, "Hanford Waste Management Area C Soil Contamination Inventory Estimates," Rev. 2, Washington River Protection Solutions, LLC, Richland, Washington.

RPP-RPT-42323, 2015, "Hanford C-Farm Tank and Ancillary Equipment Residual Waste Inventory Estimates," Rev. 3, Washington River Protection Solutions, LLC, Richland, Washington.

RPP-RPT-44042, 2010, "Recharge and Waste Release within Engineered System in Waste Management Area C," Rev. 0, Washington River Protection Solutions, LLC, Richland, Washington.

RPP-RPT-46088, 2010, "Flow and Transport in the Natural System at Waste Management Area C," Rev. 1, Washington River Protection Solutions, LLC/GSI Water Solutions, Inc., Richland, Washington.

RPP-RPT-46879, 2011, "Corrosion and Structural Degradation within Engineered System in Waste Management Area C," Rev. 2, Washington River Protection Solutions, LLC, Richland, Washington.

RPP-RPT-47479, 2011, "Exposure Scenarios for the Waste Management Area C Performance Assessment," Rev. 1, Washington River Protection Solutions, LLC, Richland, Washington.

RPP-RPT-48490, 2011, "Technical Approach and Scope for Flow and Contaminant Transport Analysis in the Initial Performance Assessment of Waste Management Area C," Washington River Protection Solutions, LLC, Richland, Washington.

RPP-RPT-49425, 2011, "Ecological Risk Assessment Approach for Hanford Waste Management Area C," Rev. 1, Washington River Protection Solutions, LLC, Richland, Washington.

RPP-RPT-56356, 2014, "Development of Alternative Digital Geologic Models of Waste Management Area C," Rev. 0, Freestone Environmental Services Inc./Washington River Protection Solutions, LLC, Richland, Washington.

RPP-RPT-58297, 2014, "Screening-Level Evaluation of Groundwater Monitoring Data Collected in Vicinity of WMA C," Rev. 0, INTERA, Inc./Washington River Protection Solutions, LLC, Richland, Washington.

RPP-RPT-58329, 2014, "Baseline Risk Assessment for Waste Management Area C," Rev. 0, INTERA, Inc./Washington River Protection Solutions, LLC, Richland, Washington.

RPP-RPT-58339, 2014, "Phase 2 RCRA Facility Investigation Report for Waste Management Area C," Draft A, Washington River Protection Solutions, LLC, Richland, Washington.

SGW-54165, 2014, "Evaluation of the Unconfined Aquifer Hydraulic Gradient Beneath the 200 East Area, Hanford Site," Rev. 0, CH2M HILL Plateau Remediation Company, Richland, Washington.

SGW-58561, 2015, "WMA C Quarterly October through December 2014 Quarterly Groundwater Monitoring Report," Rev. 0, CH2M HILL Plateau Remediation Company, Richland, Washington.

SGW-59669, 2016, "WMA C Quarterly October Through December 2015 Quarterly Groundwater Monitoring Report," Rev. 0, CH2M HILL Plateau Remediation Company, Richland, Washington.

van Genuchten, M. Th., 1980, "A Closed-form Equation for Predicting the Hydraulic Conductivity of Unsaturated Soils," Soil Science Society of America Journal, Vol. 44, No. 5, pp. 892–898.

WAC 173-303-610, "Closure and Post-Closure," Washington Administrative Code, as amended.

WAC 173-340-747, "Deriving Soil Concentrations for Groundwater Protection," Washington Administrative Code, as amended.

Washington State Department of Ecology Cleanup Levels and Risk Calculation (CLARC), Queried 08/30/2016, [CLARC Data Tables – July 2015, Chemical Parameters], https://fortress.wa.gov/ecy/clarc/FocusSheets/CLARC%20Parameters.pdf

WCH-520, 2013, "Performance Assessment for the Environmental Restoration Disposal Facility, Hanford Site, Washington," Rev. 1, Washington Closure Hanford, Richland, Washington.

WHC-EP-0645, 1995, "Performance Assessment for the Disposal of Low-Level Waste in the 200 West Area Burial Grounds," Westinghouse Hanford Company, Richland, Washington.

WHC-EP-0707, 1994, "216-U-10 Pond and 216-Z-19 Ditch Characterization Studies," Rev. 0 (formerly RHO-ST-45), Westinghouse Hanford Company, Richland, Washington.

WHC-EP-0815, 1995, "Groundwater Impact Assessment Report for the 216-T-4-2 Ditch," Westinghouse Hanford Company, Richland, Washington.

WHC-SD-EN-AP-012, 1991, "Interim-Status Groundwater Monitoring Plan for the Single-Shell Tanks," Rev. 1, Westinghouse Hanford Company, Richland, Washington.

WHC-SD-WM-EE-004, 1995, "Performance Assessment of Grouted Double-Shell Tank Waste Disposal at Hanford," Rev. 1, Westinghouse Hanford Company, Richland, Washington.

WHC-SD-WM-TI-730, 1996, "Performance Assessment for the Disposal of Low-Level Waste in the 200 East Area Burial Grounds," Rev. 0, Westinghouse Hanford Company, Richland, Washington.

WHC-SD-WM-TI-731, 1996, "Predominant Radionuclides in Hanford Site Waste Tanks," Rev. 0, Westinghouse Hanford Company, Richland, Washington.

WSRC-MS-2003-00582, 2004, "Performance Assessment/Composite Analysis Modeling to Support a Holistic Strategy for the Closure of F Area, a Large Nuclear Complex at the Savannah River Site," Rev. 1, Savannah River Technology Center, Aiken, South Carolina.

Ye, M., R. Khaleel, T. J. Yeh, 2005, "Stochastic analysis of moisture plume dynamics of a field injection experiment," Water Resources Research, Vol. 41, W03013.

Yeh, T.-C. J., M. Ye, R. Khaleel, 2005, "Estimation of effective unsaturated hydraulic conductivity tensor using spatial moments of observed moisture plume," Water Resources Research, Vol. 41, W03014.